UNIVERSITE MONTPELLIER II
SCIENCES ET TECHNIQUES DU LANGUEDOC

T H E S E

pour obtenir le grade de

DOCTEUR DE L'UNIVERSITE MONTPELLIER II

Discipline : Biochimie et Biologie Cellulaire et Moléculaire

Formation doctorale : Biologie Santé

Ecole Doctorale : Sciences Chimiques et Biologiques pour la Santé

présentée et soutenue publiquement

par

ABES SAÏD

Le 03 octobre 2007

Optimisation des vecteurs peptidiques :

application à la délivrance d'analogues d'oligonucléotides à visée thérapeutique (PNA et PMO)

JURY

M. Hans P. Merkle	Professeur, ETH Zürich Swisse	Rapporteur
M. Didier Betbeder	Professeur, Université d'Artois	Rapporteur
M. Gilles Divita	Directeur de recherche CNRS-CRBM, Montpellier	Examinateur
M. Jamal Tazi	Professeur, Université Montpellier 2	Examinateur
M. Jean-Jacques Vasseur	Directeur de recherche CNRS, Université Montpellier 2	Examinateur
M. Bernard Lebleu	Professeur, Université Montpellier 2	Directeur de Thèse

UNIVERSITE MONTPELLIER II
SCIENCES ET TECHNIQUES DU LANGUEDOC

T H E S E

pour obtenir le grade de

DOCTEUR DE L'UNIVERSITE MONTPELLIER II

Discipline : Biochimie et Biologie Cellulaire et Moléculaire

Formation doctorale : Biologie Santé

Ecole Doctorale : Sciences Chimiques et Biologiques pour la Santé

présentée et soutenue publiquement

par

ABES SAÏD

Le 03 octobre 2007

Optimisation des vecteurs peptidiques :

application à la délivrance d'analogues d'oligonucléotides à visée thérapeutique (PNA et PMO)

JURY

M. Hans P. Merkle	Professeur, ETH Zürich Swisse	Rapporteur
M. Didier Betbeder	Professeur, Université d'Artois	Rapporteur
M. Gilles Divita	Directeur de recherche CNRS-CRBM, Montpellier	Examinateur
M. Jamal Tazi	Professeur, Université Montpellier 2	Examinateur
M. Jean-Jacques Vasseur	Directeur de recherche CNRS, Université Montpellier 2	Examinateur
M. Bernard Lebleu	Professeur, Université Montpellier 2	Directeur de Thèse

A toute ma famille

Remerciements

Ce travail a été réalisé au sein du CNRS UMR5235 -Département Défenses Antivirales et Antitumorales- sous la direction du professeur Bernard LEBLEU à qui j'exprime toute ma reconnaissance pour m'avoir donné l'opportunité d'évoluer pendant ces années de thèse dans son équipe, et avant tout de m'avoir fait partager ses connaissances, sa passion pour la recherche biomédicale. Je le remercie chaleureusement pour son encadrement de haute qualité.

Je remercie les professeurs Didier Betbeder et Hans P. Merkle pour leur lecture du manuscrit, ainsi que le professeur Jamal Tazi et les Docteurs Jean-Jacques Vasseur et Gilles Divita qui ont accepté de faire partie du jury d'examen de cette thèse.

Mes chaleureux remerciements vont également aux docteurs M. J. Gait (MRC Cambridge UK), Hong Moulton (AVIBiopharma, USA), Jean-Jacques Vasseur (UMII), le professeur K. Ganesh (NCL Pune, India), les Docteurs Philippe Claire (IGF, Montpellier) et Paul Prevot (UMR5235) pour leur grande contribution à ma thèse.

Un grand merci à mon épouse, Bérénice, pour ses conseils, sans oublier tous les membres du département Défenses Antivirales et Antitumorales (Alain, Sarah, Rachida, Dina, Emilie, Georges, Caty, Annie, Danièle et Gilles) à qui j'adresse mes sincères remerciements. Merci également à Jean-philippe, Franck et José.

Pour finir je remercie la Ligue Régionale Contre le Cancer (Comité de L'Aude) pour le soutien financier dont j'ai bénéficié durant ces années de thèse.

Liste des publications (Ces publications ont été utilisées pour la rédaction de la thèse) **:**

Introduction :

- Revue I : **Abes, S.**, Richard, J. P., Thierry, A. R., Clair, P., et Lebleu, B. Tat-derived CPPs: discovery, mechanism of cell uptake and applications to the delivery of oligonucleotides, Handbook of Cell Penetrating Peptides (U.Langel,Ed.),CRC Press,Boca Raton, 2006, p(29-42)

Chapitre I :

- Article I : **Abes, S**, Ivanova, G. D, Abes, R, Arzumanov, A. A, Williams, D, Owen, D, Lebleu, B and Gait, M. J. Peptide-based delivery of steric-block PNA oligonucleotides. *Sous presse à Humana Press.*

Chapitre II :

- Article II: **Abes, S**, Williams, D., Prévot, P., Thierry, A. R., Gait, M, J., et Lebleu, B. Endosome trapping limits the efficiency of splicing correction by PNA-oligolysine conjugates. *J Control Release*, 2006, 110(3):595-604.

- Article III: Wolf, Y., Pritz, S., **Abes**, S., Bienert, M., Lebleu, B., et Oehlke, J. The mode of the chemical linkage of cell-penetrating peptides to PNAs dramatically influences the antisense activity. *Biochemistry*, 2006, 45(50):14944-54

- Article IV: Turner, J. J., Ivanova, G. D., Verbeure, B., Williams, D., Arzumanov, A. A., **Abes, S.**, Lebleu, B., et Gait, M. J. Cell-penetrating peptide conjugates of peptide nucleic acids (PNA) as inhibitors of HIV-1 Tat-dependent *trans*-activation in cells. *Nucleic Acids Res*, 2005, 33(21):6837-49.

Chapitre III :

- Article V : **Abes, S.**, Moulton, H. M., Turner, J. J., Clair, P., Richard, J. P., Iversen, P., Gait, M. J., et Lebleu, B. Peptide-based delivery of nucleic acids: Design, mechanism of uptake and application to splice-correcting oligonucleotides. *Biochemical Society Transaction*. 2007, 35(Pt 1):53-5

- Article VI: **Abes, S.**, Moulton, H. M., Clair, P., Prevot, P., Youngblood, D. S., Wu, R. P., Iversen, P. L., et Lebleu, B. Vectorization of morpholino oligomers by the (R-Ahx-R)4 peptide allows efficient splicing correction in the absence of endosomolytic agents. *J Control Release*, 2006, 116(3):304-13.

- Article VII: **Abes, S.**, Turner, J. J., Ivanova, G. D., Owen, D., Williams, D., Clair, P., Gait, M. J and Lebleu, B. Efficient splicing correction by PNA conjugation to an R6-Penetratin delivery peptide. *Nucleic Acids Res*, 2007, 1-8.

Chapitre IV :

- Article VIII: **Saïd Abes**, Hong M. Moulton[1], Philippe Clair, Rachida Abes, Paul Prevot, Derek S. Youngblood[1], Rebecca P. Wu[1], Patrick L. Iversen[1] and Bernard Lebleu. Delivery of steric block morpholino oligomers by $(R\text{-}X\text{-}R)_4$ peptides: structure-activity studies. En preparation

Chapitre V :

- Revue II: Debart, F., **Abes, S.**, Deglane, G., Moulton, H. M., Clair, P., Gait, M. J., Vasseur, J. J., et Lebleu, B. Chemical Modifications to Improve the Cellular Uptake of Oligonucleotides. *Curr Top Med Chem*, 2007, 7(7):727-37.

- Article IX: Deglane, G., **Abes, S**., Michel, T., Prévot, P., Vives, E., Debart, F., Lebleu, B., et Vasseur, J. J. Impact of the Guanidinium Group on Hybridisation and Cellular Uptake of Cationic Oligonucleotides. *Chembiochem.* 2006, 7(4):684-692.

Publications additionnelles:

- Abes, R, Arzumanov, A. A, Moulton, H. M, **Abes, S**, Ivanova, G. D, Iversen, P. L, Gait, M. J and Lebleu, B. Cell penetrating peptide-based delivery of oligonucleotides: an overview. *Biochemical Society Transaction*. 2007, 35(Pt 4):775-9.

- Moulton, H. M., Fletcher, S., Neuman B. W., McClorey, G., Stein, D A., **Abes, S.**, Wilton, S., Buchmeier, M. J., Lebleu, B and Iversen, P. L. Cell penetrating peptide–Morpholino conjugates skipped DMD exons and inhibited murine coronavirus replication in vivo. Sous presse à *Biochemical Society Transaction.* 2007, 35(Pt 4):826-8.

- Resina, S., **Abes, S.**, Turner, J. J., Prevot, P., Travo, A., Clair, P., Gait, M. J., Thierry, A. R., and Lebleu, B. Lipoplex and peptide-based strategies for the delivery of steric-block oligonucleotides. Sous presse *International Journal of Pharmaceutics.*

- Thierry, A. R., **Abes, S**., Resina, S., Travo, A., Richard, J. P., Prevot, P., et Lebleu, B. Comparison of Basic peptides- and lipid-based strategies for the delivery of splice correcting oligonucleotides. *Biochim Biophys Acta, Biomembrane*. 2006, 1758(3):364-74.

- R.Abes, A.Arzumanov, H.Moulton, **S.Abes**, G.Ivanova, M.J.Gait, P.Iversen and B.Lebleu. Arginine-rich cell penetrating peptides : design, structure-activity and applications to alter pre-mRNA splicing by steric-block oligonucleotides. Sous press à J peptide Science

Sommaire

Introduction générale

Chapitre I

Matériels et méthodes

Chapitre II

Chapitre III

Chapitre IV

Chapitre V

Chapitre VI

Sommaire figures

Sommaire tableaux

Introduction générale

1. Préface

De la fiction, de l'art ou de la science ?

Le gène comme médicament ? Soigner des maladies par des manipulations sur le génome a fait la gloire de l'imaginaire et de la fiction il y a quelques décennies. Les récentes avancées, extrêmement rapides, de nos connaissances dans le domaine de la génomique fonctionnelle et de la protéomique ont permis de mieux cerner les bases moléculaires de nombreuses maladies.

De la fiction ou de la science ? La thérapie génique consiste à remplacer un gène défectueux, responsable de pathologies souvent incurables, au sein d'une cellule d'un organisme humain par son homologue normal.

Selon les rapports de l'Office of Technology Assessment en 1984 : *« La thérapie génique est l'insertion délibérée de matériel génétique dans l'organisme d'un patient pour corriger un défaut précis à l'origine d'une pathologie, que ce soit à titre curatif ou préventif »*. Le Comité International de Bioéthique (CIB), en 1994, définit lui la thérapie génique comme *« la modification délibérée du matériel génétique de cellules vivantes pour prévenir ou guérir les maladies »*. Au cours de la précédente décennie, de grands espoirs ont été placés dans la thérapie génique. Cependant à ce jour, cette stratégie ne s'est montrée efficace que pour les enfants atteints d'un déficit immunitaire sévère combiné lié au chromosome X (DISC-X), ou *maladie des enfants Bulle* (Cavazzana-Calvo et Fischer 2004). De plus, récemment, des problèmes liés au traitement sont apparus, conduisant à l'arrêt de l'utilisation de cette technique et suscitant un vif débat au sein de la communauté scientifique sur le futur de la thérapie génique. Néanmoins, une stratégie alternative pour traiter les pathologies liées à des gènes défectueux commence à voir le jour. Le but de cette stratégie est d'identifier les mutations et de les cibler avec des oligonucléotides (ON) à visées thérapeutiques afin de les détruire (silencing) ou de les corriger. Il est en particulier possible de concevoir et de synthétiser des ON interférant spécifiquement et efficacement avec l'expression d'un gène. C'est la *stratégie antisens*. Cette stratégie permet par l'effet antisens de l'acide nucléique

utilisé l'arrêt, la correction ou le déroutage de la machinerie de transcription/traduction d'un gène anormal. Grâce aux progrès de la chimie, plusieurs analogues d'acides nucléiques avec des propriétés physico-chimiques et pharmacocinétiques très prometteuses ont été développés. Toutefois plusieurs obstacles limitent leurs utilisations : les problèmes de ciblage, d'internalisation cellulaire, et de trafic intracellulaire limitent leur efficacité. Aujourd'hui, la plupart des travaux dans le domaine de l'utilisation de stratégies antisens concernent la résolution des problèmes suscités.

2. La stratégie antisens : les oligonucléotides antisens (ONs)

2.1. Introduction

Les oligonucléotides antisens (ONs) sont de courts fragments d'acides nucléiques (de 15-20 nucléotides) complémentaires ou antisens à leur cible (ADN, ARN). Par une hybridation spécifique sur la cible, ils corrigent une mutation au niveau du génome par action sur la machinerie d'expression des gènes (transcription, épissage ou traduction) (voir Tableau I).

Les travaux de Paterson et de ses collègues ont montré qu'il est possible d'arrêter l'expression d'un gène dans un système acellulaire (Cell-free system) par hybridation d'un acide nucléique exogène (Paterson et al. 1977). En 1978, Zamecnik et Stephenson ont montré qu'il est possible de stopper la réplication d'un rétrovirus dans des cellules en culture (Zamecnik et Stephenson 1978).

A l'époque, les scientifiques ont expliqué cet effet par un arrêt de la progression du ribosome ou de la polymérase par la formation d'un complexe ON/Cible. Mais des travaux ont montré par la suite que la cible est détruite par intervention de la RNaseH suite à l'hybridation avec l'ON (Dash et al. 1987; Minshull et Hunt 1986; Walder et Walder 1988).

Dans les années 80, Simons et Mizuno ont montré l'existence d'un mécanisme naturel utilisant des ARNs antisens (Mizuno et al. 1984; Simons et Kleckner 1983). Ces molécules jouent un rôle dans la régulation de l'expression de leurs propres gènes.

De la même manière, Izant a montré que ce même mécanisme est présent chez les cellules eucaryotes (Izant et Weintraub 1984).

Plus récemment et chez de nombreux eucaryotes, il a été montré que l'expression de petits ARNs doubles brins, de 21 nucléotides, régulent négativement l'expression génique. C'est l'interférence par l'ARN (voir Figure 1).

Tableau I : Stratégies antisens : Mécanisme d'action des antisens. Adapté de (Que-Gewirth et Sullenger 2007)

Oligonucléotides antisens (ONs-AS)	Mécanisme d'action	Références
ARN antisens	**Inhibition de l'expression du gène** : Dégradation de la cible par la RNaseH **Correction de l'expression du gène** : Détournement de l'épissage ou saut d'exon.	(Kurreck 2003; Mercatante et al. 2001)
Ribozyme	**Idem ARN antisens**	(Li et al. 2007)
siRNA et miRNA	**Inhibition de l'expression du gène :** dégradation de l'ARNm par le complexe RISC/DICER ou inhibition de la traduction	(Filipowicz 2005; Pillai 2005)
Aptamer	**Inhibitions de protéines** : ARNs ou ADNs structurés et antagonistes de protéine	(Que-Gewirth et Sullenger 2007)

2.2. Evolution

Le premier problème rencontré avec cette nouvelle stratégie est la stabilité des ONs dans les fluides biologiques. Ces ONs sont dégradés facilement et rapidement, dans le sang et la cellule, par les exonucléases et endonucléases. C'est ainsi que la première génération d'analogues d'oligonucléotides avec des propriétés pharmacocinétiques, de stabilité biologique, d'hybridation et de haute affinité pour la cible, très prometteuses est produite: on parle de phosphorothioate (PS) (Campbell et al. 1990; Cossum et al. 1993; Crooke 2004; Hoke et al. 1991). En réalité, les PS (Voir Tableau II) sont synthétisés pour la première fois en 1968 par Eckstein et ses collègues (Matzura et Eckstein 1968). Ce sont les analogues qui ont été les plus étudiés et les plus utilisés à ce jour (Eckstein 2000), comme inhibiteurs de la réplication du virus HIV par exemple (Matsukura et al. 1987).

Comme évoqué précédemment, ces analogues d'ONs possèdent des caractéristiques intéressantes pour une application thérapeutique. Non seulement ces PS activent la RNaseH, mais la liaison phosphorothioate leur confère une résistance accrue aux nucléases et augmente

leur stabilité dans le sérum et le milieu intracellulaire (Campbell et al. 1990; Gewirtz et al. 1998). Toutefois, ces PS présentent des inconvénients tels que des interactions non spécifiques avec les polycations comme les Heparin-binding proteins (Brown et al. 1994; Guvakova et al. 1995; Rockwell et al. 1997), qui peuvent être cytotoxiques (Levin 1999).

De nouveaux ONs aux propriétés pharmacologiques améliorées ont donc été développés : les ONs de seconde génération comme les ARN 2'OMethyle et les ARN 2'OMethoxyethyl, et de la troisième génération comme les Peptides Nucleic Acids (PNA), les Phosphoramidates Morpholino (PMO), les Locked Nucleic Acids (LNA), les Phosphoramidates et d'autres encore (voir tableau II).

La plupart de ces ONs n'activent pas cependant la RNaseH [comme revue (Kurreck 2003)] mais permettent néanmoins d'interférer avec l'expression d'un gène par blocage stérique. Ceci est à l'origine d'une nouvelle approche thérapeutique qui se base sur l'altération ou le déroutage d'un épissage alternatif. De nombreuses applications sont envisageables dans la mesure où ce processus de maturation des ARN messagers (ARNm) est à l'origine de plusieurs maladies liées à des gènes défectueux (Garcia-Blanco et al. 2004; Venables 2004; Venables 2006), sans oublier que la majorité des virus utilisent ce processus. L'utilisation d'ONs qui n'activent pas la RNaseH peut corriger l'épissage et augmenter ainsi l'expression de la variante souhaitée de la protéine.

Tableau II : Les analogues d'acides nucléiques : tableau récapitulatif de quelques analogues d'oligonucléotides [pour revue voir (Kurreck 2003; Mercatante et al. 2001)]

<table>
<tr><th>ADN non modifié</th><th colspan="5">Première génération</th></tr>
<tr><td>ADN phosphodiester
 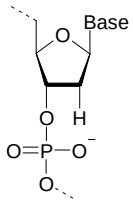 </td><td colspan="5">ADN Phosphorothioate (PS)
 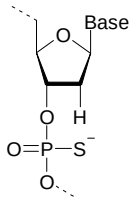 </td></tr>
<tr><th colspan="6">Deuxième génération</th></tr>
<tr><td colspan="3">ARN 2'O-methyl
 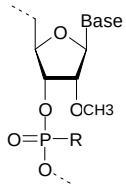 </td><td colspan="3">ARN 2'O-methoxy-ethyl
 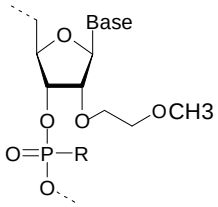 </td></tr>
<tr><th colspan="6">Troisième génération</th></tr>
<tr><td>Peptide Nucleic Acid (PNA)
 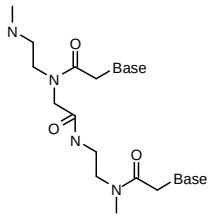 </td><td>Phosphoramidate
 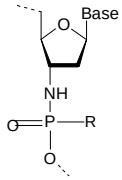 </td><td>Locked Nucleic Acid (LNA)
 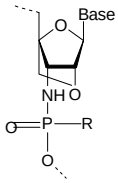 </td><td>Morpholino phophoramidate (PMO)
 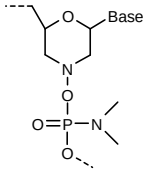 </td><td>Cyclohexene nucleic Acid (CeNA)
 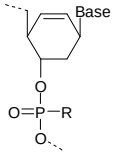 </td><td>2'Fluoro-Arabino Nucleic Acid
 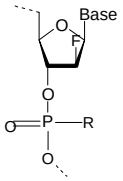 </td></tr>
</table>

NB : R = O^- ou S^-

2.3. Internalisation cellulaire, trafic intracellulaire et biodisponibilité

L'internalisation cellulaire de l'ADN ainsi que son mécanisme d'entrée sont documentés depuis les années 50. Plusieurs travaux datant de cette période montrent la possibilité de transformer des cellules, procaryotes ou eucaryotes, par de l'ADN purifié.

A titre d'exemple, une étude montre qu'il est possible avec de l'extrait d'ADN purifié à partir de cellules saines de la moëlle osseuse de restaurer le phénotype normal de cellules d'un patient atteint d'anémie (Kraus 1961).

Le caractère anionique des ONs à visée thérapeutique n'est pas vraiment un avantage pour leur internalisation et leur trafic intracellulaire (Pichon et al. 1997). Pour être efficace, les ONs doivent rentrer dans le cytoplasme ou le noyau. Or, la membrane plasmique constitue une barrière contre toute tentative d'entrée dans la cellule de macromolécules chargées et est imperméable aux polyanions (Budker et al. 1992). Cependant une localisation vésiculaire cytoplasmique, péri-nucléaire, a été observée après incubation d'ONs fluorescents avec des cellules en culture (Ceruzzi et al. 1990).

Plusieurs récepteurs potentiels d'ONs ont été caractérisés (Beltinger et al. 1995; de Diesbach et al. 2000; de Diesbach et al. 2002; Geselowitz et Neckers 1992; Kole et al. 2004). D'autre part, dans certains types cellulaires comme les cellules rénales, les ONs utilisent les canaux ioniques membranaires (Hanss et al. 1998).

Plusieurs études ont indiqué que l'internalisation des ONs se fait par un processus actif dépendant de l'énergie, de la dose, de la température et du temps (Clark 1995; Pichon et al. 1997; Shi et Hoekstra 2004; Temsamani et al. 1994). Beltinger et ses collègues ont révélé que l'internalisation des ONs est réalisée par endocytose à très haute concentration alors qu'à des doses de 1µM leur entrée est récepteur dépendant (Beltinger et al. 1995). Dans le cas où l'endocytose est utilisée, la séquestration dans les endosomes limite l'efficacité de ces oligonucléotides (Akhtar et Juliano 1992).

A l'arrivée dans le compartiment cytoplasmique, l'accumulation dans le noyau est rapide (Beltinger et al. 1995; Clarenc et al. 1993; Gao et al. 1993). Les travaux réalisés notamment par notre équipe ont indiqué qu'une localisation nucléaire est observée rapidement après une micro-injection cytoplasmique d'ONs fluorescents (Leonetti et al. 1991).

La majorité des travaux sur la biodisponibilité des ONs ont rapporté que les ONs ou leurs analogues s'accumulent en grosse partie dans les reins et le foie après une injection intraveineuse ou intrapéritonéale chez la souris (Agrawal et al. 1995; Butler et al. 1997; Srinivasan et Iversen 1995). Chez le singe, les ONs se retrouvent en majorité dans les reins et le foie, mais aussi dans le thymus, la moëlle osseuse, les glandes salivaires et le pancréas. Une accumulation modérée est également observée dans le muscle, dans l'appareil gastro-intestinal ainsi que dans la trachée. Une faible accumulation est remarquée dans le cerveau, la peau et la prostate (Iversen et al. 1995).

2.4. Application en clinique

Cette dernière décennie, les développements récents et rapides de nos connaissances de l'organisation des génomes et de leur expression ont permis de mieux cerner les bases moléculaires de nombreuses maladies (Garcia-Blanco et al. 2004; Venables 2004; Venables 2006) et de proposer de nouvelles cibles pour le développement d'agents thérapeutiques. Comme déjà décrit brièvement, les antisens possèdent un immense potentiel thérapeutique. Ils peuvent détruire (Silencing), perturber ou corriger, d'une manière spécifique, leur cible à différents niveaux de la machinerie transcription/traduction (Figure 1).

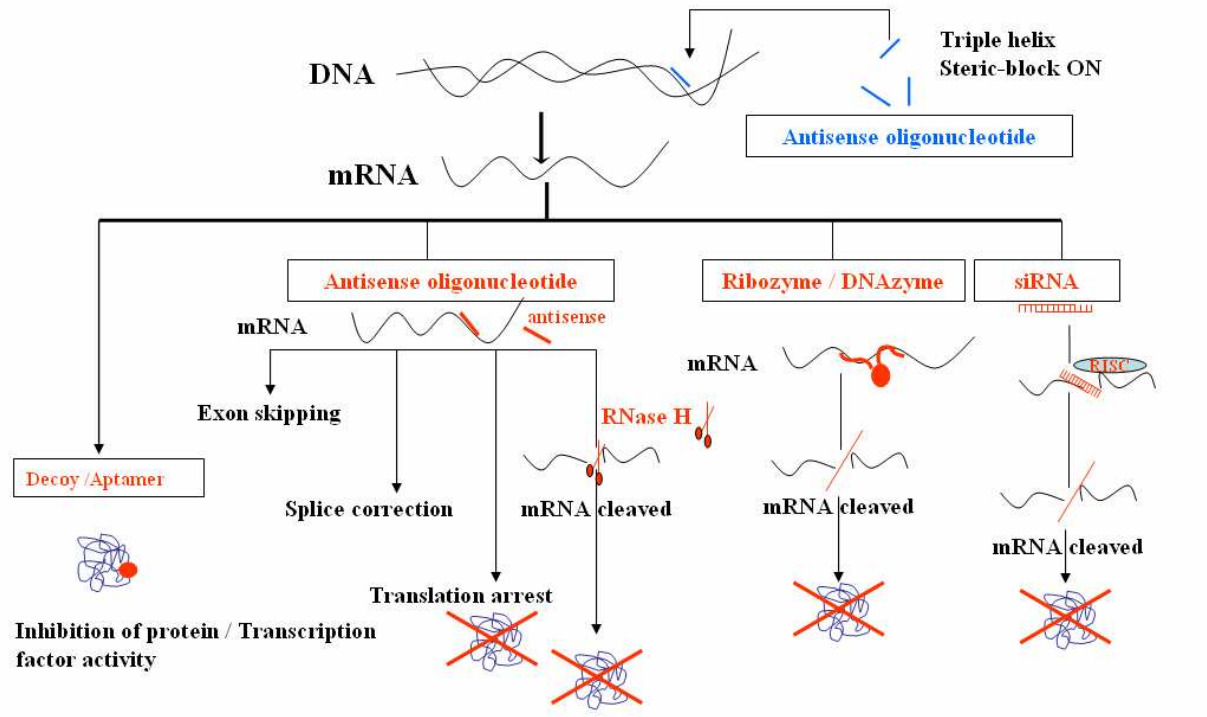

Figure 1 : *Stratégie antisens :* Les ONs s'hybrident spécifiquement à leur cible et peuvent entraîner leur destruction (Silencing), le blocage de leur expression (steric-block ON) ou même la correction d'une expression défectueuse (exon skipping, splice correction). Les stratégies les plus utilisées pour l'instant concernent la destruction ciblée d'un ARN par un ON antisens (par recrutement de la RNaseH), par un siRNA (par recrutement de l'endonucléase associée au complexe RISC), par un ribozyme ou par un DNAzyme

Comme décrit dans la première partie de l'introduction, l'efficacité de ces ONs est limitée par plusieurs facteurs. Premièrement, le caractère polyanionique des ONs rend peu efficace leur internalisation par les cellules. Deuxièmement, la séquestration des ONs dans des vésicules d'endocytose aboutit à leur dégradation par les nucléases des lysosomes. Troisièmement, la biodisponibilité des ONs est limitée à certains organes. Après injection, la plus grande partie des ONs sont éliminés par les reins et le foie, principaux organes du

métabolisme médicamenteux et l'augmentation de la dose injectée provoque des toxicités cellulaires.

Ces limites n'ont pas empêché le démarrage d'essais cliniques pour le traitement de plusieurs maladies. Vitarvene^{TM}, est un ON de première génération (phosphorothioate) commercialisé par ISIS/Novartis. Cet ON antisens inhibe l'infection de la rétine par le cytomégalovirus après une injection intra-vitréenne [pour revue (Crooke 2004)]. D'autres ON antisens sont en cours d'évaluation (voir tableau III) [pour revue (Crooke 2004), données supplémentaires], mais aucune stratégie à base d'ON antisens n'a pour l'instant été couronnée de succès mis à part le cas très particulier du traitement des maladies oculaires.

Tableau III : Oligonucléotides antisens à visée thérapeutique et essais cliniques [pour revue (Crooke 2004), données supplémentaires]

Nom	Chimie	Cible	Pathologie	Phase clinique	Biopharma
Vitravene ™	Phosphorothioate	IE2	Retinitis virale (CMV)	Sur le Marché	Isis/Novartis
Affintak™	Phosphorothioate	PKC-α	Cancer	III	Isis/Lilly
Alicaforsen™	Phosphorothioate	ICAM-1	Maladie de Crohn's	III	Isis
ISIS 2503	Phosphorothioate	H-ras	Cancer du pancréas et autres	II	Isis
MG98	Non communiqué (chimère)	ADNMeTase	Cancers du sein, colon et poumons	I	Mythygene/ Hybridon
Genasense™ (G3139)	Phosphorothioate	Bcl-2	Cancer	II/III	Genta
Resten-NG	NeuGene (Morpholino)	c-myc	Réstenose	III	AVIBioPharma
Oncomyc-NG	NeuGene (Morpholino)	c-myc	Cancer	II	AVIBioPharma
AVI-4014	NeuGene (Morpholino)	NFκB	Inflammation	I	AVIBioPharma
HEPTAZYME™	Ribozyme	HCV	VHC	II	RPI
ANGIOZYME™	Ribozyme	VEGFR-1	Cancer du sein	I/II	RPI
Product R	Peptide nucleic acids (PNA)	CCR5	VIH	I/II	Advanced Viral PNA Research Corp.
R-95288	Aptamer	HIV-1	VIH	I	Sankyo KK

3. Les stratégies de délivrance : Application à la délivrance d'oligonucléotides antisens

3.1. Introduction

Dans la première partie, nous avons vu le grand potentiel thérapeutique des oligonucléotides antisens, ainsi que les limites de leur utilisation *in vitro* en culture cellulaire ou *in vivo* dans des modèles animaux. La délivrance des oligonucléotides antisens reste un grand problème d'actualité. Le vecteur idéal doit assurer un adressage vers un type cellulaire cible, une internalisation efficace et une accumulation dans le compartiment souhaité de l'ON antisens. Le vecteur ne doit pas être toxique.

Ces dernières années, plusieurs travaux sur différentes stratégies de délivrance physique, virale et non virale, dans le but d'augmenter l'efficacité des ON antisens ont été proposés [comme revue (Luo et Saltzman 2000)]. Les méthodes physiques telles que la microinjection (Kola et Sumarsono 1995; Leonetti et al. 1991) et l'électroporation (Bergan et al. 1996; Flanagan et Wagner 1997) sont peu ou pas envisageables en thérapeutique.

Des stratégies alternatives qui se basent sur l'utilisation des vecteurs viraux (Mancheno-Corvo et Martin-Duque 2006; Zhang et Godbey 2006) ou synthétiques non-viraux (Torchilin 2006) sont en cours de développement. Une des stratégies qui semble très intéressante est la cationisation des ONs antisens, les premiers résultats montrant de bonnes capacités d'internalisation cellulaire (Debart et al. 2007; Deglane et al. 2006).

3.2. Les vecteurs viraux

Un vecteur viral doit être un cheval de Troie, doté d'une capside identique à celle du virus de départ, mais qui renferme un génome viral modifié (recombinant) porteur du gène thérapeutique. À l'encontre de l'infection virale, son entrée dans la cellule ne conduira pas à la production de nouvelles particules, mais permettra le transfert du gène thérapeutique. Les rétrovirus, adénovirus, les virus adéno-associés et le virus de l'herpes sont largement étudiés comme systèmes de délivrance de gènes thérapeutiques [pour revue récente (Zhang et Godbey 2006)].

3.2.1. Les rétrovirus :

Les rétrovirus ont été les premiers à être utilisés (Ellis et Bernstein 1989; Guild et al. 1988; Miller et al. 1993). Les rétrovirus sont des virus à ARN enveloppé (Zhang et Godbey 2006). Le virus sauvage provoque des infections chroniques. Le provirus rétroviral profite de la mitose pour rentrer dans le noyau, ce qui entraîne une limitation de transduction aux cellules en prolifération (Roe et al. 1993). Après internalisation nucléaire de l'ARN viral, ce dernier est rétrotranscrit en ADN ensuite intégré au génome de la cellule hôte. Cette intégration permet de conserver l'information génétique durant les divisions cellulaires [pour revue récente (Zhang et Godbey 2006)].

Toutefois, l'insertion se fait d'une manière aléatoire ce qui augmente le risque de mutation par altération du fonctionnement d'un gène actif, et la possibilité de transmettre cette mutation à la descendance. De plus, le nombre de copies qui s'intègrent dans le génome est faible. La faible efficacité de transfert *in vivo*, ainsi que la non fiabilité de l'insertion de cette méthode peuvent provoquer de multiples effets pathogènes et immunogènes (Anson 2004; Yi et al. 2005).

3.2.2. Les adénovirus :

Les adénovirus sont des virus sans enveloppes, à ADN linéaire double brin d'environ 36Kb (Zhang et Godbey 2006). Le tropisme cellulaire de ce virus est très large : il transduit efficacement de nombreux types cellulaires en prolifération ou quiescentes (Wu et Ataai 2000). Cependant, le génome viral reste épisomal et son expression est transitoire et faible. Cette limitation n'est pas un avantage pour le traitement de pathologies chroniques. En outre, les cellules infectées par ce type de vecteur sont éliminées rapidement par le système immunitaire (Mizuguchi et Hayakawa 2004). Toutefois l'utilisation de ces vecteurs pour l'expression d'un gène suicide, dans l'optique d'éliminer par exemple des cellules cancéreuses, est envisageable.

3.2.3. Les virus adéno-associés (AAV) :

L'AAV est un parvovirus de petit taille de (20-25nm), non enveloppé et avec une capside. Le matériel génétique de ce virus est un simple brin d'ADN, linéaire de 4.7Kb

(Zhang et Godbey 2006). Ce virus a besoin du virus de l'Herpès ou de l'adénovirus pour se répliquer. Les vecteurs dérivant de ce virus transduisent efficacement plusieurs types cellulaires (Hendrie et Russell 2005). Comme ils transduisent des cellules prolifératives et quiescentes, ils permettent une expression à long terme du transgène, qui peut être intégré au génome de la cellule hôte ou rester épisomal (Zhang et Godbey 2006). Ils sont non pathogènes et non immunogènes. Cependant leur production est difficile et le risque de mutation suite à une mauvaise insertion est élevé. Leur dépendance de l'adénovirus ou du virus de l'Herpès pour se répliquer s'ajoute à ces complications.

3.3. Les vecteurs non-viraux

Ces dernières années, les avancées enregistrées dans le développement des vecteurs non-viraux restent modestes et limitées au développement de vecteurs à base de lipides cationiques et de peptides basiques. La délivrance d'acides nucléiques avec différents vecteurs, comme la polyethyleneimine (PEI), les lipides cationiques, les peptides cationiques et les protéines, a été documentée *in vivo* et *in vitro* (Debart et al. sous presse; Luo et Saltzman 2000; Wiethoff et Middaugh 2003).

3.3.1. Délivrance par des lipides cationiques :

Cette méthode est l'une des plus populaires, à côté des nanoparticules et des dendrimères, pour la délivrance d'ONs. Le chlorure de *N*-[1-(2,3dioleyloxy)propyl]-*N*,*N*,*N*-trimethylammonium (DOTMA) fut le premier à être développé comme vecteur synthétique de gène (Felgner et al. 1987). Les lipides cationiques sont des molécules amphiphiles (Wasungu et Hoekstra 2006). Trois parties composent les lipides cationiques utilisés dans la délivrance d'acides nucléiques : un domaine basique, un domaine hydrophobe et un domaine hydrophile. Les charges cationiques de ces lipides permettent des interactions électrostatiques avec les charges négatives des groupements phosphates des acides nucléiques. Cette interaction aboutit à la formation de complexes (lipides cationiques-acides nucléiques) connus sous le nom de ***lipoplexes***.

Ces complexes sont en général cationiques, facilitant ainsi les interactions avec les membranes cellulaires vraisemblablement au niveau des glycoprotéoglycanes. Ces interactions sont suivies d'une internalisation cellulaire par endocytose (Figure 2). Les travaux réalisés au laboratoire ont révélé une localisation vésiculaire des lipoplexes après une

incubation de 6h avec des cellules en culture. Cette localisation est nucléaire après 12h d'incubation (Resina et al. 2007; Thierry et al. 2006). L'effet cytotoxique de cette stratégie lipidique est souvent associé à la nature cationique de ces lipides [revue récente (Lv et al. 2006)], au rapport de charge des lipides et des acides nucléiques qui forment le complexe ainsi qu'à la dose du complexe à transfecter (Dass 2002).

Plusieurs tentatives afin de réduire cette toxicité, basées sur les modifications chimiques sur la partie hydrophilique du lipide, ont été testées. Elles consistent à utiliser un groupement imidazolium ou pyridinium comme groupement polaire (Roosjen et al. 2002; Solodin et al. 1995). Ces travaux ont montré une réduction de la toxicité cellulaire et une transfection efficace. D'autre part, les protéines sériques limitent l'efficacité de cette stratégie par des interactions avec les complexes, ce qui augmente la taille des particules et peut être à l'origine de toxicités cellulaires (Friend et al. 1996).

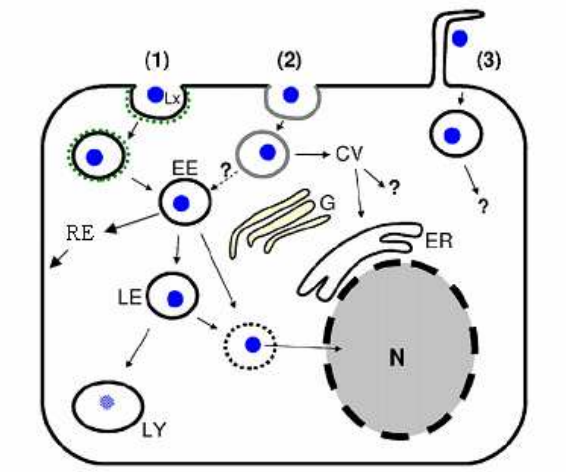

Figure 2 : *Mécanisme d'internalisation des lipoplexes :* (1) Endocytose clathrine dépendante. (2) Endocytose cavéoline dépendante. (3) macropinocytose.
EE : endosomes précoces ; RE : endosomes de recyclage; LE: endosomes tardifs; LY: lysosomes; CV: cavéosomes; G: golgi; ER: réticulum endoplasmique; N: noyau. (Wasungu et Hoekstra 2006)

3.3.2. Délivrance par des polymères cationiques :

La différence entre les polymères cationiques et les lipides cationiques est l'absence de la partie hydrophobe, ce qui les rend facilement solubles dans l'eau. Les plus étudiés et utilisés pour la délivrance de gènes sont : le PEI (Polyethyleneimine) et le PLL (polylysines) [revue récente (Lv et al. 2006)].

Le PEI est un vecteur efficace d'acides nucléiques (Figure 3). Il engendre des cytotoxicités très importantes sous une forme libre ou complexé à l'ADN (Godbey et al. 1999; Kim et al. 2005), toxicité liée à la taille du polymère. Une basse masse moléculaire (10Kd) du polymère permet une transfection efficace et réduit la toxicité (Fischer et al. 1999; Godbey et al. 1999).

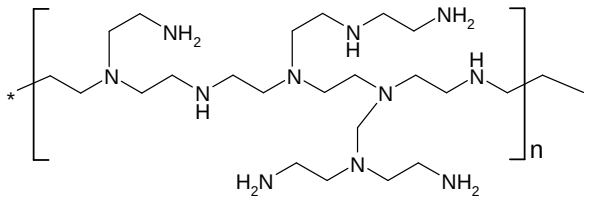

Figure 3 : *Structure du Polyethyleneimine (PEI)*

3.3.3. Délivrance par des peptides cationiques :

En 1965, Ryser HJ et Hanocock R montrent que les polypeptides basiques augmentent l'internalisation de l'albumine par des cellules tumorales. La poly(L-Lysine) (PLL) est un des premiers polypeptides utilisés pour le transfert de gènes (Wu et Wu 1987) et d'autres biomolécules (Arnold 1985; Ryser et Shen 1978; Shen et Ryser 1981). De hauts niveaux de transfection avec le PLL sont observés sur des cellules en culture. Cependant plusieurs paramètres conditionnent leur efficacité *in vivo*, tels que la taille du complexe. Il faut noter que la taille du complexe dépend aussi de la taille du PLL, de l'ADN, du rapport de charge (cationique/anionique), sans oublier les conditions de formation du complexe (Perales et al. 1994). A l'instar des polypeptides, les PLL sont facilement dégradés par les cellules. Lemaitre et Leonetti ont démontré qu'il est possible d'inhiber efficacement la réplication virale par des ONs délivrés par des PLL (Lemaitre et al. 1987; Leonetti et al. 1988).

L'endocytose est le mécanise par lequel les conjugués PLL-ONs sont internalisés dans les cellules (Lemaitre et al. 1987; Leonetti et al. 1990; Leonetti et al. 1988). Toutefois ces complexes exhibent une toxicité cellulaire rendant envisageable une utilisation *in vivo* (Leonetti et al. 1988).

Des travaux récents montrent que les PLL à structure dendritique (Figure 4) montrent une grande capacité de transfection sans toxicité significative (Ohsaki et al. 2002; Okuda et al. 2004). L'immunogénicité des PLL reste un sujet de controverse, malgré que des travaux de

plusieurs groupes montrent que le potentiel immunogène du PLL ainsi que des complexes PLL-acides nucléiques est faible ou nul (Ferkol et al. 1996).

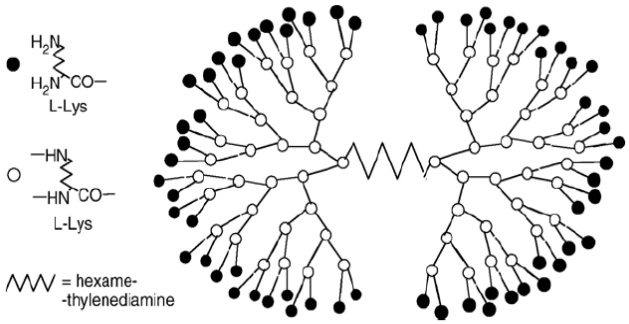

Figure 4 : *Poly(L-Lysine) à structure dendritique (KG6 pour 6^{éme} génération)*

4. Les peptides vecteurs

Les travaux récents montrent que des peptides à caractère basique peuvent traverser la membrane plasmique et pénétrer dans la cellule. Ces peptides sont regroupés sous le nom de Cell Penetrating Peptides (CPPs), Protein Transduction Domain (PTD) ou même Trojan Peptides (voir tableau IV).

Les CPPs sont des peptides de 7 à 30 acides aminés, naturels ou synthétiques capables de promouvoir la délivrance de biomolécules, de toutes tailles depuis des drogues anti-cancéreuses de petits poids moléculaires jusqu'à des nanoparticules ou des liposomes. Les CPPs traversent les membranes plasmiques d'une manière non spécifique, ce qui est un désavantage dans le cas où un ciblage est souhaité (Niesner et al. 2002). Les études récentes montrent que l'internalisation cellulaire de ces CPPs n'est pas totalement non spécifique mais dépend du type cellulaire utilisé (Mai et al. 2002; Violini et al. 2002; Ye et al. 2002). De plus, des stratégies associant des CPPs à un ciblage sont envisageables.

Historiquement, un mécanisme de translocation au travers de la membrane plasmique indépendant de l'endocytose et de l'énergie a été envisagé. La question du mécanisme d'entrée de ces CPPs dans les cellules suscite toujours un vif débat entre plusieurs équipes de recherches. Actuellement, les travaux sur le mécanisme d'internalisation des CPPs indiquent que les deux types, dépendant et indépendant de l'endocytose, peuvent être observés (Richard

et al. 2005; Richard et al. 2003; Simeoni et al. 2003), selon les CPPs et les concentrations expérimentales (concentration locale en particules) utilisées.

4.1. Le peptide Tat :

Le peptide Tat a été le plus utilisé des CPPs pour la délivrance de biomolécules variées [pour publication recente voir revue I (Abes et al. 2007)]. En 1988, des travaux ont rapporté que la protéine Tat du virus de l'immunodéficience humain (HIV-1) traverse la membrane par un mécanisme indépendant de l'énergie (Frankel et Pabo 1988; Green et Loewenstein 1988), mais des travaux plus récents plaident pour une endocytose de la protéine Tat via des vésicules à clathrine (Vendeville et al. 2004).

Les études de structures activités sur la protéine Tat ont indiqué qu'un fragment d'environ 12 acides aminés, fragment 48-60, est responsable de l'internalisation de la protéine Tat (Vives et al. 1997), résultat confirmé par d'autres groupes (Futaki et al. 2001; Wender et al. 2000). Les données initiales semblaient indiquer que l'internalisation cellulaire du peptide Tat est rapide et indépendante de la température (Vives et al. 1997). De même, Suzuki et ses collègues ont montré que les inhibiteurs d'endocytose n'affectent pas l'entrée du peptide Tat dans les cellules (Suzuki et al. 2002). Ces données faisaient penser que la pénétration de ce peptide dans les cellules était indépendante de l'endocytose (Futaki 2002). En 2003, Richard et ses collègues ont remis en question les données initiales et démontré que le processus utilisé par le peptide Tat pour entrer dans les cellules est bien l'endocytose (Richard et al. 2003) et que les protocoles utilisés initialement donneraient lieu à des artefacts expérimentaux. Ce mécanisme est dépendant de l'énergie, de la température et des héparanes sulfates membranaires. L'utilisation d'inhibiteurs de l'endocytose ou de mutants affectés dans l'expression des glycoprotéoglycanes diminue significativement l'internalisation du peptide Tat (Richard et al. 2005; Richard et al. 2003). La microscopie de fluorescence a révélé une co-localisation vésiculaire entre le peptide Tat et la transferrine (marqueur de l'endocytose) (Abes et al. 2007; Richard et al. 2005).

4.2. La pénétratine :

La pénétratine est un peptide vecteur dérivant de l'homéodomaine d'Antennapedia (43-58), une homéoprotéine de drosophile. Ce facteur de transcription interagit avec l'ADN via les 60 acides aminés conservés de l'homéodomaine (Gehring et al. 1994).
Les aminoacides de ce domaine adoptent une structure d'alpha hélice, l'homéodomaine étant formé de 3 hélices-α.

Ce peptide entre dans les cellules d'une manière énergie indépendante (Joliot et al. 1991) et de manière indépendante de l'endocytose (Derossi et al. 1996; Prochiantz 1996). Derossi et ses collaborateurs ont mis en évidence l'importance de la troisième hélice longue de 16 acides aminés, dans l'entrée de cet homéodomaine (Derossi et al. 1994).

Trois résultats particulièrement importants ont été obtenus :

- Le premier indique le rôle du résidu tryptophane 48 (W_{48}) qui ne peut être remplacé par aucun autre acide aminé hydrophobe sans diminution considérable de l'internalisation de l'homéodomaine.
- Le second montre qu'il n'y a pas de récepteur chiral qui assure l'entrée cellulaire du peptide dans la mesure où le peptide en série dextrogyre entre d'une manière aussi efficace dans les cellules.
- Le troisième révèle l'importance de la structure en hélice α pour l'internalisation. Une mutation (Q_{50}-P) déstabilise la structure en hélice et diminue dramatiquement l'efficacité d'entrée cellulaire de la pénétratine (Derossi et al. 1996; Derossi et al. 1994).

4.3. Autres peptides vecteurs :

Plusieurs peptides vecteurs issus de protéines naturelles ont été caractérisés, comme par exemple le Transportan, un peptide chimère dont la séquence est composée de la partie N terminale du neuropeptide galanine liée via une lysine à un peptide du venin de guêpe, le mastoparan. Il semble que l'internalisation du Transportan soit indépendante de la température, de l'énergie et de récepteur (Pooga et al. 2001). A l'origine le transporatan est issu d'une étude sur de nouveaux ligands pour le récepteur de la galanine. En 1996, Langel et ses collègues produisent un ligand chimère nommé galapran (Langel et al. 1996). Les travaux

de Zorko ont révélé que le galapran entre dans les cellules d'une manière indépendante de récepteur et active la protéine G (Zorko et al. 1998). La seule différence entre le Transportan et le galapran est la substitution de la proline 13 par une lysine (Pooga et al. 1998). Des analogues du Transportan n'activant pas les protéines G ont été produits, comme le TP10 (Soomets et al. 2000).
D'autre CPPs dérivés de protéines ont été proposés comme le peptide 9-32 de la calcitonine humaine ou le peptide VP22 dérivant de la protéine de l'enveloppe du virus Herpès Simplex (Elliott et O'Hare 1997; Schmidt et al. 1998). Une autre catégorie de peptides vecteurs issus de peptides antimicrobiens, comme la série SynB, dérivée de la protégrine (Drin et al. 2003; Drin et Temsamani 2002; Rousselle et al. 2003), peuvent traverser efficacement les membranes plasmiques.

D'autres peptides vecteurs synthétiques ont été développés sur la base de l'importance des charges cationiques dans l'internalisation cellulaire. Parmi ces peptides, citons les oligoarginines (Rothbard et al. 2000; Wender et al. 2000), les oligolysines (Siwkowski et al. 2004) et les polyhistidines (Pichon et al. 2001).

Une autre catégorie de vecteurs peptidiques regroupe les peptides amphipathiques dont il existe deux types : amphipathiques primaires et secondaires. Les amphipathiques primaires sont composés de deux domaines bien distincts, une partie hydrophobe liée par un bras espaceur à une partie hydrophile. Celle-ci, riche en lysine, est composée de la séquence de localisation nucléaire de l'antigène T du virus simien (SV40), et est responsable de l'adressage nucléaire de la molécule à délivrer. Quant à la partie hydrophobe qui assure l'interaction avec la membrane plasmique ainsi que l'internalisation, elle est composée soit de la séquence hydrophobe de la protéine gp41 du VIH pour le peptide MPG, soit d'une séquence riche en tryptophane (W) pour le peptide Pep-1 (Morris et al. 2001; Morris et al. 1997). Le bras espaceur assure une certaine flexibilité entre les deux domaines. Les amphipathiques secondaires possèdent une structure en hélice-α. On peut citer le peptide MAP (Oehlke et al. 1998), le peptide GALA (Li et al. 2004) et son dérivé KALA (Wagner 1999), JST1 (Wagner 1999) ainsi que des peptides vecteurs dont la séquence est riche en prolines (Pujals et al. 2006).

Tableau IV : Séquences et propriétés de quelques peptides vecteurs

	Peptide vecteur	Origine	Séquence	Référence
Peptides vecteurs naturels	Pénétratine (pAntp)	Protéine Antennapedia de la Drosophile	RQIKIWFQNRRMKWKK	(Derossi et al. 1994)
	Tat (48-60)	Protéine Tat du VIH	GRKKRRQRRRPPQ	(Vives et al. 1997)
	VP22	Protéine de l'enveloppe du Virus Herpès Simplex	DAATATRGRSAARPTERPRAPARS ASRPRRPVE	(Elliott et O'Hare 1997)
	hCT(9-32)	Calcitonine humaine	LGTYTQDFNKFHTFPQTAIGVGAP -amide	(Schmidt et al. 1998)
	PrP	Protéine du prion de souris	MANLGYWLLALFVTMWTDVGLC KKRPKP	(Lundberg et al. 2002)
Peptides vecteurs synthétiques	Transportan	Galanin(1-12)-Lys-Mastoparan	GWTLNSAGYLLGKINLKALAALA KKIL-amide	(Pooga et al. 1998)
	TP10	Transportan tronqué	AGYLLGKINLKALAALAKKIL-amide	(Soomets et al. 2000)
	MAP	Peptide Amphipathique modèle	KLALKLALKALKAALKLA-amide	(Oehlke et al. 1998)
	Pep-1	Séquence NLS + Séquence hydrophobe	KETWWETWWTEWSQPKKKRKV-cysteamide	(Morris et al. 2001)
	MPG	Séquence NLS + Séquence hydrophobe	GALFLGWLGAAGSTMGAPKKKR KV-cysteamide	(Morris et al. 1997)
	Oligoarginine		$(R)_n$ (R = Arginine)	(Rothbard et al. 2000)
Peptides vecteurs dérivant de peptides antibactériens	Magainin 2		GIGKFLHSAKKFGKAFVGEIMNS	(Takeshima et al. 2003)
	Buforin 2		TRSSRAGLQFPVGRVHRLLRK	(Park et al. 1998)

4.4. Mécanismes d'internalisation cellulaire des peptides vecteurs :

Le mécanisme d'entrée des CPPs dans les cellules a longtemps été un sujet de controverse (voir tableau V). Comme déjà évoqué, les travaux initiaux ont montré que l'internalisation cellulaire des CPPs est insensible à la température, à la déplétion d'ATP et aux inhibiteurs de l'endocytose (Derossi et al. 1996; Futaki et al. 2001; Suzuki et al. 2002; Vives et al. 1997).

Deux modèles d'entrée cellulaire basés sur ces résultats et inspirés des données expérimentales concernant les peptides antimicrobiens ont été proposés [comme revue (Henriques et al. 2006)]. Dans le premier, le peptide traverse directement la membrane plasmique et dans le second le peptide forme des pores dans la membrane cellulaire. La forte perméabilisation cellulaire semble être l'argument majeur pour expliquer l'internalisation des CPPs. La question qui se pose est d'expliquer la faible cytotoxicité de la majorité des CPPs comparés à celle des peptides antimicrobiens.

Un autre modèle a été proposé par l'équipe de Prochiantz pour expliquer l'internalisation de la pénétratine. Dans ce modèle, le peptide interagirait grâce à ses charges cationiques avec les charges négatives présentes au niveau de la membrane plasmique. Les résidus tryptophanes (W_{48} et W_{56}) assurent des interactions hydrophobes avec les phospholipides membranaires. La concentration du peptide au niveau de la membrane provoquerait une invagination de la membrane conduisant à la formation d'une micelle inverse suivie d'une libération dans le milieu intracellulaire (Derossi et al. 1996). Cependant des travaux récents sur l'importance de ces résidus tryptophanes ont montré que leur mutation par des phénylalanines n'influe pas sur l'efficacité d'internalisation, résultat qui contredit ceux de Derossi. Par contre, la mutation des deux arginines en lysines abolit complètement l'entrée cellulaire de la pénétratine (Thoren et al. 2003).

Le consensus initial concernant un mécanisme d'internalisation indépendant de l'endocytose a été remis en question à la suite de travaux mettant en évidence des artefacts expérimentaux liés à l'utilisation de ces peptides fortement chargés. Par exemple, la fixation des cellules provoque une redistribution des CPPs (Richard et al. 2003). De même, l'association forte des ces peptides basiques à la surface cellulaire biaise l'interprétation des données de cytométrie de flux (Richard et al. 2003). De nouveaux protocoles qui permettent de s'affranchir de ces problèmes méthodologiques ont été proposés (Richard et al. 2003). Avec ces nouveaux protocoles, le mécanisme d'endocytose a été confirmé comme étant au moins majoritaire pour la plupart des CPPs (Pujals et al. 2006). Toutefois, l'addition d'un résidu W à un heptarginine ou la substitution d'une proline par un résidu W dans la séquence du peptide Tat améliore son internalisation. L'entrée cellulaire de ces deux peptides est insensible à la température (Thoren et al. 2003).

Tableau V : Quelques possibilités de mécanismes d'internalisation cellulaire des CPPs. [adapté de (Henriques et al. 2006)]

	CPPs	Séquences	Références	Mécanisme d'internalisation cellulaire	Références
Peptides naturels	Tat	GRKKRRQRRRPPQ	(Vives et al. 1997)	Principalement de l'endocytose	(Richard et al. 2005; Richard et al. 2003)
	Pénétratine	RQIKIWFQNRRMKWKK	(Derossi et al. 1994)	Principalement de l'endocytose	(Thoren et al. 2000)
Peptides chimères	Pep-1	KETWWETWWTEWSQPKKKRKV	(Morris et al. 2001)	Formation de pores membranaires ou translocation directe au travers de la membrane sans formation de pores	(Deshayes et al. 2004; Henriques et Castanho 2004)
	$S4_{13}$-PV	ALWKTLLKKVLKAPKKKRKV	(Hariton-Gazal et al. 2002)	Principalement par une déstabilisation transitoire de la membrane	(Mano et al. 2006)
Peptides antibactériens	Buforin 2	TRSSRAGLQFPVGRVHRLLRK	(Park et al. 1998)	Structures ressemblantes à des pores, ne perméabilise pas la membrane	(Kobayashi et al. 2004)
	Magainin 2	GIGKFLHSAKKFGKAFVGEIMNS	(Zasloff 1987)	Formation de pores	(Matsuzaki et al. 1995)

4.5. Application à la délivrance de biomolécules :

Un obstacle majeur au développement de nouvelles stratégies thérapeutiques est l'inefficacité de la majorité des biomolécules à traverser les membranes cellulaires. Dès la découverte des CPPs, de nombreux travaux se sont focalisés sur leur utilisation comme vecteurs pour l'internalisation de protéines, de peptides et d'oligonucléotides à visée thérapeutique. Une sélection de ces différentes molécules délivrées par les CPPs est exposée dans le tableau VI [comme revue (Dietz et Bahr 2004)].

Différentes stratégies d'association entre le peptide vecteur et la molécule transportée ont été proposées : couplages stables, couplages labiles (pH sensible ou réductible), fusion ou association par interactions électrostatiques. Chacune de ces stratégies a ses avantages et ses inconvénients. Par exemple, la molécule à transporter peut défavoriser l'internalisation du vecteur peptidique, ou le CPP peut inhiber l'effet biologique de la biomolécule vectorisée.

Le choix du type de lien et du vecteur peptidique à utiliser est donc essentiel et doit être adapté à chaque cas. Dans certain cas, des interactions électrostatiques entre le peptide vecteur et l'entité biologique à vectoriser suffisent, comme par exemple pour la vectorisation de plasmides (Morris et al. 1999), de protéines (Morris et al. 2001) ou de siRNAs (Simeoni et al. 2003), par des peptides de la famille MPG et Pep1. Le couplage covalent a été généralement utilisé pour la délivrance de peptides (Chen et al. 1999) et la production de protéines recombinantes fusionnées au peptide vecteur pour celle des protéines (Peitz et al. 2002).

Tableau VI : Sélection de quelques biomolécules délivrées dans des cellules par des CPPs [comme revue (Dietz et Bahr 2004)].

Peptide vecteur	Biomolécule transportée		Type de couplage	Référence
	Type	Nom		
R_7	Petite molécule	Cyclosporine A	Lien covalent pH sensible	(Rothbard et al. 2000)
Peptide Tat et la pénétratine	Peptide	Fragment de la protéine p53	Synthèse sur le même squelette peptidique	(Snyder et al. 2004)
Peptide Tat	Peptide	Fragment de la PKC	Pont disulfure	(Begley et al. 2004)
Pep-1	Protéine	GFP	Non covalent	(Morris et al. 2001)
Pep-1	Protéine	Superoxide dismutase	Fusion	(Eum et al. 2004)
Peptide Tat	Protéine	Cre recombinase, Rho GTPase	Fusion	(Chellaiah et al. 2000; Peitz et al. 2002)
Peptide Tat	Poly-anions	ADN et Héparane sulfate	Interactions électrostatiques	(Sandgren et al. 2002)
Pep-1, peptide Tat, LL-37	Plasmide	Luciferase, GFP	Interactions électrostatiques	(Morris et al. 1999; Sandgren et al. 2004; Tung et al. 2002)
Peptide Tat	Virus	Phage λ	Expression à la surface du phage	(Eguchi et al. 2001)
Peptide Tat	Nanoparticules	_____	Pont disulfure	(Josephson et al. 1999)

4.6. Applications à la délivrance d'oligonucléotides à visée thérapeutique :

Curieusement, la délivrance d'oligonucléotides à visée thérapeutique par des peptides vecteurs n'a été documentée que par quelques groupes (Tableau VII). Les premiers résultats ont montré qu'il est possible de réguler négativement, *in vitro* dans des cellules neuronales en culture ou *in vivo* chez la souris, et d'une manière spécifique le récepteur de la galanine par des conjugués PNA-Transportan (Pooga et al. 1998).

D'autres travaux indiquent qu'il est possible de corriger un épissage défectueux par des analogues d'oligonucléotides antisens couplés à des peptides vecteurs (Astriab-Fisher et al. 2002; Kang et al. 1998; Thierry et al. 2006). Une sélection de différents oligonucléotides antisens délivrés par des peptides vecteurs est présentée dans le tableau VII.

Tableau VII : Sélection de quelques oligonucléotides antisens vectorisés par des peptides vecteurs [comme revue (Dietz et Bahr 2004; El-Andaloussi et al. 2005)].

.

	Type d'analogue antisens	Effet biologique	Référence
Peptide Tat, Pep-1, NLS	PMO	Régulation négative de l'expression c-myc et correction de l'épissage	(Moulton et al. 2003)
MPG	ARN 2'Omethyl	Délivrance cellulaire	(Morris et al. 1997)
Penetratine	PNA	Inhibition de la télomerase dans des cellules du mélanome en culture	(Villa et al. 2000)
Transportan	PNA	Inhibition de la réplication HIV (inhibition de transactivation par la protéine Tat)	(Kaushik et al. 2002)
Peptide Tat, Penetratine, oligoarginin	LNA et RNA 2'Omethyl	Inhibition de la réplication HIV (inhibition de transactivation par la protéine Tat)	(Arzumanov et al. 2001; Turner et al. 2005)
Peptide Tat et pénétratine	RNA 2'Omethyl Phosphorothioate	Inhibition de l'expression de la protéine de surface P-glycoprotéine, correction de l'épissage	(Astriab-Fisher et al. 2002; Astriab-Fisher et al. 2000)
NLS	PNA	Inhibition de l'expression de c-myc, apoptose	(Cutrona et al. 2000)
Transportan, TP10	Oligonucléotide decoy	Blocage de l'induction de l'IL-1β par NFκB	(Fisher et al. 2004)
Pep-2	PNA	Blocage du cycle cellulaire	(Morris et al. 2004)
MAP	PNA	Diminution de l'activité dans les cardiomyocytes	(Oehlke et al. 2004)

Comme nous le verrons dans la partie expérimentale de cette thèse, les principaux obstacles rencontrés ont été la difficulté d'associer de manière covalente un ON chargé négativement et un CPP à caractère basique, ainsi que la ségrégation des conjugués dans les vésicules d'endocytoses.

5. Quelques mots sur le mécanisme d'endocytose :

5.1. Principe de l'endocytose :

L'endocytose désigne un ensemble de processus utilisés par les cellules pour internaliser divers molécules ou même des microorganismes (voir Figure 5). Différents types d'endocytose ont été caractérisés chez les eucaryotes. Tous sont caractérisés par la formation de vésicules, les endosomes, où se retrouvent au moins transitoirement les molécules ou les organismes à internaliser.

L'endocytose clathrine-dépendante ou indépendante est utilisée pour l'internalisation de protéines, d'hormones, des facteurs de croissance, de virus ou de toxines. Si la voie d'endocytose dépendante de la clathrine a longtemps été considérée comme la voie d'internalisation des récepteurs *trans*-membranaires, d'autres travaux ont aussi soutenu l'existence de voies d'endocytose différentes, dites « indépendantes de la clathrine ».
La mise au point d'inhibiteurs moléculaires nouveaux, comme la filipine et la nystatine, ont permis d'établir sans ambiguïté l'existence de voies indépendantes de la clathrine et de caractériser leur contribution dans les phénomènes d'internalisation (Benmerah et Lamaze 2002).

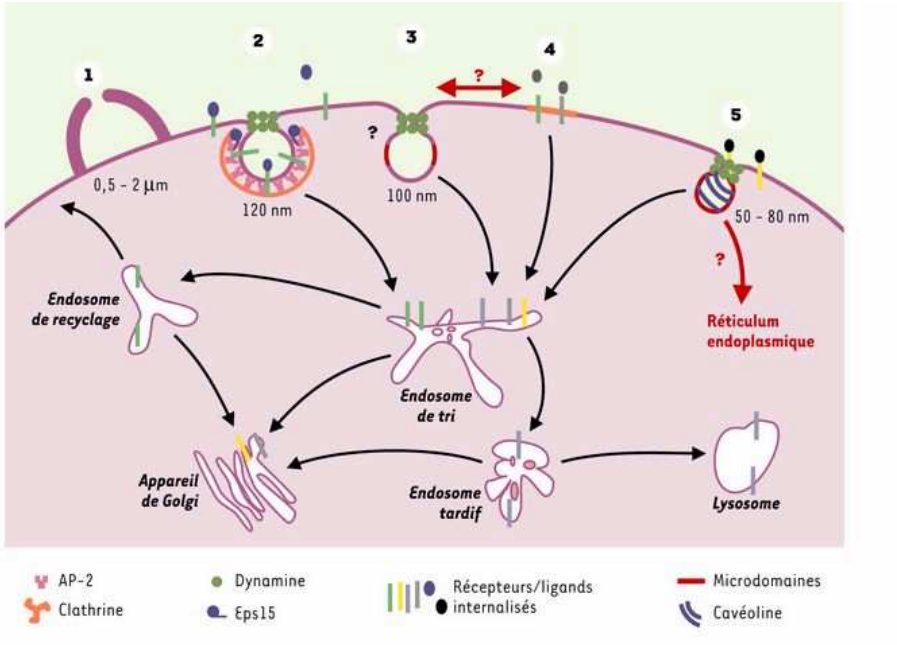

Figure 5. *Les différentes voies d'endocytose*. A côté de l'endocytose dépendante de la clathrine (2), quatre voies d'endocytose peuvent être distinguées d'un point de vue morphologique et moléculaire. La macropinocytose (1) contribue de façon induite et transitoire à l'endocytose de phase fluide en formant de grosses vésicules de tailles hétérogènes. La présence de vésicules lisses (3) dépourvues de manteau a été observée depuis longtemps en microscopie électronique. Ces vésicules contribuent surtout à l'endocytose constitutive des fluides et des solutés (pinocytose en phase fluide). Les microdomaines (4) et les cavéoles (5) sont enrichis en cholestérol et en sphingolipides. La cavéoline est un marqueur spécifique qui permet de distinguer cette voie des autres microdomaines. Le passage par les endosomes précoces, également appelés endosomes de tri, est l'étape essentielle et commune à toutes les voies d'endocytoses. La sortie des endosomes est le facteur limitant principal [d'après (Benmerah et Lamaze 2002)].

5.2. Propriétés des endosomes :

Les endosomes sont de larges vésicules d'endocytose formées par l'invagination de la membrane plasmique suite à la fixation d'un ligand sur la membrane. Trois types d'endosomes ont été caractérisés. Les endosomes précoces se forment suite à la dissociation de la vésicule de la membrane plasmique. Ces endosomes ont 200-300 nm de diamètre et sont très proches de la surface cellulaire. Les endosomes de recyclage assurent la reconduite à la surface cellulaire des récepteurs ou des molécules recyclables. Les endosomes tardifs, ou prélysosomes, sont le site d'accumulation des enzymes lysosomales (voir Figure 6).

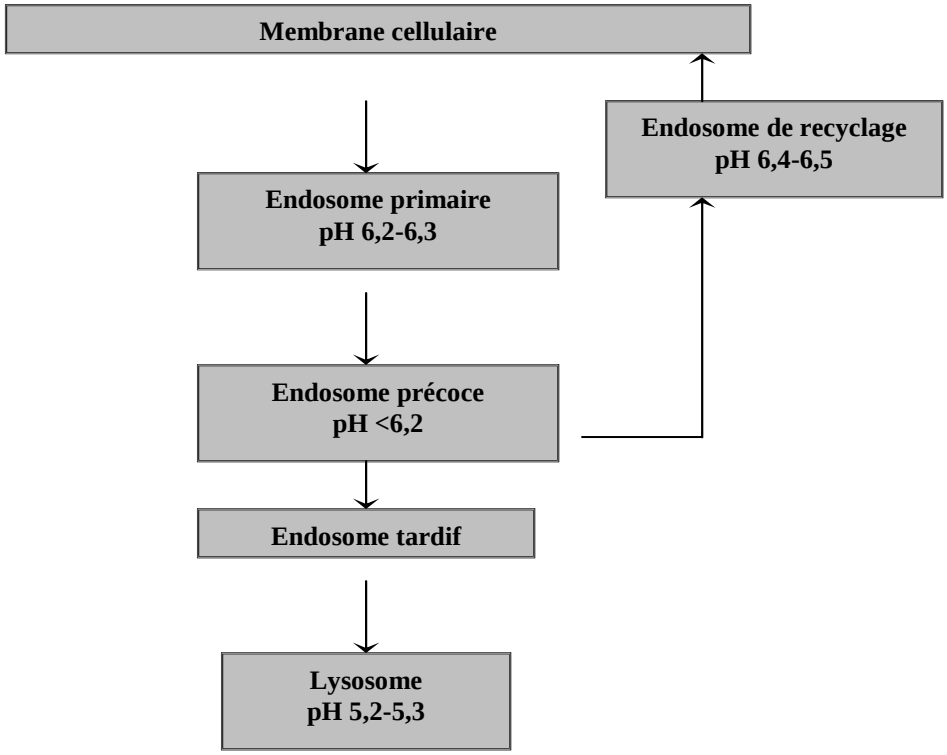

Figure 6 : *Evolution de l'endosome*

L'acidification est la propriété la plus importante qui caractérise les endosomes. Plusieurs publications montrent que l'acidité endosomale est différente selon les types d'endosomes (voir Figure 6) avec des pH variant de 5,0 à 6,5 (Tycko et al. 1983; Tycko et Maxfield 1982; Van Renswoude et al. 1982; Yamashiro et Maxfield 1984; Yamashiro et Maxfield 1987). Cette acidification se fait par une pompe à proton ATP-dépendante membranaire (Yamashiro et al. 1983). Le mécanisme qui maintient le pH stable dans chaque type d'endosome n'est pas encore élucidé. Toutefois, il est possible que la présence de canaux ioniques sur les membranes vésiculaires permette cette stabilité de pH (Al-Awqati 1986; Nelson 1987). Cette acidification des endosomes provoque la dissociation des ligands de leurs récepteurs, comme établie pour le récepteur de l'EGF et pour le récepteur des asialoglycoprotéines (DiPaola et Maxfield 1984). Le traitement des cellules par des ionophores comme la monensine, qui stoppe l'acidification des endosomes, inhibe la dissociation des complexes ligands-récepteurs (Harford et al. 1983). D'autre part, des études ont démontré qu'une forme mutée du récepteur de l'insuline ne permet pas la libération de l'insuline dans un environnement acide (Taylor et Leventhal 1983). En fait, le ligand se fixe à son récepteur à pH physiologique dans le milieu extracellulaire. Une fois que le complexe est dans l'endosome tardif, l'acidification du milieu provoque un changement de conformation du

récepteur. Ce changement de structure diminue dramatiquement l'affinité du récepteur pour son ligand et ce dernier est libéré. D'une autre manière, il a été montré qu'une forme défectueuse du récepteur à l'insuline ne libère pas l'insuline. Ce type de libération pH-dépendant est démontré pour la plupart des ligands qui utilisent l'endocytose récepteur dépendante comme voie d'internalisation cellulaire. De plus, la majorité des toxines, comme la toxine diphtérique (Raso et al. 1997), et la majorité des virus à enveloppe, comme le virus de l'Influenza (Root et al. 2000), profitent de l'acidification du milieu endosomal pour sortir vers le cytoplasme.

2 Tat-Derived Cell-Penetrating Peptides: Discovery, Mechanism of Cell Uptake, and Applications to the Delivery of Oligonucleotides

Saïd Abes, Jean-Philippe Richard, Alain Thierry, Philippe Clair, and Bernard Lebleu

CONTENTS

2.1 INTRODUCTION

Peptide and nucleic acid-based drugs offer a large array of strategies to regulate very specifically gene expression or to rescue deficient gene expression. A major limitation is, however, the poor efficiency with which these large hydrophilic biomolecules cross biological barriers.

For a long time cationic vectors have been proposed to improve the bioavailability of nucleic acid-based drugs (antisense oligonucleotides (ON), ribozymes, siRNA, plasmid DNA) since (1) they associate spontaneously with negatively charged nucleic acids through electrostatic interactions to form polyplexes and (2) these positively charged complexes allow binding to the negatively charged cell surface and further internalization.

These cationic carriers include cationic lipids, synthetic polymers as polyethyleneimine, dendrimers, and basic peptides.

Homopolymers and, in particular, poly (L-lysine) have been extensively investigated as nucleic acid delivery systems following pioneering work by Ryser et al. (see Lochmann et al.[1] for a recent review). Our own group has documented the enhanced cellular uptake via adsorptive endocytosis of antisense ON covalently bound to poly (L-lysine) in several in vitro models.[2] As an example, a sequence-specific antiviral activity has been achieved with an IC50 in the low micromolar concentration range in an HIV-1 acute infection cell assay. Further work by several groups has indicated that cell addressing can be achieved and that targeted in vivo delivery of the transported antisense ON or plasmid DNA was possible. As an example, mannosylated poly (L-lysine) has been successfully used to deliver antisense ON to macrophages in cell culture and in mice following binding to mannose-specific membrane receptors in these cells.[3]

Despite encouraging preliminary data these cationic homopolymers are rarely used nowadays due to their cytotoxicity in some cell types, their propensity to activate complement, and their heterodispersity.

A new era began when it was realized that purified proteins, such as the Drosophila Antennapedia transcription factor[4] or the HIV-1 Tat transactivating protein,[5,6] were able to cross cellular membranes and find their way to the nucleus. These experiments have paved the way to the first cell-penetrating peptides (CPPs), also named protein transduction domain (PTD). Before describing the history of Tat (48–60) PTD discovery and investigations on its still controversial mechanism of internalization we felt it useful to summarize a few relevant properties of the HIV-1 Tat protein and its mechanism of cellular uptake.

2.2 THE HIV-1 TAT PROTEIN: GENERAL PROPERTIES AND MECHANISM OF CELL UPTAKE

Tat protein transactivation requires binding to a conserved TAR element at the 5′ end of HIV-1 coded mRNAs. RNA binding is due to a stretch of basic amino acids (RKKRRYRRR) within Tat domain 4, while nuclear tropism depends on its GRKKR nuclear localization signal (NLS).[7] Early studies by Mann and Frankel[8]

had already proposed an endocytotic mechanism of Tat uptake involving heparan sulfate binding followed by adsorptive endocytosis. The role of cell surface proteoglycans in the uptake of the Tat protein has been largely confirmed in recent studies.[9] Alternative binding sites have, however, been described, such as the low-density lipoprotein receptor-related protein in neurons[10] or the Flk-1/KDR receptor on vascular endothelial cells.[11] Such observations might explain Tat-associated toxicity for some tissues. Tat is thereafter internalized through an endocytotic mechanism, whose details are still controversial. In a recent comprehensive study using both genetic and pharmacological tools available for the characterization of endocytosis, Vendeville et al.[12] proposed a clathrin-coated pits-dependent uptake followed by early escape from endocytic vesicles.

2.3 FROM FULL-SIZE TAT PROTEIN TO TAT PTD

A first step towards the molecular dissection of the Tat protein was provided by Fawell et al.[13] when they discovered that a 36 amino acid-long Tat fragment (Tat 37–72) could be conjugated to β-galactosidase and was able to promote the uptake of this 177 kDa protein in mammalian cells. This Tat peptide included two potentially interesting domains with respect to delivery, namely the basic domain and the adjacent α-helix.[14] Interestingly, the Antennapedia-derived PTD also included a cluster of basic amino acids and its α-helix conformation was thought at that time to be important for cellular uptake.[4]

A series of fluorochrome-tagged Tat peptides with deletions in the basic domain or in the α-helix domain were synthesized, and their cellular uptake was monitored by fluorescence microscopy. Cellular internalization was clearly associated with the cationic domain and not with the α-helix, thus leading to the prototype GRKKRRQRRR Tat PTD,[15] which includes the Tat RNA binding and NLS motifs mentioned in Section 2.2. Further trimming of this Tat-derived PTD or replacements of any one of its basic amino acids by alanine rapidly decreases translocation efficiency.[16,17] Interestingly, removal of the α-helix domain abolished the cytotoxicity of Tat, as monitored by MTT assays,[15] a key feature for any potential development of Tat PTD as a delivery vector. This SAR study was performed on formaldehyde-fixed cells but its key elements have now been confirmed in experimental conditions that did not lead to artifactual peptide redistribution (Richard, unpublished data).

The core GRKKRRQRRR Tat PTD has often been used with extensions allowing chemical conjugation to various biomolecules. As an example, several groups, including our own, have used a GRKKRRQRRRPPQC whose C-terminal extension includes the PPQ sequence from the Tat protein and a terminal cysteinyl residue to allow coupling to peptides or to ON through a disulfide bridge.[18] Since disulfide bridges are unstable within the reductive intracellular environment, they should open after cell entry and release their cargo, as demonstrated elegantly by Hällbrink et al.[19] Whether dissociation of the cargo from Tat PTD takes place in endocytic vesicles or in the cytoplasm has not, to our knowledge, been established.

Other versions of Tat PTD carrying various N- or C-terminal extensions have been used for the delivery of various cargoes, as reviewed in Brooks et al.[20]

Whether a stable or a labile (as the disulfide bridge) bond between Tat PTD and the transported biomolecules is preferable has seldom been investigated and will anyway depend on the nature of the cargo, as discussed extensively by Brooks et al.[20] In some instances, Tat PTD may conceivably impair target recognition by the attached cargo. In other instances, a positively charged entity might reinforce target recognition. This could become an advantage when delivering steric block ON analogs, such as peptide nucleic acids (PNAs) or morpholino ON derivatives (PMOs).[21]

2.4 TAT-MEDIATED DELIVERY OF OLIGONUCLEOTIDES

Chemical conjugation or fusion to Tat PTD has been exploited by an increasing number of groups in recent years in order to improve the cellular uptake or the bioavailability of low molecular weight drugs, biomolecules, and even large molecular weight material (such as liposomes or nanoparticles for imaging), as reviewed in Snyder and Dowdy.[22] In their comprehensive review, Dietz and Bähr[23] listed 124 examples of Tat PTD-mediated transport, and the number of published applications has increased exponentially over the last 2 years. Several chapters in this book are concerned with various applications of the CPP concept to macromolecular drugs delivery.

We will therefore not attempt to review comprehensively this aspect of the field and will thus focus on ON delivery. As stated in Section 2.1, antisense ON and related strategies are valuable tools to regulate gene expression in a very specific way and have become routine tools in functional genomics. Cellular delivery in cell culture experiments has been achieved by electroporation or by complexation with commercially available cationic lipids or PEI.[24,25] While easy to implement in vitro with most established cell lines, these strategies proved to be more cumbersome in vitro with some primary cells and in vivo for problems of toxicity or poor efficiency in the presence of serum proteins, as reviewed in Refs. [26,27]. The low toxicity of CPPs, such as Tat PTD, and the possibility of delivering a protein cargo to its intracellular target in vivo in various organs, has fostered searches for applications in ON delivery.

A comprehensive survey of the literature reveals less than a dozen publications describing the use of Tat PTD for ON delivery, which is rather low when compared to the large number of publications dealing with peptides and proteins delivery (see reviews by Lindsay[28] for peptide delivery and by Wadia and Dowdy[29] for protein transfection).

Key initial data have been provided by Langel and colleagues[30] for transportan-conjugated PNAs. The PNA antisense–CPP conjugate was delivered into cultured neuronal cells and was able to downregulate a galanin receptor in a sequence-specific manner. Most impressively, these same constructions were effective after injection in mice, thus indicating that the transportan CPP was able to cross the blood–brain barrier together with its PNA cargo.

Juliano and colleagues[18] were the first to demonstrate a sequence-specific and energy-dependent antisense response with Tat PTD-conjugated 2′Omet phosphorothioate antisense ON.

PMO are steric block ON analogs that have been widely used in gene development analysis (reviewed in Heasman[31]). Despite their interest, however, cellular delivery remains problematic for these uncharged ON analogs. The ability to deliver PMO after conjugation to the Tat PTD has been analyzed in a splicing-correction assay, described by Kang et al.[32] (*vide infra*), and in an assay monitoring the downregulation of a c-myc reporter gene expression.[33] Sequence-specific upregulation of luciferase and downregulation of c-myc expression were achieved with the appropriate peptide-conjugated PMO. Tat conjugates were 10 to 20 times more efficient than Pep-1 or NLS conjugates while free PMOs were almost not active in these assays.[21] Requested Tat conjugate concentrations remained, however, relatively high in keeping with entrapment of internalized material in endocytic vesicles.

The potential of CPP conjugation for steric block ON delivery has been extensively evaluated by Gait and colleagues.[34] They have capitalized on a well-controlled assay monitoring the inhibition of Tat-dependent transactivation by 12-mer 2′OMet/LNA mixmer ON analogs complementary to the TAR region of a HIV-1 LTR promoter. Fluorescein-labeled ON mixmers were conjugated to various CPPs (including Tat PTD) through a disulfide bridge. Cellular uptake of the conjugates was largely increased as compared to free ON but was confined to cytoplasmic vesicles, at variance with previous data.[18] No nuclear delivery was detected, and accordingly, no specific inhibition of transactivation could be monitored.[35] As a control, these ON mixmers could be delivered to the nuclei and could promote a sequence-specific transactivation inhibition when delivered with cationic lipids.

The paucity of data obtained with Tat PTD conjugation of antisense ON or PNA could be due to numerous reasons. Among these, poor escape from endocytic vesicles and degradation by nucleases appear the most plausible explanations, as noted above. Likewise, we have shown[36,37] that Tat PTD conjugated to a fluorescent PNA derivative rapidly accumulated within endocytotic vesicles in unfixed HeLa or HUVEC cells, and could barely be detected in the cytosol or in the nuclei. It should be pointed out, however, that fluorescence microscopy may not be able to detect a small proportion of antisense ON (or PNA) escaping from the endocytic vesicles or entering the cytoplasm through a nonendocytotic mechanism. A rather different distribution has, on the other hand, been observed when monitoring in parallel the intracellular distribution of antisense ON delivered with cationic DLS lipoplexes.[38] Antisense ON initially localized in endocytic vesicles and redistributed thereafter to the cytoplasm and the nuclei.[37]

Monitoring an unequivocal and easy-to-quantify biological response seems critical for the assessment of nuclear or cytoplasmic delivery of antisense ON. Most antisense ON assays suffer from the following drawbacks. First, it has proved difficult to delineate whether an antisense ON has been interacting with its target in the nuclei (thereby interfering with pre-mRNA processing or with mRNA nucleocytoplasmic transport) or in the cytoplasm (interfering with mRNA

translation and inducing mRNA degradation). Second, antisense ON (or siRNA) action leads, in general, to the downregulation of the target RNA, and it has often been difficult to discriminate between a bona fide antisense effect and side effects.

Recent work by Kole et al.[39] has provided an elegant assay with a positive readout that is now considered the most reliable to assess the nuclear delivery of an antisense ON analog and also to assay for new ON delivery vectors. It capitalizes on studies dealing with abnormalities in the splicing of a human thalassemic β-globin gene. Intron 2 mutations lead to the activation of an intronic cryptic splice site, and as a consequence, to the incomplete removal of the mutated intron. Masking of these cryptic splice sites by RNase H-incompetent ON analogs restores, at least in part, normal splicing and allows the production of a functional globin mRNA.[40] To convert these observations in antisense in vitro and in vivo assays, this mutated intron has been introduced in the coding region of luciferase or EGFP reporter genes, respectively.[32,41] The nuclear delivery of RNase H-incompetent ON (as 2′OMet ON analogs, PNA or PMO) leads to the production of functional luciferase or EGFP, which can be quantitated by biochemical assays or by FACS analysis, respectively.

In a series of recent publications, splicing correction has been documented using this assay both in cell culture experiments[41] and in vivo in a transgenic mouse model expressing the EGFP construction described above.[42] Impressively, appending as few as four lysine residues to the splice correcting PNA allowed functional delivery. A systematic further survey in a slightly different biological model for splicing correction pointed to an optimal length of eight lysines for PNA delivery.[43]

In our hands, however, similar $(Lys)_4$–PNA–Lys (unpublished observations) or $(Lys)_8$–PNA–Lys conjugates[44] were only slightly efficient in splicing correction although they were efficiently taken up by cells. Likewise, a $(Lys)_8$–PNA–Lys construct was ineffective in a Tat/TAR transactivation assay.[45] These disappointing data strongly suggest that the conjugates were taken up by endocytosis and remained entrapped in endocytotic vesicles, as directly evidenced by fluorescence microscopy. In keeping with this hypothesis, a lysosomotropic agent, such as chloroquine, significantly increased biological responses in the splicing-correction assay.[44] That endosome entrapment was limiting ON availability in the nuclei has also been substantiated in recent work by Gait's group. Treatment with chloroquine, according to the protocol defined by Abes et al.[44] did promote transactivation inhibition by ON mixmers and led to significant redistribution of endosome-entrapped material.[45]

Chloroquine has been frequently used to improve the delivery of various drugs entrapped in endocytotic vesicles. For example, it has been shown to improve gene transfer by various nonviral vectors including CPPs.[46]

Likewise, Nielsen and colleagues[47] have carefully investigated the uptake of PNAs conjugated to CPPs (pTat or pAnt) via a stable maleimide or via a reducible disulfide bridge in a panel of cell lines using confocal scanning microscopy. An energy- and concentration-dependent uptake was clearly documented but little if any material was found outside of endocytic vesicles, at variance with the data reported

in Astriab-Fisher et al.[18] In agreement with these observations, free PNA or Tat-conjugated PNAs did not promote any significant splicing-correction in HeLa pLuc 705 cells. Interestingly, coincubation of the Tat–PNA conjugate and 6 m*M* Ca^{2+} led to a large increase (44-fold) in luciferase expression and to a significant redistribution of fluorochrome-labeled dextran from endocytic vesicles towards the cytosol, in keeping with the Ca^{2+}-associated increase of plasmid DNA transfection efficiency by nonviral vectors.[48] Likewise, an effect of chloroquine treatment on luciferase expression and a redistribution of dextran has been documented by Shiraishi et al.[49]

All together, these data point to a bottleneck in the delivery of nucleic acid-based drugs by most basic amino acid-rich CPP, for example, escape from endocytic vesicles, a problem also encountered in gene therapy with nonviral vectors.

None of the endosome-destabilizing tools described above will be easily implemented in an in vivo situation, however. Alternative strategies might include co-treatment with fusogenic or membrane-destabilizing peptides and second-generation CPPs with intrinsic membrane-destabilizing properties. A large number of natural or synthetic fusogenic peptides have been described and some of them have been used to improve the expression of plasmid DNA by nonviral delivery vectors. The most interesting ones are peptides, whose fusogenic (or membrane-destabilizing) potential is pH dependent.

One of the most studied families of pH-sensitive fusogenic peptides is derived from the N-terminal region of the influenza virus hemagglutinin. This region of the viral protein is buried at neutral pH and reorganizes in an amphipathic helix at the slightly acidic pH of the endosomes. Although details of the mechanism are still not understood, these conformational changes ultimately lead to the cytoplasmic release of the viral nucleocapsid.[50] Along these lines, a significant increase of Tat-Cre recombinase activity has been obtained when cotreating cells in culture with the fusion protein and with the influenza hemagglutinin fusogenic peptide.[51] A series of synthetic peptides modeled on that of the influenza hemagglutinin one has been proposed in order to increase their fusogenic potential for this type of application, as comprehensively reviewed in Lochmann et al.[1]

A series of synthetic peptides undergoing pH-dependent conformational rearrangements from random coil to amphipathic α-helix has also been proposed by Szoka and colleagues.[52] Q4

Several natural peptides lead to membrane fusion or destabilization at neutral pH but they are generally rather cytotoxic and might be difficult to use for delivery purposes. An interesting derivative of the highly potent melittin peptide with pH-dependent membrane-destabilizing properties has recently been described and has been successfully incorporated in a plasmid DNA delivery vector.[53]

Many options to optimize nucleic acids delivery vectors thus remain open. The main problem will be to introduce, within a single entity, determinants required for cell binding (and eventually for cell targeting), for cell endocytosis, and for endosomal escape without compromising target recognition in the cytoplasm or in the nucleus and without becoming too complicated.

2.5 MECHANISM OF INTERNALIZATION OF TAT PTD AND TAT–CARGO CONJUGATES

2.5.1 From an Energy-Independent to an Endocytotic Mechanism of Uptake

A receptor- and energy-independent mechanism of cell uptake was initially proposed for the cellular uptake of Tat PTD and Tat–cargo conjugates, as for all cell penetrating peptides.

This model was proposed in several classes of experimental argument (as reviewed in Vives et al.[54]), namely:

1. CPP analogs including amino acids in D-configuration or retro-inverso forms are internalized as efficiently as the parent peptide, thus indicating that no chiral receptor is involved.
2. Inhibitors of endocytosis do not significantly alter cell uptake.
3. CPPs interact with the charged heads of phospholipids in model lipid bilayers.

These early conclusions have been questioned for methodological reasons. Indeed, fluorescence microscopy and fluorescence-activated cell sorter (FACS) analysis proved to lead to initially unforeseen artifacts when dealing with these highly cationic CPPs. Basic CPPs strongly bind to negatively charged cell surface determinants (proteoglycams essentially) as well as to plastic and glass surfaces. Extensive washing before FACS analysis is therefore not sufficient to eliminate membrane-bound material.[36] Early experimental data have thus addressed cell-bound as well as cell-internalized CPPs. Likewise, supposedly mild fixation protocols (with paraformadehyde) lead to artifactual redistribution of cell surface-bound peptides and peptide conjugates.[55] Finally, model lipid bilayers used to assess membrane interaction and reorganization are far from representative of the complexity of a biological membrane.

Two elements led us to challenge the validity of the then-prevailing nonendocytotic mechanism of Tat uptake. First, cell fractionation experiments with an iodinated radioactive derivative of Tat PTD indicated that most of the material was membrane bound and that little (if any) was associated with the cell nuclei in Hep G2 hepatoma cells (Courtoy et al., unpublished observations). Q3
Second, it became rapidly evident, in keeping with the proposal made by Lundberg and Johanson[55] for the VP22 protein PTD, that paraformaldehyde treatment leads to an artifactual redistribution of membrane-bound material and to its nuclear concentration, probably through nonspecific electrostatic interactions with nucleic acids.[36] Various solutions were thereafter proposed to overcome these methodological problems. They include enzymatic removal (through trypsin or pronase treatment)[36,56] or fluorescence quenching[57] of cell surface-bound peptides.

In order to avoid artifacts linked with fixation protocols, most recent studies rely only on live-cells imaging. Unfortunately, this complicates

protocols and precludes interesting strategies such as the use of Tat-specific antibodies to reveal the intracellular distribution of Tat PTD while avoiding the conjugation of a fluorochrome to the Tat peptide.[15] We still have to keep in mind possible artifacts linked to the conjugation of a bulky fluorochrome to the CPPs.

Recent developments have capitalized on the conjugation of cargoes whose biological activity could easily be monitored. Examples include fusion of Tat PTD to the Cre recombinase[51] or Tat conjugation to a splicing-correcting PNA as described in the previous section.[44] In both cases, nuclear delivery of the Tat-associated cargo can be quantified with sensitive biochemical assays providing a positive read-out over a low background.

2.5.2 Cell Surface Binding

As mentioned in Section 2.4.2. and Section 2.5.1, most early studies on the involvement of proteoglycans were biased by methodological problems. For example, we erroneously concluded that a GST–Tat–GFP construct behaved differently from Tat PTD[58] using FACS analysis, most probably because high ionic strength washings were able to remove cell-bound Tat–GST efficiently while not allowing complete removal of Tat PTD. Indeed, inclusion of a brief proteolytic treatment before FACS analysis led us to conclude that cell surface proteoglycans were involved in Tat–PTD cellular internalization using two commonly used tools, for example, CHO-mutant cells altered in proteoglycan biosynthesis and treatment with heparan sulfate lyases.[56] Several independent studies, as extensively reviewed,[20,59] have led to similar conclusions over the past few years, whether dealing with fluorochrome-linked Tat PTD or with various Tat constructions.

This is unsurprising, because cell surface (and, in particular, heparan sulfate) proteoglycans play a key role in the internalization of molecular entities as diverse as viruses, growth factors, cationic lipoplexes, and basic CPPs (for a recent review see Ref. [60]) While cell surface heparan sulfate proteoglycans (HSPG) serve as a major (but not necessarily exclusive) binding site for Tat PTD, for Tat–cargo conjugates, and importantly for the Tat protein itself, biological implications are still far from being understood. Does initial docking to HSPG precede transfer to higher-affinity receptors, as established for bFGF,[61] or to plasma membrane-charged lipids? Does HSPG binding trigger endocytosis and subsequent nuclear translocation, as suggested by Sandgren et al.,[62] and in this case, how does HSPG-bound Tat escape from endocytotic vesicles? These are important questions whose solutions might help to define more efficient second-generation Tat-derived peptides.

HSPGs are rather ubiquitous, which might explain why Tat-based delivery vectors are able to deliver their associated cargoes in a large number of cell types. On the other hand, the large variability of glycosaminoglycan motifs might ultimately allow tissue-targeting with CPP–cargo conjugates.

2.5.3 Which Pathway(s) of Endocytosis Are Involved in the Uptake of Tat PTD Tat–Cargo Conjugates?

Endocytosis can occur through various mechanisms, including phagocytosis, clathrin-dependent and -independent pathways as reviewed in Ref. [63]. Recently, several studies have addressed this point for the Tat protein, Tat PTD, or for various Tat–cargo constructions. Little consensus has emerged and the underlying reasons could be several. First, discrimination between various endocytic pathways mostly capitalizes on the use of pharmacological agents whose specificity is rarely complete. Second, the nature of the cargo and the cell type might influence the fate of the conjugates.

Our own group has investigated the uptake of Tat PTD conjugated to fluorochromes[56] and of Tat–PNA conjugates (Richard et al., unpublished observations). Q3 Pharmacological agents inhibiting clathrin-dependent endocytosis (such as chlorpromazine and potassium depletion) decrease the uptake of Tat and transferrin, a specific marker of this pathway. In contrast, inhibitors of lipid raft-dependent endocytosis, such as nystatin or filippin, did not significantly affect Tat uptake while reducing the internalization of a fluorochrome-labeled lactosylceramide-specific marker of this pathway. Similar conclusions have been reached independently by Potocky et al.[64] when investigating the fate of the Tat PTD and by Vendeville et al.[12] for the full-size Tat protein. Different conclusions have been reached upon studying the uptake of Tat PTD fused to Cre recombinase[65] or of a GST–Tat–GFP construct.[66] Macropinocytosis and caveolin-dependent endocytosis have been proposed in these two cases.

Altogether, these seemingly conflicting data probably reflect the possibility for basic CPPs to interact with various cell membrane microdomains and thereafter to be internalized by any type of endocytic vesicle.[20,56,59]

Conflicting data can also be found concerning the major issue of escape from endocytic vesicles. A few publications have reported cytoplasmic or nuclear accumulation of Tat-conjugates,[64,67] while in other studies,[35,51,56] no material could be detected outside of endocytic vesicles. These latter data do not necessarily eliminate the possibility of a small proportion of the endocytosed cargoes escaping endocytic vesicles before being destroyed in liposomes or recycled to the cell surface. Whatever the case, it seems that endosome entrapment limits the efficiency of Tat-mediated delivery. In keeping with this hypothesis, lysomotropic agents such as chloroquine or endosome-disrupting agents such as the influenza hemagglutinin fusogenic peptide significantly increase the functional delivery of Tat-conjugated oligonucleotides[35,44,49] or of Tat PTD-fused proteins,[51,68] as already noted in Section 2.4. A notable exception to endosome segregation of Tat-conjugated material is dendritic cells, in keeping with efficient antigen presentation by DCs after Tat PTD-mediated peptide transport.[69]

ACKNOWLEDGMENTS

Work in the authors' laboratory has been financed by the CNRS and by EEC grant QLK3-CT-2002-01989. S.Abes holds a predoctoral fellowship from the Ligue contre le Cancer.

REFERENCES

1. Lochmann, D., Jauk, E., and Zimmer, A., Drug delivery of oligonucleotides by peptides, *Eur. J. Pharm. Biopharm.*, 58, 237, 2004.
2. Leonetti, J.P. et al., Biological activity of oligonucleotide-poly(L-lysine) conjugates: Mechanism of cell uptake, *Bioconjug. Chem.*, 1, 149, 1990.
3. Mahato, R.I. et al., Physicochemical and disposition characteristics of antisense oligonucleotides complexed with glycosylated poly(L-lysine), *Biochem. Pharmacol.*, 53, 887, 1997.
4. Derossi, D. et al., The third helix of the Antennapedia homeodomain translocates through biological membranes, *J. Biol. Chem.*, 269, 10444, 1994.
5. Frankel, A.D. and Pabo, C.O., Cellular uptake of the tat protein from human immunodeficiency virus, *Cell*, 55, 1189, 1988.
6. Green, M. and Loewenstein, P.M., Autonomous functional domains of chemically synthesized human immunodeficiency virus tat trans-activator protein, *Cell*, 55, 1179, 1988.
7. Jeang, K.T., Xiao, H., and Rich, E.A., Multifaceted activities of the HIV-1 transactivator of transcription, Tat, *J. Biol. Chem.*, 274, 28837, 1999.
8. Mann, D.A. and Frankel, A.D., Endocytosis and targeting of exogenous HIV-1 Tat protein, *EMBO J.*, 10, 1733, 1991.
9. Tyagi, M. et al., Internalization of HIV-1 tat requires cell surface heparan sulfate proteoglycans, *J. Biol. Chem.*, 276, 3254, 2001.
10. Liu, J. et al., Expression of low and high density lipoprotein receptor genes in human adrenals, *Eur. J. Endocrinol.*, 142, 677, 2000.
11. Albini, A. et al., The angiogenesis induced by HIV-1 tat protein is mediated by the Flk-1/KDR receptor on vascular endothelial cells, *Nat. Med.*, 2, 1371, 1996.
12. Vendeville, A. et al., HIV-1 Tat enters T cells using coated pits before translocating from acidified endosomes and eliciting biological responses, *Mol. Biol. Cell.*, 15, 2347, 2004.
13. Fawell, S. et al., Tat-mediated delivery of heterologous proteins into cells, *Proc. Natl Acad. Sci. U.S.A.*, 91, 664, 1994.
14. Loret, E.P. et al., Activating region of HIV-1 Tat protein: Vacuum UV circular dichroism and energy minimization, *Biochemistry*, 30, 6013, 1991.
15. Vives, E., Brodin, P., and Lebleu, B., A truncated HIV-1 Tat protein basic domain rapidly translocates through the plasma membrane and accumulates in the cell nucleus, *J. Biol. Chem.*, 272, 16010, 1997.
16. Vives, E. et al., Structure activity relationship study of the plasma membrane translocating potential of short peptide from HIV-1 Tat protein, *Lett. Pept. Sci.*, 4, 429, 1997.
17. Suzuki, T. et al., Possible existence of common internalization mechanisms among arginine-rich peptides, *J. Biol. Chem.*, 277, 2437, 2002.
18. Astriab-Fisher, A. et al., Conjugates of antisense oligonucleotides with the Tat and antennapedia cell-penetrating peptides: Effects on cellular uptake, binding to target sequences, and biologic actions, *Pharm. Res.*, 19, 744, 2002.
19. Hällbrink, M. et al., Cargo delivery kinetics of cell-penetrating peptides, *Biochim. Biophys. Acta*, 1515, 101, 2001.
20. Brooks, H., Lebleu, B., and Vives, E., Tat peptide-mediated cellular delivery: Back to basics, *Adv. Drug Deliv. Rev.*, 57, 559, 2005.
21. Moulton, H.M. and Moulton, J.D., Peptide-assisted delivery of steric-blocking antisense oligomers, *Curr. Opin. Mol. Ther.*, 5, 123, 2003.

22. Snyder, E.L. and Dowdy, S.F., Cell penetrating peptides in drug delivery, *Pharm. Res.*, 21, 389, 2004.
23. Dietz, G.P. and Bahr, M., Delivery of bioactive molecules into the cell: The Trojan horse approach, *Mol. Cell Neurosci.*, 27, 85, 2004.
24. Mir, L.M. et al., Electric pulse-mediated gene delivery to various animal tissues, *Adv. Genet.*, 54, 83, 2005.
25. Lungwitz, U. et al., Polyethylenimine-based non-viral gene delivery systems, *Eur. J. Pharm. Biopharm.*, 60, 247, 2005.
26. Martin, B. et al., The design of cationic lipids for gene delivery, *Curr. Pharm. Des.*, 11, 375, 2005.
27. Thierry, A.R. et al., Cellular uptake and intracellular fate of antisense oligonucleotides, *Curr. Opin. Mol. Ther.*, 5, 133, 2003.
28. Lindsay, M.A., Peptide-mediated cell delivery: Application in protein target validation, *Curr. Opin. Pharmacol.*, 2, 587, 2002.
29. Wadia, J.S. and Dowdy, S.F., Modulation of cellular function by TAT mediated transduction of full length proteins, *Curr. Protein Pept. Sci.*, 4, 97, 2003.
30. Pooga, M. et al., Cell penetrating PNA constructs regulate galanin receptor levels and modify pain transmission in vivo, *Nat. Biotechnol.*, 16, 857, 1998.
31. Heasman, J., Morpholino oligos: Making sense of antisense?, *Dev. Biol.*, 243, 209, 2002.
32. Kang, S.H., Cho, M.J., and Kole, R., Up-regulation of luciferase gene expression with antisense oligonucleotides: Implications and applications in functional assay development, *Biochemistry*, 37, 6235, 1998.
33. Hudziak, R.M. et al., Antiproliferative effects of steric blocking phosphorodiamidate morpholino antisense agents directed against c-myc, *Antisense Nucleic Acid Drug Dev.*, 10, 163, 2000.
34. Arzumanov, A. et al., Inhibition of HIV-1 Tat-dependent trans activation by steric block chimeric 2′-O-methyl/LNA oligoribonucleotides, *Biochemistry*, 40, 14645, 2001.
35. Turner, J.J., Arzumanov, A.A., and Gait, M.J., Synthesis, cellular uptake and HIV-1 Tat-dependent trans-activation inhibition activity of oligonucleotide analogues disulphide-conjugated to cell-penetrating peptides, *Nucleic Acids Res.*, 33, 27, 2005.
36. Richard, J.P. et al., Cell-penetrating peptides. A reevaluation of the mechanism of cellular uptake, *J. Biol. Chem.*, 278, 585, 2003.
37. Thierry, A.R. et al., Comparison of basic peptides- and lipid-based strategies for the delivery of splice correcting oligonucleotides. *BBA — Biomembranes*, in press. Q6
38. Lavigne, C. et al., Cationic liposomes/lipids for oligonucleotide delivery: Application to the inhibition of tumorigenicity of Kaposi's sarcoma by vascular endothelial growth factor antisense oligodeoxynucleotides, *Methods Enzymol.*, 387, 189, 2004.
39. Kole, R., Vacek, M., and Williams, T., Modification of alternative splicing by antisense therapeutics, *Oligonucleotides*, 14, 65, 2004.
40. Lacerra, G. et al., Restoration of hemoglobin A synthesis in erythroid cells from peripheral blood of thalassemic patients, *Proc. Natl. Acad. Sci. U.S.A.*, 97, 9591, 2000.
41. Sazani, P. et al., Nuclear antisense effects of neutral, anionic and cationic oligonucleotide analogs, *Nucleic Acids Res.*, 29, 3965, 2001.
42. Sazani, P. et al., Systemically delivered antisense oligomers upregulate gene expression in mouse tissues, *Nat. Biotechnol.*, 20, 1228, 2002.

43. Siwkowski, A.M. et al., Identification and functional validation of PNAs that inhibit murine CD40 expression by redirection of splicing, *Nucleic Acids Res.*, 32, 2695, 2004.
44. Abes, S. et al., Endosome trapping limits the efficiency of splicing correction by PNA–oligolysine conjugates, *J. Controlled Release*, in press. Q6
45. Turner, J.J. et al., Cell-penetrating peptide conjugates of peptide nucleic acids (PNA) as inhibitors of HIV-1 Tat-dependent trans-activation in cells, *Nucleic Acids Res.*, in press. Q6
46. Manickam, D. et al., Influence of TAT-peptide polymerization on properties and transfection activity of TAT/DNA polyplexes, *J. Controlled Release*, 102, 293, 2005.
47. Koppelhus, U. et al., Cell-dependent differential cellular uptake of PNA, peptides, and PNA-peptide conjugates, *Antisens Nucleic Acid Drug Dev.*, 12, 51, 2002.
48. Zaitsev, S. et al., Histone H1-mediated transfection: Role of calcium in the cellular uptake and intracellular fate of H1–DNA complexes, *Acta Histochem.*, 104, 85, 2002.
49. Shiraishi, T., Pankratova, S., and Nielsen, P.E., Calcium ions effectively enhance the effect of antisense peptide nucleic acids conjugated to cationic tat and oligoarginine peptides, *Chem. Biol.*, 12, 923, 2005.
50. Skehel, J.J. and Wiley, D.C., Influenza haemagglutinin, *Vaccine*, 20, S51, 2002.
51. Wadia, J.S., Stan, R.V., and Dowdy, S.F., Transducible TAT-HA fusogenic peptide enhances escape of TAT-fusion proteins after lipid raft macropinocytosis, *Nat. Med.*, 10, 310, 2004.
52. Wyman, T.B. et al., Design, synthesis, and characterization of a cationic peptide that binds to nucleic acids and permeabilizes bilayers, *Biochemistry*, 36, 3008, 1997.
53. Boeckle, S., Wagner, E., and Ogris, M., C- versus N-terminally linked melittin–polyethylenimine conjugates: The site of linkage strongly influences activity of DNA polyplexes, *J. Gene. Med.*, 7, 1335, 2005.
54. Vives, E. et al., TAT peptide internalization: Seeking the mechanism of entry, *Curr. Protein. Pept. Sci.*, 2, 125, 2003.
55. Lundberg, M. and Johansson, M., Positively charged DNA-binding proteins cause apparent cell membrane translocation, *Biochem. Biophys. Res. Commun.*, 291, 367, 2002.
56. Richard, J.P. et al., Cellular uptake of unconjugated TAT peptide involves clathrin-dependent endocytosis and heparan sulfate receptors, *J. Biol. Chem.*, 280, 15300, 2005.
57. Drin, G. et al., Studies on the internalization mechanism of cationic cell-penetrating peptides, *J. Biol. Chem.*, 278, 31192, 2003.
58. Silhol, M. et al., Different mechanisms for cellular internalization of the HIV-1 Tat-derived cell penetrating peptide and recombinant proteins fused to Tat, *Eur. J. Biochem.*, 269, 494, 2002.
59. Melikov, K. and Chernomordik, L.V., Arginine-rich cell penetrating peptides: From endosomal uptake to nuclear delivery, *Cell. Mol. Life. Sci.*, in press. Q6
60. Belting, M., Heparan sulfate proteoglycan as a plasma membrane carrier, *Trends. Biochem. Sci.*, 28, 145, 2003.
61. Colin, S. et al., In vivo involvement of heparan sulfate proteoglycan in the bioavailability, internalization, and catabolism of exogenous basic fibroblast growth factor, *Mol. Pharmacol.*, 55, 74, 1999.
62. Sandgren, S., Cheng, F., and Belting, M., Nuclear targeting of macromolecular polyanions by an HIV-Tat derived peptide. Role for cell-surface proteoglycans, *J. Biol. Chem.*, 277, 38877, 2002.

63. Pelkmans, L. and Helenius, A., Insider information: What viruses tell us about endocytosis, *Curr. Opin. Cell. Biol.*, 15, 414, 2003.
64. Potocky, T.B., Menon, A.K., and Gellman, S.H., Cytoplasmic and nuclear delivery of a TAT-derived peptide and a beta-peptide after endocytic uptake into HeLa cells, *J. Biol. Chem.*, 278, 50188, 2003.
65. Kaplan, I.M., Wadia, J.S., and Dowdy, S.F., Cationic TAT peptide transduction domain enters cells by macropinocytosis, *J. Controlled Release*, 102, 247, 2005.
66. Fittipaldi, A. et al., Cell membrane lipid rafts mediate caveolar endocytosis of HIV-1 Tat fusion proteins, *J. Biol. Chem.*, 278, 34141, 2003.
67. Fischer, R. et al., A stepwise dissection of the intracellular fate of cationic cell-penetrating peptides, *J. Biol. Chem.*, 279, 12625, 2004.
68. Caron, N.J., Quenneville, S.P., and Tremblay, J.P., Endosome disruption enhances the functional nuclear delivery of Tat-fusion proteins, *Biochem. Biophys. Res. Commun.*, 319, 12, 2004.
69. Loison, F., A ubiquitin-based assay for the cytosolic uptake of protein transduction domains, *Mol. Ther.*, 11, 205, 2005.

6. Objectif de la thèse :

Un des obstacles majeurs à l'utilisation d'oligonucléotides (antisens, siRNA) comme outils d'analyse des mécanismes d'expression des gènes et à leur éventuel développement comme outil thérapeutique est l'efficacité faible avec laquelle ils passent les barrières membranaires dans la majorité des types cellulaires. Ces limitations concernant la délivrance et l'adressage mobilisent les scientifiques de la recherche publique et privée.

Il est nécessaire de développer des vecteurs efficaces non cytotoxiques capables de délivrer les ONs dans le compartiment cellulaire souhaité, sans être séquestrés dans les vésicules d'endocytose. L'utilisation des peptides vecteurs comme alternative à l'emploi d'autres stratégies non virales de délivrance ainsi que leur optimisation constituerait une avancée majeure dans le domaine de la délivrance des ONs. De même, les peptides et les protéines peuvent donner lieu à de nombreuses applications, limitées elles aussi par une mauvaise biodisponibilité.

Mon projet de thèse a donc pour but :

- de poursuivre l'étude du mécanisme d'internalisation des CPPs et de leurs conjugués à des ONs ;
- d'optimiser des peptides vecteurs afin de favoriser leur libération des endosomes ou de contourner l'endocytose ;
- d'utiliser ces nouveaux peptides pour vectoriser des analogues d'ONs à visée thérapeutique.

Nous avons évalué ces conjugués dans le modèle cellulaire HeLa pLuc705 de correction d'épissage initialement proposé par le Dr. R. Kole (Figure 7).

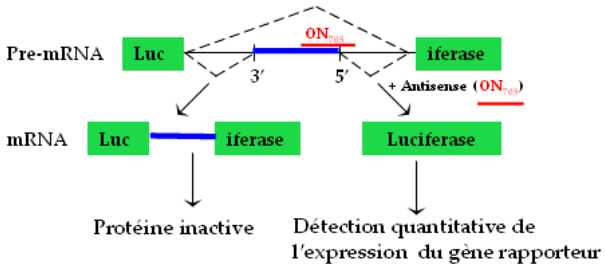

Figure 7 : *Modèle de Kole de correction d'épissage* (Kang et al. 1998).

Le modèle est issu de travaux sur une β-thalassémie où une mutation intronique crée un site cryptique d'épissage au niveau de l'intron 2 du gène de la β-globine. L'hybridation d'un oligonucléotide antisens n'activant pas la RNaseH (Steric Blocking Oligonucleotide) à ce site aberrant d'épissage masque le site, restaure l'épissage normal et permet la production de β-globine fonctionnelle. Cet intron muté a été introduit dans la séquence codante d'un gène rapporteur luciférase dont l'expression est conditionné par la délivrance nucléaire de l'ON correcteur d'épissage (Sazani et al. 2002). De telles constructions ont été établies de manière stable dans des lignées cellulaires et le Dr. Kole nous a fourni cette lignée (Kang et al. 1998).
L'énorme avantage de ce modèle est que la délivrance de l'ON antisens entraîne l'apparition d'un signal (Positive Readout Assay) alors que la plupart des essais conventionnels pour un ON antisens ou pour un siRNA se traduisent par un blocage d'expression, avec les nombreuses possibilités d'artefacts expérimentaux associés.
Avec la collaboration des équipes du Dr MJ Gait (MRC Cambridge), du Dr JJ Vasseur (Université Montpellier2), du Dr. P. Iversen (AviBioPharma, USA) et du Dr K Ganesh (National chemistry Laboratory, Pune, Inde), nous avons comparé différentes stratégies de délivrances, proposé de nouveaux peptides vecteurs et de nouvelles chimies d'ONs. Les outils sélectionnés seront testés sur d'autres modèles à relevance clinique (Garcia-Blanco et al. 2004; Kole et al. 2004; Mercatante et al. 2002), et sur des modèles animaux.

Chapitre I

Matériels et Méthodes

Chapitre I : Matériels et méthodes

Introduction :

Dans ce chapitre nous décriverons sous forme d'article de méthodologie les techniques de synthèse et d'évaluation des peptides vecteurs que nous avons utilisées le plus souvent. Cette publication, sous presse à Humana Press, expose les principaux protocoles utilisés pour évaluer l'efficacité de délivrance de ces peptides.

Les protocoles expérimentaux utilisés plus ponctuellement sont décrits dans les rubriques matériels et méthodes des publications.

Article I: Peptide-based delivery of steric-block PNA oligonucleotides

[1]**Saïd Abes**, [2]Gabriela D. Ivanova, [1]Rachida Abes, [2]Andrey A. Arzumanov, [2]Donna Williams, [2]David Owen, [1,*]Bernard Lebleu and [2]Michael J. Gait

[1]UMR 5235 CNRS, Université Montpellier 2, Place Eugene Bataillon, 34095 Montpellier cedex 5, France and [2] Medical Research Council, Laboratory of Molecular Biology, Hills Road, Cambridge CB2 2QH UK

Corresponding author: B.Lebleu,UMR 5235 CNRS, CC086,Université Montpellier 2, Place Eugene Bataillon, 34095 Montpellier cedex 5, France tel 33-467149203 fax 33-467149201 e-mail: blebleu@univ-montp2.fr

Abbreviated title: CPP ON delivery vectors

Abstract

Several strategies based on synthetic oligonucleotides (ON) have been proposed to control gene expression. As for most biomolecules however delivery has remained a major roadblock for in vivo applications. Conjugation of steric-block neutral DNA mimics as peptide nucleic acids (PNA) or phosphorodiamidate morpholino oligonucleotides (PMO) to cell penetrating peptides (CPP) has recently been proposed as a new delivery strategy. It is particularly suitable to interfere sequence-specifically with pre mRNA splicing thus offering various applications in fundamental research and in therapeutics. The chemical synthesis of these CPP conjugates as well as methodologies to monitor their cellular uptake and their efficiency in a reliable and easy to implement assay of splicing correction will be described.

1. Introduction

Synthetic oligonucleotides (ON) such as antisense ON, ribozymes, small interfering RNA, micro RNA, triple-helix forming ON or aptamers have been widely used to control gene expression through

specific interactions with RNA, DNA or even proteins. Numerous modifications have been proposed to improve the pharmacological properties of synthetic ON, for example to improve their metabolic stability or their affinity, or to increase their selectivity in target recognition. Moreover, the targeted macromolecule is in most cases intracellular. Further, free ONs are not taken up efficiently by most cell types unless associated with nucleic acids-delivery vectors. Several transfection protocols (such as for instance electroporation or lipofection) are easily implemented with cultured established cell lines. Unfortunately, most transfection methods are unsuitable for in vivo use. Thus, delivery is still considered as a major roadblock for clinical applications of synthetic ON ***(1,2)***.

The comparative evaluation of ON analogues and ON-delivery vectors in a reliable and easy to implement assay is now possible with the splicing correction assay proposed by Kole et al ***(3,4)***. Intronic point mutations in a β-thalassemic globin gene activate cryptic splice sites leading to the aberrant splicing of this intron and as a consequence to a non functional protein. Masking of the mutated site with a steric-block ON re-orients the splicing machinery towards complete removal of the intron and leads to the production of a correctly spliced mRNA. This mutated intron has been introduced in the coding region of a reporter luciferase gene and the construction has been stably transfected in HeLa cells (Fig.1). This splicing correction assay has now been widely adopted since it has a low background and provides a positive read-out with a large dynamic response. Neutral steric-block ON, such as peptide nucleic acids (PNA) ***(5)*** or (PMO) ***(6)***, are particularly suitable for this purpose since they cannot recruit RNase H, they hybridize with high affinity and selectivity to complementary RNA, and they are metabolically very stable. However, they cannot be transfected with most commercially available delivery vectors.

New strategies for the delivery of biomolecules have emerged with the discovery of cell penetrating peptides (CPP), which are small, generally basic amino acid-rich peptides that are internalized within most cell types. More importantly, they allow the cellular uptake of chemically conjugated biomolecules of various types, including ON, peptides or proteins ***(7,8)***.

PNAs are synthesised by solid phase Fmoc/Bhoc chemistry ***(9-11)***. One to three Lys residues are generally added at the C-terminus to enhance aqueous solubility. After assembly (C to N), one additional Lys residue is added, followed by either a Cys residue (for disulfide conjugation) or by bromoacetylation (for thioether conjugation). Peptides are synthesised also by solid phase Fmoc chemistry as C-terminal amides, which may help to enhance bio-stability, and with a Cys residue at the C-terminus for conjugation by either disulfide or thioether methods. It is possible to place a Cys residue anywhere in the peptide sequence should conjugation be desired at other sites.

It is important to emphasize that the majority of human genes undergo alternative splicing and that several acquired (eg. cancers, viral infections) or genetic diseases (e.g. β-thalassemia, Duchenne muscular dystrophy) can potentially be treated through ON-based control of splicing ***(12)***. Once again, the efficient nuclear delivery of the correcting ON remains a major issue, and this is addressed by

CPP-mediated delivery. Conjugation chemistries and assays to monitor the cellular uptake and the biological activity in a splicing correction assay of these PNA conjugates will be described.

2. Materials

2.1. Cell culture and cell dissociation

1. HeLa cell cultures are propagated in Dulbecco's Modified Eagle Medium (D-MEM) (500ml) (Gibco) supplemented with 10% fetal bovine serum (BioWest), 5 ml MEM Non Essential Amino Acids (100X) (Gibco), 5ml sodium pyruvate MEM (100 mM, Gibco) and 5ml Penicillin-Streptomycin-Neomycin (PSN) Antibiotic Mixture (Gibco).
2. Mycoplasma Detection Kit from Roche Applied Science for routine screening of eventual mycoplasma contaminations.
3. Opti-MEM® I Reduced Serum Medium (1X) with L-Glutamine (Gibco) for serum-free experiments.
4. Trypsin-Ethylenediamine-tetraacetic acid (0.05% Trypsin with 0.35mM EDTA 4Na) 1X (Gibco) or Pronase Powder (Sigma-Aldrich).
5. Dulbecco's Phosphate Buffered Saline (D-PBS) (1X) (Gibco) for cell washing.
6. Forma Direct Heat CO_2 Incubator HEPA Class 100 (Thermo Electron Corporation) for cell cultures.
7. Laboratory laminar airflow cabinet BH-EN 2004-S. Type II, Catégorie 2 (Microbiological Safety Cabinets) for cell manipulations in sterile conditions.
8. Allegra^{TM} 25R low-speed Beckmann centrifuge or Eppendorf Centrifuge 5417R for cell recovery.
9. Axiovert 40 C (transmitted light) (Carl Zeiss, Oberkochen, Germany) and Thoma cell for cell integrity routine checking and counting.

2.2. Synthesis of PNA-peptide conjugates

1. PNA synthesis reagents and materials: use Fmoc-PAL-PEG-PS amide support (Applied Biosystems), and Fmoc (Bhoc) PNA monomers (Panagene or Link Technologies) and Fmoc(Boc)Lys from Novobiochem. Final Cys coupling is with Boc-Cys(Npys)-OH (Bachem) for Cys-terminated PNA or bromoacetic anhydride (made with bromoacetic acid and diisopropylcarbodiimide, both from Aldrich) for *N*-bromoacetyl PNA. Other synthesis reagents are piperidine (Romil, >99.5%), *N*,*N*-diisopropylethylamine (DIPEA, 99+%, Applied Biosystems), PyBop (Novabiochem), *N*-methylpyrrolidinone (NMP, ≥ 99,5% Aldrich), 2,6-lutidine (≥ 99%, Aldrich), acetic anhydride (Aldrich), and DMF (Merck/BDH). For final deprotection, use trifluoroacetic acid (TFA) obtained from Romil (>99.9%) and triisopropylsilane (TIS) from Aldrich (>99%). Use a polyethylene syringe (IST Empty Reservoir 1ml, Kinesis) fitted with a 10 µm polyethylene frit and plastic tap (Kinesis). Carry

out reversed phase HPLC, for example using a Phenomenex Proteo C-18 column (analytical or semi-preparative) fitted with a heating jacket. Acetonitrile (Fisher Scientific, HPLC grade) and water (HPLC grade) are used as solvents.

2. Peptide synthesis reagents and materials: Use NovaSyn TGR resin (Novabiochem) for C-terminal amide synthesis and Fmoc amino acid monomers (Novabiochem) including Fmoc-Arg(Pbf)-OH, Fmoc-Asn(Trt)-OH, Fmoc-Cys(Trt)-OH, Fmoc-Gln(Trt)-OH, Fmoc-Glu(O*t*Bu)-OH, Fmoc-His(Trt)-OH, Fmoc-Lys(Boc)-OH and Fmoc-Trp(Boc)-OH. Other peptide synthesis reagents are as for PNA (above) with the addition of 1,2-ethanedithiol (EDT, >98%, Fluka). A Phenomenex Jupiter C-18 column (analytical and semi-preparative) may be used for reversed phase HPLC.

3. Conjugation reagents: Formamide (>99.5%, Fluka) BisTris.HBr, ammonium acetate. HPLC columns are as for peptide and PNA synthesis and columns are immersed in a water bath (45 °C) or surrounded by a very efficient heating jacket.

2.3 FACS analysis of PNA and PNA-peptide conjugates cellular uptake and cells permeability

1. FACSCanto™ flow cytometer (BD Biosciences, San Jose, CA) using Facs Diva® software for PNA-peptide conjugates uptake.
2. WinMDI 2.8 free software to analyse the results.
3. Propidium Iodide (Molecular Probes, Eugene, OR) used at final concentration of 0.05 µg/ml for cell permeability quantification.

2.4 Fluorescence microscopy analysis of PNA-peptide intracellular distribution

1. Alexa fluor® 546-labelled Transferrin conjugate from Molecular Probes, Eugene, OR to stain endosomes.
2. Hoechst 33342 (Trihydrochloride, Trihydrate 10mg/ml) from Molecular Probes, Eugene, OR, to stain nuclei (permeant nuclear counterstain).
3. Zeiss Axiovert 200 M fluorescence microscope (Carl Zeiss, Oberkochen, Germany).
4. Adobe Photoshop CS2 software, ImageJ free software (N.I.H, USA, public domain) and Matrox Inspector software (Matrox Electronic System Ltd) for image treatment.

2.5 Luciferase assay of splicing correction by PNA and PNA-peptide conjugates

1. Chloroquine from Sigma Aldrich to increase endosome release of CPP-ON conjugates.

2. BCA™Protein Assay Kit (Pierce, Rockford, IL) and ELISA plate reader (Dynatech MR 5000, Dynatech Labs, Chantilly, VA) for the quantification of cellular protein concentrations.
3. Berthold Centro LB 960 luminometer (Berthold Technologies, Bad Wildbad, Germany) and Luciferase Assay System with Reporter Lysis Buffer from Promega for luciferase activity quantification.

2.6 RT-PCR evaluation of splicing correction by PNA and PNA-peptide conjugates

1. Forward 5′ TTG ATATGT GGA TTTCGA GTC GTC 3′ and reverse 5′ TGT CAA TCA GAG TGC TTT TGG CG 3′ luciferase primers from Eurogentec, Belgium.
2. RNA extraction using TRI REAGENT^{TM} from Sigma Aldrich. Chloroform, isopropanol and ethanol from Carlo Erba reagents.
3. Concentrator 5301 from Eppendorf for RNA pellets drying.
4. SuperScript III one-step RT-PCR system with Platinum ® Taq polymerase (Invitrogen) and MJ Research PTC200 Peltier Thermal cycler for amplification.
3. Eppendorf BioPhotometer for amplification products quantification.
4. Agarose and ethidium bromide Powder from Sigma Aldrich for gel electrophoresis using Amilabo electrophoresis Power supply st 1006T.
5. Lumi imager F1 Roche for image acquisition.
6. DpnI, AvaI and XbaI restriction enzymes for Promega pLuc705 plasmid DNA digestion.

3. Methods

3.1. Cell culture and cell dissociation

1. Culture HeLa pLuc 705 cells (may be purchased from Gene Tools ,USA) as exponentially growing subconfluent monolayers in DMEM medium (Gibco) supplemented with 10% fetal calf serum, sodium pyruvate, non essential amino-acids and antibiotics.
2. Wash cells twice with PBS and passage with Trypsin/EDTA every other day on 175cm^2 flasks for routine maintenance for a maximum of 10 passages. For experiments, plate cells overnight on 24 wells plates (1.75 10^5 cells/well).

3.2 Synthesis of PNA-peptide conjugates

3.2.1 Synthesis of N-terminal Cys functionalised and N-bromoacetyl PNA

PNA with the desired N-terminal Cys or bromoacetyl functionalities may be purchased from Panagene (Korea). Alternatively PNA synthesis may be achieved using an APEX 396 Robotic

Peptide Synthesizer. Following final deprotection, the PNA is analysed and purified using HPLC, and the molecular mass verified by MALDI-TOF mass spectrometry.

1. Dissolve each Fmoc-PNA monomer in NMP to give 0.2 M solutions (allow 200 µL per PNA or amino acid residue). Warming may be necessary in some cases.
2. Dissolve the PyBop in DMF to give a 0.2 M solution (allow 200 µL per PNA or amino acid residue).
3. Make a 0.2 M DIPEA, 0.2 M 2,6-lutidine solution in DMF (allow 200 µL per PNA or amino acid residue).
4. Make a 20% piperidine solution in DMF (allow 1.6 mL per PNA or amino acid residue).
5. Make a capping solution with 5% acetic anhydride, 6% 2,6-lutidine solution in DMF.
6. Weigh out 10 µmol solid support, put this into a reactor well and swell the support with 1 ml DMF for 15 min.
7. Programme the Synthesizer for the desired sequence (Lys residues are usually added to the C-terminus and N-terminus, to aid solubility, followed by the activated Cys monomer or bromacetic anhydride for the final coupling).
8. Start the synthesis. Each synthesis cycle consists of Fmoc-deprotection, double coupling and capping (**Table 1**). Continue until the sequence is completed.
9. For Cys-terminated PNA, carry out the final coupling with Boc-Cys(Npys)-OH. Do not carry out a subsequent Fmoc deprotection step. For *N*-bromoacetyl PNA, carry out Fmoc deprotection followed by the final coupling as follows. Dissolve bromoacetic acid (2mmol) in dichloromethane (5 mL) and add diisopropylcarbodiimide (2 mL, 0.5 M). Stir for 15 min and filter off the white precipitate (diisopropylurea) and evaporate the filtrate to approx. 2.5 mL. Adjust the volume to 6 mL with DMF and evaporate to approx. 4 mL by bubbling Argon gas through the solution. Filter the solution a second time. Use the resultant bromoacetic anhydride in DMF for coupling to the support.
10. Wash the support with DMF, then methanol and dry the support under vacuum in a desiccator.
11. Place the support in a polyethylene syringe fitted with 10 µm frit and tap.
12. Simultaneously cleave the PNA oligomer from the support and deprotect by adding 4 mL of a 95% TFA, 2.5% water, 2.5% triisopropylsilane solution for 4 h.
13. Filter into a 15 mL Falcon tube, washing the support with additional TFA (0.5 ml). Concentrate the filtrate to approx. 200 µL and precipitate the PNA oligomer with cold (4 ˚C) diethyl ether.
14. Vortex the mixture and compact the precipitate by centrifugation (2500 rpm). Decant off the ether solution carefully and wash the precipitate with ether a further 3 times, compacting the residue and decanting off each time. *CAUTION: It is necessary to use sealed buckets when centrifuging solutions of flammable liquids such as ether.*

15. Analyse the crude product and purify by reversed phase HPLC using an analytical or semi-preparative column, as appropriate, heated to 45 ˚C. Monitor by UV at 260 nm. Buffer A: 0.1% TFA (aq.), Buffer B: 90% acetonitrile + 10% Buffer A (v/v).
16. A typical gradient for a 16-18 mer with 4 Lys residues is 5-20% buffer B over 25 minutes.
17. Collect appropriate fractions, lyophilize, redissolve in water/acetonitrile as required and analyse by HPLC and MALDI-TOF mass spectrometry.
18. Quantify the product by measuring the UV absorbance of an aliquot at 260 nm.

3.2.2 Synthesis of C-terminal Cys-containing Peptides

Peptides may be readily purchased from custom peptide synthesis suppliers. Alternatively, assemble the peptide (as a C-terminal amide) using a Peptide Synthesiser. The following protocol is designed for an Apex 396 robotic Synthesiser.

1. Dissolve each amino acid derivative in DMF to give 0.5 M solutions (allow 600 µL per amino acid residue).
2. Dissolve the PyBop in DMF to give a 0.5 M solution (allow 600 µL per amino acid residue).
3. Make a 1 M DIPEA solution in DMF (allow 600 µL per amino acid residue).
4. Make a 20% piperidine solution in DMF (allow 2 mL per amino acid residue).
5. Weigh out 50 mg support (10 µmol), put into a reactor well and swell the support with 2 × 1 mL DMF (5 min each). Drain off the DMF from the well.
6. Programme the Synthesizer for the desired sequence and start the synthesis beginning with Fmoc deprotection and subsequent double couplings, but omitting the capping step (**Table 1**), and continue until the sequence is completed finishing with an Fmoc deprotection.
7. Wash the support with DMF, then propan-2-ol, and dry under vacuum in a desiccator.
8. Simultaneously cleave the peptide from the support and deprotect with 94% TFA, 2.5% water, 2.5% EDT and 1% triisopropylsilane for 3-6 h.
9. Filter off the support and wash with additional TFA. Concentrate the filtrate to approx. 10% of the original volume and precipitate the peptide with cold (4 ˚C) diethyl ether.
10. Vortex the mixture and compact the precipitate by centrifugation (2500 rpm). Decant off the ether solution carefully and wash the precipitate with ether a further 5 times, compacting the residue and decanting off each time. *CAUTION: It is necessary to use sealed buckets when centrifuging solutions of flammable liquids such as ether*.
11. Analyse the crude product and purify by use of reversed phase HPLC using an analytical or semi-preparative column, as appropriate. Buffer A: 0.1% TFA (aq), Buffer B: 90% acetonitrile + 10% Buffer A (v/v).
12. Collect appropriate fractions, lyophilise, redissolve in water or Buffer A and analyse by HPLC and MALDI-TOF mass spectrometry.

3.2.3 Synthesis of disulfide-linked conjugates (Fig.2)

1. Put into a microfuge tube 50 µL formamide (for lipophilic peptides add instead 25 µL formamide and 25 µL acetontrile).
2. Add 20 nmol (2 µL of a 10 mM aqueous solution) of the (NPys)Cys-PNA oligonucleotide (from Section 3.2.1) and then 50 nmol (5 µL of a 10 mM stock solution, 2.5 equivalents) of the Cys-functionalised peptide to be conjugated (from Section 3.2.2).
3. Add 1 M NH_4Ac solution (10 µL).
4. Mix the solution by vortexing, centrifuge briefly and leave for 30-60 min at room temperature.
5. Purify the resulting conjugate by reversed phase HPLC at 45 °C using a single injection at flow rate 1.5 ml/min. Use a gradient 15-35% B buffer over 25 minutes when conjugating to highly basic peptides or a gradient 10-60% B buffer when conjugating to more lipophilic peptides. Buffers are the same as for peptides (see section 3.2.2).
5. Collect the product and lyophilize.
6. Dissolve the residue in sterile water, analyse by HPLC and by MALDI-TOF mass spectrometry and quantify by measuring the absorbance at 260 nm.

3.2.4 Synthesis of thioether-linked conjugates (Fig.3)

1. Dissolve 50 nmol bromoacetyl PNA in 45 µl formamide and 10 µl BisTris.HBr buffer (pH 7.5).
2. Add 15.6 µl C-terminal Cys-containing peptide (8 mM, 125 nmol, 2.5 equivalents).
3. Heat the solution at 40 °C for 2 h.
4. Purify the product by reversed phase HPLC at 45 °C. Gradients are similar to those in section 3.2.3.
5. Collect the product and lyophilize.
6. Analyse by HPLC and by MALDI-TOF mass spectrometry and quantify by measuring the absorbance at 260 nm.

3.3 FACS analysis of PNA-peptide conjugates cellular uptake and cell permeability assay

1. Wash exponentially growing HeLa pLuc705 cells with PBS to remove cell culture medium, treat with trypsin/EDTA for 5 min, centrifuge at 900xg at 4°C for 5 min, wash twice with PBS, centrifuge again, resuspend in DMEM , plate on 24 wells plates ($1.75\ 10^5$ cells/well) and culture overnight.
2. Discard the culture medium and wash cells twice with PBS.
3. Discard PBS and incubate cells with fluorescently-labeled conjugates diluted in Opti-MEM or D-MEM.

4. After incubation for the appropriate period of time, wash the cells twice with PBS and treat with Trypsin/EDTA (5 min, 37°C) or Pronase (0.1%) /EDTA (1 mM) (5 min, 4°C).
5. Resuspend cells in PBS 5% FCS, centrifuge at 900 x g (5 min, 4°C) and resuspend in PBS 0.5% FCS containing 0.05 µg/ml propidium iodide (PI).
   Note: use PI to analyse the effects of CPP-ON conjugates on cell permeability.
6. Analyse fluorescence with a FACS fluorescence activated sorter (BD Bioscience) for cellular uptake and PI permeabilization using WinMDI 2.8 free software. Exclude PI-stained cells from further analysis by appropriate gating. Analyse a minimum of 20,000 events per sample.

3.4 Fluorescence microscopy analysis of PNA-peptide intracellular distribution

1. Detach exponentially growing HeLa pLuc705 cells (3.5×10^5) with trypsin (0.05%)/EDTA.4Na (0.35mM), centrifuge at 900 x g for 5 min, resuspend in 2 ml OptiMEM and incubate with the fluorochrome-labeled conjugates (between 1-2.5 µM) for 30 to 120 min.
2. Treat the cells with trypsin and rinse twice with PBS.
3. Incubate the cells with transferrin-Alexa 546 (10 µg/ml diluted in OptiMEM) for 10 min at 37°C to stain endosomes.
4. Wash twice with PBS.
5. Incubate with Hoechst (blue fluorescence) for 5 min to stain nuclei.
6. Wash twice with PBS and add 1ml of complete medium.
7. Analyse the distribution of fluorescence in live unfixed cells on a Zeiss Axiovert 200 M fluorescence microscopy with 63x plan-apochromat objective, an AxioCam MRm camera and Axiovision software.

3.5 Luciferase assay of splicing correction by PNA and PNA-peptide conjugates

1. Detach exponentially growing HeLa pLuc705 cells with trypsin/EDTA, plate on 24 wells plates ($1.75\ 10^5$ cells/well) and culture overnight.
2. Wash twice with PBS and incubate with the splice correcting conjugates or its scrambled version at the appropriate concentrations usually between 0.5-4 h in OptiMEM medium.
3. Wash cells and continue incubation for 20 h in complete DMEM medium containing 10% FCS.
4. Wash cells twice with PBS and lyse with Reporter Lysis Buffer (Promega, Madison, WI).
5. Quantify luciferase activity in a Berthold Centro LB 960 luminometer (Berthold Technologies, Bad Wildbad, Germany) using the Luciferase Assay System substrate (Promega, Madison, WI). Perform all experiments in triplicate.

6. Measure cellular protein concentrations with the BCA™Protein Assay Kit (Pierce, Rockford, IL) and read using an ELISA plate reader (Dynatech MR 5000, Dynatech Labs, Chantilly, VA) at 550 nm. Perform all experiments in triplicate.
7. Express luciferase activities as relative luminescence units (RLU) per µg protein. Average each data point over the three replicates.

3.6 RT-PCR evaluation of splicing correction by PNA and PNA-peptide conjugates

1. Extract total RNA using 1ml of TRI REAGENT^{TM}/well after measurement of luciferase. Add 300 µl of chloroform, mix gently and incubate 10 min at room temperature.
2. Centrifuge at 12,000 x g for 15 min at 4°C and add an equal volume of isopropanol to the aqueous phase. Mix gently and incubate for 10 min at room temperature.
3. Centrifuge at 12,000 x g for 15 min at 4°C and resuspend the pellet in 1 ml of 75% ethanol. Mix and centrifuge at 12,000 x g for 5 min at 4°C. Discard the supernatant. Evaporate off the ethanol using an Eppendorf Concentrator 5301 for 1 min at 60°C.
4. Add 50µl of Nuclease Free Water.
5. Quantify total RNA using Eppendorf BioPhotometer and control quality by 1% agarose gel electrophoresis on Amilabo electrophoresis Power supply st 1006T.
6. Amplify total RNA using SuperScript III one step RT-PCR system with Platinum ® Taq polymerase in the presence of Luciferase specific primers with MJ Research PTC200 Peltier Thermal cycler.
7. Analyse PCR products by electrophoresis using 2% agarose gel. Use digestion products of the plasmid pLuc705 by DpnI, XbaI and AvaI restriction enzymes as molecular weight markers.

4. Notes

4.1 Cell culture and cell dissociation

HeLa pLuc 705 cells are stably transfected by a luciferase construction allowing the quantitative assessment of PNA-peptide conjugates nuclear delivery and biological activity (Fig.1). Cells should not be passaged more than 10 times and should be controlled routinely (1-2 times per month) for the absence of mycoplasma contamination

4.2 Synthesis of PNA-peptide conjugates

1. There is no commercial Synthesiser currently recommended for PNA synthesis. We have found acceptable results using an Apex 396 robotic Peptide Synthesiser and we have recently obtained good PNA assembly using a Liberty microwave Peptide Synthesiser. Key to success is minimisation of times for piperidine treatment. Extended treatments can lead to a trans-acylation side reaction that will

result in lower yields. PyBop must be dissolved freshly and on no account should be used after standing for greater than 2 days.

2. In conjugation reactions, it is essential to maintain full solubility. Although not entirely essential in all cases, we prefer to maintain the presence of formamide in all conjugations reactions to ensure total solubility of both starting PNA and peptide and final conjugate. In the case of a very hydrophobic peptide (eg Transportan), the use of a mixture of formamide and acetonitrile may be helpful to maintain full solubility. Following conjugation, PNA-peptides can generally be purified by reversed phase HPLC under acidic conditions, similarly to the purification of both peptides and PNA. Some adjustment to the acetonitrile gradient conditions may be necessary from case to case. We recommend that conjugates are purified in one injection (i.e. as fast as possible after conjugation) and with use of a heated column (45 °C) for optimal peak characteristics. Typically 60-80 % conjugation yields should be achieved.

4.3 FACS analysis of PNA-peptide conjugates cellular uptake and cell permeability assay

1. For mechanistic studies, different drugs or treatments interfering with endocytosis may be used. In this case, pre-treat the cells with the inhibitors for the appropriate time and concentration. Inhibitors should also be present during incubation with the PNA-peptide conjugates. Most endocytosis inhibitors tend to be cytotoxic and should be used for the shortest possible period of time ***(13)***.

2. Treatment with trypsin or pronase before FACS analysis is required to eliminate membrane-bound PNA-peptide conjugates ***(14)***. Pronase is advantageous for some experiments (as for example when monitoring energy-dependence by low temperature incubation) since it is able to act at 4°C.

4.4 Fluorescence microscopy analysis of PNA-peptide intracellular distribution

Experiments have to be performed on live cells, since most cell fixation protocols lead to artefactual re-distribution of PNA-peptide conjugates ***(14)***.

4.5 Luciferase assay of splicing correction by PNA and PNA-peptide conjugates

1. Co-treatment with 100 µM chloroquine may be included to improve endosomal release and to increase splicing correction. Chloroquine is required to achieve significant PNA or PMO nuclear delivery and splicing correction with Penetratin, $(Arg)_9$ or Tat_{48-60} at low concentrations. It is not required with recently described basic CPPs as R6Pen ***(15)*** or $(R\text{-}Ahx\text{-}R)_4$ ***(16)***.

2. PNA-peptide conjugates should preferably be used at low concentrations (below 2.5µM) to avoid cell permeabilization.

4.6 RT-PCR evaluation of splicing correction by PNA and PNA-peptide conjugates

1. R6Pen ***(15)*** or $(R\text{-}Ahx\text{-}R)_4$ ***(16)*** PNA and PMO conjugates allow splicing correction in this assay with submicromolar EC_{50} values.

2.Programme used for reverse transcription and amplification:

a) Reverse Transcription: 1 cycle
   - cDNA production: 30 min at 55°C
   - Denaturation: 2 min at 94°C

b) Amplification: 30 cycles
   - Denaturation: 20 sec at 94°C
   - Hybridization: 30 sec at 60°C
   - Elongation: 30 sec at 68°C

c) Elongation: 1 cycle for 5 min at 68°C

d) Stock PCR products at -20°C.

5. References

1. Torchilin, V. P. **(2006)** Recent approaches to intracellular delivery of drugs and DNA and organelle targeting. *Annu Rev Biomed Eng.* **8,** 343-375.

2. Zhang, X., and Godbey, W. T. **(2006)** Viral vectors for gene delivery in tissue engineering. *Adv Drug Deliv Rev.* **58,** 515-534.

3. Kang, S. H., Cho, M. J., and Kole, R. **(1998)** Up-regulation of luciferase gene expression with antisense oligonucleotides: implications and applications in functional assay development. *Biochemistry*. **37,** 6235-6239.

4. Kole, R., and Sazani, P. **(2001)** Antisense effects in the cell nucleus: modification of splicing. *Curr Opin Mol Ther.* **3,** 229-234.

5. Rasmussen, F. W., Bendifallah, N., Zachar, V., Shiraishi, T., Fink, T., Ebbesen, P., Nielsen, P. E., and Koppelhus, U. **(2006)** Evaluation of transfection protocols for unmodified and modified peptide nucleic acid (PNA) oligomers. *Oligonucleotides.* **16,** 43-57.

6. Summerton, J. **(1999)** Morpholino antisense oligomers: the case for an RNase H-independent structural type. *Biochim Biophys Acta.* **1489,** 141-158.

7. Abes, S., Richard, J. P., Thierry, A. R., Clair, P., and Lebleu, B. **(2007)** Tat-Derived Cell-Penetrating Peptides: Discovery, Mechanism of Cell Uptake, and Applications to the Delivery of Oligonucleotides. *Handbook of Cell-Penetrating Peptides (second edition).* 29-42.

8. Debart, F., Abes, S., Deglane, G., Moulton, H. M., Clair, P., Gait, M. J., Vasseur, J. J., and Lebleu, B. **(2007)** Chemical modifications to improve the cellular uptake of oligonucleotides. *Curr Top Med Chem.* **7,** 727-737.

9. Thomson, S. A., Josey, J. A., Cadilla, R., Gaul, M. D., Hassman, C. F., Luzzio, M. J., Pipe, A. J., Reed, K. L., Ricca, D. J., and Wiethe, R. W. e. a. **(1995)** Fmoc mediated synthesis of peptide nucleic acids. *Tetrahedron.* **51,** 6179-6194.

10. Braasch, D. A., Nulf, C. J., and Corey, D. A., 4.11.1-4.11.18. **(2002)** Synthesis and purification of peptide nucleic acids. *Curr. Protocols Nucleic Acids Chemistry.* 4.11.11-14.11.18.

11. Turner, J. J., Ivanova, G. D., Verbeure, B., Williams, D., Arzumanov, A. A., Abes, S., Lebleu, B., and Gait, M. J. **(2005)** Cell-penetrating peptide conjugates of peptide nucleic acids (PNA) as inhibitors of HIV-1 Tat-dependent trans-activation in cells. *Nucleic Acids Res.* **33,** 6837-6849.

12. Garcia-Blanco, M. A., Baraniak, A. P., and Lasda, E. L. **(2004)** Alternative splicing in disease and therapy. *Nat Biotechnol.* **22,** 535-546.

13. Richard, J. P., Melikov, K., Brooks, H., Prevot, P., Lebleu, B., and Chernomordik, L. V. **(2005)** Cellular uptake of unconjugated TAT peptide involves clathrin-dependent endocytosis and heparan sulfate receptors. *J Biol Chem.* **280,** 15300-15306.

14. Richard, J. P., Melikov, K., Vives, E., Ramos, C., Verbeure, B., Gait, M. J., Chernomordik, L. V., and Lebleu, B. **(2003)** Cell-penetrating peptides. A reevaluation of the mechanism of cellular uptake. *J Biol Chem.* **278,** 585-590.

15. Abes, S., Turner, J. J., Ivanova, G. D., Owen, D., Williams, D., Arzumanov, A., Clair, P., Gait, M. J. and Lebleu, B. **(2007)** Efficient splicing correction by PNA conjugation to an R6-Penetratin delivery peptide. *Nucleic Acids Res.* ***35***, in press.

16. Abes, S., Moulton, H. M., Clair, P., Prevot, P., Youngblood, D. S., Wu, R. P., Iversen, P. L., and Lebleu, B. **(2006)** Vectorization of morpholino oligomers by the (R-Ahx-R)4 peptide allows efficient splicing correction in the absence of endosomolytic agents. *J Control Release*. **116,** 304-313.

Acknowledgements

We thank R. Kole (University North Carolina) for providing the pLuc705 cell line. Studies funded by EC grant QLK3-CT-2002-01989 and CEFIPRA grant 3205. S. Abes had a pre-doctoral fellowship from the Ligue Regionale contre le Cancer and R. Abes had a Region Languedoc-Roussillon training fellowship.

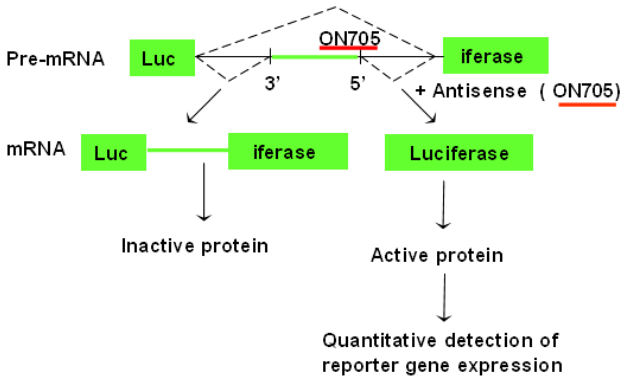

Fig.1 Outline of the luciferase splicing-correction assay

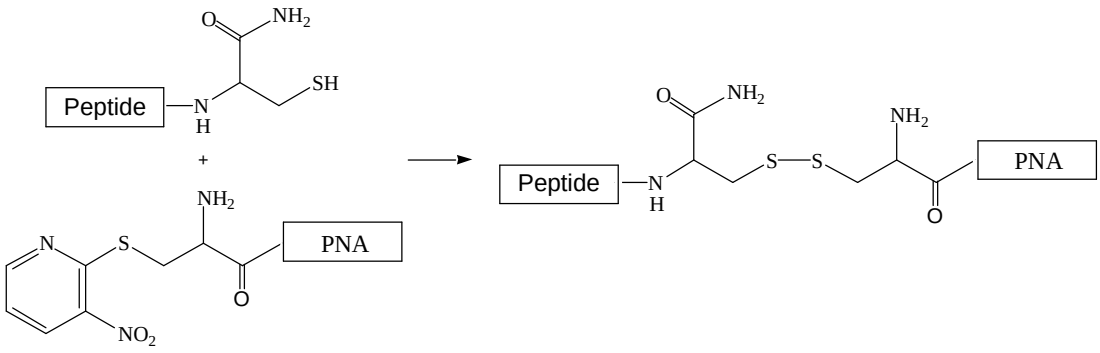

Figure 2 Formation of a Disulfide linkage

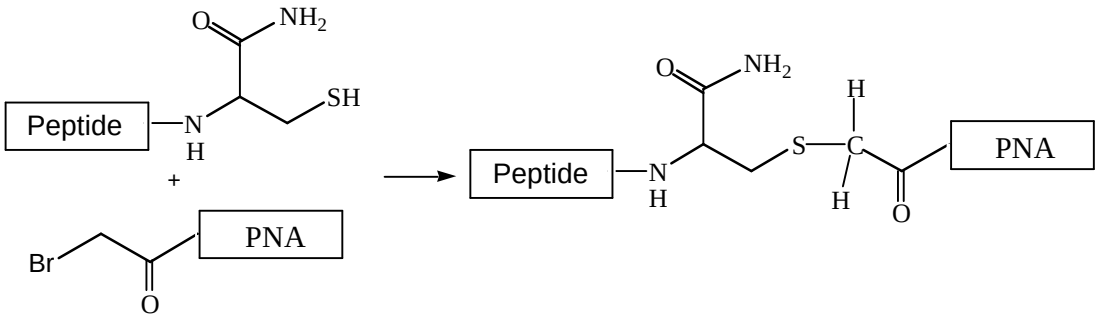

Figure 3 Formation of a thioether linkage

A

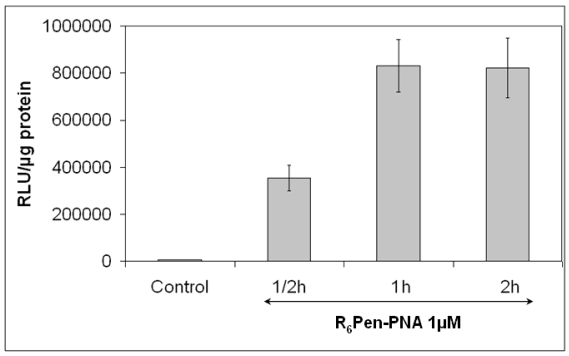

B

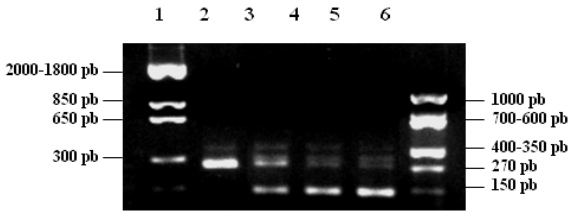

1. pLuc705 plasmid + Xba1 and Ava1
2. Control
3. R6Pen-PNA, 1µM, 1/2h
4. R6Pen-PNA, 1µM, 1h
5. R6Pen-PNA 705, 1µM, 2h
6. pLuc705 plasmid + Dnp1

Fig.4. Assay of splicing correction: Luciferase activity (**A**) and RT-PCR evaluation (**B**)

Table 1 Synthesis Cycle for PNA or peptide synthesis on the APEX 396 synthesizer.

Synthesis Step	Reagents and volumes (μL)	Time (min)
Deprotection	20% piperidine soln. (800) 20% piperidine soln. (800)	1 4
Wash (× 5)	DMF (1000)	1
Couple (×2)	PNA or amino acid (100) PyBop (100) DiPEA/lutidine (100) DMF (100)	30
Wash (× 5)	DMF (1000)	1
Cap (×2)	PNA Capping Solution (1000)	5
Wash (× 5)	DMF (1000)	1

Chapitre II

Réévaluation de la mécanistique d'internalisation cellulaire et de l'efficacité des conjugués antisens-CPP

Chapitre II

Réévaluation de la mécanistique d'internalisation cellulaire et de l'efficacité des conjugués antisens-CPP

Article II: Endosome trapping limits the efficiency of splicing correction by PNA-oligolysine conjugates

Saïd Abes, Donna Williams[1], Paul Prevot, Alain Thierry, Michael J. Gait[1], Bernard Lebleu, UMR 5124 CNRS, CC 086, Université Montpellier 2, Place Eugène Bataillon, 34095 Montpellier, France
[1]Medical Research Council, Laboratory of Molecular Biology, Hills Road, Cambridge, CB2 2 QH, UK

Article III: Structural Requirements for Cellular Uptake and Antisense Activity of Peptide Nucleic Acids Conjugated with Various Peptides

Yvonne Wolf, Stephan Pritz, **Saïd Abes**[1], Michael Bienert, Bernard Lebleu[1], and Johannes Oehlke
Leibniz-Institute of Molecular Pharmacology, Robert-Roüssle-Strasse 10, D-13125 Berlin, Germany, and UMR 5124 CNRS,
[1]Université Montpellier 2, Place Eugène Bataillon, 34095 Montpellier, France

Article IV: Cell-penetrating peptide conjugates of peptide nucleic acids (PNA) as inhibitors of HIV-1 Tat-dependent trans-activation in cells

John J. Turner, Gabriela D. Ivanova, Birgit Verbeure, Donna Williams,
Andrey A. Arzumanov, **Saïd Abes**[1], Bernard Lebleu[1] and Michael J. Gait*
Laboratory of Molecular Biology, Medical Research Council, Hills Road, Cambridge CB2 2QH, UK and
[1]UMR 5124 CNRS, CC 086, Université Montpellier 2, Place Eugène Bataillon, 34095 Montpellier, France

1. Introduction :

Comme évoqué dans l'introduction et largement admis dans la communauté scientifique, la mise au point de vecteurs efficaces et non toxiques pour la délivrance de toutes sortes de biomolécules (voir Figure 8) reste un problème majeur pour leur utilisation en génomique fonctionnelle et pour leur développement en clinique.

Les CPPs apparaissent comme des vecteurs de biomolécules attractifs vu leur faible toxicité et leur grande diversité, comme l'atteste l'abondante littérature consacrée à ce domaine au cours des dernières années (Abes et al. 2007; Jarver et Langel 2004; Thierry et al. 2003).

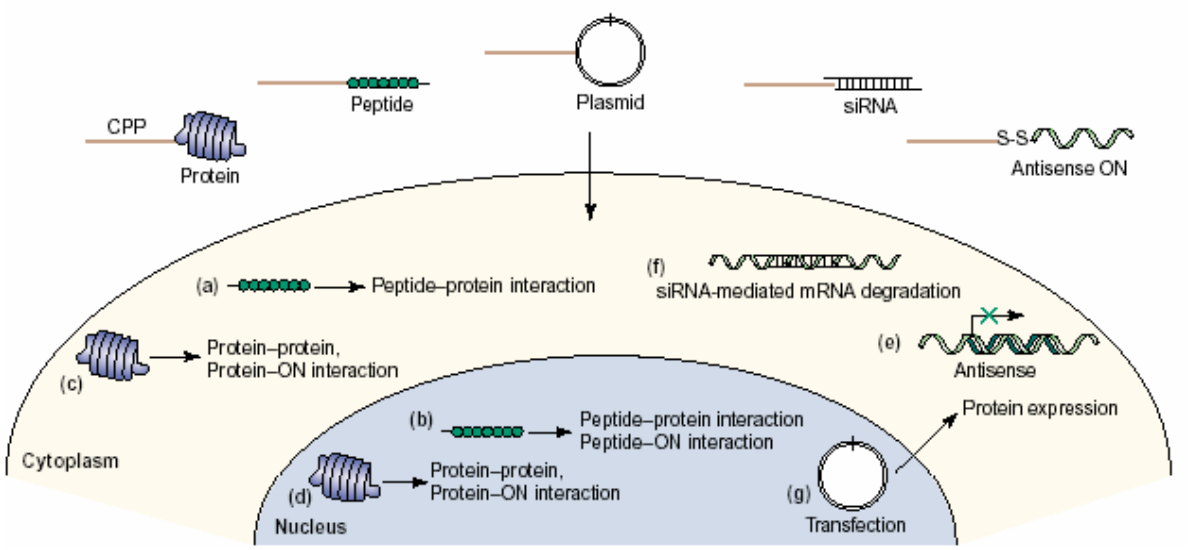

Figure 8: *La délivrence par les CPPs :* Les CPPs sont capables d'internaliser plusieurs biomolécules au travers de la membrane plasmique et/ou nucléaire des cellules. [Adapté de (Jarver et Langel 2004)]

Les mécanismes mis en jeu dans l'internalisation des CPPs et de leurs conjugués à des cargos restent cependant très controversés. Le rationnel de notre démarche est qu'une meilleure compréhension des mécanismes mis en jeu permettra vraisemblablement d'optimiser ces vecteurs peptidiques.

2. Utilisation des CPPs pour la délivrance de PNA :

Le premier objectif de cette thèse a été de déterminer la mécanistique d'internalisation ainsi que les effets biologiques des conjugués CPPs-PNA sur des cellules en culture. Le modèle biologique utilisé est celui de la correction d'épissage initialement proposé par le Dr. R. Kole (Kole et al. 2004) (voir Figure 7).

Précédemment, plusieurs publications (Sazani et al. 2001; Siwkowski et al. 2004) avaient décrit la possibilité de corriger l'épissage dans ce modèle à l'aide d'analogues en série 2'OMéthyl ou de PNA conjugués à une courte chaîne (4 à 8 résidus) de lysines. Ceci n'était à priori pas surprenant dans la mesure où l'étude structure activité (SAR) réalisée sur des CPPs

comme Tat 48-60 [comme revue récentes (Abes et al. 2007)], dans notre laboratoire en particulier, avait démontré le rôle critique joué par les acides aminés basiques lors de la pénétration.

Plus surprenant néanmoins, la correction de l'épissage avec ces conjugués ne paraissait pas dépendante de la température dans les conditions utilisées, ce qui suggérait la mise en jeu d'un mécanisme indépendant de l'endocytose (Siwkowski et al. 2004).

Il nous a donc semblé important de vérifier ces données expérimentales. Le PNA_{705} (**CCTCTTACCTCAGTTACA)**, corrigeant l'épissage dans le modèle de Kole, a été conjugué chimiquement à une chaîne de 8 résidus Lysine (K), dans le cadre d'une collaboration avec l'équipe du Dr.M.GAIT (MRC Cambridge). Pour les études de microscopie de fluorescence, la même construction est conjuguée à une fluorescéine (voir Figure 9).

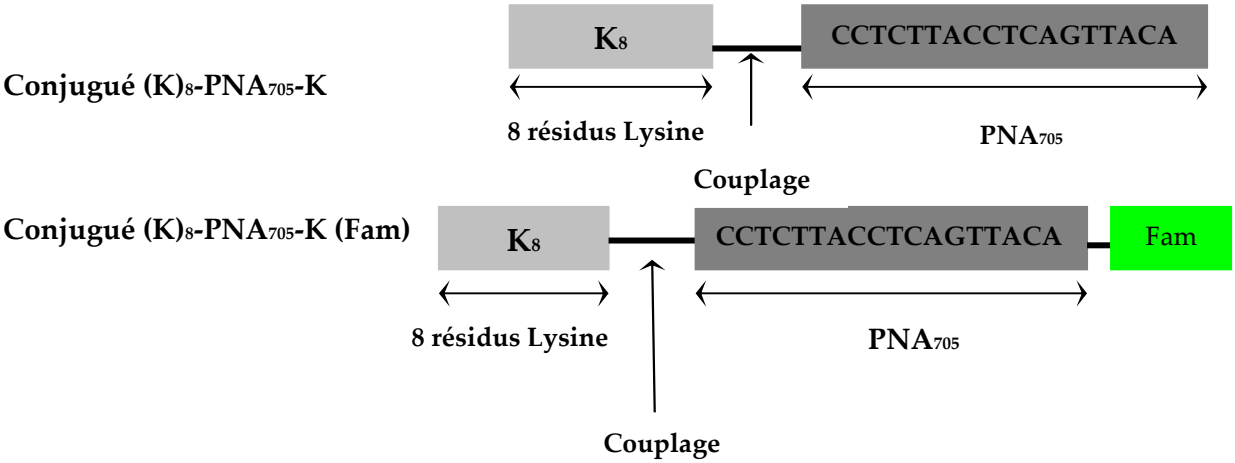

Figure 9 : *Conjugués K_8-PNA et K_8-PNA-Fam* (K= lysine, Fam = fluorescéine)

3. Bilan sur la réévaluation :

La pénétration du K_8-PNA-K-(Fam) dans les cellules HeLa pLuc705 (utilisées pour analyser la correction de l'épissage) a été analysée par cytométrie de flux en fonction du temps, de la concentration ou de la température. La cytotoxicité des conjugués a été déterminée par co-incubation avec de l'iodure de propidium (PI). La quantité de matériel K_8-PNA-K-(Fam) internalisé augmente avec la concentration en conjugué, mais une perméabilisation des

cellules au PI est observée à des concentrations supérieures à 2,5 µM. A faible concentration (2 µM), la pénétration est dépendante de la température (Abes et al. 2006).

Par contre, à des concentrations plus élevées (5 et 10 µM), aucun effet de la température n'est observé en accord avec la forte perméabilisation observée (Abes et al. 2006). Il faut noter ici que les résultats publiés dans ce domaine (Sazani et al. 2001; Siwkowski et al. 2004) ont été réalisés à des concentrations élevées.

L'activité de correction d'épissage de ces conjugués a été déterminée ensuite par mesure de l'activité luciférase. Le conjugué $(Lys)_8$-PNA_{705}-Lys est plus efficace que le PNA_{705} seul, mais cette activité de correction d'épissage reste très faible si on la compare à celle obtenue avec des analogues en série 2'OMethyl vectorisés par des lipoplexes (Abes et al. 2006; Thierry et al. 2006).

Comme ces conjugués semblent internalisés par un mécanisme d'endocytose, nous nous sommes demandés si ils ne restent pas bloqués dans les endosomes / lysosomes.
Nous avons donc utilisé des agents lysosomotropiques comme la chloroquine, déjà connus pour augmenter fortement l'efficacité de transfection de plasmides par des vecteurs non viraux (Ciftci et Levy 2001; Fredericksen et al. 2002).

La co-incubation du conjugué $(Lys)_8$-PNA_{705}-Lys avec la chloroquine (100 µM) augmente très fortement l'activité luciférase. Aucun effet n'est obtenu avec le PNA_{705} libre ou avec une version mutée du conjugué $(Lys)_8$-PNA_{705} scrambled-Lys.

Nous avons vérifié par microscopie de fluorescence et par FACS que ces conditions expérimentales ne perméabilisaient pas les cellules. Le même type de résultat a été obtenu par un traitement au sucrose 0,5 M qui est également supposé déstabiliser les vésicules d'endocytose (Abes et al. 2006). D'autre part nous avons vérifié par RT-PCR que le traitement par la chloroquine ou par le sucrose permettait de déceler de l'ARN messager correctement épissé, bien que la bande correspondant à l'ARN messager anormal ne disparaisse pas (Abes et al. 2006).

Nous avons vérifié si ce problème limite également l'efficacité d'autres conjugués. Sur le même modèle de correction d'épissage, nos travaux en collaboration avec l'équipe du Dr. J.

Oehlke confirment la faible efficacité de correction d'épissage liée à une séquestration dans les vésicules d'endocytose (Wolf et al. 2006). Le couplage du PNA correcteur de l'épissage, dans le modèle de Kole, avec le peptide amphipatique MAP ou la pénétratine permet de dérouter l'épissage vers la forme active de la luciférase. L'addition d'un agent endosomolytique, comme la chloroquine ou le calcium, augmente significativement l'effet de correction. De plus, les études de microscopie confirment une localisation essentiellement vésiculaire pour les deux conjugués en absence d'agents endosomolytiques (Wolf et al. 2006).

En collaboration avec l'équipe du Dr. M. J. Gait nous avons testé différents vecteurs peptidiques. Le modèle utilisé se base sur l'arrêt par la protéine Tat du VIH de la transactivation de TAR. Cet arrêt se traduit par l'inhibition de l'expression de la luciférase. Trois plasmides ont été transfectés d'une manière stable dans des cellules HeLa. Le premier code pour la protéine Tat du VIH sous contrôle d'un promoteur inductible, le second pour la *Firefly luciferase*. Il dépend de la transactivation de la région TAR par la protéine Tat. Le troisième est un contrôle de spécificité d'inhibition qui code pour la *Renilla Luciférase* sous contrôle du promoteur CMV (Turner et al. 2005). L'efficacité de plusieurs peptides vecteurs a été testée sur ce modèle : le peptide Tat (48-60), la pénétratine, la séquence NLS du SV40, l'octalysine et la nonarginine. Aucune inhibition de synthèse de la luciférase n'a été enregistrée. L'addition de la chloroquine augmente l'effet d'inhibition de l'expression de la luciférase dans ce modèle. La microscopie de fluorescence montre une localisation vésiculaire dominante pour tous ces conjugués (Turner et al. 2005).

Ces résultats indiquent que le couplage de PNA aux peptides vecteurs est nécessaire pour l'internalisation mais pas suffisant pour une correction d'épissage ou une inhibition d'expression efficace.
D'autres travaux, réalisés par les équipes du Dr. P. Nielsen et du Dr. U. Langel, ont confirmé que la rétention de ces conjugués dans les compartiments d'endocytose est une limitation majeure à leur activité (El-Andaloussi et al. 2005; Shiraishi et Nielsen 2006).

4. Discussion :

La première partie du bilan expose l'influence de la concentration du conjugué sur le processus d'internalisation cellulaire. Ce mécanisme devient insensible à la température à des

concentrations supérieures à 5µM. Cette insensibilité s'explique par la forte perméabilisation de la membrane cellulaire (voir Figure 10).

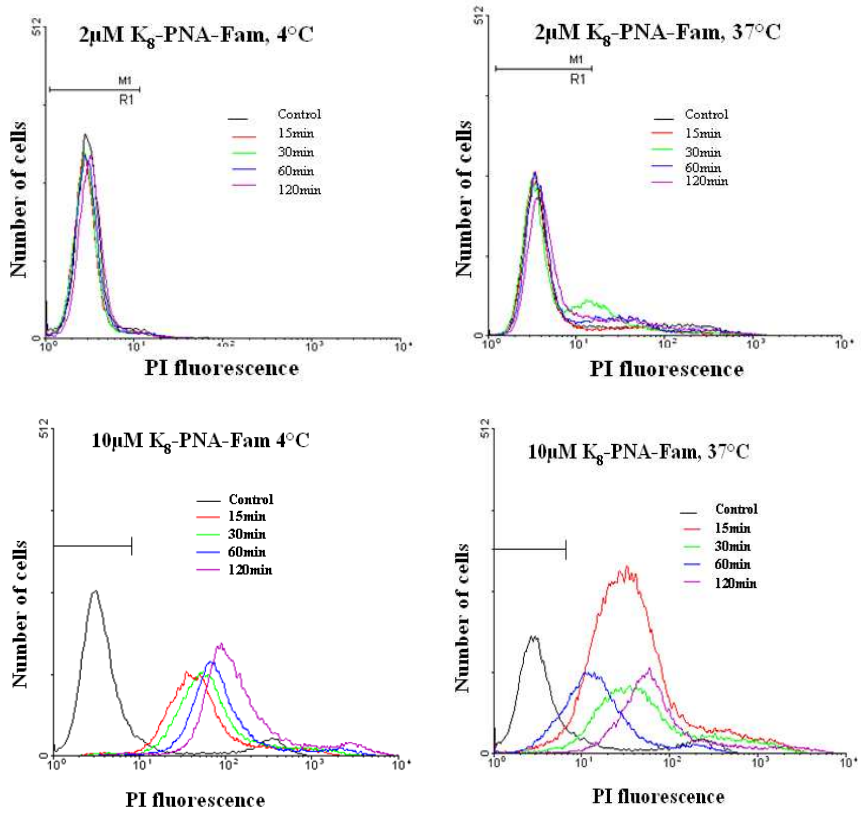

Figure 10 : *Effet de la concentration du K_8-PNA-Fam sur la permeabilité cellulaire :* profil d'internalisation de l'iodure de propidium au cours du temps après incubation des cellules avec 2µM ou 10µM de K_8-PNA-Fam à 37°C ou à 4°C.

Les résultats que nous présentons suggèrent fortement que deux processus dépendant de la dose du conjugué antisens peuvent être mis en jeu : le premier, à basse concentration, dépendant de la température et qui ne perméabilise pas les membranes ; le second à forte concentration, indépendant de la température et qui perméabilise fortement les membranes.
Les différents travaux présentés dans ce premier chapitre s'accordent à démontrer que la séquestration dans les vésicules d'endocytose limite l'efficacité des analogues antisens. Ces endosomes s'acidifient au cours de leur évolution en lysosomes (voir Figure 6). Une fois dans le lysosome, les conjugués antisens sont dégradés par les enzymes lysosomales.

Nos expériences montrent que la chloroquine ou le sucrose augmentent nettement la correction d'épissage. Cette augmentation n'est pas le résultat d'une internalisation accrue (Abes et al. 2006). Il faut savoir que la chloroquine, médicament antipaludéen, est une amine qui traverse la membrane plasmique sous sa forme non protonée et qui s'accumule dans les compartiments acides de la cellule, comme l'endosome tardif ou le lysosome. Cette accumulation permet de réguler le pH du lysosome, ce qui entraîne l'inhibition de l'activité enzymatique. De plus, les vésicules éclatent par pression osmotique et leur charge se libère (de Duve et al. 1974). Les travaux d'amélioration de l'efficacité de délivrance de protéines recombinantes fusionnées au peptide Tat avaient montré qu'il est possible de l'augmenter significativement par déstabilisation des endosomes à l'aide de peptides fusogènes ou de la chloroquine (Caron et al. 2004; Wadia et al. 2004).

Toutefois, la microscopie de fluorescence ne permet pas de déceler une redistribution significative des conjugués après traitement avec la chloroquine et la grande partie des conjugués fluorescents restent séquestrés dans les vésicules d'endocytose (voir Figure 11).

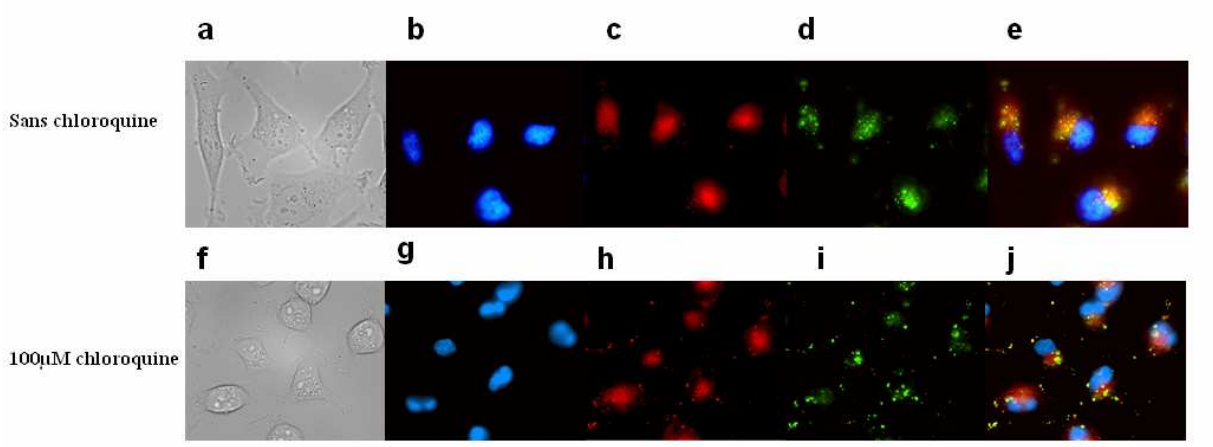

Figure 11 : *Effet de la chloroquine sur la localisation intracellulaire du conjugué fluorescent Tat-PNA :*
La chloroquine ne provoque pas une redistribution intracellulaire du conjugué fluorescent. Les cellules HeLapLuc705 ont été incubées pendant 4 heures à 37°C avec le conjugué fluorescent Tat-PNA à une concentration de 2µM en absence (a, b, c, d et e) de chloroquine ou en présence (f, g, h, i et j) de 100µM chloroquine (co-incubation). Les noyaux sont colorés en bleu (Hoeschst), les vésicules d'endocytose en rouge (transferrine-Alexa 545). La couleur verte indique la localisation du conjugué. Les images **e** et **j** sont des superposition de (b, c, d) et (g, h, i) respectivement.

Une certaine localisation cytoplasmique et nucléaire a été observée après co-traitement avec la chloroquine par l'équipe du Dr. M. J. Gait (Turner et al. 2005). Cela laisse penser que seul une faible proportion de conjugués antisens s'échappent des endosomes, mais que ceci suffit à corriger l'épissage d'une manière spécifique et significative.

5. Conclusion :

La présente étude (article II) ainsi que nos travaux de collaboration (article III et IV) sur l'utilisation des peptides vecteurs démontre que des conjugués PNA-CPPs sont peu efficaces, car les conjugués internalisés restent enfermés dans les vésicules d'endocytose. L'addition d'agents endosomolytiques, comme la chloroquine, augmente significativement la correction de l'épissage. Malheureusement, l'utilisation de tels agents *in vivo* n'est pas envisageable vu leurs nombreux effets indésirables.

Available online at www.sciencedirect.com
SCIENCE DIRECT
Journal of Controlled Release 110 (2006) 595 – 604
journal of controlled release
www.elsevier.com/locate/jconrel

Endosome trapping limits the efficiency of splicing correction by PNA-oligolysine conjugates

Saïd Abes [a], Donna Williams [b], Paul Prevot [a], Alain Thierry [a], Michael J. Gait [b], Bernard Lebleu [a,*]

[a] UMR 5124 CNRS, CC 086, Université Montpellier 2, Place Eugène Bataillon, 34095 Montpellier, France
[b] Medical Research Council, Laboratory of Molecular Biology, Hills Road, Cambridge, CB2 2 QH, UK

Received 4 August 2005; accepted 17 October 2005
Available online 27 December 2005

Abstract

Splicing correction by steric-blocking oligonucleotides (ON) might lead to important clinical applications but requires efficient delivery to cell nuclei. The conjugation of short oligolysine tails has been used to deliver a correcting peptide nucleic acid (PNA) sequence in a positive readout assay in which ON hybridization to the cryptic splice site is strictly required for the expression of a luciferase reporter gene. We have investigated the mechanism of cellular uptake and the efficiency of a $(Lys)_8$-PNA-Lys construction in this model system. Cell uptake is temperature-dependent and leads to sequestration of the conjugate in cytoplasmic vesicles in keeping with an endocytic mechanism of internalization. Accordingly a significant and sequence-specific splicing correction is achieved only in the presence of endosome-disrupting agents as chloroquine or 0.5 M sucrose. These endosome-disrupting agents do not affect the activity of free PNA, and do not increase $(Lys)_8$-PNA-Lys uptake.

Keywords: Conjugation; Oligolysine; PNA; Splicing correction; Endocytosis

1. Introduction

The majority of human genes undergo alternative splicing (reviewed in 1). Mutations in splicing cis-acting regulatory elements are associated with many human diseases such as for instance thalassemias, Alzheimer's disease, cystic fibrosis, muscular dystrophies or cancers [1]. As an example, several forms of β-thalassemia are due to mutations in the β globin gene intron 2 which activate cryptic splice sites and lead to the production of non-functional β globin mRNA and protein [2].

Several experiments have established that the masking of these cryptic splice sites by antisense oligonucleotides (ON) restores normal splicing in cell culture experiments [reviewed in [3]]. To be effective the correcting ON should be metabolically stable, hybridize to its target with high affinity and specificity, be delivered efficiently to the cell nucleus, and not trigger the activation of a nuclease. The use of RNase H activating oligodeoxynucleotides as phosphorothioate ON derivatives, or of siRNAs is therefore precluded for splicing correction. RNase H incompetent analogues (or steric blocking ON) as phosphorodiamidate morpholino oligomers (PMO) [4] or peptide nucleic acids (PNA) [5] have favorable pharmacologic properties in terms of nuclease resistance and affinity for a complementary RNA sequence. Cellular delivery remains however a limitation as for most nucleic acids-based strategies. Moreover neutral PMO and PNA cannot be administered by cationic delivery vectors such as PEI or cationic lipids.

A series of recent experiments has established that the chemical conjugation of RNase H incompetent ON to cell penetrating peptides (CPP) [6,7] or even to short oligolysine tails [8–10] could lead to splicing correction. Most of these experiments have been performed with a reporter splicing assay which is considered as the most reliable to assess the nuclear delivery of steric-blocking ON analogues since it gives rise to a positive read-out over a very low background [11]. In brief, the coding sequence of a reporter gene is interrupted by a human β globin intron 2 carrying a cryptic splice site. The aberrant splice site prevents proper processing of the reporter pre-mRNA unless the cryptic splice site is masked by the steric blocking ON analogue. Relatively high concentrations were

* Corresponding author. Tel.: +33 4 67 16 33 03; fax: +33 4 67 16 33 01.
E-mail address: blebleu@univ-montp2.fr (B. Lebleu).

0168-3659/$ - see front matter © 2005 Elsevier B.V. All rights reserved.
doi:10.1016/j.jconrel.2005.10.026

used in these experiments and little has been documented in terms of cell uptake mechanism [8–10].

Interestingly PNA-oligolysine conjugates were reported to lead to splicing correction by a temperature-independent mechanism at variance with most recent data with cationized delivery vectors of nucleic acids [8].

The present study was aimed at re-evaluating the mechanism of uptake and the splicing correction efficiency of a $(Lys)_8$-PNA-Lys conjugate in this model. Lysosomotropic agents largely increased splicing correction efficiency in keeping with an endocytic mechanism of cellular uptake and entrapment within endocytic vesicles.

2. Experimental methods

2.1. Cells and cell culture

HeLa pLuc 705 cells were cultured as exponentially growing subconfluent monolayers in DMEM medium (Gibco) supplemented with 10% fetal calf serum, 1 mM sodium pyruvate and non essential amino-acids.

2.2. Synthesis of PNA 705, $(Lys)_8$-PNA-Lys, $(Lys)_8$-PNA-Lys (scrambled) and $(Lys)_8$-PNA-Lys (Fam)

These were synthesized by Fmoc chemistry on 5 μmol scale on an APEX 396 Robotic Peptide Synthesizer with a Fmoc-PAL-PEG-PS resin and Fmoc (Bhoc) PNA monomers purchased from Applied Biosystems (0.2 M dissolved in *N*-methylpyrollidone (NMP)). The activator was 0.2 M PyAOP (or PyBOP) in DMF, and a mixture of DIPEA and 2,6-lutidine to give a 0.4 M solution in DMF was used as the base solution (reagent mix A). Amino acid couplings were carried out with 0.2 M PyBOP in DMF and 0.4 M DIPEA (660 μl in 10 ml) in DMF (reagent mix B). The resin was washed 5× with DMF after each coupling. Fmoc deprotection was carried out with 20% piperidine in DMF (1 min, then 4 min), amino acid deprotection with 20% piperidine in DMF (3 then 12 min). After 5× washes with DMF, PNA was double coupled using reagent mix A and amino acids were double coupled using reagent mix B, each with a reaction time of 30 min per coupling. Fmoc-Lys(Boc) was used for the $(Lys)_8$ sequence and Fmoc-Lys(Mmt) for the residue for fluorescent labelling. After washing 5× with DMF, a capping step was carried out using 5% acetic anhydride, 6% 2,6-lutidine in DMF (2 × 5 min), followed by washing 5× with DMF. The N-terminal Fmoc group needs to be removed (as above) before final cleavage.

In the case of $(Lys)_8$-PNA-Lys(Mmt), the resin was washed with DCM and the Mmt group removed by treatment with 9 aliquots of 2% trifluoroacetic acid, 5% triisopropylsilane (TIS) in DCM (5 min incubation for every aliquot, 45 min in total). The resin was washed with 1 × DCM and 1 × DMF. To 6-carboxyfluorescein diacetate (6-CDFA, Sigma, 10 eq. relative to resin loading) dissolved in a minimal volume of NMP was added HOAt (10 eq.) dissolved in DMF and DIC (10 eq.), premixed for 10 min, and reacted with the resin for at least 16 h at room temperature, the resin washed thoroughly and then de-acetylated by treatment with 20% piperidine in DMF (as above).

The resin was treated with 95% TFA, 2.5% H_2O, 2.5% TIS with addition of 10% phenol as scavenger for a minimum of 90 min. PNAs were analysed and purified by RP-HPLC on a Phenomenex Jupiter C18 column (see below) with buffer A: 0.1% TFA in water, buffer B: 10% buffer A in acetonitrile and monitoring at 260 nm with a gradient of 10–50% B gradient over 30 min. MALDI-TOF mass spectrometry was carried out on a Voyager DE Pro BioSpectrometry workstation with a matrix of α-cyano-4-hydroxycinnamic acid, 10 mg ml^{-1} in acetonitrile–3% aqueous trifluoroacetic acid (1:1, *v*/*v*). The accuracy of the mass measurement is regarded as ±0.05%.

2.3. Flow cytometry

To analyse the internalization of fluorochrome-labeled $(Lys)_8$-PNA-Lys by FACS, exponentially growing HeLa pLuc705 cells were detached with nonenzymatic cell dissociation medium (Sigma). 3×10^5 cells were plated and cultured overnight on 30 mm plates. The cultured medium was discarded, and the cells were washed with PBS. PBS was discarded and the cells were incubated with 2 μM $(Lys)_8$-PNA-Lys (Fam). After different times of incubation at 37 °C in the presence of the fluorescent conjugate, the cells were washed twice with PBS, treated with Pronase (0.1%)/EDTA (1 mM) (5 min, 4 °C), resuspended in PBS 5% FCS, centrifuged at 900 ×*g* (5 min, 4 °C) and resuspended in PBS 0.5% FCS containing 0.05 μg/ml propidium iodide (PI) (Molecular Probes). Fluorescence analysis was performed with FACS fluorescence activated sorter (BD Bioscience). Cells stained with PI were excluded from further analysis. A minimum of 20,000 events per sample was analysed.

2.4. Fluorescence microscopy

Exponentially growing HeLa pLuc705 cells were dissociated with nonenzymatic cell dissociation medium, centrifuged at 900 ×*g* and resuspended in OptiMEM. 5×10^5 cells in 250 μl of OptiMEM were then incubated with 2 μM $(Lys)_8$-PNA-Lys (Fam). Cells were then treated with Pronase (0.1%)/EDTA (1 mM) and rinsed twice for 5 min with PBS. The distribution of fluorescence was analysed on a Zeiss Axiovert 200 M fluorescence microscope without fixation.

2.5. Splicing correction assay

To analyse splicing correction by free PNA or by $(Lys)_8$-PNA-Lys, exponentially growing HeLa pLuc705 cells were detached with nonenzymatic cell dissociation medium. 3.5×10^5 cells were plated and cultured overnight on 6 wells plates. The cultured medium was discarded, and the cells were washed with PBS. PBS was discarded and the cells were incubated for 4 h with free PNA or with $(Lys)_8$-PNA-Lys (diluted in OptiMEM at the appropriate concentration).Incubation was continued for 20 h in complete DMEM medium containing 10% FCS. Cells were washed twice with PBS and

lysed with the RLB Reporter lysis buffer (Promega). Luciferase activity was quantified using a Berthold Centro LB 960 luminometer. Total cellular protein concentrations were measured with BCA™ Protein Assay Kit (PIERCE, PERBIO) and read using ELISA plates reader Dynatech MR 5000 at a wavelength of 550 nm. Data were expressed as luciferase relative luminescence per microgram protein. All experiments were done in triplicate. Each data point was averaged over the three replicates.

2.6. RT-PCR

To confirm that the luciferase signal was indeed due to sequence-specific restoration of splicing by the conjugates $(Lys)_8$-PNA-Lys, cells were processed as indicated in Section 2.5. Total RNA was isolated from the cells using the High pure RNA isolation Kit (Roche Applied Science) and examined by RT-PCR (MJ Research PTC200 Peltier Thermal cycler). Forward (TTGATATGTGGATTTCGAGTCGTC) and reverse (TGTCAATCAGAGTGCTTTTGGCG) primers were used.

3. Results

Previous studies by Sazani et al. [8] have established that as little as four lysine residues appended to a PNA allowed improved cellular uptake and splicing correction in the splicing correction assay summarized in Fig. 1A. This assay makes use of HeLa pLuc 705 cells stably transfected with a construction (a generous gift from Dr. R. Kole) in which the coding sequence of a reporter (luciferase in our experiments) gene is interrupted by the mutated intron 2 from a thalassemia human β globin gene [11]. This intron carries a mutation which creates an aberrant splice site and prevents the normal processing of the chimeric pre mRNA. The hybridization of a steric-blocking antisense ON analogue (PNA 705 or 2'Omet ON with the sequence indicated in Fig. 1B) masks the cryptic splice site and redirects the splicing machinery towards complete intron 2 removal thereby allowing correct luciferase pre mRNA processing and luciferase expression (Fig. 1A).

In a recent comprehensive study by Siwkowski et al. [10], a $(Lys)_8$-PNA-Lys (Fam) construct was found optimal to redirect CD40 mRNA splicing in a murine B cell lyphoma cell line and in

A

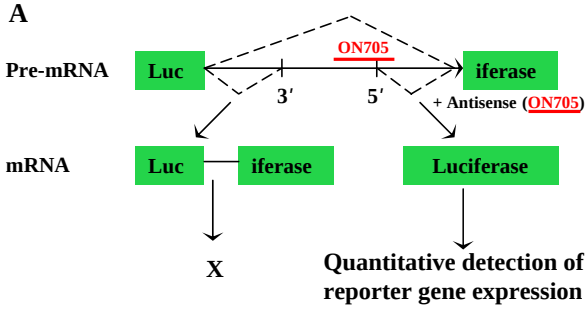

B

PNA 705: N terminal-CCT CCT ACC TCA GTT ACA-Lys
PNA 705 scrambled: N terminal-CCTGCT ATACCACTT ACA-Lys
2′OMet 705: 3′-CCT CCT ACC TCA GTT ACA-5′
2′OMet 705 scrambled: 3′-CCT GCT ATA CCA CTT ACA-5′

C

$(Lys)_8$-PNA-Lys(Fam) :
Lys-Lys-Lys-Lys-Lys-Lys-Lys-Lys-CCTCTTACCTCAGTTACA–Lys(ε-FAM)

$(Lys)_8$-PNA-Lys:
Lys-Lys-Lys-Lys-Lys-Lys-Lys-Lys-CCTCTTACCTCAGTTACA–Lys

$(Lys)_8$-PNA(Scr)-Lys:
Lys-Lys-Lys-Lys-Lys-Lys-Lys-Lys-CCTGTTATACCACTTACA-Lys

$(Lys)_8$-PNA(Scr)-Lys (Fam):
Lys-Lys-Lys-Lys-Lys-Lys-Lys-Lys-CCTGTTATACCACTTACA-Lys(ε-FAM)

Fig. 1. (A) Splicing correction assay: HeLa pLuc 705 cells were stably transfected with a construction in which the coding sequence of the luciferase gene is interrupted by a mutated intron 2 of the human β-globin gene. This mutation creates a 5′splice site and activates a 3′splice site. Masking of the 5′splice site by a RNase H-incompetent antisense ON (705) restores the production of functional luciferase mRNA and protein. (B) Sequences of ON 705 and scrambled controls: (C) Structures of $(Lys)_8$-PNA-Lys conjugates and fluorescent (Fam) derivatives.

primary murine macrophages. In line with increased efficiency in terms of splicing correction, these oligolysine-tailed PNAs were taken up more efficiently than free PNA-lys [10]. Little has been reported in terms of mechanism of cellular uptake for these oligolysine-tailed conjugates. Intriguingly however the efficiency of splicing correction in the Kole model by PNA-Lys_4 conjugates remained unchanged when the cells were incubated with the conjugates at 37 or at 4 °C [8] at variance with the data obtained with free PNA [12]. As pointed by the authors themselves, these results suggested an energy- and most probably endocytosis-independent mechanism of uptake for these positively charged PNAs.

3.1. Cellular uptake mechanism of $(Lys)_8$-PNA-Lys (Fam) conjugates

The uptake of $(Lys)_8$-PNA-Lys (Fam) (Fig. 1C) in HeLa pLuc cells was monitored by FACS analysis. Cells were treated with pronase at low temperature before FACS analysis to remove plasma membrane-associated material and to take into account cell internalized material only [13]. Propidium iodide (PI) uptake was monitored in parallel to assess cell permeabilisation. A concentration-dependant increase in $(Lys)_8$-PNA-Lys (Fam) cellular uptake has been observed (Fig. 2A).

Importantly however, a significant increase in PI uptake occurred when the cells were incubated at concentrations superior to 2 μM (Fig. 2B). Along the same line the monitoring of cell size distribution by FACS analysis indicated that significant alterations took place at high $(Lys)_8$-PNA-Lys concentrations (data not shown).

In order to gain insight into the mechanism of internalization of these conjugates, HeLa pLuc705 cells were incubated with the $(Lys)_8$-PNA-Lys (Fam) conjugate at 4 or at 37 °C for increasing period of times and cellular uptake was monitored by FACS analysis as above. As shown in Fig. 3A, the uptake of $(Lys)_8$-PNA-Lys (Fam) at low (2 μM) concentration is temperature- and time-dependent in keeping with an endocytic process.

A completely different behavior was observed when monitoring uptake at higher (5 or 10 μM) conjugate concentrations (Fig. 3B). Cellular uptake was much faster and was not affected by the incubation temperature in line with the observations reported by Sazani et al. [8] for PNA Lys_4 at 10 μM. Two different routes might therefore be used for the cellular internalization of Lys-tailed PNAs. At low concentration endocytosis prevails in keeping with most published data for free and CPP-conjugated PNAs [reviewed in 14]. At higher concentration, an energy-independent mechanism occurs possibly due to peptide-induced membrane permeabilization as also indicated by PI uptake (Fig. 3B) and by increased cell mortality (data not shown).

Further experiments were therefore performed with low (2 μM) concentrations of the conjugates.

3.2. Splicing correction by $(Lys)_8$-PNA-Lys conjugates

As already mentioned, the splicing correction assay described in Fig. 1A is considered as the most reliable to assess the effectiveness of oligonucleotide chemistries and/or delivery strategies [reviewed in [3]].

Splicing correction was monitored in terms of luciferase activity. Data were standardized per microgram of total cellular protein. The absence of significant alterations in total cellular proteins and the absence of PI uptake were taken as indicators of the absence of cytotoxicity of the PNA conjugates. A scrambled version of PNA 705 (Fig. 1B) was used to assess the sequence specificity of the antisense effect.

Free PNA Lys 705 led to a slight but concentration-dependent increase in luciferase activity (Fig. 4A) in keeping with the inefficient cellular uptake reported in previous studies. Surprisingly, however, splicing correction by the $(Lys)_8$-PNA-Lys conjugate was only slightly (although significantly) improved as compared to free PNA and still required high concentrations. Likewise, a $(Lys)_8$-PNA-Lys construct of appropriate sequence was found ineffective in a TAT/TAR

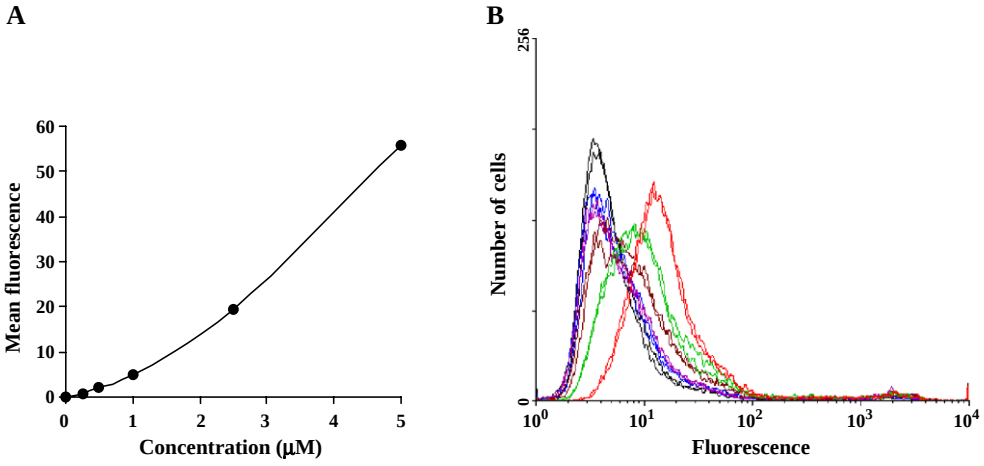

Fig. 2. FACS analysis of $(Lys)_8$ -PNA-Lys (Fam) uptake in HeLa pLuc 705 cells. (A) Cells were incubated with $(Lys)_8$-PNA-Lys (Fam) at the indicated concentrations for 2 h at 37 °C, and analysed by FACS. (B) FACS analysis of PI fluorescence in cells incubated alone (black curve) or in the presence of 250 nM (blue curve), 500 nM (brown curve), 1 μM (violet curve), 2.5 μM (green curve) or 5 μM (red curve) $(Lys)_8$-PNA-Lys (Fam) for 2 h at 37 °C. (For interpretation of the references to colour in this figure legend, the reader is referred to the web version of this article.)

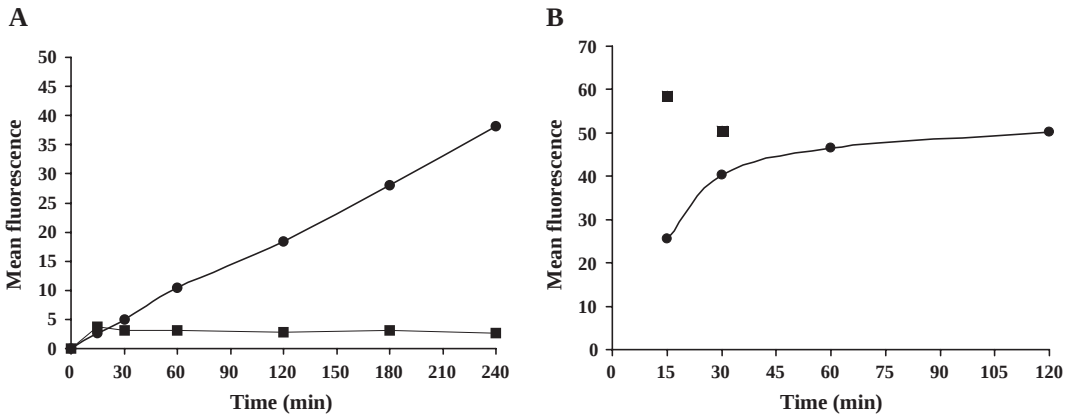

Fig. 3. FACS analysis of $(Lys)_8$-PNA-Lys (Fam) uptake as a function of temperature. (A) Cells were incubated with 2 μM $(Lys)_8$ -PNA-Lys (Fam) at 37 °C (●) or at 4 °C (■) for the indicated times. (B) Cells were incubated with 10μM $(Lys)_8$ -PNA-Lys (Fam) at 37 (●) or at 4 °C (■) for the indicated times. Cytotoxicity of the conjugate at this concentration precluded significant measurements at longer incubation times.

transactivation inhibition assay in a parallel study (Turner, J.J. et al., submitted).

As a point of comparison, negatively charged 2' O Met ON analogues (uncharged PNA cannot be delivered this way) were evaluated in the same assay using DLS cationic liposomes [15] as a delivery vector. As shown in Fig. 4B, a sequence-specific and much more efficient correction has been obtained. When drawn at the same scale luciferase expression with the oligolysine-tailed PNA cannot be distinguished from the background level.

3.3. Endosome disrupting agents increase the efficiency of splicing correction by $(Lys)_8$-PNA-Lys conjugates.

The low biological activity of $(Lys)_8$-PNA-Lys in the splicing correction assay could result from entrapment of the conjugates in endocytic compartments and/or from degradation by lysosomal enzymes (although the modified backbone of PNAs renders them rather resistant to proteases and nucleases).

In keeping with this hypothesis fluorescence microscopy analysis of live unfixed HeLa pLuc 705 cells incubated with $(Lys)_8$-PNA-Lys (Fam) (2 μM, 4 h, 37 °C) together with an Alexa546-tagged Transferrin marker (which is internalized by clathrin-coated pits endocytosis) reveals a characteristic cytoplasmic punctate distribution. Little if any $(Lys)_8$-PNA-Lys (Fam) staining could be detected in cell nuclei (Fig. 5).

The most commonly used pharmacological agent to promote increased delivery of drugs entrapped in endocytic compartments is chloroquine [16]. It has in particular been used in several studies to improve the functional delivery of plasmid DNA by non-viral vectors [17,18]. Chloroquine is a lysosomo-

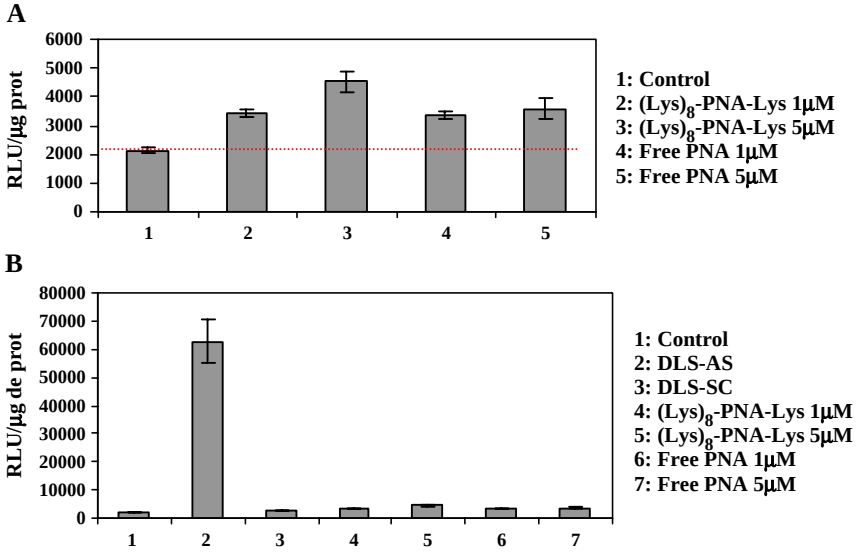

Fig. 4. Splicing corrections in the absence of chloroquine. (A) HeLa pLuc 705 cells were incubated in OptiMEM in the absence of correcting ON (1), in the presence of 1 (2) or 5 μM (3) $(Lys)_8$-PNA-Lys conjugate, or in the presence of 1 (4) or 5 μM (5) free PNA during 4 h. Luciferase expression was analysed 24 h later and expressed in RLU/μg protein. Each experiment was made in triplicate and error bars are indicated. (B) Comparison of the efficiency of splicing correction by $(Lys)_8$-PNA-Lys conjugate at 1 (4) or 5 μM (5) concentrations, by free PNA at 1 (6) or 5 μM (7), and by 2'OMet lipoplexes (30 nM) (2). Lane 1: untreated cells (control); Lane 3: Lipoplexes with a scrambled 2'OMet ON. Data are expressed in RLU/μg protein. Notice the different scales in panel (A) and panel (B).

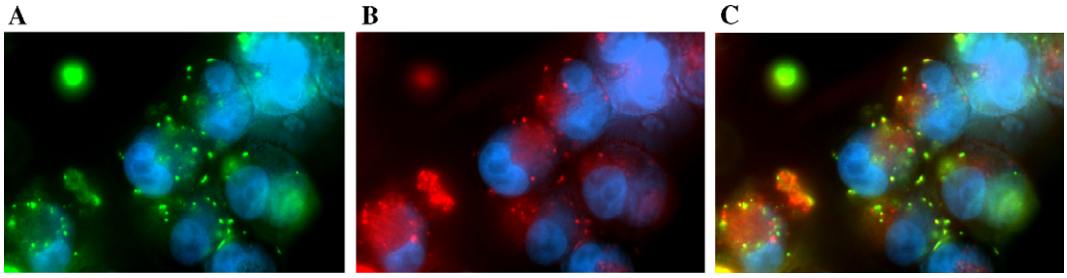

Fig. 5. Fluorescence microscopy images in unfixed HeLa pLuc 705 cells incubated with 2 μM Fam tagged (green fluorescence $(Lys)_8$-PNA-Lys (panel A) for 4 h and there after with Alaxa 546-tagged (red fluorescence) transferrin (panel B) for 5 min. Nuclei were stained with Hoechst (blue fluorescence) for 5 min. Co-localization was revealed in panel (C) (yellow staining). (For interpretation of the references to colour in this figure legend, the reader is referred to the web version of this article.)

tropic amine acting as a buffering agent and preventing endosome acidification. Chloroquine also slows down endocytosis thus leaving more time for endosome escape. Finally, preventing the acidification of endocytic compartments inhibits associated degradative activities.

Choroquine has been used at concentrations varying from 100 to 500 μM in various studies. In a first set of experiments we have evaluated a range of chloroquine concentrations extending from 50 to 200 μM on the splicing correction activity of $(Lys)_8$-PNA-Lys conjugates. No significant difference in splicing correction enhancement was observed between 100 and 200 μM chloroquine concentrations (data not shown). Cell mortality was however important after 24 h incubation of the cells with 200 μM chloroquine while no cell alteration occurred with 100 μM chloroquine as attested by fluorescence microscopy monitoring of PI uptake (data not shown). A protocol in which cells were co-incubated with the $(Lys)_8$-PNA-Lys conjugate and 100 μM chloroquine for 4 h has been used in further experiments.

As shown in Fig. 6A, chloroquine co-treatment very significantly increased splicing correction by $(Lys)_8$-PNA-Lys conjugates and correction reached comparable levels than with 2'OMet ON delivered with DLS lipoplexes. Chloroquine did not increase the efficiency of free PNA as expected since neutral PNAs are very poorly internalized [12]. The sequence-specificity of splicing correction was verified with a scrambled version of the $(Lys)_8$-PNA-Lys construct which does not lead to any significant luciferase activity even in the presence of chloroquine (Fig. 6B). Splicing correction by $(Lys)_8$-PNA-Lys in the presence of chloroquine was dose-dependent (Fig. 6B and data not shown) but relatively high concentrations (500 nM or more) of the conjugate were required to achieve a significant increase in luciferase activity even in the presence of chloroquine. Although it is difficult to compare steric blocking agents which differ in their chemistry, 2'OMet ON were active in the low (30 nM) nanomolar range when delivered with DLS lipoplexes (data not shown). On the other hand, correction by $(Lys)_8$-PNA-Lys conjugates was as efficient when the entire experiment was carried out in serum-containing culture medium (Fig. 6C) while DLS lipoplex delivery was strongly inhibited by serum proteins (data not shown) in keeping with previous studies with cationic lipid formulations [19].

Cell incubation in the presence of high sucrose concentration is an alternative strategy to promote endosome destabilization and to increase release of endosome-entrapped material [17]. Indeed sucrose accumulates in endocytic vesicles and leads to vesicles swelling [20]. As shown in Fig. 6D, co-incubation with 0.5 M sucrose largely increased luciferase expression in $(Lys)_8$-PNA-Lys treated cells but not in cells treated with the scrambled version of the conjugate.

Although agents acting by different mechanisms (chloroquine and sucrose treatment) promoted endosome destabilization and lead to increased splicing correction by $(Lys)_8$-PNA-Lys, we could not exclude possible effects on cellular uptake. We therefore incubated the cells with the $(Lys)_8$-PNA-Lys conjugate for 4 h in the absence of chloroquine, replaced the cell culture medium and then added chloroquine for 1 or 4 h. As seen in Fig. 7A, chloroquine did not have to be co-incubated with the $(Lys)_8$-PNA-Lys conjugate to promote splicing correction. These data do strongly suggest that chloroquine is not increasing cellular uptake but favors release from endocytic compartments. Along the same lines, chloroquine (Fig. 7B) or sucrose (Fig. 7C) did not increase the cellular uptake of fluorescein-tagged $(Lys)_8$-PNA-Lys (Fam) whether added simultaneously or after the conjugate.

In order to confirm that the increased luciferase activity in chloroquine treated cells was due to splicing correction, RNAs were analysed by RT-PCR using a set of primers allowing the amplification of both correctly spliced and aberrant luciferase mRNAs. As shown in Fig. 8, chloroquine treatment is required to achieve significant splicing correction by the $(Lys)_8$-PNA-Lys conjugate and the antisense effect is sequence-specific.

4. Discussion

This manuscript essentially aimed at gaining insight into the mechanism of cellular uptake of oligolysine-tailed PNA [8–10] which appeared as an elegant and simple strategy to improve the pharmacological properties of neutral steric-blocking ON as PNAs. One could indeed expect increased cellular uptake as amply demonstrated for steric-blocking PMO and PNA conjugated to basic amino-acids-rich CPPs [7,21]. Moreover the stable conjugation of a positively-charged tail to a PNA should lead to accelerated hybridization rate and increased affinity for a complementary RNA sequence [22].

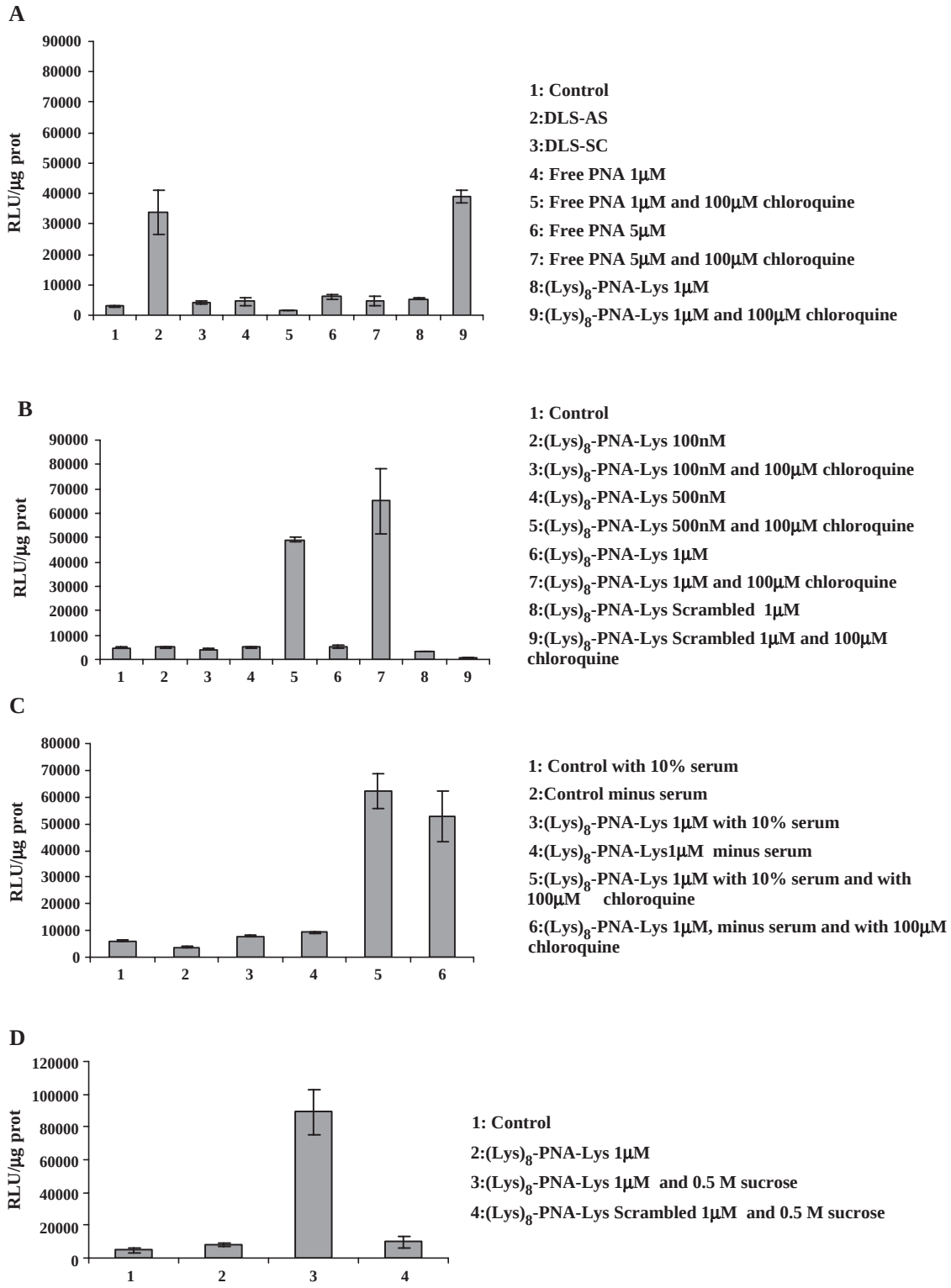

Fig. 6. Effect of chloroquine on splicing correction by $(Lys)_8$-PNA-Lys conjugate. (A) HeLa pLuc 705 were incubated in the absence of correcting ON (1), in the presence of antisense (2) or scrambled (3) 2'OMet delivered as lipoplexes, in the presence of 1 μM free PNA without (4) or with (5) chloroquine (100 μM), in the presence of 5 μM free PNA without (6) or with (7) chloroquine (100 μM), or in the presence of 1 μM $(Lys)_8$-PNA-Lys without (8) or with (9) chloroquine (100 μM). Data are expressed in RLU/μg protein. Experiments have been made in triplicate and averaged. Error bars are indicated. (B) Concentration dependence and specificity of splicing correction. Cells were incubated with (3, 5, 7) or without (2, 4, 6, 8) chloroquine (100 μM) and $(Lys)_8$-PNA-Lys conjugate at 100 nM (2, 3), 500 nM (4, 5) or 1 μM (6, 7), or with 1 μM of the scrambled version of the conjugate (8, 9). Control in with no addition (1). Data are expressed as in panel (A). (C) Effect of serum on splicing correction. Cells were incubated in serum (10% FCS) containing (1, 3, 5) or in serum free (2, 4, 6) media without any addition (1, 2), with 1 μM $(Lys)_8$-PNA-Lys (3, 4) or with 1 μM $(Lys)_8$-PNA-Lys and 100 μM chloroquine (5, 6) for 4 h. Data are expressed as in panel (A). (D) Effect of sucrose on splicing correction. Cells were incubated in OptiMEM in the absence of correcting ON (1), in the presence of 1 μM $(Lys)_8$-PNA-Lys without (2) or with (3) 0.5 M sucrose, or in the presence of scrambled version of the conjugate and 0.5 M sucrose (4).

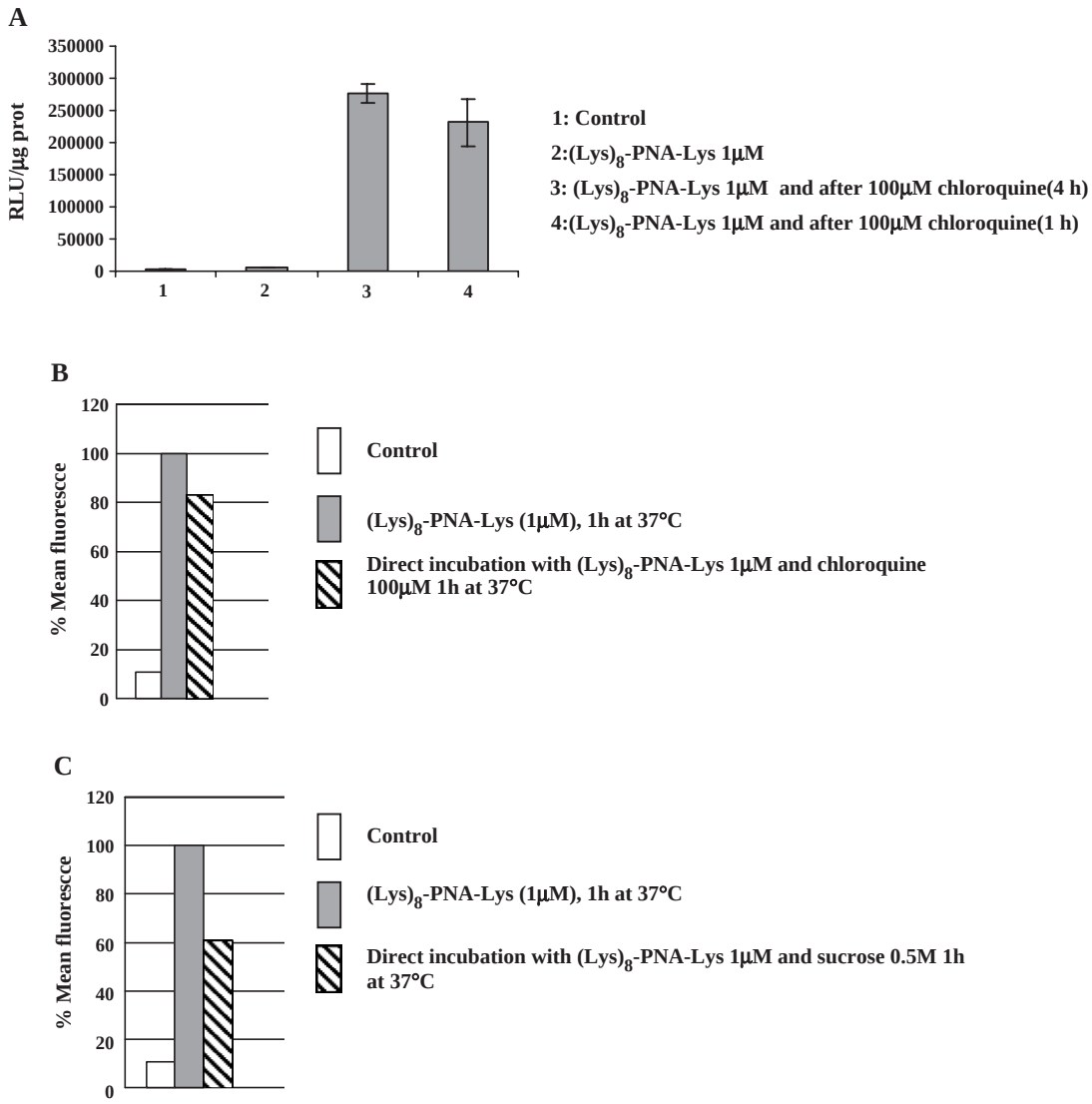

Fig. 7. Chloroquine treatment does not increase $(Lys)_8$-PNA-Lys cell uptake. (A) Sequential addition of $(Lys)_8$-PNA-Lys and chloroquine increases splicing correction. HeLa pLuc 705 cells were incubated in the absence of correcting ON (1), or in the presence of 1 μM $(Lys)_8$-PNA-Lys (2) for 4 h. In 3 and 4, cells were incubated with 1 μM $(Lys)_8$-PNA-Lys for 4 h, cells were then washed and incubated for 1 (4) or 4 h (3) with 100 μM chloroquine. Cells were then washed and incubated with fresh medium. Luciferase assays were performed after 24 h total incubation. Data are expressed in RLU/μg protein. (B) FACS analysis of $(Lys)_8$-PNA-Lys (Fam) uptake without (■) or with (▧) 1 μM chloroquine for 1 h at 37 °C. untreated cells (□). (C) FACS analysis of $(Lys)_8$-PNA-Lys (Fam) uptake without (■) or with (▧) 0.5 M sucrose for 1 h at 37 °C. untreated cells (□).

In a first series of papers with an assay closely related to the present one, Sazani et al. [8,9] established that PNA oligomers appended at their C-termini with a $(Lys)_4$ tail were taken up more efficiently than free PNA (PNA-Lys). The calculated EC50 for splicing correction was not dramatically improved however since it was decreased from 4.7 μM for the free PNA to 2.1 μM for the PNA Lys_4 conjugate [8]. Intriguingly the positively charged PNA $(Lys)_4$ was taken up by a temperature independent mechanism in contrast to the endocytic mechanism of uptake described for free PNAs [12], as well as with recent data on Tat CPP-conjugated PNAs [23]. In a recent study, Siwkowski et al. [10] evaluated CD 40 antigen splicing redirection by a series of conjugates in which oligolysine tails of increased lengths were appended to the N-terminal end of a PNA steric-blocking ON. The eight-lysine PNA conjugate was the most efficient inhibitor of CD40 expression in this assay with an EC_{50} in the 1–2 μM range. No insight into the mechanism of uptake was provided except for an improved cellular uptake as compared to free PNA.

We have chosen to re-evaluate the mechanism of cellular uptake and the efficacy of splicing correction of $(Lys)_8$-PNA-Lys conjugate in the Kole model [11]. It indeed provides a positive read out while the CD 40 redirection model [10] leads to an inhibition of CD40 expression. FACS analysis of $(Lys)_8$-PNA-Lys (Fam) uptake at increasing concentrations did reveal that these conjugates could alter cellular permeability at high concentration as evidenced by propidium iodide staining. This

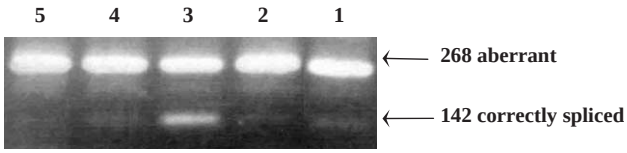

1: Control

2: $(Lys)_8$-PNA-Lys 1 μM

3: $(Lys)_8$-PNA-Lys 1 μM (4h) + 100 μM chloroquine (4h)

4: $(Lys)_8$-PNA-Lys Scrambled 1 μM

5: $(Lys)_8$-PNA-Lys Scrambled 1 μM (4h) + 100 μM chloroquine (4h)

Fig. 8. RT-PCR detection of splicing correction by $(Lys)_8$-PNA-Lys: effect of chloroquine and sequence specificity. HeLa pLuc 705 cells were untreated (1), incubated 4 h with 1 μM $(Lys)_8$-PNA-Lys without (2) or with (3) 100 μM chloroquine, or incubated 4 h with 1 μM of scrambled conjugate version without (4) or with (5) chloroquine. RT-PCR detection of splicing correction as described in Experimental methods. The upper band corresponds to the aberrantly spliced luciferase mRNA and lower band to the correctly spliced mRNA.

could possibly be responsible for the seemingly temperature-independent mechanism of uptake reported by Sazani et al. [8]. They indeed evaluated temperature dependence of the PNA$(Lys)_4$ conjugates uptake at concentration (10 μM) for which we also found evidence for a fast and temperature-independent cell internalization process. The two sets of experiments have however been performed with different conjugates (Lys_4 at the C-terminus or Lys_8 at the N-terminus) and cannot be strictly compared. In any case we have focused on experimental conditions (e.g. conjugate concentration 2 μM) in which cellular uptake was strictly temperature-dependent and did not cause any significant cell permeabilisation as judged by PI uptake.

Splicing correction data in terms of luciferase expression were rather disappointing where compared to the RLU values recorded with lipoplex-delivered 2'OMet ON of identical sequence. Again differences in ON chemistries do not allow a direct comparison but 2'OMet ON should be less efficient than PNAs in binding RNA except at high salt concentration (e.g. binding of the TAR element) [24]. Whatever the case there was an apparent contradiction between the increased uptake of the $(Lys)_8$-PNA-Lys conjugates and their very modest splicing correction efficiency in our experimental conditions in an otherwise highly sensitive assay. Along the same lines PNA conjugated to a $(Lys)_8$ tail or to various CPPs were inefficient in a HIV-1 Tat-dependent *trans*-activation assay [27].

As already mentioned, the initial view of a direct membrane translocation of CPP-conjugated biomolecules has recently been challenged [23]. It is now generally accepted that at least basic amino acid-rich CPPs and their conjugated biomolecules are taken up by endocytosis. As an example, Tat PNA conjugates are taken up by endocytosis and accumulate in endocytic vesicles [23]. Entrapment within these compartments and cargo degradation by associated nucleases and proteases could therefore limit the efficiency of CPP-based delivery strategy, as known for plasmid DNA delivery by non-viral vectors. In keeping with this hypothesis, it has recently been shown that endosome destabilization by lysosomotropic agents or by fusogenic peptides enhanced the functional delivery of Cre recombinase-Tat fusion proteins [25,26]. Our experiments clearly establish that sucrose or chloroquine treatment very significantly increases splicing correction by $(Lys)_8$-PNA-Lys in a sequence-specific way, in line with the well-established endosome-destabilizing activity of these two different pharmacological agents. Importantly, sucrose or chloroquine increased luciferase expression similarly whether co-incubated with the $(Lys)_8$-PNA-Lys conjugate or added after conjugate removal. On the other hand, decreased (and not increased) $(Lys)_8$-PNA-Lys (Fam) uptake was monitored by FACS upon incubation with chloroquine or sucrose treatment.

Likewise chloroquine treatment significantly enhanced the inhibition of HIV-1 Tat-dependent *trans*-activation in a HeLa cell assay involving stably integrated plasmids for several PNA-peptide conjugates composed of a PNA 16-mer either stably polyether linked or disulfide linked to a cell-penetrating peptide [27].

Interestingly not all tested peptide conjugates were found to be efficient in the HIV-1 Tat dependent *trans*-activation assay and the $(Lys)_8$-PNA-Lys construction in particular was inactive even in the presence of chloroquine. This is not contradictory with the data reported here since the luciferase splice correction assay is very sensitive and probably more so than the Tat-dependent *trans*-activation assay where a substantial decrease in reporter luciferase expression is needed for activity to be observed. Small amounts of $(Lys)_8$-PNA-Lys released from endocytic vesicles upon chloroquine (or sucrose) treatment might conceivably be sufficient to correct luciferase splicing while inefficient to compete out Tat binding to the TAR element in the *trans*-activation assay. In keeping with this hypothesis, splicing correction in chloroquine-treated cells is still partial as shown in the RT-PCR analysis of luciferase gene transcripts. Moreover, chloroquine treatment does not lead to a significant redistribution of $(Lys)_8$-PNA-Lys as shown by fluorescence microscopy in our experiments (data not shown) and in parallel experiments on the Tat-dependent *trans*-activation model [27]. In contrast, chloroquine treatment led to a significant cytoplasmic and nuclear release of Tat conjugated PNA [27].

Future directions will include the screening of various peptidic constructions and/or fusogenic elements in this reliable and sensitive splicing correction assay, searching for optimal cellular uptake end endosomal release of the conjugated steric blocking ON.

Acknowledgements

We thank John Turner and Andrey Arzumanov (Cambridge) for helpful discussions and Sarah Resina for producing 2'OMet lipoplex formulation. This work was funded by grants from the EC framework 5 (contract QLK3-CT-2002-01989) and from IFCPAR (contract 3205-A). Saïd Abes is the recipient of pre-doctoral fellowship from the Ligue contre le Cancer. We thank Dr. R. Kole for the generous gift of the HeLa pLuc 705 cell line.

References

[1] M.A. Garcia-Blanco, A.P. Baraniak, E.L. Lasda, Alternative splicing in disease and therapy, Nat. Biotechnol. 22 (5) (2004) 535–546.

[2] N.F. Olivieri, The beta-thalassemias, N. Engl. J. Med. 341 (2) (1999) 99–109.

[3] R. Kole, M. Vacek, T. Williams, Modification of alternative splicing by antisense therapeutics, Oligonucleotides 14 (1) (2004) 65–74.

[4] J. Summerton, Morpholino antisense oligomers: the case for an RNase H-independent structural type, Biochim. Biophys. Acta. 1489 (1) (1999) 141–158.

[5] L. Bastide, B. Lebleu, I. Robbins, Modulation of nucleic acid information processing by PNAs: potential use in anti-viral therapeutics, Lett. Pept. Sci. 10 (2004) 149–159.

[6] A. Astriab-Fisher, D. Sergueev, M. Fisher, B.R. Shaw, R.L. Juliano, Conjugates of antisense oligonucleotides with the Tat and antennapedia cell-penetrating peptides: effects on cellular uptake, binding to target sequences, and biologic actions, Pharm. Res. 19 (6) (2002) 744–754.

[7] H.M. Moulton, M.C. Hase, K.M. Smith, P.L. Iversen, HIV Tat peptide enhances cellular delivery of antisense morpholino oligomers, Antisense Nucleic Acid Drug Dev. 13 (2003) 31–43.

[8] P. Sazani, S.H. Kang, M.A. Maier, C. Wei, J. Dillman, J. Summerton, M. Manoharan, R. Kole, Nuclear antisense effects of neutral, anionic and cationic oligonucleotide analogs, Nucleic Acids Res. 29 (19) (2001) 3965–3974.

[9] P. Sazani, F. Gimignani, S.H. Kang, M.A. Maier, M. Manoharan, M. Persmark, D. Bortner, R. Kole, Systemically delivered antisense oligomers upregulate gene expression in mouse tissues, Nat. Biotechnol. 20 (12) (2002) 1228–1233.

[10] A.M. Siwkowski, L. Malik, C.C. Esau, M. Maier, E.V. Wancewicz, K. Albertshofer, B.P. Monia, C.F. Bennett, A.B. Eldrup, Identification and functional validation of PNAs that inhibit murine CD40 expression by redirection of splicing, Nucleic Acids Res. 32 (9) (2004) 2695–2706.

[11] S.H. Kang, M.J. Cho, R. Kole, Up-regulation of luciferase gene expression with antisense oligonucleotides: implications and applications in functional assay development, Biochemistry 37 (1998) 6235–6239.

[12] U. Koppelhus, S.K. Awasthi, V. Zachar, H.U. Holst, P. Ebbeson, P.E. Nielsen, Cell-dependant differential cellular uptake of PNA, peptides and PNA-peptide conjugates, Antisense Nucleic Acid Drug Dev. 12 (2002) 51–63.

[13] J.P. Richard, K. Melikov, H. Brooks, P. Prevot, B. Lebleu, L.V. ChernomordiK, Cellular uptake of unconjugated TAT peptide involves clathrin-dependent endocytosis and heparan sulfate receptors, J. Biol. Chem. 280 (15) (2005) 5300–5306.

[14] A.R. Thierry, E. Vives, J.P. Richard, P. Prevot, C. Martinand-Marie, I. Robbins, B. Lebleu, Cellular uptake and intracellular fate of antisense oligonucleotides, Curr. Opin. Mol. Ther. 5 (2) (2003) 133–138.

[15] C. Lavigne, Y. Lunardi-Iskandar, B. Lebleu, A.R. Thierry, Cationic liposomes/lipids for oligonucleotide delivery, Methods Enzymol. 387 (2004) 189–212.

[16] V. Ferrari, D.J. Cutler, Kinetics and thermodynamics of chloroquine and hydroxychloroquine transport across the human erythrocyte membrane, Biochem. Pharmacol. 41 (1991) 23–30.

[17] K. Ciftci, R.J. Levy, Enhanced plasmid DNA transfection with lysosomotropic agents in cultured fibroblasts, Int. J. Pharm. 218 (2001) 81–92.

[18] D.S. Manickam, H.S. Bisht, L. Wan, G. Mao, D. Oupicky, Influence of TAT-peptide polymerization on properties and transfection activity of TAT/DNA polyplexes, J. Control. Release 102 (2005) 293–306.

[19] O. Zelphati, L.S. Uyechi, L.G. Barron, F.C. Szoka Jr., Effect of serum components on the physico-chemical properties of cationic lipid/oligonucleotide complexes and on their interaction with cells, Biochim. Biophys. Acta 1390 (1998) 119–133.

[20] T. Kato, S. Okada, T. Yutaka, H. Yabuuchi, The effects of sucrose loading on lysosomal hydrolases, Mol. Cell. Biochem. 60 (1) (1984) 83–98.

[21] P. Järver, Ü. Langel, The use of cell-penetrating peptides as a tool for gene regulation, Drug Discov. Today 9 (2004) 395–402.

[22] D.R. Corey, 48000-fold acceleration of hybridization by chemically modified oligonucleotides, J. Am. Chem. Soc. 117 (36) (1995) 9373–9374.

[23] J.P. Richard, K. Melikov, E. Vives, E. Ramos, B. Verbeure, M.J. Gait, L.V. Chernomordik, B. Lebleu, Cell-penetrating peptides. A reevaluation of the mechanism of cellular uptake, J. Biol. Chem. 278 (1) (2003) 585–590.

[24] A. Arzumanov, A.P. Walsh, V.K. Rajwanshi, R. Kumar, J. Wengel, M.J. Gait, Inhibition of HIV-1 Tat-dependent trans activation by steric block chimeric 2′-*O*-methyl/LNA oligoribonucleotides, Biochemistry 40 (2001) 14645–14654.

[25] N.J. Caron, S.P. Quenneville, J.P. Tremblay, Endosome disruption enhances the functional nuclear delivery of Tat-fusion proteins, Biochem. Biophys. Res. Commun. 319 (2004) 12–20.

[26] J.S. Wadia, R.V. Stan, S.F. Dowdy, Transducible TAT-HA fusogenic peptide enhances escape of TAT-fusion proteins after lipid raft macropinocytosis, Nat. Med. 10 (3) (2004) 310–315.

[27] J. Turner, G.D. Ivanova, B. Verbeure, D. Williams, A.A. Arzumanov, S. Abes, B. Lebleu, M.J. Gait, Cell-penetrating peptide conjugates of peptide nucleic acids (PNA) as inhibitors of HIV-1 Tat-dependent trans-activation in cells, Nucleic Acids Res. 33 (21) (2005) 6837–6849.

Structural Requirements for Cellular Uptake and Antisense Activity of Peptide Nucleic Acids Conjugated with Various Peptides†

Yvonne Wolf,*,‡ Stephan Pritz,‡ Saïd Abes,§ Michael Bienert,‡ Bernard Lebleu,§ and Johannes Oehlke‡

Leibniz-Institute of Molecular Pharmacology, Robert-Rössle-Strasse 10, D-13125 Berlin, Germany, and UMR 5124 CNRS, Université Montpellier 2, Place Eugène Bataillon, 34095 Montpellier, France

Received April 10, 2006; Revised Manuscript Received October 6, 2006

ABSTRACT: Peptide nucleic acids (PNAs) have shown great promise as potential antisense drugs; however, poor cellular delivery limits their applications. Improved delivery into mammalian cells and enhanced biological activity of PNAs have been achieved by coupling to cell-penetrating peptides (CPPs). Structural requirements for the shuttling ability of these peptides as well as structural properties of the conjugates such as the linker type and peptide position remained controversial, so far. In the present study an 18mer PNA targeted to the cryptic splice site of a mutated β-globin intron 2, which had been inserted into a luciferase reporter gene coding sequence, was coupled to various peptides. As the peptide lead we used the cell-penetrating α-helical amphipathic peptide KLAL KLAL KAL KAAL KLA-NH_2 [model amphipathic peptide (MAP)] which was varied with respect to charge and structure-forming properties. Furthermore, the linkage and the localization of the attached peptide (C- vs N-terminal) were modified. Positive charge as well as helicity and amphipathicity of the KLA peptide was all required for efficient dose-dependent correction of aberrant splicing. The highest antisense effect was reached within 4 h without any transfection agent. Stably linked conjugates were also efficient in correction of aberrant splicing, suggesting that a cleavable disulfide bond between CPP and PNA is clearly not essential. Moreover, the placement of the attached peptide turned out to be crucial for attaining antisense activity. Coadministration of endosome disrupting agents such as chloroquine or Ca^{2+} significantly increased the splicing correction efficiency of some conjugates, indicating the predominant portion to be sequestered in vesicular compartments.

Peptide nucleic acids (PNAs)[1] have shown great promise as potential antisense drugs since they are potent and metabolically stable RNA- and DNA-binding ligands (*1*). However, cellular delivery remains a limitation as for most nucleic acid-based strategies (*2*). Moreover, uncharged PNAs cannot straightforward be administered by cationic vectors such as polyethylenimine (PEI) or cationic lipids. Complexation with cationic lipids and a DNA carrier is efficient but complicates the approach (*3*). Recently discovered cell-penetrating peptides (CPPs) have gained a lot of attention because of their ability to cross cellular membranes and to transport conjugated cargos, thus possessing great potential for drug delivery (for recent reviews, see refs *4* and *5*). Even though the mechanism of translocation of CPPs is not fully understood yet, a number of promising studies have been published showing enhanced cellular delivery of CPP conjugated with various types of cargo (reviewed in refs *6* and *7*). PNAs covalently attached to simple cationic sequences such as lysine residues have been shown to enter cultured cells efficiently and to affect splicing (*8*−*11*) as well as inhibit gene expression (*12*). Moreover, synthetic peptides such as transportan or model amphipathic peptide (MAP) promoted an enhanced biological activity of PNAs targeted to various intracellular sites (*13*, *14*). Because of the high diversity of these peptides, the structural requirements for the shuttling ability of CPPs are controversial. Additionally, available data may be influenced by the methodology applied for the determination of internalization. CPP−cargo internalization should be evaluated by a reliable biological assay, allowing unequivocal evidence about the delivery of the transported oligonucleotide to its intracellular site of action. Our current study addresses the important question of how the structural properties of PNA−peptide conjugates such as the type of peptide, its placement, and the type of linkage relate to its ability to attain antisense activity evaluated by the splicing-correction assay developed by Kole et al. (*15*). This assay is considered as the most reliable for evaluating

† This work was supported by the European Commission framework 5 (QLK3-CT-2002−01989).

* To whom correspondence should be addressed. Telephone: +49-30-94793240. Fax: +49-30-94793159. E-mail: wolf@fmp-berlin.de.

‡ Leibniz-Institute of Molecular Pharmacology.

§ UMR 5124 CNRS, Université Montpellier 2.

[1] Abbreviations: AEEA, o-linker, 2-[2-(Fmoc-amino)ethoxy]ethoxyacetic acid; CLSM, confocal laser scanning microscopy; CPP, cell-penetrating peptide; DAPI, 4′,6-diamidino-2-phenylindole; DIC, 1,3-diisopropylcarbodiimide; DIPEA, *N*,*N*-diisopropylethylamine; DMEM, Dulbecco's modified Eagle's medium; DMF, *N*,*N*-dimethylformamide; FAM, 5-carboxyfluorescein; FCS, fetal calf serum; Fmoc, *N*-(9-fluorenylmethoxycarbonyl); HATU, *N*-[(dimethylamino)-1*H*-1,2,3-triazolo[4,5-*b*]pyridin-1-ylmethylene]-*N*-methylmethanaminium hexafluorophosphate *N*-oxide; HBTU, *N*-[(1*H*-benzotriazol-1-yl)(dimethylamino)methylene]-*N*-methylmethanaminium hexafluorophosphate *N*-oxide; HOBt, 1-hydroxybenzotriazole; MAP, model amphipathic peptide, KLAL KLAL KAL KAAL KLA-NH_2; MTT, 3-(4,5-dimethylthiazol-2-yl)-2,5-diphenyltetrazolium bromide; NMP, *N*-methylpyrrolidone; PNA, peptide nucleic acid; TCEP, tris(2-carboxyethyl)phosphine; TFA, trifluoroacetic acid; RLU, relative luminescence units.

10.1021/bi0606896 CCC: $33.50
Published on Web 11/18/2006

Table 1: Sequences of PNAs and Peptides Used for Conjugation

	sequence[a]	structural properties[b] and charge
PNA	Ac-C-ooo-cct ctt acc tca gtt aca-ooo-NH_2[c]	
	Ac-ooo-cct ctt acc tca gtt aca-ooo-LPKTGGR-NH_2[d]	
	FAM-ooo-cct ctt acc tca gtt aca-ooo-LPKTGGR-NH_2[d]	
	H-GGG-ooo-cct ctt acc tca gtt aca-ooo-NH_2[d]	
PNA scr	Ac-ooo-tcc ttc cca act ttg aca-ooo-LPKTGGR-NH_2[d]	
	H-GGG-ooo-tcc ttc cca act ttg aca-ooo-NH_2[d]	
KLA	Dns-GC-KLAL KLAL KAL KAAL KLA-NH_2[c]	amphipathic, α-helical, 5+
	H-KLAL KLAL KAL KAAL KLA LPKTGGR-NH_2[d]	
	H-GGG KLAL KLAL KAL KAAL KLA-NH_2[d]	
KGL	Dns-GC-KGLK LKGG LGL LGKL KLG-NH_2[c]	unstructured, 5+
	H-KGLK LKGG LGL LGKL KLG LPKTGGR-NH_2[d]	
KAL	Dns-GC-KALK LKAA LAL LAKL KLA-NH_2[c]	nonamphipathic, α-helical, 5+
	H-KALK LKAA LAL LAKL KLA LPKTGGR-NH_2[d]	
ELA	Dns-GC-ELAL ELAL EAL EAAL ELA-NH_2[c]	amphipathic, α-helical, 5−
	H-ELAL ELAL EAL EAAL ELA LPKTGGR-NH_2[d]	
	H-GGG ELAL ELAL EAL EAAL ELA-NH_2[d]	
RLA	Dns-GC-RLAL RLAL RAL RAAL RLA-NH_2[c]	amphipathic, α-helical, 5+
	H-RLAL RLAL RAL RAAL RLA LPKTGGR-NH_2[d]	
Pen	Dns-GC-RQI KIW FQN RRM KWK K-NH_2[c]	poor α-helical amphipathic, 7+
	H-RQI KIW FQN RRM KWK KLPKTGGR-NH_2[d]	
	H-GGG RQI KIW FQN RRM KWK K-NH_2[d]	

[a] Key: lower case letters = PNA bases; upper case letters = amino acids; Dns = dansyl; FAM = 5-carboxyfluorescein; o = ethylene glycol spacer. [b] According to CD measurements in 50% trifluoroethanol (TFE) in water (*46*). [c] Used for disulfide coupling. [d] Used for sortase-mediated ligation.

the nuclear delivery of steric blocking oligonucleotide analogues since it is a positive read-out assay and only the appearance of a specific oligonucleotide within the nucleus of a viable cell will allow correct splicing. In brief, the coding sequence of a luciferase reporter gene is interrupted by a mutated β-globin intron 2 (IVS2−705) carrying a cryptic splice site. This mutation causes aberrant splicing of luciferase pre-mRNA and therefore prevents translation of luciferase. However, masking the cryptic splice site by steric blocking oligonucleotide analogues induces correct splicing, restoring luciferase expression. In the present study an 18mer PNA (cct ctt acc tca gtt aca) targeted to the cryptic splice site was covalently attached to various peptides. As the peptide lead, we used the cell-penetrating α-helical amphipathic peptide KLAL KLAL KAL KAAL KLA-NH_2, also known as model amphipathic peptide (MAP) (*16*, *17*), which was varied with respect to structure-forming properties and charge (Table 1). Additionally, we investigated the well-known cell-penetrating peptide penetratin (*18*). As the conjugation approach, disulfide coupling was performed, which is a commonly used method for the assembly of peptide−cargo conjugates. The disulfide bond is thought to be cleaved rapidly once within the reducing environment of the cell. However, it is not yet clear whether the use of biolabile bonds such as a disulfide bridge offers advantages or may be essential for attaining antisense activity. Therefore, a series of conjugates with stable linkages was synthesized by a sortase-mediated ligation approach (*19*). Moreover, the localization of the peptide (C- vs N-terminal) was modified since influences of the attached peptide on the biological activity of oligonucleotide conjugates have been occasionally reported (*20*, *21*). In order to contribute to the elucidation of the mechanism of internalization, we also investigated the influence of the known lysosomotropic agent chloroquine (*22*, *23*) as well as Ca^{2+} (*24*, *25*) on the ability of the conjugates to correct aberrant splicing.

EXPERIMENTAL PROCEDURES

General. Chemicals and reagents were purchased from Sigma (Deisenhof, Germany) or Bachem (Heidelberg, Germany) unless specified otherwise.

Synthesis of PNAs, Peptides, and PNA−Peptide Conjugates. (A) PNA and Peptide Solid-Phase Synthesis. PNAs were synthesized manually by Fmoc [*N*-(9-fluorenylmethoxycarbonyl)] chemistry (*26*, *27*). Fmoc (Bhoc) PNA monomers were purchased from Applied Biosystems and used at 0.5 M dissolved in *N*-methylpyrrolidone (NMP). Before and after PNA assembly six AEEA spacers [o-linker, 2-[2-(Fmoc-amino)ethoxy]ethoxyacetic acid; Fluka], three at the C-terminus and three at the N-terminus, were coupled to a TentaGel S RAM resin (0.22 mmol/g; Rapp) in the same manner as the PNA monomers. For the sortase-mediated ligation (*19*) either a LPKTGGR motif or a triglycine had to be inserted before or after PNA assembly, respectively (sequences of the PNAs are shown in Table 1). The amino groups were deprotected by 20% piperidine in *N*,*N*-dimethylformamide (DMF) for 6 min. After five washes with DMF the monomers were coupled to the resin by *N*-[(dimethylamino)-1*H*-1,2,3-triazolo[4,5-*b*]pyridin-1-ylmethylene]-*N*-methylmethanaminium hexafluorophosphate *N*-oxide (HATU, 0.45 M) in DMF and 5 equiv of *N*,*N*-diisopropylethylamine (DIPEA) and *sym*-collidine (2,4,6-trimethylpyridine) for 20 min. A double coupling was performed. The resin was washed five times with DMF after each coupling step. A capping step followed using 4% acetic anhydride and 4% DIPEA in DMF. Then the resin was split into two portions. To one portion a Cys (StBu) residue was attached at the N-terminus for disulfide coupling; to the other portion a triglycine was coupled for the sortase-mediated ligation. In order to obtain 5-carboxyfluorescein- (FAM-) labeled PNAs, the Fmoc-deprotected resin was treated with 5 equiv of 5-carboxyfluorescein (FAM), 1-hydroxybenzotriazole (HOBt, 5 equiv), and 1,3-diisopropylcarbodiimide (DIC, 4.8 equiv) in DMF for at least 24 h. The coupling of FAM was repeated

twice. The N-terminal Fmoc group was removed before final cleavage. Finally, the product was cleaved from the resin by 20% *m*-cresol in trifluoroacetic acid (TFA). PNAs were purified and analyzed by RP-HPLC on a PolyEncap A300 column with eluent A, 0.1% TFA in water, and eluent B, 80% acetonitrile in 0.1% TFA (gradient: 5−95% B in 45 min), and monitoring at 260 nm. MALDI-TOF mass spectrometry was performed on a Voyager DE STR workstation using a matrix of α-cyanohydroxycinnamic acid (5 mg/mL) in 60% acetonitrile/0.3% TFA and provided the expected $[M + H]^+$. The sequences of the PNAs are shown in Table 1.

Peptides were synthesized automatically on a 433A peptide synthesizer (Applied Biosystems) by the solid-phase method using standard Fmoc chemistry. Syntheses were carried out on TentaGel S RAM resin (0.22 mmol/g; Rapp) using N^{α}-Fmoc-protected amino acid derivatives (5 equiv, 0.5 M) and *N*-[(1*H*-benzotriazol-1-yl)(dimethylamino)methylene]-*N*-methylmethanaminium hexafluorophosphate *N*-oxide (HBTU, 4.9 equiv, 0.5 M) as coupling reagent in the presence of DIPEA (10 equiv, 2.0 M) in DMF. Double couplings for 20 min were allowed to proceed; N-terminal deblocking was carried out twice with 20% piperidine in DMF for 5 min. All washes were made with DMF. Final cleavage from the resin and deprotection of side chain functionalities were achieved by a mixture of 5% phenol, 2% triisopropylsilane, and 5% water in TFA for 2 h. Purification and characterization were carried out as described for PNAs. For the sortase-mediated ligation peptide sequences were elongated with either a LPKTGGR motif or a triglycine at the C- or N-terminus, respectively. Peptides used were either KLA, also known as model amphipathic peptide (MAP), which is a positively charged, α-helical amphipathic peptide, ELA, wherein the lysine residues are replaced by glutamic acid, KGL, which is an unstructured peptide moiety, KAL, an nonamphipathic analogue of KLA, RLA, which is even more basic than KLA due to the replacement of the lysine residues by arginines, or penetratin. The sequences of all synthesized peptides are shown in Table 1.

(B) Assembly of the Disulfide-Linked PNA−Peptide Conjugates. (1) Activation of the PNA with 2,2′-Dithiodipyridine. To remove the protecting group (StBu) from the cysteine residue to a solution of PNA (sequence is shown in Table 1; 1 mg dissolved in 200 μL of ammonium bicarbonate buffer, pH 9.0), 250 μL of β-mercaptoethanol was added, and the reaction mixture was left to stand for 1 h at room temperature. Then the PNA was precipitated with ether. To the precipitate, isolated by centrifugation, was added a solution of tris(2-carboxyethyl)phosphine (TCEP, 0.5 mg/mL in ammonium acetate buffer, pH 7.0) to cleave probably generated PNA dimers into monomers. The reaction mixture was kept for 30 min at 50 °C. Next, a solution of 2,2′-dithiodipyridine (10 mg/mL in ammonium acetate buffer, pH 7.0) was added, and the reaction mixture was left to stand for 3 h at 50 °C. The product was precipitated with ether and dissolved in ammonium acetate buffer, pH 7.0.

(2) Formation of the Disulfide Bond. To a solution of 10 nmol of the activated PNA in ammonium acetate buffer (pH 7.0) was added a 5-fold excess of the peptide. In the case of the MAP-derived peptides (KLA, RLA, ELA) acetonitrile (1:1 v/v) had to be added to the reaction mixture to prevent precipitation. The reaction mixture was kept for 30−45 min at 50 °C. Purification and analysis of the conjugates were carried out on an analytical PolyEncap C18 column (heated at 50 °C) using a gradient of 5−95% eluent B in 45 min (eluent A, 0.1% TFA in water; eluent B, 80% acetonitrile in 0.1% TFA). Detection was performed at 260 and 220 nm, respectively. The lyophilized products were dissolved in 0.1% TFA and stored in the freezer. MALDI-TOF mass spectrometry was performed on a Voyager DE STR workstation using a matrix of α-cyanohydroxycinnamic acid (5 mg/mL) in 60% acetonitrile/0.3% TFA and provided the expected $[M + H]^+$.

(C) Assembly of PNA−Peptide Conjugates with Stable Linkages. The syntheses of the stably linked PNA−peptide conjugates were carried out using a sortase-mediated ligation strategy (*19*). The detailed procedure will be reported elsewhere (S. Pritz, in preparation). In brief, ligations were carried out in aqueous buffered solutions containing 50 mM Tris-HCl, 150 mM NaCl, and 5 mM $CaCl_2$ at pH 7.5. Solutions (600 μL) containing 1.66 mM CPP, 0.33 mM PNA, and 6 μM sortase were dialyzed against 1 L of the aqueous buffer (mentioned above) for 24 h at ambient temperature through a membrane with a molecular mass cutoff of 2000 Da. Purification of these conjugates was carried out on a semipreparative PolyEncap C18 column (heated at 50 °C) using a gradient of 10−80% eluent B in 70 min (eluent A, 0.1% TFA in water; eluent B, 80% acetonitrile in 0.1% TFA; flow rate, 4 mL/min) and monitoring at 220 nm. The appropriate fractions were lyophilized and analyzed by analytical HPLC and MALDI-TOF mass spectrometry as described above. Conjugates of KLA with a scrambled sequence of the PNA (KLA−PNA scr and PNA−KLA scr, respectively) were synthesized to assess the sequence specificity of the antisense effect. For the synthesis of FAM-labeled PNA conjugates with KLA, ELA, and penetratin, a PNA labeled with 5-carboxyfluorescein (FAM) at the N-terminus was used to enable fluorescence microscopy studies.

Cell Culture. HeLa pLuc 705 cells were cultured in Dulbecco's modified Eagle's medium (DMEM) containing 4.5 g/L glucose (Gibco) supplemented with 10% (v/v) fetal calf serum (FCS) and 1% (v/v) nonessential amino acids in a humidified atmosphere containing 5% CO_2.

Splicing Correction Assay. For assessing the splicing correction, HeLa pLuc 705 cells were plated in 96-well plates at a density of 2×10^4 cells per well and cultured overnight. The culture medium was discarded, and the cells were washed twice with PBS. The cells were incubated for 4 h either with the naked PNA or with the PNA−peptide conjugates at various concentrations diluted in OptiMEM. Incubation was continued for another 20 h in DMEM containing 10% FCS. For chloroquine and Ca^{2+} experiments conjugates were prepared at 1 μM in OptiMEM containing 100 μM chloroquine and 6 mM $CaCl_2$, respectively, and added to the cells for 4 h incubation. After the cells were washed, incubation was continued for another 20 h in DMEM/10% FCS. In the case of chloroquine and Ca^{2+} treatment the growth medium was supplemented with 100 μM chloroquine or 6 mM $CaCl_2$, respectively. After 24 h cells were washed twice with PBS and lysed with the reporter lysis buffer (Promega). The plates were stored at −80 °C for at least 4 h to ensure complete lysis. Luciferase activity was quantified by using the luciferase assay system from Promega and measuring the luminescence by a GENios Pro

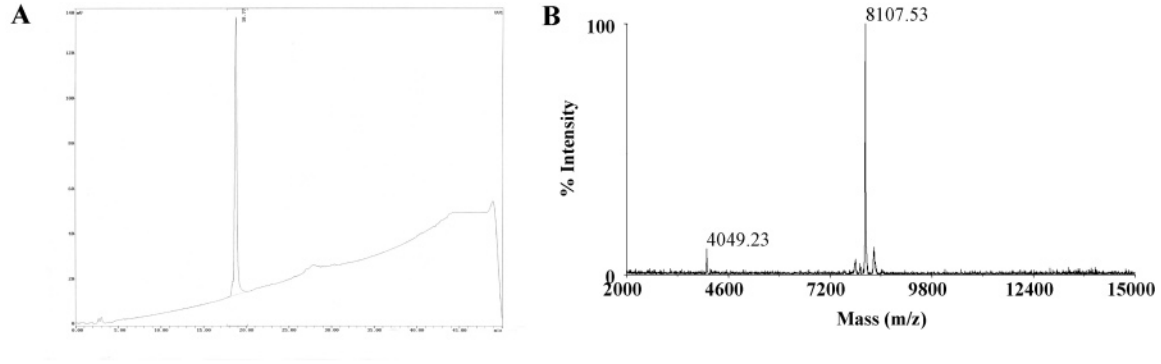

C

conjugate	sequence	mw calculated	mw found
KLA-PNA	H-KLAL KLAL KAL KAAL KLA LPKTGGG ooo-cct ctt acc tca gtt aca-ooo-NH_2	8106.7	8107.5
PNA-KLA	Ac-ooo-cct ctt acc tca gtt aca-ooo-LPKTGGG KLAL KLAL KAL KAAL KLA-NH_2	8148.7	8150.6
FAM-PNA-KLA	FAM-ooo-cct ctt acc tca gtt aca-ooo-LPKTGGG KLAL KLAL KAL KAAL KLA-NH_2	8464.9	8472.9
KLA-PNA scr	H-KLAL KLAL KAL KAAL KLA LPKTGGG ooo-tcc ttc cca act ttg aca-ooo-NH_2	8106.7	8104.3
PNA-KLA scr	Ac-ooo-tcc ttc cca act ttg aca-ooo-LPKTGGG KLAL KLAL KAL KAAL KLA-NH_2	8148.7	8149.6
KGL-PNA	H-KGLK LKGG LGL LGKL KLG LPKTGGG ooo-cct ctt acc tca gtt aca-ooo-NH_2	8022.5	8026.0
KAL-PNA	H-KALK LKAA LAL LAKL KLA LPKTGGG ooo-cct ctt acc tca gtt aca-ooo-NH_2	8106.7	8107.0
ELA-PNA	H-ELAL ELAL EAL EAAL ELA LPKTGGG ooo-cct ctt acc tca gtt aca-ooo-NH_2	8111.4	8112.7
PNA-ELA	Ac-ooo-cct ctt acc tca gtt aca-ooo-LPKTGGG ELAL ELAL EAL EAAL ELA-NH_2	8153.4	8155.1
FAM-PNA-ELA	FAM-ooo-cct ctt acc tca gtt aca-ooo-LPKTGGG ELAL ELAL EAL EAAL ELA-NH_2	8469.7	8475.4
RLA-PNA	H-RLAL RLAL RAL RAAL RLA LPKTGGG ooo-cct ctt acc tca gtt aca-ooo-NH_2	8246.7	8253.3
Pen-PNA	H-RQI KIW FQN RRM KWK KLPKTGGG ooo-cct ctt acc tca gtt aca-ooo-NH_2	8475.9	8471.7
PNA-Pen	Ac-ooo-cct ctt acc tca gtt aca-ooo-LPKTGGG RQI KIW FQN RRM KWK K-NH_2	8518.0	8515.7
FAM-PNA-Pen	FAM-ooo-cct ctt acc tca gtt aca-ooo-LPKTGGG RQI KIW FQN RRM KWK K-NH_2	8834.2	8835.6

FIGURE 1: Analytical data of the stably linked conjugates. HPLC chromatogram (A) and MALDI-TOF mass spectrum (B) of KLA−PNA. (C) Calculated and found molecular masses of all stably linked conjugates.

luminometer (Tecan). Total cellular protein quantities were measured by Bradford protein assay according to the manufacturer's protocol and read using a Safire plate reader (Tecan) at a wavelength of 595 nm. Data were expressed as relative luminescence units (RLU) per microgram of protein. Each data point is the average of the three replicates. Cell viability was assessed using the MTT [3-(4,5-dimethylthiazol-2-yl)-2,5-diphenyltetrazolium bromide] assay.

Confocal Laser Scanning Microscopy Studies. For confocal microscopy studies HeLa pLuc 705 cells (10^5/well) were plated on coverslips and cultured in growth medium overnight. The medium was discarded, and the cells were washed with PBS followed by incubation with the conjugates at 1 μM in 500 μL of OptiMEM for 4 h. In the case of chloroquine or Ca^{2+} treatment the incubation solution was supplemented with either 100 μM chloroquine or 6 mM Ca^{2+}. Then the cells were washed two times with PBS and cultured for another 20 h in DMEM/10% FCS, in the case of chloroquine or Ca^{2+} treatment supplemented with 100 μM chloroquine or 6 mM Ca^{2+}, respectively. CLSM measurement was performed using a LSM 510 invert confocal laser scanning microscope (Carl Zeiss Jena GmbH, Jena, Germany; software, LSM 510 META image examiner, version 3.2, Carl Zeiss Jena GmbH, Jena, Germany). Nuclei were stained with 1 μg/mL DAPI (4′,6-diamidino-2-phenylindole; Sigma-Aldrich, Germany) (*28*). Subsequent to the observation, the viability of the cells was assessed by Trypan Blue staining. Excitation was performed at 488 nm (FAM), 345 nm (DAPI), and 543 nm (Trypan Blue), and emission was measured at 515, 455, and 570 nm, respectively.

RESULTS

Synthesis of Disulfide and Stably Linked PNA−Peptide Conjugates. PNA−peptide conjugates were designed to test the influence of the attached peptides on the antisense activity and cellular uptake of PNAs. The PNA sequence (shown in Table 1) was flanked by three ethylene glycol spacers (o-linker) at each side to increase solubility and minimize aggregation of the PNA−peptide conjugates. The sequences of the PNA−peptide conjugates synthesized by the sortase-mediated ligation approach are shown in Figure 1 (panel C). These conjugates carry a LPKTGGG motif between the peptide and the PNA which was required for the enzyme (sortase) recognition. Panels A and B of Figure 1 show a

A

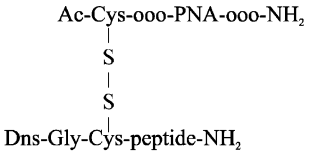

B

conjugate	mw calculated	mw found
PNA-SS-KLA	8049.6	8053.4
PNA-SS-KGL	7965.5	7961.9
PNA-SS-KAL	8049.6	8049.6
PNA-SS-ELA	8054.4	8050.5
PNA-SS-RLA	8189.7	8195.9
PNA-SS-Pen	8418.9	8415.5

FIGURE 2: Analytical data of the disulfide-linked conjugates. (A) Structure of disulfide-linked conjugates. The linkage is in all cases between the N-terminus of the PNA and the N-terminus of the peptides. (B) Calculated and found molecular masses of all disulfide-linked conjugates.

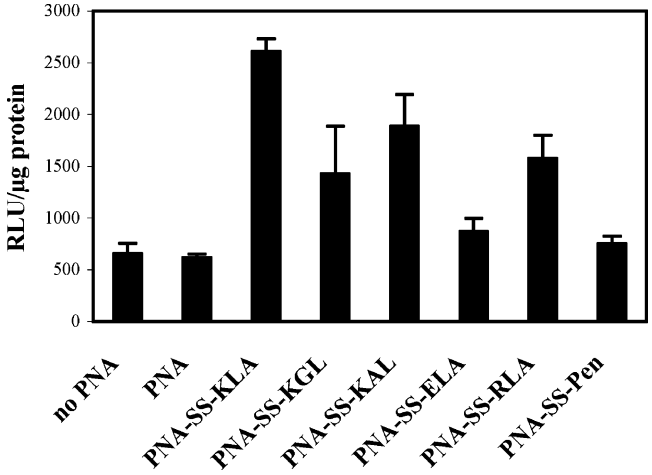

FIGURE 3: Splicing correction of the disulfide-linked PNA−peptide conjugates. HeLa pLuc 705 cells were incubated in OptiMEM in the absence of PNA (no PNA) or in the presence of 1 μM naked PNA or various disulfide-linked PNA−peptide conjugates for 4 h. Luciferase expression was analyzed 24 h later and expressed in relative luminescence units (RLU)/μg of protein. Each experiment was done in triplicate, and error bars are indicated.

HPLC chromatogram and a mass spectrum of the stably linked KLA−PNA conjugate. In all cases purity was >95%. MALDI-TOF mass spectrometry provided the correct mass for all conjugates (Figure 1, panel C).

The structure of the disulfide-bridged conjugates is displayed in Figure 2 (panel A); in each case the Cys residue is located at the N-terminus of the peptide. Precipitation of the MAP-derived peptide conjugates was reduced by adding acetonitrile to the reaction mixture and heating it at 50 °C. Purification of the disulfide-linked conjugates was also carried out by reverse-phase HPLC, and characterization was performed by MALDI-TOF mass spectrometry, providing the correct mass for the conjugates (Figure 2, panel B).

Helicity, Amphipathicity, and Positive Charge of the Peptides Attached to the PNA Are Requested for Promoting an Efficient Splicing Correction. We investigated the ability of the PNA−peptide constructs in correction of aberrant splicing using HeLa pLuc 705 cells which carry a mutated luciferase gene (*15*). As shown in Figure 3 in the case of the unconjugated PNA there was no significant increase of luciferase luminescence. Conjugation of the PNA with the cationic, α-helical amphipathic peptide KLA via a disulfide bond (PNA−SS−KLA) led at 1 μM to a 5-fold enhanced

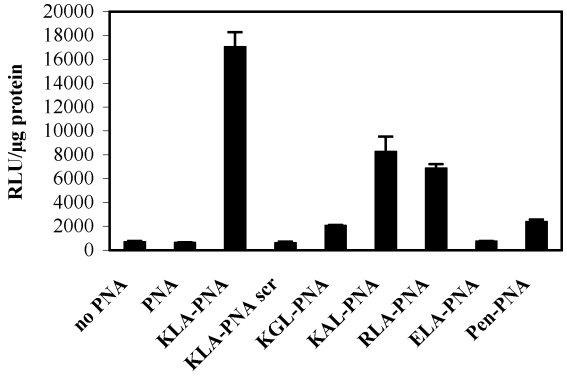

FIGURE 4: Splicing correction of the stably linked PNA−peptide conjugates. HeLa pLuc 705 cells were incubated in OptiMEM in the absence of PNA (no PNA) or in the presence of 1 μM naked PNA or various stably linked PNA−peptide conjugates for 4 h. Luciferase expression was analyzed 24 h later and expressed in relative luminescence units (RLU)/μg of protein. Each experiment was done in triplicate, and error bars are indicated.

biological activity compared to the naked PNA. The corresponding unstructured KGL (PNA−SS−KGL) and nonamphipathic KAL (PNA−SS−KAL) constructs were less effective (2.3-fold and 3-fold, respectively) in correction of splicing than KLA. For PNAs conjugated to the negatively charged ELA (PNA−SS−ELA) wherein the lysine residues have been replaced by glutamic acid and surprisingly for PNA attached to the well-known cell-penetrating peptide penetratin (PNA−SS−Pen), no activity could be observed. It has been repeatedly reported that peptides containing arginine residues are better taken up by cells (*29*−*31*) and thus are more potent than lysine analogues (*32*). Therefore, we also tested a PNA conjugate with a KLA analogue wherein the lysine residues have been replaced by arginines (PNA−SS−RLA). Interestingly, this modification did not lead to a higher antisense effect than the lysine derivative.

A Cleavable Disulfide Bond, Allowing the Release of the PNA Oligomer, Is Not Required To Restore Aberrant Splicing. Next, we addressed the issue whether a linker as a disulfide bridge, which is expected to be cleaved rapidly once within the reducing environment of the cell, is advantageous or essential for achieving antisense activity. Interestingly, as shown in Figure 4 the stable conjugates were also effective in correction of splicing, suggesting a cleavable disulfide bridge not to be essential for attaining antisense activity. For the stably linked conjugates derived from the MAP peptide moiety a similar pattern to that obtained for the disulfide-linked conjugates was found. Highest luciferase activity was observed for the PNA conjugated with KLA (KLA−PNA), possessing cationic as well as α-helical amphipathic properties, followed by those with the nonamphipathic KAL (KAL−PNA) and highly basic RLA peptides (RLA−PNA). The constructs with the unstructured KGL (KGL−PNA) and penetratin (Pen−PNA), respectively, showed a slightly enhanced antisense activity. No effect was observed for the negatively charged ELA−PNA. The sequence specificity of the effect was ascertained by the inactivity of a conjugate of KLA with a scrambled PNA sequence (KLA−PNA scr). In order to find out whether the LPKTGGG motif, which was required for the synthesis of the stably linked conjugates by the sortase-mediated ligation approach, has an influence on cellular uptake and antisense activity, a stably linked KLA−PNA conjugate (H-KLALKLALKALKAALKLAoooc-

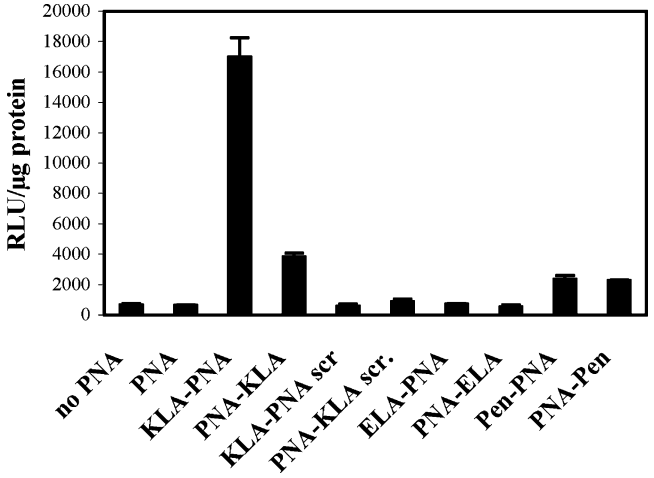

FIGURE 5: Influence of the position of the peptide attached to the PNA on the splicing correction of the conjugates. HeLa pLuc 705 cells were incubated in OptiMEM in the absence of PNA (no PNA) or in the presence of 1 μM naked PNA or various stably linked PNA−peptide conjugates for 4 h. Luciferase expression was analyzed 24 h later and expressed in relative luminescence units (RLU)/μg of protein. Each experiment was done in triplicate, and error bars are indicated.

ctcttacctcagttacaooo-NH_2) lacking this motif was synthesized by straightforward solid-phase synthesis. Antisense activity of this conjugate in Kole's splicing-correction assay was found to be comparable with the KLA−PNA construct carrying the LPKTGGG sequence (data not shown). Moreover, the six ethylene glycol spacers (o-linker) which were inserted to increase solubility and minimize aggregation did not influence the biological activity since a KLA−PNA conjugate (H-KLALKLALKALKAALKLAcctcttacctcagttaca-NH_2) showed similar correction of aberrant splicing as the one used in this study containing six o-spacers (data not shown).

The Position of the Peptide Attached to the PNA Influences the Antisense Efficiency of the Conjugates. Considering the orientation of the peptide attached to the PNA (C- vs N-terminal), the conjugate bearing the KLA peptide moiety at the C-terminus of the PNA (PNA−KLA) was much less effective in splicing correction than the analogue coupled to the N-terminus of the PNA (KLA−PNA) as shown in Figure 5. In case of the penetratin conjugates Pen−PNA (coupled to the N-terminus of the PNA) and PNA−Pen (attached to the C-terminus), no significant difference in antisense activity could be observed. The negatively charged ELA peptide, no matter if attached to the N- or C-terminus of the PNA, did not promote any antisense activity of the PNA. The scrambled PNAs conjugated to KLA (KLA−PNA scr, PNA−KLA scr) did not show any biological activity, confirming the sequence specificity of the obtained effects. These results clearly demonstrate that a cleavable disulfide bond between CPP and PNA is not essential for biological activity. However, the orientation of the coupling (C- vs N-terminal) seems to have an impact on achieving activity. As shown in Figures 6 and 7, respectively, the ability of the KLA conjugates (PNA−SS−KLA, KLA−PNA, and PNA−KLA) to correct aberrant splicing exhibited a strong dependence on the incubation concentration and time. The naked PNA did not show any activity up to 2.5 μM. The antisense effect of KGL and KAL conjugates was only slightly enhanced at higher concentrations (up to 2.5 μM) (data not

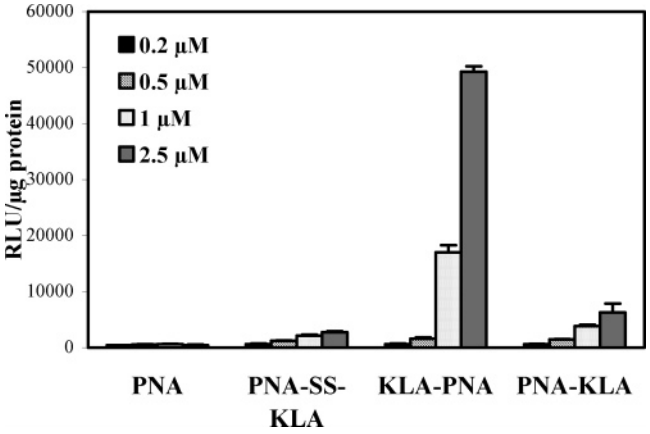

FIGURE 6: Concentration dependence of splicing correction. HeLa pLuc 705 cells were incubated in OptiMEM with 0.2 (black bars), 0.5 (striped bars), 1 (dotted bars), or 2.5 μM (gray bars) naked PNA or various PNA−KLA conjugates (PNA−SS−KLA, KLA−PNA, and PNA−KLA, respectively) for 4 h. Data are expressed in relative luminescence units (RLU)/μg of protein.

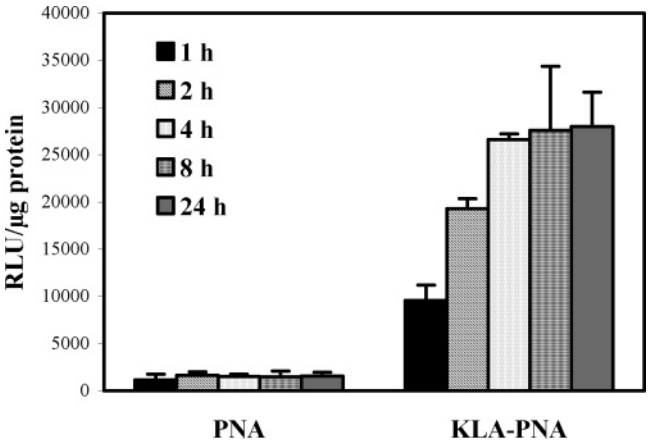

FIGURE 7: Time−course experiment. Splicing correction of 1 μM naked PNA or KLA−PNA incubated for 1, 2, 4, 8, or 24 h, respectively, with HeLa pLuc 705 cells. Luciferase expression was analyzed 24 h later and expressed in relative luminescence units (RLU)/μg of protein.

shown). One should note that MAP-derived PNA conjugates showed rather high cytotoxicity at higher concentrations (20% cell viability at 4 μM; data not shown) assessed by the MTT assay. The maximum of luciferase activity of the stable KLA−PNA construct was reached within 4 h, the time point at which the set of data in Figures 3−6 and 8 was taken. There was no significant increase in luciferase activity after incubating the cells for 8 and 24 h, respectively. We also tested the influence of serum on the splicing correction. The presence of serum had no impact on the splicing activity (data not shown).

The Antisense Effect of the Conjugates Is Enhanced by Lysosomotropic Agents. It has been repeatedly reported that agents, known to mediate a release from endosomes, could significantly enhance the antisense activity of oligonucleotide− and PNA−CPP conjugates (*11*, *33*). The most commonly used pharmacological agent for such purpose is chloroquine (*22*, *23*). Similar effects were observed after addition of 6 mM Ca^{2+} (*24*, *32*). In order to gain insight into the mechanism of the delivery of PNA−peptide conjugates used in this study, we also investigated the antisense activity in the presence of chloroquine (100 μM)

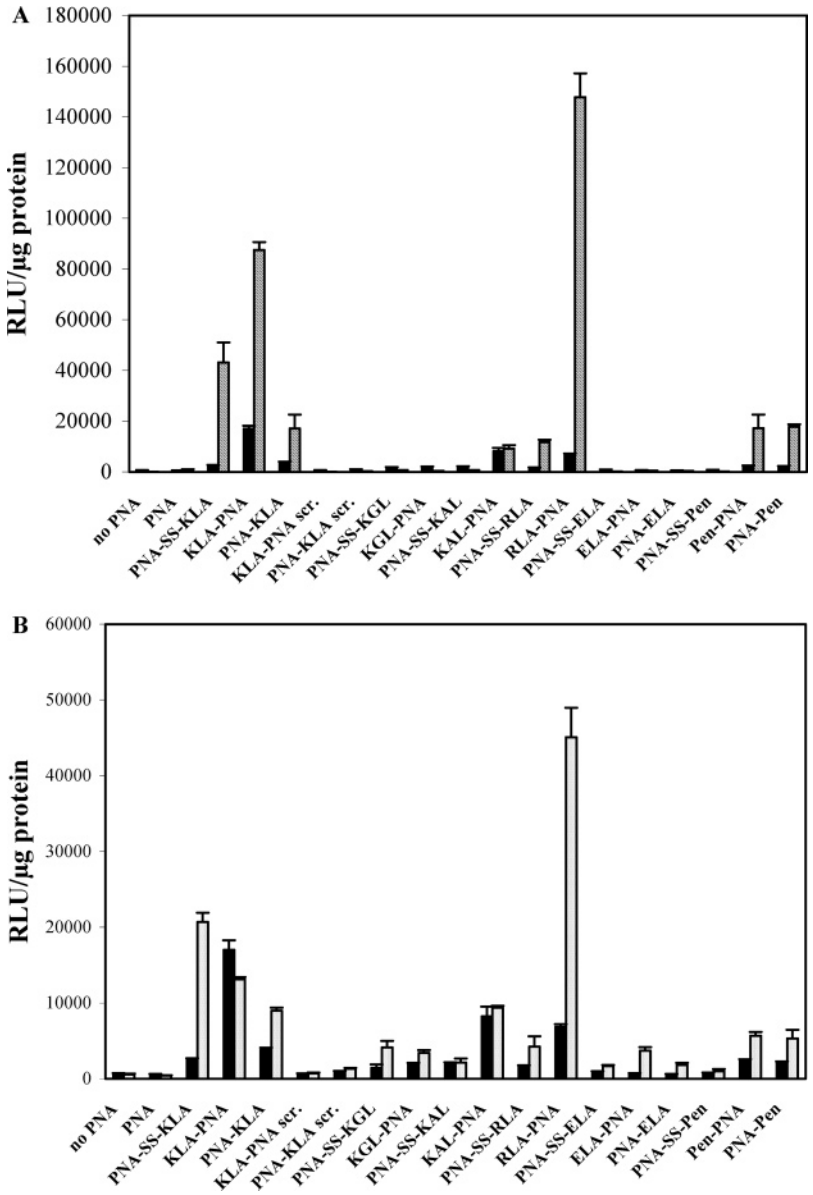

FIGURE 8: Effect of lysosomotropic agents on the splicing correction of the conjugates. (A) Chloroquine treatment. HeLa pLuc 705 cells were incubated in the absence of PNA (no PNA) or in the presence of 1 μM naked PNA and various PNA−peptide conjugates without (black bars) or with 100 μM chloroquine (striped bars) for 4 h. Cells were then grown in DMEM/10% FCS, in the case of chloroquine treatment containing 100 μM chloroquine, for a further 20 h. Data are expressed in relative luminescence units (RLU)/μg of protein. Experiments have been done in triplicate. Error bars are indicated. (B) Ca^{2+} treatment. HeLa pLuc 705 cells were incubated in the absence of PNA (no PNA) or in the presence of 1 μM naked PNA and various PNA−peptide conjugates without (black bars) or with 6 mM $CaCl_2$ (dotted bars) for 4 h. Cells were then grown in DMEM/10% FCS, in case of calcium treatment supplemented with 6 mM $CaCl_2$, for 20 h. Data are expressed in relative luminescence units (RLU)/μg of protein. Error bars are indicated.

and Ca^{2+} (6 mM). In a first set of experiments 100 μM chloroquine was coadministered with the conjugates and has been left on the cells for 4 h. No significant difference in splicing correction could be observed (data not shown). However, when chloroquine (100 μM) has been supplemented to the medium containing 10% FCS as a posttreatment and left in total on the cells for 24 h, tremendous effects became apparent for the amphipathic KLA peptide disulfide-linked to the PNA (PNA−SS−KLA) and stably linked at the N-terminus of the PNA (KLA−PNA) (47- and 96-fold, respectively, related to the naked PNA) (Figure 8, panel A). An even greater enhancement (162-fold) was found for the RLA−PNA, the arginine analogue of KLA. The stably linked conjugates of penetratin (Pen−PNA and PNA−Pen) as well as PNA−KLA revealed only slightly enhanced antisense activities. No significant enhancement in biological activity was observed for the naked PNA and conjugates with other peptides such as KGL, ELA, and KAL. Coadministration of chloroquine had no influence on the sequence specificity since scrambled PNAs attached to KLA (KLA−PNA scr, PNA−KLA scr) remained ineffective in splicing correction. Moreover, chloroquine treatment did not affect the cell viability assessed by the MTT test (data not shown). These data infer a rather huge amount at least of some conjugates (PNA−SS−KLA, KLA−PNA, and RLA−PNA) to be sequestered in vesicular compartments.

A slightly different pattern to that obtained with chloroquine treatment could be observed after co-incubation with 6 mM Ca^{2+} (Figure 8, panel B). A great enhancement of the biological effect was seen again for the stably linked

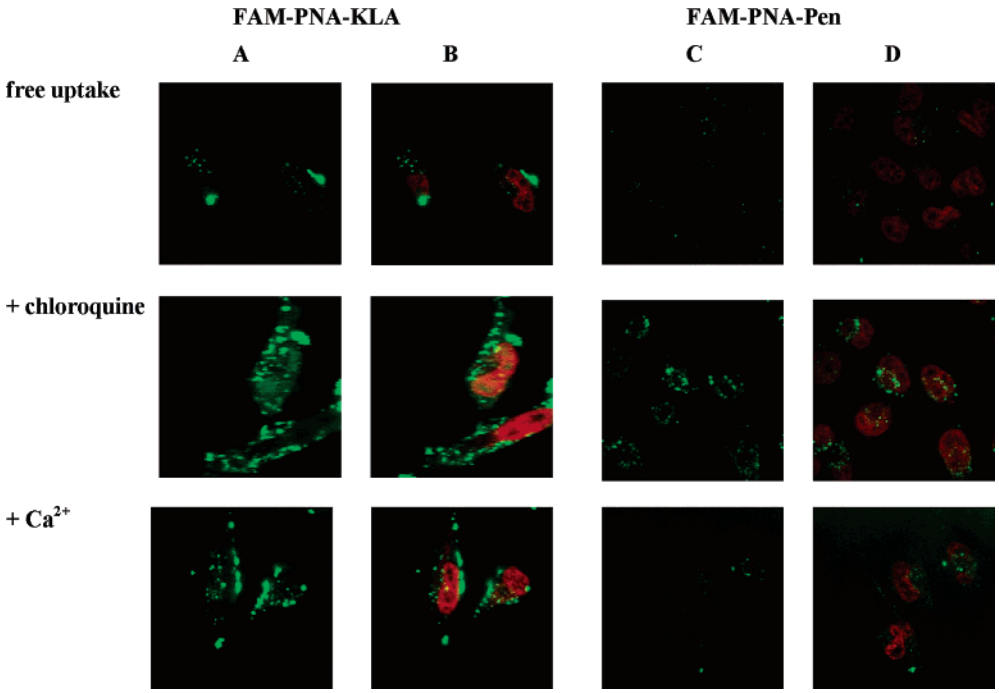

FIGURE 9: Confocal microscopy studies. Confocal microscopy images of the uptake of FAM-labeled, stably linked PNA−CPP conjugates when incubated for 4 h at 1 μM in the absence and presence of lysosomotropic agents. Cells were then cultured for another 20 h in DMEM/10% FCS, in the case of chloroquine or Ca^{2+} treatment supplemented with 100 μM chloroquine or 6 mM Ca^{2+}, respectively. Nuclei are stained red with DAPI. (For DAPI a pseudocolor is used.) In green color (A and C) fluorescein fluorescence is shown. (B) and (D) are overlaid images of DAPI staining (red color) and fluorescein fluorescence (green color). Colocalization can be seen in yellow. The first line represents the internalization without any lysosomotropic agents (free uptake) while the second and third lines show images of the uptake in the presence of chloroquine or Ca^{2+}, respectively.

RLA−PNA conjugate. However, for the stably linked KLA−PNA no enhancement of luciferase activity was found in the presence of Ca^{2+} whereas the activity of PNA−SS−KLA and PNA−KLA showing little splicing correction in the absence of chloroquine or Ca^{2+} did increase. In context, our data suggest more complex factors additionally to sequestration within and release from endosomes to influence the splicing correction activity of the conjugates and the action of chloroquine and Ca^{2+}.

Indication of Endosomal Release by Confocal Microscopy in the Presence of Chloroquine. To obtain visual evidence for conjugate release from endosomal compartments by adding chloroquine (100 μM) or Ca^{2+} (6 mM), we performed confocal microscopy of FAM-labeled PNAs conjugated with KLA, ELA, and penetratin (PNA−KLA, PNA−ELA, PNA−Pen) in the absence and presence of these reagents. Only live, nonfixed cells were used to prevent artifacts caused by cell fixation (*34*). To facilitate visualization of any nuclear uptake, DAPI (4′,6-diamidino-2-phenylindole) was used to stain the cell nucleus. By using the same experimental setup as taken for the antisense activity experiments, we were unable to detect any uptake for the naked PNA and the negatively charged PNA−ELA (data not shown). In the absence of lysosomotropic agents PNA−KLA and PNA−Pen showed a punctate fluorescence (Figure 9, first line, panels A−D) in the cytosol, suggesting endosomal sequestration. However, the PNA conjugated with KLA (Figure 9, first line, panels A and B) showed higher uptake and a quite different distribution compared to the PNA−Pen conjugated, being concentrated in large aggregates at the cell membrane (accumulation was observed within 5 min) as well as inside the cytoplasm. By analyzing the internalization by the CLSM software (*35*), significant nuclear uptake was detected for PNA−KLA whereas the PNA conjugated to penetratin could not be seen inside the nucleus, which is consistent with the lack of activity in the splicing-correction assay. Coadministration of chloroquine led to significant nuclear uptake of both conjugates. The PNA−KLA conjugate (second line, panels A and B) appeared diffusively distributed whereas the PNA−Pen (second line, panels C and D) showed a punctate fluorescence within the nucleus. Addition of 6 mM Ca^{2+} resulted in an enhanced accumulation of the PNA−KLA conjugate (Figure 9, third line, panels A and B) at the cell membrane, outside as well as inside the cell, as large aggregates, with a few spots being located within the nucleus. The effect of Ca^{2+} on the distribution of the PNA−Pen conjugate (Figure 9, third line, panels C and D) was less strong compared to that of chloroquine. Overall, the confocal microscopy data provide evidence for sequestration of a dominant part of PNA−CPP conjugates in endosomes.

DISCUSSION

The current study addresses important questions about structural properties of PNA−peptide conjugates requested for attaining antisense activity such as the peptide sequence, its placement, and the type of linkage. Our data clearly demonstrate that nuclear delivery and antisense activity of PNAs can be enhanced by the attachment of cell-penetrating peptides. The KLA−PNA conjugates, possessing cationic as well as α-helical amphipathic properties, showed highest nuclear activity in Kole's splicing-correction assay (*15*). This effect was dose- as well as time-dependent. It has been repeatedly reported that replacement of lysine by arginine residues resulted in an increased cellular uptake as well as biological activity (*29*−*32*). Probably this is due to the ability of the guanidinium group of arginine to form hydrogen bonds

with sulfate, phosphate, and carboxylate groups in the membrane (*36*, *37*), thereby producing less polar ion pair complexes capable of diffusing into the membrane (*36*). As demonstrated in this study, replacement of the lysine residues of the KLA peptide by arginines (RLA) did not lead to a higher antisense activity of the corresponding PNA conjugate. We assume that the guanidinium side chain which seems to be preferred for simple basic peptide sequences such as oligoarginines (e.g., Arg_9) is less important for the KLA peptide, and other structural properties such as amphipathicity and helicity also seem to contribute to cellular uptake and biological activity. Indeed, conjugates of peptides lacking amphipathicity or helicity (KAL and KGL, respectively) were less effective in restoring aberrant splicing. Conjugation of the PNA with a negatively charged peptide, ELA, did not lead to any enhanced biological effect. These data, which are consistent with reports of others (*12*, *21*, *38*), indicate that structure requirements such as positive charge and amphipathicity, being regarded to be characteristic of cell-penetrating peptides (*5*, *39*, *40*), seem to be essential for attaining an enhanced antisense activity of corresponding PNA−peptide conjugates. The important question whether the intracellular release of the PNA by cleavage of the linkage of the conjugate is advantageous or even essential for biological activity remained unresolved so far. In the present study we gained clear evidence that a disulfide bond between the peptide and the PNA which is expected to be rapidly cleaved within the cell is not essential for biological activity. This is in line with our recent studies showing equal antisense activity of a disulfide- and an amide-bound PNA−KLA conjugate targeted to the nociceptin/orphanin FQ receptor of spontaneously beating neonatal rat cardiomyocytes (*14*), (Y. Wolf, submitted for publication). In the current study the stably linked conjugates showed an even higher antisense activity than the disulfide-bridged ones (Figures 3 and 4). Even though the additional LPKTGGG motif of the stably linked conjugates, which had to be inserted into the conjugate sequence for enzymatic ligation, had no significant impact on the antisense activity, we cannot exclude that other structural differences of the conjugates (positioning of PNA to peptide sequence) also contribute to their activity, and further investigations are needed.

We observed a tremendous decrease of the antisense effect when the peptide has been attached to the C-terminus of the PNA (Figure 5), suggesting the position of the peptide (C- vs N-terminal) to play an important role for the biological activity of the conjugates. Even though the PNA−KLA conjugate has been efficiently delivered into the nucleus after endosomal release by chloroquine treatment (Figure 9), the antisense activity was only little increased (Figure 8, panel A). These data indicate that, apparently, the N-terminus of the PNA is the preferred attachment site for the peptides, which might be understood in terms of PNA−RNA binding. Indeed, PNAs modify mRNA processing by steric blocking (*41*). Recently, Moulton et al. also observed a dramatic decrease of antisense activity of a phosphorodiamidate morpholino oligomer (PMO) when cationic peptides or bulky moieties such as carboxyfluorescein or cholesterol had been coupled to the 3′-end of the oligos (*20*). The authors hypothesized steric interferences of the PMO−RNA binding to be the reason for this phenomenon. In order to gain insight into the role of the peptide attached to the PNA and its position, studies on the binding affinity of PNA−peptide conjugates to the target sequence using the surface plasmon resonance technique are currently under way.

Overall, however, peptide features such as positive charge and amphipathicity seem not to be sufficient to promote biological activity of PNAs. Indeed, there are also examples of PNA conjugates with well-known CPPs such as penetratin, as shown in our study, or Tat (*32*, *33*) being inactive. The lack of activity seems not to be due to cellular uptake since an enhanced internalization into HeLa cells for a PNA attached to penetratin has been detected by means of CE-LIF in our recent study (Y. Wolf, submitted for publication) being in line with others (*42*, *43*). This is also consistent with our confocal microscopy data presented in the current study revealing efficient uptake into HeLa cells for PNA−KLA as well as PNA−Pen conjugates. One of the reasons for the absence of activity could be that only a minor portion of the conjugates is internalized by a nonendocytic pathway formerly regarded to be characteristic of CPPs (*39*, *40*) while the predominant portion is taken up by endocytosis and remains sequestered within endosomal compartments. It has recently been reported that endosome destabilization by lysosomotropic agents (*11*, *32*) or fusogenic peptides such as, for instance, hemagglutinin peptide (*44*) led to enhanced biological effects of CPP−cargo conjugates. In order to gain insight into mechanistic aspects of the intracellular delivery of the PNA−peptide conjugates evaluated in the current study, we also investigated the antisense activity in the presence of the lysosomotropic agent chloroquine as well as Ca^{2+}. Treatment with chloroquine has shown great effect on the ability of some peptide conjugates to restore correct splicing (Figure 7, panel A). In contrast to the experiments conducted without chloroquine the stably linked RLA−PNA conjugate, wherein the lysine residues had been replaced by arginine, became more efficient than its lysine analogue KLA after addition of chloroquine or Ca^{2+}. A modulation of the target affinity of the PNA caused by the cationic peptides might be the reason for this enhanced activity. Without chloroquine assistance the RLA conjugate seems to be sequestered in endosomes and therefore less active in splicing correction compared to the KLA−PNA conjugate which might more efficiently escape the endosomes itself. Furthermore, nonendocytotic pathways are possibly involved in the uptake of the KLA−PNA conjugate being in line with our previous CE-LIF studies (*14*) (Y. Wolf, submitted for publication). This has also been recently discussed by Shiraishi et al. (*45*), who observed an antisense activity in Kole's model for a stably linked KLA−PNA conjugate. The antisense activity could even be enhanced by photochemical treatment facilitating endosomal release. We gained clear evidence for conjugate release from endosomes and enhanced nuclear uptake by confocal microscopy for the FAM-labeled stably linked PNA−KLA conjugate when chloroquine was coadministered. However, for the PNA−KLA there was only a little enhancement of splicing activity after chloroquine treatment while the antisense activity of the KLA−PNA conjugate has dramatically increased. This supports the assumption that the peptide attached at the C-terminus of the PNA might hinder the binding of the PNA to its target probably due to steric interferences. In contrast to the diffused chloroquine-induced distribution, Ca^{2+} seems more to stimulate the accumulation of the PNA−KLA at the cell mem-

brane. Therefore, the mechanism of the Ca^{2+} effect to increase the splicing activity seems to be more complex and cannot be simply explained an increased endosomal release. These observations are consistent with those of Shiraishi et al. (*32*), who found an enhanced antisense activity in Kole's splicing model for $(Arg)_9$−PNA and Tat−PNA conjugates in the presence of Ca^{2+}. Overall, these data indicate that there is no direct correlation between uptake and antisense activity, suggesting other factors (e.g., the binding affinity to intracellular targets) also to be crucial for attaining biological activity. Therefore, our current work is focused on binding studies of PNAs linked to various peptides using the surface plasmon resonance technique.

ACKNOWLEDGMENT

We thank D. Krause, B. Pisarz, and H. Lerch for excellent technical assistance. Burkhard Wiesner is thanked for support with the confocal microscopy studies.

REFERENCES

1. Egholm, M., Buchardt, O., Christensen, L., Behrens, C., Freier, S. M., Driver, D. A., Berg, R. H., Kim, S. K., Norden, B., and Nielsen, P. E. (1993) PNA hybridizes to complementary oligonucleotides obeying the Watson-Crick hydrogen-bonding rules, *Nature 365*, 566−568.
2. Pooga, M., Land, T., Bartfai, T., and Langel, U. (2001) PNA oligomers as tools for specific modulation of gene expression, *Biomol. Eng. 17*, 183−192.
3. Hamilton, S. E., Simmons, C. G., Kathiriya, I. S., and Corey, D. R. (1999) Cellular delivery of peptide nucleic acids and inhibition of human telomerase, *Chem. Biol. 6*, 343−351.
4. Vives, E. (2005) Present and future of cell-penetrating peptide mediated delivery systems: "is the Trojan horse too wild to go only to Troy?", *J. Control Release 109*, 77−85.
5. Zorko, M., and Langel, U. (2005) Cell-penetrating peptides: mechanism and kinetics of cargo delivery, *Adv. Drug Deliv. Rev. 57*, 529−545.
6. Gait, M. J. (2003) Peptide-mediated cellular delivery of antisense oligonucleotides and their analogues, *Cell. Mol. Life Sci. 60*, 844−853.
7. Lochmann, D., Jauk, E., and Zimmer, A. (2004) Drug delivery of oligonucleotides by peptides, *Eur. J. Pharm. Biopharm. 58*, 237−251.
8. Sazani, P., Kang, S. H., Maier, M. A., Wei, C. F., Dillman, J., Summerton, J., Manoharan, M., and Kole, R. (2001) Nuclear antisense effects of neutral, anionic and cationic oligonucleotide analogs, *Nucleic Acids Res. 29*, 3965−3974.
9. Sazani, P., Gemignani, F., Kang, S. H., Maier, M. A., Manoharan, M., Persmark, M., Bortner, D., and Kole, R. (2002) Systemically delivered antisense oligomers upregulate gene expression in mouse tissues, *Nat. Biotechnol. 20*, 1228−1233.
10. Siwkowski, A. M., Malik, L., Esau, C. C., Maier, M. A., Wancewicz, E. V., Albertshofer, K., Monia, B. P., Bennett, C. F., and Eldrup, A. B. (2004) Identification and functional validation of PNAs that inhibit murine CD40 expression by redirection of splicing, *Nucleic Acids Res. 32*, 2695−2706.
11. Abes, S., Williams, D., Prevot, P., Thierry, A., Gait, M. J., and Lebleu, B. (2006) Endosome trapping limits the efficiency of splicing correction by PNA-oligolysine conjugates, *J. Control Release 110*, 595−604.
12. Kaihatsu, K., Huffman, K. E., and Corey, D. R. (2004) Intracellular uptake and inhibition of gene expression by PNAs and PNA-peptide conjugates, *Biochemistry 43*, 14340−14347.
13. Pooga, M., Soomets, U., Hallbrink, M., Valkna, A., Saar, K., Rezaei, K., Kahl, U., Hao, J. X., Xu, X. J., WiesenfeldHallin, Z., Hokfelt, T., Bartfai, A., and Langel, U. (1998) Cell penetrating PNA constructs regulate galanin receptor levels and modify pain transmission in vivo, *Nat. Biotechnol. 16*, 857−861.
14. Oehlke, J., Wallukat, G., Wolf, Y., Ehrlich, A., Wiesner, B., Berger, H., and Bienert, M. (2004) Enhancement of intracellular concentration and biological activity of PNA after conjugation with a cell-penetrating synthetic model peptide, *Eur. J. Biochem. 271*, 3043−3049.
15. Kang, S. H., Cho, M. J., and Kole, R. (1998) Up-regulation of luciferase gene expression with antisense oligonucleotides: Implications and applications in functional assay developments, *Biochemistry 37*, 6235−6239.
16. Oehlke, J., Scheller, A., Wiesner, B., Krause, E., Beyermann, M., Klauschenz, E., Melzig, M., and Bienert, M. (1998) Cellular uptake of an alpha-helical amphipathic model peptide with the potential to deliver polar compounds into the cell interior non-endocytically, *Biochim. Biophys. Acta 1414*, 127−139.
17. Oehlke, J., Lorenz, D., Wiesner, B., and Bienert, M. (2005) Studies on the cellular uptake of substance P and lysine-rich, KLA-derived model peptides, *J. Mol. Recognit. 18*, 50−59.
18. Derossi, D., Joliot, A. H., Chassaing, G., and Prochiantz, A. (1994) The third helix of the Antennapedia homeodomain translocates through biological membranes, *J. Biol. Chem. 269*, 10444−10450.
19. Mao, H. Y., Hart, S. A., Schink, A., and Pollok, B. A. (2004) Sortase-mediated protein ligation: A new method for protein engineering, *J. Am. Chem. Soc. 126*, 2670−2671.
20. Moulton, H. M., Nelson, M. H., Hatlevig, S. A., Reddy, M. T., and Iversen, P. L. (2004) Cellular uptake of antisense morpholino oligomers conjugated to arginine-rich peptides, *Bioconjugate Chem. 15*, 290−299.
21. Albertshofer, K., Siwkowski, A. M., Wancewicz, E. V., Esau, C. C., Watanabe, T., Nishihara, K. C., Kinberger, G. A., Malik, L., Eldrup, A. B., Manoharan, M., Geary, R. S., Monia, B. P., Swayze, E. E., Griffey, R. H., Bennett, C. F., and Maier, M. A. (2005) Structure-activity relationship study on a simple cationic peptide motif for cellular delivery of antisense peptide nucleic acid, *J. Med. Chem. 48*, 6741−6749.
22. Midoux, P., Mendes, C., Legrand, A., Raimond, J., Mayer, R., Monsigny, M., and Roche, A. C. (1993) Specific gene transfer mediated by lactosylated poly-L-lysine into hepatoma cells, *Nucleic Acids Res. 21*, 871−878.
23. Erbacher, P., Roche, A. C., Monsigny, M., and Midoux, P. (1996) Putative role of chloroquine in gene transfer into a human hepatoma cell line by DNA/lactosylated polylysine complexes, *Exp. Cell Res. 225*, 186−194.
24. Haberland, A., Knaus, T., Zaitsev, S. V., Stahn, R., Mistry, A. R., Coutelle, C., Haller, H., and Bottger, M. (1999) Calcium ions as efficient cofactor of polycation-mediated gene transfer, *Biochim. Biophys. Acta 1445*, 21−30.
25. Zaitsev, S., Buchwalow, I., Haberland, A., Tkachuk, S., Zaitseva, I., Haller, H., and Bottger, M. (2002) Histone H1-mediated transfection: role of calcium in the cellular uptake and intracellular fate of H1-DNA complexes, *Acta Histochem. 104*, 85−92.
26. Thomson, S. A., Josey, J. A., Cadilla, R., Gaul, M. D., Hassman, C. F., Luzzio, M. J., Pipe, A. J., Reed, K. L., Ricca, D. J., Wiethe, R. W., and Noble, S. A. (1995) Fmoc mediated synthesis of peptide nucleic-acids, *Tetrahedron 51*, 6179−6194.
27. Braasch, D. A., and Corey, D. R. (2001) Synthesis, analysis, purification, and intracellular delivery of peptide nucleic acids, *Methods 23*, 97−107.
28. Kapuscinski, J., and Szer, W. (1979) Interactions of 4′,6-diamidine-2-phenylindole with synthetic polynucleotides, *Nucleic Acids Res. 6*, 3519−3534.
29. Futaki, S., Suzuki, T., Ohashi, W., Yagami, T., Tanaka, S., Ueda, K., and Sugiura, Y. (2001) Arginine-rich peptides−An abundant source of membrane-permeable peptides having potential as carriers for intracellular protein delivery, *J. Biol. Chem. 276*, 5836−5840.
30. Mitchell, D. J., Kim, D. T., Steinman, L., Fathman, C. G., and Rothbard, J. B. (2000) Polyarginine enters cells more efficiently than other polycationic homopolymers, *J. Pept. Res. 56*, 318−325.
31. Rothbard, J. B., Garlington, S., Lin, Q., Kirschberg, T., Kreider, E., McGrane, P. L., Wender, P. A., and Khavari, P. A. (2000) Conjugation of arginine oligomers to cyclosporin A facilitates topical delivery and inhibition of inflammation, *Nat. Med. 6*, 1253−1257.
32. Shiraishi, T., Pankratova, S., and Nielsen, P. E. (2005) Calcium ions effectively enhance the effect of antisense peptide nucleic acids conjugated to cationic tat and oligoarginine peptides, *Chem. Biol. 12*, 923−929.
33. Turner, J. J., Ivanova, G. D., Verbeure, B., Williams, D., Arzumanov, A. A., Abes, S., Lebleu, B., and Gait, M. J. (2005) Cell-penetrating peptide conjugates of peptide nucleic acids (PNA)

as inhibitors of HIV-1 Tat-dependent trans-activation in cells, *Nucleic Acids Res. 33*, 6837−6849.
34. Richard, J. P., Melikov, K., Vives, E., Ramos, C., Verbeure, B., Gait, M. J., Chernomordik, L. V., and Lebleu, B. (2003) Cell-penetrating peptides. A reevaluation of the mechanism of cellular uptake, *J. Biol. Chem. 278*, 585−590.
35. Wiesner, B., Lorenz, D., Krause, E., Beyermann, M., and Bienert, M. (2002) Measurement of intracellular fluorescence in the presence of a strong extracellular fluorescence using confocal laser scanning microscopy, *LAMSO 3*, 1−17.
36. Sakai, N., and Matile, S. (2003) Anion-mediated transfer of polyarginine across liquid and bilayer membranes, *J. Am. Chem. Soc. 125*, 14348−14356.
37. Salvatella, X., Martinell, M., Gairi, M., Mateu, M. G., Feliz, M., Hamilton, A. D., de Mendoza, J., and Giralt, E. (2004) A tetraguanidinium ligand binds to the surface of the tetramerization domain of protein P53, *Angew. Chem., Int. Ed Engl. 43*, 196−198.
38. Tripathi, S., Chaubey, B., Ganguly, S., Harris, D., Casale, R. A., and Pandey, V. N. (2005) Anti-HIV-1 activity of anti-TAR polyamide nucleic acid conjugated with various membrane transducing peptides, *Nucleic Acids Res. 33*, 4345−4356.
39. Lindgren, M., Hällbrink, M., Prochiantz, A., and Langel, Ü. (2000) Cell-penetrating peptides, *Trends Pharmacol. Sci.* 21, 99−103.
40. Langel, Ü. Ed. (2002) Cell-penetrating peptides, *Handbook of Cell-Penetrating Peptides*, CRC Press LLC, Boca Raton, FL.
41. Braasch, D. A., and Corey, D. R. (2002) Novel antisense and peptide nucleic acid strategies for controlling gene expression, *Biochemistry 41*, 4503−4510.
42. Simmons, C. G., Pitts, A. E., Mayfield, L. D., Shay, J. W., and Corey, D. R. (1997) Synthesis and membrane permeability of PNA-peptide conjugates, *Bioorg. Med. Chem. Lett. 7*, 3001−3006.
43. Koppelhus, U., Awasthi, S. K., Zachar, V., Holst, H. U., Ebbesen, P., and Nielsen, P. E. (2002) Cell-dependent differential cellular uptake of PNA, peptides, and PNA-peptide conjugates, *Antisense Nucleic Acid Drug Dev. 12*, 51−63.
44. Wadia, J. S., Stan, R. V., and Dowdy, S. F. (2004) Transducible TAT-HA fusogenic peptide enhances escape of TAT-fusion proteins after lipid raft macropinocytosis, *Nat. Med. 10*, 310−315.
45. Shiraishi, T., and Nielsen, P. E. (2006) Photochemically enhanced cellular delivery of cell penetrating peptide-PNA conjugates, *FEBS Lett. 580*, 1451−1456.
46. Scheller, A., Oehlke, J., Wiesner, B., Dathe, M., Krause, E., Beyermann, M., Melzig, M., and Bienert, M. (1999) Structural requirements for cellular uptake of alpha-helical amphipathic peptides, *J. Pept. Sci. 5*, 185−194.

BI0606896

Nucleic Acids Research, 2005, Vol. 33, No. 21 ***6837–6849***
doi:10.1093/nar/gki991

Cell-penetrating peptide conjugates of peptide nucleic acids (PNA) as inhibitors of HIV-1 Tat-dependent *trans*-activation in cells

John J. Turner, Gabriela D. Ivanova, Birgit Verbeure, Donna Williams, Andrey A. Arzumanov, Saïd Abes[1], Bernard Lebleu[1] and Michael J. Gait*

Laboratory of Molecular Biology, Medical Research Council, Hills Road, Cambridge CB2 2QH, UK and [1]UMR 5124 CNRS, CC 086, Université Montpellier 2, Place Eugène Bataillon, 34095 Montpellier, France

Received October 6, 2005; Revised and Accepted November 14, 2005

ABSTRACT

The *trans*-activation response (TAR) RNA stem–loop that occurs at the 5′ end of HIV RNA transcripts is an important antiviral target and is the site of interaction of the HIV-1 Tat protein together with host cellular factors. Oligonucleotides and their analogues targeted to TAR are potential antiviral candidates. We have investigated a range of cell penetrating peptide (CPP) conjugates of a 16mer peptide nucleic acid (PNA) analogue targeted to the apical stem–loop of TAR and show that disulfide-linked PNA conjugates of two types of CPP (Transportan or a novel chimeric peptide R_6-Penetratin) exhibit dose-dependent inhibition of Tat-dependent *trans*-activation in a HeLa cell assay when incubated for 24 h. Activity is reached within 6 h if the lysosomotropic reagent chloroquine is co-administered. Fluorescein-labelled stably-linked conjugates of Tat, Transportan or Transportan TP10 with PNA were inactive when delivered alone, but attained *trans*-activation inhibition in the presence of chloroquine. Confocal microscopy showed that such fluorescently labelled CPP–PNA conjugates were sequestered in endosomal or membrane-bound compartments of HeLa cells, which varied in appearance depending on the CPP type. Co-administration of chloroquine was seen in some cases to release fluorescence from such compartments into the nucleus, but with different patterns depending on the CPP. The results show that CPP–PNA conjugates of different types can inhibit Tat-dependent *trans*-activation in HeLa cells and have potential for development as antiviral agents. Endosomal or membrane release is a major factor limiting nuclear delivery and *trans*-activation inhibition.

INTRODUCTION

Efficient delivery of oligonucleotides and their analogues through cell membranes to allow interaction with intracellular RNA targets and to control gene expression has proved to be a significant challenge. Oligonucleotide analogues that carry negative charges (e.g. phosphodiesters or phosphorothioates) are often delivered into common laboratory cell lines in culture (such as HeLa cells) by complexation with cationic lipids (1), of which there is now a wide choice. However, there are usually limiting lipid-associated cell toxicities and stability disadvantages for therapeutic use. Charge-neutral peptide nucleic acids (PNAs) (2) and phosphorodiamidate morpholino oligomers (PMO) (3) have been developed as oligonucleotide analogues that are unaffected by cellular nucleases and which have strong RNA binding. It was hoped that the lack of negative charge might facilitate cell uptake, but cell membrane translocation of unmodified PNA and PMO has proved to be as inefficient as for phosphate-containing oligonucleotides and analogues (4).

Recently, certain peptides [known as cell penetrating peptides (CPPs) or protein transduction domains] have been identified that have strong cell translocation properties and potential for drug delivery (5). A number of promising cell delivery studies have focussed on covalent conjugates of CPPs with various types of cargo [reviewed in Refs (6–8)] including oligonucleotides and their analogues [reviewed in Refs (9–11)]. Whereas conjugates of CPPs with negatively charged

*To whom correspondence should be addressed. Tel: +44 1223 248011; Fax: +44 1223 402070; Email: mgait@mrc-lmb.cam.ac.uk
Present address:
Birgit Verbeure, Centre for Intellectual Property Rights, Catholic University of Leuven, Minderbroederstraat 5, B-3000 Leuven, Belgium

phosphodiester or phosphorothioate oligonucleotides have had mixed results in recent cell delivery studies (12–15), several reports have showed enhanced cellular delivery and biological activity of PNA covalently attached to CPPs [reviewed in Refs (9,11)].

In common with many other steric block oligonucleotide analogue types, PNA does not induce RNase H-dependent RNA cleavage when bound to an RNA target. Therefore stoichiometric amounts must be delivered into either the cytosol of cells [e.g. to block translation (16)] or into the nucleus [e.g. to redirect splicing (17)] compared with the amount of target RNA. Thus, efficient delivery is of paramount importance to observe strong gene expression control effects.

For some years we have studied the *trans*-activation activity of the HIV-1 *trans*-activator protein Tat which interacts with the HIV *trans*-activation responsive element (TAR) stem–loop RNA and other cellular factors to strongly stimulate transcriptional elongation from the viral long terminal repeat (LTR) (18,19). Inhibitors of these RNA–protein interactions block full-length transcription and resultant HIV-1 gene expression, and thus are potential candidates for anti-HIV therapies. Despite much effort to date, no small molecule inhibitors [reviewed in Refs (20)] have emerged as clinical candidates.

Several years ago, we showed that 12mer steric block oligonucleotide analogues of a number of types [e.g. 2′-*O*-methyl (OMe), a mixmer oligonucleotide containing OMe and some 5-methyl C locked nucleic acid (LNA) units, or a PNA oligomer] targeted to the apical part of the TAR stem–loop, which is highly sequence-conserved (Figure 1), were able to inhibit sequence-specifically Tat-dependent *in vitro* transcription directed by HeLa cell nuclear extract on a DNA template containing the HIV-1 LTR (21–23). We then showed that, when delivered by a cationic lipid or surfactant, 12mer and 16mer OMe/LNA mixmer oligonucleotides could dose-dependently and sequence-dependently inhibit Tat-dependent HIV LTR *trans*-activation from a stably integrated plasmid system in HeLa cells with a firefly luciferase reporter, but without effect on a control *Renilla* luciferase reporter (22,23). Fluorescein-labelled OMe/LNA oligonucleotides were found by confocal microscopy to be located in both cytosolic and nuclear compartments when delivered by a range of cationic lipid reagents (23).

Recently, we described the chemical synthesis and purification of disulfide conjugates of a range of CPPs with fluorescein-labelled OMe/LNA oligonucleotides and reported that in all cases such conjugates were unable to inhibit Tat-dependent *trans*-activation in our HeLa cell reporter assay involving stably integrated reporter plasmids (15). Whereas in most cases attachment of a CPP significantly enhanced unassisted HeLa cell uptake of the oligonucleotides, their uptake was confined to cytosolic (presumably endosomal) compartments. Exclusion from the cell nucleus correlated with the lack of inhibition of Tat-dependent *trans*-activation, suggesting that the barrier to nuclear activity is due to insufficient release from endosomal compartments. Similar cytosolic entrapment was also a feature of OMe/LNA oligonucleotide lipid-free uptake studies into human fibroblasts (15).

Kaushik *et al*. (24) found that 15mer and 16mer steric block PNAs targeted to the TAR RNA, when electroporated into CEM lymphocytes, were able to inhibit Tat-dependent *trans*-activation in a transient luciferase reporter assay and also block expression of luciferase from CEM cells pre-infected with pseudotyped HIV-1 virions. 16mer PNA disulfide conjugated to the CPP Transportan [a synthetic chimeric peptide derived from the neuropeptide galanin and wasp venom toxin mastoparan (25)] inhibited Tat-dependent *trans*-activation in Jurkat or CEM cells or Jurkat cells transiently transfected with luciferase reporters (IC_{50} of ~0.5 μM), and also inhibited HIV-1 production in chronically infected H9 cells (IC_{50} of ~1 μM), where it appeared to be acting by inhibition at the transcriptional level (26). Subsequently, Chaubey *et al*. (27) have shown improved activity levels of the same PNA-Transportan conjugate in an antiviral assay in blocking synthesis of proviral DNA and significantly higher level of activity (IC_{50} of ~40 nM) by inhibition of viral infectivity by pre-treatment of HIV virions.

Our current studies address the important question of how the chemical structure of a CPP–PNA (the type of CPP, its placement and the type of linkage) relates to its ability to penetrate HeLa cells, enter the nucleus and inhibit Tat-dependent *trans*-activation, which is one of the proposed mechanisms for attaining antiviral activity. We now report the chemical synthesis of a range of CPPs conjugated either through a stable polyether or through a cleavable disulfide linkage to a 16mer PNA targeted to the HIV-1 TAR apical loop. We study their ability to inhibit Tat-dependent *trans*-activation when incubated with HeLa cells using a rigorous, double-luciferase reporter system that involves stably integrated plasmids. We show that disulfide-linked CPP–PNA conjugates with two types of CPP (Transportan or a novel chimeric peptide R_6-Penetratin) are able to inhibit Tat-dependent *trans*-activation when incubated with HeLa cells for 24 h. Co-administration of the lysosomotropic reagent chloroquine allowed activity to be seen within 6 h. In addition, *trans*-activation inhibition could be attained for several FAM-labelled, stably-linked CPP–PNA conjugates, notably Tat-PNA, in the presence of chloroquine, which were inactive in its absence. Confocal microscopy showed that such CPP–PNA conjugates, when incubated with Hela cells in the absence of chloroquine, were sequestered in endosomal or membrane-bound compartments of HeLa cells, which varied in appearance depending on the CPP type. In some cases, co-administration of chloroquine was seen to release fluorescence from such compartments into the nucleus, but with different patterns depending on the CPP. The results are significant in that CPP–PNA conjugates of different types can inhibit Tat-dependent *trans*-activation in cells and that endosome or membrane release is a major factor limiting nuclear delivery and *trans*-activation inhibition. The results contribute towards improved design of biologically active CPP–PNA.

MATERIALS AND METHODS

Assembly of FAM–PNA–peptide conjugates with stable linkages

These were synthesized manually on a 5 μmol scale using a polyethylene syringe fitted with a 10 μm polyethyelene

frit (Isolute SPE Accessories) attached to a manifold multi-filtration device, and Fmoc chemistry (28). Fmoc-PAL-PEG-PS resin and Fmoc (Bhoc) PNA monomers were purchased from Applied Biosystems and used at 0.2 M dissolved in *N*-methylpyrollidone (NMP). The activator was 0.2 M PyAOP (or PyBOP) in DMF, and a mixture of DIPEA and 2,6-lutidine to give a 0.4 M solution in DMF was used as the base solution (reagent mix A). For conjugates **1**–**4** (Figure 2), after PNA assembly an Fmoc-AEEA spacer (O-linker, Applied Biosystems) was coupled followed by amino acid couplings, each carried out with 0.2 M PyBOP in DMF and 0.4M DIPEA (660 µl in 10 ml) in DMF (reagent mix B). For conjugates **5** and **6**, peptide synthesis was carried out before PNA synthesis and for conjugates **7** and **8**, peptide assembly was both before and after PNA assembly with spacers between each. Both PNA monomers and amino acid monomers were double coupled for 30 min per coupling. The resin was washed five times with DMF after each coupling. Fmoc deprotection was carried out with 20% piperidine in DMF (3 min, then 12 min) and resin washed again five times with DMF. 6-Carboxyfluorescein diacetate (6-CDFA; Sigma) (four equivalents relative to resin loading) was dissolved in a minimal volume of NMP and four equivalents of PyBOP dissolved in DMF added followed by four equivalents of DIPEA. The mixture was left for 10 min and another 4 equivalents of DIPEA added to the resin. After 16 h, the resin was washed thoroughly with DMF and deacetylated by treatment with 20% piperidine in DMF.

Assembly of $(K)_8$–PNA–K(FAM) (conjugate 9) and Cys(Npys)–PNA (towards conjugates 10–15)

These were synthesized on 5 µmol scale on an APEX 396 Robotic Peptide Synthesizer using the same reagents and resin as for manual synthesis. Fmoc deprotection was carried out with 20% piperidine in DMF (1 min, then 4 min), amino acid deprotection with 20% piperidine in DMF (3 min then 12 min). After five times washing with DMF, PNA was double coupled using reagent mix A and amino acids were double coupled using reagent mix B, each with a reaction time of 30 min per coupling. Boc-Cys(NPys) was used in the synthesis of PNAs required for disulfide coupling. Fmoc-Lys(Boc) was used for the $(Lys)_8$ sequence and Fmoc-Lys(Mmt) for the residue for fluorescent labelling. After washing five times with DMF, a capping step was carried out using 5% acetic anhydride, 6% 2,6-lutidine in DMF (2×5 min), followed by washing five times with DMF. The N-terminal Fmoc group needs to be removed (as above) before final cleavage.

In the case of $(Lys)_8$–PNA–Lys(Mmt), the resin was washed with DCM and the Mmt group removed by treatment with nine aliquots of 2% trifluoroacetic acid, 5% triisopropylsilane (TIS) in DCM (5 min incubation for every aliquot, 45 min in total). The resin was washed with 1× DCM and 1× DMF. To 6-CFDA (10 equivalents relative to resin loading) dissolved in a minimal volume of NMP was added HOAt (10 equivalents) dissolved in DMF and diisopropylcarbodiimide (DIC) (10 equivalents), premixed for 10 min, and reacted with the resin for at least 16 h at room temperature, the resin washed thoroughly and then deacetylated by treatment with 20% piperidine in DMF (as above).

Deprotection and purification of PNA

The resin was treated with 95% TFA, 2.5% H_2O, 2.5% TIS with addition of 10% phenol as scavenger for a minimum of 90 min. PNAs were analysed and purified by reversed phase high-performance liquid chromatography (HPLC) on a Phenomenex Jupiter C18 column (see below) with buffer A, 0.1% TFA in water; buffer B, 10% buffer A in acetonitrile and monitoring at 260 nm with a gradient of 10–50% B gradient over 30 min. MALDI-TOF mass spectrometry was carried out on a Voyager DE Pro BioSpectrometry workstation with a matrix of α-cyano-4-hydroxycinnamic acid, 10 mg ml^{-1} in acetonitrile-3% aqueous TFA (1:1, v/v). The accuracy of the mass measurement is regarded as ±0.05%.

Synthesis of Cys peptides

Tat-Cys, R_9F_2-Cys, Penetratin-Cys and R_6-Penetratin-Cys were purchased as C-terminal amides from Southampton Polypeptides. Transportan-Cys peptides were synthesized on a PerSeptive Biosystems Pioneer peptide synthesiser (100 µmol scale) using standard Fmoc/*tert*-butyl solid phase synthesis techniques as C-terminal amide peptides using NovaSyn TGR resin (Novabiochem). Deprotection of all peptides and cleavage from solid support was achieved by treatment with TFA in the presence of triethylsilane and water (each 3%). Purification was carried out by reversed phase HPLC as described previously (15) and MALDI-TOF mass spectrometry with the same matrix as for PNA.

Disulfide conjugates of Cys(NPys)–PNA with Cys-peptides (conjugates 10–15)

To an eppendorf tube containing the Npys-activated PNA oligomer (20 nmol in 25 µl water) was added 1 M NH_4Ac (pH 7, 10 µl) followed by the Cys-peptide to be conjugated (40 nmol, 4 µl of 10 mM stock solution). In the case of Transportan and derivatives, 50 µl of acetonitrile was added prior to peptide addition to prevent precipitation of the peptide at neutral pH. The solution was thoroughly mixed and allowed to stand for 30 min, whereupon the conjugate was purified in one aliquot by reversed phase HPLC using a Phenomenex Jupiter C18 column (5 µm, 300 Å, 250×4.6 mm^2) heated to 45°C: Flow rate 1.5 ml min^{-1}, Buffer A—0.1% TFA (aqueous), Buffer B—90% acetonitrile, 10% Buffer A. Gradient 5–30% B buffer in 25 min for Penetratin, R_9F_2, and R_6-Penetratin conjugates (**11**, **12** and **13**, respectively). A gradient of 5–50% B buffer was used for Transportan conjugates **14** and **15**. For conjugate 10, a step gradient was necessary because of close elution of conjugate, Tat and PNA: 5–10% B (2 min); 10–12.5% B (2 min); 12.5% B (4 min); 12.5–15% B (2 min); 15% B (4 min); 15–17.5% B (2 min); 17.5% B (4 min); 17.5–20% B (2 min); 20% B (4 min). The product was collected, lyophilized and analysed by MALDI-TOF mass spectrometry as described above for PNA alone. As an example, the HPLC purification profile for the R_6–PenC–PNA conjugate **13** (Supplementary Figure 1A), the HPLC analytical profile of the purified product (Supplementary Figure 1B) and mass spectrum (Supplementary Figure 2) are shown.

Inhibition of Tat-dependent *trans*-activation in cells

Inhibition of HIV-1 Tat-mediated *trans*-activation by CPP–PNA conjugates in HeLa cells (Figure 3) was carried out

similarly to that described previously (22,23). Briefly, in each experiment two identical 96-well plates were prepared with 10×10^3 HeLa Tet-Off/Tat/luc-f/luc-R cells per well and incubated at 37°C for 24 h. One of the plates was used for the luciferase assay and the other for the cytotoxicity assay. Conjugates were prepared at 2.5 μM concentration in Opti-MEM (Invitrogen), subsequently diluted and added to the cells for 6 or 24 h incubation, cells washed in phosphate-buffered saline (PBS) and followed by 18 h incubation in DMEM/10% fetal bovine serum (FBS). For chloroquine experiments (Figure 4), conjugates were prepared at 2.5 μM concentration and 100 μM chloroquine in Opti-MEM, subsequently diluted by 100 μM chloroquine in Opti-MEM and added to the cells for 6 h incubation, cells washed as before, followed by 18 h incubation in DMEM/10% FBS. For the time course study (Figure 5), incubations with conjugates and 100 μM chloroquine were carried out for 2, 4, 6 and 8 h, respectively, before treatment as above.

Luciferase assay. Cell lysates were prepared and analysed using the Dual Luciferase Reporter Assay System (Promega) and relative light units for both firefly and *Renilla* luciferase read sequentially using a Berthold Detection Systems Orion Microplate luminometer. Each data point was averaged over two replicates of three separate experiments.

Toxicity assay. The extent of toxicity was determined by measurement of the proportion of live cells colorimetrically using CellTiter 96 AQ_{ueous} One Solution Assay (Promega). The absorbance at 490 nm was read using a Molecular Devices Emax Microplate Reader.

Each data point was averaged over two replicates of three separate experiments. The relative light units in the luciferase assays were normalized to the absorbance data from the toxicity assay, which reflects the amount of live cells and then expressed as a percentage compared with the luciferase activities of HeLa cells treated in the absence of CPP–PNA. The error bars reflect the full range of the experimental values and are not SDs. It is common to normalize the firefly luciferase levels to that of the *Renilla* luciferase levels when co-transfection of plasmids is used. However in this stably integrated system, the level of *Renilla* luciferase is 20-fold lower than that of firefly luciferase and is thus much more sensitive to fluctuations resulting from small changes in cell growth conditions. Showing a simple ratio of the two levels unreasonably amplifies these fluctuations. We have therefore found it more beneficial to show the two sets of luciferase data separately (Figures 3 and 4) and to assess the extent of level changes or otherwise in each set.

Confocal microscopy

HeLa cells (15×10^3) were plated on an 8-well Lab-Tek chambered coverglass (Fisher Scientific) in DMEM/10%FBS and cultured overnight. The medium was discarded and cells were washed with PBS followed by incubation with 300 μl of 2.5 μM CPP–PNA conjugate or 2.5 μM CPP–PNA conjugate/100 μM chloroquine in OptiMEM for 5.5 h. For nuclear staining, 50 μl OptiMEM containing hydroethidine (50 μg ml^{-1}) was added to each well and incubated for 0.5 h at 37°C. After two washes, 200 μl of OptiMEM (without phenol red) (Invitrogen) medium containing HEPES buffer was added into the wells for observation of living cells.

The cells were observed with a Radiance 2100 confocal system on a Nikon Eclipse TE300 inverted microscope using a 60× Planapo objective N.A. 1.4.A 488 nm Argon laserline was used to excite fluorescein and a HQ 515/30 emission filter was used for observation of the green emission. Hydroethidine was excited with a 543 nm (green) HeNe laser and detected using a HQ 570LP (orange) emission filter. A dual fluorescence method was used with a differential interference contrast transmission channel. The images in the three channels were acquired sequentially at ~1 frame/s with a scanning resolution of 512 × 512 pixels and a Kalman average of 10 frames was used. When comparing the uptake or activity of the PNA conjugates the imaging conditions (such as photomultiplier gain/offset, laser intensities and confocal aperture size) were kept constant for the observation of the different conjugates, so that the intensities represent the true differences in uptake/activity.

RESULTS

In our earlier work, we reported that a 12mer PNA targeted to residues 24–35 of the apical loop of the HIV-1 TAR (Figure 1A) blocked Tat binding *in vitro* as well as Tat-dependent *in vitro* transcription in HeLa cell extract (21). More recently we have studied Tat-dependent *trans*-activation activity in HeLa cells and showed that a 16mer OMe/LNA steric block oligonucleotide was ~2-fold more inhibitory than a 12mer (22,23). Since Kaushik *et al*. (24) showed that a 16mer PNA targeted to TAR (residues 20–34) had several fold larger inhibitory activity than a 12mer PNA in reverse transcription, Tat-dependent *trans*-activation and HIV production assays, we have focussed our CPP–PNA conjugate studies on a similar 16mer PNA targeted to HIV-1 TAR (residues 21–35) (Figure 1A).

Our HeLa cell line carrying stably integrated luciferase reporters, used by us in several previous studies (22,23,29), has significant advantages for the study of the inhibition of Tat-dependent *trans*-activation activity (Figure 1B). In this 3-plasmid system, HIV-1 Tat is produced in *trans* to control production of GL3-firefly luciferase from the HIV-1 LTR, whilst a control *Renilla* luciferase is under constitutive CMV promoter direction. In contrast to the transient plasmid reporter system of Kaushik *et al*. (24), in order to see significant steric block inhibition of the TAR RNA system, oligonucleotides or PNA must be delivered efficiently to the nucleus of almost all cells, since each cell contains the three plasmids. The integrated plasmid system would be expected to mimic more closely an integrated HIV-1 provirus than transient transfection. Since unconjugated PNA is not taken up by cells, conjugation with a CPP, minimally a few Lys residues (17), is essential to achieve at least some cell binding and entry. We wished to determine how the nature of the CPP and the way it is linked to the PNA influences the ability of the PNA component to enter the cell, reach the nucleus and inhibit Tat-dependent *trans*-activation.

Synthesis of stably-linked and disulfide-linked conjugates of CPPs to 16mer PNA

A series of stably-linked CPP–PNA conjugates was synthesized using the Fmoc method (28), where the linkage between

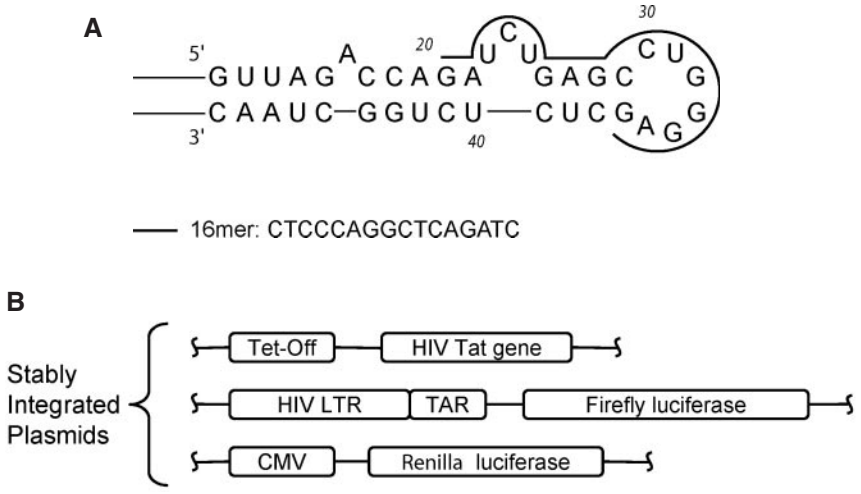

Figure 1. (**A**) Secondary structure of the TAR RNA apical stem–loop, the binding site on TAR and sequence of the PNA 16mer. (**B**) Stably integrated plasmids within the HeLa Tet-Off/Tat/luc-f/luc-R cell line used for *trans*-activation inhibition studies.

the PNA and peptide parts consisted of a short polyether linkage (AEEA, 8-amino-3,5-dioxo-octanoic acid, also known as an O-linker) (Figure 2A, conjugates **1**–**8**). All conjugates were purified by reversed phase HPLC and characterized by MALDI-TOF mass spectrometry. CPPs used were either the Tat peptide (residues 48–58) (30), an SV40 nuclear localization signal (NLS) (31,32), Transportan (25) or a shorter 21mer version of Transportan [known as TP10 or Transportan 21 (33)]. In conjugates **1**–**4**, a single CPP (Tat, Transportan, TP10 or NLS, respectively) was linked to the N-terminus of the 16mer PNA, spaced by an O-linker (Figure 2A). In conjugates **5** and **6**, a single CPP (TP10 or NLS) was linked to the C-terminus of the PNA, spaced by an O-linker. In conjugates **7** and **8**, both NLS and Tat CPPs were added, one on each end in different order, each spaced by an O-linker. A carboxyfluorescein (FAM) label was coupled to the N-terminus of each conjugate to enable cell fluorescence uptake studies.

A different type of stably-linked CPP–16mer PNA conjugate was also synthesized that carried eight lysine residues on the N-terminus [Figure 2A, conjugate **9**]. Conjugate **9** was prompted by the work of Siwkowski *et al*. (34) who showed that a K_8–PNA construct was very effective at redirection of splicing of a CD40 mRNA when added to BCL_1 or macrophage cells, and that this was due to enhanced cell uptake resultant from the use of the K_8 conjugate acting effectively as a CPP. In conjugate **9**, the FAM label was attached to the PNA moiety on the C-terminus via the ε-amino group of a single K residue.

In order to compare with the Transportan-PNA conjugate of Kaushik *et al*., (26) which utilized a disulfide linkage, we synthesized a range of CPP–PNA conjugates that contained a disulfide linkage (Figure 2B). These were synthesized by conjugation of Cys–peptides with Cys–PNA activated with a nitropyridylsulfenyl (NPys) group, purified by reversed phase HPLC and characterized by MALDI-TOF mass spectrometry. Six such conjugates were prepared (Figure 2B) from PNA 16mer containing three C-terminal K residues and as CPPs either Tat (30), Penetratin (35), R_9F_2 (36), Transportan or a novel R_6-Penetratin chimeric peptide that we have described recently (15). In four cases (**10–13**) the Cys residue was located on the C-terminus of the peptide, in one case Transportan was placed at the N-terminus (**14**) [which is similar to that described previously by Kaushik *et al*. (26)], and in the case of construct **15**, a Cys residue replaced K-13 in Transportan.

Inhibition of Tat-dependent *trans*-activation by CPP–PNA

We tested the ability of CPP–PNA constructs to inhibit Tat-dependent *trans*-activation by incubation with HeLa Tet-Off/Tat/luc-f/luc-R cells (21,23) for 6 or 24 h in the absence of any transfection agent. Cells were then washed and subsequently grown for 18 h. Firefly luciferase activity results from HIV-1 Tat-dependent transcription, whilst *Renilla* luciferase activity acts as an internal control to check that there is no inhibition of general transcription/translation.

In the case of stably-linked conjugates **1**–**9**, there was no significant reduction seen either of firefly luciferase or *Renilla* luciferase expression up to 2.5 μM tested (data not shown). We then tested the six disulfide-linked CPP–PNA conjugates. Tat, Penetratin and R_9F_2 conjugates **10**–**12** showed no activity up to 2.5 μM tested (data not shown). For 6 h incubation (Figure 3A, upper panel), the R_6-Penetratin disulfide conjugate **13** showed no activity, but both Transportan disulfide conjugates **14** and **15** showed a small dose-dependent reduction of firefly luciferase activity (Figure 3A, upper panel). The *Renilla* luciferase activity did not drop significantly over the same concentration range (Figure 3A, lower panel). Note that the absolute level of *Renilla* luciferase activity in terms of light units is only 5–10% of that of the firefly luciferase in this cell line. Sporadic increases in *Renilla* luciferase fluorescence for particular constructs are occasionally observed, e.g. construct **14**, reflecting the much higher sensitivity of the *Renilla* luciferase to additives or cell growth conditions compared with firefly luciferase. A significant reduction in *Renilla* luciferase expression would have been expected had there been any non-specific transcription/translation suppressive effect upon addition of the CPP–PNA, which is clearly not the case. Cell viability for 6 h incubation with the highest concentration

A. Stably-linked conjugates

Conjugate	Description	Calculated molecular mass	Observed MALDI molecular mass
1	FAM-Tat-*O*-PNA-$CONH_2$	6253.06	6254.49
2	FAM-TP-*O*-PNA-$CONH_2$	7598.75	7603.61
3	FAM-TP10-*O*-PNA-$CONH_2$	6941.04	6945.60
4	FAM-SV40 NLS-*O*-PNA-$CONH_2$	5642.42	5644.12
5	FAM-PNA-*O*-TP10-$CONH_2$	6941.04	6945.24
6	FAM-PNA-*O*-SV40 NLS-$CONH_2$	5642.42	5643.52
7	FAM-SV40 NLS-*O*-PNA-*O*-Tat-$CONH_2$	7263.36	7262.32
8	FAM-Tat-*O*-PNA-*O*- SV40 NLS-$CONH_2$	7263.36	7263.50
9	NH_2-K_8-PNA-K(FAM)-$CONH_2$	5785.69	5791.78

FAM = Carboxyfluorescein label
O = -NH-$(CH_2CH_2O)_2CH_2CO$-
Tat = GRKKRRQRRRP
TP = GWTLNSAGYLLGKINLKALAALAKKIL
TP10 = AGYLLGKINLKALAALAKKIL
SV40 NLS = PKKKRKV

B. Disulfide-linked conjugates

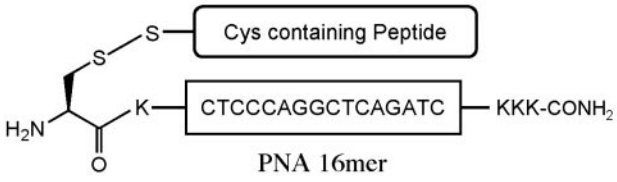

Conjugate	Peptide[a]	Calculated molecular mass	Observed MALDI molecular mass
10	Tat-**C**	6483.88	6486.43
11	Pen-**C**	7350.95	7355.68
12	R_9F_2-**C**	6708.22	6711.56
13	R_6Pen-**C**	8288.07	8288.17
14	**C**-TP	7831.56	7836.82
15	TP(int **C**)[b]	7703.38	7704.88

[a] **C** denotes where disulfide linkage is
[b] Internal **C** replaces K 13 in Transportan (TP) i.e. GWTLNSAGYLLG-**C**-INLKALAALAKKIL
Pen = RQIKIWFQNRRMKWKKGG

Figure 2. (**A**) Structures of various FAM-labelled stably-linked CPP–PNA and PNA–CPP conjugates **1–9** and their calculated and observed mass values. (**B**) Structure of various disulfide-linked CPP–PNA conjugates **10–15** and their calculated and observed mass values. The linkage is in all cases between an N-terminal Cys residue on the PNA and a Cys residue within the peptide either on the C-terminus (**10–13**) N-terminus (**14**) or an internal residue (**15**). These conjugates do not carry a FAM label.

(2.5 μM) of the stably-linked CPP–PNA was >95% in all cases and for disulfide-linked conjugates was >90%.

For 24 h delivery of the CPP–PNAs, a strong dose-dependent reduction of firefly luciferase activity was seen for all three conjugates **13–15** (Figure 3B, upper panel), whilst no significant reduction in *Renilla* luciferase activity was seen in any case (Figure 3B, lower panel, note that in this case there was no significant sporadic increase for the same conjugate **14**). Thus the R_6-Penetratin and the two Transportan conjugates of PNA 16mer, in contrast to Tat, Penetratin and R_9F_2 conjugates, must in some way assist significant amounts of PNA to reach the nucleus and interact with TAR RNA during the extended time 24 h time period in order to show such strong inhibition of Tat-dependent *trans*-activation.

Effect of chloroquine addition on CPP–PNA conjugates

In common with most types of biomolecules, it is well known that oligonucleotides and their analogues enter most cells via an endocytotic pathway, of which there are many types (37). In our previous studies with CPP conjugates of LNA/OMe oligonucleotides, confocal microscopy evidence was obtained that the most probable limiting factor in obtaining *trans*-activation inhibition was sequestration within endosomal or other membrane-bound cytosolic compartments (15). We

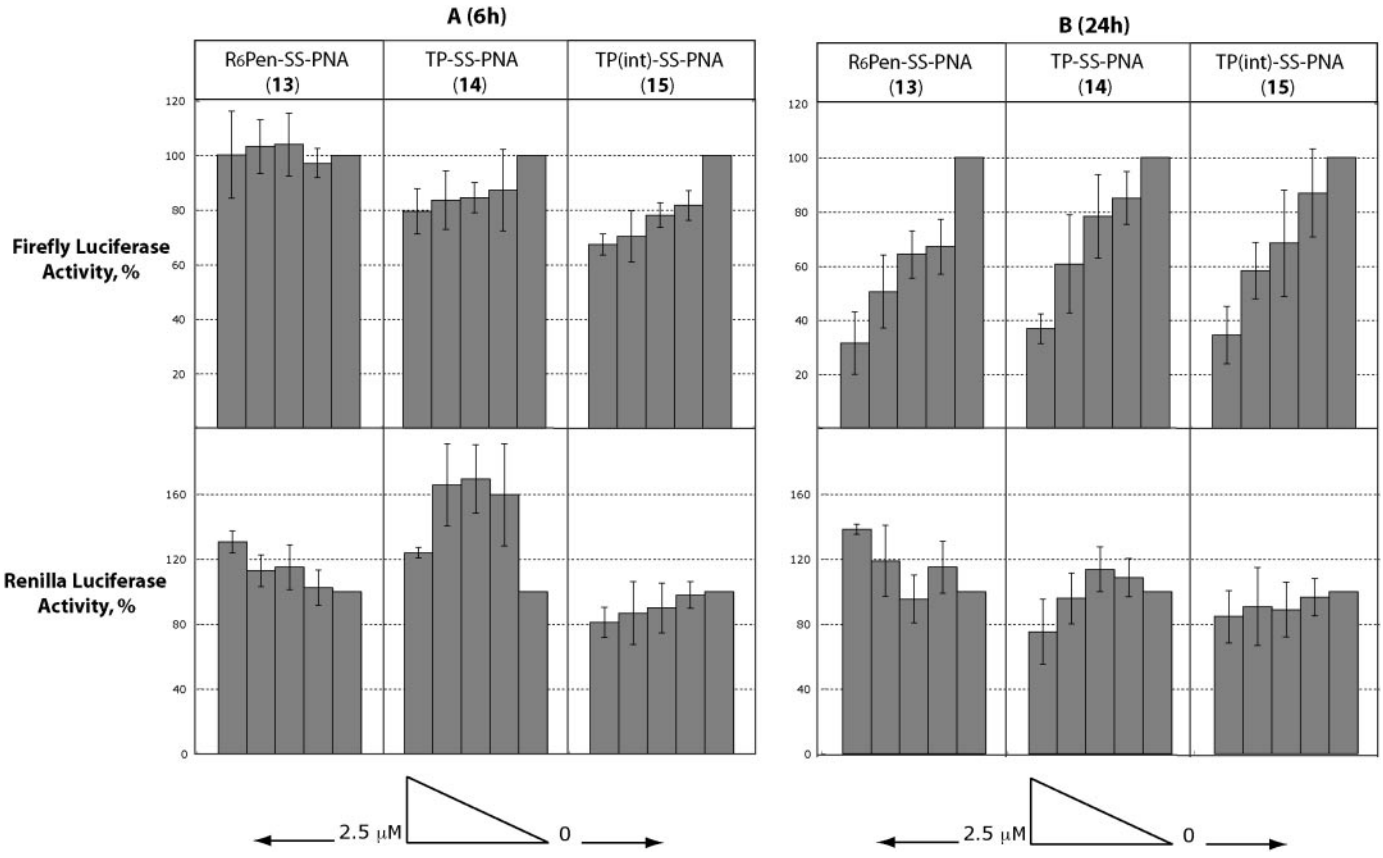

Figure 3. *Trans*-activation inhibitory effects of disulfide-linked CPP–PNA conjugates **13**–**15** in the HeLa cell reporter assay with 6 h delivery (**A**) or 24 h (**B**). Firefly luciferase activity represents Tat-TAR dependent expression whilst *Renilla* luciferase activity represents control constitutive expression. Bars (left to right) in each case represent 2.5, 1.25, 0.625, 0.312 and 0 μM CPP–PNA concentrations.

therefore asked if addition of a known lysosomotropic reagent could enhance the release of CPP–PNA conjugates from such compartments. Chloroquine is an anti-malarial drug and a weak base that passes through membranes in its unprotonated form and accumulates in acidic compartments, such as lysosomes and endosomes, where it leads to osmotic swelling (38). The reagent has been used to study endosomal uptake of antisense oligodeoxynucleotides (1,39,40). The reagent is thought to promote the disruption of endosomal compartments. Similarly lysosomotropic agents increase the efficiency of transgene expression by non-viral delivery vectors (41,42).

We therefore carried out the *trans*-activation inhibition assay with the HeLa cell reporter system with addition of CPP–PNA for 6 h in the presence of 100 μM chloroquine, cells washed and grown for a further 18 h. For stably-linked Tat-PNA conjugate (**1**), there was now seen a significant level of reduction of firefly luciferase (Figure 4A). A smaller reduction (reduction most noticeable at the highest CPP–PNA concentration used) was seen for Transportan-PNA (**2**), TP10–PNA (**3**), NLS–PNA–Tat (**7**) (Figure 4A) and also for PNA–TP10 (**5**) and Tat–PNA–NLS (**8**) (data not shown). No inhibitory activity was observed for NLS–PNA (**4**) or PNA–NLS (**6**) or for K_8–PNA (**9**) (data not shown). No reduction was seen of *Renilla* luciferase activity in any case (data not shown). Cell viability was >85% for all stably-linked CPP–PNAs in the presence of chloroquine.

The three CPP–PNA disulfide conjugates (**13–15**) that had previously shown high firefly luciferase inhibition activity at 24 h in the absence of chloroquine (Figure 3B) showed a strong dose-dependent inhibition of firefly luciferase expression when chloroquine was co-administered with the CPP–PNA for 6 h (Figure 4B). No reduction was seen in any case in *Renilla* luciferase expression as conjugate concentration was increased (data not shown). A small increase in *Renilla* luciferase activity was again seen at high CPP–PNA concentration in occasional cases (data not shown). Cell viability was >70% for the disulfide-linked conjugates in the presence of chloroquine.

To show that sequence-specificity is maintained when chloroquine is co-administered, we tested controls of R_6-Pen-S-S-PNA (**13**) with scrambled and mismatched PNA sequences and both of these showed no inhibitory activity of firefly luciferase expression (Figure 4B). Similar scrambled and mismatched controls for Transportan disulfide PNA conjugate **14** were also inactive (data not shown). Thus chloroquine addition has no effect on the sequence-specificity of the inhibition of Tat-dependent *trans*-activation of the active CPP–PNAs. No effect was seen of 100 μM chloroquine on HeLa cell viability (data not shown) and the level of firefly luciferase activity was not significantly affected by chloroquine alone (Figure 4A and B, minus chloroquine control). However, chloroquine alone treatment did show a reduction

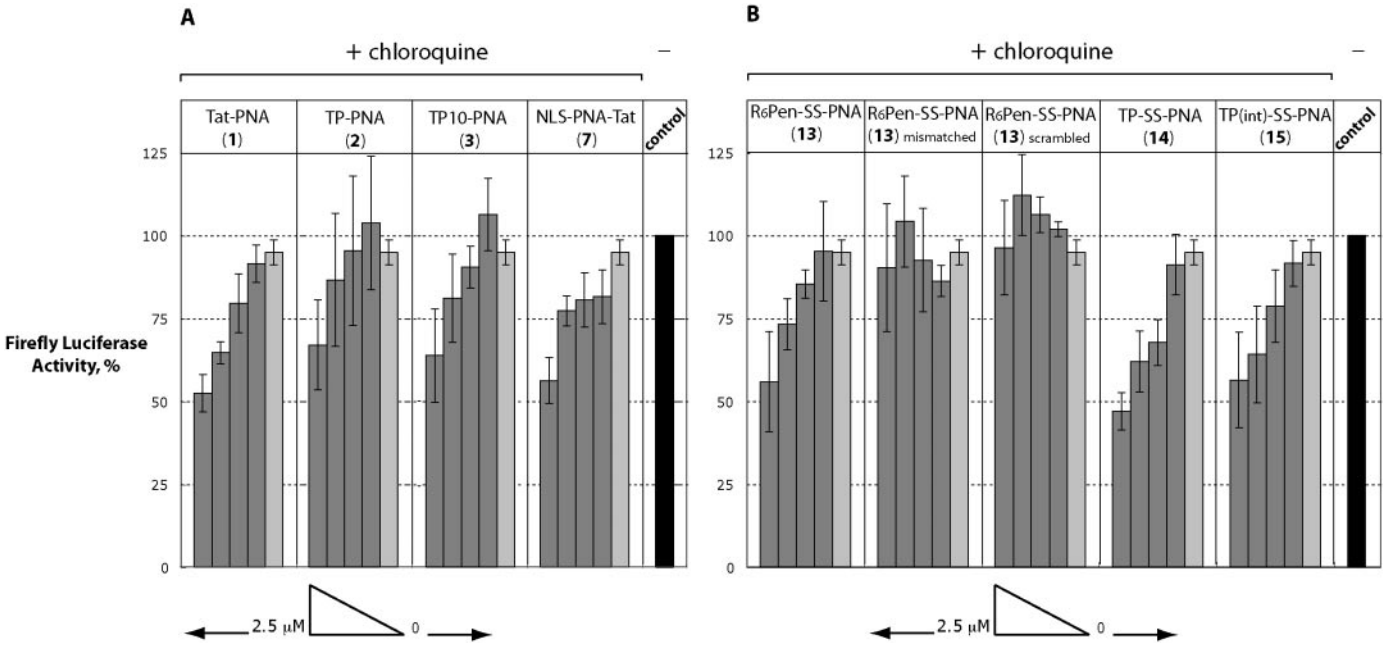

Figure 4. *Trans*-activation inhibitory effects (firefly luciferase activity) of CPP–PNA conjugates in the HeLa cell reporter assay with delivery for 6 h in the presence of 100 μM chloroquine. (**A**) Stably-linked conjugates Tat–PNA (**1**), TP–PNA (**2**), TP10–PNA (**3**) and NLS–PNA–Tat (**7**). (**B**) Disulfide-linked conjugates R_6–Pen-S-S–PNA (**13**), mismatched conjugate **13** (PNA sequence, CTCCGCAGCTCAGATC), scrambled conjugate **13** (PNA sequence, ATCGCTCGCACCATGC), TP–S-S–PNA (**14**) and TP(int)–S-S–PNA (**15**). Bars (left to right) in each case represent 2.5, 1.25, 0.625, 0.312 and 0 μM (light shaded bar) CPP–PNA concentrations. Control (black bar), absence of CPP–PNA and absence of chloroquine.

in the level of *Renilla* luciferase (but no further reduction when CPP–PNA was added) (data not shown).

Overall the chloroquine co-administration data are consistent with the hypothesis that release from endosomal or membrane-bound compartments is limiting in attaining *trans*-activation inhibition activity for CPP–PNA conjugates. Since some stably-linked CPP–PNAs gained activity when chloroquine was co-administered (Figure 4A), a cleavable disulfide bond between CPP and PNA is clearly not essential. However, there is not as yet a fully consistent structure–activity relationship, since no significant inhibition of firefly luciferase was seen with co-administration of chloroquine with Tat-S-S-PNA, Penetratin–S-S–PNA and R_9F_2–S-S–PNA disulfide conjugates **10**–**12** for 6 h (data not shown), which were also inactive in the absence of chloroquine (data not shown).

To look at the time course for the effect of chloroquine on nuclear Tat-dependent *trans*-activation inhibition activity, we co-incubated 2.5 μM of the most active stably-linked conjugate, Tat-PNA (**1**), with 100 μM chloroquine for different times, washed the cells and continued growth in each case for 18 h. The results showed that the majority of the inhibitory effect is seen within 6 h with very little additional reduction in firefly luciferase activity after 8 h (Figure 5). Similar time courses were seen for lower concentrations of Tat-PNA, with correspondingly smaller firefly luciferase expression reductions (data not shown). This shows that 6 h co-administration, the time point when the set of data in Figure 4 was taken, was reasonably well chosen to see most of any observable *trans*-activation inhibition enhancement effect.

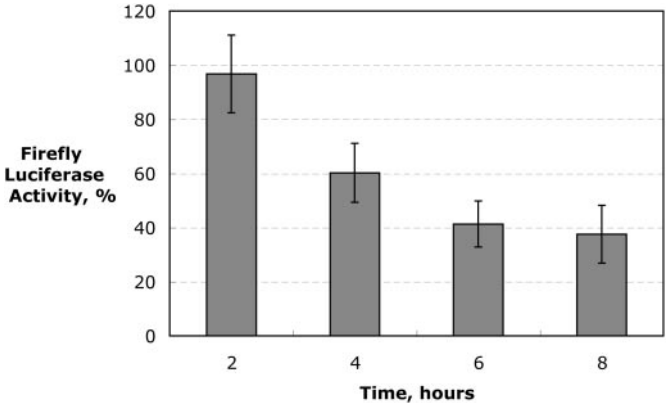

Figure 5. *Trans*-activation inhibitory effects (firefly luciferase activity) of 2.5 μM Tat-PNA (**1**) incubated for 2, 4, 6 or 8 h, respectively, with HeLa reporter cells, cells washed and grown for 18 h before assay.

Confocal microscopy of FAM-labelled CPP–PNA in the absence and presence of chloroquine

To obtain visual evidence for chloroquine release from endosomal or membrane-bound compartments, we examined by live-cell confocal microscopy the ability of FAM-labelled constructs to enter the HeLa cells after 5.5 h, a similar time to that used for the activity experiments (Figure 6). A hydroethidine dye was used to stain the cell nucleus, which makes it easier to observe any nuclear uptake (green colour or yellow colour when overlayed), but also only the nuclei of live cells are stained red, ensuring that only healthy cells are included

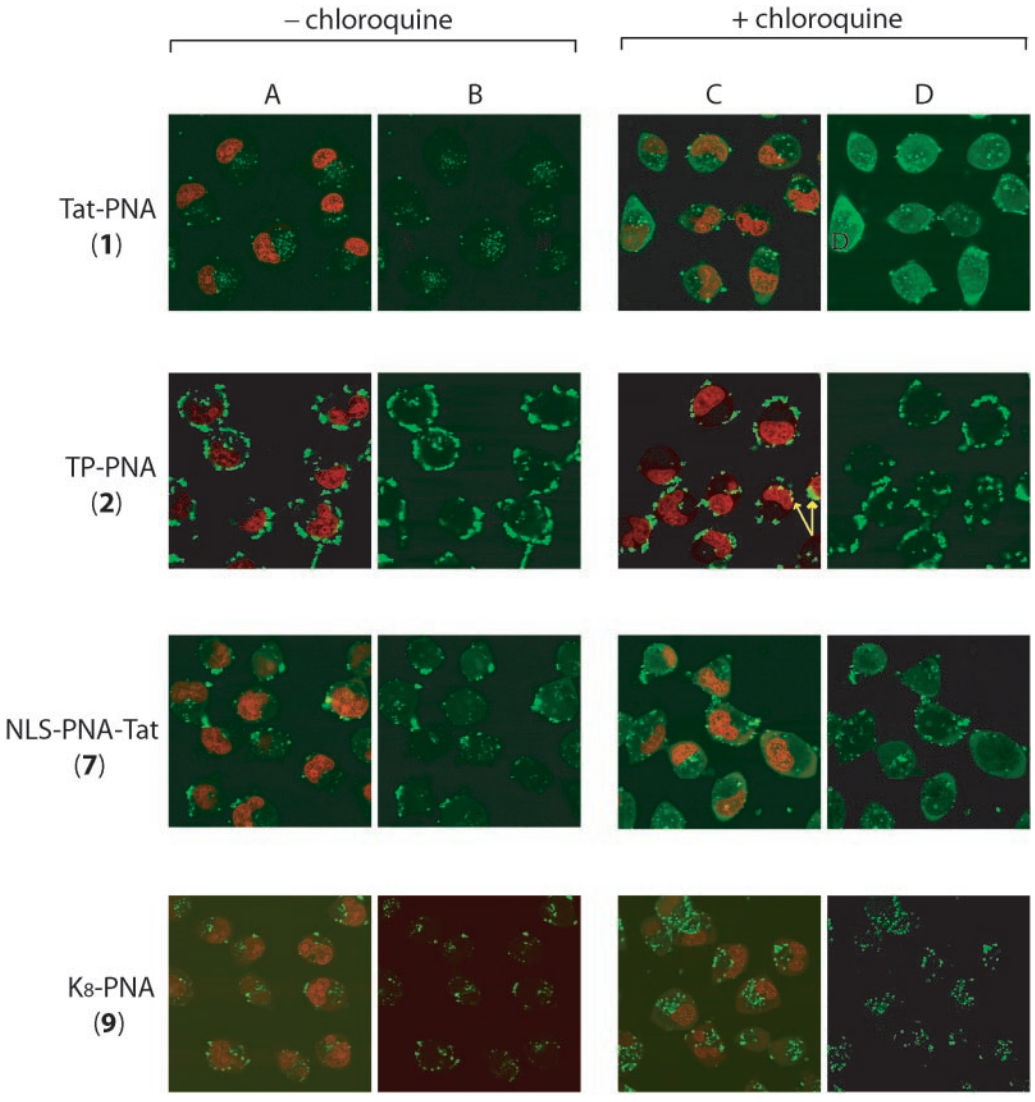

Figure 6. Confocal microscopy images of the uptake of fluorescein (FAM)-labelled CPP–PNA conjugates when incubated for 5.5 h with unfixed HeLa cells. Nuclei are stained red with hydroethidine. (**A** and **C**) Orange filter to view both the red colour of hydroethidine and the fluorescein fluorescence. (**B** and **D**) Green filter to view only the fluorescein fluorescence. (A and B) Show incubations in the absence of chloroquine, (C and D) Show incubations in the presence of 100 μM chloroquine. First line Tat–PNA (**1**); second line Transportan–PNA (**2**); third line NLS–PNA–Tat (**7**); fourth line K_8–PNA (**9**). In (C), second line, yellow dots are marked with arrows showing co-localization of hydroethidine dye and fluorescein fluorescence on the inner wall of the nucleus in several nuclei.

in observations (Figure 6A and C, orange filter). Figure 6B and D shows green emission only. Note that all confocal microscopy experiments used live cells that are unfixed and which are not subject to artefacts of cell fixation (43).

All FAM-labelled CPP–PNA constructs **1**–**9** showed significant cell uptake. For example in the absence of chloroquine, Tat-PNA (**1**) showed a punctate distribution of fluorescence in the cytosol with rather small puncta that were quite well distributed and typical of endosomal sequestration (Figure 6A and B, first line). In contrast Transportan–PNA conjugate (**2**) (Figure 6A and B, second line) and TP10–PNA (**3**) (data not shown) showed strong uptake but a quite different distribution, being concentrated either at or close to the cell surface in large aggregates, with just a few large puncta seen within the cytosol. FAM-labelled constructs containing both NLS and Tat peptides showed a punctate distribution more akin to that of Tat–PNA. For example NLS–PNA–Tat (conjugate **7**, Figure 6A and B, third line) showed both small and large cytosolic puncta. The K_8-PNA uptake pattern (conjugate **9**) (Figure 6A and B, fourth line) looked very similar to that of Tat–PNA conjugate **1**. Since the FAM label in the case of K_8–PNA is on the C-terminus of the PNA (compared with the N-terminus of the peptide in the case of Tat–PNA), this gives confidence that any fluorescence seen is due to intact CPP–PNAs during the 5.5 h delivery period and not as a result of FAM label release. The lack of significant nuclear fluorescence seen in all four conjugate cases is consistent with the lack of activity of the stably-linked CPP conjugate constructs in the *trans*-activation inhibition assay in the absence of chloroquine.

Confocal microscopy of HeLa cells treated for 5.5 h with FAM-labelled Tat–PNA in the presence of 100 μM chloroquine was informative. Conjugate **1** (Figure 6C and D, first line) showed in addition to punctate structures in the cytosol,

a significant and uniform fluorescence in the cytosol and nucleus. This is particularly apparent in the image taken with green emission (Figure 6D), where the hydroethidine red colour is not visible. In contrast, Transportan–PNA (conjugate **2**) in the presence of chloroquine showed the majority of the fluorescence as large aggregates at or close to the cell surface (Figure 6C and D, second line), similar to that seen in the absence of chloroquine (Figure 6A and B). However with hydroethidine staining (Figure 6C) some of the nuclei showed yellow spots (owing to overlay of red and green) just inside the nuclear membrane (yellow arrows). There was very little green fluorescence seen in the cytosol under the green emission (Figure 6D). This suggests that the Transportan–PNA conjugate **2** may have quite different characteristics of cell uptake and trafficking.

NLS–PNA–Tat (**7**) (Figure 6C and D) showed general fluorescence release very similar to that of Tat–PNA (**1**), but less strongly. The same result was seen for Tat–PNA–NLS (**8**) (data not shown). Other constructs such as K_8–PNA (**9**) (Figure 6C and D) did not show strong evidence of uniform cell fluorescence when chloroquine was co-administered and the fluorescence remained punctate, similar to that in the absence of chloroquine (Figure 6A and B). The overall fluorescence in the cytosol (either in endosomes or general) appeared to be higher in many cases when chloroquine was used, but one should note that the overall levels of fluorescence cannot be directly compared in the presence and absence of chloroquine, because fluorescein has substantially reduced fluorescence at the low pH value found within endosomes and chloroquine itself (being a base) is also likely to affect pH.

Overall, the confocal microscopy results show that the nature of the CPP attached stably to the PNA by O-linker affected both the type of vesicular structure seen in the cytosol (mostly punctate or mostly aggregates at the cell surface) as well as whether and how the fluorescence is released by chloroquine addition. It is clear that basic peptides such as Tat promote a radically different cell uptake pattern of PNA (conjugate **1**) from that of Transportan (conjugate **2**). In general, confocal microscopy data provides additional evidence for sequestration of CPP–PNA in endosomal or membrane-bound compartments.

DISCUSSION

The importance of this study centres on how the type of CPP and the way it is linked to a PNA 16mer directed against a HIV-1 TAR target affects the ability of PNA to inhibit Tat-dependent *trans*-activation in HeLa cell nuclei using our stably integrated, double-luciferase reporter plasmid system. The TAR apical stem–loop is a well-validated, steric block antisense target by us (15,22,23,29) and by others (24,44,45). Dose-dependence and sequence-specificity in cells was established previously using lipid-delivered oligonucleotide analogues. Inhibition at the RNA level was verified using a Tat-dependent transcription assay with HeLa cell nuclear extract (22,23). In the current study, we found that two disulfide-linked conjugates of 16mer anti-TAR PNA to Transportan (linked in different ways) or a novel R_6-Penetratin chimeric peptide (conjugates **13**–**15**) were able to inhibit intracellular *trans*-activation at a significant level when incubated for 24 h (Figure 3). In contrast, PNA conjugates disulfide-linked to Tat, Penetratin and R_9F_2 (**10–12**) and a range of CPP conjugates having stable O-linkers between CPP and PNA components (**1–9**) were unable to elicit *trans*-activation inhibition (data not shown).

We have used co-administration of the lysosomotropic reagent chloroquine to provide strong evidence that the barrier to high *trans*-activation inhibition activity in the nucleus is poor release from endosomes or other membrane-bound compartments. The three disulfide-linked CPP–PNA conjugates **13**–**15** that showed inhibition on their own when incubated with cells for 24 h also showed substantial activity within 6 h in the presence of chloroquine, and the sequence-specificity of the inhibitory activity was maintained (Figure 4B). Some stably-linked conjugates that were inactive when delivered alone, e.g. Tat–PNA conjugate **1**, were able to gain significant inhibitory activity in the presence of chloroquine (Figure 4A). The time course of the *trans*-activation inhibitory activity showed that most of the effect occurred within 6 h (Figure 5). Thus an unstable disulfide linkage is not a prerequisite for activity if endosomal release can be enhanced by chloroquine. Surprisingly, activity was not enhanced significantly for some other conjugates, notably PNA disulfide-linked to Tat, Penetratin and R_9F_2 (conjugates **10**–**12**, data not shown). This shows that the structure–function relationship of inhibition activity and chloroquine enhancement is complex and not just a matter of cleavable versus stable linkage. Clearly though, disulfide-linked CPP–PNA **13**–**15** were the only ones that worked in the absence of chloroquine.

Folini *et al*. (46) described recently a photochemical approach to trigger endosomal release from adenocarcinoma cells DU145 of a naked PNA targeted to hTERT mRNA. Incubation of 18 h with high PNA concentration (10 μM) and a photosensitizer was used followed by a 60–80 s fluorescent light treatment. A significant reduction in telomerase activity was observed in cell extracts and some microscopy evidence was obtained for fluorescent PNA redistribution into cytosol and nucleus from endosomal vesicles. A stably-linked Tat–PNA was only slightly active at 2 μM when incubated for 48 h but these authors did not test photochemical release of Tat–PNA (46). Whilst consistent with Folini *et al*. (46), our data is important in that we have used CPP–PNAs, which have much better cell uptake and therefore can be used at lower concentration, short delivery periods (6 h) and a definite nuclear target (hTERT mRNA could have been inhibited either in cytosol or nucleus), as well as a known drug, chloroquine, to demonstrate endosomal release is limiting in attaining *trans*-activation inhibition in HeLa cells.

We observed endosomal and/or membrane sequestration for several stably-linked FAM-labelled CPP–PNA tested (Figure 6). This is consistent with previous observations by others in several cell lines for fluorescently labelled Tat–PNA and Penetratin–PNA, whereas no uptake was observed for PNA alone (4). The very different confocal microscopy uptake patterns of Tat–PNA (**1**) and Transportan–PNA (**2**) confirm previous suggestions that there are at least two classes of CPP, one broadly encompassed by Arg-rich domains, such as Tat (47) and our novel chimeric peptide R_6-Penetratin (15), and another by the more hydrophobic peptide Transportan (25,26,48). We found clear evidence for conjugate release from endosomes by confocal microscopy in the cases of

FAM-labelled stably-linked Tat–PNA (**1**) and NLS–PNA–Tat (**7**) (Figure 6). There was also some evidence of release into the nucleus for stably-linked Transportan–PNA (**2**). In this case there was no general cytosolic fluorescence but instead a different localization pattern that suggests an alternative trafficking pathway for Transportan–PNA.

Our experiments here do not address directly the issue of the type of uptake pathway(s) for the two types of CPP–PNA conjugate nor the precise role of chloroquine in facilitating activity and nuclear delivery. The punctate endosomal location of Tat–PNA **1**, the fluorescence release (Figure 6) and the gain of *trans*-activation inhibition activity (Figure 4) are all completely consistent with our previous data on Tat peptide and Tat–PNA showing sequestration in acidic endosomal compartments (43). In contrast, Transportan clearly directs the PNA into membrane-bound vesicular compartments that are different to those of Tat–PNA conjugates (compare conjugates **1** and **2** in Figure 6). Recently published studies with several cell lines using FACS analysis concluded that a TAMRA-labelled disulfide-linked Transportan–PNA was not taken up by a receptor-mediated or endocytotic process because the kinetics of uptake were not affected by low temperature or by the addition of phenylarsine oxide (27). Our results on chloroquine enhancement of *trans*-activation activity of two types of disulfide-linked TP–PNAs (**13** and **14**, Figure 4B) suggest that some sort of endosomal routing may nevertheless occur, at least in part. However, the clearly different pattern of uptake seen for stably-linked TP–PNA (**2**) in the absence and presence of chloroquine to that of Tat–PNA (**1**) and other cationic peptides (Figure 6) implies that a non-endocytic pathway of delivery is possible in the case of TP–PNA. Further comparative data between the two types of conjugate using specific classes of endocytosis inhibitor, as well as other cell trafficking analysis techniques, will be required to address this point with sufficient clarity.

We found that minimal CPPs, such as a stably-linked K_8–PNA conjugate **9** which was FAM-labelled at the C-terminus of the PNA, were not active in our assay up to 2.5 μM tested, even in the presence of chloroquine (data not shown). Nor did we see evidence for cytosolic release (Figure 6, fourth line). The fact that similar punctate fluorescence patterns were observed in the absence of chloroquine for both N-terminal FAM-labelled Tat–PNA and C-terminally labelled K_8–PNA (Figure 6, compare first and fourth lines) suggests that the fluorescence observed reflects intact CPP–PNA conjugate. It should be noted that biotin labelled Tat, Penetratin and R_9 peptides internalized in cells for several hours and rapidly isolated from cells without chance of proteolysis during isolation were found to be predominantly intact (49).

In work carried out in parallel using a K_8–PNA construct directed to a splice site to redirect splicing and up-regulate production of luciferase, chloroquine co-treatment allowed partial splicing correction and increased luciferase expression in keeping with partial release of the conjugate entrapped within endosomal compartments (50). Treatment with sucrose (which is also believed to promote endocytic vesicles swelling and destabilization) gave similar data. We believe that the splicing correction assay is probably much more sensitive than the anti-TAR *trans*-activation inhibition assay described here. We note that in a different splicing assay IC_{50}s for similar K_n–PNA conjugates were in the micromolar range (34).

Our work complements well previous studies using a disulfide-linked Transportan–PNA conjugate which was shown to inhibit HIV-1 production in chronically infected H9 cells (IC_{50} of 1 μM) when treated in culture for 6 h (26). In our Tat-dependent *trans*-activation assay, two different disulfide-linked Transportan–PNA conjugates and also an R_6–Penetratin–PNA conjugate showed similar inhibition levels (IC_{50} of 0.5–1 μM) (Figure 3) but in each case strong inhibition was only seen after 24 h delivery. Our evidence suggests that CPP–PNA conjugates are sequestered in endosomal or membrane-bound compartments and thus only slowly released. For further studies, we are currently constructing disulfide-linked PNA–peptide conjugates fluorescently labelled on the N-terminus of the PNA. Preliminary confocal microscopy studies on a Tat conjugate showed punctate endosomal sequestration similar to the stably-linked conjugates **1** and **9** (A.A. Arzumanov, unpublished data).

Our studies are important also in consideration as to what extent antiviral effects of PNA-peptides might be due to inhibition of Tat-dependent *trans*-activation. Chaubey *et al.* (27) found recently that their disulfide-linked Transportan–PNA conjugate was active with IC_{50} of 500 nM in an HIV infection inhibition assay when HIV-1 was used to infect CEM cells in the presence of conjugate. Because these experiments were carried out by co-incubation of virus and conjugate with cells, antiviral activity could arise for several reasons, such as interference with viral uptake, inhibition of reverse transcription within partially uncoated virions within the cytosol of infected cells, or by inhibition of Tat-dependent *trans*-activation once the proviral DNA has been integrated into the host. Blocking of reverse transcription *in vitro* by steric block oligonucleotides and PNA complementary to TAR has been well known for some years (51,52) but to what extent this can occur within cells is currently unclear. Our results show that blocking Tat-dependent *trans*-activation is a possible activity in cells, as evidenced by our robust integrated plasmid assay, and that this can be effected by two types of disulfide-linked TP–PNA and a new R_6–Penetratin–PNA. However, this cell activity was only obtained strongly after 24 h incubation.

Our results suggest that entrapment within endosomal or membrane compartments is probable to limit the antiviral activities of many PNA–peptide conjugates and thus there would now be great benefit in investigation of a much wider CPP range that might further enhance endosomal or membrane release. For example, our disulfide-linked R_6–Penetratin–PNA conjugate clearly belongs to a different class to Transportan–PNA conjugates. This peptide is a chimera between Penetratin and a short poly-Arg sequence (53), which is thought to act similarly to Tat peptide. This chimera is therefore a double CPP. We hope to extend our studies to antiviral activities of this and other similar CPP–PNA conjugates in the future.

Chaubey *et al.* (27) also showed that their TP–PNA conjugate was much more highly effective as a virucidal agent with a dose median of 66 nM when HIV-1 virions were pretreated with conjugate before infection of cells. This activity cannot be due therefore to *trans*-activation inhibition. The conjugate was shown to cause abortive termination of reverse transcription within virions, but only when treated at the much higher dose of 0.5 or 1.0 μM. Thus it is not

yet clear if the conjugate binds also to the viral envelope to prevent cell attachment or entry. Further, during preparation of this manuscript, Tripathi *et al*. (54) reported synthesis of Transportan, Transportan TP10 and C-terminally truncated Transportan-linked through a Cys residue added to ε-amino group of Lys-13, as well as Penetratin and Tat peptides linked through their N-termini, in each case to the N-terminus of fluorescein-labelled 16mer PNA. Interestingly, the HIV-1 virucidal activities all fell within a narrow range (28–72 nM dose median) with the Penetratin conjugate being the best, whilst antiviral activities varied from 400 nM IC_{50} for full-length Transportan conjugate to 1.1 μM for truncated Transportan conjugates. Penetratin and Tat conjugates showed 800 and 720 nM IC_{50} respectively. There was no clear correlation of the level of cell uptake as measured by FACS analysis with antiviral activity, and no cell localization experiments were reported.

Contrary to the observations of Tripathi *et al*. (54), who suggested that all these disulfide-linked conjugates are taken up by cells by similar non-endocytotic pathways, because uptake was not seen to be inhibited at 4°C, our confocal microscopy data (Figure 6) suggest sequestration of CPP–PNA in endosomal or membrane-bound compartments and release in the presence of the lysosomotropic reagent chloroquine. Clearly our *trans*-activation inhibition data (Figures 3 and 4) show that two classes of CPP (Transportan and R_6–Penetratin) disulfide-linked to PNA enable nuclear activity to be attained. No clear literature data are available as to whether intracellular cleavage of their disulfide linkages occurs or if PNA–peptide conjugates are released intact from the endosome or other membrane-bound compartment. Confocal microscopy studies of disulfide-linked conjugates carrying different fluorophores on PNA and peptide parts (32) may help to address this issue. But our important data show that a cleavable bond is not essential in principle since stably-linked Tat–PNA **1** is strongly active when chloroquine is co-administered (Figure 4B).

Whilst this manuscript was undergoing review, a paper was published showing that 6 mM calcium ions or 60–120 μM chloroquine co-administration increased the ability of stably-linked Tat-*O*-PNA or R_7–PNA to correct mis-splicing of luciferase mRNA 44- and 8-fold, respectively, in the nucleus of HeLa pLuc 705 cells, but no effect was observed for naked PNA (55). Evidence was presented that the mechanism involves endosomal release. The results presented are fully consistent with our data.

The TAR apical stem–loop target is highly sequence-conserved and is one of several potential targets in the HIV-1 RNA leader suitable for development of oligonucleotide antiviral agents. For example, we reported recently that 16mer OMe/LNA oligonucleotides targeted to TAR, when delivered by cationic lipids, could inhibit HIV replication in a HeLa T4 β-galactosidase cell line (56). PNA–peptides have particularly high potential because of their dual potential for antiviral and virucidal activities and the lack of need for a transfection agent. We are now in a position to improve on such activities by carrying out structure–activity relationships with further peptide–PNA conjugates, concentrating on improving their membrane penetration and endosomal release properties.

SUPPLEMENTARY DATA

Supplementary data are available at NAR Online.

ACKNOWLEDGEMENTS

We thank Martin Fabani for helpful discussions and David Owen for advice on peptide synthesis. This work is funded in part by a grant from EC Framework 5 (contract QLK3-CT-2002-01989). Funding to pay the Open Access publication charges for this article was provided by the EC Framework 5 grant.

Conflict of interest statement. None declared.

REFERENCES

1. Bennett,C.F., Chiang,M.-Y., Chan,H., Shoemaker,J.E.E. and Mirabelli,C.K. (1992) Cationic lipids enhance cellular uptake and activity of phosphorothioate antisense oligonucleotides. *Mol. Pharmacol*., **41**, 1023–1033.
2. Egholm,M., Buchardt,O., Christensen,L., Behrens,C., Freier,S.M., Driver,D.A., Berg,R.H., Kim,S.K., Norden,B. and Nielsen,P. (1993) PNA hybridizes to complementary oligonucleotides obeying the Watson–Crick hydrogen bonding rules. *Nature*, **365**, 566–568.
3. Summerton,J., Stein,D., Huang,S.B., Matthews,P., Weller,D.D. and Partridge,M. (1997) Morpholino and phosphorothioate antisense oligomers compared in cell-free and in cell systems. *Antisense Nucleic Acid Drug Dev*., **7**, 63–70.
4. Koppelhus,U., Awasthi,S.K., Zachar,V., Holst,H.U., Ebbeson,P. and Nielsen,P.E. (2002) Cell-dependent differential cellular uptake of PNA, peptides and PNA–peptide conjugates. *Antisense Nucleic Acid Drug Dev*., **12**, 51–63.
5. Lochmann,D., Jauk,E. and Zimmer,A. (2004) Drug delivery of oligonucleotides by peptides. *Eur. J. Pharm. Biopharm*., **58**, 237–251.
6. Lindsay,M.A. (2002) Peptide-mediated cell delivery: application in protein target validation. *Curr. Opin. Pharmacol*., **2**, 587–594.
7. Wadia,J.S. and Dowdy,S.F. (2002) Protein transduction technology. *Curr. Opin. Biotechnol*., **13**, 52–56.
8. Zorko,M. and Langel,U. (2005) Cell-penetrating peptides: mechanism and kinetics of cargo delivery. *Adv. Drug Deliv. Rev*., **57**, 529–545.
9. Gait,M.J. (2003) Peptide-mediated cellular delivery of antisense oligonucleotides and their analogues. *Cell. Mol. Life Sci*., **60**, 1–10.
10. Thierry,A.R., Vivès,E., Richard,J.-P., Prevot,P., Martinand-Mari,C., Robbins,I. and Lebleu,B. (2003) Cellular uptake and intracellular fate of antisense oligonucleotides. *Curr. Opin. Mol. Ther*., **5**, 133–138.
11. Zatsepin,T.S., Turner,J.J., Oretskaya,T.S. and Gait,M.J. (2005) Conjugates of oligonucleotides and analogues with cell penetrating peptides as gene silencing agents. *Curr. Pharm. Des*., **11**, 3639–3654.
12. Antopolsky,M., Azhayeva,E., Tengvall,U., Auriola,S., Jääskeläinen,I., Rönkkö,S., Honkakoski,P., Urtti,A., Lönnberg,H. and Azhayev,A. (1999) Peptide-oligonucleotide phosphorothioate conjugates with membrane translocation and nuclear localization properties. *Bioconjug. Chem*., **10**, 598–606.
13. Astriab-Fisher,A., Sergueev,D., Fisher,M., Ramsay Shaw,B. and Juliano,R.L. (2002) Conjugates of antisense oligonucleotides with the Tat and Antennapedia cell-penetrating peptides: effect on cellular uptake, binding to target sequences, and biologic actions. *Pharm. Res*., **19**, 744–754.
14. Chen,C.-P., Zhang,L.-R., Peng,Y.-F., Wang,X.-B., Wang,S.-Q. and Zhang,L.-H. (2003) A concise method for the preparation of peptide and arginine-rich peptide-conjugated antisense oligonucleotides. *Bioconjug. Chem*., **14**, 532–538.
15. Turner,J.J., Arzumanov,A.A. and Gait,M.J. (2005) Synthesis, cellular uptake and HIV-1 Tat-dependent *trans*-activation inhibition activity of oligonucleotide analogues disulphide-conjugated to cell-penetrating peptides. *Nucleic. Acids Res*., **33**, 27–42.
16. Dias,N., Dheur,S., Nielsen,P.E., Gryaznov,S., Van Aerschot,A., Herdewijn,P., Hélène,C. and Saison-Behmoaras,T.E. (1999) Antisense

PNA tridecamers targeted to the coding region of Ha-ras mRNA arrest polypeptide chain elongation. *J. Mol. Biol.*, **294**, 403–416.
17. Sazani,P., Kang,S.-H., Maier,M.A., Wei,C., Dillman,J., Summerton,J., Manoharan,M. and Kole,R. (2001) Nuclear antisense effects of neutral, anionic and cationic analogs. *Nucleic Acids Res.*, **29**, 3965–3974.
18. Karn,J. (1999) Tackling Tat. *J. Mol. Biol.*, **293**, 235–254.
19. Rana,T.M. and Jeang,K.-T. (1999) Biochemical and functional interactions between HIV-1 Tat protein and TAR RNA. *Arch. Biochem. Biophys.*, **365**, 175–185.
20. Krebs,A., Ludwig,V., Boden,O. and Göbel,M.W. (2003) Targeting the HIV *trans*-activation responsive region-approaches towards RNA-binding drugs. *Chembiochem*, **4**, 972–978.
21. Arzumanov,A., Walsh,A.P., Liu,X., Rajwanshi,V.K., Wengel,J. and Gait,M.J. (2001) Oligonucleotide analogue interference with the HIV-1 Tat protein–TAR RNA interaction. *Nucleosides Nucleotides Nucleic Acids*, **20**, 471–480.
22. Arzumanov,A., Walsh,A.P., Rajwanshi,V.K., Kumar,R., Wengel,J. and Gait,M.J. (2001) Inhibition of HIV-1 Tat-dependent *trans*-activation by steric block chimeric 2′-O-methyl/LNA oligoribonucleotides. *Biochemistry*, **40**, 14645–14654.
23. Arzumanov,A., Stetsenko,D.A., Malakhov,A.D., Reichelt,S., Sørensen,M.D., Babu,B.R., Wengel,J. and Gait,M.J. (2003) A structure-activity study of the inhibition of HIV-1 Tat-dependent *trans*-activation by mixmer 2′-*O*-methyl oligoribonucleotides containing locked nucleic acid (LNA), α-LNA or 2′-thio-LNA residues. *Oligonucleotides*, **13**, 435–453.
24. Kaushik,M.J., Basu,A. and Pandey,P.K. (2002) Inhibition of HIV-1 replication by anti-transactivation responsive polyamide nucleotide analog. *Antiviral Res.*, **56**, 13–27.
25. Pooga,M., Soomets,U., Hällbrink,M., Valkna,A., Saar,K., Rezaei,K., Kahl,U., Hao,J.-X., Xu,X.-J., Wiesenfeld-Hallin,Z. *et al.* (1998) Cell penetrating PNA constructs regulate galanin receptor levels and modify pain transmission *in vivo*. *Nat. Biotechnol.*, **16**, 857–861.
26. Kaushik,N., Basu,A., Palumbo,P., Nyers,R.L. and Pandey,V.N. (2002) Anti-TAR polyamide nucleotide analog conjugated with a membrane-permeating peptide inhibits Human Immunodeficiency Virus Type I production. *J. Virol.*, **76**, 3881–3891.
27. Chaubey,B., Tripathi,S., Ganguly,S., Harris,D., Casale,R.A. and Pandey,V.N. (2005) A PNA–Transportan conjugate targeted to the TAR region of the HIV-1 genome exhibits both antiviral and virucidal properties. *Virology*, **331**, 418–428.
28. Thomson,S.A., Josey,J.A., Cadilla,R., Gaul,M.D., Hassman,C.F., Luzzio,M.J., Pipe,A.J., Reed,K.L., Ricca,D.J., Wiethe,R.W. *et al.* (1995) Fmoc mediated synthesis of peptide nucleic acids. *Tetrahedron*, **51**, 6179–6194.
29. Holmes,S.C., Arzumanov,A. and Gait,M.J. (2003) Steric inhibition of human immunodeficiency virus type-1 Tat-dependent *trans*-activation *in vitro* and in cells by oligonucleotides containing 2′-O-methyl G-clamp ribonucleoside analogues. *Nucleic Acids Res.*, **31**, 2759–2768.
30. Vivès,E., Brodin,P. and Lebleu,B. (1997) A truncated HIV-1 Tat protein basic domain rapidly translocates through the plasma membrane and accumulates in the cell nucleus. *J. Biol. Chem.*, **272**, 16010–16017.
31. Brandén,L.J., Mohamed,A.J. and Smith,C.I. (1999) A peptide nucleic acids-nuclear localization signal fusion that mediates nuclear transport of DNA. *Nat. Biotechnol.*, **17**, 784–787.
32. Braun,K., Peschke,P., Pipkorn,R., Lampel,S., Wachsmuth,M., Waldeck,W., Friedrich,E. and Debus,J. (2002) A biological transporter for the delivery of peptide nucleic acids (PNAs) to the nuclear compartment of living cells. *J. Mol. Biol.*, **318**, 237–243.
33. Soomets,U., Kilk,T. and Langel,U. (2001) Transportan, its analogues and their applications. In Epton,R. (ed.), *Innovations and Perspectives in Solid Phase Synthesis and Combinatorial Libraries 2000*. Mayflower Press, Kingswinford, UK, pp. 131–136.
34. Siwkowski,A.M., Malik,L., Esau,C.C., Maier,M.A., Wancewicz,E.V., Albertshofer,K., Monia,B.P., Bennett,C.F. and Eldrup,A.B. (2004) Identification and functional validation of PNAs that inhibit murine CD40 expression by redirection of splicing. *Nucleic Acids Res.*, **32**, 2695–2706.
35. Allinquant,B., Hantraye,P., Mailleux,P., Moya,K., Bouillot,C. and Prochiantz,A. (1995) Downregulation of amyloid precursor protein inhibits neurite outgrowth *in vitro*. *J. Cell Biol.*, **128**, 919–927.
36. Moulton,H.M., Nelson,M.H., Hatlevig,S.A., Reddy,M.T. and Iversen,P.L. (2004) Cellular uptake of antisense morpholino oligomers conjugated to arginine-rich peptides. *Bioconjug. Chem.*, **15**, 290–299.
37. Connor,S.D. and Schmidt,S.L. (2003) Regulated portals of entry into the cell. *Nature*, **422**, 37–44.
38. De Duve,C., De Barsy,T., Poole,B., Trouet,A., Tulkens,P. and Van Hoof,F. (1974) Lysosomotropic agents. *Biochem. Pharmacol.*, **23**, 2495–2510.
39. Stewart,A.J., Pichon,C., Meunier,L., Midoux,P., Monsigny,M. and Roche,A.C. (1996) Enhanced biological activity of antisense oligonucleotides complexed with glycosylated poly-L-lysine. *Mol. Pharmacol.*, **50**, 1487–1494.
40. de Diesbach,P., N'Kuli,F., Berens,C., Sonveaux,E., Monsigny,M., Roche,A.C. and Courtoy,P.J. (2002) Receptor-mediated endocytosis of phosphodiester oligonucleotides in the HepC2 cell line: evidence for non-conventional intracellular trafficking. *Nucleic Acids Res.*, **30**, 1512–1521.
41. Ciftci,K. and Levy,R.J. (2001) Enhanced plasmid DNA transfection with lysosomotropic agents in cultured fibroblasts. *Int. J. Pharm.*, **218**, 81–92.
42. Rudolph,C., Plank,C., Lausier,J., Schillinger,U., Müller,R.H. and Rosenecker,J. (2003) Oligomers of the arginine-rich motif of the HIV-1 TAT protein are capable of transferring plasmid DNA into cells. *J. Biol. Chem.*, **278**, 11411–11418.
43. Richard,J.-P., Melikov,K., Vivès,E., Ramos,C., Verbeure,B., Gait,M.J., Chernomordik,L.V. and Lebleu,B. (2003) Cell-penetrating peptides. A re-evaluation of the mechanism of cellular uptake. *J. Biol. Chem.*, **278**, 585–590.
44. Mayhood,T., Kaushik,N., Pandey,P.K., Kashanchi,F., Deng,L. and Pandey,V.N. (2000) Inhibition of Tat-mediated transactivation of HIV-1 LTR transcription by polyamide nucleic acid targeted to the TAR hairpin element. *Biochemistry*, **39**, 11532–11539.
45. Hamma,T., Saleh,A., Huq,I., Rana,T.M. and Miller,P.S. (2003) Inhibition of HIV Tat-TAR interactions by an antisense oligo-2′-*O*-methylribonucleoside methylphosphonate. *Bioorg. Med. Chem. Lett.*, **13**, 1845–1848.
46. Folini,M., Berg,K., Millo,E., Villa,R., Prasmickaite,L., Daidone,M.G., Benatti,U. and Zaffaroni,N. (2003) Photochemical internalization of a peptide nucleic acid targeting the catalytic subunit of human telomerase. *Cancer Res.*, **63**, 3490–3494.
47. Brooks,H., Lebleu,B. and Vivès,E. (2005) Tat peptide-mediated cellular delivery: back to basics. *Adv. Drug Deliv. Rev.*, **57**, 559–577.
48. Kilk,K., Elmquist,A., Saar,K., Pooga,M., Land,T., Bartfai,T., Soomets,U. and Langel,U. (2004) Targeting of antisense PNA oligomers to human galanin receptor type 1 mRNA. *Neuropeptides*, **38**, 316–324.
49. Burlina,F., Sagan,S., Bolbach,G. and Chassaing,G. (2005) Quantification of the cellular uptake of cell-penetrating peptides by MALDI-TOF mass spectrometry. *Angew. Chem. Int. Ed. Engl.*, **44**, 4244–4247.
50. Abes,S., Williams,D., Prevot,P., Thierry,A.R., Gait,M.J. and Lebleu,B. (2005) Endosome trapping limits the efficiency of splicing correction by PNA–oligolysine conjugates. *J. Controlled Release*, in press.
51. Boulmé,F., Perälä-Heape,M., Sarih-Cottin,L. and Litvak,S. (1997) Specific inhibition of *in vitro* reverse transcription using antisense oligonucleotides targeted to the TAR regions of HIV-1 and HIV-2. *Biochim. Biophys. Acta*, **1351**, 249–255.
52. Boulmé,F., Freund,F., Moreau,S., Nielsen,P., Gryaznov,S., Toulmé,J.-J. and Litvak,S. (1998) Modified (PNA, 2′-O-methyl and phosphoramidate) anti-TAR antisense oligonucleotides as strong and specific inhibitors of *in vitro* HIV-1 reverse transcriptase. *Nucleic Acids Res.*, **26**, 5492–5500.
53. Futaki,S. (2005) Membrane-permeable arginine-rich peptides and the translocation mechanisms. *Adv. Drug Deliv. Rev.*, **57**, 547–558.
54. Tripathi,S., Chaubey,B., Ganguly,S., Harris,D., Casale,R.A. and Pandey,P.K. (2005) Anti-HIV-1 activity of anti-TAR polyamide nucleic acid conjugated with various membrane transducing peptides. *Nucleic Acids Res.*, **33**, 4345–4356.
55. Shiraishi,T., Pankratova,S. and Nielsen,P.E. (2005) Calcium ions effectively enhance the effect of antisense peptide nucleic acids conjugated to cationic Tat and oligoarginine peptides. *Chem. Biol.*, **12**, 923–929.
56. Brown,D., Arzumanov,A., Turner,J.J., Stetsenko,D.A., Lever,A.M.L. and Gait,M.J. (2005) Antiviral activity of steric-block oligonucleotides targeting the HIV-1 *trans*-activation response and packaging signal stem-loop RNAs. *Nucleosides Nucleotides Nucleic Acids*, **5-7**, 393–396.

Chapitre III

Alternatives pour la déstabilisation des vésicules d'endocytose

Chapitre III

Alternatives pour la déstabilisation des vésicules d'endocytose

1. Introduction :

Nos travaux récents (voir chapitre II), confortés par la majorité des travaux publiés récemment dans le domaine de la délivrance de biomolécules par des CPPs, font état d'une faible efficacité liée à la séquestration dans les vésicules d'endocytose. Ceci ne constitue pas un handicap insurmontable pour la délivrance de biomolécules requises en quantité faible comme par exemple l'ADN plasmidique ou une protéine enzymatique (Cre-recombinase par exemple). Dans les applications qui nous intéressent et, en particulier, pour la délivrance d'oligonucléotides agissant par blocage stérique sur l'épissage de pré-ARNm, la délivrance de quantités plus importantes de matériel est requise et la séquestration dans les vésicules d'endocytose est une limitation importante. La plupart des travaux réalisés *in vitro* indiquent en effet qu'un traitement par la chloroquine, le sucrose ou le calcium comme agents endosomolytiques reste nécessaire pour promouvoir une réponse antisens significative. Ces agents endosomolytiques agissent sur le pH de l'endosome en bloquant son acidification.
La photoinduction provoque également une déstabilisation des endosomes et une libération de leur contenu (Maiolo et al. 2004). Ce procédé a été utilisé pour augmenter l'efficacité de délivrance par des CPPs (Folini et al. 2003; Matsushita et al. 2004; Shiraishi et Nielsen 2006). Le mécanisme par lequel cette méthode perturbe l'intégrité des endosomes est mal connu. Il semble que l'apparition de dérivés oxygénés suite à l'induction par le laser est à l'origine de cette déstabilisation (Maiolo et al. 2004). Toutefois, l'étude de toxicité liée à la photoinduction indique que ce procédé affecte la viabilité des cellules (Shiraishi et Nielsen 2006). Cependant, ces agents ne sont pas applicables en thérapeutique, et le développement d'une méthode alternative de déstabilisation constituerait une avancée majeure.

2. Partie I : Déstabilisation des endosomes par des peptides fusogènes

2.1. Bilan bibliographique :

Une alternative pour perturber les endosomes est l'exploitation de leur pH légèrement acides. Une telle capacité de déstabilisation pH dépendante est exploitée par des virus et des bactéries qui profitent de l'acidification des vésicules d'endocytose pour s'en échapper. La présence à

leur surface de protéines comportant des domaines qui se structurent d'une manière pH dépendante en hélices amphipatiques, est à l'origine de la déstabilisation de la membrane vésiculaire (Dimitrov 2000; Pecheur et al. 1999). La protéine la mieux documentée est l'hémaglutinine (HA2) du virus Influenza. Sa partie N terminale change de conformation au pH acide des endosomes, conduisant à son insertion dans la membrane de l'endosome et à la fusion des membranes du virus et de l'endosome (Isin et al. 2002). De la même façon, la toxine diphtérique interagit avec la membrane suite à l'exposition de la partie hydrophobe de son domaine d'interaction membranaire (Sandvig et Olsnes 1981).

Plusieurs travaux ont indiqué la possibilité de délivrer des acides nucléiques par association au domaine d'interaction membranaire des toxines (Sandvig et van Deurs 2005). D'autres travaux mentionnent une augmentation de la délivrance de conjugués Tat-Cre recombinase après un co-traitement avec le peptide de fusion Tat-HA2 (Wadia et al. 2004). Cette stratégie d'échappement, pH-dépendante, a également été utilisée pour augmenter l'efficacité de transfection du complexe peptide (4_6)-plasmide suite à une co-incubation avec un peptide de synthèse 4_3E conçu pour se structurer d'une manière pH-dépendante (Ohmori et al. 1997).

Plusieurs peptides possédant cette capacité d'adopter une conformation en hélice-α à pH acide ont été synthétisés et étudiés, comme le peptide GALA (Li et al. 2004) et son dérivé KALA (Wagner 1999), le peptide JST1 (Wagner 1999) ou les polyhistidines (Pichon et al. 2001). Tous ces peptides possèdent la capacité de déstabiliser les membranes phospholipidiques à pH acide.

2.2. Résultats et discussion :

Les travaux de cette partie font l'objet d'une publication (voir article V)

<u>Article V:</u> Peptide-based delivery of nucleic acids: design, mechanism of uptake and applications to splice-correcting oligonucleotides.

Saïd. Abes[1], Hong. M. Moulton[2], John. J. Turner[3], Philippe. Clair[1], Jean philippe. Richard[1], Patrick. Iversen[2], Michael. J. Gait[3] and Bernard. Lebleu[1]

[1]Université Montpellier 2, UMR 5124 CNRS, place Eugene Bataillon, 34095 Montpellier cedex 5, France; [2]AVI BioPharma, 4575 SW Research Way, Corvallis, OR 97330

USA ;[3]Medical Research Council, Laboratory of Molecular Biology, Hills Road, Cambridge, CB2 2 QH, UK

Au cours de cette étude, nous avons testé différents peptides endosomolytiques (voir Tableau VIII).

Tableau VIII : Peptides endosomolytiques utilisés

Peptide déstabilisant	Séquence	Référence
H5WYG	GLFHAIAHFIHGGWHGLIHGWYG	(Midoux et al. 1998)
LR2	RLLRRLLRRLLRLLRR	_____
Palmitoyl-LR2	Palm-RLLRRLLRRLLRLLRR	_____
K_9-LR2	KKKKKKKKKRLLRRLLRRLLRLLRR	_____
Magainine	GIGKFLHSAKKFGKAFVGEIMNS	(Matsuzaki 1998)
Tachyplesine	KWCFRVCYRGICYRRCR	(Doherty et al. 2006)
SynB4 (dérivé de latachyplesine)	AWSFRVSYRGISYRRSR	(Day et al. 2003)
Palmitoyl-SynB4	Palm-AWSFRVSYRGISYRRSR	_____
Protegrine	RGGRLCYCRRRFCVCVGR	(Lam et al. 2006)
SynB1	RGGRLSYSRRRFSTSTGR	(Drin et al. 2003)
Palmitoyl-SynB1	Palm-RGGRLSYSRRRFSTSTGR	_____
Ahx-SynB3	Ahx-RRLSYSRRRF	(Drin et al. 2003)
Palmitoyl-Ahx-SynB3	Palm-Ahx-RRLSYSRRRF	_____
Indolicidine	ILPWKWPWWPWRR	(Chan et al. 2006)

H5WYG est un analogue du domaine N terminal de la sous unité HA2 de l'hémaglutinine dont les acides aminés G_4, G_8, E_{11}, T_{15} et D_{19} sont substitués par des histidines (Midoux et al. 1998; Pichon et al. 2001). Après protonation des résidus histidine à pH ~ 6-7, ce peptide acquière une structure en hélice-α et perturbe les membranes cellulaires.

Nous avons également expérimenté des peptides lytiques, antibactériens. Ces peptides sont généralement cationiques, amphiphiles de 20 à 50 acides aminés. Leur diversité structurale est à l'origine de trois grandes familles : les peptides en hélice-α, les peptides riches en cystéine avec un ou plusieurs ponts disulfures et les peptides riches en tryptophane, comme proposé dans la classification d'Andrès et Dimarcq (Andres et Dimarcq 2007). Nous avons choisi quelques peptides caractéristiques de chacune de ces trois familles :

- La magainine, qui est composée de 23 acides aminés structurés en hélice-α (Matsuzaki 1998).

- La tachyplesine et la protegrine composées de 17 et 18 acides aminés respectivement, avec deux ponts disulfures qui stabilisent leur structure (Doherty et al. 2006; Lam et al. 2006) ainsi que leurs dérivés, la famille SynB (Drin et al. 2003).

- L'indolicidine qui est riche en résidus tryptophane (Chan et al. 2006).

Comme déjà évoqué, le but de cette étude est de trouver un moyen pour s'affranchir de l'utilisation de la chloroquine.
Nous avons rajouté en trans, en présence du conjugué Tat-PNA correcteur d'épissage ces différentes peptides endosomolytiques à des concentrations croissantes, comme schématisé dans la Figure 12. Malheureusement, la co- ou post-incubation des peptides endosomolytiques avec le conjugué correcteur, Tat-PNA, n'augmente pas significativement l'efficacité de correction dans les cellules HelapLuc705 [voir Figure 13 et (Abes et al. 2007)]. Les peptides lytiques utilisés ne sont pas efficaces et de fortes toxicités sont observées aux concentrations supérieures à 0,5µM. Les effets observés avec le Palm-LR2 et K_9LR2 sont effectivement associés à de fortes perméabilisations cellulaires (Abes et al. 2007).

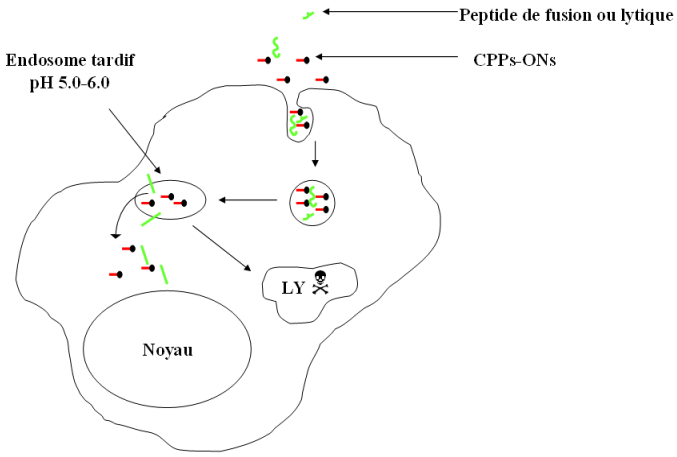

Figure 12 : Stratégie de déstabilisation des endosomes par des peptides de fusion (couleur verte) qui adoptent une structure en hélice-α d'une manière pH dépendante ou qui possèdent une structure en hélice d'une manière permanente. LY correspond au lysosome, ☠ correspond à la dégradation par les enzymes lysosomales.

Comme déjà évoqué, le peptide H5WYG est un analogue de la sous unité HA2 de l'hémaglutinine. Il déstabilise plus efficacement les membranes à pH acide en comparaison à la sous unité HA2 de l'hémaglutinine (Pichon et al. 2001). Les travaux du Dr. F. Dowdy et ses collègues ont mis en évidence une recombinaison efficace par la protéine de fusion Tat-Cre recombinase en présence du conjugué Tat-HA2. L'utilisation de peptide HA2 seul à la même concentration (5µM) n'est pas efficiente. Le couplage Tat-HA2 réduit la concentration de HA2 nécessaire pour perturber les endosomes (Wadia et al. 2004). Des travaux récents ont montré que le peptide hémaglutinine est fonctionnel après oligomérisation (Lau et al. 2004).
Nos expériences montrent qu'entre 0,1 et 0,5µM, soit à des concentrations inférieures à celles décrites dans la littérature, on n'observe aucun effet significatif dans notre modèle de correction d'épissage. Le choix de faibles concentrations se justifie néanmoins par le fait que l'agent endosomolytique ne doit pas affecter la viabilité des cellules.

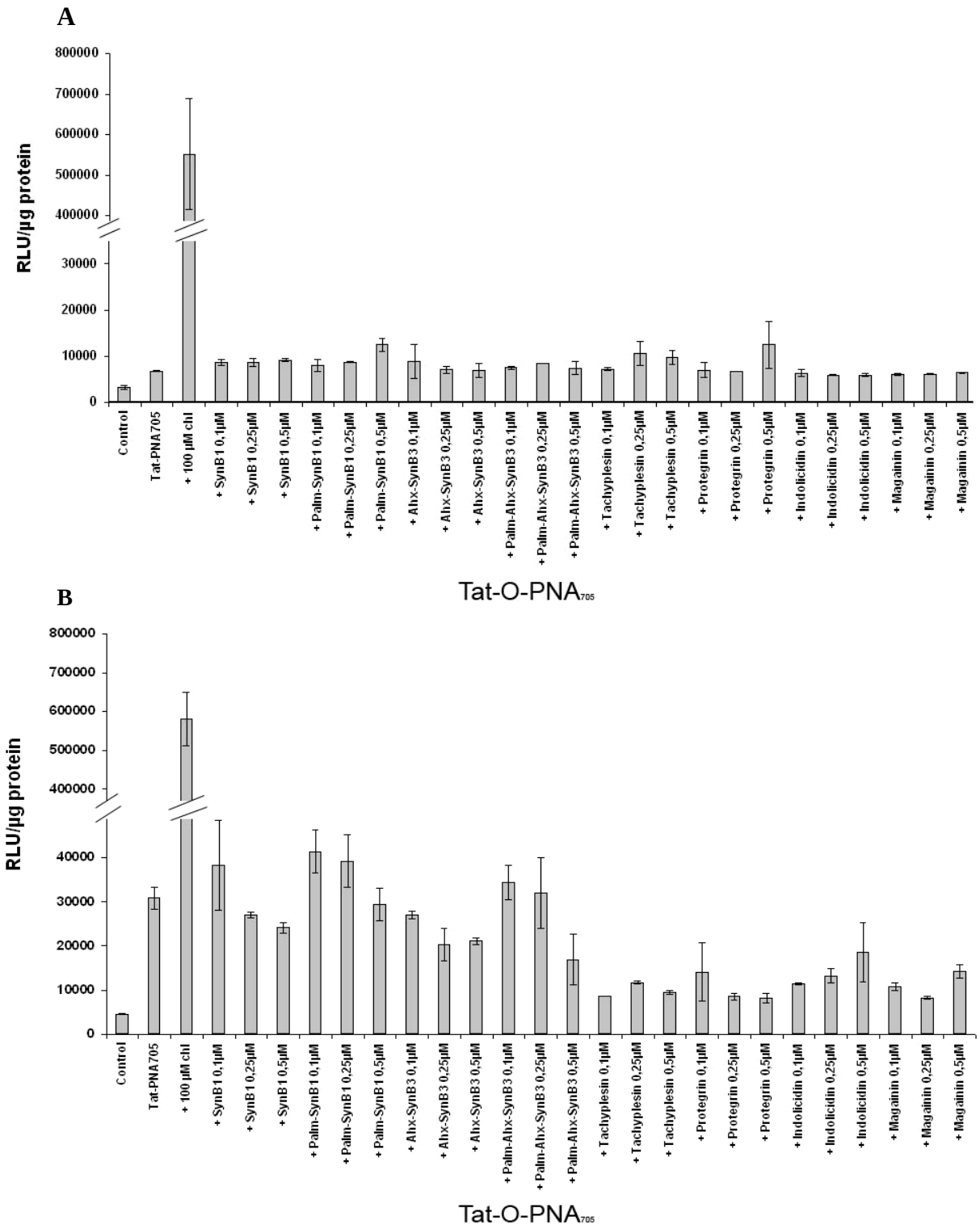

<u>Figure 13</u> : *Effets des peptides endosomolytiques sur la correction d'épissage par le conjugué Tat-PNA :*

Les cellules HeLapLuc705 ont été incubées en absence de conjugué (contrôle négatif) ou avec 1µM du conjugué Tat-PNA correcteur en absence ou en présence de 100µM de chloroquine (contrôle positif), ou en présence de différentes concentrations de peptides endosomolytiques. **(A)** Correspond au protocole de post-incubation où les agents endosomolytiques ont été rajoutés après 4h d'incubation des cellules avec le conjugué correcteur. **(B)** Correspond au protocole de co-incubation où les agents endosomolytiques ont été rajoutés au même temps que le conjugué correcteur.

2.3. Conclusion :

Les travaux présentés dans ce chapitre indiquent la faible efficacité des peptides fusogènes à pouvoir déstabilisant des endosomes dans notre modèle de cellules en culture. Cette stratégie de déstabilisation ne semble donc pas encourageante, mais il est important de noter que les concentrations des peptides endosomolytiques utilisées sont très faibles par rapport à celles décrites dans la littérature.

3. Partie II : Vers de nouveaux peptides vecteurs endosomolytiques

Dans cette stratégie de déstabilisation nous avons opté pour l'utilisation de nouveaux peptides vecteurs. En collaboration avec les équipes du Dr. H. Moulton et du Dr. M. J. Gait, nous avons sélectionné deux peptides riches en arginine très prometteurs : $(R\text{-}Ahx\text{-}R)_4$ et R_6Pen. Rappelons ici que les charges cationiques des CPPs sont nécessaires pour l'internalisation cellulaire, mais que les charges seules ne sont pas suffisantes pour une pénétration efficace.
Nous avons également contribué à la caractérisation d'un peptide amphipathique appelé MAP en collaboration avec l'équipe du Dr. J. Oehlek (Berlin). Ce peptide permet une correction d'épissage en absence de chloroquine lorsqu'il est couplé au PNA705 par un lien stable ou par un pont disulfure (Wolf et al. 2006). Ce peptide amphipathique devient rapidement cytotoxique et nous n'avons pas poursuivi sa caractérisation.

3.1. Bilan bibliographique :

Rothbard et ses collègues ont montré que l'internalisation cellulaire des nonarginines est plus efficace que celle des nonalysines et des nonahistidines (Mitchell et al. 2000; Wender et al. 2000). L'importance des groupements guanidinium a été confirmée par la comparaison des efficacités de pénétration des nonarginines et des nonacitrullines ou nonaornithines (Mitchell et al. 2000). De plus, plusieurs travaux ont établi une délivrance augmentée d'oligonucléotides et de leurs analogues par un greffage de groupements guanidines aux phosphates internucléotidiques (Deglane et al. 2006; Zhou et al. 2003).

Des études de structure-activité ont montré que la longueur de la chaîne d'arginine a une influence sur l'internalisation cellulaire du CPP, avec un optimum pour un squelette de 7 à 15

carbones (Futaki et al. 2001; Mitchell et al. 2000). En outre, l'ajout d'un espaceur entre la chaîne latérale et le squelette peptidique dans des peptoïdes dérivants de la nonarginine augmente d'une manière importante l'entrée cellulaire (Goun et al. 2006; Wender et al. 2000). Des travaux similaires ont indiqué que la longueur du squelette peptidique lui-même affecte significativement la pénétration cellulaire. Enfin, et d'une manière très intéressante, l'espacement entre les arginines augmente l'entrée cellulaire de la polyarginine (Rothbard et al. 2002). Les travaux de Rothbard indiquent par ailleurs que des résidus arginines peuvent être remplacés par des acides aminés non chargés ou même par des acides aminés non naturels sans perte d'efficacité en terme d'internalisation cellulaire. Ceci se comprend à l'examen d'un modèle de la nonarginine qui indique que l'organisation dans l'espace des groupements guanidinium ne leur permet pas d'interagir tous avec les récepteurs membranaires : têtes polaires des phospholipides et / ou l'héparanes sulfates membranaires, comme indiqué récemment par les travaux de plusieurs groupes dont le nôtre (Richard et al. 2005). Le remplacement de résidus arginine par des acides aminés non naturels devrait par ailleurs avoir deux avantages complémentaires : diminuer la densité de charges ainsi que la cytotoxicité associée et augmenter la stabilité métabolique du peptide.

Le processus de pénétration cellulaire utilisé par les nonarginines est un mécanisme endocytotique dépendant de l'énergie, de la température et des glycoprotéoglycanes membranaires (Fuchs et Raines 2004). Leur efficacité d'internalisation se baserait sur les interactions électrostatiques du groupement guanidinium avec les groupements anioniques de la membrane plasmique. Ces interactions sont à l'origine de l'augmentation de l'hydrophobicité du polyarginine ainsi que sa pénétration et sa libération dans la cellule (Goun et al. 2006; Rothbard et al. 2004).

3.2. Résultats et discussions :

Les travaux de cette partie II du chapitre III ont été réalisés en collaboration avec l'équipe du Dr. H. Moulton et l'équipe du Dr. M. J. Gait. Les résultats obtenus font l'objet de deux publications article VI et VII respectivement.

<u>Article VI</u> : Vectorization of morpholino oligomers by the (R-Ahx-R)$_4$ peptide allows efficient splicing correction in the absence of endosomolytic agents.

Saïd Abes, Hong M. Moulton[1], Philippe Clair, Paul Prevot, Derek S. Youngblood[1], Rebecca P. Wu[1], Patrick L. Iversen[1] and Bernard Lebleu
UMR 5124 CNRS, Université Montpellier 2, place Eugene Bataillon, 34095 Montpellier cedex 5, France and [2]AVI BioPharma, 4575 SW Research Way, Suite 200, Corvallis, OR 97330, USA.

Notre étude a porté sur deux aspects importants non abordés dans les travaux de Rothbard :

- L'efficacité de (R-Ahx-R)$_4$ comme vecteur de délivrance de biomolécules en utilisant un modèle de correction d'épissage.
- L'étude du mécanisme d'internalisation de ce conjugué en comparaison avec deux conjugués de références Tat (48-60) et R_9F_2 (Voir Figure 14).

Les trois peptides ont été conjugués au PMO_{705} correcteur d'épissage. Ce travail a indiqué qu'il n'existe aucune corrélation entre l'internalisation cellulaire et l'expression de la luciférase. L'internalisation cellulaire de ces trois conjugués fluorescents a été analysée par microscopie de fluorescence et par cytometrie en flux. Les résultats de microscopie ont montré une localisation vésiculaire extranucléaire des trois peptides. La cytométrie en flux à mis en évidence une pénétration cellulaire plus importante du conjugué R_9F_2-PMO que des deux autres conjugués. D'une manière très intéressante, les résultats de correction d'épissage ont indiqué un ordre d'efficacité indépendant du taux de conjugués internalisés. Cet ordre décroît de (R-Ahx-R)$_4$-PMO > Tat-PMO > R_9F_2-PMO.

(R-Ahx-R)$_4$

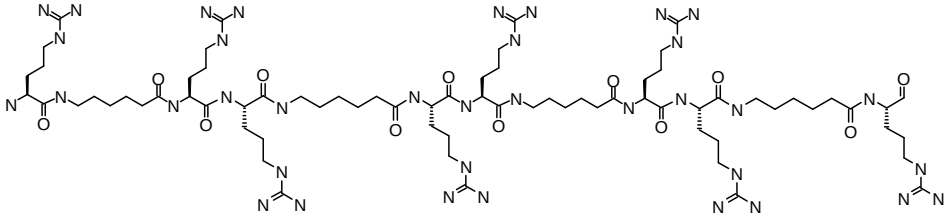

Tat (48-60)

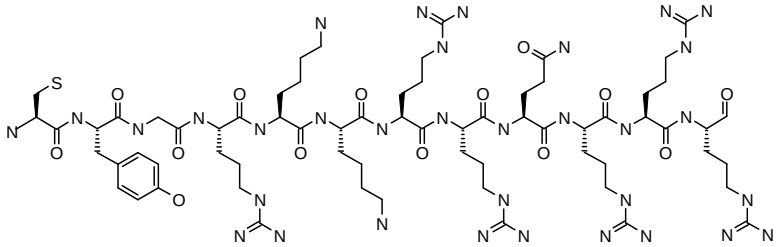

R_9F_2C

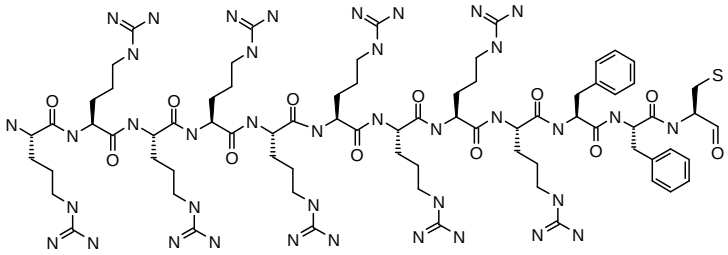

Figure 14 : *Structures linéaires des peptides utilisés*

Afin de mieux comprendre cette différence d'activité, plusieurs hypothèses ont été envisagées. La première se base sur une résistance aux enzymes lysosomales. La présence d'acides aminés non naturels dans le peptide vecteur (R-Ahx-R)$_4$ limite l'activité des protéases. Cette résistance accrue permettrait au conjugué (R-Ahx-R)$_4$-PMO d'être libéré avant une dégradation par les enzymes du lysosome. La seconde est l'affinité pour les héparanes sulfates membranaires qui conditionne l'internalisation cellulaire et peut être à l'origine de la libération des endosomes. En effet, une trop forte affinité pour les héparanes sulfates membranaires pourrait défavoriser la dissociation rapide du complexe conjugué-héparane sulfate après internalisation et empêche ainsi leur libération des compartiments d'endocytose.

Les travaux de nos collaborateurs d'AVIBiopharma sur la stabilité des conjugués (R-Ahx-R)$_4$-PMO et R_9F_2-PMO ont montré que les deux peptides sont dégradés de la même façon dans les cellules après 24 heures (Nelson et al. 2005), mais que la partie PMO reste intacte. Nous

avons exploré les affinités que présente chaque conjugué pour l'héparine, prise comme modèle d'héparanes sulfates. Les trois conjugués étudiés dans cet article présentent des affinités différentes pour l'héparine. Celui qui a le plus d'affinité est le conjugué R_9F_2-PMO ensuite le Tat-PMO et enfin le $(R\text{-}Ahx\text{-}R)_4$-PMO.

Les résultats de la RT-PCR sur le conjugué $(R\text{-}Ahx\text{-}R)_4$-PMO, correcteur d'épissage, ainsi que sa version brouillée ont confirmé que le déroutage de l'épissage est séquence spécifique et qu'il dépend de la concentration du conjugué correcteur (voir Figure 15). Une correction complète est obtenue à la correction de 2,5µM du conjugué $(R\text{-}Ahx\text{-}R)_4$-PMO, confirmant ainsi les donnés obtenues en terme d'activité luciférase.

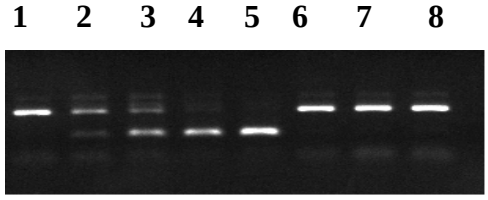

ARNm aberrant

ARNm correctement épissé

1: Contrôle (Cellules non traitées)
2: 0.5µM $(R\text{-}Ahx\text{-}R)_4$-PMO
3: 1µM $(R\text{-}Ahx\text{-}R)_4$-PMO
4: 2.5µM $(R\text{-}Ahx\text{-}R)_4$-PMO
5: 5µM $(R\text{-}Ahx\text{-}R)_4$-PMO
6: 1µM $(R\text{-}Ahx\text{-}R)_4$-PMOsc
7: 5µM $(R\text{-}Ahx\text{-}R)_4$-PMOsc
8: 10µM $(R\text{-}Ahx\text{-}R)_4$-PMOsc

Figure 15 : *Analyse par RT-PCR de l'effet de la concentration du $(R\text{-}Ahx\text{-}R)_4$-PMO705 sur la correction d'épissage :* les cellules HeLapLuc705 ont été incubées avec différentes concentrations du conjugué $(R\text{-}Ahx\text{-}R)_4$-PMO705 correcteur d'épissage ou avec sa version brouillée $R\text{-}Ahx\text{-}R)_4$-PMO705SC. Les cellules ont été lysées, les ARN totaux ont été purifiés et analysés par RT-PCR.

Article VII: Efficient splicing correction by PNA conjugation to an R_6-Penetratin delivery peptide

Saïd Abes, John J. Turner[1], Gabriela D. Ivanova[1], David Owen[1], Donna Williams[1], Philippe Clair, Michael J. Gait[1] and Bernard Lebleu

UMR 5135 CNRS, Université Montpellier 2, Place Eugene Bataillon, 34095 Montpellier cedex 5, France and [1] Medical Research Council, Laboratory of Molecular Biology, Hills Road, Cambridge CB2 2QH UK

Cette partie concerne le travail réalisé en collaboration avec l'équipe du Dr. Mike Gait. Nous y avons testé l'efficacité du peptide R_6-Penetratine (voir Figure 16) pour la délivrance de PNA correcteur d'épissage dans le modèle de Kole.

R_6Pen

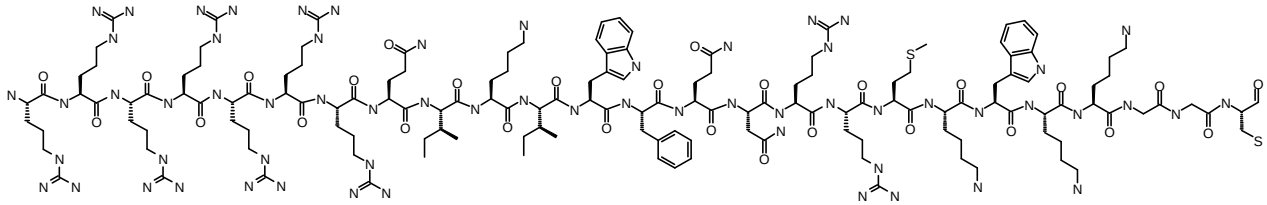

Figure 16 : *Structure linéaire du peptide R_6Pen.*

Comme déjà signalé, la majorité des conjugués correcteurs d'épissage testés dans notre laboratoire ne sont significativement actifs qu'en présence de la chloroquine. La comparaison entre ces différents conjugués et le R_6-Pen-PNA en absence d'agents endosomolytiques a montré une efficacité très intéressante à une concentration qui ne perméabilise pas la membrane cellulaire (voir Tableau IX). Toutefois, l'addition de la chloroquine augmente l'effet de correction par le conjugué R_6Pen-PNA_{705}. La spécificité de correction a été testée par l'utilisation d'une version brouillée du conjugué R_6Pen-PNA_{705}.

Nous avons également étudié l'effet du lien entre le PNA et le CPP. Les résultats ont montré qu'il y a peu de différence entre un lien stable et un pont réductible dans la cellule. Les mêmes résultats ont été obtenus sur un modèle d'inhibition de la transactivation par le peptide Tat (Turner et al. 2005). De même, nos travaux sur les conjugués MAP-PNA_{705} en collaboration avec l'équipe du Dr. J Oehlke ont montré qu'en présence de la chloroquine la version réductible du conjugué est plus efficace que le conjugué stable.

Tableau IX : Pourcentage de cellules non perméabilisées : Les cellules HeLapLuc705 ont été incubées pendant 4 heures en présence des différents conjugués aux concentrations indiquées. Les cellules sont ensuite lavées, trypsinisées et analysées par cytométrie en flux après ajout d'iodure de propidium à une concentration finale de 0,05µg/ml.

		% de cellules non perméabilisées
Control (Non treated cells)	**0µM**	97,9%
Pen-PNA705	**0,5µM**	97,3%
	1µM	97,6%
	2,5µM	98,0%
R3Pen-s-s-PNA705	**0,5µM**	98,1%
	1µM	98,0%
	2,5µM	94,3%
R6Pen-PNA705	**0,5µM**	98,2%
	1µM	97,8%
	2,5µM	96,6%
R6Pen-s-s-PNA705	**0,5µM**	98,4%
	1µM	95.0%
	2,5µM	89,1%
R6Pen(W-L)-s-s-PNA705	**0,5µM**	96,8%
	1µM	96,7%
	2,5µM	93,9%
R9Pen-s-s-PNA705	**0,5µM**	97,4%
	1µM	97,2%
	2,5µM	93,1%

L'analyse de l'effet de la longueur de la queue d'arginine a montré qu'un optimum d'activité est obtenu avec une hexaarginine. Il faut savoir que l'importance des W dans l'internalisation cellulaire est discutée. Les travaux de Prochiantz et ses collègues ont montré l'importance de l'interaction membranaire des résidus tryptophane W_{48} et W_{56} de la pénétratine lors de son internalisation cellulaire. A l'inverse, de Thoren et al (2003) ont démontré que la substitution des tryptophanes par des phénylalanines n'a aucun effet sur la pénétration cellulaire de la pénétratine (Thoren et al. 2003). D'une manière intéressante, une version mutée du conjugué R_6Pen-PNA_{705} dans laquelle le résidu W_{48} est substitué par une Leucine est plus efficace en correction d'épissage que la version non mutée.

L'analyse par RT-PCR a confirmé que la correction d'épissage est spécifique de séquence. Le déroutage de l'épissage par les conjugués correcteurs permet l'apparition de la bande

d'ARNm correctement épissée et la disparition partielle de la bande aberrante à faible concentration (voir Figure 17).

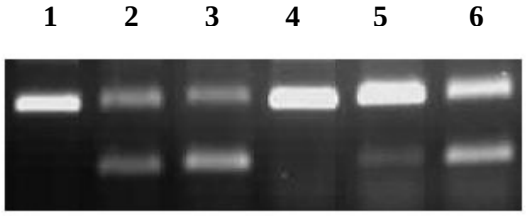

Figure 17 : *Analyse par RT-PCR de l'efficacité de correction par les conjugués R6Pen-PNA :* les cellules HeLapLuc705 ont été incubées avec différents conjugués correcteurs. Les cellules ont été lysées, les ARN totaux ont été purifiés et analysés par RT-PCR.

3.3. Conclusion :

La question posée dans ce chapitre était de savoir comment s'affranchir d'un traitement par des agents endosomolytiques pour délivrer efficacement des oligonucléotides à l'aide de CPPs à des concentrations faibles et sans cytotoxicité. Deux stratégies ont été testées.

La première est basée sur l'utilisation des peptides connus pour leur potentiel de déstabilisation membranaire. Les résultats obtenus après une co- ou post-incubation en trans de ces peptides avec le conjugué correcteur d'épissage ne sont pas encourageants.

La seconde a consisté à utiliser de nouveaux peptides vecteurs. Avec nos collaborateurs nous avons sélectionné deux peptides prometteurs : le R_6Pen et le $(R\text{-}Ahx\text{-}R)_4$. Les deux peptides permettent de délivrer efficacement différents analogues d'ONs correcteurs d'épissage. La correction d'épissage est spécifique de la séquence et est indépendante de l'addition d'agents endosomolytiques. Néanmoins, l'addition de la chloroquine augmente l'effet de correction. Les études de structure activité sur le R_6Pen-PNA ont montré qu'un optimum de correction est obtenu avec une hexaarginine, le type de couplage entre le CPP et l'ON influençant peu l'activité de correction. La mutation W_{48}-L n'a quant à elle pas d'effet sur la correction. Nous avons également démontré qu'il n'y a pas de corrélation positive entre l'internalisation cellulaire et l'efficacité de correction. En revanche, une forte affinité à l'héparine semble entraîner une forte pénétration cellulaire et une faible correction d'épissage.

Peptide-based delivery of nucleic acids: design, mechanism of uptake and applications to splice-correcting oligonucleotides

S. Abes*, H. Moulton†, J. Turner‡, P. Clair*, J.P. Richard*, P. Iversen†, M.J. Gait‡ and B. Lebleu*[1]

*Université Montpellier 2, UMR 5124 CNRS, place Eugene Bataillon, 34095 Montpellier cedex 5, France, †AVI BioPharma, 4575 SW Research Way, Corvallis, OR 97330, U.S.A., and ‡Medical Research Council, Laboratory of Molecular Biology, Hills Road, Cambridge CB2 2QH, U.K.

Abstract

CPPs (cell-penetrating peptides) have given rise to much interest for the delivery of biomolecules such as peptides, proteins or ONs (oligonucleotides). CPPs and their conjugates were initially thought to translocate through the cell membrane by a non-endocytotic mechanism which has recently been re-evaluated. Basic-amino-acid-rich CPPs first interact with cell-surface proteoglycans before being internalized by endocytosis. Sequestration and degradation in endocytotic vesicles severely limits the cytoplasmic and nuclear delivery of the conjugated biomolecules. Accordingly, splicing correction by CPP-conjugated steric-block ON analogues is inefficient in the absence of endosomolytic agents. New arginine-rich CPPs allowing efficient splicing correction by conjugated PNAs (peptide nucleic acids) or PMO (phosphorodiamidate morpholino oligomer) steric blockers in the absence of endosomolytic agents have recently been defined in our group and are currently being characterized. They offer promising leads for the development of efficient cellular delivery vectors for therapeutic steric-block ON analogues.

Synthetic ONs (oligonucleotides) allow an efficient and specific control of gene expression and they have therefore been extensively used in functional genomics. Likewise several ON-based strategies [antisense ONs, aptamers, siRNA (small interfering RNA)] are currently under clinical evaluation for the treatment of cancers, pathogenic infections and genetic diseases. A major limitation of ON-based therapy is poor ON bioavailability, hence the search for delivery vehicles [1,2].

Among the many strategies for delivery of biomolecules, conjugation to CPPs (cell-penetrating peptides) has received a wide audience. The CPP concept emerged when it was realized that the *Drosophila Antennapedia* transcription factor [3] or the HIV-1 Tat (transactivator of transcription) [4] was able to cross biological membranes. In both cases, cellular uptake of the proteins is due to a short and basic-amino-acid-rich stretch of residues (GRKKRRQRRRP for the Tat-derived peptide [5]). Importantly for biotechnological applications, CPP conjugation or fusion enhances the delivery of membrane-impermeant biomolecules, such as peptides, proteins or ONs [6].

A mechanism of direct translocation across the plasma membrane has initially been proposed for CPP uptake. However, this view has been revised at least for basic-amino-acid-rich CPPs, such as penetratin, oligoarginine and Tat-(48–60) [7]. It is now generally accepted that arginine- or lysine-rich CPP–cargo conjugates first interact with membrane-associated proteoglycans and are then internalized by endocytosis [8,9]. Whether clathrin-coated pits, caveosomes or macropinocytosis is involved is still controversial and may depend on cell type, conjugated cargo and other factors [10].

As long as endocytosis is involved, segregation and degradation of the CPP–cargo conjugates within endocytotic compartments are anticipated. This could explain why CPP-mediated delivery of antisense ON has been unsuccessful in several instances. For example, Turner et al. [11] surveyed a large collection of CPP–ON conjugates with the aim of inhibiting the Tat transactivation of an HIV promoter. No significant inhibition was obtained, consistent with a cytoplasmic-dotted distribution of the fluorochrome-tagged CPP–ON conjugates. In another study, oligolysine-tagged PNAs (peptide nucleic acids) were inactive in the splicing correction assay developed by Kole's group [12], at variance with earlier data by other groups [13,14]. In this assay, a mutated intron carrying a cryptic splice site was inserted in the coding region of a luciferase reporter gene and the chimaeric plasmid was stably transfected in HeLa $pLuc_{705}$ cells. Luciferase expression is conditional on the hybridization of an SSO (splice-switching ON), thus providing a well-controlled assay for the nuclear delivery of the SSO.

Chemical and physical agents known to destabilize endocytotic vesicles largely increased splicing correction [15–17] or transactivation inhibition [18] by various CPPs conjugated to steric-block ON which further indicates that endosomal trapping limits CPP-based ON delivery. As an example, splice-correcting PNA_{705} (Figure 1) or PMO_{705} (PMO is

Key words: cell-penetrating peptide (CPP), endocytosis, nucleic acid delivery, peptide-based delivery, splice-correcting oligonucleotide.

Abbreviations used: Ahx, 6-aminohexanoic acid; CPP, cell-penetrating peptide; ON, oligonucleotide; PMO, phosphorodiamidate morpholino oligomer; PNA, peptide nucleic acid; SSO, splice-switching ON; Tat, transactivator of transcription.

[1]**To whom correspondence should be addressed (email blebleu@univ-montp2.fr).**

Figure 1 | Splicing correction by Tat CPP–SSO conjugate

(**A**) Effect of chloroquine on splicing correction by Tat–O–PNA_{705}. HeLa $pLuc_{705}$ cells were incubated with Tat–O–PNA_{705} at the indicated concentrations in the absence or the presence of 100 μM chloroquine. (**B**) Effects of the linker between Tat and PNA_{705} on splicing correction. HeLa $pLuc_{705}$ cells were incubated with 1 μM Tat–O–PNA_{705} or Tat–Cys-s–s-PNA_{705} in the absence or in the presence of 100 μM chloroquine. Luciferase activities were expressed as relative luminescence units (RLU) per μg of protein. All experiments were performed in triplicate. Results are means ± S.D.

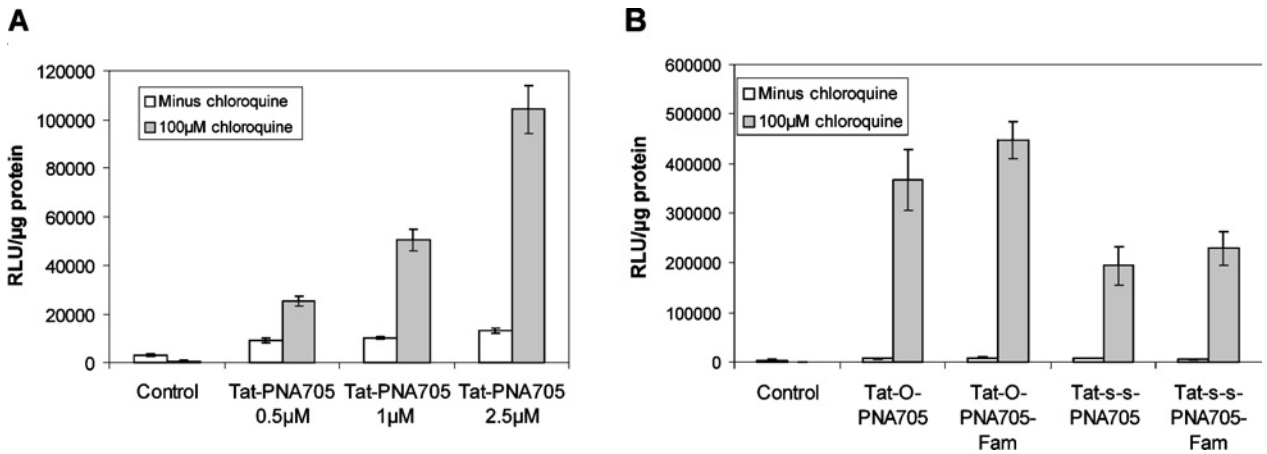

Figure 2 | Effect of membrane-destabilizing peptides on splicing correction

HeLa $pLuc_{705}$ cells were incubated with 1 μM Tat–O–PNA_{705} in the absence (control) or in the presence of 100 μM chloroquine, or in the presence of membrane-destabilizing peptide at the indicated concentration. (**A**) Post-incubation protocol: chloroquine or membrane-destabilizing peptide was added after incubation of cells with 1 μM Tat–O–PNA_{705}. (**B**) Co-incubation protocol: chloroquine or membrane-destabilizing peptide was added together with 1 μM Tat–O–PNA_{705}. Luciferase activity was quantified as described in Figure 1.

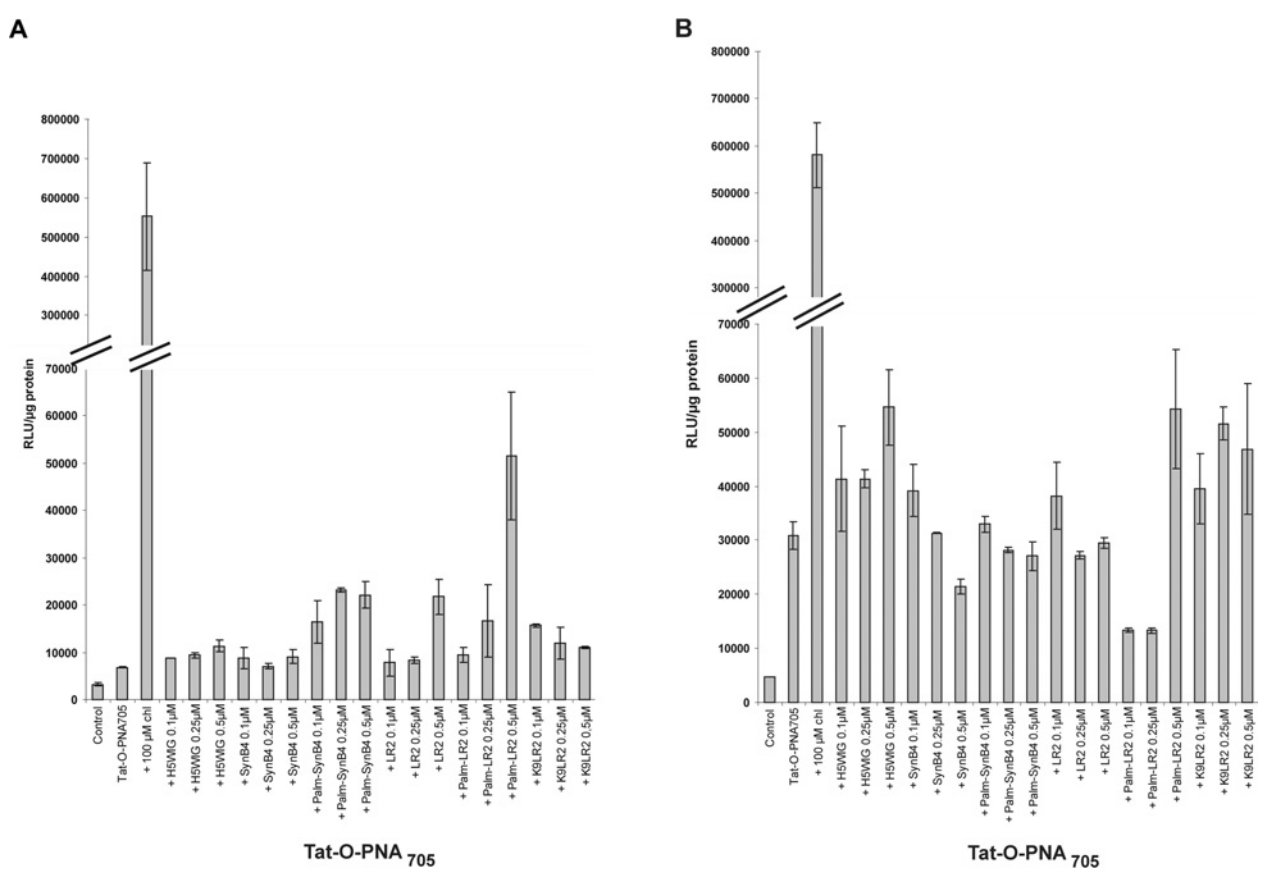

Figure 3 | Splicing correction with (R–Ahx–R)$_4$–PNA$_{705}$

HeLa pLuc$_{705}$ cells were incubated with (R–Ahx–R)$_4$–PNA$_{705}$ at the indicated concentrations in the absence of chloroquine, and luciferase activity was quantified as described in Figure 1.

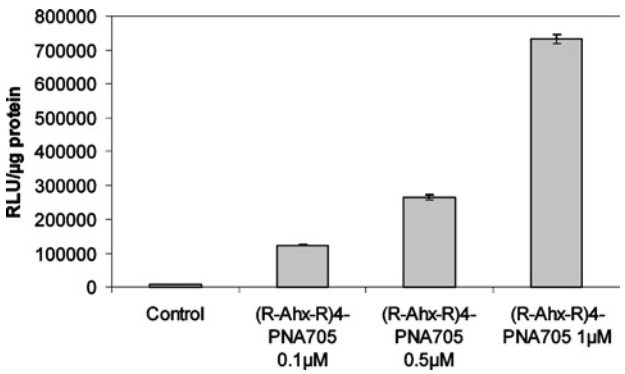

phosphorodiamidate morpholino oligomer) [19] have been conjugated to Tat-(48–60) through either stable or reducible linkers. No significant luciferase expression was achieved in the absence of treatment with chloroquine, an endosomolytic drug.

It is now generally accepted that endosome trapping limits CPP-based ON delivery and that strategies are needed to overcome this limitation. Indeed, most of the endosomolytic agents reported so far cannot be envisaged easily for *in vivo* treatments.

Co- or post-incubation of the Tat–PNA$_{705}$ conjugate with membrane-destabilizing or fusogenic peptides was first explored following an earlier report showing enhanced protein transfection by Tat–Cre recombinase in the presence of the influenza haemagglutinin fusogenic peptide [20]. Treatment of HeLa pLuc$_{705}$ cells with Tat–PNA$_{705}$ in the presence of these peptides did not result in significant enhancement of luciferase expression compared with the treatment with chloroquine (Figure 2). The only active peptide, namely a palmitoylated Leu–Arg repeat [(LR)$_2$], was unfortunately cytotoxic at its active dose.

Most studies have pointed to the key role played by guanidinium groups of arginine side chains for the binding and internalization of CPPs. Accordingly, short oligoarginine stretches enhance the cellular internalization of conjugated low-molecular-mass drugs or biomolecules [21]. An oligoarginine CPP was slightly more efficient than Tat CPP in promoting the nuclear delivery of the splicing-correcting PMO$_{705}$, but became cytotoxic rapidly [21]. Molecular modelling by Rothbard et al. [22] has revealed that not all guanidinium groups in a stretch of consecutive arginine residues are able to interact with a model membrane. The same authors systematically surveyed the cellular uptake of peptides in which arginine residues alternated with natural or unnatural amino acids. One of the most efficient was (R–Ahx–R)$_3$–Arg (where Ahx is 6-aminohexanoic acid). Conjugation of PMO$_{705}$ [19] or PNA$_{705}$ (Figure 3) to (R–Ahx–R)$_4$ leads to very significant splicing correction in Kole's model in the absence of chloroquine.

Since these conjugates are not cytotoxic when tested over a large range of concentrations, the (R–Ahx–R)$_4$ CPP might represent an interesting lead for the development of therapeutic ONs. Structure–activity relationship studies are currently being undertaken to improve the cytoplasmic and nuclear ON delivery.

Work in our groups has been funded by grants from IFCPAR (Indo-French Centre for the Promotion of Advanced Research) (B.L.) and EC Framework 5 (B.L. and M.G.). S.A. holds a pre-doctoral fellowship from the Ligue Contre le Cancer. R. Kole (University of North Carolina) is acknowledged for providing the HeLa pLuc$_{705}$ strain for the splicing-correction assay, and P. Prevot (Université Montpellier) is thanked for his help with fluorescence microscopy.

References

1 Gewirtz, A.M., Sokol, D.L. and Ratajczak, M.Z. (1998) Blood **92**, 712–736
2 Lochmann, D., Jauk, E. and Zimmer, A. (2004) Eur. J. Pharm. Biopharm. **58**, 237–251
3 Joliot, A. and Prochiantz, A. (2004) Nat. Cell Biol. **6**, 189–196
4 Frankel, A.D. and Pabo, C.O. (1988) Cell. Mol. Biol. Lett. **55**, 1189–1193
5 Vives, E., Brodin, P. and Lebleu, B. (1997) J. Biol. Chem. **272**, 16010–16017
6 Mae, M. and Langel, U. (2006) Curr. Opin. Pharmacol. **6**, 509–514
7 Richard, J.P., Melikov, K., Vives, E., Ramos, C., Verbeure, B., Gait, M.J., Chernomordik, L.V. and Lebleu, B. (2003) J. Biol. Chem. **278**, 585–590
8 Richard, J.P., Melikov, K., Brooks, H., Prevot, P., Lebleu, B. and Chernomordik, L.V. (2005) J. Biol. Chem. **280**, 15300–15306
9 Jones, S.W., Christison, R., Bundell, K., Voyce, C.J., Brockbank, S.M., Newham, P. and Lindsay, M.A. (2005) Br. J. Pharmacol. **145**, 1093–1102
10 Pujals, S., Fernandez-Carneado, J., Lopez-Iglesias, C., Kogan, M.J. and Giralt, E. (2006) Biochim. Biophys. Acta **1758**, 264–279
11 Turner, J.J., Arzumanov, A.A. and Gait, M.J. (2005) Nucleic Acids Res. **33**, 27–42
12 Kang, S.H., Cho, M.J. and Kole, R. (1998) Biochemistry **37**, 6235–6239
13 Sazani, P., Kang, S.H., Maier, M.A., Wei, C., Dillman, J., Summerton, J., Manoharan, M. and Kole, R. (2001) Nucleic Acids Res. **29**, 3965–3974
14 Siwkowski, A.M., Malik, L., Esau, C.C., Maier, M.A., Wancewicz, E.V., Albertshofer, K., Monia, B.P., Bennett, C.F. and Eldrup, A.B. (2004) Nucleic Acids Res. **32**, 2695–2706
15 Abes, S., Williams, D., Prevot, P., Thierry, A., Gait, M.J. and Lebleu, B. (2006) J. Controlled Release **110**, 595–604
16 Shiraishi, T., Pankratova, S. and Nielsen, P.E. (2005) Chem. Biol. **12**, 923–929
17 Shiraishi, T. and Nielsen, P.E. (2006) FEBS Lett. **580**, 1451–1456
18 Turner, J.J., Ivanova, G.D., Verbeure, B., Williams, D., Arzumanov, A.A., Abes, S., Lebleu, B. and Gait, M.J. (2005) Nucleic Acids Res. **33**, 6837–6849
19 Abes, S., Moulton, H.M., Clair, P., Prevot, P., Youngblood, D.S., Wu, R.P., Iversen, P.L. and Lebleu, B. (2006) J. Controlled Release **116**, 304–313
20 Wadia, J.S., Stan, R.V. and Dowdy, S.F. (2004) Nat. Med. **10**, 310–315
21 Wright, L.R., Rothbard, J.B. and Wender, P.A. (2003) Curr. Protein Pept. Sci. **4**, 105–124
22 Rothbard, J.B., Kreider, E., VanDeusen, C.L., Wright, L., Wylie, B.L. and Wender, P.A. (2002) J. Med. Chem. **45**, 3612–3618

Received 18 August 2006

Available online at www.sciencedirect.com
ScienceDirect
Journal of Controlled Release 116 (2006) 304–313
journal of controlled release
www.elsevier.com/locate/jconrel

Vectorization of morpholino oligomers by the (R-Ahx-R)$_4$ peptide allows efficient splicing correction in the absence of endosomolytic agents☆

Saïd Abes [a,1], Hong M. Moulton [b,1], Philippe Clair [a], Paul Prevot [a], Derek S. Youngblood [b], Rebecca P. Wu [b], Patrick L. Iversen [b], Bernard Lebleu [a,*]

[a] UMR 5124 CNRS, Université Montpellier 2, place Eugene Bataillon, 34095 Montpellier cedex 5, France
[b] AVI BioPharma, 4575 SW Research Way, Suite 200, Corvallis, OR 97330, USA

Received 11 July 2006; accepted 14 September 2006
Available online 30 September 2006

Abstract

The efficient and non-toxic nuclear delivery of steric-block oligonucleotides (ON) is a prerequisite for therapeutic strategies involving splice correction or exon skipping. Cationic cell penetrating peptides (CPPs) have given rise to much interest for the intracellular delivery of biomolecules, but their efficiency in promoting cytoplasmic or nuclear delivery of oligonucleotides has been hampered by endocytic sequestration and subsequent degradation of most internalized material in endocytic compartments. In the present study, we compared the splice correction activity of three different CPPs conjugated to PMO$_{705}$, a steric-block ON targeted against the mutated splicing site of human β-globin pre-mRNA in the HeLa pLuc705 splice correction model. In contrast to Tat48–60 (Tat) and oligoarginine (R_9F_2) PMO$_{705}$ conjugates, the 6-aminohexanoic-spaced oligoarginine (R-Ahx-R)$_4$–PMO$_{705}$ conjugate was able to promote an efficient splice correction in the absence of endosomolytic agents. Our mechanistic investigations about its uptake mechanisms lead to the conclusion that these three vectors are internalized using the same endocytic route involving proteoglycans, but that the (R-Ahx-R)$_4$–PMO$_{705}$ conjugate has the unique ability to escape from lysosomial fate and to access to the nuclear compartment. This vector, which has displays an extremely low cytotoxicity, the ability to function without chloroquine adjunction and in the presence of serum proteins. It thus offers a promising lead for the development of vectors able to enhance the delivery of therapeutic steric-block ON in clinically relevant models.

Keywords: Splice correction; PMO antisens; CPPs; (R-Ahx-R) 4; Endosomolytic agents

1. Introduction

Promising oligonucleotide (ON)-based strategies leading to sequence-specific control of gene expression have been proposed but their applications are limited by poor delivery into cytoplasm and nuclear compartments [1]. The most popular tools for nucleic acids delivery are cationic vectors such as lipoplexes or PEI. However they are not devoid of cytotoxicity, and most are not effective in the presence of serum proteins [2,3] Moreover, they cannot easily be used to transfect neutral ON analogs such as peptide nucleic acids (PNAs) [4] or phosphorodiamidate morpholino oligomers (PMOs) [5].

Cell penetrating peptides (CPPs) have been of much interest as delivery vectors for biomolecules such as peptides or nucleic acids [6]. Many publications describe the use of CPPs for protein or peptide transfection [7] but, surprisingly, relatively little has been documented for the CPP-based delivery of antisense ON analogs [8]. A series of independent studies have established recently that CPPs rich in basic amino acids (oligolysine, oligoarginine or Tat) did not efficiently promote the nuclear delivery of conjugated antisense ON analogs [9–11]. This might

Abbreviations: CHO, Chinese hamster ovary; CPP, cell penetrating peptide; Fam, carboxyfluorescein; FCS, Fetal calf serum; HPLC, high pressure liquid chromatography; PI, propidium iodide; PBS, phosphate buffered saline; PMO, phosphorodiamidate morpholino oligomers; PEI, polyethylene imine; PNA, peptide-nucleic acid; ON, oligonucleotide.

☆ This work was funded by EC framework 5 (QLK3-CT-2002-01989) and CEFIPRA (3205-1) grants to B. Lebleu. S. Abes holds a PhD fellowship from the Ligue contre le Cancer.

* Corresponding author. Tel.: +33 4 67 163 303; fax: +33 4 67 163 301.
E-mail address: blebleu@univ-montp2.fr (B. Lebleu).

[1] These authors contributed equally to this work.

0168-3659/$ - see front matter © 2006 Elsevier B.V. All rights reserved.
doi:10.1016/j.jconrel.2006.09.011

be due to the internalization mechanism of CPP–ON conjugate, which involves endocytotic pathways rather than direct membrane translocation as initially thought [12].

Most studies about ON delivery by CPPs capitalized on the splicing correction assay initially described by the group of R. Kole [13], which is considered as the most reliable to assess the nuclear delivery of an antisense ON. The coding sequence of a luciferase reporter gene is interrupted by the human β-globin thalassemic intron 2 which carries a crytic splice site. This aberrant splice site prevents total removal of the intron unless the site is masked by a steric blocking (RNase H-independent) ON analogue. The advantage of this easy to implement assay is that the nuclear delivery of the correcting ON analogue gives rise to a positive read-out over a very low background.

Using this model, it was demonstrated that CPP–ON conjugates were efficiently taken up but largely remained trapped within endocytic vesicles [9,11]. Inefficient endosome release and/or lysosome degradation were therefore proposed as the major limitation for the cytoplasm/nuclear delivery of ONs. Consistent with this hypothesis, various treatments known to promote endosome leakage or endosome disruption such as chloroquine, Ca^{2+} treatment, high sucrose concentration or photochemical activation strongly increased splice correction by CPP–PNA conjugates [9,11,14]. Similar conclusions were reached for the CPP-mediated delivery of ON analogues designed to interfere with Tat transactivation by binding to the HIV-1 TAR element [10].

Since most of these endosomolytic agents are not easy to use in an *in-vivo* setting, alternative strategies had to be searched for. Co-treatment with a CPP conjugate and an endosome-destabilizing peptide is a possibility as proposed by Wadia et al. [15], but it has the potential disadvantage of complicating the delivery vector formulation.

Screening analogs of existing CPPs for more efficient cellular uptake is an alternative strategy. An interesting structure activity relationship (SAR) study has been described by Rothbard et al. [16]. Knowing the seemingly key role of arginine's guandinium headgroups for CPP uptake, they evaluated the influence of backbone spacing on cellular uptake. One of the most efficient arginine-based CPP included a 6-aminohexanoic spacer, most probably because it provided both increased flexibility and metabolic stability to the peptide. However, this SAR study was carried out using fluorescein as the probe and no biologically functional cargos were used. As the materials trapped in endosomes can fluoresce, it is unknown whether intensity of cell fluorescence directly correlates with the amount of cargo in the cytoplasm/nucleus.

PMOs have proven to be effective steric blockers in various studies [17,18]. They have, in particular, been used successfully to promote exon skipping in skeletal muscles of the mdx dystrophic mice [19]. Although CPPs have had some success in enhancing the cellular delivery of PMOs in the virology field [20–23], it still requires much more investigation to understand SAR in terms of delivery efficiencies, internalization mechanisms and cellular toxicity of CPP–PMO conjugates.

In the present study, we compared the nuclear delivery efficiencies of three different CPPs namely the 6-aminohexanoic-spaced oligoarginine ((R-Ahx-R)$_4$), Tat48–60 (Tat), and oligoarginine (R_9F_2) in the absence of endosomolytic agents. Each peptide was conjugated to the PMO targeted to the mutated splicing site of human β-globin pre-mRNA in Kole's splice correction model. In addition, we investigated the internalization mechanisms of these CPP–PMO conjugates and hypothesized mechanisms explaining why (R-Ahx-R)$_4$–PMO is more effective in splicing correction than Tat or R_9F_2 conjugates.

2. Experimental methods

2.1. Synthesis of peptides and of morpholino-peptide conjugates

PMOs were synthesized as described elsewhere [24,25]. CPPs were synthesized using standard FMOC chemistry and purified to >95% purity at AVI BioPharma (Corvallis, OR). R_9F_2–PMO and Tat–PMO were synthesized and purified as described previously [26,27]. The synthesis and purification of (R-Ahx-R)$_4$–PMO is described below. The peptide was conjugated to the nitrogen of a piperazine ring at the 5′-terminus of the PMO. First, a C-terminally reactive peptide-benzotriazolyl ester was prepared by dissolving the peptide acid with 2-(1H-benzotriazole-1-yl)-1,1,3,3-tetramethylaminium hexafluorophosphate (HBTU) and 1-hydroxybenzotriazole (HOBT) in 1-methyl-2-pyrrolidinone (NMP). The concentration of the peptide was 50 mM. Diisopropylethylamine (DIEA) was added to the peptide solution. The molar ratios of peptide acid:HBTU:HOBt:DIEA were 1.0:1.2:1.3:1.9, respectively. Immediately after the addition of DIEA, the peptide solution was added to a DMSO solution containing either 5′-piperazine-functionalized, 3′-acetyl–PMO or 3′-fluorescein–PMO (13 mM) at 1:1 molar ratio. After stirring at 37 °C for 2 h, the reaction was stopped by adding a four-fold volumetric excess of water. The resulting solution was loaded onto a CM-sepharose (Sigma, St. Louis, MO) column. The unconjugated PMO and other reaction product were washed from the column using 10-column volumes of water. The conjugate was eluted from the column by 3-column volumes of 2 M guanidinium–HCl. The conjugate/salt solution was then loaded onto a HLB column (Waters, Milford, MA), which was subsequently washed with 10-column volumes of water to remove salt. Finally, the CPP–PMO conjugate was eluted off the HLB column with 3-column volumes of 50% CH_3CN and lyophilized. The final products were analyzed by matrix assisted laser desorption ionization time of flight mass spectrometry and HPLC. The purities of the final products were >85%.

2.2. Cells and cell culture

HeLa pLuc705 cells (a generous gift from Dr. R. Kole) were cultured as exponentially growing subconfluent monolayers in DMEM medium (Gibco, Carlsbad, CA) supplemented with 10% FCS, 1 mM Na pyruvate and nonessential amino-acids. CHO-K1, CHO-pgs745 cells were cultured as exponentially growing subconfluent monolayers in F-12K medium (Invitrogen) supplemented with 10% (v/v) fetal calf serum and 2 mM glutamine.

2.3. Flow cytometry

To analyze CPP–PMO conjugates cell internalization, exponentially growing HeLa pLuc705 cells (3×10^5 cells seeded and grown overnight in 30-mm plates) were incubated with the Fam-labelled (R-Ahx-R)$_4$–PMO$_{705}$, Tat–PMO$_{705}$ or R_9F_2–PMO$_{705}$. The cells were then washed twice with PBS, detached by incubating with trypsin for 5 min at 37 °C (0.5 mg/ml)/EDTA.4Na (0.35 mM), and washed by centrifugation (5 min, 900 ×*g*) in ice-cold PBS containing 5% FCS. The resulting cell pellet was resuspended in ice-cold PBS containing 0.5% FCS and 0.05 μg/ml PI (Molecular Probes, Eugene, OR). Fluorescence analysis was performed in a Faxcalibur flow cytometer (BD Biosciences, San Jose, CA). Cells stained with PI were excluded from further analysis. A minimum of 20,000 events per sample was analyzed. Kinetic studies were performed by incubating the conjugates (2 μM) in OptiMEM (Gibco, Carlsbad, CA) medium for indicated times, whereas dose-response studies were performed by incubating the conjugates at indicated concentrations for 30 min in OptiMEM medium or in complete medium.

2.4. Fluorescence microscopy

Exponentially growing HeLa pLuc705 cells were trypsinized, centrifuged at 900 ×*g* for 2 min and resuspended in OptiMEM. 5×10^5 cells in 250 μl OptiMEM were incubated with 2 μM of the Fam labelled conjugates. Cells were then treated with trypsin (0.05%)/EDTA.4Na (0.35 mM) and rinsed twice for 5 min with PBS/heparin (1 mg/ml). LysoTracker®Red DND-99 and Hoechst dye (Molecular Probes, Eugene, OR) were used to stain lysosomes/endosomes and nuclei, respectively. The distribution of fluorescence in live unfixed cells was analysed on a Zeiss Axiovert 200 M fluorescence microscope (Carl Zeiss, Oberkochen, Germany).

2.5. Splicing correction assay

The conjugates (R-Ahx-R)$_4$–PMO$_{705}$, Tat–PMO$_{705}$, R_9F_2–PMO$_{705}$, or the scrambled version (R-Ahx-R)$_4$–PMOsc$_{705}$ were incubated for 4 h in OptiMEM medium in the absence or in the presence of 100 μM chloroquine with exponentially growing HeLa pLuc705 cells (3.5×10^5 cells/well seeded and cultivated overnight in 6 wells plates). The conjugates were then washed and incubation continued for 20 h in complete DMEM medium containing 10% FCS. Cells were washed twice with ice-cold PBS and lysed with Reporter Lysis Buffer (Promega, Madison, WI). Luciferase activity was quantified in a Berthold Centro LB 960 luminometer (Berthold Technologies, Bad Wildbad, Germany) using the Luciferase Assay System substrate (Promega, Madison, WI). Cellular protein concentrations were measured with the BCA™ Protein Assay Kit (Pierce, Rockford, IL) and read using an ELISA plate reader (Dynatech MR 5000, Dynatech Labs, Chantilly, VA) at 550 nm. Luciferase activities were expressed as relative luminescence units (RLU) per μg protein. All experiments were performed in triplicate. Each data point was averaged over the three replicates.

2.6. RT-PCR

HeLa pLuc705 cells plated at 30,000 cells/well in a 24-well plate 24 h before treatment. To treat cells, media was replaced with the culture media containing indicated concentrations of (R-Ahx-R)$_4$–PMO$_{705}$ and cells were incubated for 24 h. Cells were harvested by trypsin treatment and washed with PBS. Total RNA was extracted from the cells using the RNeasy Mini Kit (Qiagen; Valencia, CA) as outlined by the manufacturer. The extracted RNA was amplified by RT-PCR (Icycler, BioRad; Hercules, CA) with forward primer 5′TTG ATA TGT GGA TTT CGA GTC GTC3′and reverse primer 5′TGT CAA TCA GAG TGC TTT TGG CG3′ with the following RT-PCR program: (50 °C, 35 min)×1 cycle, (95 °C, 5 min)×1 cycle, (95 °C, 30 s; 55 °C, 30 s; 72 °C, 30 s)×30 cycles. The products were analyzed on a 2% agarose gel and visualized by washing in an ethidium bromide bath. The image was captured with a Polaroid camera (Model DS-34, Polaroid, Waltham, MA) and digitized with a psc750 (Hewlett Packard; Houston, TX) scanner.

2.7. Heparin-affinity chromatography

3 μg of each CPP–PMO conjugate were injected in triplicate on a HiTrap Sepharose/heparin 1 ml column (Amersham Biosciences, Freiburg, Germany), fitted on a Beckman–Gold HPLC chromatography (Beckman Coulter, Fullerton, CA). The conjugates were eluted at a flow rate of 1 ml/min of 2.5 mM phosphate buffer pH 7 by a linear gradient of NaCl from 70 to 970 mM, in 30 min. Elution of the conjugates was followed by UV absorption at 260 nm. Results were presented as eluting NaCl concentrations and expressed as the mean and standard deviation of triplicate measurements.

3. Results

3.1. Splicing correction by (R-Ahx-R)$_4$–PMO$_{705}$ conjugate

Previous studies have reported the delivery of uncharged steric-block ON (PNA or PMO) conjugated to cell penetrating peptides such as Tat or to short oligolysine tails [26,28]. However, several recent studies came to the conclusion that the conjugated PNA derivatives were essentially taken up by endocytosis and that their nuclear delivery was severely limited by entrapment within endocytic vesicles [9–11]. These studies and the present one have been carried out with the splicing correction assay proposed by Kang et Al. (1998), which is now considered as the most reliable to quantitate the nuclear delivery of steric blocking ON. It makes use of HeLa pLuc705 cells stably transfected with a construct in which the coding sequence of a reporter luciferase gene is interrupted by the mutated intron 2 from a thalassemic human β globin gene. This intron carries a mutation which creates an aberrant splice site and prevents the normal processing of the chimeric pre mRNA. The hybridization of a steric-blocking antisense ON analogue masks the cryptic splice site and redirects the splicing machinery towards the complete removal of intro 2, thereby allowing correct pre-mRNA processing and expression of luciferase.

Table 1
Sequences and nomenclature of CPPs and morpholino oligos

Name	Sequences
$(R\text{-}Ahx\text{-}R)_4$	CH_3CO-RAhxRRAhxRRAhxRRAhxRAhxB-COOH
R_9F_2	NH_2-RRRRRRRRRFFC-$CONH_2$
Tat	NH_2-CYGRKKRRQRRR-$CONH_2$
PMO_{705}	5′-CCT CTT ACC TCA GTT ACA-3′
PMO_{705}sc	5′-CTC TCT CAC CAT TGA CAT-3′

Ahx = 6-Aminohexanoic acid. B = β-Alanine.

Similar problems could be anticipated for the delivery of PMO ON derivatives, another class of steric-blocking ON analogues. A splice-correcting PMO sequence (refered to as PMO_{705}) has therefore been conjugated to commonly used CPPs such as Tat 48–60 (Tat–PMO_{705}) or R9 (R_9F_2–PMO_{705}) (see Table 1 for PMO and CPP sequences). Splice correction has been monitored by luciferase activity and data have been standardized per microgram of total cellular protein. As shown in Fig. 1 (panel 1A, splicing correction by Tat–PMO_{705} or by R_9F_2–PMO_{705} was only slightly improved at low concentration. A dose-dependent increase was observed for the Tat–PMO_{705} conjugate when raising the concentration from 1 to 10 μM (Fig. 1, panel B) while the R_9F_2–PMO_{705} could not validly be used within this range of concentration since it was too cytotoxic in serum-free medium (Fig. 2). Although disappointing, these data are in line with the poor efficiency of

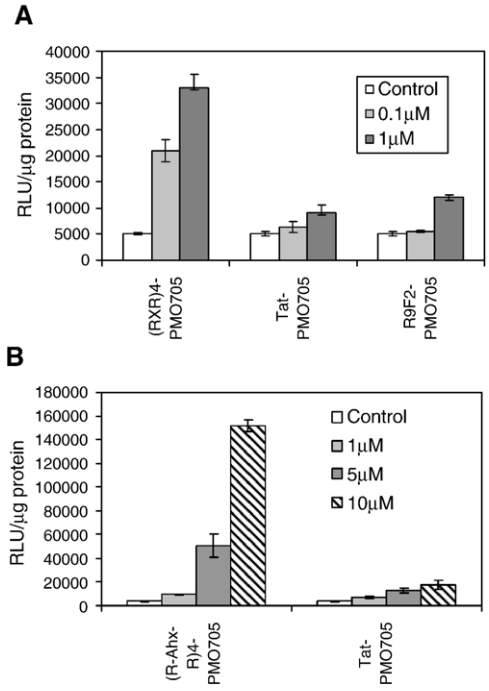

Fig. 1. Splicing correction by $(R\text{-}Ahx\text{-}R)_4$–$PMO_{705}$ conjugate: dose-response and comparison to Tat–PMO and R_9F_2–PMO. HeLa pLuc705 cells were incubated for 4 h in OptiMEM in the absence (control) or in the presence of CPP–PMO_{705} conjugates at the indicated concentrations. CPP–PMO conjugates were tested between 0.1 and 1 μM (panel A) or between 1 and 10 μM (panel B). Luciferase expression was quantified 20 h later and was expressed as RLU/μg protein. Each experiment was made in triplicate and error bars (standard derivations) are indicated.

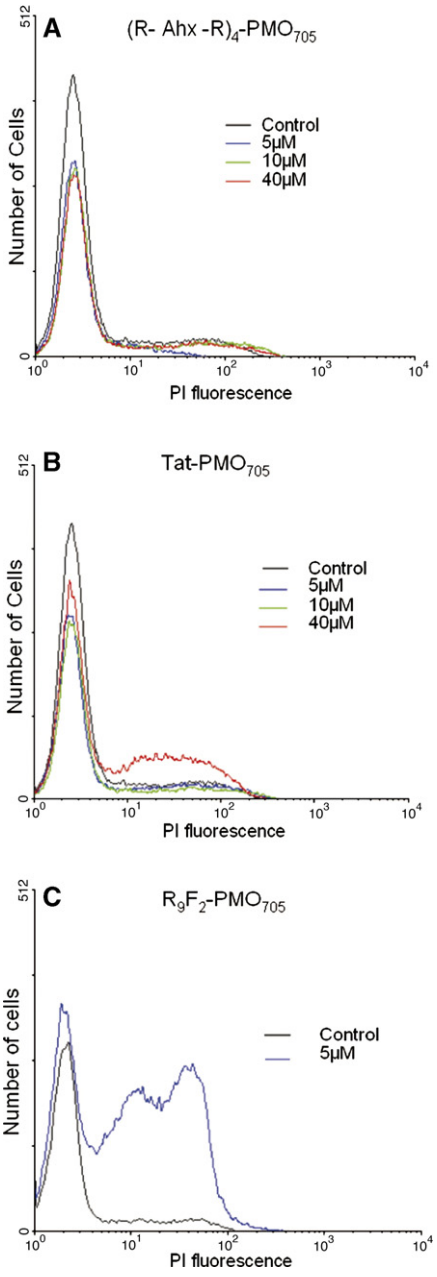

Fig. 2. CPP–PMO induced cell permeabilization. Cells were incubated with $(R\text{-}Ahx\text{-}R)_4$–$PMO_{705}$, Tat–$PMO_{705}$ or R_9F_2–PMO_{705} at the indicated concentrations for 2 h at 37 °C in the presence of 0.05 μg/ml PI. Cells were washed and trypsinised. PI uptake was monitored by flow cytometry.

CPP–PNA conjugates which we and others have observed in the absence of endosomolytic agents.

A rather different situation has been observed with PMO_{705} conjugated to $(R\text{-}Ahx\text{-}R)_4$. As seen in Fig. 1 (panels A and B) much higher levels of luciferase activity were obtained. A significant correction was already achieved at low conjugate concentration (100 nM) and increased nearly linearly up to 10 μM. The sequence-specificity of the $(R\text{-}Ahx\text{-}R)_4$–$PMO_{705}$-mediated splice correction was verified with a scrambled version of the conjugate (see Table 1 for PMO_{705}sc sequence) (Fig. 3). Luciferase expression remained at its basal level even

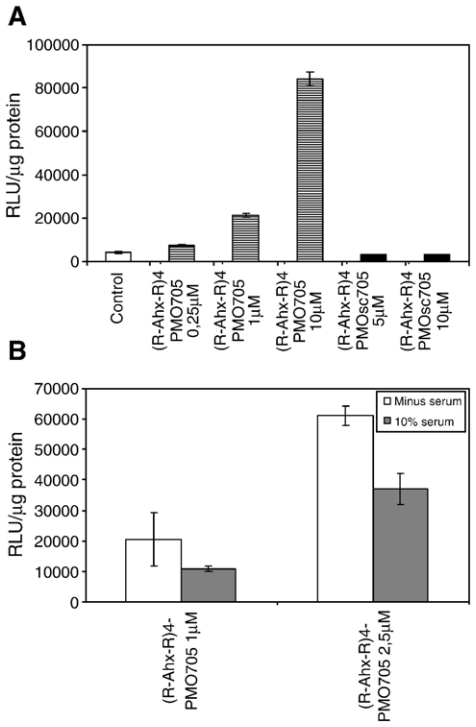

Fig. 3. Specificity (panel A) and serum dependence (panel B) of splicing correction by (R-Ahx-R)$_4$–PMO$_{705}$ A. HeLa pLuc705 cells were incubated for 4 h in OptiMEM at the indicated concentrations in the absence (control) or in the presence of (R-Ahx-R)$_4$–PMO$_{705}$ or (R-Ahx-R)$_4$–PMO$_{705}$sc. B. HeLa pLuc705 cells were incubated with 1 or 2.5 µM of (R-Ahx-R)$_4$–PMO$_{705}$ in the absence or presence of 10% serum. Luciferase expression was quantified 20 h later and was expressed as RLU/µg protein. Each experiment was made in triplicate and error bars are indicated.

in cells treated with high concentrations (10 µM) of (R-Ahx-R)$_4$–PMO$_{705}$sc.

Importantly, (R-Ahx-R)$_4$–PMO$_{705}$ did not lead to any detectable cells permeabilization even at high concentrations. Uptake of PI in the cells treated with the CPP–PMO$_{705}$

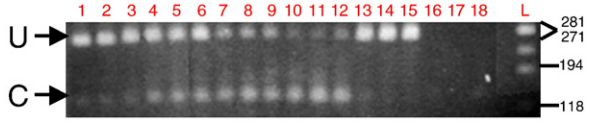

Lanes	uM	Template
1,2,3	1	+
4,5,6	2	+
7,8,9	4	+
10,11,12	8	+
13,14,15	0	+
16,17,18	0	-
L	0	φX174 DNA-HaeIII

Fig. 4. RT-PCR analysis of uncorrected (U, 268 bp) and corrected (C, 142 bp) spliced luciferase pre-mRNA. Total RNA was extracted from cells treated with 0, 1, 2, 4 or 8 µM of (R-Ahx-R)$_4$–PMO$_{705}$ for 24 h. Each line represents an individual sample.

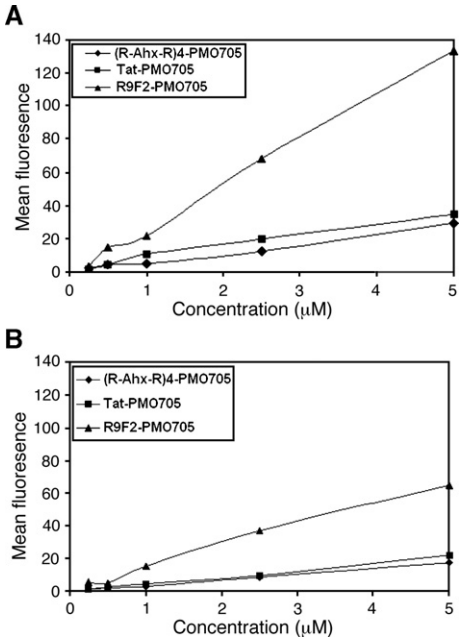

Fig. 5. Flow cytometry analysis of CPP–PMO uptake. HeLa pLuc705 cells were incubated in the absence (A) or presence (B) of 10% serum, with (R-Ahx-R)$_4$–PMO$_{705}$–Fam, (♦) Tat–PMO$_{705}$–Fam (■) or R$_9$F$_2$–PMO$_{705}$–Fam (▲) at the indicated concentration for 2 h at 37 °C. Cells were washed, trypsinised and analyzed by flow cytometry.

conjugates was used as an index for peptide-induced membrane permeabilization (Fig. 2). The (R-Ahx-R)$_4$–PMO$_{705}$ conjugate did not lead to any PI uptake at concentrations up to 40 µM (panel A), well above the concentration leading to significant splice correction. Cell permeabilization by (R-Ahx-R)$_4$–PMO$_{705}$ only became significant at concentrations >60 µM (data not shown) in contrast with Tat–PMO$_{705}$ or R$_9$F$_2$–PMO$_{705}$ (panel B and C respectively).

In experiments described so far, cells were incubated with the CPP–PMO$_{705}$ conjugates in OptiMEM serum-free medium. It was however critical to determine whether cellular uptake and splicing correction is affected by the presence of serum proteins, a well established flaw for most commercial cationic lipids

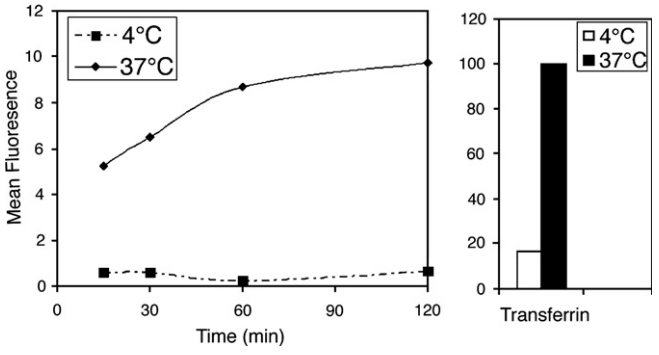

Fig. 6. Effect of temperature on the kinetics of uptake of (R-Ahx-R)$_4$–PMO$_{705}$–Fam. HeLa pLuc705 cells were incubated with 2 µM (R-Ahx-R)$_4$–PMO$_{705}$–Fam at 4 °C or 37 °C. At the indicated times, cells were washed with ice-cold PBS, trypsinised and analyzed by flow cytometry. As a control of endocytic activity, cells were incubated 5 min with 25 µg/ml FITC-labelled transferrin at 4 °C or 37 °C before being processed the same way.

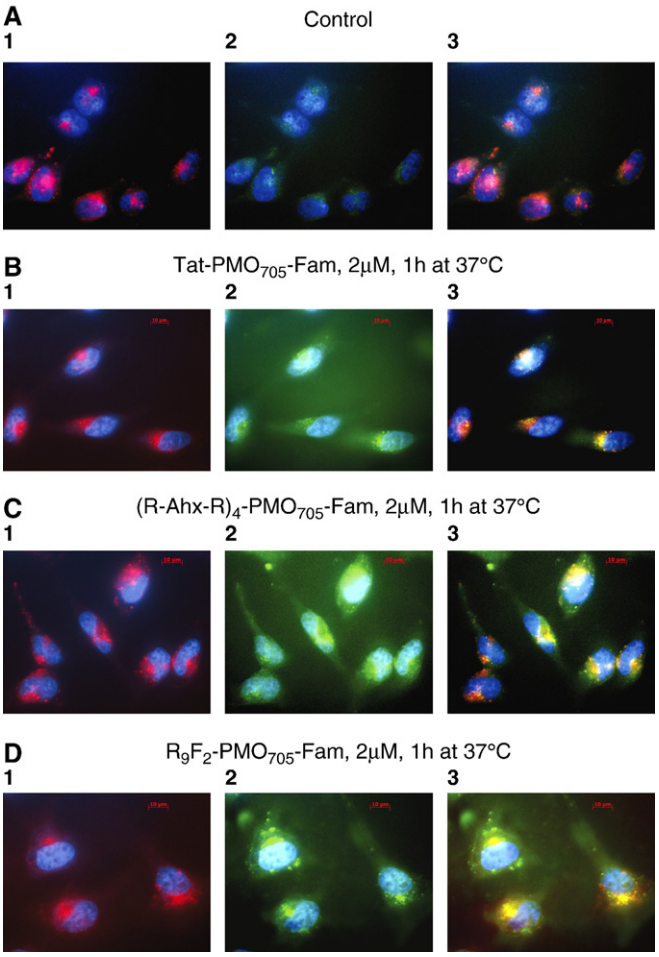

Fig. 7. Intracellular distribution of CPP–PMO_{705}–Fam. Fluorescence microscopy images in live HeLa pLuc705 cells incubated in OptiMEM in the absence (control) or presence of 2 µM conjugate (green fluorescence) for 1 h and thereafter with 50 nM LysoTracker®Red DND-99, (red fluorescence) for 5 min. Nuclei were stained with Hoechst (blue fluorescence) for 5 min. Co-localization between green and red fluorescence was revealed in panel C (yellow staining). (For the interpretation of the references to the colour in this figure legend, the reader is referred to the web version of this article.)

formulations. As shown in Fig. 3 (panel B), the luciferase signal is lower but still significant in the presence of serum.

In order to confirm that the luciferase activity was due to (R-Ahx-R)$_4$–PMO_{705} splicing correction, mRNAs were analysed by RT-PCR using primers allowing the specific amplification of both correctly spliced and aberrant luciferase mRNA. Incubation with increasing concentrations of (R-Ahx-R)$_4$–PMO_{705} led to a dose-dependent decrease of the aberrantly-spliced luciferase mRNA and to the concomitant increase of the correctly-spliced mRNA (Fig. 4).

3.2. Is the increased splice-correcting activity of (R-Ahx-R)$_4$–PMO_{705} due to higher cell uptake?

We first monitored cellular uptake of fluorescein (Fam)-tagged derivatives of the CPP–PMO conjugates by flow cytometry. A proteolytic (trypsin) treatment step was introduced prior to analysis in order to remove unwashed membrane-bound material (Richard et al. 2003). As shown in Fig. 5, the cellular uptake of all three conjugates ((R-Ahx-R)$_4$–PMO_{705}–Fam, Tat–PMO_{705}–Fam and R_9F_2–PMO_{705}–Fam increased in a dose-dependent mode whether the incubation had been done in the absence (panel A) or in the presence (panel B) of serum proteins, in keeping with splicing correction data (Fig. 1). Importantly, there is no correlation between the amount of internalized CPP conjugates and their abilities to correct splicing. R_9F_2–PMO_{705}–Fam is most efficiently taken up whereas (R-Ahx-R)$_4$–PMO_{705}–Fam and Tat–PMO_{705}–Fam are taken up about equally (Fig. 5). However, (R-Ahx-R)$_4$–PMO_{705} is largely more efficient than the other two conjugates in the splice correction assay (Fig. 1).

3.3. Is the increased splice-correcting activity of (R-Ahx-R)$_4$–PMO_{705} due to a different mechanism of cellular internalization ?

The mechanism of CPP internalization has been heavily debated, and recent data favour an energy-dependent mechanism [29]. The cellular uptake of the (R-Ahx-R)$_4$–PMO_{705}–Fam (Fig. 6),Tat–PMO_{705}–Fam or R_9F_2–PMO_{705}–Fam conjugate was completely blocked upon incubation at 4 °C in accordance with data published for Tat CPP and for Tat–PNA conjugates [9,29]. Moreover, depletion of the intracellular ATP pool by NaN_3 treatment inhibited the uptake of all three conjugates to the same extent as it does for transferrin (data not shown). In addition, the cellular uptake of these conjugates was significantly inhibited by endocytosis inhibitors such as chlorpromazine and cytochalasin-D as well as by depletion of cellular K^+ (data not shown). These observations are in line with an energy-dependent mechanism of cellular internalization involving endocytosis.

We next evaluated the intracellular distribution of these CPP–PMO_{705}–Fam conjugates by fluorescence microscopy. All experiments were performed on live unfixed cells to eliminate the re-distribution artifacts which commonly occur upon cell fixation with these cationic CPPs [12]. As seen in Fig. 7, a large proportion of these CPP–PMO conjugates was

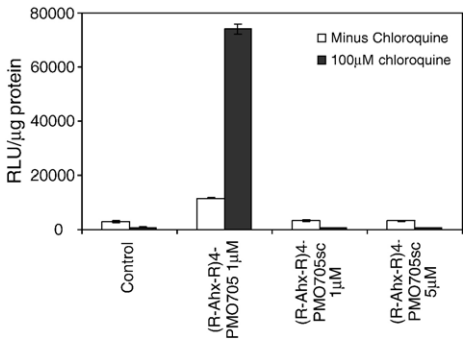

Fig. 8. Effect of chloroquine on splicing correction by (R-Ahx-R)$_4$–PMO_{705}. The splice correction assay was performed by incubating HeLa pLuc705 cells with (R-Ahx-R)$_4$–PMO_{705} or (R-Ahx-R)$_4$–PMO_{705}sc for 4 h at the indicated concentrations in the absence or in the presence of 100 µM chloroquine. Luciferase expression was quantified 20 h later and was expressed as RLU/µg protein. Each experiment was made in triplicate and error bars (standard derivations) are indicated.

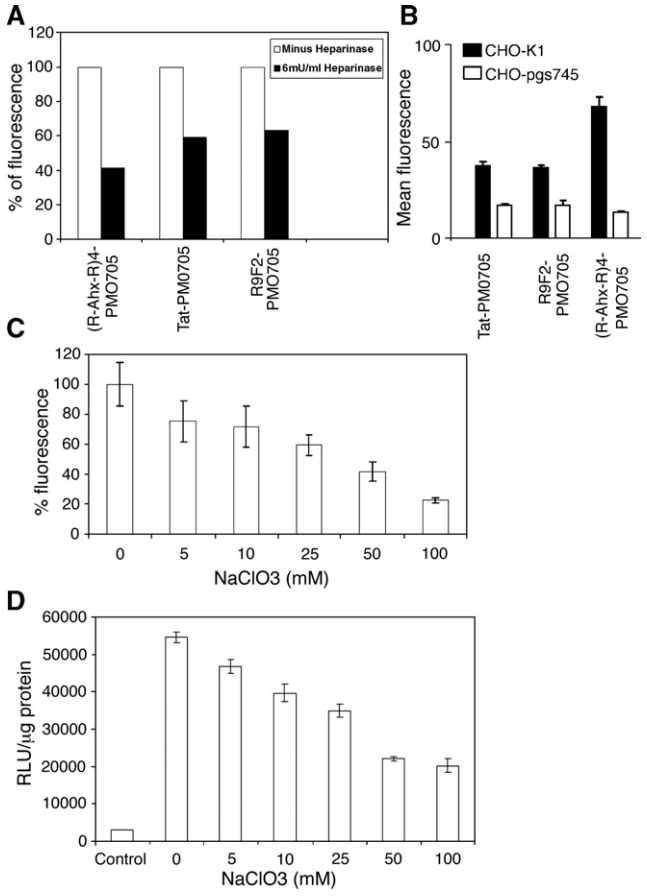

Fig. 9. Involvement of proteoglycans in the uptake of (R-Ahx-R)$_4$–PMO$_{705}$–Fam. A. HeLa pLuc 705 cells were incubated with 2 µM of each CPP–PMO$_{705}$–Fam in the absence or in the presence of 6 mU/ml of heparinase for 2 h at 37 °C. Cells were washed, trypsinised and analyzed by flow cytometry. B. Uptake of the fluorescently labelled conjugates in wild-type CHO and proteoglycan-deficient CHOpgs745. Cells were incubated with 2 µM CPP–PMO$_{705}$–Fam, washed, trypsinised and analyzed by flow cytometry. C. HeLa pLuc705 cells were incubated with 2 µM (R-Ahx-R)$_4$–PMO$_{705}$–Fam in the presence of the indicated concentration of chlorate ($NaClO_3$) for 2 h at 37 °C. Cells were washed, trypsinised and analyzed by flow cytometry. D. HeLa pLuc 705 cells were incubated with 1 µM (R-Ahx-R)$_4$–PMO$_{705}$ in the presence of the indicated concentration of chlorate ($NaClO_3$). Luciferase expression was expressed as RLU/µg protein. Each experiment was made in triplicate and error bars are indicated.

concentrated within discrete cytoplasmic structures and co-localized with a lysosomal marker, while none could be detected in the nuclei within 1 h of treatment. A rather faint diffuse fluorescence with intense punctuate fluorescence was however observed in cells after 24 h of treatment (data not shown). The microscopic analysis may not be sensitive enough to definitively reveal low amounts of escaping material.

Recent studies by several groups (including our own) have established that segregation within endocytic compartments severely limits cytoplasmic (and consequently nuclear) delivery of CPP–ON conjugates. We therefore evaluated whether treatment with endosomolytic agents would improve splicing correction by (R-Ahx-R)$_4$–PMO$_{705}$. As shown in Fig. 8, chloroquine treatment significantly increased splicing correction by (R-Ahx-R)$_4$–PMO$_{705}$ and not by its scrambled version, supporting entrapment within endocytic vesicles as a limiting factor for activity, as also demonstrated for the other conjugates (data not shown).

Altogether, these data show that the three CPP–PMO conjugates are taken up by endocytosis. However, they do not reveal differences in the mechanism of cell uptake or in the intracellular distribution which could explain why splicing correction with (R-Ahx-R)$_4$–PMO$_{705}$ is significantly more efficient than with Tat–PMO$_{705}$ in the absence of endosomolytic agents.

3.4. The (R-Ahx-R)$_4$–PMO$_{705}$ conjugate has a lower affinity for heparin than the Tat–PMO$_{705}$ conjugate

Charged biopolymers, as cationic lipoplexes or basic amino acids-rich CPPs, interact with cell surface proteoglycans before being internalized by endocytosis [30]. Therefor we used biochemical and genetic tools to unravel a possible interaction of (R-Ahx-R)$_4$–PMO$_{705}$ conjugates with cell-surface proteoglycans.

In keeping with earlier data for Tat peptide [29], pretreatment with heparinase, a glycosaminoglycan lyase, inhibited the cell internalization of the (R-Ahx-R)$_4$–PMO$_{705}$ conjugate to the same extent as for the R$_9$F$_2$-and Tat–PMO conjugates, as shown in Fig. 9 (panel A). Likewise, the uptake of all three conjugates was significantly inhibited in mutant CHO cells (CHO-pgs 745)

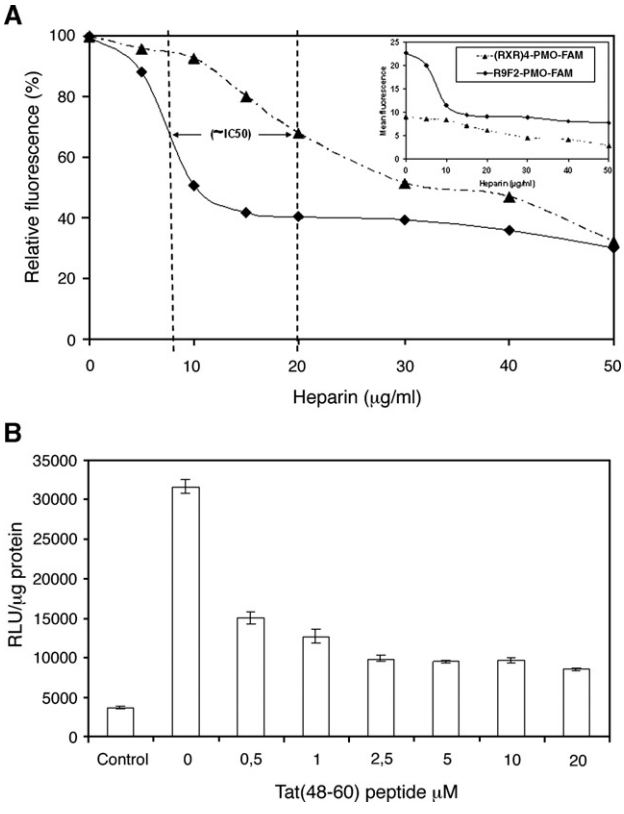

Fig. 10. (R-Ahx-R)$_4$–PMO$_{705}$–Fam binds to heparin with a lower affinity. A. HeLa pLuc705 cells were incubated with 2 µM (R-Ahx-R)$_4$–PMO$_{705}$–Fam or R$_9$F$_2$–PMO$_{705}$–Fam in the presence of the indicated concentration of heparin for 2 h at 37 °C. Cells were washed, trypsinised and analyzed by flow cytometry. B. HeLa pLuc705 cells were incubated with 1 µM (R-Ahx-R)$_4$–PMO$_{705}$ in the presence of the indicated concentration of Tat(48–60). Luciferase expression was expressed as RLU/µg protein. Each experiment was made in triplicate and error bars are indicated.

Table 2
Heparin affinity chromatography of CPP–PMO–FAM conjugates

Conjugate	[NaCl] mM	SD [NaCl] mM
(R-Ahx-R)$_4$–PMO$_{705}$–Fam	0.557	0.004
Tat–PMO$_{705}$–Fam	0.657	0.007
R_9F_2–PMO$_{705}$–Fam	0.842	0.005

Values are the mean and standard deviation of the eluting concentrations of NaCl determined in triplicate.

deficient in cell surface heparan sulfate expression (Fig. 9, panel B). Finally, chlorate pretreatment, which is known to interfere with the sulfation of cell surface proteoglycans, dose-dependently inhibited (R-Ahx-R)$_4$–PMO$_{705}$ uptake and splice correction (Fig. 9, panel C and D). Altogether, these data support the involvement of cell surface heparan sulfates.

As mentioned above, the fate of CPPs after interaction with cell surface proteoglycans remains largely debated. Whichever the mechanism, it is increasingly considered that restricted escape from endocytic vesicles severely limits nuclear delivery. In this context, the affinity of CPP conjugates to proteoglycans might be a key element. While the interaction should be strong enough to allow binding at the cell surface, release has to take place to allow endosomal escape [6]. As a first evaluation of this problem, the internalization of (R-Ahx-R)$_4$–PMO$_{705}$ has been quantitated in the presence of increasing amounts of heparin, as model proteoglycan. Significantly higher amounts of heparin were required to inhibit the uptake of (R-Ahx-R)$_4$–PMO$_{705}$–Fam as compared to R_9F_2–PMO$_{705}$–Fam (Fig. 10, panel A) or Tat–PMO$_{705}$–Fam (data not shown). In addition, the relative heparin-binding affinities of the three conjugates were compared using heparin-affinity chromatography. (R-Ahx-R)$_4$–PMO$_{705}$ eluted at a lower ionic strength (as provided by a NaCl gradient) than R_9F_2–PMO or Tat–PMO (Table 2) indicating a lower affinity for this model heparan sulfate.

However, these experiments do not provide any information about the actual relative affinities of the CPP–PMO conjugates for cell surface proteoglycans. Therefore, we undertook competition experiments using unlabelled Tat(48–60) peptide to interfere with (R-Ahx-R)$_4$–PMO$_{705}$ uptake and splice correction. Unconjugated Tat peptide dramatically inhibited in a dose-dependant fashion the splice correction by (R-Ahx-R)$_4$–PMO$_{705}$ (Fig. 10, panel B), as well as the uptake of (R-Ahx-R)$_4$–PMO$_{705}$–Fam (data not shown). This functional interference supports the existence of a common endocytotic mechanism of cell uptake for both CPPs, and suggests that the difference in their splice-correcting efficiency may be due to later events during their endosomal fate.

4. Discussion

In this work, using an *ad hoc* well standardized assay, we studied the properties of three CPPs in regard to their capacity to deliver a steric-blocking PMO to the nuclear compartment where they can mediate splicing correction.

The sequence specificity, low toxicity and biological stability of PMOs make them potential drugs for gene-specific therapies. Classic CPPs such as Tat 48–60 or oligoarginine peptides enhance cellular uptake of PMOs but with toxicity or low efficiency [20,26,31,32]. Here we found that Tat and R9 peptide–PMO conjugates behaved as expected from previous work on PNA–CPP conjugates by this and other groups [9,11]. The splicing correction efficiency of the PMO versions of these conjugates remained low at doses up to 10 μM, and higher concentrations were precluded due to their cytotoxicity. Moreover, preliminary mechanistic studies using the endosomolytic agent chloroquine demonstrated that this low efficiency was largely caused by endosomal sequestration (data not shown). In searching for more efficacious and less toxic CPPs for PMO delivery, we also took into consideration that an effective carrier should not be cleaved by enzymes in blood. One strategy to increase the metabolic stability without using costly D-amino acids is to incorporate non-α amino acids into CPP sequences. Indeed the (R-Ahx-R)$_4$ sequence, which derived by insertions of 6-aminohexanoic acid into the R8 sequence, has a greater stability than oligoarginine in human serum (data not shown).

In this study, the (R-Ahx-R)$_4$–PMO$_{705}$ conjugate was much more active than Tat(48–60) and R_9F_2 conjugates even without an endosomolytic agent and, importantly, did not lead to cell permeabilization even at high concentrations. The (R-Ahx-R)$_4$–PMO$_{705}$sc, the scrambled version of the conjugate, was inactive thus confirming that the splice-correcting activity is sequence-specific. RT-PCR confirmed the production of the correctly-spliced mRNA in cells treated with the (R-Ahx-R)$_4$–PMO$_{705}$ conjugate.

As a first step towards SAR studies aiming at the design of even more potent analogs, we have attempted to define why (R-Ahx-R)$_4$–PMO$_{705}$ was more active in this assay than the other conjugates tested so far. The trivial explanation could be an increased cellular uptake. Surprisingly, flow cytometry clearly showed that cell internalization of (R-Ahx-R)$_4$–PMO$_{705}$ was the lowest (R_9F_2 > Tat ≥ (R-Ahx-R)$_4$) of all conjugates, which is not correlated with splicing correction efficiency, where (R-Ahx-R)$_4$–PMO$_{705}$ was the most effective ((R-Ahx-R)$_4$ >> R_9F_2 > Tat). It is worth mentioning here that a previous study [16] had established that oligoarginines with non-α amino acids insertions were taken up more efficiently than oligoarginines in a Jurkat T cell line. Apparent discrepancies between the results of our and Rothbard's groups could be due to differences in cell types, in the contribution of phenylalanines in the R_9F_2 sequence and in methodologies that were used in the studies. In the present study, a proteolysis treatment prior to flow cytometry analysis was used to eliminate cell-bound material. Whatever the case, this study shows that the cellular uptake determined by flow cytometry is not necessarily correlated with the amount of cargo in the cytosolic and nuclear compartments.

It is now increasingly admitted that endocytosis is a major pathway for CPP cellular uptake although direct membrane translocation might still be an alternative route for some CPPs [33]. The involvement of an energy-dependent mechanism for the uptake of (R-Ahx-R)$_4$–PMO$_{705}$ has been definitely proven by low temperature incubation, by depletion of the cellular ATP pool (data not shown), and by co-localization of a major part of (R-Ahx-R)$_4$–PMO$_{705}$Fam with lysosomal markers as also

observed for Tat-and R_9F_2–PMO conjugates. The cytoplasmic and nuclear localization of (R-Ahx-R)$_4$–PMO$_{705}$Fam was suggested by a faint diffuse fluorescence after 24 h of incubation. This could not be quantitated in our experiments and we have to infer that some material has been escaping over time to explain the sequence-specific splice-correcting activity. It should be recalled here that a pre-mRNA target is present at a very low steady-state concentration in the nucleus and that, in theory, very low amounts of the correcting ON should be sufficient to achieve splicing correction if effectively delivered in the nucleus. For instance, we have shown that a cationic lipoplex formulation of negatively charged 2′OMe-RNA$_{705}$ was able to correct splicing in this assay at a 10 nM concentration, consistent with a nearly quantitative nuclear delivery [8].

The splice-correcting efficiency of (R-Ahx-R)$_4$–PMO$_{705}$ was strongly enhanced in the presence of chloroquine, as previously documented with other PNA– or PMO–CPP conjugates. This is consistent with the observation that uptake of (R-Ahx-R)$_4$–PMO$_{705}$ involves endocytosis and indicates that entrapment within endocytic vesicles still limits its efficiency.

However, endocytosis may proceed by different pathways which might influence the intracellular routing of the internalized CPP-conjugates. The uptakes of all three conjugates were similarly inhibited by several known endocytosis inhibitors (chlorpromazine, cytochalasin-D and ethylisopropylamiloride) as well as by depletion of cellular K^+ (data not shown). At this stage, no significant difference in endocytosis pathways was found to explain the increased splice-correcting activity of (R-Ahx-R)$_4$–PMO$_{705}$.

Therefore, we next investigated the affinity of the three CPP–PMO conjugates for cell-surface proteoglycans, a property known to be important for cell-internalisation and intracellular fate of cationic delivery vectors. Treatment of cells with heparinase to remove cell-surface proteoglycans strongly inhibited the cell uptake of all three fluorescein-labelled CPP–PMO conjugates. Comparison of cell uptake in a CHOpgs745 mutant cell-line devoid of proteoglycan versus wild-type CHO cells confirmed a dependency of all three peptides on the presence of cell-surface proteoglycans. Inhibition of proteoglycans sulfation also decreased the splice correction efficiency and the internalisation of (R-Ahx-R)$_4$–PMO$_{705}$, evidencing the importance of the sulfate negative charges for cell uptake.

We next assessed the relative heparin-binding affinity of the three CPP–PMO conjugates. The uptake of (R-Ahx-R)$_4$–PMO$_{705}$ was inhibited in a dose-dependant way by heparin, a model heparan sulfate. Interestingly, cell-internalisation assays by flow cytometry in the presence of competitive amounts of heparin showed that a higher concentration of heparin was necessary to displace (R-Ahx-R)$_4$–PMO$_{705}$ (IC50 = 20 μg/ml) than to displace the R_9F_2–PMO conjugate (IC50 = 8 μg/ml). Heparin-affinity chromatography showed that (R-Ahx-R)$_4$–PMO$_{705}$ has the lowest affinity of all three CPP–PMO conjugates for heparin.

Taken together these results suggest that internalization of all three CPP–PMO conjugates depend on cell surface proteoglycans and that (R-Ahx-R)$_4$–PMO$_{705}$ may have a lower affinity for sulfated polyanions. The competition experiments between (R-Ahx-R)$_4$–PMO$_{705}$ and Tat(48–60) peptide clearly revealed the existence of a common pathway of internalisation for these two CPPs. The difference in splice correction efficiency must therefore reside at later stages during the fate of internalized conjugates.

We can propose several hypothesis to explain this difference. First, the only true peptidic links in (R-Ahx-R)$_4$ lie between the pairs of arginines. This unusual structure may not offer an efficient binding and positioning in the active site of proteases, thus allowing a longer half-life in our assay system, and subsequently a higher probability to escape from the endosome and lysosome compartments. In keeping with this hypothesis, (R-Ahx-R)4–PMO$_{705}$ was more stable in human serum than Tat and R_9F_2 conjugates (data not shown). On the other hand, our previous studies [34] have shown that after 24 h of incubation with intact cells, the peptide moiety of (R-Ahx-R)$_4$ and R_9F_2 conjugates was entirely degraded, while the PMO moiety (which is the key element for splicing-correction) remained detectable. Nevertheless, it is still possible that these conjugates may be degraded at different rates. Second, the lower affinity of (R-Ahx-R)$_4$ for heparan sulfates could allow an easier dissociation of the proteoglycan/conjugate complex, thus allowing endosomal escape to take place, or at least preventing the rapid segregation of the conjugate in lysosomal compartments. Finally, affinity for the target RNA sequence should be a critical factor for efficient steric blocking. Several features of the (R-Ahx-R)$_4$–PMO$_{705}$ construct might be favourable in this respect. The uncharged high affinity PMO$_{705}$ is known to hybridize to complementary RNA with a high Tm of 74 °C while retaining sequence specificity [34]. In addition, the stable conjugation of a cationic, flexible and metabolically more stable CPP may provide an RNA-anchoring entity. The contribution of these various and non-exclusive possibilities deserves further work and is currently under investigation in our laboratories.

In summary, and to our knowledge, this (R-Ahx-R)$_4$–PMO construct has turned out to be the most efficient in this reliable and quantitative splicing-correction assay. Its ability to function without adjunction of chloroquine, and in the presence of serum proteins, offers a promising lead for the development of vectors able to enhance delivery of ONs in clinically relevant models. Indeed (R-Ahx-R)$_4$–PMO conjugate was found more efficient than free 2′OMe Phosphorothioate or free PMO to promote *in vitro* exon skipping in muscular cells from the Golden Retriever Muscular Distrophy model [35]. As noted however, there is room for improvement, possibly through further SAR studies, since endosomolytic agents still increase the efficiency of the conjugate.

References

[1] A.R. Thierry, E. Vives, J.P. Richard, P. Prevot, C. Martinand-Mari, I. Robbins, B. Lebleu, Cellular uptake and intracellular fate of antisense oligonucleotides, Curr. Opin. Mol. Ther. 5 (2) (2003) 133–138.

[2] O. Zelphati, L.S. Uyechi, L.G. Barron, F.C. Szoka Jr., Effect of serum components on the physico-chemical properties of cationic lipid/oligonucleotide complexes and on their interactions with cells, Biochim. Biophys. Acta 1390 (2) (1998) 119–133.

[3] S.M. Moghimi, P. Symonds, J.C. Murray, A.C. Hunter, G. Debska, A. Szewczyk, A two-stage poly(ethylenimine)-mediated cytotoxicity: implications for gene transfer/therapy, Molec. Ther. 11 (6) (2005) 990–995.

[4] K. Kaihatsu, K.E. Huffman, D.R. Corey, Intracellular uptake and inhibition of gene expression by PNAs and PNA–peptide conjugates, Biochemistry 43 (45) (2004) 14340–14347.
[5] B.L. Gebski, C.J. Mann, S. Fletcher, S.D. Wilton, Morpholino antisense oligonucleotide induced dystrophin exon 23 skipping in mdx mouse muscle, Hum. Mol. Genet. 12 (15) (2003) 1801–1811.
[6] S. Pujals, J. Fernandez-Carneado, C. Lopez-Iglesias, M.J. Kogan, E. Giralt, Mechanistic aspects of CPP-mediated intracellular drug delivery: Relevance of CPP self-assembly, Biochim. Biophys. Acta. 1758 (3) (2006) 264–279.
[7] E.L. Snyder, S.F. Dowdy, Recent advances in the use of protein transduction domains for the delivery of peptides, proteins and nucleic acids in vivo, Expert Opin. Drug Deliv. 2 (1) (2005) 43–51.
[8] A.R. Thierry, S. Abes, S. Resina, A. Travo, J.P. Richard, P. Prevot, B. Lebleu, Comparison of basic peptides-and lipid-based strategies for the delivery of splice correcting oligonucleotides, Biochim. Biophys. Acta 1758 (3) (2006) 364–374.
[9] S. Abes, D. Williams, P. Prevot, A.R. Thierry, M.J. Gait, B. Lebleu, Endosome trapping limits the efficiency of splicing correction by PNA–oligolysine conjugates, J. Control. Release 110 (3) (2006) 595–604.
[10] J.J. Turner, G.D. Ivanova, B. Verbeure, D. Williams, A.A. Arzumanov, S. Abes, B. Lebleu, M.J. Gait, Cell-penetrating peptide conjugates of peptide nucleic acids (PNA) as inhibitors of HIV-1 Tat-dependent trans-activation in cells, Nucleic Acids Res. 33 (21) (2005) 6837–6849.
[11] T. Shiraishi, S. Pankratova, P.E. Nielsen, Calcium ions effectively enhance the effect of antisense peptide nucleic acids conjugated to cationic tat and oligoarginine peptides, Chem. Biol. 12 (8) (2005) 923–929.
[12] J.P. Richard, K. Melikov, E. Vives, C. Ramos, B. Verbeure, M.J. Gait, L.V. Chernomordik, B. Lebleu, Cell-penetrating peptides. A reevaluation of the mechanism of cellular uptake, J. Biol. Chem. 278 (1) (2003) 585–590.
[13] S.H. Kang, M.J. Cho, R. Kole, Up-regulation of luciferase gene expression with antisense oligonucleotides: implications and applications in functional assay development, Biochemistry 37 (18) (1998) 6235–6239.
[14] T. Shiraishi, P.E. Nielsen, Photochemically enhanced cellular delivery of cell penetrating peptide–PNA conjugates, FEBS Lett. 580 (5) (2006) 1451–1456.
[15] J.S. Wadia, R.V. Stan, S.F. Dowdy, Transducible TAT-HA fusogenic peptide enhances escape of TAT-fusion proteins after lipid raft macropinocytosis, Nat. Med. 10 (3) (2004) 310–315.
[16] J.B. Rothbard, E. Kreider, C.L. VanDeusen, L. Wright, B.L. Wylie, P.A. Wender, Arginine-rich molecular transporters for drug delivery: role of backbone spacing in cellular uptake, J. Med. Chem. 45 (17) (2002) 3612–3618.
[17] B.W. Draper, P.A. Morcos, C.B. Kimmel, Inhibition of zebrafish fgf8 pre-mRNA splicing with morpholino oligos: a quantifiable method for gene knockdo, Genesis 30 (3) (2001) 154–156.
[18] G. Lacerra, H. Sierakowska, C. Carestia, S. Fucharoen, J. Summerton, D. Weller, R. Kole, Restoration of hemoglobin A synthesis in erythroid cells from peripheral blood of thalassemic patients, Proc. Natl. Acad. Sci. U. S. A. 97 (17) (2000) 9591–9596.
[19] J. Alter, F. Lou, A. Rabinowitz, H. Yin, J. Rosenfeld, S.D. Wilton, T.A. Partridge, Q. Lu, Systemic delivery of morpholino oligonucleotide restores dystrophin expression bodywide and improves dystrophic pathology, Nat. Med. 12 (2) (2006) 175–177.
[20] B.W. Neuman, D.A. Stein, A.D. Kroeker, M.J. Churchill, A.M. Kim, P. Kuhn, P. Dawson, H.M. Moulton, R.K. Bestwick, P.L. Iversen, M.J. Buchmeier, Inhibition, escape, and attenuated growth of severe acute respiratory syndrome coronavirus treated with antisense morpholino oligomers, J. Virol. 79 (15) (2005) 9665–9676.
[21] B.W. Neuman, D.A. Stein, A.D. Kroeker, A.D. Paulino, H.M. Moulton, P.L. Iversen, M.J. Buchmeier, Antisense morpholino-oligomers directed against the 5′ end of the genome inhibit coronavirus proliferation and growth, J. Virol. 78 (11) (2004) 5891–5899.
[22] T.S. Deas, I. Binduga-Gajewska, M. Tilgner, P. Ren, D.A. Stein, H.M. Moulton, P.L. Iversen, E.B. Kauffman, L.D. Kramer, P.Y. Shi, Inhibition of flavivirus infections by antisense oligomers specifically suppressing viral translation and RNA replication, J. Virol. 79 (8) (2005) 4599–4609.
[23] R.M. Kinney, C.Y. Huang, B.C. Rose, A.D. Kroeker, T.W. Dreher, P.L. Iversen, D.A. Stein, Inhibition of dengue virus serotypes 1 to 4 in vero cell cultures with morpholino oligomers, J. Virol. 79 (8) (2005) 5116–5128.
[24] J. Summerton, D. Weller, US Patent: (1993) 5185444.
[25] J. Summerton, D. Weller, Morpholino antisense oligomers: design, preparation, and properties, Antisense Nucleic Acid Drug Dev. 7 (3) (1997) 187–195.
[26] H.M. Moulton, M.C. Hase, K.M. Smith, P.L. Iversen, HIV Tat peptide enhances cellular delivery of antisense morpholino oligomers, Antisense Nucleic Acid Drug Dev. 13 (1) (2003) 31–43.
[27] H.M. Moulton, M.H. Nelson, S.A. Hatlevig, M.T. Reddy, P.L. Iversen, Cellular uptake of antisense morpholino oligomers conjugated to arginine-rich peptides, Bioconjug. Chem. 15 (2) (2004) 290–299.
[28] P. Sazani, S.H. Kang, M.A. Maier, C. Wei, J. Dillman, J. Summerton, M. Manoharan, R. Kole, Nuclear antisense effects of neutral, anionic and cationic oligonucleotide analogs, Nucleic Acids Res. 29 (19) (2001) 3965–3974.
[29] J.P. Richard, K. Melikov, H. Brooks, P. Prevot, B. Lebleu, L.V. Chernomordik, Cellular uptake of unconjugated TAT peptide involves clathrin-dependent endocytosis and heparan sulfate receptors, J. Biol. Chem. 280 (15) (2005) 15300–15306.
[30] M. Belting, Heparan sulfate proteoglycan as a plasma membrane carrier, Trends Biochem. Sci. 28 (3) (2003) 145–151.
[31] S. Enterlein, K.L. Warfield, D.L. Swenson, D.A. Stein, J.L. Smith, C.S. Gamble, A.D. Kroeker, P.L. Iversen, S. Bavari, E. Muhlberger, VP35 knockdown inhibits Ebola virus amplification and protects against lethal infection in mice, Antimicrob. Agents Chemother. 50 (3) (2006) 984–993.
[32] K.L. Holden, D.A. Stein, T.C. Pierson, A.A. Ahmed, K. Clyde, P.L. Iversen, E. Harris, Inhibition of dengue virus translation and RNA synthesis by a morpholino oligomer targeted to the top of the terminal 3′ stem-loop structure, Virology 344 (2) (2006) 439–452.
[33] A. Joliot, A. Prochiantz, Transduction peptides: from technology to physiology, Nat. Cell Biol. 6 (2004) 189–196.
[34] M.H. Nelson, D.A. Stein, A.D. Kroeker, S.A. Hatlevig, P.L. Iversen, H.M. Moulton, Arginine-rich peptide conjugation to morpholino oligomers: effects on antisense activity and specificity, Bioconjug. Chem. 16 (4) (2005) 959–966.
[35] G. McClorey, H.M. Moulton, P.L. Iversen, F. Fletcher, S.D. Wilton, Antisense oligonucleotide-induced exon skipping restores dystrophin expression in vitro in a canine model of DMD, Gene Therapy. 13 (19) (2006) 1373–1381.

Published online 21 June 2007

Nucleic Acids Research, 2007, Vol. 35, No. 13 ***4495–4502***
doi:10.1093/nar/gkm418

Efficient splicing correction by PNA conjugation to an R_6-Penetratin delivery peptide

Saïd Abes[1], John J. Turner[2], Gabriela D. Ivanova[2], David Owen[2], Donna Williams[2], Andrey Arzumanov[2], Philippe Clair, Michael J. Gait[2] and Bernard Lebleu[1,*]

[1]UMR 5235 CNRS, Université Montpellier 2, Place Eugene Bataillon, 34095 Montpellier cedex 5, France and [2]Medical Research Council, Laboratory of Molecular Biology, Hills Road, Cambridge CB2 2QH UK

Received January 31, 2007; Revised April 20, 2007; Accepted May 7, 2007

ABSTRACT

Sequence-specific interference with the nuclear pre-mRNA splicing machinery has received increased attention as an analytical tool and for development of therapeutics. It requires sequence-specific and high affinity binding of RNaseH-incompetent DNA mimics to pre-mRNA. Peptide nucleic acids (PNA) or phosphoramidate morpholino oligonucleotides (PMO) are particularly suited as steric block oligonucleotides in this respect. However, splicing correction by PNA or PMO conjugated to cell penetrating peptides (CPP), such as Tat or Penetratin, has required high concentrations (5–10 μM) of such conjugates, unless an endosomolytic agent was added to increase escape from endocytic vesicles. We have focused on the modification of existing CPPs to search for peptides able to deliver more efficiently splice correcting PNA or PMO to the nucleus in the absence of endosomolytic agents. We describe here R_6-Penetratin (in which arginine-residues were added to the N-terminus of Penetratin) as the most active of all CPPs tested so far in a splicing correction assay in which masking of a cryptic splice site allows expression of a luciferase reporter gene. Efficient and sequence-specific correction occurs at 1 μM concentration of the R6Pen–PNA705 conjugate as monitored by luciferase luminescence and by RT-PCR. Some aspects of the R6Pen–PNA705 structure–function relationship have also been evaluated.

INTRODUCTION

A serious limitation of the use of many types of synthetic oligonucleotides (ON) and their analogues as therapeutic antisense agents has been their poor cellular delivery (1,2). Many types of vector have been designed to aid ON delivery both for cell culture and *in vivo*. Amongst such strategies, conjugation to cell penetrating peptides (CPP) has received much recent attention (3–6).

In the case of negatively charged antisense ON, the potential of conjugated CPPs for delivery has not been realized, since there are very few publications that have shown significant biological activity (7,8). Indeed, a recent study with a well-controlled assay dealing with inhibition of *trans*-activation of the HIV-1 LTR showed some significant cell internalization of a number of CPP-ONs, but a complete lack of biological activity (9). In addition, only very modest biological activity was found for similar CPPs conjugated to synthetic short interference RNA (siRNA) targeted to a P38 MAP kinase mRNA (10).

A particularly useful HeLa cell assay for assessing the activity of CPP-ONs conjugates in a comparative manner is that established by Kole and colleagues (11) involving splice correction of an aberrant β-globin intron by 16-mer synthetic oligonucleotides (705 site) and subsequent up-regulation of firefly luciferase. This assay is straightforward to carry out and has a very high dynamic range, such that even very low activity levels can be seen as a positive luminescence read-out. CPPs conjugated to ONs that are not negatively charged, such as peptide nucleic acids (PNA) or phosphoramidate morpholino oligonucleotides (PMO) have shown significant promise in splicing correction assays and other steric block applications, for which PNA is particularly suited. For many PNA conjugates, biological activity in this and other splice alteration assays has been observed when the PNA is attached to cationic, amphipathic or other CPP peptides, but concentrations of conjugates in the 5–10 μM range almost invariably have been needed for incubation with cultured cells to see significant splice alteration activity (12–19).

Recent studies by our laboratories (19–23) and by other groups (24,25) have demonstrated that a major barrier for nuclear delivery, required for splicing correction, is the release from endocytic vesicular compartments. This was not surprising since, for polycationic CPPs such as Tat,

*To whom correspondence should be addressed. Tel: +33 467 14 92 03; Fax: +33 467 14 92 01; Email: bernard.lebleu@univ-montp2.fr
Correspondence may also be addressed to Michael J. Gait. Tel: +44 1223 248011; Fax: +441223 402070; Email: mgait@mrc-lmb.cam.ac.uk

Penetratin, R_9 or K_8, the vast majority of the material is internalized by an active mechanism of endocytosis, which involves electrostatic interactions with cellular heparan sulphates, and has little access to the nuclear compartment (20). Endosomolytic agents, such as chloroquine, calcium ions or high sucrose concentration (21,26), are necessary to obtain a significant splice correction activity (17–19,23), but the use of such agents *in vivo* is difficult to envisage. One possible solution is to complement the CPP with a membrane-destabilizing agent (e.g. viral fusogenic peptide or membrane-destabilizing peptide), such as has been proposed by Dowdy to improve CPP-mediated protein transfection (27), or to screen for a new peptide additive that might improve the biological activity of the CPP conjugate. In addition to the increased complexity of such a delivery system and to its cost, we have not been able to find to date a peptide or lipopeptide that showed substantially enhanced steric-block biological activity for a PNA ON conjugated to the Tat peptide (19). Likewise the co-incubation of 5 μM HA2–Penetratin fusion peptide with various CPP–PNA constructions had only a moderate effect on splice correction (18).

We, therefore, concluded that a better approach is to modify existing CPPs in order to search for peptides that may have enhanced intrinsic endosomolytic activity. Two vector strategies have been adopted, both taking into account the key roles played by Arg side chains in CPP uptake. We recently showed that $(R\text{-Ahx-R})_4$–PMO705 conjugate had significant splicing correction activity in the luciferase up-regulation model at 1 μM concentration in the absence of an endosomolytic agent (28). Similarly we showed that a $(R\text{-Ahx-R})_4$–PNA705 conjugate also had significant splice correction activity at 1 μM concentration (19). In parallel studies, we found substantial activity in an HIV-1 *trans*-activation inhibition assay (also requiring nuclear delivery) when a derivative of the known CPP Penetratin, in which six Arg residues were added to the N-terminus of the CPP, R_6-Penetratin (R6Pen), was disulfide-conjugated to a PNA complementary to the *trans*-activation responsive element RNA (21). We show now that this Arg-modified CPP when conjugated to a PNA targeted to the luciferase splice correction site shows by far the highest up-regulation of luciferase at both protein and RNA levels at 1 μM concentration compared to all previous CPPs studied. We also begin to characterize some aspects of the structure–function relationship and show that, for example, a W→L mutant that was reported to substantially reduce the cell penetration of Penetratin peptide (29) does not reduce the splice correction activity of the R6Pen–PNA conjugate. These results show that R6Pen might be a very good lead CPP towards further development of a suitable PNA–peptide conjugate candidate for *in vivo* studies.

MATERIALS AND METHODS

Synthesis of peptide–PNA conjugates

Synthesis of PNA. N-terminal nitropyridyl (Npys) cysteine-containing PNA oligonucleotides with additional lysine residues were synthesized on an Apex 396 Synthesizer by the Fmoc/Bhoc method as previously described (21,30) to give the general structure NH_2-Cys(NPys)-Lys-PNA-$(Lys)_3$-amide. PNA705 antisense is CCTCTTACCTCAGTTACA and PNA705 scrambled sequence is CCTGTTATACCACTTACA. Note that we have found recently that higher overall synthesis yields are obtained when the final deprotections are carried out in the absence of phenol scavenger. In some cases, N-terminal Cys-containing PNA was obtained from Panagene (www.panagen.com) and activated with dipyridyldisulfide (Pys2) as follows. To the PNA (500 nmol) was added 150 μl Pys2 (6.75 μmol, 13.5 eq.) in DMF (10 mg ml^{-1}), 15 μl 2 M triethylammonium acetate solution (pH 7) and 135 μl water. After standing for 1 h the solution was loaded on to a Sephadex NAP-10 column and eluted with 0.1% TFA solution, collecting the excluded volume. This solution was used directly in conjugation after quantification by measurement of the absorbance at 260 nm. Npys and Pys activated PNA could be used interchangeably in the conjugation reactions to form disulfide linkages.

Stably Linked K_8-PNA705 [NH_2-$(Lys)_8$-CCTCTT ACCTCAGTTACA-Lys-amide] and Tat-PNA705 [NH_2-Gly-Arg-Lys-Lys-Arg-Arg-Gln-Arg-Arg-Arg-Pro-(O-linker)-CCTCTTACCTCAGTTACA-amide] peptide–PNA conjugates were synthesized by continuous PNA/peptide synthesis as previously described (21,30). An O-linker was added with an Fmoc-AEEA spacer (Applied Biosystems). The α-N-bromoacetyl-Lys-PNA-$(Lys)_3$-amide (both 705 and scrambled 705) were obtained from Panagene (Korea).

MALDI-TOF mass spectrometry was carried out on a Voyager DE Pro BioSpectrometry workstation with a matrix of α-cyano-4-hydroxycinnamic acid, 10 mg ml^{-1} in acetonitrile/3% aqueous trifluoroacetic acid (1:1, v/v). The accuracy of the mass measurement in linear mode is regarded by the manufacturer as ±0.05%, but since internal calibration was not used, the determined values varied in a few cases from the calculated by ± 0.1%.

Synthesis of peptides. All peptides were prepared with free N-terminus and C-terminal amide and also contained an additional C-terminal cysteine residue to allow conjugation. Tat: GRKKRRQRRRPC, Pen: RQIKIWFQNRRMKWKKGGC and $(R\text{-Ahx-R})_4$-C were obtained from Southampton Polypeptides/Activotec. R_6-Pen: RRRRRRRQIKIWFQNRRMKW KKGGC, $R_6Pen_{(W\text{-}L)}$: RRRRRRRQIKILFQNRRMK WKKGGC, R_3Pen: RRRQIKIWFQNRRMKWKK GGC and R_9Pen: RRRRRRRRRQIKIWFQNRR MKWKKGGC were synthesized on a PerSeptive Biosystems Pioneer peptide synthesiser (100 μmol scale) using standard Fmoc/*tert*-butyl solid phase synthesis techniques as C-terminal amide peptides using NovaSyn TGR resin (Novabiochem). Deprotection of all peptides and cleavage from the solid support was achieved by treatment with trifluoroacetic acid (TFA) in the presence of triethylsilane (1%), ethane dithiol (2.5%) and water (2.5%). Purification was carried out by reversed phase HPLC as previously described (9) and analysed by MALDI-TOF mass spectrometry with the same matrix as for PNA.

Conjugation of peptides with PNA

Thioether conjugations. In a typical conjugation reaction, 50 nmol bromoacetyl PNA was dissolved in 45 µl formamide and 10 µl BisTris–HBr buffer (pH 7.5) and 15.6 µl C-terminal-Cys containing peptide (8 mM, 125 nmol. 2.5 eq.) was added. The solution was heated at 40°C for 2 h and the product was purified by reversed phase HPLC at 45°C using water bath heating and analysed by MALDI-TOF mass spectrometry (Supplementary Table S1).

Disulfide conjugations. These were carried out essentially as previously described usually with a 2.5-fold excess of peptide component over PNA component. Purification was carried out by reversed phase HPLC as above and analysis by MALDI-TOF mass spectrometry (21,30)(see Supplementary Table S1).

Splice correction assay

This was carried out similarly to that described previously (28). The conjugates (Table 1) were incubated for 4 h in 1 ml OptiMEM medium with exponentially growing HeLa pLuc705 cells (1.75×10^5 cells/well seeded and cultivated overnight in 24-well plates). The conjugates were then diluted with 0.5 ml complete medium (DMEM plus 10% fetal bovine serum) and incubation continued for 20 h. Cells were washed twice with ice-cold PBS and lysed with Reporter Lysis Buffer (Promega, Madison, WI, USA). Luciferase activity was quantified with a Berthold Centro LB 960 luminometer (Berthold Technologies, Bad Wildbad, Germany) using the Luciferase Assay System substrate (Promega, Madison, WI, USA). Cellular protein concentrations were measured with the BCA™Protein Assay Kit (Pierce, Rockford, IL, USA) and read using an ELISA plate reader (Dynatech MR 5000, Dynatech Labs, Chantilly, VA, USA) at 550 nm. Levels of luciferase expression are shown as relative light units (RLUs) per microgram protein. All experiments were performed in triplicate. Each data point was averaged over the three replicates.

Cell permeability assay (Flow cytometry analysis)

To analyse the cell permeabilization of CPP–PNA conjugates, exponentially growing HeLa pLuc705 cells (3×10^5 cells seeded and grown overnight in 30 mm plates) were incubated for 4 h with the CPP–PNA705 conjugates at different concentrations. The cells were then washed twice with PBS, detached by incubating with trypsin for 5 min at 37°C (0.5 mg ml^{-1})/EDTA.4Na (0.35 mM), and washed by centrifugation (5 min, 900 × *g*) in ice-cold PBS containing 5% FCS. The cell pellet was resuspended in ice-cold PBS containing 0.5% FCS and 0.05 µg/ml propidium iodide (PI) (Molecular Probes, Eugene, OR, USA). Fluorescence analysis was performed with a BD FacsCanto flow cytometer (BD Biosciences, San Jose, CA, USA). A minimum of 20 000 events per sample were analysed.

RT–PCR analysis of splice correction

HeLa pLuc705 cells were plated at 30 000 cells/well in a 24-well plate 24 h before treatment. After overnight incubation, the cells were washed with PBS and incubated in 1 ml OptiMEM containing 1 µM of the indicated conjugates (naked PNA705, Pen-s-s–PNA705, R6Pen-s-s–PNA705, R6Pen-s-s–PNA705scr or R6Pen(W–L)-s-s–PNA705) for 4 h and the conjugates were then diluted with 0.5 ml of DMEM containing 10% FCS and allowed to grow for 20 h. Cells were then washed twice with PBS. Total RNA was extracted from the cells using the High pure RNA isolation Kit (Roche Applied Science). The extracted RNA was examined by RT-PCR (MJ Research PTC200 Peltier Thermal cycler) with forward primer 5′TTG ATA TGT GGA TTT CGA GTC GTC3′ and reverse primer 5′TGT CAA TCA GAG TGC TTT TGG CG3′. The products were analysed on a 2% agarose gel (Figure 7A).

For dose-dependence experiments (Figure 7B), cells were treated as described above with increasing concentrations of R6Pen-s-s–PNA705 or R6Pen–PNA705 conjugates. After carrying out the luciferase assay and

Table 1. Sequences and nomenclature of CPP–PNA705 conjugates

Name	Sequences[a]
	Stably linked
R6Pen–PNA705 (S-CH2)[b]	**NH_2-RRRRRRRQIKIWFQNRRMKWKKGGC**-thioacetyl-**K**-CCT CTT ACC TCA GTT ACA-**KKK**-amide
R6Pen–PNA705scr (S-CH2)[b]	**NH_2-RRRRRRRQIKIWFQNRRMKWKKGGC**-thioacetyl-**K**-CCT GTT ATA CCA CTT ACA-**KKK**-amide
Tat–PNA705[c]	**NH_2-GRKKRRQRRRP**-O linker-CCT CTT ACC TCA GTT ACA-amide
K8–PNA705[c]	**NH_2-KKKKKKKK-**CCT CTT ACC TCA GTT ACA -**K**-amide
(R-Ahx-R)4–PNA705(S-CH2)[b]	**NH_2-R-Ahx-RR-Ahx-RR-Ahx-RR-Ahx-R-C**-thioacetyl-**K**-CCT GTT ATA CCA CTT ACA-**KKK**-amide
	Disulfide linked[d]
Pen-s-s–PNA705	**NH_2-RQIKIWFQNRRMKWKKGGC**-ss-**CK**-CCT CTT ACC TCA GTT ACA-**KKK**-amide
R6Pen-s-s–PNA705	**NH_2-RRRRRRRQIKIWFQNRRMKWKKGGC**-ss-**CK**-CCT CTT ACC TCA GTT ACA-**KKK**-amide
R6Pen-s-s-PNA705scr	**NH_2-RRRRRRRQIKIWFQNRRMKWKKGGC**-ss-**CK**-CCT GTT ATA CCA CTT ACA-**KKK**-amide
R6Pen(W–L)-s-s–PNA705	**NH_2-RRRRRRRQIKILFQNRRMKWKKGGC**-ss-**CK**-CCT CTT ACC TCA GTT ACA-**KKK**-amide
R3Pen-s-s–PNA705	**NH_2-RRRRQIKIWFQNRRMKWKKGGC**-ss-**CK**-CCT CTT ACC TCA GTT ACA-**KKK**-amide
R9Pen-s-s–PNA705	**NH_2-RRRRRRRRRRQIKIWFQNRRMKWKKGGC**-ss-**CK**-CCT CTT ACC TCA GTT ACA-**KKK**-amide

[a]Bold denotes amino acid residues, normal typeface for PNA residues and an underlined residue shows a W to L mutation in Penetratin.
[b]A thioacetyl linker is formed between a C-terminal cysteine on the peptide and a N-α-bromoacetyl-substituted PNA.
[c]A continuous synthesis (an O-linker is added with an Fmoc-AEEA spacer monomer from Applied Biosystems).
[d]All disulfide-linked conjugates are formed between a C-terminal Cys residue on the peptide and an N-terminal Cys residue on the PNA part.

BCA™ Protein Assay, the remaining cell lysates (about 270 µl) were transferred into 2 ml microfuge tubes and total RNA was extracted with 1 ml TRI Reagent (Sigma). Minor changes to the manufacturer's protocol were made to accommodate the presence of Reporter Lysis Buffer. Thus, 0.3 ml of chloroform was used for extraction and the amount of iso-propanol for RNA precipitation was increased to give a 1:1 mixture with the aqueous phase. The RT-PCR was carried out as described above and agarose gels were scanned using Gene Tools Analysis Software (SynGene, Cambridge, UK).

RESULTS

Figure 1 shows a comparison of the splice correction activities at 1 µM concentration of unconjugated PNA705, K8-PNA705 and Tat-PNA705, the activity of each of which is known to be chloroquine-dependent (9,17,18,23), together with R6Pen–PNA705 and (R-Ahx-R)4–PNA705 (19) in the absence of an endosomolytic agent. In all cases, PNAs were conjugated to the carrier peptides through stable amide or thioacetyl linkages (Table 1 for construct details). R6Pen conjugate, and to a lesser extent (R-Ahx-R)4 conjugate, gave rise to a strong up-regulation of luciferase under conditions where K8 and Tat peptide conjugates were essentially inactive. Note that the scale of light units is shown in relative light units per microgram protein, demonstrating the very high level of activity seen for R6Pen–PNA705. The low level of activity for Tat-PNA705 agrees with results recently reported by two other laboratories, where similarly low splice correction was seen also for Penetratin, R_9 and Transportan at 1 µM concentration (17,18) and only at 5–10 µM concentrations did some conjugates (notably Transportan) show significant splice correction activity. Thus, R6Pen appears substantially more effective as a CPP and leads to much stronger splice correction activity compared to our previously used (R-Ahx-R)4–PNA705.

The splice correction activity of the R6Pen conjugate is sequence-specific, since no splice correction activity is seen when this CPP vector is conjugated to a scrambled version of PNA705 (Figure 2). Note that luciferase activity levels vary somewhat between experiments as pointed out by Bendifallah *et al.* (17). Normalization of the data to the basal luciferase expression in untreated cells, as proposed by these authors, gives rise to much less apparent variation between experiments (see Supplementary Data, Figures 1 and 2), but we have chosen here to show un-normalized values just to demonstrate the high activity levels.

To characterize further the properties of the R6Pen–PNA705 conjugate, we monitored the dose-dependence of splice correction, as measured by luciferase up-regulation, at concentrations between 0.1 and 2.5 µM (Figure 3). R6Pen–PNA705 allows an efficient dose-dependent splice correction activity in the absence of chloroquine (Figure 3, white bars) under conditions where no toxicity was seen, as judged by measurement of PI uptake by flow cytometry (Supplementary Data, Figure 3). The proportion of permeabilized cells remained <3% as compared to the untreated controls in cells incubated with the various CPP–PNA conjugates at 1 µM (e.g. at the concentration allowing almost complete splicing correction). The addition of chloroquine improved the splice correction activity, which demonstrates that some of the conjugate still remains entrapped in endosomal compartments in keeping with an endocytotic mechanism of cell uptake. However, the incremental improvement in splice correction activity afforded by chloroquine addition was somewhat smaller at the higher concentrations (approximately 2- to 3-fold, Figure 3, grey bars), than those we obtained previously with K8 and Tat conjugates of PNA or PMO, where a 10-fold increase or more was often observed (19,23).

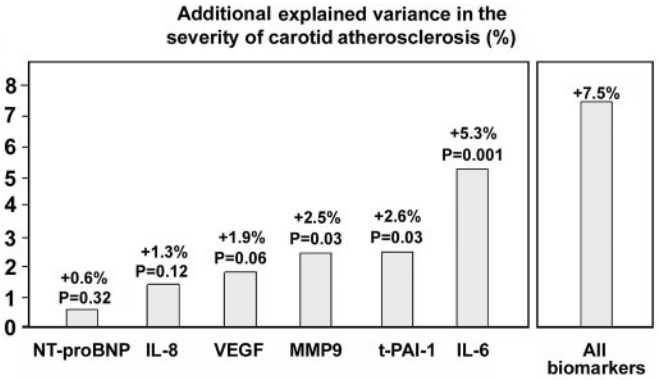

Figure 1. Comparison of splice correction efficiencies by various CPP–PNA705 conjugates. HeLa pLuc705 cells were incubated for 4 h in OptiMEM in the absence (control), in the presence of 1 µM PNA705 alone, or in the presence of 1 µM CPP–PNA705 conjugates. Luciferase expression was quantified 20 h later and was expressed as RLU per microgram protein. Each experiment was made in triplicate and error bars (standard deviations) are indicated.

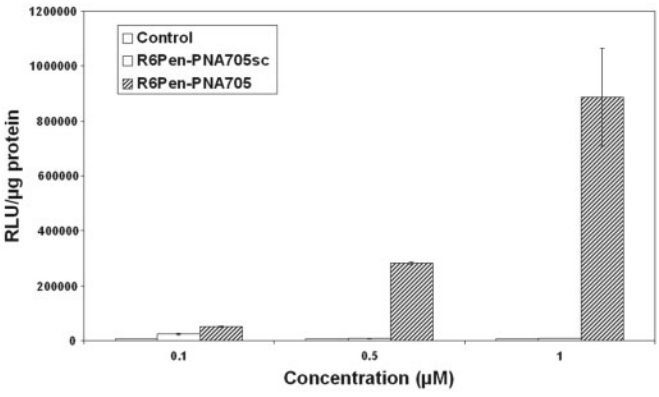

Figure 2. Splice correction specificity. HeLa pLuc705 cells were incubated for 4 h in OptiMEM in the absence (control) of correcting PNA, in the presence of the stably linked R_6Pen–PNA705 splice correcting conjugate, or in the presence of its scrambled version at the indicated concentrations. Luciferase expression was quantified 20 h later and was expressed as RLU per microgram protein. Each experiment was made in triplicate and error bars (standard deviations) are indicated.

We next investigated the importance of the stability of the linkage between the delivery peptide and the PNA cargo. It has been suggested by others that if a disulfide-linked conjugate is able to escape from the endocytic compartments and reaches the cytosol, the disulfide bridge might be reduced, thus allowing free PNA to be released (31). A new conjugate R6Pen-s-s–PNA705 (Table 1) was therefore constructed with a linker containing a disulfide bridge, similar to that which we have previously used in studies of HIV-1 Tat-dependent *trans*-activation inhibition (21). This conjugate was tested in the splice-correction assay in parallel with the stably linked R6Pen–PNA705 and indeed showed a slightly (but reproducibly) higher activity (Figure 4). However, the relatively small difference demonstrates that the nature of the linkage is not a principal factor governing splice correction activity. Nevertheless, we decided to use the more active disulfide-bridged conjugates for further studies on the structure–function relationship.

In order to determine the effect of the N-terminal Arg stretch on splice correction activity, we constructed a series of R(z)Pen-s-s–PNA705 conjugates with z {0, 3, 6 and 9}. These R(z)Pen-s-s–PNA705 conjugates were tested at 0.5 and 1 μM in the splice correction assay in the absence of chloroquine (Figure 5). Pen-s-s–PNA705 at 1 μM displays only a very weak activity, consistent with previous results of others (17,18). The activity level is strongly enhanced by the addition of an Arg tail by factors of 16, 43 and 28 for z = 3, 6 and 9, respectively. Thus, at 1 μM concentration, the optimum activity is obtained for R_6. No significant differences were seen in cell toxicity for any of the conjugates at this concentration as judged by flow cytometry and PI uptake (Supplementary Data, Figure 3).

Previous studies (29) have shown that the substitution of the tryptophan residues that occurs naturally in the *Antennapaedia* homeodomain helix 3 sequence by a leucine residue decreased the cell internalization of Penetratin peptide. Surprisingly, the R6Pen(W–L)-s-s–PNA705 conjugate displayed a slightly higher splicing correction activity than the unmodified R6Pen–PNA705 (Figure 6). This indicates that the Penetratin part of the R6Pen–PNA conjugate has a completely different effect in enhancement of membrane permeabilization when it is located within the PNA conjugate context as compared to the Penetratin peptide alone.

In most studies using the HeLa-pLuc705 model, splice-correction is monitored by the quantification of luciferase luminescence activity (17–19,22,23,28). However, this assay gives only a relative appreciation of splice correction activity between different conjugates. In contrast, use of RT-PCR allows the evaluation of the completeness of splice correction by comparison of the

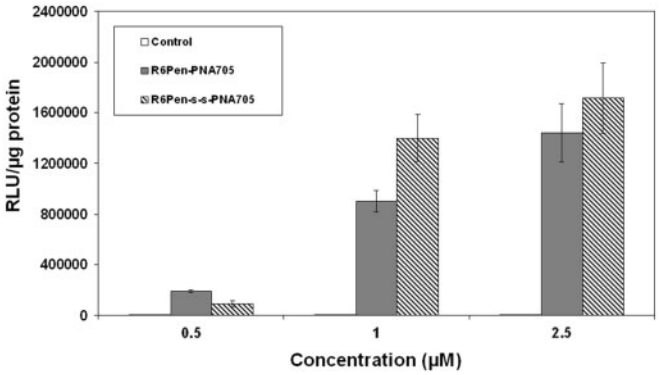

Figure 4. The effect of CPP–PNA705 linker stability on splice correction. HeLa pLuc705 cells were incubated for 4 h in OptiMEM in the absence (control) or in the presence of R_6Pen–PNA705 conjugates at the indicated concentrations. The R_6Pen and PNA705 moieties were conjugated by a stable thioacetyl or by a reducible disulfide linker. Luciferase expression was quantified 20 h later and was expressed as RLU per μg protein. Each experiment was made in triplicate and error bars (standard deviations) are indicated.

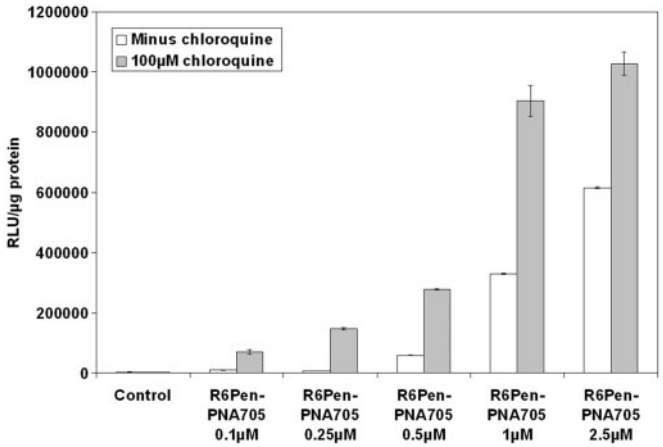

Figure 3. The effect of chloroquine on splice correction. HeLa pLuc705 cells were incubated for 4 h in OptiMEM with R_6Pen–PNA705 correcting conjugates at the indicated concentrations in the absence (white bars) or in the presence (grey bars) of 100 μM chloroquine. Luciferase expression was quantified 20 h later and was expressed as RLU per microgram protein. Each experiment was made in triplicate and error bars (standard deviations) are indicated.

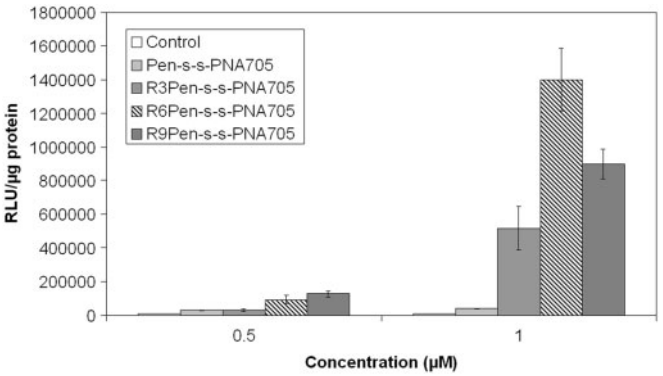

Figure 5. The effect of the number of arginine residues on splice correction. HeLa pLuc705 cells were incubated for 4 h in OptiMEM in the absence (control) or in the presence of R_zPen–PNA705 conjugates (with z = 0, 3, 6 or 9) at the indicated concentrations. Luciferase expression was quantified 20 h later and was expressed as RLU per microgram protein. Each experiment was made in triplicate and error bars (standard deviations) are indicated.

amounts of uncorrected and corrected mRNA, as has been used with this splice correction assay for cationic lipid-based transfection methods (11,32). We, therefore, carried out RT-PCR on RNA samples extracted from HeLa-pLuc705 cells incubated with various conjugates (Figure 7A). As expected, no RT-PCR products corresponding to the correctly spliced mRNA were detected in cells treated with 1 μM of free PNA705, Pen-s-s–PNA705, or scrambled control R6Pen-s-s–PNA705sc, as seen in lanes 1, 2 and 3, respectively. In contrast, a very high proportion of correctly spliced mRNA was found in cells treated with 1 μM R6Pen-s-s–PNA705 (lane 4) or with R6Pen(W–L)-s-s–PNA705 (lane 6).

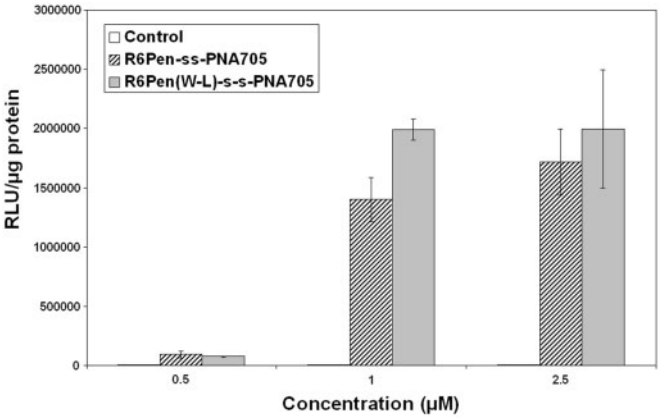

Figure 6. The effect of a W→L Penetratin mutation on splice correction. HeLa pLuc705 cells were incubated for 4 h in OptiMEM in the absence (control) or in the presence of CPP–PNA705 conjugates at the indicated concentrations. Luciferase expression was quantified 20 h later and was expressed as RLU per microgram protein. Each experiment was made in triplicate and error bars (standard deviations) are indicated.

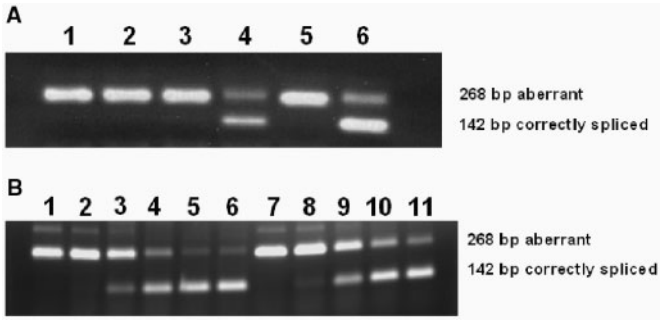

Figure 7. RT-PCR analysis of splice correction. (**A**) HeLa pLuc705 cells were incubated for 4 h in OptiMEM in the absence (control), in the presence of 1 μM PNA705 alone or in the presence of 1 μM CPP–PNA705 conjugates. Total RNA was extracted 20 h later and amplified by RT-PCR. PCR products from incorrectly (268 bp) and correctly (142 bp) spliced luciferase pre-mRNA were analysed on a 2% agarose gel. Lane 1: control, Lane 2: PNA705_alone, Lane 3: Pen-ss–PNA705, Lane 4: R_6Pen-s-s–PNA705, Lane 5: R_6Pen-s-s–scrambled PNA705, Lane 6: R_6Pen(W–L)-s-s–PNA705. (**B**) Dose dependencies of splice correction using 1 μg of total RNA extracted, amplified by RT-PCR and analyses as in (a). Lane 1: control of untreated cells, Lanes 2–6: cells treated with 0.25, 0.5, 1, 2 or 4 μM R6Pen-s-s–PNA705 respectively and Lanes 7–11: cells treated with 0.25, 0.5, 1, 2 or 4 μM stably linked R6Pen–PNA705, respectively.

The dose-dependences of splice correction for R6Pen-s-s–PNA706 and stably linked R6Pen–PNA705 were assessed by the RT-PCR assay (Figure 7B). The EC_{50}s of splice correction at the RNA level were estimated as 0.7 ± 0.3 μM and 1.0 ± 0.3 μM, respectively. EC_{50}s were also estimated from the amounts of conjugate required to raise the luciferase luminescence levels to 50% of the observed plateaux values (data not shown). These values were found to be 0.9 ± 0.2 μM and 1.0 ± 0.2 μM, respectively.

DISCUSSION

The nuclear delivery of steric-block ON analogues conjugated with most CPPs for splice correction or exon skipping has been hampered by endosome trapping, unless an endosome disturbing drug or peptide is added, or high CPP–PNA conjugate concentrations are used. Bearing in mind the key role played by cationic amino acids for CPP uptake, we have appended varying numbers of arginine residues to the N-terminal end of Penetratin, a CPP which by itself does not impart on the PNA a significant amount of splice correction ability. R6Pen turned out to be the most active. The level of activity obtained for splice correcting conjugated PNA is higher than for all other CPPs tested to date, including the recently described (R-Ahx-R)4 vector (19,28). Remarkably, R6Pen–PNA705 conjugates are highly active at 1 μM concentrations in the absence of any endosomolytic agents.

Quantification of luciferase expression, as carried out here and also in most published work to date, is a sensitive and convenient assay, which allows one to compare several conjugates quickly in terms of efficiency or specificity, and is thus the method of choice for structure–activity relationships studies. However, such data are expressed in relative light units and do not allow direct determination of the extent to which aberrant splicing has been corrected. RT-PCR products from the aberrantly and correctly spliced luciferase pre-mRNA can be separated easily by agarose gel electrophoresis, thus allowing evaluation of the extent of splice correction under various conditions. RT-PCR data closely parallel luciferase luminescence measurements and indicate that the R6Pen-ss–PNA705 and the W→L variant allow sequence-specific splicing correction at 1 μM concentration to a high level (about 60–70%), whilst PNA705 alone or Pen-s-s–PNA705 are totally inactive. The levels of activity we have obtained (EC_{50} of 0.7–1.0 μM) now start to approach those obtained with the same assay by cationic lipid transfection using leashed PNA or other modified ON types (11,32).

The achievement of a fair proportion of correction at low conjugate concentration is a key issue in the development of steric block ONs as potential therapeutics. By use of PI as an index of membrane permeabilization, we have indeed verified that R6Pen did not perturb membrane integrity of HeLa cells at the active dosage. Previous studies from our group have established that high (>5 μM) concentrations of CPP–ON as R_9 or K_8–ON

led to significant increase of PI uptake thus precluding further developments (23).

We have no explanation at this stage for the dramatically increased splice correction activity of R6Pen as compared to Pen or as compared to several Arg-rich CPPs. It is worth emphasizing in this respect that the W→L mutation in the Penetratin moiety, which is known to inhibit Penetratin peptide uptake (29), does not affect splice correction by R6Pen–PNA705 and instead gave rise to a slightly higher activity (Figures 6 and 7), thus inferring different mechanisms by which this CPP operates. Along the same lines, chloroquine has a significantly lower effect on splice correction by R6Pen–PNA705 (Figure 3) as compared to Tat-PNA705 (19) or K8-PNA705 (23), in keeping with its improved intrinsic endosomal escape. We are also able to rule out significant effects of the Lys residues on the PNA part on splice correction activity. Indeed we have found recently that R6Pen disulfide linked to a PNA 18-mer containing just one Lys residue on each end behaved identically to the corresponding conjugate containing four Lys residues (data not shown). Further mechanistic studies are in progress, but it should be noted that we have deliberately avoided on these conjugates the use of fluorescent labels, which are commonly used to track cellular uptake by confocal microscopy. Such labels alter the hydrophobicity of the conjugate at a particular region. This may alter the ability of the PNA-peptide to be released from endosomal compartments. Concerns about this have emerged recently in the case of our parallel studies on inhibition of HIV-1 Tat-dependent *trans*-activation (21). We have been unable so far to construct a conjugate that contains a fluorescein label on the PNA part of a R_6-Penetratin–PNA conjugate targeted to TAR without losing all intra-nuclear inhibition activity in the absence of chloroquine in our HeLa cell assay (Turner, J.J., Arzumanov, A.A., Ivanova, G.D. and Gait, M.J., unpublished results). Further, there does not appear to be a strong correlation of the amount of fluorescent oligonucleotide reagent seen to be taken up by cells and their biological activity (21,23,25,28), as has also become apparent in the design of lipid-based reagents for delivery of siRNA (33). Thus, more sophisticated ways of tracking locations of nucleic acids-based reagents and determining the precise compartments where activity takes place will be needed before such types of experiment become fully meaningful.

Whether CPP delivery peptides and their cargoes should be conjugated through stable or unstable linkers has often been debated, but few direct comparisons have been provided. In our case, a disulfide-linked conjugate was slightly (but reproducibly) more active than a stably conjugated PNA. Thus, we are now in the process of carrying out further more detailed structure–function analyses using such disulfide linkers to try to understand how the various parts of the R6-Penetratin peptide contribute to obtaining intra-nuclear splice correction activity. The disulfide linker strategy may also be less susceptible to problems arising from steric interference by the conjugated delivery vehicle, or from potential non-specific binding of the vector to non-targeted entities. However, use of PNA–peptide conjugates *in vivo* may require a more stable linkage and our work shows that a thioacetyl linker is also compatible with high-level splice correction activity.

The fact that strong splicing correction (as judged by the RT-PCR analysis) can be achieved at much lower (1 μM) concentration of the correcting ON than has previously proved possible opens up promising perspectives for *in vivo* applications. We hope that further optimization of the peptide–PNA construct will lead to a construct suitable for *in vivo* studies, and eventually for instance towards the treatment of disease-associated splicing defects [cancer, thalassemia, etc. (34)] or in exon-skipping strategies, as are now being considered for the treatment of Duchenne muscular dystrophy (35,36).

SUPPLEMENTARY DATA

Supplementary data are available at NAR Online.

ACKNOWLEDGEMENTS

We acknowledge a CEFIPRA (3205-1) grant to B. L. S. A. is the recipient of a fellowship from the Ligue Régionale contre le Cancer. We thank R. Kole for the generous gift of the HeLa pLuc 705 cell line. Funding for the Open Access Publication charges for this article was provided by CNRS.

Conflict of interest statement. None declared.

REFERENCES

1. Thierry,A.R., Vivès,E., Richard,J.-P., Prevot,P., Martinand-Mari,C., Robbins,I. and Lebleu,B. (2003) Cellular uptake and intracellular fate of antisense oligonucleotides. *Curr. Opinion in Mol. Therapeutics*, **5**, 133–138.
2. Shi,F. and Hoekstra,D. (2004) Effective intracellular delivery of oligonucleotides in order to make sense of antisense. *J. Controll. Release*, **97**, 189–209.
3. Gait,M.J. (2003) Peptide-mediated cellular delivery of antisense oligonucleotides and their analogues. *Cell. Mol. Life Sci.*, **60**, 1–10.
4. Juliano,R.L. (2005) Peptide-oligonucleotide conjugates for the delivery of antisense and siRNA. *Curr. Opinion in Mol. Therapeutics*, **7**, 132–138.
5. Venkatesan,N. and Kim,B.H. (2006) Peptide conjugates of oligonucleotides: synthesis and applications. *Chem. Rev.*, **106**, 3712–3761.
6. Turner,J.J., Arzumanov,A., Ivanova,G., Fabani,M. and Gait,M.J. (2006) . In Langel,U. (ed.), *Cell-Penetrating Peptides, 2nd edn.* CRC Press, Boca Raton, pp. 313–328.
7. Astriab-Fisher,A., Sergueev,D.S., Fisher,M., Ramsay Shaw,B. and Juliano,R.L. (2000) Antisense inhibition of P-glycoprotein expression using peptide-oligonucleotide conjugates. *Biochem. Pharmacol.*, **60**, 83–90.
8. Astriab-Fisher,A., Sergueev,D., Fisher,M., Ramsay Shaw,B. and Juliano,R.L. (2002) Conjugates of antisense oligonucleotides with the Tat and Antennapedia cell-penetrating peptides: effect on cellular uptake, binding to target sequences, and biologic actions. *Pharmaceutical Res.*, **19**, 744–754.
9. Turner,J.J., Arzumanov,A.A. and Gait,M.J. (2005) Synthesis, cellular uptake and HIV-1 Tat-dependent trans-activation inhibition activity of oligonucleotide analogues disulphide-conjugated to cell-penetrating peptides. *Nucleic Acids Res.*, **33**, 27–42.
10. Turner,J.J., Jones,S., Fabani,M., Ivanova,G., Arzumanov,A. and Gait,M.J. (2007) RNA targeting with peptide conjugates of oligonucleotides, siRNA and PNA. *Blood Cells Mol. Dis.*, **38**, 1–7.

11. Kang,S.-H., Cho,M.-J. and Kole,R. (1998) Up-regulation of luciferase gene expression with antisense oligonucleotides: implications and applications in functional assay development. *Biochemistry*, **37**, 6235–6239.
12. Sazani,P., Kang,S.-H., Maier,M.A., Wei,C., Dillman,J., Summerton,J., Manoharan,M. and Kole,R. (2001) Nuclear antisense effects of neutral, anionic and cationic analogs. *Nucleic Acids Res.*, **29**, 3965–3974.
13. Sazani,P., Gemignani,F., Kang,S.-H., Maier,M.A., Manoharan,M., Persmark,M., Bortner,D. and Kole,R. (2002) Systemically delivered antisense oligomers upregulate gene expression in mouse tissues. *Nature Biotech.*, **20**, 1228–1233.
14. Siwkowski,A.M., Malik,L., Esau,C.C., Maier,M.A., Wancewicz,E.V., Albertshofer,K., Monia,B.P., Bennett,C.F. and Eldrup,A.B. (2004) Identification and functional validation of PNAs that inhibit murine CD40 expression by redirection of splicing. *Nucleic Acids Res.*, **32**, 2695–2706.
15. Albertshofer,K., Siwkowski,A.M., Wancewicz,E.V., Esau,C.C., Watanabe,T., Nishihara,K.C., Kinberger,G.A., Malik,L., Eldrup,A.B. *et al.* (2005) Structure-activity relationship study on a simple cationic peptide motif for cellular delivery of antisense peptide nucleic acid. *J. Med. Chem.*, **48**, 6741–6749.
16. Maier,M.A., Esau,C.C., Siwkowski,A.M., Wancewicz,E.V., Albertshofer,K., Kinberger,G.A., Kadaba,N.S., Watanabe,T., Manoharan,M. *et al.* (2006) Evaluation of basic amphipathic peptides for cellular delivery of antisense peptide nucleic acids. *J. Med. Chem.*, **49**, 2534–2542.
17. Bendifallah,N., Rasmussen,F.W., Zachar,V., Ebbesen,P., Nielsen,P.E. and Koppelhus,U. (2006) Evaluation of cell-penetrating peptides (CPPs) as vehicles for intracellular delivery of antisense peptide nucleic acid (PNA). *Bioconjugate Chem.*, **17**, 750–758.
18. El-Andalousi,S., Johansson,H.J., Lundberg,P. and Langel,U. (2006) Induction of splice correction by cell-penetrating peptide nucleic acids. *J. Gene Medicine*, **8**, 1262–1273.
19. Abes,S., Moulton,H.M., Turner,J.J., Clair,P., Richard,J.-P., Iversen,P.L., Gait,M.J. and Lebleu,B. (2007) Peptide-based delivery of nucleic acids: design, mechanism of uptake and applications to splice-correcting oligonucleotides. *Biochem. Soc. Trans.*, **35**, 53–55.
20. Richard,J.-P., Melikov,K., Vivès,E., Ramos,C., Verbeure,B., Gait,M.J., Chernomordik,L.V. and Lebleu,B. (2003) Cell-penetrating peptides. A re-evaluation of the mechanism of cellular uptake. *J. Biol. Chem.*, **278**, 585–590.
21. Turner,J.J., Ivanova,G.D., Verbeure,B., Williams,D., Arzumanov,A., Abes,S., Lebleu,B. and Gait,M.J. (2005) Cell-penetrating peptide conjugates of peptide nucleic acids (PNA) as inhibitors of HIV-1 Tat-dependent trans-activation in cells. *Nucleic Acids Res.*, **33**, 6837–6849.
22. Wolf,Y., Pritz,S., Abes,S., Bienert,M., Lebleu,B. and Oehlke,J. (2006) Structural requirements for cellular uptake and antisense activity of peptide nucleic acids conjugated with various peptides. *Biochemistry*, **45**, 14944–14954.
23. Abes,S., Williams,D., Prevot,P., Thierry,A.R., Gait,M.J. and Lebleu,B. (2006) Endosome trapping limits the efficiency of splicing correction by PNA-oligolysine conjugates. *J. Controll. Rel.*, **110**, 595–604.
24. Koppelhus,U., Awasthi,S.K., Zachar,V., Holst,H.U., Ebbeson,P. and Nielsen,P.E. (2002) Cell-dependent differential cellular uptake of PNA, peptides and PNA-peptide conjugates. *Antisense & Nucl. Acid Drug Dev.*, **12**, 51–63.
25. Kaihatsu,K., Huffman,K.E. and Corey,D.R. (2004) Intracellular uptake and inhibition of gene expression by PNAs and PNA-peptide conjugates. *Biochemistry*, **43**, 14340–14347.
26. Shiraishi,T., Pankratova,S. and Nielsen,P.E. (2005) Calcium ions effectively enhance the effect of antisense peptide nucleic acids conjugated to cationic Tat and oligoarginine peptides. *Chem. and Biol.*, **12**, 923–929.
27. Wadia,J.S., Stan,R.V. and Dowdy,S.F. (2004) Transducible TAT-HA fusogenic peptide enhances escape of TAT-fusion proteins after lipid raft macropinocytosis. *Nat. Med.*, **10**, 310–315.
28. Abes,S., Moulton,H.M., Clair,P., Prevot,P., Youngblood,D.S., Wu,R.P., Iversen,P.L. and Lebleu,B. (2006) Vectorization of morpholino oligomers by the $(R\text{-}Ahx\text{-}R)_4$ peptide allows efficient splicing correction in the absence of endosomolytic agents. *J. Controll. Rel.*, **116**, 304–313.
29. Lindgren,M., Gallet,X., Soomets,U., Hällbrink,M., Bråkenhielm,E., Pooga,M., Brasseur,R. and Langel,U. (2000) Translocation properties of novel cell penetrating Transportan and Penetratin analogues. *Bioconjugate Chem.*, **11**, 619–626.
30. Turner,J.J., Williams,D., Owen,D. and Gait,M.J. (2005) Disulfide conjugation of peptides to oligonucleotides and their analogues. *Curr. Protocols Nucleic Acids Chem.*, 4.28.1–4.28.21.
31. Hällbrink,M., Florén,A., Elmquist,A., Pooga,M., Bartfai,T. and Langel,U. (2001) Cargo delivery kinetics of cell-penetrating peptides. *Biochim. Biophys. Acta*, **1515**, 101–109.
32. Shiraishi,T., Bendifallah,N. and Nielsen,P.E. (2006) Cellular delivery of polyheteroaromate-Peptide Nucleic Acid conjugates mediated by cationic lipids. *Bioconjugate Chem.*, **17**, 189–194.
33. Heyes,J., Palmer,L., Bremner,K. and MacLachlan,I. (2005) Cationic lipid saturation influences intracellular delivery of encapsulated nucleic acids. *J. Controll. Rel.*, **107**, 276–287.
34. Kole,R., Vacek,M. and Williams,T. (2004) Modification of alternative splicing by antisense therapeutics. *Oligonucleotides*, **14**, 65–74.
35. McClorey,G., Moulton,H.M., Iversen,P.L. and Wilton,S.D. (2006) Antisense oligonucleotide-induced exon skipping restores dystrophin expression in vitro in a canine model of DMD. *Gene Ther.*, **13**, 1373–1381.
36. McClorey,G., Fall,A.M., Moulton,H.M., Iversen,P.L., Rasko,J.E., Ryan,M., Fletcher,S. and Wilton,S.D. (2006) Induced dystrophin exon skipping in human muscle explants. *Neuromus. Disord.*, **16**, 583–590.

Chapitre IV

Etude de la structure-activité des conjugués $(R\text{-}X\text{-}R)_4$-PMO

Chapitre IV

Etude de la structure-activité des conjugués (R-X-R)$_4$-PMO

1. Introduction :

Dans cette partie, nous avons entrepris une étude de structure-activité sur les conjugués (R-X-R)$_4$-PMO en collaboration avec l'équipe du Dr. P. Iversen (AVIBiopharma). L'idée principale de cette étude est d'améliorer l'efficacité du conjugué (R-Ahx-R)$_4$-PMO en modifiant la composition du groupement espaceur **X** entre les résidus arginines.

Comme exposé dans le chapitre III (Partie II), l'internalisation cellulaire de la version fluorescente du conjugué (R-Ahx-R)$_4$-PMO dépend de l'énergie et implique les héparanes sulfates des glycoprotéoglycanes membranaires, suggérant ainsi un mécanisme de pénétration endocytotique (Abes et al. sous presse; Abes et al. 2007). De plus, la microscopie de fluorescence a montré une localisation vésiculaire de ce conjugué.

Les travaux de Rothbard ont montré qu'un accroissement de l'espacement entre les charges améliore l'internalisation cellulaire des oligoarginines (Rothbard et al. 2002). Nos résultats (article VI) confirment les travaux de Rothbard, et suggèrent, d'une manière très intéressante, que la correction d'épissage est indépendante du taux d'internalisation cellulaire et est corrélée négativement avec l'affinité des conjugués pour les héparanes sulfates membranaires. A titre d'exemple, le conjugué R_9F_2-PMO est internalisé plus efficacement que (R-Ahx-R)$_4$-PMO et son affinité pour l'héparine est supérieure (Abes et al. 2006). Par contre, le conjugué (R-Ahx-R)$_4$-PMO présente une activité de correction très supérieure à celle du R_9F_2-PMO. Ces résultats suggèrent que l'affinité des conjugués pour les héparanes sulfates est un paramètre important dans l'internalisation et surtout dans l'effet biologique obtenu.

Dans cette partie, nous avons étudié l'effet de trois paramètres structuraux sur l'efficacité de correction (voir Tableau X) :

- Longueur du groupement espaceur **X**
- Hydrophobicité et affinité pour les héparanes sulfates des conjugués
- Effet des stéréo-isomères

Tableau X : Nomenclature et structure des peptides de délivrance de la famille $(R\text{-}X\text{-}R)_4$-PMO

	ID	Séquences	Nombre de C	Spacer X	Structure
Longeure du spacer X	**1**	$(RGR)_4GB$	2	G = Glycine	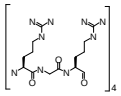
	2	$(RBR)_4BB$	3	B = b-Alanine	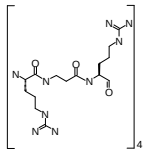
	3	$(RAbuR)_4AbuB$	4	Abu = 4-aminobutyric acid	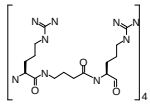
	4	$(RAvaR)_4AvaB$	5	Ava = 5-aminovaleric acid	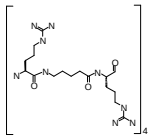
	5	$(RAhxR)_4AhxB$	6	Ahx = 6-aminohexanoic acid	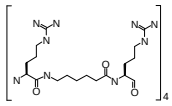
	6	$(RAhpR)_4AhpB$	7	Ahp = 7-aminoenanthic acid	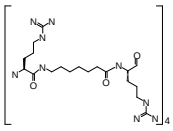
	7	$(RAcyR)_4AcyB$	8	Acy = 8-aminocaprylic acid	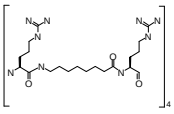
Hydrophobicité	**8**	$(RAbuFR)_4AbuFB$	6	F = Phénylalanine	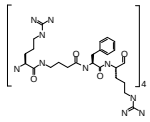
	9	$(RAbuLR)_4AbuLB$	6	L = Leucine	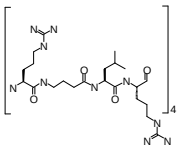
	10	$(RAbu,NLeR)_4Abu,NLeB$	6	nL = Norleucine	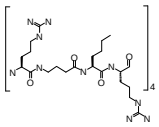
	11	$(RAbuAR)_4AbuAB$	6	A = Alanine	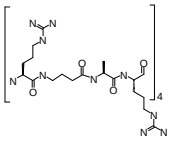
	12	$(R[AEEA]R)_4[AEEA]B$	6	[AEEA] = Ethylène glycol	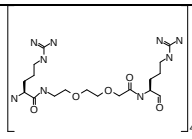
Stéréo-isomérie	**13**	$(rAhxR)_4AhxB$	6	Ahx = 6-aminohexanoic acid	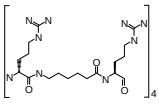

2. Résultats et discussion :

L'ensemble des résultats de ce chapitre feron l'objet d'une publication qui est en préparation (voir fin du chapitre IV).

Article VIII: Delivery of steric block morpholino oligomers by (R-X-R)$_4$ peptides: structure-activity studies

Saïd Abes, Hong M. Moulton[1], Philippe Clair, Rachida Abes, Paul Prevot, Derek S. Youngblood[1], Rebecca P. Wu[1], Patrick L. Iversen[1] and Bernard Lebleu

UMR 5124 CNRS, Université Montpellier 2, place Eugene Bataillon, 34095 Montpellier cedex 5, France and [2]AVI BioPharma, 4575 SW Research Way, Suite 200, Corvallis, OR 97330, USA.

L'ensemble des expériences de correction d'épissage dans cette étude ont été réalisées à des concentrations comprises entre 0,25µM et 1µM, de manière à éviter toute perméabilisation des membranes cellulaires (Figure 18). L'internalisation d'iodure de propidium (quantifié par analyse en FACS) a été prise comme critère de perméablisation.

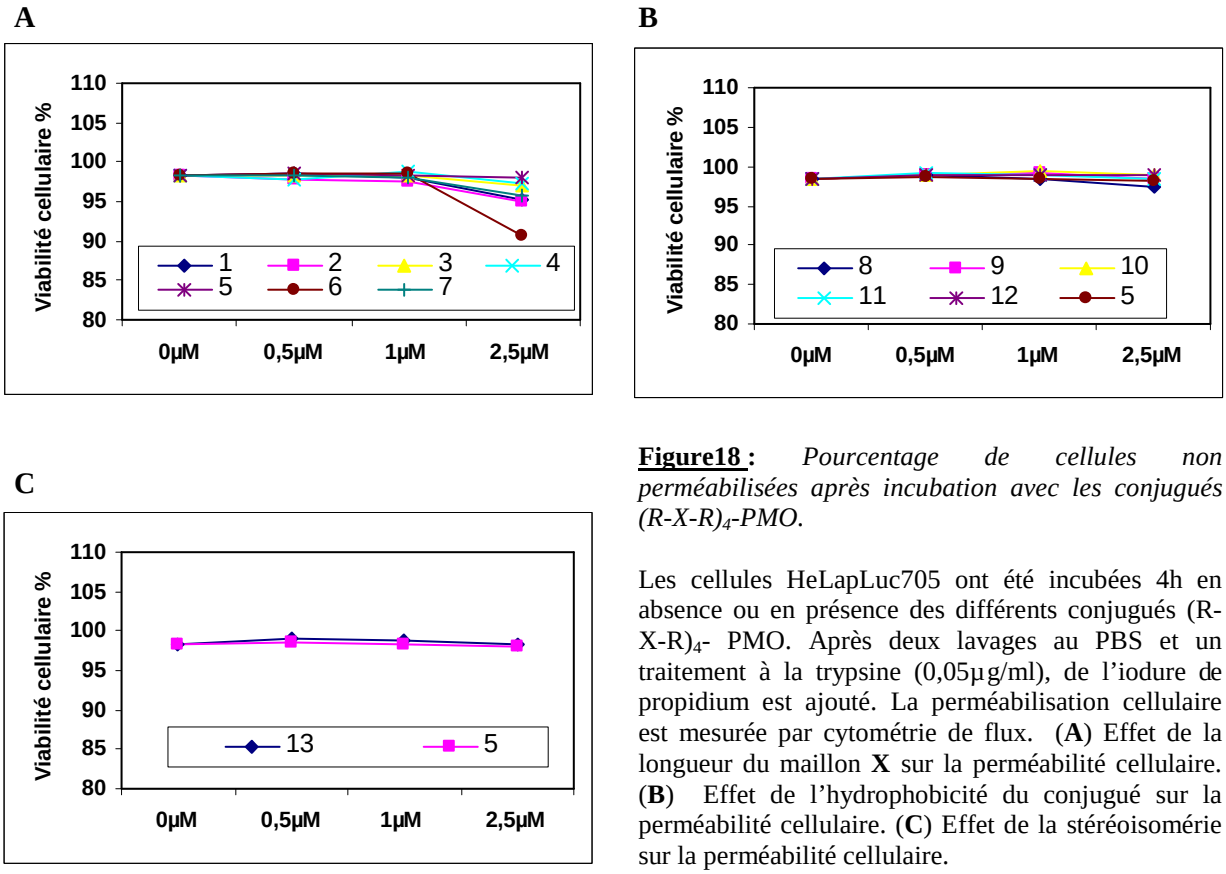

Figure18 : *Pourcentage de cellules non perméabilisées après incubation avec les conjugués (R-X-R)$_4$-PMO.*

Les cellules HeLapLuc705 ont été incubées 4h en absence ou en présence des différents conjugués (R-X-R)$_4$- PMO. Après deux lavages au PBS et un traitement à la trypsine (0,05µg/ml), de l'iodure de propidium est ajouté. La perméabilisation cellulaire est mesurée par cytométrie de flux. (**A**) Effet de la longueur du maillon **X** sur la perméabilité cellulaire. (**B**) Effet de l'hydrophobicité du conjugué sur la perméabilité cellulaire. (**C**) Effet de la stéréoisomérie sur la perméabilité cellulaire.

L'activité luciférase a été mesurée pour les conjugués **1-7** (voir Tableau X). Celle-ci augmente en fonction de la longueur du maillon **X**, avec un optimum d'activité pour un espacement des arginines compris entre 5 et 7 atomes de carbone. La microscopie de fluorescence et la cytométrie de flux sur les versions fluorescentes de ces conjugués correcteurs d'épissage ont montré d'une part une localisation vésiculaire majoritaire et d'une autre part une pénétration cellulaire dépendante de la concentration.

D'une manière très intéressante, pour des concentrations de 0,5µM à 2,5µM, plus la taille du maillon **X** augmente plus la pénétration cellulaire des conjugués diminue (voir article VII). L'analyse de l'affinité de chacun de ces conjugués par HPLC sur une colonne d'héparine a indiqué que la longueur du bras espaceur affecte négativement l'interaction conjugués-héparine. Cette diminution de la pénétration cellulaire et de l'activité de correction est probablement la résultante d'une diminution d'affinité.

Nos résultats confirment également que plus le maillon **X** est long plus la correction d'épissage est efficace. La corrélation entre l'ensemble de ces paramètres n'est pourtant pas aussi simple car la diminution d'activité des conjugués **6** et **7** est corrélée avec une augmentation de leur internalisation. Toutefois, leur affinité pour l'héparine diminue ce qui n'explique pas la diminution de l'activité de correction. L'analyse de l'hydrophobicité par HPLC sur colonne C_{18} de ces conjugués a montré que les conjugués **6** et **7** sont légèrement plus hydrophobes que le conjugué **5**. Ceci laisse supposer que l'intervention d'interactions hydrophobes contribue éventuellement à l'amélioration de l'internalisation cellulaire, mais pas à la correction d'épissage.

Il semble que plusieurs critères conditionnent l'efficacité de ces conjugués. En se basant sur les résultats précédents, nous avons sélectionné d'autres conjugués **8-11** (voir Tableau X) qui présentent la même longueur du maillon **X**, mais différents par leur hydrophobicité. De la même manière et à des concentrations qui ne perméabilisent pas les membranes cellulaires (voir Figure 18 B), leur évaluation dans le modèle de correction d'épissage a confirmé que l'hydrophobicité pénalise fortement l'activité de correction (voir article VII). L'analyse par microscopie de fluorescence et par cytométrie de flux des versions fluorescentes de ces conjugués a montré une localisation majoritairement vésiculaire comparable à celle du conjugué **5**, ainsi qu'une internalisation faible et dépendante de la concentration (Figure 19).

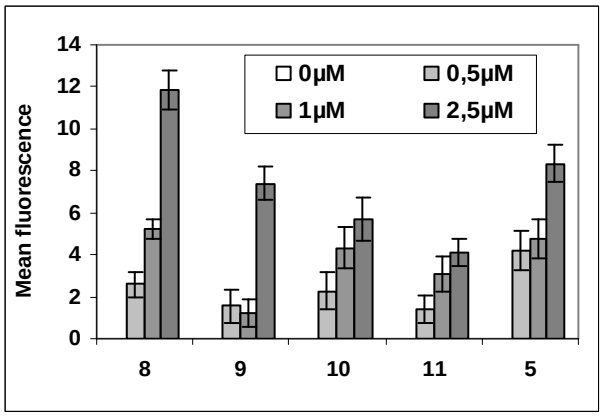

Figure 19 : *Effet de l'hydrophobicité sur l'internalisation des conjugués (RXR)$_4$-PMO.* Les cellules HeLapLuc705 ont été incubées en absence ou en présence des différents conjugués (RXR)$_4$-PMO à 37°C pendant 2h aux concentrations indiquées. Après un traitement à la trypsine et un lavage au PBS, 0,05µg/ml d'iodure de propidium a été ajouté. La fluorescence des cellules a été analysée au cytomètre de flux.

Pour expliquer cette diminution significative de l'efficacité des conjugués **8-11** nous avons comparé leur hydrophobicité, mesurée par HPLC sur une colonne C_{18}, à celle du conjugué **5**. Les conjugués **8-10** exhibent une forte hydrophobicité par rapport à celle du conjugué **5** (voir article VII), hydrophobicité vraisemblablement à l'origine de la faible activité de correction. Il est probable que ces conjugués interagissent fortement avec les membranes plasmiques par des interactions hydrophobes, ce qui rendrait difficile leur libération dans le milieu intracellulaire après une internalisation par endocytose, diminuant ainsi l'activité de correction. En ce qui concerne le conjugué **11**, il présente la même hydrophobicité que le conjugué **5** (voir article VII). Néanmoins, la correction d'épissage en sa présence est significativement plus faible comparée à l'efficacité du conjugué **5**. L'analyse de l'affinité de ce conjugué **11** pour l'héparine a mis en évidence une faible affinité comparée à celle du conjugué **5**, ce qui explique sa faible efficacité. De plus, la comparaison entre le conjugué **7** et le conjugué **12**, qui possèdent la même longueur du maillon **X** et la même affinité pour l'héparine, indique une faible efficacité du conjugué **12**. L'analyse de l'hydrophobicité montre que le conjugué **12** est moins hydrophobe. Il est donc difficile de distinguer les effets de l'affinité pour les héparanes sulfates et de l'hydrophobicité qui conditionnent tous les deux l'efficacité de correction.

Nous avons évoqué dans le chapitre II l'hypothèse de la résistance aux enzymes du lysosome pour expliquer l'efficacité du conjugué (R-Ahx-R)$_4$-PMO. En effet la présence du maillon Ahx entre les arginines crée des liens non conventionnels, ce qui peut être l'origine d'une stabilité métabolique accrue. Les travaux récents d'AVIBiopharma ont cependant indiqué que

ce conjugué est dégradé de la même manière que les conjugués R_9F_2-PMO ou Tat-PMO, probablement de par la présence de blocs d'arginines RR (Nelson et al. 2005). Le stéréo-isomère du conjugué $(RAhxR)_4$-PMO utilisé pour cette étude est $(rAhxR)_4$-PMO , dont une arginine sur deux est de série D. Cette modification élimine les blocs RR et tous les liens du conjugué sont ainsi non ordinaires, ce qui devrait augmenter sa résistance aux protéases et son activité de correction. Ce nouveau conjugué (conjugué 13) corrige efficacement l'épissage, mais cette correction est inférieure par rapport à la version L du conjugué (conjugué **5**). Les expériences de microscopie de fluorescence et de cytométrie de flux, dans des conditions de concentrations qui ne perméabilisent pas les membranes (Figure 18 C), ont mis en évidence une localisation vésiculaire et une internalisation cellulaire dépendante de la dose similaire pour les deux conjugués (Figure 20).

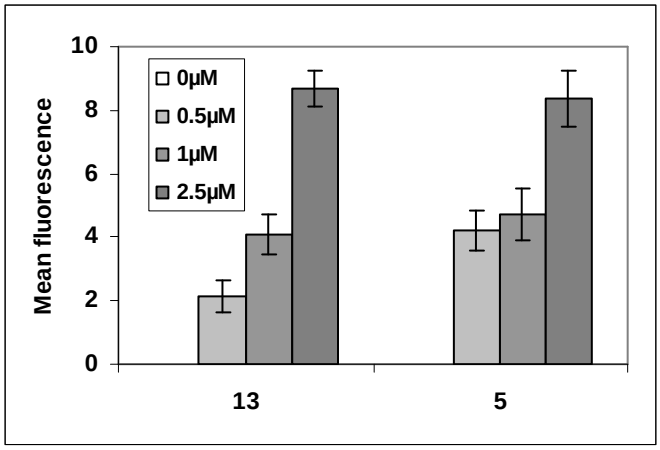

Figure 20 : *Effet de la stéréochimie sur l'internalisation des conjugués **5** et **13**.* Les cellules HeLapLuc705 ont été incubées en absence ou en présence des conjugués **5** ou **13** à 37°C pendant 2h aux concentrations indiquées. Après un traitement à la trypsine et un lavage au PBS, 0,05µg/ml iodure de propidium a été ajouté. La fluorescence des cellules a été analysée au cytomètre de flux.

L'analyse par HPLC sur colonne d'héparine ou C_{18} du conjugué **13** a montré une différence d'affinité pour l'héparine et une même hydrophobicité comparé au conjugué **5**. Le conjugué **13** a plus d'affinité pour l'héparine, ce qui pourrait expliquer une diminution de l'activité de correction malgré une stabilité métabolique normalement augmentée.

L'analyse de tous ces résultats a montré d'une manière claire l'impact de l'affinité et de l'hydrophobicité des conjugués sur la correction d'épissage. Bien que ces conjugués permettent de corriger l'épissage à des concentrations inférieures à 1µM, nous envisageons de poursuivre nos études de structure-activité en tirant part des résultats déjà obtenus et décrits

ci-dessus. Nous avons envisagé en particulier d'évaluer l'efficacité de trois peptides de la famille RXR : (RBR), (RAbuR) et (rAhxR) où les blocs de (RXR) se répètent 2 ou 3 fois. Ces peptides sont couplés à des PMO correcteurs d'épissage.

3. Conclusion :

Dans cette partie nous avons démontré que l'affinité et l'hydrophobicité des conjugués utilisés jouent un rôle crucial dans la délivrance de PMO correcteur d'épissage. Un optimum d'activité est obtenu avec le $(RAhxR)_4$-PMO. Ce conjugué possède une affinité et une hydrophobicité qui lui permettent d'interagir modérément avec les membranes plasmiques, ce qui lui permet d'être internalisé et de se dissocier facilement des membranes, se libérant ainsi dans le milieu intracellulaire. Néanmoins, et comme décrit dans le chapitre II, une partie importante du $(RAhxR)_4$-PMO reste emprisonnée dans les vésicules d'endocytose.

Delivery of steric block morpholino oligomers by (R-X-R)$_4$ peptides: structure-activity studies

Saïd Abes, Hong M. Moulton[1], Philippe Clair, Rachida Abes, Paul Prevot, Derek S. Youngblood[1], Patrick L. Iversen[1] and Bernard Lebleu

UMR 5235 CNRS, Université Montpellier 2, place Eugene Bataillon , 34095 Montpellier cedex 5, France and [1]AVI BioPharma, 4575 SW Research Way, Suite 200, Corvallis, OR 97330, USA.

1. Introduction

Protein transduction domains (PTD) as penetratin or Tat 48-60, or synthetic cell penetrating peptides (CPP) as oligoarginine have generated a large interest for their seemingly unique mechanism of membrane translocation and for their capacity to transport various biomolecules across biological membranes. Both assumptions have had to be re-visited since cellular uptake does involve endocytosis and since transport of biomolecules does not occur as efficiently as anticipated at least at low concentrations. In a series of experiments carried out independantly by several groups, CPPs mentioned above turned out rather inefficient in transporting uncharged splice correcting oligoucleotide (ON) analogs as PNA (peptide nucleic acids) or PMO (phosphorodiamidate morpholino oligomers) for a large part because CPP-conjugated material remained entrapped in endocytic vesicles. In keeping with this hypothesis, peptides or drugs (such as chloroquine) leading to endosome destabilization did significantly increase splicing correction.

We have recently described a new (R-Ahx-R)$_4$ CPP (in which Arg residues are interspersed with non-natural 6-aminohexanoic acid amino acid spacers) which leads to efficient splicing corrections at low concentration in the absence of endosomolytic agents. (R-Ahx-R)$_4$ is less cytotoxic and much more active than the parent oligoarginine peptide and than the prototypic

Tat 48-60 peptide. Importantly, (R-Ahx-R)$_4$-PMO conjugates also lead to efficient exon skipping in murine and dog DMD (Duchenne muscular dystrophy) models and inhibit the replication of viruses in several murine models of viral infection (Moulton et al 2007).

We nevertheless felt important to initiate structure-activity relationship (SAR) studies on this peptide for the following reasons. First, we do not know why (R-Ahx-R)$_4$ is more efficient than Tat 48-60 or (Arg)$_9$ in promoting the nuclear delivery of the conjugated splice correcting ON at micoromolar concentration (EC50 between 0.8 and 1μM). Second, the majority of the conjugated ON is still found entrapped in endocytic vesicles. Third, (R-Ahx-R)$_4$ PMO conjugates become cytotoxic *in vivo* at high concentrations (Fletcher et al. 2007, Moulton et al 2007).

The manuscript essentially aimed at comparing series of (R-Ahx-R)$_4$ PMO conjugates analogues differing in terms of Arg charge spacing , in hydrophobicity of the linker and in stereochemistry. Criteria for the comparative evaluations of these conjugates included cellular uptake, splicing correction efficiency , affinity for heparin and hydrophobicity.

2. Experimental methods

*2.1. Synthesis of CPP-PMO Conjugates***.** The antisense PMO (CCT CTT ACC TCA GTT ACA) is synthesized as described (Summerton and Weller 1997, 1991)., The CPPs, using standard Fmoc chemistry, were synthesized and purified to the purities of > 95% as determined by HPLC and mass spectrometry analysis. Conjugation of a CPP to a PMO through an amide linker, described previously (Abes et al., 2006), was followed with an additional purification step to remove nonconjugated peptide. Samples were loaded on source 30S resin (Amersham Biosciences, Pittsburgh, PA) in a 2 ml Biorad (Hercules, CA) MT2 column at 2 ml/min with running buffer A (20 mM Na_2HPO_4, 25% acetonitrile, pH 7.0) and purified into 45 sec fractions with 0-35% buffer gradient (buffer B: 1.5M NaCl, 20 mM

Na_2HPO_4, 25% acetonitrile, pH 7.0) over 60 min, using a high pressure liquid chromatography system. The desired faction was desalted by a method described previously (Abes et al., 2006). HPLC and MS analyses revealed that the final product contained > 93% CPP conjugated to full-length PMO, with the balance composed of CPP conjugated to incomplete PMO sequence, nonconjugated full-length or incomplete PMO.

2.2. Cells and cell culture

HeLa pLuc705 cells were cultured as exponentially growing subconfluent monolayers in DMEM medium (Gibco) supplemented with 10% fetal calf serum, 1 mM sodium pyruvate and non essential amino-acids.

2.3. Flow cytometry

To analyze (R-X-R)–PMO conjugates cell internalization, exponentially growing HeLa pLuc705 cells (1.75×10^5 cells seeded and grown overnight in 24 well plates) were incubated with the Fam-labelled (R-X-R)4–PMO. The cells were then washed twice with PBS, detached by incubating with trypsin for 5 min at 37 °C (0.5 mg/ml)/EDTA.4Na (0.35 mM), and washed by centrifugation (5 min, 900 ×g) in ice-cold PBS containing 5% FCS. The resulting cell pellet was resuspended in ice-cold PBS containing 0.5% FCS and 0.05 µg/ml propidium iodide (PI) (Molecular Probes, Eugene, OR). Fluorescence analysis was performed with a BD FacsCanto flow cytometer (BD Biosciences, San Jose, CA). Cells stained with PI were excluded from further analysis. A minimum of 20,000 events per sample was analyzed.

2.4. Splicing correction assay

The conjugates (R-X-R)4–PMO were incubated for 4 h in 1 ml OptiMEM medium with exponentially growing HeLa pLuc705 cells (1.75×10^5 cells/well seeded and cultivated

overnight in 24 wells plates). The conjugates were then diluted with 0.5 ml complete medium (DMEM plus 10% fetal bovine serum) and incubation continued for 20 h. Cells were washed twice with ice-coldPBS and lysed with Reporter Lysis Buffer (Promega, Madison,WI). Luciferase activity was quantified in a Berthold Centro LB 960 luminometer (Berthold Technologies, Bad Wildbad, Germany) using the Luciferase Assay System substrate (Promega, Madison, WI). Cellular protein concentrations were measured with the BCA™Protein Assay Kit (Pierce, Rockford, IL) and read using an ELISA plate reader (Dynatech MR 5000, Dynatech Labs, Chantilly, VA) at 550 nm. Luciferase activities were expressed as relative luminescence units (RLU) per μg protein. All experiments were performed in triplicate. Each data point was averaged over the three replicates.

2.5. Heparin-affinity chromatography

3 μg of each CPP–PMO conjugate were injected in triplicate on a HiTrap Sepharose/heparin 1 ml column (Amersham Biosciences, Freiburg, Germany), fitted on a Beckman–Gold HPLC chromatography (Beckman Coulter, Fullerton, CA). The conjugates were eluted at a flow rate of 1 ml/min of 2.5 mM phosphate buffer pH 7 by a linear gradient of NaCl from 70 to 970 mM, in 30 min. Elution of the conjugates was followed by UV absorption at 260 nm. Results were presented as eluting NaCl concentrations and expressed as the mean and standard deviation of triplicate measurements.

2.6. Hydrophobicity Reverse Phase chromatography

0.1 μg of each $(R\text{-}X\text{-}R)_4$–PMO conjugate were injected in triplicate on a C18 Waters Symmetry Shield 4.6x250 mm column, fitted on a Beckman–Gold HPLC chromatograph (Beckman Coulter, Fullerton, CA). The conjugates were eluted at a flow rate of 1 ml/min of

H2O/0.1%TFA by a linear gradient of acetonitrile from 5% to 95% in 30 min. Elution of the conjugates was followed by UV absorption at 260 nm. Results were presented as eluting acetonitrile concentrations and expressed as the mean and standard deviation of triplicate measurements.

3. Results

3.1 Criteria for the design of (R-X-R)$_4$ analogs

Most studies on basic aminoacids-rich CPP emphasized the importance of arginine-side chains and of the spacing between these guanidinium groups. Studies by Rothbard et al in particular have shown that a six carbon 6-aminohexanoic acid linker seemed optimal in terms of cellular uptake but no data concerning efficiency in terms of cytoplasmic or nuclear delivery of a payload was provided. We therefore designed a series of $(RXR)_4$ PMO conjugates with X varying from 2 to 8 carbons (compounds 1 to 7 in Table 1). As seen below, the present study did confirm a dependance of charge spacing with an optimum for $(R\text{-}Ahx\text{-}R)_4$ (in which X = 6) in terms of nuclear delivery of the PMO payload. Based on this first set of data, we designed a series of C6 linked-Arg peptides differing in terms of hydrophobicity (compounds 8 to 11 in Table 1).

Since metabolic stability has often been proposed as a factor governing CPP efficiency, the D-Arg modified $(r\text{-}Ahx\text{-}R)_4$ (compound 12 in Table 1) has been included.

3.2 Effect of charge spacing on splicing correction

Compounds 1 to 7 (Table 1) were first compared for their ability to promote luciferase expression in dose-response experiments (Fig. 1). Increasing the length of the spacer led to an increased luciferase expression with an optimum for C5 to C7-linked material. Cellular uptake data, as monitored by FACS analysis of the corresponding fluorescein-labeled conjugates,

gave rise to a rather different picture (Fig.2). Indeed, increasing the length of the spacer has a negative effect on cellular uptake while it increases splicing correction efficiency. $(R\text{-}Ahx\text{-}R)_4$ PMO in particular is the most active in terms of splicing correction and is the less efficient in terms of cellular uptake. PI uptake has been monitored in parallel as an index of cell membrane integrity. No significant PI uptake was seen at doses up to 2.5µM for any one of these compounds except for compound 7 which is slightly cytotoxic at 2.5µM concentrations. Along the same line, it is worth pointing here that $(R\text{-}Ahx\text{-}R)_4$ PMO corrects splicing more efficiently than $(Arg)_9$ PMO while taken up less efficiently (Abes et al 2006).

3.3 Effect of charge spacing on affinity for heparin and on hydrophobicity

It is now well admitted that basic CPPs interact with heparan sulfate-containing glycosaminoglycans before being internalized by endocytosis. However too much affinity for heparan sulfate might be detrimental for the release of CPP-ON conjugates from endocytic vesicles as hypothesized in our previous publications .

Compounds 1 to 7 (Table 1) have thus been compared in terms of affinity for model heparan sulfates on Hi-trap Heparin column (Fig. 3A). Increasing spacer length clearly leads to decreased affinity as monitored by the NaCl concentration required for elution. $(Arg)_9$-PMO has an even higher affinity for heparan sulfate than $(RGR)_4$-PMO and is less active in splicing correction (data not shown).

Affinity for heparan sulfates thus appears to parallel cellular uptake efficiency while being inhibitory for splicing correction efficiency. However, compounds 6 and 7 would then be expected to be more active in splicing correction than compound 5, which is not observed.

Increasing the hydrocarbon spacer length should also increase hydrophobocity which could itself be promoting membranes entrapment. Increased hydrophobocity has indeed be verified by C18- column chromatography (Fig. 4).

3.4. Influence of hydrophobicity and heparan sulfate affinity on splicng correction

In this first part of this SAR study, we have compared compounds differing by their charge spacing and as a consequence by their hydrophobocity and their affinity for heparan sulfate. We know compare a series of compounds (compounds 8 to 11 in Table 1) with the same spacing (6 atom linker as in (R-Ahx-R)$_4$- PMO) but with varying hydrophobic character.

Some compounds (11 in Table 1) have hydrophobicities comparable to the parent (R-Ahx-R)$_4$ PMO (compound 5) taken as a reference while other (compounds 8 to 10) have a significantly higher hydrophobocity than compound 5, as monitored by C18-column chromatography (Fig.6). These conjugates were then analyzed for splicing correction efficiency and for cellular uptake at various concentrations.

Splicing correction efficiency is clearly lower for more hydrophobic conjugates (compounds 8 to 10) and compound 5 remains the most active (Fig.6). Cellular uptake for this series of compounds has been monitored as well by FACS analysis but no major difference has been found (data not shown). Unexpectdly at first sight, compound 11 was less efficient than compound 5 in terms of splicing correction (Fig.6) despite a similar hydrophobocity (Fig.5). Again, affinity for heparan sulfates has to be taken into account as shown in previous section. Compounds 8 to 11 were therefore compared to reference compound 5 in this respect (Fig.7). Here again this series of compounds divides into two groups : (i) compounds 8 to 10 with a lower affinity for heparan sulfate and a higher hydrophobocity than reference compound 5 and (ii) compound 11 with a comparable hydrophobocity but a lower affinity for heparan sulfates than reference compound 5.

Altogether these experiments indicate that hydrophobicity and affinity for heparan sulfates should neither be too low nor too high for optimal splicing correction.

3.5. Influence of D-Arg residues

Increased metabolic stability should in principle improve biological efficiency and could in part explain the higher efficacy of $(R\text{-}Ahx\text{-}R)_4$ PMO as compared to (Arg PMO and Tat $_{48\text{-}60}$ PMO, as discussed previously. However the (R-Ahx-R)4 portion of $(R\text{-}Ahx\text{-}R)_4$ PMO was found to be degraded in intact cells (Youngblood et al., 2007). We therefore synthesized $(r\text{-}Ahx\text{-}R)_4$ PMO (compound 12 in Table 1) in which one of two L-Arg in the R-Ahx-R repeat was replaced by a D-Arg (r) and compared it in terms of splicing correction and cellular uptake. Surprisingly the $(r\text{-}Ahx\text{-}R)_4$ PMO was significantly less efficient in dose-response experiments on splicing correction (Fig 8) while taken up to the same extent by cells (data not shown). Both L-and D-Arg containig peptides had similar hydrophobocity (data not shown). Interestingly $(r\text{-}Ahx\text{-}R)_4$ PMO has a signficantly higher affinity for heparan sulfate than the parent $(R\text{-}Ahx\text{-}R)_4$ PMO thus pointing again to the role played by this parameter in splicing correction efficiency (Fig. 8).

References

Summerton, J. and Weller, D. (1997) Morpholino antisense oligomers: Design, preparation, and properties. *Antisense Nucleic Acid Drug Dev.*, **7,** 187-195.

Summerton, J. and Weller, D. (1991) Uncharged morpholino-based polymers having phosphorus containing chiral intersubunit linkage. Patent US-5185444.

Moulton, H. M., Fletcher, S., Neuman, B. W., McClorey, G., Stein, D. A., Abes, S., Wilton, S. D., Buchmeier, M. J., Lebleu, B., et Iversen, P. L. **(2007)**. Cell-penetrating peptide-morpholino conjugates alter pre-mRNA splicing of DMD (Duchenne muscular dystrophy) and inhibit murine coronavirus replication in vivo. *Biochem Soc Trans.* **35**(Pt 4): 826-828.

Fletcher, S., Honeyman, K., Fall, A. M., Harding, P. L., Johnsen, R. D., Steinhaus, J. P., Moulton, H. M., Iversen, P. L., et Wilton, S. D. **(2007)**. Morpholino Oligomer-Mediated Exon Skipping Averts the Onset of Dystrophic Pathology in the mdx Mouse. *Mol Ther.* **15**(9):1587-92

Abes, S., Moulton, H. M., Clair, P., Prevot, P., Youngblood, D. S., Wu, R. P., Iversen, P. L., et Lebleu, B. **(2006)**. Vectorization of morpholino oligomers by the (R-Ahx-R)4 peptide allows efficient splicing correction in the absence of endosomolytic agents. *J Control Release.* **116**(3): 304-313.

Legends to the figures

Fig. 1. Effect of charge spacing on $(RXR)_4XB$-PMO conjugates splicing correction.
HeLa pLuc705 cells were incubated for 4h in OptiMEM in the absence (white bars) or in the presence of 0.25µM (hatched bars) or 1µM (grey bars) of the various $(RXR)_4XB$-PMO conjugates. Luciferase expression was quantified 20h later and expressed as RLU/ µg protein. Each experiment was made in triplicate and error bars (standard deviations) are indicated.
1: $(RGR)_4GB$-PMO; 2: $(RBR)_4BB$-PMO; 3: $(RAbuR)_4AbuB$-PMO; 4: $(RAvaR)_4AvaB$-PMO; 5: $(RAhxR)_4AhxB$-PMO; 6: $(RAhpR)_4AhpB$-PMO; 7: $(RAcyR)_4AcyB$

Fig. 2. Flow cytometry analysis of fluorescently-labeled $(RXR)_4XB$-PMO conjugates cell uptake : effect of charge spacing .
HeLa pLuc705 cells were incubated for 1h in OptiMEM in the absence (white bars) or in the presence of 0.5µM (hatched bars) or 1µM (grey bars) of the various $(RXR)_4XB$-PMO-FAM conjugates. Cells were washed,trypsinized and analyzed by flow cytometry. Each experiment was made in triplicate and error bars (standard deviations) are indicated.
1: $(RGR)_4GB$-PMO-FAM; 2: $(RBR)_4BB$-PMO-FAM; 3: $(RAbuR)_4AbuB$-PMO-FAM; 4: $(RAvaR)_4AvaB$-PMO-FAM; 5: $(RAhxR)_4AhxB$-PMO-FAM; 6: $(RAhpR)_4AhpB$-PMO-FAM; 7: $(RAcyR)_4AcyB$-PMO-FAM

Fig. 3. Heparin affinty chromatography of $(RXR)_4XB$-PMO conjugates.
$(RXR)_4XB$-PMO conjugates were injected on a HiTrap Sepharose/heparin column and eluted by a linear gradient of NaCl. Elution was monitored by UV absorption at 260 nm. Results are presented as eluting NaCl concentrations. Each experiment was made in triplicate and error bars (standard deviations) are indicated.
1: $(RGR)_4GB$-PMO; 2: $(RBR)_4BB$-PMO; 3: $(RAbuR)_4AbuB$-PMO; 4: $(RAvaR)_4AvaB$-PMO; 5: $(RAhxR)_4AhxB$-PMO; 6: $(RAhpR)_4AhpB$-PMO; 7: $(RAcyR)_4AcyB$

Fig. 4. Hydrophobicity of $(RXR)_4XB$-PMO conjugates.
$(RXR)_4XB$-PMO conjugates were injected on a C18- Sepharose column and eluted by a linear gradient of acetonitrile. Elution was monitored by UV absorption at 260 nm. Results are presented as eluting acetonitrile concentrations. Each experiment was made in triplicate and error bars (standard deviations) are indicated.

1: (RGR)$_4$GB-PMO; 2: (RBR)$_4$BB-PMO; 3: (RAbuR)$_4$AbuB-PMO; 4: (RAvaR)$_4$AvaB-PMO; 5: (RAhxR)$_4$AhxB-PMO; 6: (RAhpR)$_4$AhpB-PMO; 7: (RAcyR)$_4$AcyB

Fig. 5. Hydrophobicity of (RXR)$_4$XB-PMO conjugates.

(RXR)$_4$XB-PMO conjugates were injected on a C18- Sepharose column and eluted by a linear gradient of acetonitrile. Elution was monitored by UV absorption at 260 nm. Results are presented as eluting acetonitrile concentrations. Each experiment was made in triplicate and error bars (standard deviations) are indicated.

8: (RAbuFR)$_4$AbuFB-PMO; 9: (RAbuLR)$_4$AbuLB-PMO; 10: (RAbu,NLeR)$_4$Abu,NLeRB-PMO; 11: (RAbuAR)$_4$AbuAB-PMO; 5: (RAhxR)$_4$AhxB-PMO

Fig. 6. Splicing correction by (RXR)$_4$XB-PMO conjugates with identical charge spacing and varying hydrophobicity.

HeLa pLuc705 cells were incubated for 4h in OptiMEM in the absence (white bars) or in the presence of 0.25µM (hatched bars) or 1µM (grey bars) of the various (RXR)$_4$XB-PMO conjugates. Luciferase expression was quantified 20h later and expressed as RLU/ µg protein.Each experiment was made in triplicate and error bars (standard deviations) are indicated.

8: (RAbuFR)$_4$AbuFB-PMO; 9: (RAbuLR)$_4$AbuLB-PMO; 10: (RAbu,NLeR)$_4$Abu,NLeRB-PMO; 11: (RAbuAR)$_4$AbuAB-PMO; 5: (RAhxR)$_4$AhxB-PMO

Fig. 7. Heparin affinty chromatography of (RXR)$_4$XB-PMO conjugates.

(RXR)$_4$XB-PMO conjugates were injected on a HiTrap Sepharose/heparin column and eluted by a linear gradient of NaCl. Elution was monitored by UV absorption at 260 nm. Results are presented as eluting NaCl concentrations. Each experiment was made in triplicate and error bars (standard deviations) are indicated.

8: (RAbuFR)$_4$AbuFB-PMO; 9: (RAbuLR)$_4$AbuLB-PMO; 10: (RAbu,NLeR)$_4$Abu,NLeRB-PMO; 11: (RAbuAR)$_4$AbuAB-PMO; 5: (RAhxR)$_4$AhxB-PMO

Fig. 8. Splicing correction by (RAhxR)$_4$AhxB-PMO and (rAhxR)$_4$AhxB-PMO.

HeLa pLuc705 cells were incubated for 4h in OptiMEM in the absence (white bars) or in the presence of 0.25µM (hatched bars) or 1µM (grey bars) of (RAhxR)$_4$AhxB-PMO and (rAhxR)$_4$AhxB-PMO conjugates. Luciferase expression was quantified 20h later and

expressed as RLU/ µg protein.Each experiment was made in triplicate and error bars (standard deviations) are indicated.
13: (rAhxR)$_4$AhxB-PMO, 5: (RAhxR)$_4$AhxB-PMO

Fig. 9. Heparin affinty chromatography of (RAhxR)$_4$AhxB-PMO and (rAhxR)$_4$AhxB-PMO. Conjugates were injected on a HiTrap Sepharose/heparin column and eluted by a linear gradient of NaCl. Elution was monitored by UV absorption at 260 nm. Results are presented as eluting NaCl concentrations. Each experiment was made in triplicate and error bars (standard deviations) are indicated.
13: (rAhxR)$_4$AhxB-PMO, 5: (RAhxR)$_4$AhxB-PMO

Fig. 10. Hydrophobicity of (RAhxR)$_4$AhxB-PMO and (rAhxR)$_4$AhxB-PMO.
Conjugates were injected on a C18- Sepharose column and eluted by a linear gradient of acetonitrile. Elution was monitored by UV absorption at 260 nm. Results are presented as eluting acetonitrile concentrations. Each experiment was made in triplicate and error bars (standard deviations) are indicated.

Table I :

	ID	Sequences	Spacer's C	Spacer	Structure
Spacer length	**1**	(RGR)$_4$GB	2	G = Glycine	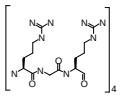
	2	(RBR)$_4$BB	3	B = b-Alanine	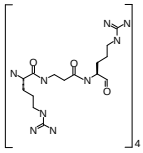
	3	(RAbuR)$_4$AbuB	4	Abu = 4-aminobutyric acid	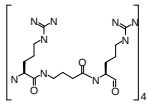
	4	(RAvaR)$_4$AvaB	5	Ava = 5-aminovaleric acid	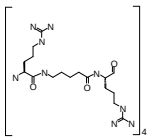
	5	(RAhxR)$_4$AhxB	6	Ahx = 6-aminohexanoic acid	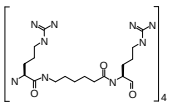
	6	(RAhpR)$_4$AhpB	7	Ahp = 7-aminoenanthic acid	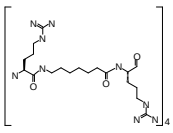
	7	(RAcyR)$_4$AcyB	8	Acy = 8-aminocaprylic acid	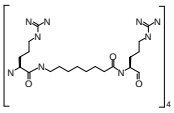
Hydrophobicity	**8**	(RAbuFR)$_4$AbuFB	6	F = Phenylalanine	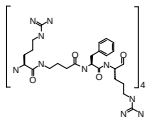
	9	(RAbuLR)$_4$AbuLB	6	L = Leucine	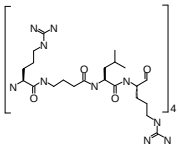
	10	(RAbu,NLeR)$_4$Abu,NLeRB	6	nL = Norleucine	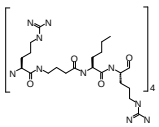
	11	(RAbuAR)$_4$AbuAB	6	A = Alanine	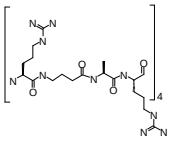
Stereo-isomeric	**12**	(rAhxR)$_4$AhxB	6	Ahx = 6-aminohexanoic acid	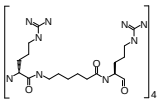

Figure 1

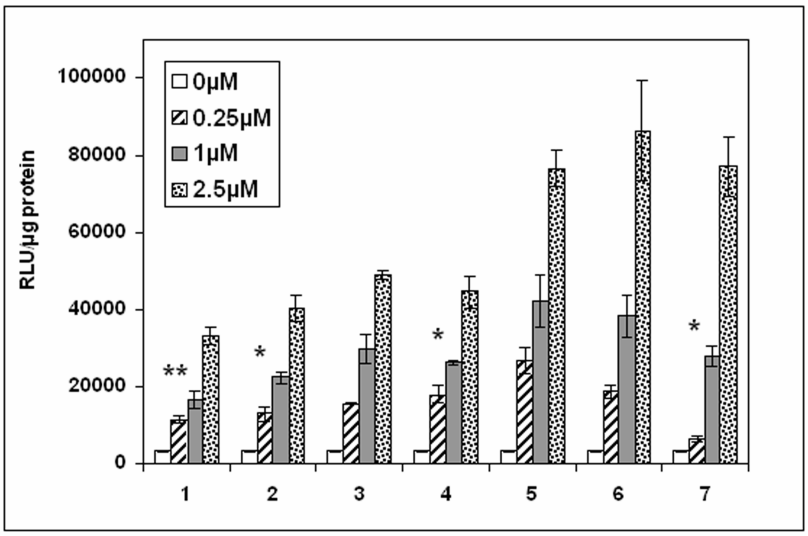

≤ 0.001 ***
≤ 0.01 **
≤ 0.05 *

Figure 2

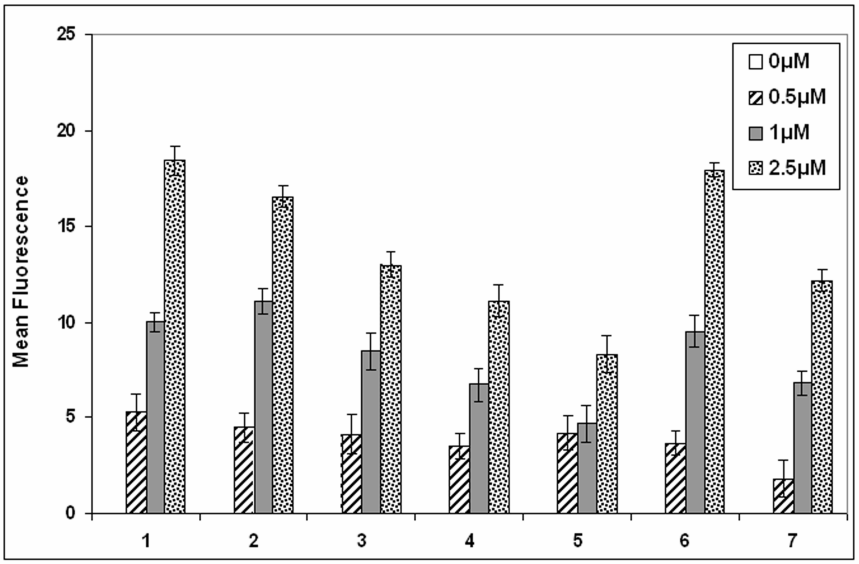

Figure 3

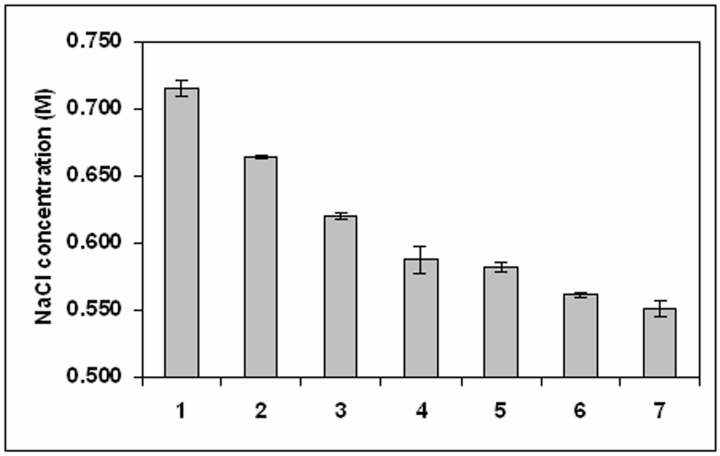

Figure 4

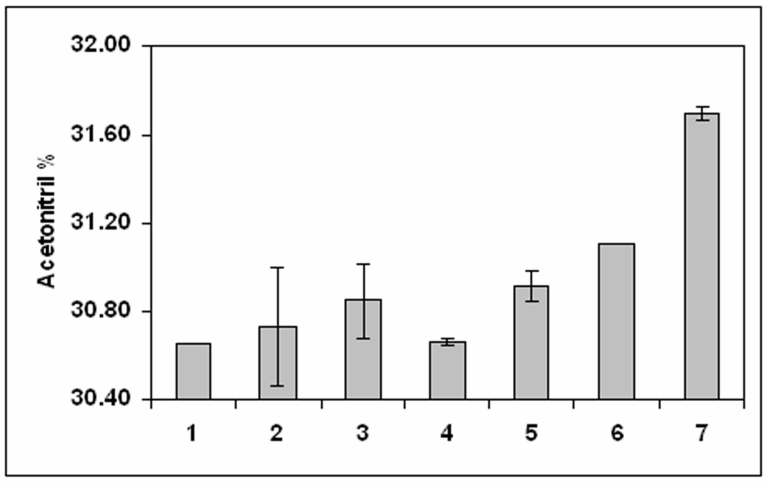

Figure 5

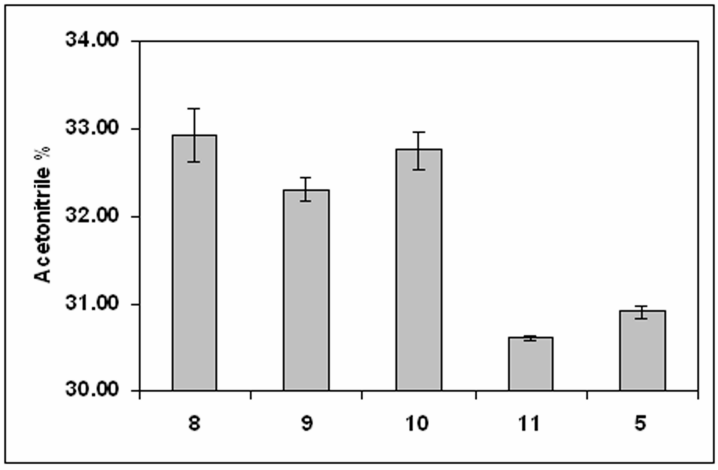

Figure 6

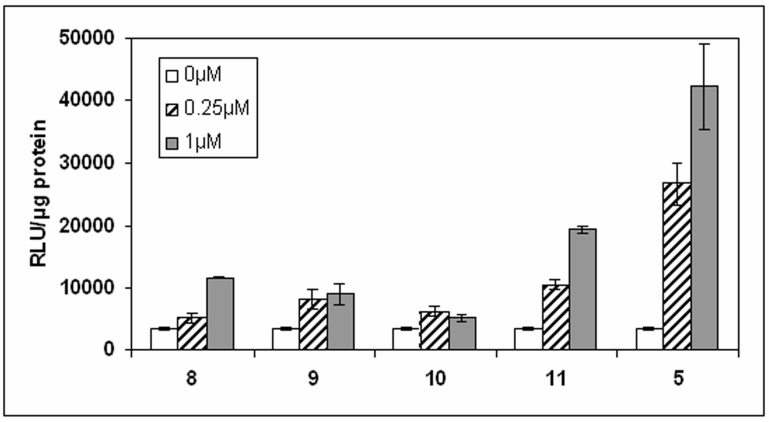

Figure 7

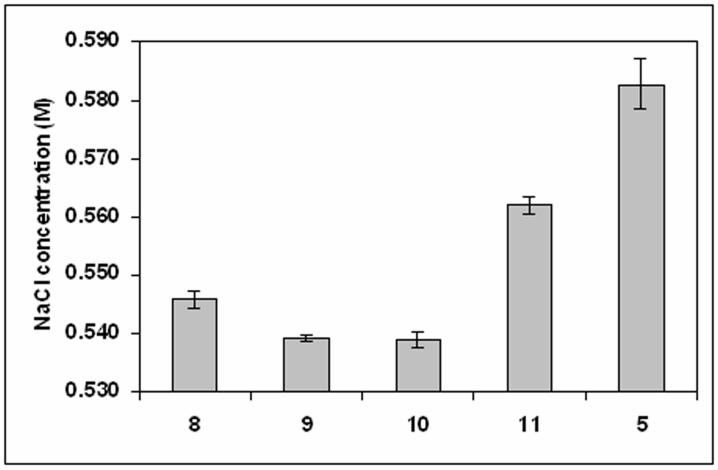

Figure 8

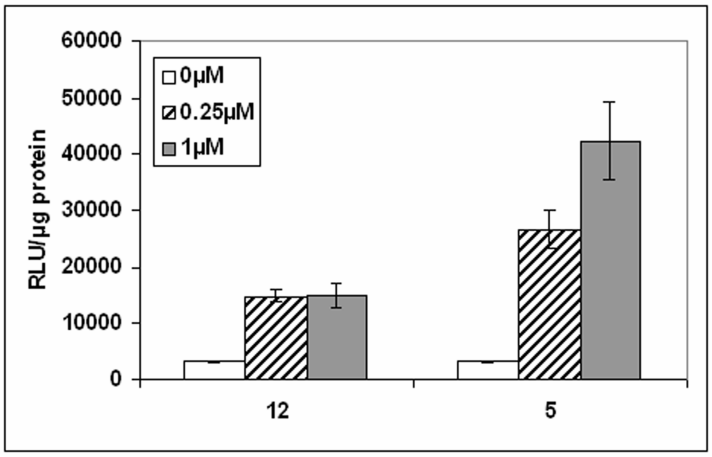

Figure 9

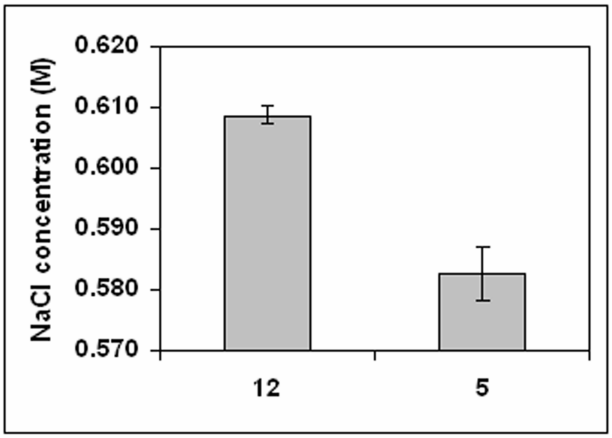

Figure 10

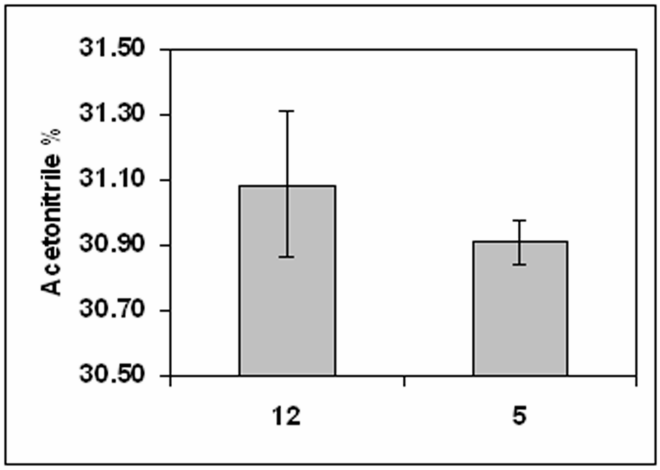

Chapitre V

Vers une nouvelle stratégie de délivrance des oligonucléotides

Chapitre V

Vers une nouvelle stratégie de délivrance des oligonucléotides

Revue II: Chemical Modifications to Improve the Cellular Uptake of Oligonucléotides

Françoise Debart[1], **Saïd Abes[2]**, Gaelle Deglane[1], Hong M. Moulton[3], Philippe Clair[2], Michael J. Gait[4], Jean-Jacques Vasseur[1] et Bernard Lebleu[2]

[1]LCOBS, UMR 5625 CNRS, [2]DAA, and UMR 5124 CNRS Université Montpellier 2, Place Eugene Bataillon, 34095 Montpellier cedex 5, France
[3]AVI Biopharma, Corvallis,OR, USA
[4]Laboratory of Molecular Biology, Medical Research Council, Cambridge, UK

Article IX: Impact of the Guanidinium Group on Hybridisation and Cellular Uptake of Cationic Oligonucleotides

Gaëlle Deglane[1], **Saïd Abes[2]**, Thibaut Michel[1], Paul Prévot[2], Eric Vives[3], Françoise Debart[1], Ivan Barvik[4], Bernard Lebleu[2] et Jean-Jacques Vasseur[1]

[1]LCOBS, UMR 5625 CNRS, [2]DAA, and UMR 5124 CNRS Université Montpellier 2, Place Eugene Bataillon, 34095 Montpellier cedex 5, France
[3] INSERM EMI0227 CRLC Val d'Aurelle-Paul Lamarque 34298 Montpellier Cedex 05 (France)
[4] Charles University, Faculty of Mathematics and Physics Institute of Physics, Ke Karlovu 5 12116 Prague 2 (Czech Republic)

The first two authors should be regarded as joint First Authors

1. Introduction :

Cette partie de la thèse a été réalisée en collaboration avec l'équipe du Dr. J.J. Vasseur (Université Montpellier 2). L'idée consiste à cationiser directement les ONs afin de rendre plus efficace leur pénétration ainsi que leur hybridation, comme décrit en détail dans la revue II.

2. Bilan bibliographique :

Nos travaux initiaux menés en collaboration avec l'équipe du Dr. Vasseur avaient montré que des analogues cationisés d'ONs, les phosphoramidates, complémentaires du site IRES de recrutement dans les ribosomes, entrent dans les cellules sans utilisation d'agents de transfection et inhibent l'expression d'un gène de la luciférase dont la traduction est sous dépendance de cet élément (Michel et al. 2003). Par ailleurs, les travaux de Rothbard et al (Rothbard et al. 2004) ont montré l'importance des groupements guanidinium des arginines dans l'internalisation cellulaire des CPPs riches en arginines. Connaissant ces propriétés, Ly et al ont montré que la guanidylation de PNA augmente significativement l'internalisation cellulaire de ce dérivé antisens (Dragulescu-Andrasi et al. 2005; Zhou et al. 2003). Curieusement, ce travail indiquait que l'internalisation cellulaire de ces PNA guanidylés est indépendante de l'énergie suggérant ainsi l'implication d'un mécanisme non endocytotique. Les groupements guanidiniums peuvent être couplés à différents endroits du nucléotide : sur le C2 du ribose (Maier et al. 2002), sur le groupement phosphate internucléosidique (Barawkar et Bruice 1998), sur le groupement phosphate (Deglane et al. 2006) ou sur la base (Robles et al. 2001; Roig et Asseline 2003).

3. Résultats et Discussion :

Dans ce travail, nous avons étudié la mécanistique ainsi que les propriétés d'hybridation des guanidinobutyl phosphoramidate polythymidines (Figure 21).

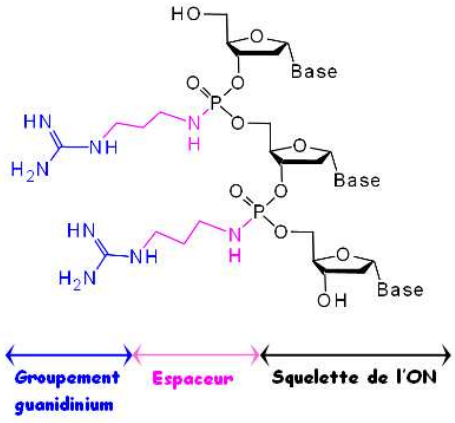

Figure 21 : *Structure linéaire du guanidinobutyl phosphoramidate.*

L'étude des propriétés d'hybridation réalisée par l'équipe du Dr. Vasseur a montré une forte affinité entre l'ON guanidylé et la cible (ADN ou ARN). Cette forte attraction résulte non seulement des interactions électrostatiques entre les groupements guanidiniums de l'ON et les

groupements phosphates de la cible, mais aussi de la formation de liaisons hydrogènes entre les deux groupes (Deglane et al. 2006).

Nos résultats ont indiqué que la guanidylation augmente significativement l'internalisation cellulaire des guanidinobutyl phosphoramidates. Cette pénétration est dépendante de la concentration et de la température. La microscopie de fluorescence a montré que la localisation de ces ONs modifiés reste vésiculaire (Deglane et al. 2006) contrairement aux résultats rapportés par les travaux de Ly et al qui montrent une localisation nucléaire. Ceci est probablement dû à un artéfact de leur protocole: la fixation des cellules (Dragulescu-Andrasi et al. 2005; Zhou et al. 2003) Zhou et al 2003). En effet, la fixation des cellules par le paraformaldéhyde 3,7% provoque une redistribution intracellulaire de l'analogue antisens (Figure 22).

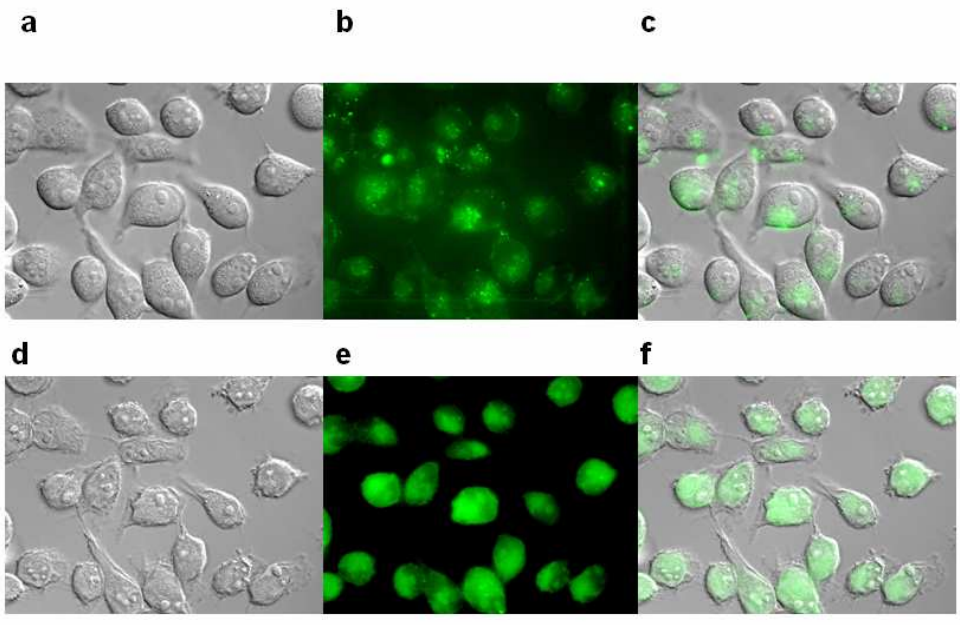

Figure 22: *Effet de la fixation sur la localisation intracellulaire de l'analogue guanidinobutyl phosphoramidate couplé à la fluorescéine.* Les cellules HeLa ont été incubées avec 1µM de l'ONs guanidylé. Après 60 minutes, les cellules sont lavées et analysées au microscope de fluorescence. a, b et c correspondent aux cellules vivantes. d, e et f correspondent aux cellules fixées avec 3,7% de paraformaldéhyde.

En parallèle de cette étude, nous avons engagé une collaboration avec le groupe du Dr. K. Ganesh (National Chemical Laboratory Pune, Inde) pour synthétiser et évaluer de nouveaux analogues de PNA. A la différence des travaux de Ly et al, ces PNA ne portent pas de groupement guanidinium, mais sont des PNA contraints (Figure 23). Certains de ces PNAs à structure contrainte (pour augmenter leur affinité pour un brin complémentaire d'ADN ou

d'ARN) sont également chargés. Ces analogues cationiques à structure contrainte de PNAs ont également l'avantage d'être plus solubles dans l'eau que les PNAs non modifiés. Enfin, la présence de groupements cationiques pourrait également permettre leur internalisation dans les cellules en l'absence d'agents de transfection.

L'équipe du Dr. K. N. Ganesh a effectivement établi que ces PNAs chargés ont une bonne solubilité dans l'eau et une meilleure hybridation à l'ADN (D'Costa et al. 2001; Govindaraju et al. 2003; Govindaraju et al. 2004; Lonkar et al. 2004). Malheureusement, la synthèse de PNAs comportant les quatre bases de tailles suffisantes (15-18 mers) pour être utilisés comme antisens est difficile et se fait avec un rendement insuffisant.

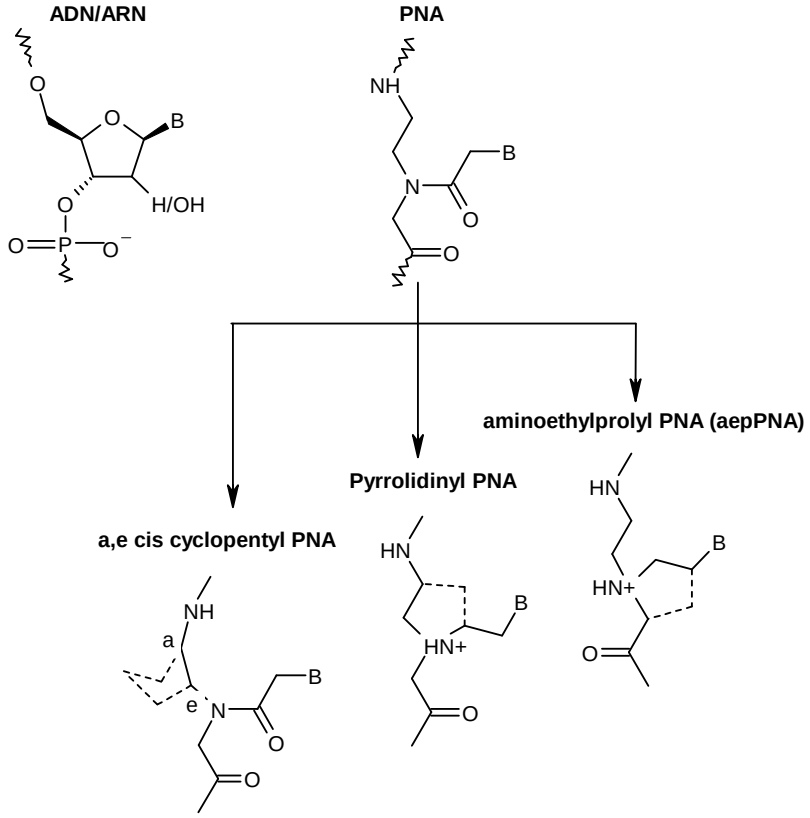

Figure 23 : *Structure de PNA contraints cationiques le aepPNA et le pyrrolidinyl PNA et non cationique le a,e cis cyclopentyl PNA.*

Un PNA contraint chargé (aepPNA), correcteur d'épissage dans le modèle de Kole a été synthétisé avec 2 ou 3 charges positives et ses propriétés ont été étudiées en parallèle avec un analogue non cationisé. Aucun des deux PNAs produits ne corrigent l'épissage dans les cellules HeLapLuc705. La première implique l'entrée dans les cellules de ces PNAs. Nous avons alors analysé leur internalisation cellulaire et les résultats préliminaires ont indiqué une très faible entrée cellulaire. Cependant, comme nous l'avons constaté avec le $(R\text{-}Ahx\text{-}R)_4$-PMO, pénétration cellulaire et efficacité de la correction d'épissage ne sont pas

nécessairement liés. La seconde concerne les propriétés d'hybridation à l'ADN et à l'ARN. Cette étude, réalisée par l'équipe du Dr. K. Ganesh, a mis en évidence une hybridation plus efficace et stable à l'ADN complémentaire qu'à l'ARN de ces deux PNAs en comparaison à un PNA classique. Cette préférence pour l'ADN détourne probablement l'antisens de sa cible ARN pré-messager.

4. Conclusion :

La collaboration avec l'équipe du Dr. J. J. Vasseur a permis d'évaluer l'efficacité de pénétration cellulaire d'oligonucléotides antisens guanidylés. L'étude des propriétés d'hybridation de ces antisens cationiques a montré une forte affinité et stabilité d'interaction apportées par la guanidylation des ONs pour la cible. L'étude de la mécanistique d'internalisation cellulaire a montré que l'analogue ONs guanidylé, guanidinobutyl phosphoramidate, entre dans les cellules d'une manière dépendante de la dose et de la température suggérant ainsi un processus de pénétration énergie dépendant. Malheureusement, la microscopie de fluorescence a indiqué une localisation vésiculaire de l'analogue ON guanidylé. Des problèmes de rendement de synthèse d'oligonucléotides guanidylés comportant les quatre bases ne nous ont malheureusement pas permis encore d'analyser leurs propriétés dans le test fonctionnel de correction d'épissage.
Les travaux sur les PNAs contraints avec l'équipe du Dr. K. Ganesh ne sont pas encourageants jusqu'ici. Entretemps l'équipe indienne a sélectionné deux nouveaux PNAs contraints cationiques (pyrrolidinyl PNA) et non cationisés (*a, e* cis cyclopentyl PNA) s'hybridant fortement à un ARN complémentaire. Nous envisageons de les coupler à des peptides vecteurs pour évaluer leur efficacité dans un test fonctionnel.

Chemical Modifications to Improve the Cellular Uptake of Oligonucleotides

Françoise Debart[a], Saïd Abes[b], Gaelle Deglane[a], Hong M. Moulton[c], Philippe Clair[b], Michael J. Gait[d], Jean-Jacques Vasseur[a] and Bernard Lebleu*[,b]

[b]*DAA, UMR 5124 CNRS and* [a]*LCOBS, UMR 5625 CNRS, Université Montpellier 2, Place Eugene Bataillon, 34095 Montpellier cedex 5, France,* [c]*AVI Biopharma, Corvallis,OR, USA,* [d]*Laboratory of Molecular Biology, Medical Research Council, Cambridge, UK*

Abstract: Specific control of gene expression by synthetic oligonucleotides (ON) is now widely used for target validation but clinical applications are limited by ON bioavailability. Moreover, most currently used strategies for physical and chemical delivery cannot be easily implemented *in vivo*. This article reviews new strategies which appear promising for ON delivery. The first part deals with ON chemical modifications aiming at improving cellular uptake as for instance the grafting of cationic groups on the ON backbone. The second part concerns ON conjugation to cell penetrating peptides.

INTRODUCTION

Synthetic oligonucleotides (ON) are recognized to be powerful tools for controlling specifically gene expression. They are now widely used for target validation in pre-clinical studies and have been considered for therapeutic applications. Several strategies targeting RNA, DNA or proteins have been proposed including antisense ON, triple helix-forming ON, rybozymes, DNAzymes, decoy ON, aptamers, immunostimulating ON and the now very popular siRNA. The first ON approved for a major clinical application, the topical ocular administration in the treatment of age-related macular degeneration, is Macugen^R, an aptamer interfering with the interaction between VEGF and its receptor.

However, ON broad therapeutic potential is limited because of poor bioavailability and cellular penetration. Cellular membranes in particular are formidable obstacles for the efficient delivery of synthetic ON into the cells, a difficulty which is widely encountered in biomolecules delivery. Although still a matter of controversy, the common belief is that the cellular uptake of ON occurs by endocytic pathways such as fluid-phase pinocytosis, adsorptive endocytosis and, in a few cases, receptor-mediated endocytosis. Escape of entrapped ON from endosomes-lysosomes eventually takes place by inefficient and unclear mechanisms.

The polyanionic nature and the size of ON are generally pointed out to explain that their passive diffusion could not take place at a significant level. Since unmodified ON and most ON analogues are negatively-charged, their cellular uptake can easily be increased by various physical (electroporation for example) and chemical (cationic lipids formulations for example) delivery strategies. However, some primary cells remain difficult to transfect and these tools cannot be easily implemented *in vivo* for systemic ON delivery. On the other hand, ON cellular uptake eventually takes place by unexpected mechanisms in some tissues thus explaining why biological responses have been observed *in vivo* with unassisted first generation phosphorothioate (PS) ON analogs. This issue remains controversial since biological effects *in vivo* might also been attributed to non specific effects as activation of TLR-mediated responses by unmethylated CpG stretches in ODN or by dsRNA structures in siRNA.

Whatever the case it is now increasingly being considered that poor delivery is limiting many *in vivo* applications of ON-based strategies.

As delivering by passive transport should in principle lead to more efficient drugs, chemists have developed neutral and more hydrophobic backbone-modified ON based on the assumption that neutral ON would resolve the uptake problem. Well-known examples are methylphosphonates, peptide nucleic acids (PNA) and phosphorodiamidate morpholino oligomers (PMO) as shown in Fig (**1**). However, it was quickly discovered that these neutral analogues were not taken up by cells more readily than anionic ON and that their cellular uptake was even lower than charged PS ON analogues.

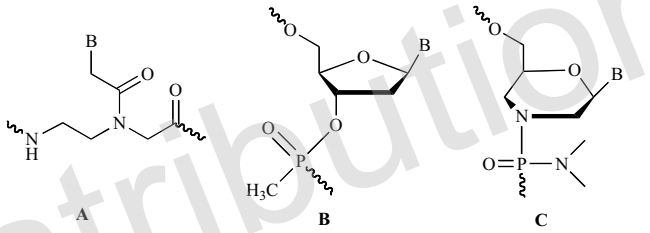

Fig. (1). Neutral hydrophobic backbone-modified ON: A) PNA unit, B) methylphosphonate nucleotide unit, C) PMO unit.

Today, three strategies to chemically assist the delivery of ON and their analogues are investigated. One is the design of ON-complexing delivery vehicles as already mentioned. The literature concerning these carriers is extensively documented and will not be deeply discussed here. Molecular, macromolecular and even supramolecular carriers constituted of cationic lipids, dendrimers [1], polymers, cyclodextrins [2, 3, 4] and even carbon nanotubes [5, 6] have been designed to improve ON cellular uptake. Despite an enhanced efficiency compared to naked ONs, it emerges that virtually all the complexes formed between the ONs and these vehicles enter cells via endocytosis [7].

The second strategy to improve delivery efficacy is to chemically link the ON at its 5' or 3' end to various conjugated groups. In these conjugates, the ON to be delivered becomes part of the vehicle. Most of these conjugates have been listed in 2002 in a comprehensive review by Manoharan [8]. Conjugation to cell penetrating peptides (CPP) is one of the most popular and will be described in the third section of this article. Conjugation with lipophilic moieties such as cholesterol, aminoglycosides, polyethylene glycols, acridine, etc… has been also described. In ON-complexes, the ON moiety is not covalently bound and an excess of the complexing agent is generally required. Consequently, low ON concentrations are available for delivery. In principle, higher concentrations can be achieved with ON-conjugates. However, the covalent attachment of the transporter group could be disadvantageous as it may influence the intracellular distribution of the ON moiety and its hybridization to its targets. Both strategies (complexation and conjugation) can eventually be combined. The third strategy concerns chemical modifications that alter the intrinsic nature of the ON in order to improve cellular uptake (even without assistance). This approach where the chemically-modified ON becomes its own vehicle is in line with the research of new

*Address correspondence to this author at the DAA, UMR 5124 CNRS, Université Montpellier 2, Place Eugene Bataillon, 34095 Montpellier Cedex 5, France; E-mail: bernard.lebleu@univ-montp2.fr

1568-0266/07 $50.00+.00

analogues that gave rise in the past to modifications like PNA and PMO. Several examples will be discussed in the following section.

ON CHEMICAL MODIFICATIONS AIMING AT IMPROVING DELIVERY

The aim of this part is not to discuss the abundant literature concerning chemically-assisted cellular uptake of ON that has already been reported in several reviews. Instead, our purpose is to focus on new concepts that have been recently applied to ON and their analogues. In this regard, the delivery of ONs facilitated by ON is one of the unusual ways to perform it and several examples will be given. The use of ON-conjugates with "molecular umbrellas" [7] constituted of amphiphilic sterols allowing interactions both with a lipid bilayer and with the ON has never been tested on cell cultures but is a promising and original approach that may circumvent an endocytotic delivery route. Finally, we will concentrate our attention to cationic ON and more specifically to analogues bearing guanidine functions found to be critical for the delivery of basic amino acids-rich CPPs. Although the exact mechanism responsible for the transport of guanidine-rich molecules is still unclear, introducing guanidine groups within ON analogues could be a clue for improving their cellular uptake.

ASSISTED DELIVERY OF OLIGONUCLEOTIDES WITH OLIGONUCLEOTIDES

Several ON-assisted ON delivery approaches are reviewed here, including the use of sense strand, appending a poly deoxyguanosine tail to an ON and the ON co-incubating treatments.

PNAs have a high therapeutic potential because of their high affinity and specificity for nucleic acid targets in addition to nuclease resistance. However, these analogues suffer from a low aqueous solubility and more importantly are poorly taken up by cells. Moreover, assisted delivery of naked PNA by complexation with cationic lipids is impossible because neutral PNAs cannot interact with the charges of the lipids. Complexation with cationic liposomes is however possible using PNA-DNA hybrids. The anionic DNA moiety hybridized to the PNA sequence is then able to complex via electrostatic interactions with the cationic lipids. This approach has been initially proposed by the group of D. Corey [9, 10] and recently used by the team of P.Nielsen [11]. Because protocols based on lipid transfection are well established, annealing of PNA to DNA and subsequent complexation with lipofectamine or other commercially available lipid formulations appears a general method for delivering PNA into the cells. Noteworthy, however, hybridization to complementary DNA was not necessary for lipoplex complexation when the PNA was conjugated to the 9-aminoacridine (Acr) intercalator [11]. The antisense activity in cells of these Acr-PNA lipofectamine complexes was dose-dependant, sequence-specific and comparable to the activity obtained with the PNA-DNA lipofectamine strategy. To explain these results, it has been proposed that the acridine in its non-protonated form behaves like the adamantyl moiety reported several years ago to enhance the cellular uptake of PNA conjugates [12]. Both compounds are adequately lipophilic to permit complexation with cationic lipids.

The opportunity of delivering a DNA antisense ON analogue hybridized with a complementary sense sequence using a cationic lipid (lipofectamine) as vehicle was also investigated by Juliano and Herdewijn[13]. In their approach, the antisense ON was a gapmer made of 2'-*O*-methyl PS wings (to enhance resistance towards nucleases) and of a deoxynucleotide PS gap (to provide RNAse H activity). The sense ON was a short phosphodiester ON whose hydrolysis by cellular nucleases releases the active and metabolically-stable antisense ON. The reduction of the MDR1 gene encoded P-glycoprotein expression in NIH 3T3 and MDR-3T3 cells was found to be greater than with the single-stranded antisense ON delivered with lipofectin. Confocal microscopy analysis of the cellular distribution of the hybrid using different fluorescent tags for the antisense (Fluorescein) and for the sense (Texax Red) strands indicated that the antisense moiety but not the sense strand was transported to the nucleus. However, it is not easy to figure out if the enhanced biological effect observed with these DNA duplexes compared to the antisense ON alone could be explained by only one or several factors such as an increased cell uptake, a reduced release from the cell or a higher metabolic stability.

Conjugation of cholesterol to a sense strand has been tried to improve the biological activity of antisense ONs. Due to its lipophilic character, the cholesterol moiety interacts with the lipid vehicle and enhances the amount of ON incorporated in the lipoplexes. Moreover, connecting cholesterol to the sense and not to the antisense strand prevents it to influence the intracellular distribution and the hybridization to nucleic acid targets of the antisense strand and, consequently, to affect the biological effect of the antisense ON. Juliano and Herdewijn [14] thus tried to improve their initial concept by derivatization of the sense sequence with cholesterol. A cholesterol molecule was linked to 1-4 number of sense ON through an oligolysine linker as shown in Fig. (**2**). A 20 PS ON gapmer with 2'-methoxyethyl nucleotide wings, a gap of 8 PS nucleotides and a 3'-propanediol moiety was used as the antisense ON. In comparison to non conjugated double-stranded complexes, the cholesterol-double stranded DNA-lipofectamin complexes gave only a small, although significant, reduction of P-glycoprotein expression in MDR 3T3 cells compared to the formulation without cholesterol conjugation. Cholesterol conjugation increased the amount of antisense ON in the cationic lipolexes when formulated with a 11mer sense strand but not with a 18mer sense strand. Higher antisense ON concentrations in the lipoplexes were achieved with a long sense sequence than with a short one. This suggested that the electrostatic interaction is the most important factor for the complex formation when formulated with a longer sense ON, while the weak hydrophobic interaction between the cholesterol and the transfection agent may have a role for the lipoplex formation when formulated with a shorter sense ON. One cannot preclude however that longer double-stranded ON are thermodynamically more stable than shorter ones and could moderate the DNA helix denaturation induced by cationic lipids as reported by Prasad and col [15, 16].

Along the same lines, Lorenz and col [17]. reported a greater down-regulation of gene expression with a siRNA in which the sense strand was conjugated to cholesterol than with cholesterol-linked antisense strand or with two modified strands. The conjugation of the sense strand to a cholesterol moiety was also the strategy of Soutshek and col [18] for gene silencing using siRNA.

CpG DNA are potent immunostimulatory agents able to activate cells of the immune system. Interestingly for innate immunity, CpG DNA recognition of Toll-like receptor 9 (TLR-9) seems to happen inside endosomes and the delivery of CpG DNA to the endosomes followed by endosomal maturation is decisive for immune activation.

Specific membrane receptors of CpG DNA have not been found in Antigen-presenting cell. However, it is known that poly deoxyguanosine binds to the scavenger receptor mainly expressed in the monocyte lineage. Two independent groups [19] [20, 21, 22] showed that the conjugation of a CpG ON to a dG run constituted of 5 to 6 consecutive nucleotide units increased their cellular uptake in monocytes and B-cells without vehicle and enhanced immuno-stimulation. It was outlined that the supramolecular structures induced by the formation of G base tetrads could influence ON uptake possibly through scavenger receptor. The cellular internalization of the dG run-CpG ON conjugates was more efficient for 3'-CpG conjugates than for 5'-conjugates [22]. The G tetraplex could also protect CpG ON from nuclease degradation thus enhancing their half-life in biological media.

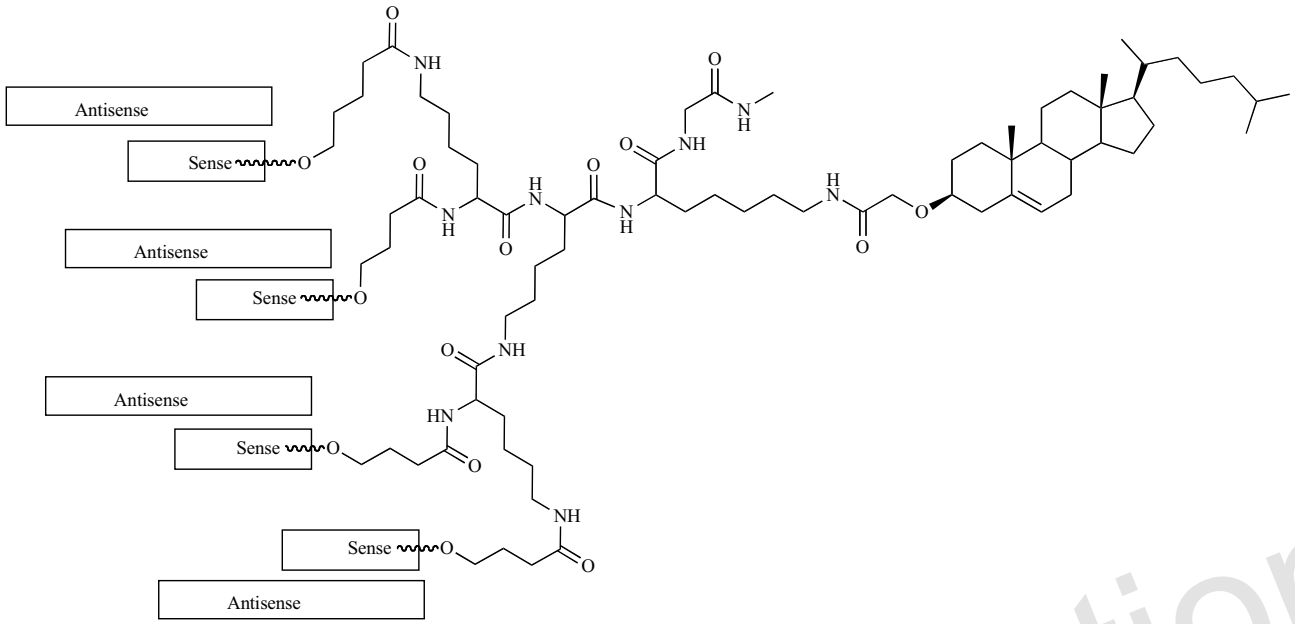

Fig. (2). Cholesterol-linked ON constructions for complexation with cationic lipids.

Small interfering RNA (siRNA) [23] which are composed of double-stranded RNA ON very efficiently inhibit gene expression in mammalian cells through the specific degradation of the targeted mRNA. Since they appear to be more efficient than RNaseH-competent antisense ON they are now considered as potential drugs for medical applications [18]. A crucial limiting factor for their therapeutic use will probably be delivery as for DNA ON. However, it has been shown that unassisted cellular uptake of siRNA occurs in mammalian cells [24, 25]. It could be more due to their double-stranded structure than to chemical differences between RNA and DNA [13]. The authors hypothesized that the improved uptake of the double-stranded siRNA as compared to the single-stranded DNA may be at least partly responsible of the higher biological activity. The examples of delivery enhancement by hybridization to a complementary sequence shown above support this hypothesis. Along the same lines, it was shown that naked long-chain double-stranded DNA can be delivered to mammalian cells without carriers and that this process was enhanced by sequence-specific single stranded ON [26].

In light of these results, Overhoff and Sczakiel explored the stimulation of siRNA delivery by co-incubation with ONs [27]. The delivery efficiency was tested with several ON analogues i.e. phosphodiester DNA and RNA, 2'-O-methyl, PS DNA and RNA. Only PS DNA was able to efficiently increase the uptake of siRNA. The phenomenon was not sequence-specific but was concentration-dependant and increased with the ON length. Compared to free siRNAs uptake as reported before by the same group [25] and by an independent one [25], the efficiency of siRNA delivery by co-incubation with a PS ON was estimated to be 30 -50 times higher. Confocal microscopy revealed that siRNA delivered with this strategy showed a perinuclear and dotted distribution. In comparison, without PS stimulation, the siRNA distribution was homogeneous and disseminated over the cytoplasm. This is likely due to a different route of delivery with PS ON stimulation as inhibitors of caveolin-mediated endocytosis reduced siRNA uptake whereas an activator of this pathway increased it. It has been postulated that PS DNA interacts with PS ON-specific membrane receptors and stimulate the internalization of siRNA in caveosomal vesicles carrying them to a perinuclear location.

ASSISTED ON DELIVERY WITH "MOLECULAR UMBRELLAS"

Despite the broad number of ligands linked to ON and whatever their hydrophilic, lipophilic or amphipathic character, none were able to allow cell delivery by passive transport. In this respect, the work done by the group of Regen on molecular umbrella-assisted transport of ON [7, 28] across phospholipid bilayers deserves attention.

Cholic and deoxycholic acids are amphipatic sterols with a hydrophobic (the carbon face of the sterol) and a hydrophilic face (the OH group of the sterol). Regen's group introduced several years ago [29, 30] the concept of molecular umbrellas constituted of several sterols linked together through a central scaffold to the compound of interest. When a hydrophilic compound is in a hydrophilic environment, the umbrella is in a fully exposed conformation in which the hydrophobic faces of the sterols interact together favouring hydrophilic interactions between hydrophilic faces and the solvent. In contrast, in a hydrophobic environment such as a lipid bilayer, the umbrella is closed on the compound in a shielded conformation so that the hydrophilic faces of the sterols now interact with the compound while the hydrophobic faces interact with the lipid tails. This concept was applied with success to the transport of small hydrophilic peptides [31, 32] and of adenosine 5'-triphosphate [33, 34] through synthetic phospholipids bilayers.

For ON transport, molecular umbrellas were designed as shown in Fig. (**3**). They are constituted of 2 to 4 cholic or deoxycholic acids linked by a scaffold made of lysines linked to a spermidine. 2-nitro 5-mercaptobenzoic was used as the linker between the central amino group of the spermidine (amide bond) and the thiol function of a thio ON (disulfide bond) [7, 28]. This bond is interesting since it is cleaved when gluthatione is trapped into the liposomes as done in this study. This will most probably happen also in cells as gluthatione is present in the cytoplasm. It could be noted that a similar gluthatione-sensitive prodrug approach was recently employed for polyethyleneglycol conjugates of ON linked through a disulfide bond [35].

The problem of using molecular umbrellas conjugates of ON is that they are larger molecules than previously studied ones, and it is

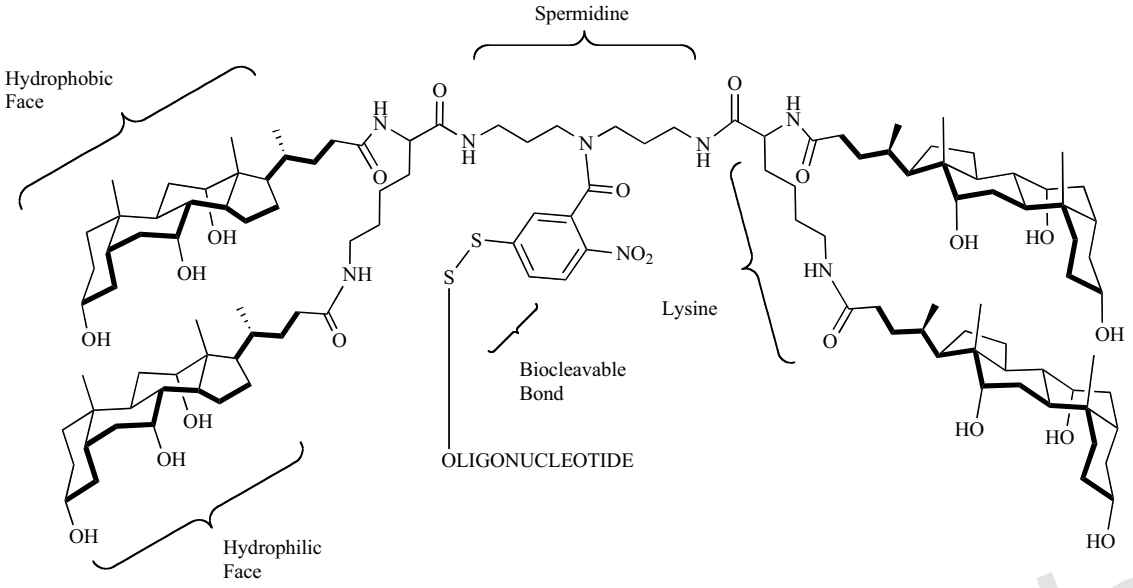

Fig. (3). Molecular umbrella constituted of four cholic acids linked to an ON through a central scaffold of lysines bound to spermidine and 2-nitro 5-mercaptobenzoic.

not possible for the umbrella to shield the whole ON. Nonetheless, the effective transport a 16-mer ON-molecular umbrella conjugate across a synthetic cholesterol-rich lipid bilayer has been demonstrated.

The use of molecular umbrellas thus appears as a hopeful approach to transport ON by passive diffusion. If transport happens in natural cell membranes, this strategy will be worth being pursued for the development of ON as therapeutics.

CATIONIC AMINO AND GUANIDINO ON

The introduction of positive charges into ON is expected to favour hybridization with nucleic acid targets, due to the partial or complete replacement of the electrostatic repulsion between polyanionic single strands by an electrostatic attraction. This concept has been validated with base-modified analogues bearing 5-propynylamino uridines instead of thymines [36, 37], with sugar modified 2'-*O*-ethylamino ON [38], with phosphate-modified deoxyribonucleic guanidine oligomers (DNG) [39, 40] and with aminoalkyl derivatives in an alpha-nucleosidic configuration as reported by our group [41, 42] (Fig. (**4**)).

It has been also suggested that the positive charges may increase the permeability of the cell membrane though electrostatic interaction of the cationic ON with polar heads of membrane phospholipids [43]. This might not be the case since cationized biomolecules are likely to interact first with negatively charged membrane-associated proteoglycans as heparan sulfates. However, it is amazing that despite a lot of studies concerning the hybridization of these ON analogues, little information concerning their mechanism of cell penetration in their free form is available. Generally, these ON analogues have been delivered by physical means more than with conventional carriers. Concerning cationic sugar modifications for example, electroporation was used to deliver a PS 20-mer antisense ON capped with nine 2'-*O*-propylamino nucleotides. This ON analogue reduced C-*raf* expression by a 10-fold factor in comparison with a PS ON [44]. Similarly, several gene knockouts by 2'-*O*-ethylamino triplex-forming ON were observed after simultaneous electroporation with the targeted reporter gene into various cell lines [45, 46, 47, 48, 49]. Microinjected dimethylaminopropyl phosphoramidate cationic ON analogues inhibited gene expression in *Xenopus* oocytes in both the antigene (as fully modified) [50] and antisense (as a zwitterionic

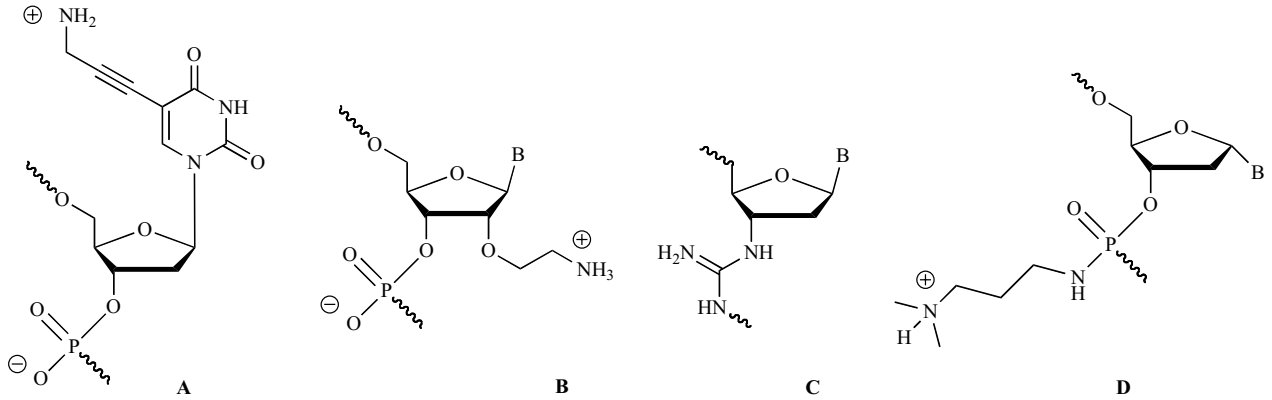

Fig. (4). Positively-charged ON analogues enhancing hybridization properties : A) 5-aminopropinyl 2'-deoxyuridine 3'-phosphate, B) 2'-*O*-aminoethyl nucleotide unit, C) deoxyribonucleic guanidine unit (DNG), D) 3'dimethylaminopropylphosphoramidate α-nucleotide.

gapmer) [51] modes. Dagle and col. suggested that the net charge of the analogues could affect their localization into the cell and favour their nuclear transport. More recently [52], we tested the capacity of cationic dimethylaminopropylphosphoramidate alpha-ON to sterically block IRES-mediated translation of a luciferase reporter gene in a HepG2 hepatoma cell line. A cationic ON complementary to the III-d loop of the IRES (Internal Ribosome Entry Site) inhibited gene expression in a dose-dependant and specific manner. This antisense effect was only moderate since a 30% decrease of the targeted luciferase activity was observed after 24 hours of incubation but, interestingly, it did not require the use of physical delivery techniques or of transfection agents. Under similar conditions a neutral phosphoramidate ON as well as an anionic 2'-*O*-methyl were inefficient. This result demonstrated for the first time the unassisted uptake of a cationic ON and, consequently, their potential as antisense agents. There are several reasons to connect guanidino instead of amino groups to ON in order to make them zwitterionic of cationic. The guanidinium group is highly basic (pKa 12.5) and guanidino ON should remain protonated under a wider range of pH than amino analogues [53]. This should enhance their affinity for complementary nucleic acid targets. The other reason is to improve their intrinsic uptake properties by mimicking the now well established role of arginine side chains in the internalization of CPPs such as the human HIV-1 Tat [54] and the *Drosophila* Antennapedia [55]. Based on this approach, Ly s' group [56, 57] hypothesized that incorporation of guanidino functions into the PNA backbone will facilitate the free uptake of PNA into mammalian cells (Fig. (**5**)). Moreover, the high solubility in water of GPNA with an arginine backbone instead of the conventional glycine backbone of PNA is a clear advantage. The chemistry of theses compounds needs to be stereoselective, since the authors showed a better affinity for RNA targets with GPNA with a D- than with GPNA with an L-configuration.

The free-uptake effectiveness of fully or partially modified GPNA was followed by fluorescence microscopy on fluorescein conjugates. Ly and col. [56] demonstrated the nuclear uptake of these analogues in a HCT116 cell line [57] as well as in HeLa cells and primary ES cells. As already known, the corresponding unmodified PNA was not internalized. Surprisingly, a PNA conjugated with a tetraargine peptide was not taken up by either cell lines, whereas Sazani and col. [58] showed a few years ago that a PNA conjugated with a tetralysine peptide was taken up by Hela cells in the absence of transfection reagents. Moreover, it was found that the free uptake of GPNA was as efficient at 37°C than at 4°C suggesting that endocytosis or membrane receptor mediated recognition were not involved in their delivery. However, the cells were fixed with formaldehyde before analysis by fluorescence microscopy. It has to be recalled at this point that artefacts of redistribution into the nucleus have been encountered with cationic CPP when chemical fixation was used [59]. The role of the guanidinium group on the cellular uptake of modified ON was also demonstrated with DNA analogues incorporating 5-[(6-guanidinohexylcarbamoyl)methyl] uracyle instead of thymine nucleobases [60]. Free cell uptake was monitored by fluorescence on fixed and unfixed HeLa cells. Both showed that the cellular distribution of the DNA analogues was mainly cytoplasmic and it was suggested that cellular uptake occurred through endocytosis. The guanidino function is responsible since the amino ON derivative was taken up much less efficiently than the guanidino ON. Interestingly, the uptake was less efficient with a 20mer ON bearing six guanidino base modifications than with the one bearing four.

We have reported the efficient postsynthesis guanidination of amino groups linked to a phosphoramidate backbone [41]. The cellular uptake of these fully backbone-modified ON was studied recently [61]. Here again, the guanidinium significantly improved the cellular uptake of DNA analogues. A cationic guanidino 12mer ON was taken up about six times more efficiently than an anionic PS ON analogue (Fig. (**6A**)). These experiments were performed with and without formaldehyde fixation of the cells. When cells were fixed, a nuclear localization was predominant whereas a dotted mainly cytoplasmic distribution occurred with non-fixed cells (Fig. (**6B**)). This is in agreement with an endocytotic pathway of internalisation with material, at least in part, trapped in endocytic vesicles. Furthermore, Fluorescence Activating Cell Sorting analyses indicated that, in contrast to what was observed at 37°C, the internalization at 4°C for both PS and guanidino phosphoramidate analogues was negligible and did not increase with incubation time in keeping with endocytosis.

These three recent reports dealing with the delivery of guanidino ON analogues do show that introducing guanidinium functions on the nucleobases or on the backbone improves the cellular uptake of these compounds without the use of any vehicle. However, two of these reports support an endocytotic mechanism of internalization whereas the third one is in favour of direct translocation through the cell membrane. Whatever the case, these cationic guanidino ON open the way to a new strategy for the non-assisted delivery of ON.

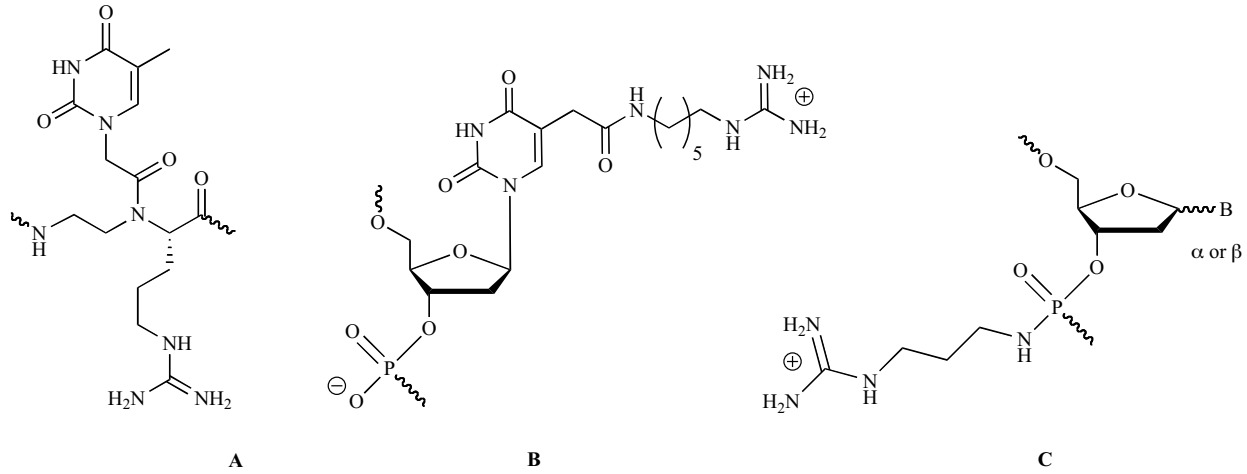

Fig. (5). Guanidino ON Motifs: A) guanidine-based PNA (GPNA) unit, B) 5-[(6-guanidinohexycarbamoyl)methyl]-2'-deoxyuridine 3'-phosphate, C) 3'-guanidinobutyl phosphoramidate nucleoside unit.

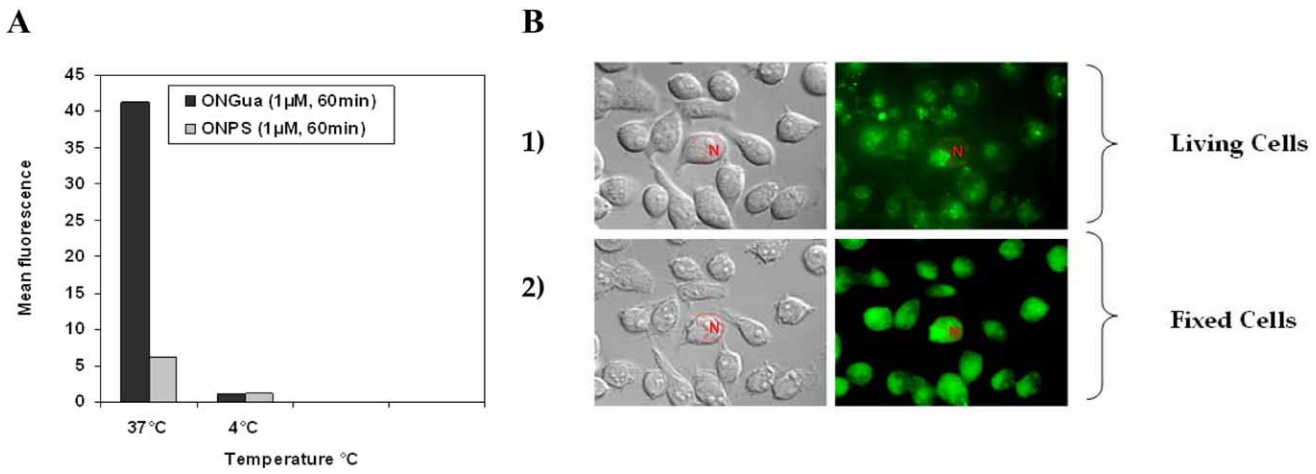

Fig. (6). Cellular uptake of Guanidino ON analogues.
A) Flow cytometry analysis of the cells uptake of fluorescently labelled guanidylated ON (ONGua) or phosphorothioate ON (ONPS) at 37°C and 4°C. **B**) Fluorescence microscopy analysis of guanidylated ON cell uptake. Live unfixed HeLa cells were incubated with fluorescein-labelled ONGua (panel 1). Paraformaldehyde (3.7%) fixation was then performed under the microscope and cells were again observed 10 min later (panel 2) in order to document redistribution after cell fixation. N represents nucleus.

DELIVERY OF ANTISENSE ON BY CELL PENETRATING PEPTIDES

General Outline

Homopolymers as poly (L-lysine) have been extensively investigated as nucleic acids delivery systems following pioneering work by Ryser *et al* [62]. ([63] for a recent review). Our own group has documented the enhanced cellular uptake via adsorptive endocytosis of antisense ON covalently bound to poly (L-lysine) in several *in vitro* models [64]. As an example, a potent sequence-specific antiviral activity has been achieved in a HIV-1 acute infection cell assay. Further work by several groups has indicated that targeted *in vivo* delivery of the transported antisense ON was possible [65]. However, these cationic heterodisperse homo-polymers are rarely used nowadays due to their cytotoxicity and to complement activation. The concept of basic-peptide delivery was revived when it was realized that purified proteins as the Drosophila Antennapedia transcription factor [66] or the HIV-1 Tat transactivating protein [67, 68] were able to cross cellular membranes and to find their way to the nucleus. These experiments have paved the way to the first cell penetrating peptides (CPP) also named PTD for protein transduction domain. It rapidly became evident that cellular internalization was associated with a short stretch of aminoacids in the Antennapedia and Tat proteins. In this latter case, cellular uptake is due to the GRKKRRQRRR cationic domain [54] which includes the Tat RNA binding motif and a nuclear localization signal. Importantly, it was rapidly realized that chemical conjugation or fusion to these PTD could be exploited to improve the cellular uptake or the bioavailability of low molecular weight drugs, biomolecules (as peptides, proteins or oligonucleo-tides) and even large molecular weight material (as liposomes or nanoparticles for imaging) as reviewed in [69]. As an example, Dietz and Bähr [70] listed 124 applications of Tat PTD-mediated transport in their comprehensive review of the CPP field two years ago. Research in this area did not limit to natural PTD and a large number of synthetic CPPs have been designed and studied in terms of mechanism of cellular uptake and applications over the last years as briefly accounted in Table **1**.

CPP-Mediated Delivery of Antisense ON: A Few Examples

Surprisingly, the CPP-mediated delivery of antisense ON has not been largely documented despite promising initial data. The impetus has been provided by Langel and his colleagues [75] with Transportan-conjugated PNAs. The PNA antisense-CPP conjugate was delivered into cultured neuronal cells and was able to down-regulate in a sequence-specific way its galanin receptor target. Most impressively, these same constructions were effective after injection in mice thus indicating that the transportan CPP was able to cross the blood brain barrier. Likewise, Juliano and his colleagues [83] demonstrated a sequence-specific and energy-dependent down-regulation of P-glycoprotein expression with Antp- or Tat -conjugated 2'Omet PS antisense ON. Intriguingly the antisense activity of these conjugates was more pronounced in the presence of serum.

The ability to deliver steric-blocking PMO after CPP conjugation has been analysed in a splicing correction assay described by Kang *et al.* [84] (vide infra) and in an assay monitoring the down regulation of a c-myc reporter gene expression [85]. Sequence-specific upregulation of luciferase and down-regulation of c-myc expression were achieved with CPP-conjugated PMO. Tat conjugates were 10-20 times more efficient than Pep-1 or NLS conjugates while free PMOs were almost not active in these assays [86]. Requested Tat conjugate concentrations remained however relatively high. The potential of CPP conjugation for steric block ON delivery has also been extensively evaluated by M. Gait and his colleagues [87] using on a well-controlled assay monitoring the inhibition of Tat-dependent transactivation by 12-mer 2'OMet/LNA (Locked Nucleic Acid) mixmer ON analogues complementary to the TAR region of a HIV-1 LTR promoter. Fluorescein-labelled ON mixmers were conjugated to various CPPs through a disulfide bridge. Cellular uptake of the conjugates was largely increased as compared to free ON but confined to cytoplasmic vesicles [83]. No nuclear delivery was detected and accordingly no specific inhibition of trans-activation could be monitored [88].

As will be detailed in the following section, entrapment within endocytotic vesicles now appears to be the main problem encountered in CPP-mediated delivery of ON.

A different strategy has been followed by G. Divita and his colleagues with the MPG CPP family. These bipartite CPPs (see Table **1**) combine a hydrophobic fusion peptide and a cationic nuclear localization signal. At variance with PTD and most other CPPs, MPG derived CPPs form non covalent complexes with nucleic acids. Physico-chemical studies with synthetic lipid bilayers

Table 1. Examples of Cell Penetrating Peptides

Cells Penetrating Peptides (CPPs)	Sequences	References
Natural CPPs		
Penetratin	RQIKIWFQNRRMKWKK	[66]
Tat (48-60)	GRKKRRQRRRPPQ	[54]
VP22	DAATATRGRSAASRPTERPRAPARSASRPRRVD	[71]
LL-37	LLGDFFRKSKEKIGKEFKRIVQRIKDFLRNLVPRTES	[72]
Mouse PrP (1-28)	MANLGYWLLALFVTMWTDVGLCKKRPKPamide	[73]
pVEC	LLIILRRRIRKQAHAHSKamide	[74]
Synthetic CPPs		
Transportan (TP)	GWTLNSAGYLLGKINLKALAALAKKILamide	[75]
TP10	AGYLLGKINLKALAALAKKILamide	[76]
Polyarginine	RRRRRRRRRR	[77]
MAP	KLALKLALKALKAALKLAamide	[78]
Pep-1	KETWWETWWTEWSQPKKKRKV	[79]
Pep-2	KETWFETWFTEWSQPKKKRKV	[80]
MPG	GALFLGWLGAAGSTMGAPKKKRKV	[81]
KALA	WEAKLAKALAKALAKHLAKALAKALKACEA	[82]

have led to a mechanism involving direct membrane translocation through pore formation ([89] for a recent review), although arguments for an endocytotic mechanism have also been proposed [90]. Whatever the mechanism, various versions of these bipartite amphipathic peptides have been used successfully for the delivery of charged antisense ON [81], uncharged PNA [79] or siRNA [91].

Splicing Correction as a Model System for the Evaluation of CPP-ON Conjugates

Monitoring an unequivocal and easy-to-quantify biological response is critical to evaluate the activity of ON-delivery vectors. Indeed, antisense ON or siRNA lead in general to a decreased expression of the targeted gene and it has often been difficult to discriminate between an authentic antisense effect and side effects.

Recent work by R. Kole and his colleagues (as reviewed in [92]) has provided an elegant assay with a positive readout which is now considered as the most reliable model for assessing the efficiency of ON delivery vectors. It capitalizes on studies dealing with splicing abnormalities of the β-globin gene in a human thalassemia. An intronic mutation gives rise to a cryptic splice site and as a consequence to the incomplete removal of the mutated intron. Masking of this abnormal splice site by specific hybridization with a RNase H-incompetent ON analogue (coined SSO for splicing switching oligonucleotide) restores normal splicing and allows the production of a functional protein [93]. This mutated intron has been introduced in the coding region of either luciferase or EGFP reporter genes thus providing an elegant model for the evaluation of splicing correction *in vitro* or *in vivo* [58, 84]. Indeed, the nuclear delivery of RNase H-incompetent ON analogues (as 2'OMet ON, PNA or PMO) leads to the production of functional luciferase or EGFP which can be quantitated by a biochemical assay or by FACS analysis, respectively, as outlined in Fig. (**7**).

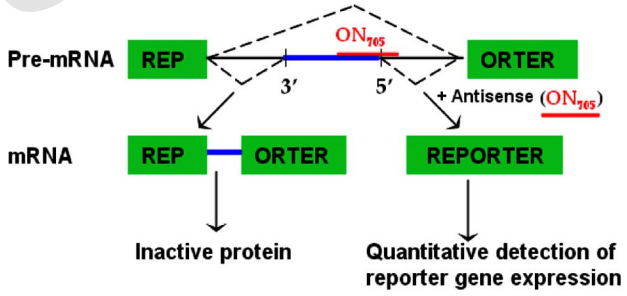

Fig. (7). Splicing correction assay (adapted from Kang *et al*, 1998).

Apart from being an interesting assay, splicing correction has several potential clinical applications. It has to be recalled here that most human genes undergo alternative splicing and that, in some cases, a delicate balance between splicing products is requested for appropriate gene regulation. Not surprisingly several inherited or acquired important human diseases are already known to be linked with deficient splicing mechanisms [94, 95]. RNaseH-incompetent antisense ON have already demonstrated their potential at least *in vitro*. As an example, overexpression of the anti-apoptotic version of Bcl-X in prostate or breast cancer cells is associated with resistance to chemotherapy. The appropriate balance between the pro- and anti-apoptotic versions of Bcl-X can be restored by the *in vitro* transfection of SSOs and consequently sensitivity to chemotherapy can be restored [96, 97]. An equally promising strategy has been proposed for the treatment of Duchenne muscular dystrophy. In this case SSO hybridization induces the skipping of the mutated exon thus leading to the production of a shorter but functional version of dystrophin [98, 99]. In both cases the

bioavailability of the SSOs is a limiting factor since delivery with cationic lipids was proved to be toxic (in particular for muscular cells) and free SSOs had to be given in high quantities.

Entrapment in Endocytic Vesicles Limits the Efficiency of CPP Delivery

The paucity of data obtained with CPP conjugation of antisense ON could be due to several reasons. Among these, poor escape from endocytotic vesicles and degradation by lysosomal nucleases are the most plausible. Indeed most recent studies on basic amino-acids-rich CPP mechanism of cell internalization have pointed to endocytosis after initial binding to membrane proteoglycans as reviewed in [100]. Moreover, we have shown that CPP-conjugated to fluorochrome-tagged PNA or PMO accumulate within endocytotic vesicles in unfixed cells [59, 101, 102, 103, 104].

In a series of recent publications, splicing correction has been documented using the assay described above both *in vitro* [58] and in a transgenic mouse model [104]. Impressively, appending as few as four lysine residues to the splice correcting PNA allowed functional delivery. A systematic further survey in a slightly different biological model for splicing correction pointed to an optimal length of eight lysine for PNA delivery [106]. In our hands, however similar $(Lys)_4$ –PNA-Lys (unpublished observations) or $(Lys)_8$ –PNA-Lys conjugates [103] were not efficient in Kole's model despite they were taken up by cells. Likewise, a $(Lys)_8$ – PNA-Lys construct was ineffective in a Tat/TAR transactivation assay. [102] These disappointing data strongly suggested that the conjugates remained trapped in endocytotic vesicles as verified by fluorescence microscopy. In keeping with this hypothesis, an endosomolytic agent as chloro-quine largely increased splicing correction in this model [103]. Similar data were obtained with PNA or PMO SSOs conjugated to various CPPs as briefly outlined in Fig. (**8**). Likewise, chloroquine treatment lead to trans-activation inhibition by ON mixmers [102].

Recent independant studies by several groups have essentially lead to similar conclusions namely that segregation of ON-CPP in endocytotic vesicles was the limiting factor for cytoplasmic or nuclear delivery, as reviewed by Pujals *et al* [107]. In all cases treatment by endosomolytic physical (as light photoactivation) or chemical (as chloroquine, high concentrations of sucrose or Ca^{2+} ions) agents was required to achieve an efficient biological effect [103, 108, 109, 110]. Unfortunately the *in vivo* use of these agents is difficultly envisaged. An interesting alternative strategy of counteranion–mediated delivery has been proposed by S.Futaki *et al.,* [111]. They have demonstrated that the complexation of arginine side-chains in CPPs to the aromatic moieties of pyrene butyrate allowed direct translocation across the plasma membrane and subsequent cytoplasmic delivery of the CPP-associated cargo. The validity of the concept has however not be established for the CPP-mediated transport of ON analogues.

The CPP-association or co-delivery of fusogenic peptides has been explored by Dowdy *et al.,* [112]. A significant increase in Tat CPP-mediated expression of the fused Cre-recombinase has been achieved. We have screened several membrane destabilizing peptides for their ability to improve splicing correction when co-delivered with a Tat-PNA conjugate but data have not been encouraging sofar (Abes, Clair *et al*., unpublished).

Several groups have capitalized on the splicing correction assay described above to screen for efficient CPP-mediated delivery of PNA or PMO. Nielsen *et al.,* [113] have systematically analysed splicing correction by 16 CPP-PNA conjugates including various versions of transportan,penetratin, polyarginines of various lengths or Tat. Transportans and to a lower extent $(Arg)_9$ were by far the most actives in this assay but, unfortunately, became rapidly cytotoxic and were inhibited by serum. Our group has exploited studies by Rothbard *et al.,* [114] which has systematically investigated a series of polyArg analogues in terms of cell uptake. Molecular modelling had indicated that not all Arg side chains in polyArg would be able to interact with a model membrane. Based on this assumption, they synthesized a series of peptides nonamers in which Arg residues were interspersed with non α-amino acids allowing a modulation in the spacing of guanidinium groups. One of the most efficient derivative which came out of their evaluation was $(R\text{-}Ahx\text{-}R)_3R$, a peptide in which Arg residues are interspersed with aminohexanoic acid. An analogue of this peptide, $(R\text{-}Ahx\text{-}R)_4$-Ahx-βAla, allowed an efficient and sequence-specific splicing correction in the absence of endosomolytic agents when conjugated to PMO_{705} [104] as shown in Fig. (**8B**). Notewhorthy these

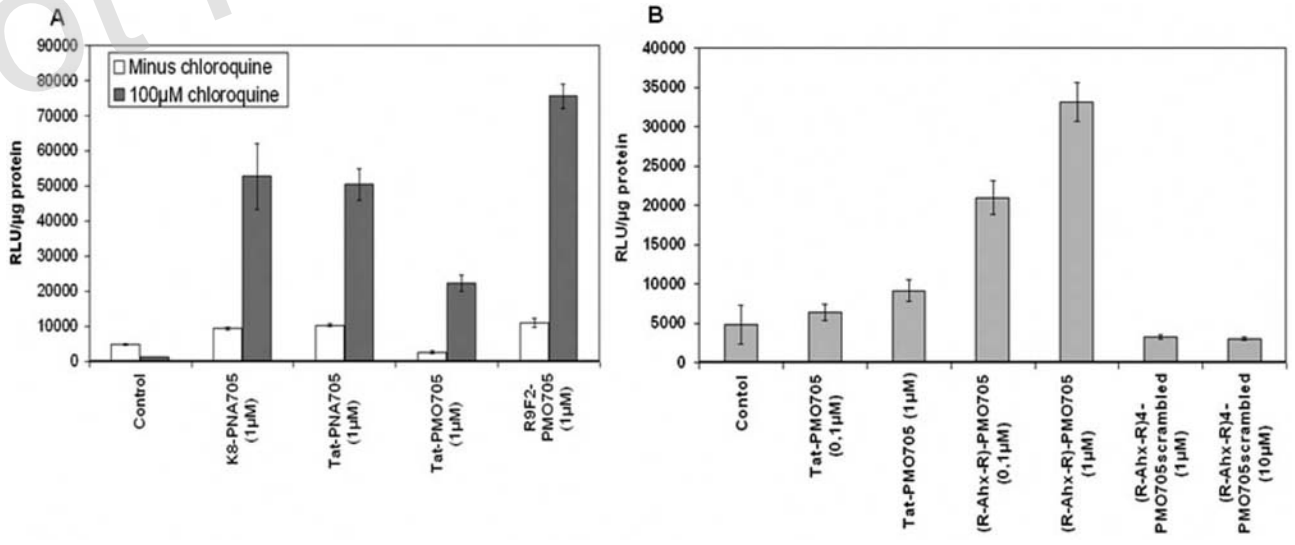

Fig. (8). Evaluation of CPPs conjugates using the splice correction assay. Panel (A), splicing correction using the indicated CPPs-ON conjugate at 1µM in the absence of chloroquine (white bars) or in the presence of 100µM chloroquine (gray bars). Panel (B), splicing correction using (R-Ahx-R)-PMO705 or Tat-PMO705 conjugates at the indicated concentration without endosomolytic agents.

conjugates were not cytotoxic over a large concentration range and remained active in the presence of serum thus offering an interesting prospect for *in vivo* applications.

CONCLUSIONS AND PERSPECTIVES

Several new strategies have thus been proposed to improve the cellular delivery of ON. Whatever their originality and their demonstrated efficiency *in vitro* mostly on laboratory cell cultures, much remains to be achieved before considering their development for clinical applications. Their potential still has to be evaluated *in vivo* on well controlled biological models and to be compared in terms of efficiency, cytotoxicity and selectivity with more classical delivery vectors as nanoparticles or liposomes. As stated initially in this article, however, it is increasingly considered that ON-based strategies offer unique possibilities to control specifically gene expression but then their full potential will probably not be met if their bioavailability is not improved. A concerted investment by chemists and biologists in this field is therefore worth being continued.

ACKNOWLEDGMENTS

Work in the authors groups has been funded by grants from IFCPAR (BL) and EEC (BL and MG). S. Abes and G.Deglane hold pre-doctoral fellowships from the Ligue Contre le Cancer and from the Ministère de la Recherche et de la Technologie, respectively. R. Kole (Univ.North Carolina) is acknowledged for providing the HeLa pLuc 705 strain for the splicing correction assay and P.Prevot for his help with fluorescence microscopy.

REFERENCES

[1] Dufes, C.; Uchegbu, I. F.; Schatzlein, A. G. Dendrimers in gene delivery. *Adv. Drug Deliv. Rev.* **2005**, *57(15),* 2177-2202.

[2] Lysik, M. A.; and Wu-Pong, S. Innovations in oligonucleotide drug delivery. *J. Pharm. Sci.* **2003**, *92(8),* 1559-1573.

[3] Patil, S. D.; Rhodes, D. G.; Burgess, D. J. DNA-based therapeutics and DNA delivery systems: A comprehensive review. *AAPS J.* **2005**, *7(1),* E61-E77.

[4] Shoji, Y.; Nakashima, H. Current status of delivery systems to improve target efficacy of oligonucleotides. *Curr. Pharmaceut. Des.* **2004**, *10(7),* 785-796.

[5] Kam, N. W. S.; Liu, Z.; Dai, H. J. Functionalization of carbon nanotubes via cleavable disulfide bonds for efficient intracellular delivery of siRNA and potent gene silencing. *J. Am. Chem. Soc.* **2005**, *127(36),* 12492-12493.

[6] Gao, L.; Nie, L.; wang, T.; Qin, Y.; Guo, Z.; Yang, T.; Yan, X. Carbon nanotube delivery of the GFP gene into mammalian cells. *ChemBioChem.* **2006**, *7,* 239-242.

[7] Janout, V.; Jing, B. W.; Regen, S. L. Molecular umbrella-assisted transport of an oligonucleotide across cholesterol-rich phospholipid bilayers. *J. Am. Chem. Soc.* **2005**, *127(45),* 15862-15870.

[8] Manoharan, M. Oligonucleotide conjugates as potential antisense drugs with improved uptake, biodistribution, targeted delivery, and mechanism of action. *Antisense Nucleic Acid Drug Dev.*. **2002**, *12(2),* 103-128.

[9] Hamilton, S. E.; Simmons, C. G.; Kathiriya, I. S.; Corey, D. R. Cellular delivery of peptide nucleic acids and inhibition of human telomerase. *Chem. Biol.* **1999**, *6(6),* 343-351.

[10] Doyle, D. F.; Braasch, D. A.; Simmons, C. G.; Janowski, B. A.; Corey, D. R. Inhibition of gene expression inside cells by peptide nucleic acids: Effect of mRNA target sequence, mismatched bases, and PNA length. *Biochemistry* **2001**, *40(1),* 53-64.

[11] Shiraishi, T.; Nielsen, P. E. Down-regulation of MDM2 and activation of p53 in human cancer cells by antisense 9-aminoacridine-PNA (peptide nucleic acid) conjugates. *Nucleic Acids Res.* **2004**, *32(16),* 4893-4902.

[12] Ljungstrom, T.; Knudsen, H.; Nielsen, P. E. Cellular uptake of adamantyl conjugated peptide nucleic acids. *Bioconj. Chem.* **1999**, *10(6),* 965-972.

[13] Astriab-Fisher, A.; Fisher, M. H.; Juliano, R.; Herdewijn, P. Increased uptake of antisense oligonucleotides by delivery as double stranded complexes. *Biochem. Pharmacol.* **2004**, *68(3),* 403-407.

[14] Chaltin, P.; Margineanu, A.; Marchand, D.; Van Aerschot, A.; Rozenski, J.; De Schryver, F.; Herrmann, A.; Mullen, K.; Juliano, R.; Fisher, M. H.; Kang, H. M.; De Feyter, S.; Herdewijn, P. Delivery of antisense oligonucleotides using cholesterol-modified sense dendrimers and cationic lipids. *Bioconj. Chem.* **2005**, *16(4),* 827-836.

[15] Prasad, T. K.; Gopal, V.; Rao, N. M. Cationic lipids and cationic ligands induce DNA helix denaturation: detection of single stranded regions by KMnO4 probing. *FEBS Lett.* **2003**, *552(2-3),* 199-206.

[16] Prasad, T. K.; Gopal, V.; Rao, N. M. Structural changes in DNA mediated by cationic lipids alter in vitro transcriptional activity at low charge ratios. *Biochim. Biophys. Acta Gen. Sub.* **2003**, *1619(1),* 59-69.

[17] Lorenz, C.; Hadwiger, P.; John, M.; Vornlocher, H. P.; Unverzagt, C. Steroid and lipid conjugates of siRNAs to enhance cellular uptake and gene silencing in liver cells. *Bioorg. Med. Chem. Lett.* **2004**, *14(19),* 4975-4977.

[18] Soutschek, J.; Akinc, A.; Bramlage, B.; Charisse, K.; Constien, R.; Donoghue, M.; Elbashir, S.; Geick, A.; Hadwiger, P.; Harborth, J.; John, M.; Kesavan, V.; Lavine, G.; Pandey, R. K.; Racie, T.; Rajeev, K. G.; Rohl, I.; Toudjarska, I.; Wang, G.; Wuschko, S.; Bumcrot, D.; Koteliansky, V.; Limmer, S.; Manoharan, M.; Vornlocher, H. P. Therapeutic silencing of an endogenous gene by systemic administration of modified siRNAs. *Nature* **2004**, *432(7014),* 173-178.

[19] Lee, S. W.; Song, M. K.; Baek, K. H.; Park, Y. J.; Kim, J. K.; Lee, C. H.; Cheong, H. K.; Cheong, C.; Sung, Y. C. Effects of a hexameric deoxyribo-guanosine run conjugation into CpG oligodeoxynucleotides on their immunostimulatory potentials. *J. Immunol.* **2000**, *165(7),* 3631-3639.

[20] Dalpke, A. H.; Zimmermann, S.; Albrecht, I.; Heeg, K. Phosphodiester CpG oligonucleotides as adjuvants: polyguanosine runs enhance cellular uptake and improve immunostimulative activity of phosphodiester CpG oligonucleotides in vitro and *in vivo*. *Immunology* **2002**, *106(1),* 102-112.

[21] Zimmermann, S.; Heeg, K.; Dalpke, A. Immunostimulatory DNA as adjuvant: efficacy of phosphodiester CpG oligonucleotides is enhanced by 3 ' sequence modifications. *Vaccine* **2003**, *21(9-10),* 990-995.

[22] Bartz, H.; Mendoza, Y.; Gebker, M.; Fischborn, T.; Heeg, K.; Dalpke, A. Poly-guanosine strings improve cellular uptake and stimulatory activity of phosphodiester CpG oligonucleotides in human leukocytes. *Vaccine* **2004**, *23(2),* 148-155.

[23] Elbashir, S. M.; Harborth, J.; Lendeckel, W.; Yalcin, A.; Weber, K.; Tuschl, T. Duplexes of 21-nucleotide RNAs mediate RNA interference in cultured mammalian cells. *Nature* **2001**, *411(6836),* 494-498.

[24] Lingor, P.; Michel, U.; Scholl, U.; Bahr, M.; Kugler, S. Transfection of "naked" siRNA results in endosomal uptake and metabolic impairment in cultured neurons. *Biochem. Biophys. Res. Commun.* **2004**, *315(4),* 1126-1133.

[25] Overhoff, M.; Wunsche, W.; Sczakiel, G. Quantitative detection of siRNA and single-stranded oligonucleotides: relationship between uptake and biological activity of siRNA. *Nucleic Acids Res.* **2004**, *32(21),* e170.

[26] Lehmann, M. J.; Sczakiel, G. Spontaneous uptake of biologically active recombinant DNA by mammalian cells via a selected DNA segment. *Gene Ther.* **2005**, *12(5),* 446-451.

[27] Overhoff, M.; Sczakiel, G. Phosphorothioate-stimulated uptake of short interfering RNA by human cells. *EMBO Rep.* **2005**, *6(12),* 1176-1181.

[28] Janout, V.; Regen, S. L. A needle-and-thread approach to bilayer transport: Permeation of a molecular umbrella-oligonucleotide conjugate across a phospholipid membrane. *J. Am. Chem. Soc.* **2005**, *127(1),* 22-23.

[29] Janout, V.; Lanier, M.; Regen, S. L. Molecular umbrellas. *J. Am. Chem. Soc.* **1996**, *118(6),* 1573-1574.

[30] Shawaphun, S.; Janout, V.; Regen, S. L. Chemical evidence for transbilayer movement of molecular umbrellas. *J. Am. Chem. Soc.* **1999**, *121(25),* 5860-5864.

[31] Janout, V.; Di Giorgio, C.; Regen, S. L. Molecular umbrella-assisted transport of a hydrophilic peptide across a phospholipid membrane. *J. Am. Chem. Soc.* **2000**, *122(11),* 2671-2672.

[32] Janout, V.; Zhang, L. H.; Staina, I. V.; Di Giorgio, C.; Regen, S. L. Molecular umbrella-assisted transport of glutathione across a phospholipid membrane. *J. Am. Chem. Soc.* **2001**, *123(23),* 5401-5406.

[33] Janout, V.; Jing, B. W.; Regen, S. L. Molecular umbrella-assisted transport of thiolated AMP and ATP across phospholipid bilayers. *Bioconj. Chem.* **2002**, *13(2),* 351-356.

[34] Janout, V.; Jing, B. W.; Staina, I. V.; Regen, S. L. Selective transport of ATP across a phospholipid bilayer by a molecular umbrella. *J. Am. Chem. Soc.* **2003**, *125(15),* 4436-4437.

[35] Oishi, M.; Nagatsugi, F.; Sasaki, S.; Nagasaki, Y.; Kataoka, K. Smart polyion complex micelles for targeted intracellular delivery of PEGylated antisense oligonucleotides containing acid-labile linkages. *Chembiochem* **2005**, *6(4),* 718-725.

[36] Bijapur, J.; Keppler, M. D.; Bergqvist, S.; Brown, T.; Fox, K. R. 5-(1-propargylamino)-2'-deoxyuridine (UP): a novel thymidine analogue for generating DNA triplexes with increased stability. *Nucleic Acids Res.* **1999**, *27(8),* 1802-1809.

[37] Gowers, D. M.; Bijapur, J.; Brown, T.; Fox, K. R. DNA triple helix formation at target sites containing several pyrimidine interruptions: stabilization by protonated cytosine or 5-(1- propargylamino)dU. *Biochemistry* **1999**, *38(41),* 13747-13758.

[38] Cuenoud, B.; Casset, F.; Hüsken, D.; Natt, F.; Wolf, R. M.; Altmann, K.-H.; Martin, P.; Moser, H. E. Dual recognition of double-stranded DNA by 2'-aminoethoxy-modified oligonucleotides. *Angew. Chem. Int. Ed.* **1998**, *37(9),* 1288-1291.

[39] Dempcy, R. O.; Almarsson, O.; Bruice, T. C. Design and synthesis of deoxynucleic guanidine: a polycation analogue of DNA. *Proc. Natl. Acad. Sci. USA.* **1994**, *91(17),* 7864-7868.

[40] Toporowski, J. W.; Reddy, S. Y.; Bruice, T. C. Comparison of positively charged DNG with DNA duplexes: a computational approach. *Bioorg. Med. Chem.* **2005**, *13(11),* 3691-3698.

[41] Michel, T.; Debart, F.; Vasseur, J. J. Efficient guanidination of the phosphate linkage towards cationic phosphoramidate oligonucleotides. *Tetrahedron Lett.* **2003**, *44(35),* 6579-6582.

[42] Michel, T.; Debart, F.; Heitz, F.; Vasseur, J. J. Highly stable DNA triplexes formed with cationic phosphoramidate pyrimidine alpha-oligonucleotides. *Chembiochem* **2005**, *6(7),* 1254-1262.

[43] Linkletter, B. A.; Bruice, T. C. Solid-phase synthesis of positively charged deoxynucleic guanidine (DNG) modified oligonucleotides containing neutral urea linkages: effect of charge deletions on binding and fidelity. *Bioorg. Med. Chem.* **2000**, *8(8),* 1893-1901.

[44] Griffey, R. H.; Monia, B. P.; Cummins, L. L.; Freier, S. M.; Greig, M. J.; Guinosso, C. J.; Lesnik, E.; Manilili, S. M.; Mohan, V.; Owens, S.; Ross, B. R.; Sasmor, H.; Wancewicz, E.; Weiler, K.; Wheeler, P. D.; Cook, P. D. 2'-O-Aminopropyl ribonucleotides: a zwitterionic modification that enhances the exonuclease resistance and biological activity of antisense oligonucleotides. *J. Med. Chem.* **1996**, *39(26),* 5100-5109.

[45] Puri, N.; Majumdar, A.; Cuenoud, B.; Natt, F.; Martin, P.; Boyd, A.; Miller, P. S.; Seidman, M. M. Targeted gene knockout by 2'-O-aminoethyl modified triplex forming oligonucleotides. *J. Biol. Chem.* **2001**, *276(31),* 28991-28998.

[46] Stutz, A. M.; Hoeck, J.; Natt, F.; Cuenoud, B.; Woisetschlager, M. Inhibition of interleukin-4- and CD40-induced IgE germline gene promoter activity by 2'-aminoethoxy-modified triplex-forming oligonucleotides. *J. Biol. Chem.* **2001**, *276(15),* 11759-11765.

[47] Puri, N.; Majumdar, A.; Cuenoud, B.; Natt, F.; Martin, P.; Boyd, A.; Miller, P. S.; Seidman, M. M. Minimum number of 2'-O-(2-aminoethyl) residues required for gene knockout activity by triple helix forming oligonucleotides. *Biochemistry* **2002**, *41(24),* 7716-7724.

[48] Majumdar, A.; Puri, N.; Cuenoud, B.; Natt, F.; Martin, P.; Khorlin, A.; Dyatkina, N.; George, A. J.; Miller, P. S.; Seidman, M. M. Cell Cycle Modulation of Gene Targeting by a Triple Helix-forming Oligonucleotide. *J. Biol. Chem.* **2003**, *13(*11072-11077.

[49] Puri, N.; Majumdar, A.; Cuenoud, B.; Miller, P. S.; Seidman, M. M. Importance of clustered 2'-O-(2-aminoethyl) residues for the gene targeting activity of triple helix-forming oligonucleotides. *Biochemistry* **2004**, *43(5),* 1343-1351.

[50] Bailey, C. P.; Dagle, J. M.; Weeks, D. L. Cationic oligonucleotides can mediate specific inhibition of gene expression in Xenopus oocytes. *Nucleic Acids Res.* **1998**, *26(21),* 4860-4867.

[51] Dagle, J. M.; Littig, J. L.; Sutherland, L. B.; Weeks, D. L. Targeted elimination of zygotic messages in Xenopus laevis embryos by modified oligonucleotides possessing terminal cationic linkages. *Nucleic Acids Res.* **2000**, *28(10),* 2153-2157.

[52] Michel, T.; Martinand-Mari, C.; Debart, F.; Lebleu, B.; Robbins, I.; Vasseur, J. J. Cationic phosphoramidate alpha-oligonucleotides efficiently target single-stranded DNA and RNA and inhibit hepatitis C virus IRES-mediated translation. *Nucleic Acids Res.* **2003**, *31(18),* 5282-5290.

[53] Roig, V.; Asseline, U. Oligo-2 '-deoxyribonucleotides containing uracil modified at the 5-position with linkers ending with guanidinium groups. *J. Am. Chem. Soc.* **2003**, *125(15),* 4416-4417.

[54] Vives, E.; Brodin, P.; Lebleu, B. A truncated HIV-1 Tat protein basic domain rapidly translocates through the plasma membrane and accumulates in the cell nucleus. *J. Biol. Chem.* **1997**, *272(25),* 16010-16017.

[55] Derossi, D.; Calvet, S.; Trembleau, A.; Brunissen, A.; Chassaing, G.; Prochiantz, A. Cell internalization of the third helix of the antennapedia homeodomain is receptor-independent. *J. Biol. Chem.* **1996**, *271(30),* 18188-18193.

[56] Dragulescu-Andrasi, A.; Zhou, P.; He, G. F.; Ly, D. H. Cell-permeable GPNA with appropriate backbone stereochemistry and spacing binds sequence-specifically to RNA. *Chem. Commun.* **2005**, (*2),* 244-246.

[57] Zhou, P.; Wang, M. M.; Du, L.; Fisher, G. W.; Waggoner, A.; Ly, D. H. Novel binding and efficient cellular uptake of guanidine-based peptide nucleic acids (GPNA). *J. Am. Chem. Soc.* **2003**, *125(23),* 6878-6879.

[58] Sazani, P.; Kang, S. H.; Maier, M. A.; Wei, C.; Dillman, J.; Summerton, J.; Manoharan, M.; Kole, R. Nuclear antisense effects of neutral, anionic and cationic oligonucleotide analogs. *Nucleic Acids Res.* **2001**, *29(19),* 3965-3974.

[59] Richard, J. P.; Melikov, K.; Vives, E.; Ramos, C.; Verbeure, B.; Gait, M. J.; Chernomordik, L. V.; Lebleu, B. Cell-penetrating peptides. A reevaluation of the mechanism of cellular uptake. *J. Biol. Chem.* **2003**, *278(1),* 585-590.

[60] Ohmichi, T.; Kuwahara, M.; Sasaki, N.; Hasegawa, M.; Nishikata, T.; Sawai, H.; Sugimoto, N. Nucleic acid with guanidinium modification exhibits efficient cellular uptake. *Angew. Chem. Int. Edit.* **2005**, *44(41),* 6682-6685.

[61] Deglane, G.; Abes, S.; Michel, T.; Prevot, P.; Vives, E.; Debart, F.; Barvik, I.; Lebleu, B.; Vasseur, J. J. Impact of the guanidinium group on hybridization and cellular uptake of cationic oligonucleotides. *Chembiochem* **2006**, *7(4),* 684-692.

[62] Ryser, H. J.; Shen, W. C.; Merk, F.B. Membrane transport of macromolecules: new carrier functions of proteins and poly(amino acids). *Life Sci.* **1978**, *22(13-15),* 1253-1260.

[63] Lochmann, D.; Jauk, E.; Zimmer, A. Drug delivery of oligonucleotides by peptides. *Eur. J. Pharm. Biopharm.* **2004**, *58 (2)*, 237-51.

[64] Leonetti, J. P.; Degols, G.; Lebleu, B. Biological activity of oligonucleotide-poly(L-lysine) conjugates: mechanism of cell uptake. *Bioconjug. Chem.* **1990**, *1(2),* 149-153.

[65] Mahato, R. I.; Takemura, S.; Akamatsu, K.; Nishikawa, M.; Takakura, Y.; Hashida, M. Physicochemical and disposition characteristics of antisense oligonucleotides complexed with glycosylated poly(L-lysine). *Biochem. Pharmacol.* **1997**, *53(6),* 887-895.

[66] Derossi, D.; Joliot, A. H.; Chassaing, G.; Prochiantz, A. The third helix of the Antennapedia homeodomain translocates through biological membranes. *J. Biol. Chem.* **1994**, *269(14),* 10444-10450.

[67] Frankel, A. D.; Pabo, C. O. Cellular uptake of the tat protein from human immunodeficiency virus. *Cell* **1988**, *55(6),* 1189-1193.

[68] Green, M.; Loewenstein, P. M. Autonomous functional domains of chemically synthesized human immunodeficiency virus tat trans-activator protein. *Cell* **1988**, *55(6),* 1179-1188.

[69] Snyder, E. L.; Dowdy, S. F. Cell penetrating peptides in drug delivery. *Pharm. Res.* **2004**, *21(3),* 389-393.

[70] Dietz, G. P.; Bahr, M. Delivery of bioactive molecules into the cell: the Trojan horse approach. *Mol. Cell Neurosci.* **2004**, *27(2),* 85-131.

[71] Elliott, G.; O'Hare, P. Intercellular trafficking and protein delivery by a herpesvirus structural protein. *Cell* **1997**, *88(2),* 223-233.

[72] Sandgren, S.; Wittrup, A.; Cheng, F.; Jonsson, M.; Eklund, E.; Busch, S.; Belting, M. The human antimicrobial peptide LL-37 transfers extracellular DNA plasmid to the nuclear compartment of mammalian cells via lipid rafts and proteoglycan-dependent endocytosis. *J. Biol. Chem.* **2004**, *279(17),* 17951-17956.

[73] Lundberg, P.; Magzoub, M.; Lindberg, M.; Hallbrink, M.; Jarvet, J.; Eriksson, L. E.; Langel, U.; Graslund, A. Cell membrane translocation of the N-terminal (1-28) part of the prion protein. *Biochem. Biophys. Res. Commun.* **2002**, *299(1),* 85-90.

[74] Elmquist, A.; Lindgren, M.; Bartfai, T.; Langel, Ü. VE-cadherin-derived cellpenetrating peptide, pVEC, with carrier functions. *Exp. Cell Res.* **2001**, *269,* 237-244.

[75] Pooga, M.; Hallbrink, M.; Zorko, M.; Langel, U. Cell penetration by transportan. *FASEB J.* **1998**, *12(1),* 67-77.

[76] Soomets, U.; Lindgren, M.; Gallet, X.; Hallbrink, M.; Elmquist, A.; Balaspiri, L.; Zorko, M.; Pooga, M.; Brasseur, R.; Langel, U. Deletion analogues of transportan. *Biochim. Biophys. Acta* **2000**, *1467(1),* 165-176.

[77] Rothbard, J. B.; Garlington, S.; Lin, Q.; Kirschberg, T.; Kreider, E.; McGrane, P. L, Wender, P. A.; Khavari, P. A. Conjugation of arginine oligomers to cyclosporin A facilitates topical delivery and inhibition of inflammation. *Nat. Med.* **2000**, *6(11),* 1253-1257.

[78] Oehlke, J. S. A.; Wiesner, B.; Krause, E.; Beyermann, M.; Klauschenz, E.; Melzig, M.; Bienert, M. Cellular uptake of an alpha-helical amphipathic model peptide with the potential to deliver polar compounds into the cell interior non-endocytically. *Biochim. Biophys. Acta* **1998**, *1414(1-2),* 127-139.

[79] Morris, M. C.; Depollier, J.; Mery, J.; Heitz, F.; Divita, G. A peptide carrier for the delivery of biologically active proteins into mammalian cells. *Nat. Biotechnol.* **2001**, *19(12),* 1173-1176.

[80] Morris, M. C.; Chaloin, L.; Choob, M.; Archdeacon, J.; Heitz, F.; Divita, G. Combination of a new generation of PNAs with a peptide-based carrier enables efficient targeting of cell cycle progression. *Gene Ther.* **2004**, *11(9),* 757-764.

[81] Morris, M. C.; Vidal, P.; Chaloin, L.; Heitz, F.; Divita, G. A new peptide vector for efficient delivery of oligonucleotides into mammalian cells. *Nucleic Acids Res.* **1997**, *25(14),* 2730-2736.

[82] Wyman, T. B.; Nicol, F.; Zelphati, O.; Scaria, P. V.; Plank, C.; Szoka, F. C. Jr. Design, synthesis, and characterization of a cationic peptide that binds to nucleic acids and permeabilizes bilayers. *Biochemistry* **1997**, *36(10),* 3008-3017.

[83] Astriab-Fisher, A.; Sergueev, D.; Fisher, M.; Shaw, B. R.; Juliano, R. L. Conjugates of antisense oligonucleotides with the Tat and antennapedia cell-penetrating peptides: effects on cellular uptake, binding to target sequences, and biologic actions. *Pharm. Res.* **2002**, *19(6),* 744-754.

[84] Kang, S. H.; Cho, M. J.; and Kole, R. Up-regulation of luciferase gene expression with antisense oligonucleotides: implications and applications in functional assay development. *Biochemistry* **1998**, *37(18),* 6235-6239.

[85] Hudziak, R. M.; Summerton, J.; Weller, D. D.; Iversen, P. L. Antiproliferative effects of steric blocking phosphorodiamidate morpholino antisense agents directed against c-myc. *Antisense Nucleic Acid Drug Dev.* **2000**, *10(3),* 163-176.

[86] Moulton, H. M.; Hase, M. C.; Smith, K.M.; Iversen, P. L. HIV Tat peptide enhances cellular delivery of antisense morpholino oligomers. *Antisense Nucleic Acid Drug Dev.* **2003**, *13(1),* 31-43.

[87] Arzumanov, A.; Walsh, A. P.; Rajwanshi, V. K.; Kumar, R.; Wengel, J.; Gait, M. J. Inhibition of HIV-1 Tat-dependent trans activation by steric block chimeric 2'-O-methyl/LNA oligoribonucleotides. *Biochemistry* **2001**, *40(48),* 14645-14654.

[88] Turner, J. J.; Arzumanov, A. A.; Gait, M. J. Synthesis, cellular uptake and HIV-1 Tat-dependent trans-activation inhibition activity of oligonucleotide analogues disulphide-conjugated to cell-penetrating peptides. *Nucleic Acids Res.* **2005**, *33(1),* 27-42.

[89] Gros, E.; Deshayes, S.; Morris, M. C.; Aldrian-Herrada, G.; Depollier, J.; Heitz, F.; Divita, G. A non-covalent peptide-based strategy for protein and peptide nucleic acid transduction. *Biochim. Biophys. Acta* **2006**, *1758(3),* 384-393.

[90] Weller, K.; Lauber, S.; Lerch, M.; Renaud, A.; Merkle, H. P.; Zerbe, O. Biophysical and biological studies of end-group-modified derivatives of Pep-1. *Biochemistry* **2005**, *44(48),* 15799-15811.

[91] Simeoni, F.; Morris, M. C.; Heitz, F.; Divita, G. Insight into the mechanism of the peptide-based gene delivery system MPG: implications for delivery of siRNA into mammalian cells. *Nucleic Acids Res.* **2003**, *31(11),* 2717-2724.

[92] Kole R, V. M.; Williams T. Modification of alternative splicing by antisense therapeutics. *Oligonucleotides* **2004**, *14(1),* 65-74.

[93] Lacerra, G.; Sierakowska, H.; Carestia, C.; Fucharoen, S.; Summerton, J.; Weller, D.; Kole, R. Restoration of hemoglobin A synthesis in erythroid cells from peripheral blood of thalassemic patients. *Proc. Natl. Acad. Sci. USA* **2000**, *97(17),* 9591-9596.

[94] Garcia-Blanco, M. A.; Baraniak, A. P.; Lasda, E. L. Alternative splicing in disease and therapy. *Nat. Biotechnol.* **2004**, *22(5),* 535-546.

[95] Venables, J. P. Unbalanced alternative splicing and its significance in cancer. *Bioessays* **2006**, *28(4),* 378-386.

[96] Mercatante DR, S. P.; Kole R. Modification of alternative splicing by antisense oligonucleotides as a potential chemotherapy for cancer and other diseases. *Curr. Cancer Drug Targets* **2001**, *1(3),* 211-230.

[97] Mercatante, D. R.; Mohler, J. L.; Kole, R. Cellular response to an antisense-mediated shift of Bcl-x pre-mRNA splicing and antineoplastic agents. *J. Biol. Chem.* **2002**, *277(51),* 49374-49382.

[98] McClorey, G.; Moulton, H. M.; Iversen, P. L.; Fletcher, S.; Wilton, S. D. Antisense oligonucleotide-induced exon skipping restores dystrophin expression in vitro in a canine model of DMD. *Gene Ther.* **2006**, *13*(19), 1373-81.

[99] Alter, J.; Lou, F.; Rabinowitz, A.; Yin, H.; Rosenfeld, J.; Wilton, S.D.; Partridge, T.A.; Lu, Q. Systemic delivery of morpholino oligonucleotide restores dystrophin expression bodywide and improves dystrophic pathology. *Nat. Med.* **2006**, *12(2),* 175-177.

[100] Belting, M.; Sandgren, S.; Wittrup, A. Nuclear delivery of macromolecules: barriers and carriers. *Adv. Drug Deliv. Rev.* **2005**, *57(4),* 505-527.

[101] Thierry, A. R.; Abes, S.; Resina, S.; Travo, A.; Richard, J. P.; Prevot, P.; Lebleu, B. Comparison of basic peptides- and lipid-based strategies for the delivery of splice correcting oligonucleotides. *Biochim. Biophys. Acta* **2006**, *1758(3),* 364-374.

[102] Turner, J. J.; Ivanova, G. D, Verbeure, B.; Williams, D.; Arzumanov, A. A.; Abes, S.; Lebleu, B.; Gait, M. J. Cell-penetrating peptide conjugates of peptide nucleic acids (PNA) as inhibitors of HIV-1 Tat-dependent trans-activation in cells. *Nucleic Acids Res.* **2005**, *33(21),* 6837-6849.

[103] Abes, S.; Williams, D.; Prevot, P.; Thierry, A.; Gait, M.J.; Lebleu, B. Endosome trapping limits the efficiency of splicing correction by PNA-oligolysine conjugates. *J. Control Rel.* **2006**, *110(3),* 595-604.

[104] Abes, S.; Moulton, H. M.; Clair, P.; Prevot, P.; Youngblood, D. S.; Wu, R. P.; Iversen, P. L.; Lebleu, B. Vectorization of morpholino oligomers by the (R-Ahx-R)4 peptide allows efficient splicing correction in the absence of endosomolytic agents. *J. Control Rel. submitted.*

[105] Sazani, P.; Gemignani, F.; Kang, S. H.; Maier, M. A.; Manoharan, M.; Persmark, M.; Bortner, D.; Kole, R. Systemically delivered antisense oligomers upregulate gene expression in mouse tissues. *Nat. Biotechnol.* **2002**, *20(12),* 1228-1233.

[106] Siwkowski, A. M.; Malik, L.; Esau, C. C.; Maier, M. A.; Wancewicz, E. V.; Albertshofer, K.; Monia, B. P.; Bennett, C. F.; Eldrup, A. B. Identification and functional validation of PNAs that inhibit murine CD40 expression by redirection of splicing. *Nucleic Acids Res.* **2004**, *32(9),* 2695-2706.

[107] Pujals, S.; Fernandez-Carneado, J.; Lopez-Iglesias, C.; Kogan, M. J.; Giralt, E. Mechanistic aspects of CPP-mediated intracellular drug delivery: Relevance of CPP self-assembly. *Biochim. Biophys. Acta* **2006**, *in press*

[108] Shiraishi, T.; Nielsen, P. E. Photochemically enhanced cellular delivery of cell penetrating peptide-PNA conjugates. *FEBS Lett.* **2006**, *580(5),* 1451-1456.

[109] Shiraishi, T.; Pankratova, S.; Nielsen P. E. Calcium ions effectively enhance the effect of antisense peptide nucleic acids conjugated to cationic tat and oligoarginine peptides. *Chem. Biol.* **2005**, *12(8),* 923-929.

[110] Wolf, Y.; Pritz, S.; Abes, S.; Bienert, M.; Lebleu, B.; Oehlke, J. Structural requirements for cellular uptake and antisense activity of PNAs conjugated with various peptides. *Biochemistry. submitted*

[111] Takeuchi, T.; Kosuge, M.; Tadokoro, A.; Sugiura, Y.; Nishi, M.; Kawata, M.; Sakai, N.; Matile, S.; Futaki, S. Direct and Rapid Cytosolic Delivery Using Cell-Penetrating Peptides Mediated by Pyrenebutyrate. *ACS Chem. Biol.* **2006**, *1(5),* 299-303.

[112] Wadia, J. S.; Stan, R. V.; Dowdy, S. F. Transducible TAT-HA fusogenic peptide enhances escape of TAT-fusion proteins after lipid raft macropino-cytosis. *Nat. Med.* **2004**, *10(3),* 310-315.

[113] Bendifallah, N.; Rasmussen, F. W.; Zachar, V.; Ebbesen, P.; Nielsen, P. E.; Koppelhus, U. Evaluation of cell-penetrating peptides (CPPs) as vehicles for intracellular delivery of antisense peptide nucleic acid (PNA). *Bioconjug. Chem.* **2006**, *17(3),* 750-758.

[114] Rothbard, J. B.; Kreider, E.; VanDeusen, C. L.; Wright, L.; Wylie, B. L.; Wender, P. A. Arginine-rich molecular transporters for drug delivery: role of backbone spacing in cellular uptake. *J. Med. Chem.* **2002**, *45(17),* 3612-3618.

Received: November 16, 2006 Accepted: November 28, 2006

CHEMBIOCHEM

DOI: 10.1002/cbic.200500433

Impact of the Guanidinium Group on Hybridization and Cellular Uptake of Cationic Oligonucleotides

Gaëlle Deglane,[a] Saïd Abes,[b] Thibaut Michel,[a] Paul Prévot,[b] Eric Vives,[b, c] Françoise Debart,*[a] Ivan Barvik,[d] Bernard Lebleu,[b] and Jean-Jacques Vasseur[a]

The grafting of cationic groups to synthetic oligonucleotides (ONs) in order to reduce the charge repulsion between the negatively charged strands of a duplex or triplex, and consequently to increase a complex's stability, has been extensively studied. Guanidinium groups, which are highly basic and positively charged over a wide pH range, could be an efficient ON modification to enhance their affinity for nucleic acid targets and to improve cellular uptake. A straightforward post-synthesis method to convert amino functions attached to ONs (on sugar, nucleobase or backbone) into guanidinium tethers has been perfected. In comparison to amino groups, such cationic groups anchored to α-oligonucleotide phosphoramidate backbones play important roles in duplex stability, particularly with RNA targets. This high affinity could be explained by dual recognition resulting from Watson–Crick or Hoogsteen base pairing combined with cationic/anionic backbone recognition between strands involving H-bond formation and salt bridging. Molecular-dynamics simulations corroborate interactions between the cationic backbones of the α-ONs and the anionic backbones of the nucleic acid targets. Moreover, ONs with guanidinium modification increased cellular uptake relative to negatively charged ONs. The cellular localization of these new cationic phosphoramidate ONs is mainly cytoplasmic. The uptake of these ON analogues might occur through endocytosis.

Introduction

A large number of oligonucleotide (ON) analogues have been synthesized and studied in the contexts of diagnostic or therapeutic applications.[1–3] Important goals in designing efficient antisense compounds or more recently siRNA[4,5] include high hybridization affinity while maintaining specificity of recognition, resistance to enzymatic degradation and ability to penetrate into cells. Many chemical modifications satisfactorily increase nuclease stability of the ONs and their affinity toward complementary nucleic acid sequences, but little has been achieved regarding efficient cellular uptake.[3]

Charge repulsion disfavours the hybridization of negatively charged ONs to RNA or DNA targets. Accordingly, ON analogues containing neutral backbones, such as morpholino derivatives[6] or peptide nucleic acids (PNAs),[7] hybridize with a higher affinity than their negatively counterparts without loss of specificity. Along the same lines, it was anticipated that ON analogues carrying a net positive charge should even be more beneficial in terms of binding efficiency and should also give hybridization with increased association rates. A few examples of cationic ONs (with positively charged backbones)[8–12] or zwitterionic ONs (with positively charged tethers attached to the nucleobases or to the 2′-position of the sugars)[13–22] have been described. Strategies have included the incorporation of amino groups prone to protonation under physiological conditions or of the guanidinium group (pK_a 12.5), which is highly basic and positively charged over a wide pH range.[17,22–24] In particular, deoxynucleic guanidine (DNG) oligomers in which the internucleoside phosphate linkages have been replaced by cationic guanidinium groups have been extensively studied.[10,25] These DNG analogues are resistant to nucleases and bind to complementary DNA sequences with high affinity without compromising the specificity of binding. The guanidinium group from the arginine side chain has also been introduced into a PNA backbone as a replacement for glycine.[26] These PNA analogues, known as guanidine-based peptide nucleic acids (GPNAs), are much more highly soluble in water than unmodified PNAs, which have a strong tendency to aggregate in

[a] *G. Deglane,[+] Dr. T. Michel, Dr. F. Debart, Dr. J.-J. Vasseur*
LCOBS, UMR 5625 CNRS-UMII, CC 008, Université Montpellier II
Place Eugène Bataillon, 34095 Montpellier Cedex 05 (France)
Fax: (+33) 4-6704-2029
E-mail: debart@univ-montp2.fr

[b] *S. Abes,[+] P. Prévot, Dr. E. Vives, Prof. B. Lebleu*
UMR 5124 CNRS-UMII, CC 086, Université Montpellier II
Place Eugène Bataillon, 34095 Montpellier Cedex 05 (France)

[c] *Dr. E. Vives*
Present address : INSERM EMI0227
CRLC Val d'Aurelle-Paul Lamarque
34298 Montpellier Cedex 05 (France)

[d] *Dr. I. Barvik*
Charles University, Faculty of Mathematics and Physics, Institute of Physics
Ke Karlovu 5, 12116 Prague 2 (Czech Republic)

[+] *These authors contributed equally to this work*

aqueous solution. Furthermore, these GPNA analogues have been claimed to exhibit remarkable cellular uptake properties while maintaining sequence-specific recognition of a single-stranded DNA target. This strategy was clearly inspired by recent studies on cell-penetrating peptides (CPPs) such as the human HIV-1 Tat[27] and the *Drosophila* Antennapedia (Ant)[28] transduction domains, which have been extensively exploited for their ability to transport conjugated biomolecules across cell membranes.[29] A common feature of these CPPs is their high positively charged amino acid content, and particularly the key role of arginines. Several natural or synthetic arginine-rich peptides are able to transport chemically conjugated biomolecules into cells,[30–33] while several nonpeptidic compounds bearing guanidinium groups—including guanidinoglycosides,[34] a cationic methacrylate polymer,[35] or polyguanidine peptoid derivatives[36]—have also been reported to enhance the cellular uptake of conjugated biomolecules. Very recently, ONs with guanidinium modification attached to the nucleobases exhibited efficient cellular uptake.[37] Collectively, these studies suggest that the guanidinium groups are critical for transport through biological barriers. Although the mechanism responsible for transport mediated by guanidine-rich molecules is still controversial, the design of new ON analogues bearing guanidinium groups could be of interest.

Some years ago, we applied an efficient method for the post-synthesis conversion of primary amino functions into guanidinium groups to the assembly of ONs with β- or α-anomeric configurations,[24] successfully synthesizing several β- or α-anomeric ON analogues with phosphoramidate internucleotide linkages ending in guanidinium tethers. In this report, we establish their ability to form duplexes and triplexes with complementary RNA or DNA targets, and to penetrate into live cells more efficiently than the corresponding negatively charged ONs. Molecular dynamics simulations were performed to tentatively explain the hybridization efficiency of guanidino ONs. Moreover, this convenient method of guanidination allows conversion of amino groups either at the 2′-position of nucleotides or on the nucleobase within an oligonucleotide.

Results and Discussion

Post-synthesis guanidination of oligonucleotides

Several modified ONs bearing guanidinium tethers have recently been obtained through different methods. In particular, 2′-*O*-guanidinium ethyl modified ONs were synthesized by using a phosphoramidite synthon of 5-methyluridine bearing a protected guanidinium group in the 2′-position.[23] In this case, a novel guanidinating reagent was used to convert the amino groups and the *N*-(2-cyanoethoxycarbonyl) group[38] to protect the guanidinium groups for ON synthesis on solid support. Unfortunately, this method is time-consuming and requires tedious multistep preparation of each phosphoramidite synthon, since these are not commercially available.

In contrast, the approach described in our initial work[24] allows the post-synthesis guanidination of amino groups linked to the 2′-position in nucleotides, to the 5-position of uracil or to the phosphoramidate backbone within an ON. In this paper, the guanidination procedure has been improved as follows.

Aminobutylphosphoramidate ($PNHBuNH_2$) ONs **4**–**6** (Table 1) were treated with freshly prepared solution of *O*-methylisourea

Table 1. Oligonucleotides synthesized and targets used in melting and cellular uptake experiments

ON	Anomeric configure	Sequence 5′→3′[a]	Internucleotide linkages[b]
1	β	TTTCTTCCTCTT	PO
2	α	T·T·C·T·C·C·T·T·C·T·T·T	(·) PNHDMAP
3	α	T·C·T·T·A·A·C·C·C·A·C·A	(·) PNHDMAP
4	α	T+T+C+T+C+C+T+T+C+T+T+T	(+) $PNHBuNH_2$
5	α	T+C+T+T+A+A+C+C+C+A+C+A	(+) $PNHBuNH_2$
6	α	Fluo-T+T+T+T+T+T+T+T+T+T+T+T	(+) $PNHBuNH_2$
7	α	T*T*C*T*C*C*T*T*C*T*T*T	(*) PNHBuGua
8	α	T*C*T*T*A*A*C*C*C*A*C*A	(*) PNHBuGua
9	α	Fluo-T*T*T*T*T*T*T*T*T*T*T*T	(*) PNHBuGua
10	β	Fluo-TTTTTTTTTTTT	PS
11	β	TU_{AP}TCTU_{AP}CCU_{AP}CU_{AP}T	PO
12	β	TU_{GP}TCTU_{GP}CCU_{GP}CU_{GP}T	PO
13	β	TX^{NH_2}TCTX^{NH_2}CCX^{NH_2}CX^{NH_2}T	PO
14	β	TX^{Gua}TCTX^{Gua}CCX^{Gua}CX^{Gua}T	PO
I	β	AAAGAAGGAGAA TTTCTTCCTCTT	PO
II	β	GC**AAAGAAGGAGAA**C-T_4- G**TTCTCCTTCTTT**GC	PO
III	β	AGAATTGGGTGT	PO
IIIa		AGAA<u>A</u>TGGGTGT	PO
IIIb		AGAA<u>G</u>TGGGTGT	
IV	β	agaauugggugu	PO
IVa		agaa<u>c</u>ugggugu	

[a] Fluo = fluorescein; uppercase = DNA; lowercase = RNA; underlined = mismatch position; U_{AP} = 2′-*O*-(3-aminopropyl)uridine; U_{GP} = 2′-O-[3-(guanidinium)propyl]uridine; X^{NH_2} = 5-[*N*-(6-aminohexyl)-3-acrylimido]-2′-deoxyuridine; X^{Gua} = 5-[*N*-(6-guanidinium hexyl)-3-acrylimido]-2′-deoxyuridine. [b] (·) PNHDMAP = dimethylaminopropylphosphoramidate; (+) $PNHBuNH_2$ = aminobutylphosphoramidate; (*) PNHBuGua = guanidinobutylphosphoramidate; PO = phosphodiester; PS = phosphorothioate.

chloride in aqueous ammonia for 45 min at 65 °C (Scheme 1). The previously used hemisulfate salt was replaced by the chloride salt to enhance the solubility of the resulting guanidinobutylphosphoramidate (PNHBuGua) ONs **7**–**9** in water. Moreover, side products corresponding to the incomplete guanidination of some internucleotide linkages were minimized with this reagent.

To extend this method, we applied the guanidination procedure to the conversion of amino groups linked to 2′-position in nucleotides or to the 5-position of uracil components within ONs. Some years ago, ONs containing 2′-*O*-aminopropyl modifications were extensively studied[39] since these modifications enhance the exonuclease resistance and accordingly increase the biological activity of these antisense ON analogues. These results prompted us to replace the primary amino group by the more basic guanidinium group, as already done with 2′-*O*-aminohexyl ONs[22] or with 2′-*O*-aminoethyl ONs.[23] In brief, we synthesized the phosphodiester dodecamer **11**, containing

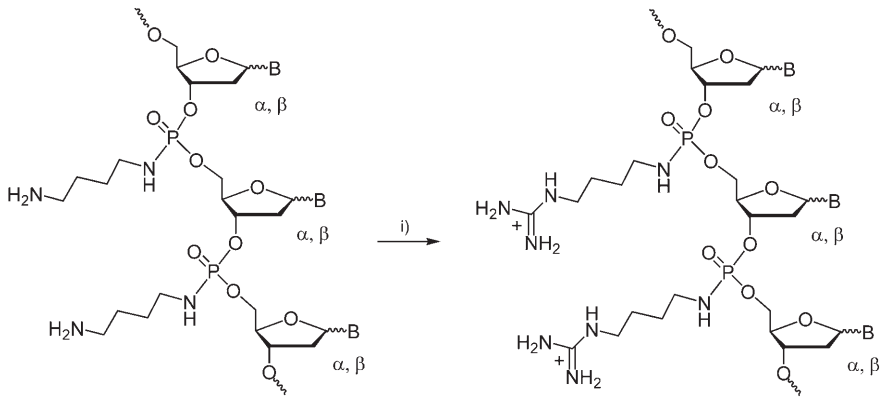

Scheme 1. Application of the guanidination reaction to the conversion of aminobutylphosphoramidate ($PNHBuNH_2$) ONs into guanidinobutylphosphoramidate (PNHBuGua) ONs. i) *O*-Methylisourea chloride, NH_4OH, 65 °C, 45 min.

four 2′-*O*-(aminoethyl)-uridine units (U_{AP}; Scheme 2), by phosphoramidite chemistry. After deprotection under standard conditions, the suitably pure ON **11** was directly guanidylated by

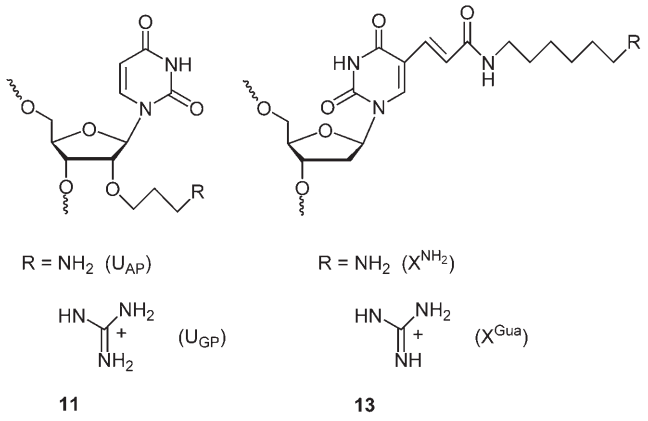

Scheme 2. Structures of 2′-*O*- and base-modified oligonucleotides bearing guanidinium groups.

our convenient method to afford ON **12** in quantitative yield. This guanidination reaction was also effectively performed on ON **13**, containing four 2′-deoxyuridine moieties modified at their 5-position with a linker ending in an amino group (X^{NH_2}; Scheme 2). Other modified ONs containing guanidinium derivatives linked to the nucleobases had previously been synthesized by treatment with 1*H*-pyrazole-1-carboxamidine, which was able to convert an amino group within an ON into a guanidinium group in 90% yield.[17] In our case, ON **14** containing four guanidinium residues (X^{gua}) was obtained in quantitative yield. The conversion of amino groups linked to the nucleobase, the 2′-position of the sugar or the backbone by this post-synthesis guanidination is not only complete, but also more straightforward and convenient to achieve than those previously described.

Duplex formation with DNA and RNA targets

To determine the impact of the guanidinium groups on the hybridization properties of these cationic analogues, the pairing of $PNHBuNH_2$ α-ON **5** and PNHBuGua α-ON **8** with their complementary DNA (**III**) and RNA (**IV**) targets (Table 1) was investigated by UV melting experiments. The thermal stabilities of these duplexes were compared to those of the natural PO β-ON or of another previously studied cationic PNHDMAP α-ON **3** (Figure 1).[12] All tested cationic α-ONs, whatever the phosphoramidate backbone modification, formed much more stable duplexes than those formed with the natural PO β-ON with DNA **III** or RNA **IV**. The introduction of $PNHBuNH_2$ or PNHBuGua linkages into α-ONs **5** or **8** greatly increased the thermal stabilities of the DNA duplexes ($\Delta T_m = +29\,^{\circ}C$). The average stabilization (ΔT_m per mod) was 2.6 °C per modification. These T_m values were slightly higher than those obtained with PNHDMAP α-ON **3**. Remarkably, the PNHDMAP modification increased the stability of the duplex with RNA target **IV** by only 10.5 °C (ΔT_m per mod. $= +0.95\,^{\circ}C$) whereas $PNHBuNH_2$ α-ON **5** showed a substantial enhancement of duplex stability ($\Delta T_m = +20.5\,^{\circ}C$). The increase in T_m (+24.5 °C) was even greater when PNHBuGua α-ON **8** was hybridized to RNA **IV**. The average stabilization of 2.2 °C per PNHBuGua modification, was the highest among all the phosphoramidate modifications tested on α-ONs.[12,40] Thus, with RNA targets, the duplex stability was significantly affected by the type of phosphoramidate linkages (neutral PNHME[40] or cationic PNHDMAP,[12] $PNHBuNH_2$, PNHBuGua). Both the pendant tether (methoxyethyl, dimethylammonium, ammonium or guanidinium) connected to the phosphoramidate function through an alkyl chain and the length of the

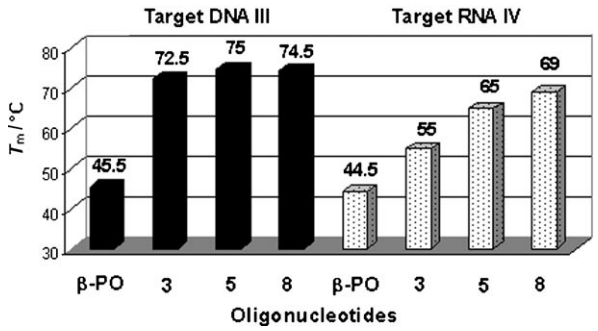

Figure 1. Thermal stabilities of fully cationic phosphoramidate (PNHDMAP, $PNHBuNH_2$, PNHBuGua) α-ONs with DNA target **III** or RNA target **IV** in comparison with phosphodiester (PO) β-ON. Experiments were carried out at 3 μM concentration for each strand in sodium cacodylate (10 mM)/NaCl (100 mM)/pH 7.

alkyl chain (C3 or C4) seem to play important roles in the stabilization of duplexes with RNA. Cationic PNHBuGua α-ON exhibits the highest affinity for RNA targets among all the backbone-modified α-ONs studied. In contrast, with DNA targets, the various cationic groups have the same effect on hybrid stability. Differences between the hybridization stability of the duplex cationic α-ON/DNA-target or cationic α-ON/RNA-target could tentatively be explained by molecular modeling (see Molecular Modeling section).

Determination of the thermodynamic parameters from the melting curves, to evaluate the impact of the guanidinium groups on the hybridization, was not possible because the upper absorbance baselines of the melting curves were not well defined, due to high transition relative to the high stability of the complexes (T_m duplex around 70 °C).

If the electrostatic interaction between PNHBuGua α-ON and anionic DNA or RNA target in a duplex is significant, the binding could become nonspecific and independent of Watson–Crick base-pairing recognition. To study the sequence specificity of the binding, α-ON **8** was allowed to form duplexes with DNA **IIIa** and **IIIb** or with RNA **IVa**. Introduction of one A:A or G:A mismatch in the DNA duplex or one C:A mismatch in the RNA duplex did not prevent the duplex formation but did destabilize the structures. It is noteworthy that the duplex transitions were shifted to lower temperatures and were very broad, so accurate determination of the respective T_m values was consequently difficult. These broad transitions indicate a loss of cooperativity and probably result from a decrease in specificity due to ionic interactions competing with base-pairing recognition.

Triplex formation in the pyrimidine motif

The effect of the guanidinium groups on the thermal stability of the triplex formed between PNHBuGua α-ON **7** and double-stranded DNA **I** (Table 1) in comparison to the triplex formed with another cationic PNHDMAP α-ON **2** and PNHBuNH$_2$ α-ON **4** was also investigated. Furthermore the stability of the 2′-*O*-guanidinopropyl-modified β-ON **12** hybridized to DNA target **II** was studied. For cationic phosphoramidate α-ONs **4** and **7**, and the previously studied PNHDMAP α-ON **2**,[41] we observed strong enhancement of triplex stability in relation to the triplex formed with PO β-ON **1** (Figure 2). An increase in T_m of about 39 °C, corresponding to 3.5 °C per modification, was observed for all the cationic α-ONs (**2**, **4** and **7**). Triplex stability was not affected by the nature of the cationic pendent group (dimethylaminopropyl, aminobutyl or guanidinobutyl) anchored to the phosphoramidate function; guanidinium groups do not stabilize triplexes more efficiently than amino groups. Similar data were obtained when the guanidinium group was joined to the 2′-position through a propyl chain in β-ON **12** containing four modified nucleotides dispersed in the ON chain. A similar increase in triplex stability (ΔT_m +9 °C and ΔT_m per mod. 2.3 °C) was obtained with 2′-*O*-aminopropyl-modified ON **11** and 2′-*O*-guanidino-modified ON **12**. These results are in agreement with those obtained by Asseline et al.,[17] who described ONs containing uracil modified at the 5-position with linkers ending in guanidinium groups. In this case, triplex stability was not improved when amino groups were replaced by guanidinium groups.

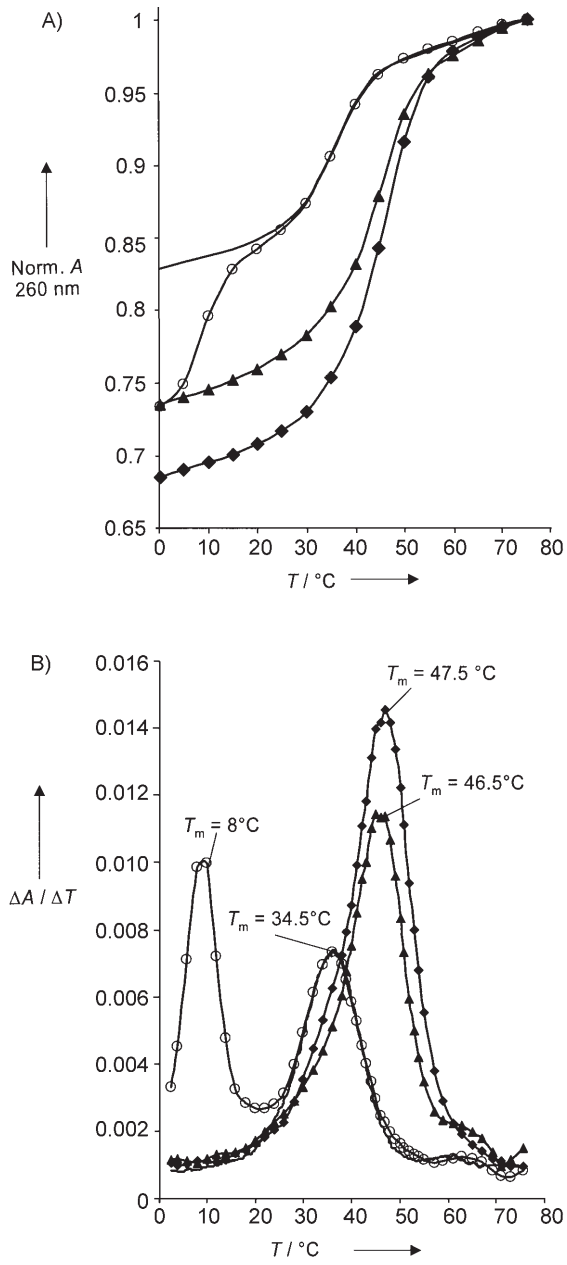

Figure 2. A) UV melting curves (260 nm) and B) first derivative plots of duplex **I** (plain line) and of the complexes formed with target **I** and β-TFO **1** (○), α-TFO **4** (◆) or α-TFO **8** (▲). ONs and targets were used at final concentrations of 3 μM in sodium cacodylate (10 mM)/NaCl (100 mM)/pH 7. Curves were normalized at the absorbance of **1**.

Molecular modeling

Molecular dynamics simulations of fully solvated ONs revealed that both types of tethers (either amino- or guanidiniumalkyl chains) are indeed able to bridge the minor grooves of dA·dT and dA·rU duplexes (as well as the minor–major groove in the case of the triplex structure). Cationic tethers interact efficient-

ly with phosphate groups (position *i*+12+3) in the complementary DNA or RNA strands. Direct hydrogen bonds between positively charged heads of linkers and negatively charged oxygen atoms in phosphate groups were established within the MD runs (Figures 3 and 4).

Stabilizing interactions, quantified by use of the THY/URA:N2–O1P:ADE interatomic distance distributions produced in 5 ns MD runs, showed remarkable differences, however (Figure 5). Firstly, the narrower minor groove in dA_{12}·dT_{12} duplexes results in a more pronounced distribution at its maximum in the vicinity of ~3 Å distance. This indicated direct hydrogen bonding between the N2 imino group and the O1P phosphate group atom for both tethers. Furthermore, several local distribution maxima should be noted in the case of the guanidinium tether, corresponding either to stabilizing hydrogen bonds produced by N3 or N4 amino groups (~4–5 Å) or less common binding toward *i*+12+2 phosphate groups (~8 Å).

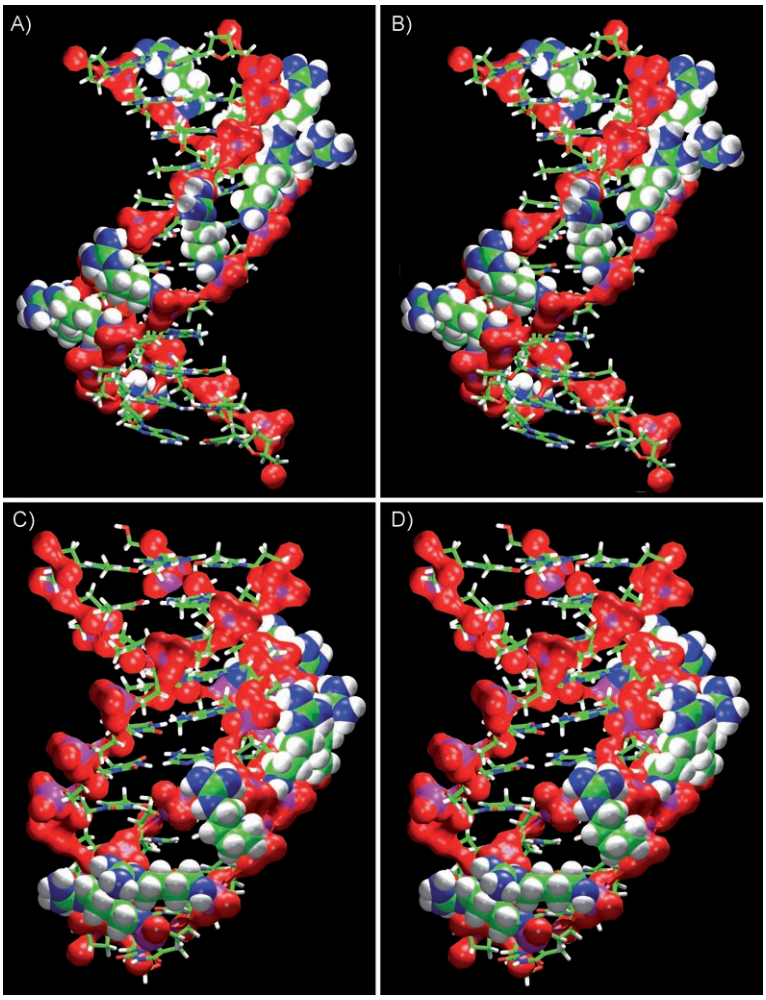

Figure 3. Stereo figures of the α-guanidinium-dA_{12}·β-dT_{12} duplex (top) and α-guanidinium-dT_{10}* β-dA_{10}·β-dT_{10} triplex (bottom) structures at the end of MD simulations. Bases and ribose moieties are depicted as sticks. The phosphate groups are shown as their solvent-accessible surfaces. The guanidinium phosphoramidate substitutions are highlighted with space-filling spheres. Color coding of sticks, spheres and solvent-accessible surfaces is given by their underlying atom type: N = blue, O = red, P = purple, C = green, H = white.

Overall, these results are consistent with the specific effects displayed by the phosphoramidate modified oligonucleotides for DNA/RNA binding, and corroborate the existence of interstrand contact between the protonated side chains and one phosphodiester oxygen atom of the DNA or RNA backbone.

Furthermore, molecular modeling could also be useful to explain differences between the hybridization of cationic α-ONs with DNA or RNA targets.

Indeed, a DNA/DNA duplex has a relatively narrow minor groove, so all tethers are able to bridge it effectively. In contrast, a DNA/RNA hybrid has a minor groove a little bit wider, so longer tethers are more advantageous. T_m values and lengths of the tethers correlate: the longer the tethers, the higher the T_m. PNHDMAP α-ON forms a less stable duplex than $PNHBuNH_2$ α-ON, which forms a less stable duplex than PNHBuGua α-ON. Poorer contacts between cationic heads of tethers and phosphate groups in the case of RNA counterparts are quantified in Figure 5.

Guanidinium groups are able to exploit their extension for more efficient and versatile binding.

Cellular uptake of cationic ON analogues

The time courses of cellular uptake for cationic ON **9** and for a negatively charged phosphorothioate ON analogue of identical sequence (ON **10**) were monitored in cultured HeLa cells by fluorescence-activated cell sorting (FACS). On a molar basis, the cationic ON **9** was taken up about six times more efficiently than its anionic counterpart **10** (Figure 6, left panel). No significant toxicity was observed since the size distribution of HeLa cells remained essentially unchanged in relation to untreated cells (data not shown). Similarly no significant uptake of propidium iodide was observed upon FACS analysis (data not shown).

To characterize the uptake mechanism further, the kinetics of cellular internalization of ONs **9** and **10** were also monitored at 4 °C, a temperature at which energy-dependent processes such as endocytosis are severely impaired. Cellular uptake at low temperature was negligible and did not increase with incubation time, in keeping with an energy-dependent mechanism of internalization (Figure 6, right panel). Similar data were obtained in HepG2 hepatoma cells (data not shown).

Cellular internalization can also be monitored by fluorescence microscopy, which gives an estimation of intracellular compartmentalization. These experiments were first performed in live cells (that is, in the absence of any chemical fixation). It should be borne in mind here that artefacts of redistribution have been encountered when dealing with cationic biomolecules as cell penetrating peptides.[42] Figure 7, panel A indicates that ON **9** does not accumulate in the nuclei but remains mainly cytoplasmic with a nonhomogeneous distribution. This is characteristic of material taken up by endocytosis and retained, at

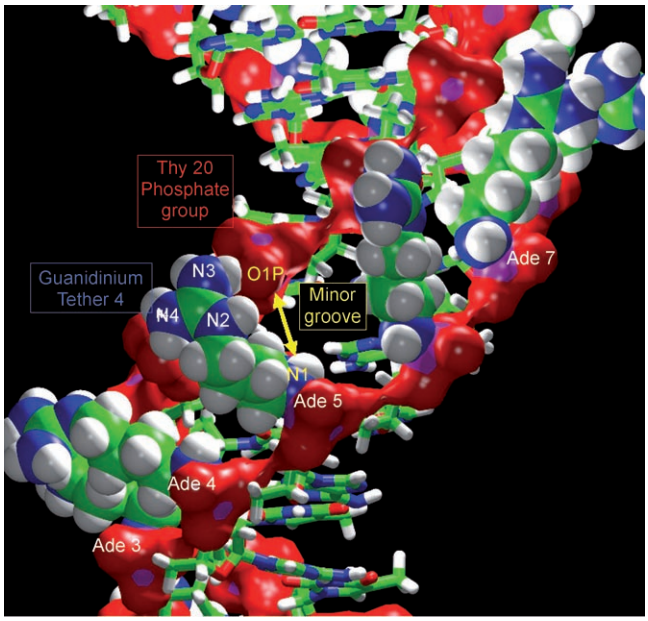

Figure 4. Molecular model showing interactions between the guanidinium phosphoramidate tethers (highlighted with space-filling spheres) and the O1P nonbridging phosphate oxygen atoms in the complementary natural strand.

least in part, in endocytic vesicles. Although not surprising, the distribution of guanidylated ON analogue **9** is rather different from the data reported for GPNAs, which were essentially found in nuclei.[26] These differences in intracellular distribution could be due to differences in the backbone (sugar-phosphate versus pseudopeptide) on which the guanidinium groups have been grafted. Another possibility could be that the formaldehyde fixation procedure used by Zhou et al.[26] results in an artefactual redistribution of cell-associated material, as seen for cationic CPPs. In keeping with this possibility, cells in which ON **9** had been internalized were gently fixed with formaldehyde and further observed by fluorescence microscopy. As is evident from Figure 7, panel B, a rather different distribution was obtained and nuclear accumulation had become detectable after cell fixation.

Conclusion

Previous work had shown that the anchorage of cationic pendant tethers to phosphoramidate α-oligonucleotides resulted in the formation of highly stable and specific duplexes and triplexes.[12,41] Here, we have demonstrated that guanidinium groups as cationic tethers significantly increase the affinity of phosphoramidate α-ONs toward nucleic acid targets, in particular toward RNA. This high affinity could be explained in terms of the dual recognition resulting from Watson–Crick or Hoogsteen base-pairing, combined with cationic/anionic backbone recognition between strands, involving H-bond formation and salt bridging. Furthermore, this guanidinium modification improves the cellular uptake, and the cellular localization of these cationic phosphoramidate ONs is mainly cytoplasmic, in keep-

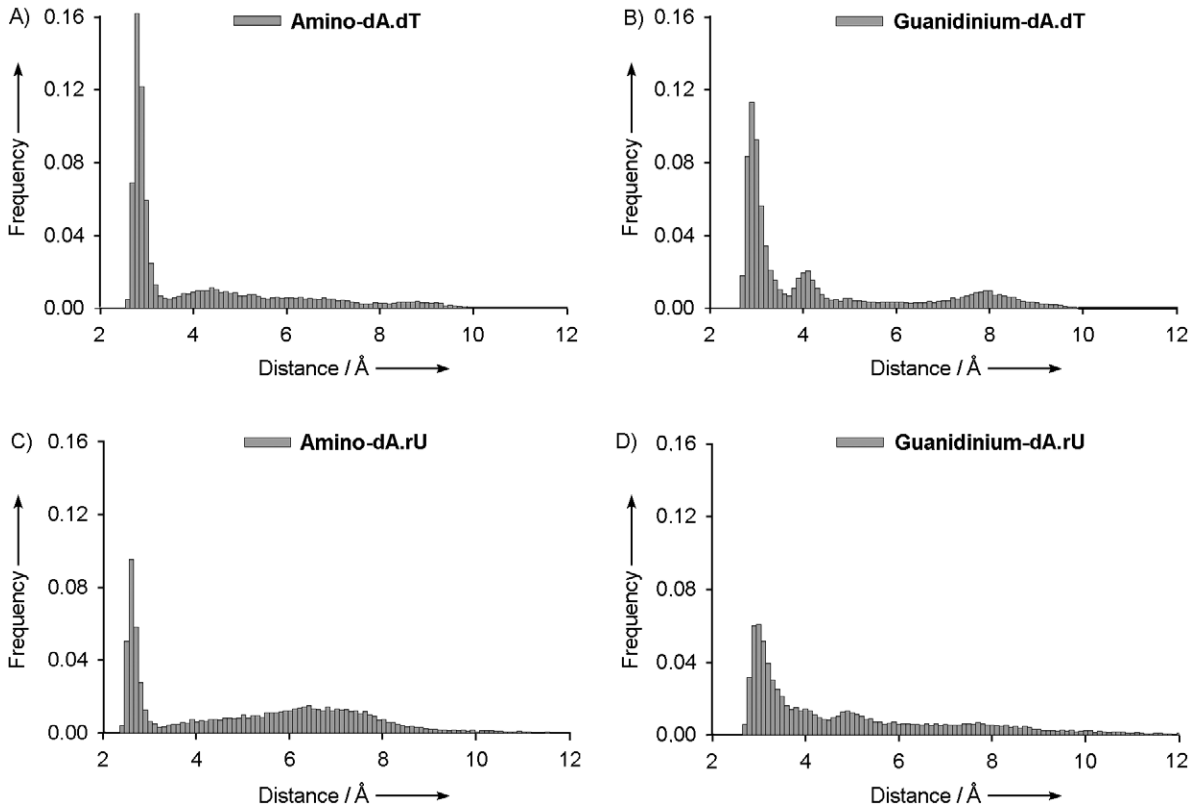

Figure 5. Stabilizing interactions of the phosphoramidate tethers directed across the minor groove with the phosphate groups in the complementary strand, quantified by use of the THY/URA:N2–O1P:ADE interatomic distance distributions. Values produced within the whole 5 ns MD runs were taken into account.

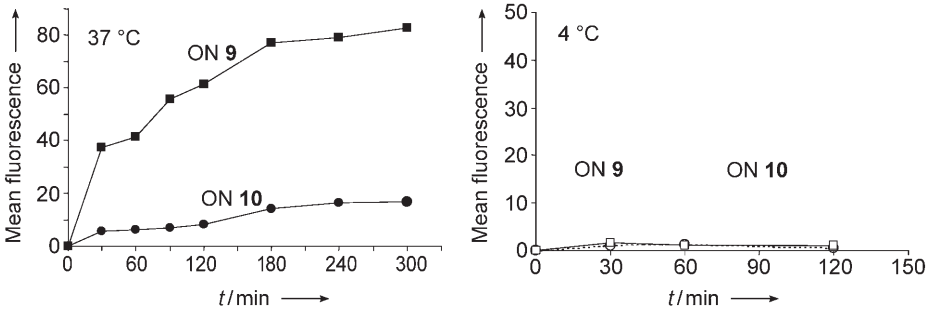

Figure 6. Cell uptake kinetics of ONs **9** and **10** at 4 °C (□, ○) and 37 °C (■, ●). HeLa cells were incubated at 4 °C or at 37 °C with cationic PNHBuGua ON **9** (squares) or with PS ON **10** (circles) at 1 μM. Cells were processed and analyzed by FACS as described in the Experimental Section.

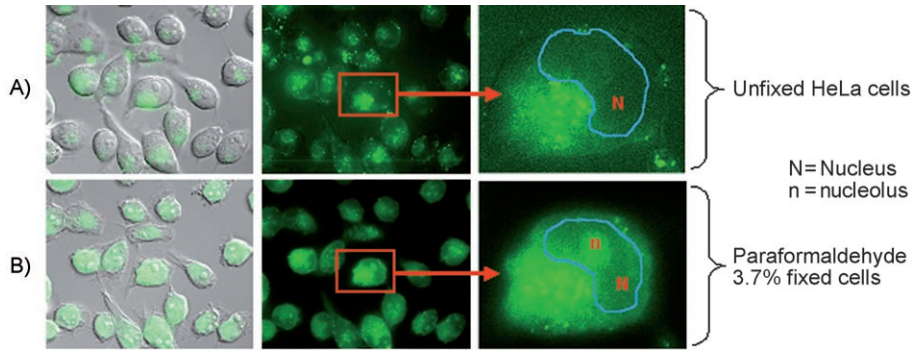

Figure 7. Fluorescence microscopy analysis of ON **9** cell uptake. Live unfixed HeLa cells were incubated with fluorescein-labelled ON **9** (panel A) as indicated in the Experimental Section. Formaldehyde fixation was then performed under the microscope and cells were again observed 10 min later (panel B). In each case a cell was also observed at a larger magnification (see arrows in the figures) in order better to document redistribution after cell fixation.

ing with an endocytotic mechanism of internalization. Finally, these PNHBuGua analogues are highly soluble in water and nuclease-resistant. Taken together, these properties indicate that this new class of cationic ONs has promise as gene-expression inhibitors.

Experimental Section

Target oligonucleotides DNA duplex **I**, hairpin DNA **II**, single-stranded DNA **III** and RNA **IV**, and PO β-ON **1** were purchased from Eurogentec (Seraing, Belgium).

Oligonucleotide synthesis and purification: It is well established that α-ONs and their backbone-modified phosphoramidate analogues hybridize to the purine strand of the duplex DNA target with an antiparallel orientation.[43–45] For this reason, PNHDMAP **2**, $PNHBuNH_2$ **4** and PNHBuGua α-ON **7** (Table 1) were designed with antiparallel orientations with respect to the purine strands of DNA targets **I** and **II**. In contrast, phosphoramidate α-ONs bind to single-stranded DNA or RNA targets with a parallel orientation,[12] so PNHDMAP **3**, $PNHBuNH_2$ **5** and PNHBuGua α-ONs **8** were therefore designed with parallel orientations with respect to the targets **III** or **IV**.

Phosphoramidate ONs (Table 1) were synthesized (1 μmol scale) with an ABI model 394 DNA synthesizer by *H*-phosphonate chemistry[46] with protected α-nucleoside 3′-*H*-phosphonates for **2**–**6**.[47,48] Oxidative amidation of hydrogen phosphonate diesters was performed manually by using a solution of dimethylaminopropylamine for **2** and **3** or *N*-1-trifluoroacetylbutyldiamine (100 mg, 0.54 mmol) for **4**–**6** in CCl_4 (0.8 mL) and pyridine (0.2 mL) as previously described.[12,24] After deprotection, PNHDMAP and $PNHBuNH_2$ ONs **2**–**6** were purified by cationic exchange HPLC (Dionex DX 600)) with a Nucleogel SCX 1000–8 column (50×4.6 mm; Macherey–Nagel) with a 25 min linear gradient of NaCl (0–1 M) in KH_2PO_4 (pH 5.8, 20 mM) containing CH_3CN (20%) at a flow rate of 1.5 mL min^{-1}. For guanidination of purified $PNHBuNH_2$, we applied an improved variant of the procedure described in the literature.[24] ONs **4**–**6** (about 10 O.D) were treated with a mixture of a freshly prepared solution (125 μL) of *O*-methylisourea chloride (100 mg, 0.81 mmol) in water (100 μL) and aqueous ammonia (30%, 125 μL). The reaction mixtures were incubated for 45 min at 65 °C in sure seal flasks. ONs **7**–**9** were further purified under the same conditions as described above, except that PNHBuGua **7**–**9** were eluted with a 45 min linear gradient of KCl (0–1.35 M) in KH_2PO_4 (pH 5.8, 20 mM) containing CH_3CN (20%) at a flow rate of 1.5 mL min^{-1}. All cationic ONs were desalted with Chromafix PS-RP cartridges (Macherey–Nagel). Their final purities were checked by HPLC and their characterizations were performed by MALDI-TOF MS. To obtain α-ON **6**, the fluorescein phophoramidite was coupled to $PNHBuNH_2$ α-dT_{12} on solid support and the phosphite-triester linkage was oxidized with iodine in pyridine.

Phosphorothioate β-ON **10** and phosphodiester β-ONs **11** and **13** were prepared (1 μmol scale) with an ABI model 394 DNA synthesizer by standard phosphoramidite chemistry. The coupling time of 2′-*O*-(3-aminopropyl)uridine phosphoramidite (Chem Genes, USA) for ON **11** was set to 10 min. The crude ON **11** was directly guanidylated with *O*-methylisourea chloride to afford **12** with high purity. The crude ON **13** was purified by reversed-phase HPLC with a Nucleosil C_{18} column (150×4.6 mm, Macherey–Nagel) with use of a 25 min linear gradient of CH_3CN (5–15%) in TEAAc (pH 7, 50 mM). Guanidination of **13** afforded **14**, which was further HPLC-purified under the same conditions.

UV melting experiments: Optical measurements were carried out on a Uvikon 943 spectrophotometer (Kontron) as previously described.[12] Prior to the experiments, the ONs, each at a final concentration of 3 μM, were mixed in NaCl (100 mM)/sodium cacodylate (pH 7, 10 mM). A heating–cooling–heating cycle in the 5–90 °C temperature range with gradients of 0.3 °C min^{-1} (for triplex studies) or 0.5 °C min^{-1} (for duplex studies) was applied. T_m values were determined from the maxima of the first derivative plots of absorbance versus temperature.

Molecular modeling: Molecular dynamics simulations are a well established tool for atomic detail level studies of nucleic acids[49,50] including modified systems.[51] The initial α-dA_{12}·β-dT_{12} duplex structure was constructed by using the CHIMERA software package.[52,53] The natural dT_{12} strand in canonical Arnott B-type geometry was coiled around by the α-anomeric counterpart, which was constructed by stepwise addition of the individual α-anomeric residues. They were manipulated by hand to achieve a suitable arrangement of both strands allowing Watson–Crick hydrogen bonding of bases. It was established despite unusual, but experimentally evidenced, parallel orientation of both strands. Furthermore, a resulting .pdb file was adjusted by several atomic insertions/omissions to produce the α-dA_{12}·β-rU_{12} duplex. Moreover, the α-dA_{12} strand was converted into the α-dT_{10} one, which was coiled around into the major groove of the usual canonical β-dA_{12}·β-dT_{12} duplex. Either amino- or guanidium-alkyl tethers were anchored to phosphorus atoms in place of one of the nonbridging oxygens in all α-anomeric strands discussed above. In summary, the α-amino-dA_{12}·β-dT_{12}, α-guanidino-dA_{12}·β-dT_{12}, α-amino-dA_{12}·β-rU_{12} and α-guanidino-dA_{12}·β-rU_{12} duplexes and the α-guanidino-dT_{10}*β-dA_{10}·β-dT_{10} triplex structure were prepared. Finally, explicit Na^+ counterions were placed at the phosphates of nucleotides by use of the EDIT module of AMBER 5.0.[49] Nucleic acids with Na^+ counterions were surrounded by ~4000 TIP3P water molecules, which extended to a distance of approximately 10 Å (in each direction) from the nucleic acid atoms. This gives a periodic box size of $\sim 60 \times \sim 40 \times \sim 40$ Å^3. New .inpcrd (initial coordinates) and .prmtop (molecular topology, force field etc.) files for the whole simulated system, including the α-anomeric residues as well as cationic tethers, were created by use of the LINK, EDIT and PARM modules; this required necessary completion and modification of all nuc94.in and parm.dat files. Several bond (NS–P), angle and dihedral angle (CT-NS-P-OS, X-CT-NS-P) terms were taken from ref. [51], in which the AMBER parameters for the similar internucleotide linkage modification were developed. Remaining charges, as well as bond, angle and dihedral terms for the side chains, were taken from the AMBER 5.0 database[54] and did not require modification (similarity of cationic tethers with protein lysine/arginine side chains was exploited). Such approximation was judged sufficient for the geometrical factors analyzed here. Fully solvated trajectories (lasting for 5 ps) were computed with the aid of the SANDER module of the AMBER 5.0 software package,[49] with use of the implemented Particle Mesh Ewald summation method for electrostatic interactions.[55] Conventional computational procedures were used.[56] Figures were produced with the aid of the VMD[57,58] and RASTER3D software packages.[59,60]

Cells and cell cultures: Cells were cultured as exponentially growing subconfluent monolayers on 90 mm plates in D-MEM medium (Gibco) supplemented with 10% (*v*/*v*) fetal calf serum and non-essential amino acids.

Flow cytometry: To analyze the internalization of fluorochrome-labelled ONs by FACS, exponentially growing HeLa cells were dissociated with nonenzymatic cell dissociation medium, centrifuged at 900 *g* and resuspended in Opti-MEM. HeLa cells (5×10^5) in Opti-MEM (250 µL) were then incubated with the ON at the concentrations indicated in the Figure legends. After incubation at 37 °C or 4 °C in the presence of the ON, the cell suspension was centrifuged at 1000 *g*. The cell pellet was washed twice with NaCl/Pi before incubation with pronase (1 µg mL^{-1})/EDTA (1 mM) for 5 min at 4 °C. Cells were then washed once more with NaCl/Pi and were finally resuspended in NaCl/Pi (500 µL).

Fluorescence analysis for both cell lines was performed with a FACScan fluorescence-activated cell sorter (Becton Dickinson). A minimum of 20000 events per sample was analyzed.

Fluorescence microscopy: Exponentially growing cells were dissociated with nonenzymatic cell dissociation medium (Sigma) and 2.5×10^5 cells were plated and cultured overnight on 30 mm plates with a glass bottom. The culture medium was discarded and the cells were washed with NaCl/Pi (pH 7.3), the NaCl/Pi was discarded, and the cell monolayer was incubated with the ON dissolved in Opti-MEM at the appropriate concentration. Cells were subsequently rinsed three times for 5 min. with NaCl/Pi for the observation of the living cells. For the fixed cells, the protocol was the same, but cells were also fixed in formaldehyde (3.7% *v*/*v*) in NaCl/Pi for 5 min. at room temperature. The distribution of fluorescence was analyzed on a Zeiss Axiophot 200 M fluorescence microscope.

Acknowledgements

We (G.D, T.M, F.D, J.-J.V) thank the Association pour la Recherche contre le Cancer (ARC) for financial support. Uptake studies were financed by EEC grant QLK3-CT-2002 to B.L. S.A. is the recipient of a LNFCC (Ligue Nationale Française Contre le Cancer) fellowship. Molecular modeling work was supported by a Grant from the Ministry of Education, Youth and Sports of the Czech Republic (project MSM 0021620835) and the Grant Agency of the Czech Republic (project No. 202/02/D114). Results were partially obtained with computer facilities of the Metacentrum of the Czech Universities.

Keywords: cellular uptake · DNA recognition · guanidinium · molecular dynamics · oligonucleotides

[1] P. Herdewijn, *Antisense Nucleic Acid Drug Dev.* **2000**, *10*, 297–310.
[2] C. J. Leumann, *Bioorg. Med. Chem.* **2002**, *10*, 841–854.
[3] J. Kurreck, *Eur. J. Biochem.* **2003**, *270*, 1628–1644.
[4] S. M. Hammond, A. A. Caudy, G. J. Hannon, *Nat. Rev. Genet.* **2001**, *2*, 110–118.
[5] T. Tuschl, *ChemBioChem* **2001**, *2*, 239–245.
[6] P. L. Iversen, *Curr. Opin. Mol. Ther.* **2001**, *3*, 235–238.
[7] P. E. Nielsen in *Methods in Enzymology: Antisense Technology Part A: General Methods, Methods of Delivery, and RNA Studies, Vol. 313* (Ed.: M. I. Phillips), Academic Press, San Diego, **2000**, pp. 156–164.
[8] S. Chaturvedi, T. Horn, R. L. Letsinger, *Nucleic Acids Res.* **1996**, *24*, 2318–2323.
[9] J. M. Dagle, D. L. Weeks, *Nucleic Acids Res.* **1996**, *24*, 2143–2149.
[10] D. A. Barawkar, T. C. Bruice, *Proc. Natl. Acad. Sci. USA* **1998**, *95*, 11047–11052.
[11] P. M. Reddy, T. C. Bruice, *Bioorg. Med. Chem. Lett.* **2003**, *13*, 1281–1285.
[12] T. Michel, C. Martinand-Mari, F. Debart, B. Lebleu, I. Robbins, J.-J. Vasseur, *Nucleic Acids Res.* **2003**, *31*, 5282–5290.
[13] T. Thomas, T. J. Thomas, *Biochemistry* **1993**, *32*, 14068–14074.
[14] D. A. Barawkar, K. J. Rajeev, V. A. Kumar, K. N. Ganesh, *Nucleic Acids Res.* **1996**, *24*, 1229–1237.
[15] J. Bijapur, M. D. Keppler, S. Bergqvist, T. Brown, K. R. Fox, *Nucleic Acids Res.* **1999**, *27*, 1802–1809.
[16] J. Robles, A. Grandas, E. Pedroso, *Tetrahedron* **2001**, *57*, 179–194.
[17] V. Roig, U. Asseline, *J. Am. Chem. Soc.* **2003**, *125*, 4416–4417.
[18] C. J. Wilds, M. A. Maier, V. Tereshko, M. Manoharan, M. Egli, *Angew. Chem.* **2002**, *114*, 123–125; *Angew. Chem. Int. Ed.* **2002**, *41*, 115–117.
[19] B. Cuenoud, F. Casset, D. Hüsken, F. Natt, R. M. Wolf, K.-H. Altmann, P. Martin, H. E. Moser, *Angew. Chem.* **1998**, *110*, 1350–1353; *Angew. Chem. Int. Ed.* **1998**, *37*, 1288–1291.

[20] N. Puri, A. Majumdar, B. Cuenoud, F. Natt, P. Martin, A. Boyd, P. S. Miller, M. M. Seidman, *Biochemistry* **2002**, *41*, 7716 – 7724.
[21] M. Sollogoub, R. A. J. Darby, B. Cuenoud, T. Brown, K. R. Fox, *Biochemistry* **2002**, *41*, 7224 – 7231.
[22] M. A. Maier, I. Barber-Peoc'h, M. Manoharan, *Tetrahedron Lett.* **2002**, *43*, 7613 – 7616.
[23] T. P. Prakash, A. Puschl, E. Lesnik, V. Mohan, V. Tereshko, M. Egli, M. Manoharan, *Org. Lett.* **2004**, *6*, 1971 – 1974.
[24] T. Michel, F. Debart, J.-J. Vasseur, *Tetrahedron Lett.* **2003**, *44*, 6579 – 6582.
[25] H. Challa, T. C. Bruice, *Bioorg. Med. Chem.* **2004**, *12*, 1475 – 1481.
[26] P. Zhou, M. Wang, L. Du, G. W. Fisher, A. Waggoner, D. H. Ly, *J. Am. Chem. Soc.* **2003**, *125*, 6878 – 6879.
[27] E. Vivès, P. Brodin, B. Lebleu, *J. Biol. Chem.* **1997**, *272*, 16010 – 16017.
[28] D. Derossi, S. Calvet, A. Trembleau, A. Brunissen, G. Chassaing, A. Prochiantz, *J. Biol. Chem.* **1996**, *271*, 18188 – 18193.
[29] Astriab-Fisher, D. Sergueev, M. Fisher, B. Ramsay Shaw, R. L. Juliano, *Pharm. Res.* **2002**, *19*, 744 – 754.
[30] J. B. Rothbard, E. Kreider, C. L. VanDeusen, L. Wright, B. L. Wylie, P. A. Wender, *J. Med. Chem.* **2002**, *45*, 3612 – 3618.
[31] H. M. Moulton, M. H. Nelson, S. A. Hatlevig, M. T. Reddy, P. L. Iversen, *Bioconjugate Chem.* **2004**, *15*, 290 – 299.
[32] T. Suzuki, S. Futaki, M. Niwa, S. Tanaka, K. Ueda, Y. Sugiura, *J. Biol. Chem.* **2002**, *277*, 2437 – 2443.
[33] S. Futaki, T. Suzuki, W. Ohashi, T. Yagami, S. Tanaka, K. Ueda, Y. Sugiura, *J. Biol. Chem.* **2001**, *276*, 5836 – 5840.
[34] N. W. Luedtke, P. Carmichael, Y. Tor, *J. Am. Chem. Soc.* **2003**, *125*, 12374 – 12375.
[35] A. M. Funhoff, C. F. van Nostrum, M. C. Lok, M. M. Fretz, D. J. A. Crommelin, W. E. Hennink, *Bioconjugate Chem.* **2004**, *15*, 1212 – 1220.
[36] P. A. Wender, D. J. Mitchell, K. Pattabiraman, E. T. Pelkey, L. Steinman, J. B. Rothbard, *Proc. Natl. Acad. Sci. USA* **2000**, *97*, 13003 – 13008.
[37] T. Ohmichi, M. Kuwahara, N. Sasaki, M. Hasegawa, T. Nishikata, H. Sawai, N. Sugimoto, *Angew. Chem.* **2005**, *117*, 6840 – 6843; *Angew. Chem. Int. Ed.* **2005**, *44*, 6682 – 6685.
[38] M. Manoharan, T. P. Prakash, I. Barber-Peoc'h, B. Bhat, G. Vasquez, B. S. Ross, P. D. Cook, *J. Org. Chem.* **1999**, *64*, 6468 – 6472.
[39] R. H. Griffey, B. P. Monia, L. L. Cummins, S. Freier, M. J. Greig, C. J. Guinosso, E. Lesnik, S. M. Manalili, V. Mohan, S. Owens, B. S. Ross, H. Sasmor, E. Wancewicz, K. Weiler, P. D. Wheeler, P. D. Cook, *J. Med. Chem.* **1996**, *39*, 5100 – 5109.
[40] A. Laurent, M. Naval, F. Debart, J.-J. Vasseur, B. Rayner, *Nucleic Acids Res.* **1999**, *27*, 4151 – 4159.
[41] T. Michel, F. Debart, F. Heitz, J.-J. Vasseur, *ChemBioChem* **2005**, *6*, 1254 – 1262.
[42] J. P. Richard, K. Melikov, E. Vives, C. Ramos, B. Verbeure, M. J. Gait, L. V. Chernomordik, B. Lebleu, *J. Biol. Chem.* **2003**, *278*, 585 – 590.
[43] B.-W. Sun, F. Geinguenaud, E. Taillandier, M. Naval, A. Laurent, F. Debart, J.-J. Vasseur, *J. Biomol. Struct. Dyn.* **2002**, *19*, 1073 – 1082.
[44] S. B. Noonberg, J. C. François, D. Praseuth, A.-L. Guieysse-Peugeot, J. Lacoste, T. Garestier, C. Hélène, *Nucleic Acids Res.* **1995**, *23*, 4042 – 4049.
[45] T. Michel, F. Debart, J.-J. Vasseur, F. Geinguenaud, E. Taillandier, *J. Biomol. Struct. Dyn.* **2003**, *21*, 435 – 445.
[46] B. C. Froehler in *Methods in Molecular Biology. Protocols for Oligonucleotides and Analogs, Vol. 20* (Ed.: S. Agrawal), Humana Press, Totowa, **1993**, pp. 63 – 80.
[47] V. Ozola, C. B. Reese, Q. Song, *Tetrahedron Lett.* **1996**, *37*, 8621 – 8624.
[48] A. Laurent, M. Naval, F. Debart, J.-J. Vasseur, B. Rayner, *Nucleic Acids Res.* **1999**, *27*, 4151 – 4159.
[49] D. A. Pearlman, D. A. Case, J. W. Caldwell, W. R. Ross, T. E. Cheatham III, S. DeBolt, D. Ferguson, G. Seibel, P. Kollman, *Comput. Phys. Commun.* **1995**, *91*, 1 – 41.
[50] T. E. Cheatham III, M. A. Young, *Biopolymers* **2001**, *56*, 232 – 256.
[51] P. Cieplak, T. E. Cheatham III, P. A. Kollman, *J. Am. Chem. Soc.* **1997**, *119*, 6722 – 6730.
[52] E. F. Pettersen, T. D. Goddard, C. C. Huang, G. S. Couch, D. M. Greenblatt, E. C. Meng, T. E. Ferrin, *J. Comput. Chem.* **2004**, *25*, 1605 – 1612.
[53] CHIMERA, http://www.cgl.ucsf.edu/chimera
[54] D. W. Cornell, P. Cieplak, C. I. Bayly, I. R. Gould, K. M. Merz, D. M. Ferguson, D. C. Spellmeyer, T. Fox, J. W. Caldwell, P. A. Kollman, *J. Am. Chem. Soc.* **1995**, *117*, 5179 – 5197.
[55] T. Darden, D. York, L. J. Pedersen, *J. Chem. Phys.* **1993**, *98*, 10089 – 10092.
[56] AMBER, http://amber.scripps.edu
[57] W. Humphrey, A. Dalke, K. Schulten, *J. Mol. Graphics* **1996**, *14*, 33 – 38.
[58] VMD, http://www.ks.uiuc.edu/Research/vmd
[59] E. A. Merritt, D. J. Bacon, in *Methods in Enzymology, Vol. 277* (Eds.: C. W. Carter, Jr., R. M. Sweet), **1997**, pp. 505 – 524.
[60] RASTER3D, http://www.bmsc.washington.edu/raster3d

Received: October 24, 2005
Published online on March 6, 2006

Chapitre VI

Discussion générale

Chapitre VI

Discussion générale :

Comme évoqué dans l'introduction, la découverte des propriétés de passage membranaire d'un certain nombre de protéines a ouvert une nouvelle alternative très prometteuse de délivrance de biomolécules. Les études de structure activité faites sur ces protéines ont mis en évidence que seule une séquence peptidique courte (10-30 résidus en général) et riche en acides aminés basiques est responsable de la pénétration cellulaire.
Ces peptides issus de protéines ont été regroupés sous le nom de **C**ell **P**enetrating **P**eptide (**CPP**) ou **P**rotein **T**ransduction **D**omain (**PTD**). Ces vecteurs peptidiques sont naturels (Tat (48-60), pénétratine…) ou synthétiques (MPG, Pep, MAP, Transportan…).
Si les développements biotechnologiques de ces peptides comme vecteurs sont divers et importants, la mécanistique d'internalisation cellulaire de ces peptides reste mal comprise et est toujours un sujet de débat. Cette controverse porte sur la mise en jeux d'un mécanisme d'endocytose et sur un processus de translocation au travers de la membrane plasmique.

Le premier mécanisme décrit est indépendant de l'endocytose et mène à une localisation nucléaire de ces peptides. Toutefois, les protocoles de traitement cellulaire utilisés conduisaient à plusieurs artefacts faussant l'interprétation des données expérimentales.
Les travaux menés récemment par notre équipe dans des conditions éliminant ces artéfacts ont indiqué que la pénétration cellulaire de plusieurs peptides de délivrance dépend d'un mécanisme endocytotique impliquant une liaison aux héparanes sulfates membranaires suivi d'une endocytose et d'une localisation vésiculaire extranucléaire, résultats confirmés par plusieurs équipes. Toutefois, le mécanisme d'entrée dans les cellules pourrait varier en fonction du peptide, du cargo transporté et des conditions expérimentales. Un des résultats les plus intéressants de cette thèse dans ce contexte est l'effet de la concentration du conjugué utilisé sur le mécanisme de pénétration cellulaire.

En effet, dans l'étude de l'efficacité de l'octalysine couplée à un PNA correcteur d'épissage, deux types de comportements ont été observés. A basse concentration, les conjugués K_8-PNA pénètrent par un processus endocytotique et restent pour une large part ségrégés dans les vésicules d'endocytoses. La correction d'épissage ne se fait efficacement qu'après ajout

d'agents endosomolytiques comme la chloroquine. A plus forte concentration, l'internalisation des conjugués ne dépend pas de la température et permet une correction d'épissage en absence de chloroquine. Cette différence de mécanisme est probablement le résultat d'une perméabilisation membranaire causée par la forte concentration des conjugués Il faut souligner que la majorité des publications concernent des travaux réalisés aux concentrations auxquelles nous avons mis en évidence une perméabilisation membranaire. Notre objectif étant à terme d'utiliser ces peptides comme vecteurs pour la délivrance de biomolécules dans un contexte clinique, nous ne retiendrons que les résultats obtenus à basse concentration en l'absence de perméabilisation membranaire.

L'utilisation de ces peptides pour la délivrance de biomolécules a été documentée par plusieurs groupes. Comme évoqué dans l'introduction, bon nombre de publications décrivent des activités biologiques efficaces en présence de ces peptides, soit couplés chimiquement par des interactions covalentes à l'agent thérapeutique, soit par des interactions électrostatiques.

Au commencement de la présente thèse, nous avons réévalué l'efficacité d'un certain nombre de peptides vecteurs pour la délivrance d'analogues d'oligonucléotides antisens dans le modèle de correction d'épissage décrit dans les travaux de l'équipe du Dr. R. Kole.

Brièvement, ce modèle implique un gène de luciférase où est inséré un intron muté provenant de la β-thalassémie. Cette mutation crée un site cryptique d'épissage utilisé préférentiellement aboutissant à une forme inactive de la protéine. L'hybridation d'un oligonucléotide antisens masque ce site cryptique et déroute l'épissage vers une forme fonctionnelle de la luciférase. L'intérêt de ce modèle réside dans le fait que la réponse biologique obtenue est un signal positif reflétant la production de luciférase active après une correction d'épissage par l'analogue antisens.

Nos travaux de collaboration avec les équipes du Dr. M. J. Gait (Cambridge) et du Dr. J. Oehlke (Berlin) ainsi que les travaux d'autres équipes (équipe du Dr. P. E. Nielsen et du Pr. Ü. Langel) ont mis l'accent sur les limitations liées à l'utilisation des peptides vecteurs qui utilisent l'endocytose comme mécanisme d'entrée cellulaire. Une fois ces conjugués correcteurs d'épissage internalisés par endocytose, ils restent bloqués dans des endosomes et l'évolution de ces vésicules en lysosomes conduit à une dégradation enzymatique des conjugués. L'utilisation d'agents endosomolytiques, comme la chloroquine, le sucrose et les ions calciques, déstabilise les endosomes et permet la libération des conjugués séquestrés, améliorant ainsi l'efficacité de correction d'épissage.

Le mode d'action de ces agents peut s'expliquer de différentes manières. La plus couramment proposée est que l'accumulation de ces agents dans les vésicules d'endocytose entraine l'éclatement de ces dernières par effet osmotique. Malheureusement, la microscopie de fluorescence faite sur les cellules incubées avec les conjugués correcteurs d'épissage en présence ou en absence de chloroquine n'a montré aucune différence de localisation significative, observation confirmée par les travaux du Dr. S. Dowdy (communication personnelle) sur la transfection des protéines.
La deuxième est que la chloroquine retarde l'évolution endosome/lysosome, ce qui augmente la durée de vie des conjugués ainsi que la probabilité d'être relachés dans le cytoplasme cellulaire. Il faut savoir qu'avec d'autres modes de transfection sur le même modèle, une correction d'épissage est obtenue avec des concentrations de 10-20nM. Si l'on se rapporte à la dose utilisée dans nos expériences, qui est de l'ordre du µmolaire, il suffit d'une infime quantité qui se libère des endosomes après addition de la choloroquine pour avoir une correction d'épissage efficace. Enfin, la neutralisation du pH des vésicules d'endocytose.

Cependant, il n'est pas envisageable d'utiliser la chloroquine *in vivo* car les effets indésirables associés à son utilisation sont importants malgré qu'elle soit utilisée comme médicament antipalludique. La question qui s'est posée à ce niveau est donc comment s'affranchir de la chloroquine ? Et quelles sont les stratégies alternatives qui peuvent être utilisées pour améliorer l'efficacité de ces conjugués sans addition de la chloroquine ?

Nous avons envisagé deux possibilités : la première implique l'utilisation de peptides à caractère fusogène ou perturbateur des vésicules d'endocytose. La seconde consiste à optimiser les peptides de délivrance déjà existants ou à concevoir de nouveaux vecteurs plus efficaces en terme de libération des endosomes.

Plusieurs travaux ont documenté le rôle de peptides fusogènes comme la partie N terminale du peptide de fusion HA2 du virus de l'Influenza. Les résultats obtenus avec ce peptide décrivent une augmentation de la délivrance de protéines ou d'ADN plasmidique. Nos expériences d'ajout en trans de peptides fusogènes ne sont pas encourageantes, malgré l'utilisation de toute une panoplie de peptides décrits comme déstabilisants des membranes biologiques.

Le mode d'action de ces peptides est cependant compliqué. Plusieurs publications décrivent pour un certain nombre de ces peptides une activité dépendante d'une oligomérisation (ou d'une topologie particulière) ou à des concentrations dépassant le µmolaire, qui sont toxiques dans notre modèle cellulaire. Nous avons alors opté pour l'optimisation des vecteurs déjà existants. Avec nos collaborateurs d'AVIBiopharma (USA), nous nous somme basés sur les résultats du Dr. J. Rothbard concernant le rôle des groupements guanidinium des arginines dans l'internalisation cellulaire et avons sélectionné un nouveau peptide de délivrance. Ce vecteur $(R\text{-}Ahx\text{-}R)_4$, couplé à un PMO, un analogue d'oligonucléotide antisens, augmente d'une manière significative la correction de l'épissage sans addition d'agents endosomolytiques. Le $(R\text{-}Ahx\text{-}R)_4$ entre dans les cellules par endocytose avec implication des héparanes sulfates membranaires. Néanmoins, l'internalisation cellulaire de ce conjugué est faible par rapport à celle du conjugué poly-arginine (R_9F_2-PMO). Différentes hypothèses ont été envisagées pour expliquer cette forte activité de correction apportée par le conjugué $(R\text{-}Ahx\text{-}R)_4$-PMO. La première concerne la résistance du conjugué aux protéases/nucléases cellulaires. La présence de liaisons non peptidiques dans la structure du $(R\text{-}Ahx\text{-}R)_4$-PMO peut être à l'origine de cette résistance et de l'augmentation de sa demi-vie. Les données expérimentales présentées par l'équipe du Dr. P. L. Iversen (AviBiopharma, USA) ont cependant montré que la dégradation cellulaire du $(R\text{-}Ahx\text{-}R)_4$-PMO est similaire à celle du Tat-PMO ou du R_9F_2-PMO. La seconde hypothèse est une corrélation entre l'activité biologique et l'internalisation cellulaire. Nos expériences, présentées dans le chapitre II, ont indiqué que ce n'est pas le conjugué le mieux internalisé qui corrige efficacement l'épissage. La troisième hypothèse concerne un lien possible entre affinité du conjugué pour ses récepteurs membranaires et effet biologique. Nos résultats préliminaires indiquent une faible affinité du conjugué $(R\text{-}Ahx\text{-}R)_4$-PMO à des héparanes sulfates. Cette faible affinité est probablement la résultante de l'espacement entre les groupements guanidiniums des arginines. Notre hypothèse actuelle est qu'il faut une certaine affinité suffisante pour permettre une fixation du conjugué aux glycoprotéoglycanes membranaires suivie d'une entrée cellulaire. Par contre, l'affinité doit être suffisamment faible pour permettre une dissociation du conjugué rapide conditionnant sa sortie des endosomes.

Les études en cours de structure activité tendent à confirmer cette hypothèse de travail. Les résultats obtenus ont indiqué qu'il y a un effet de l'espacement des arginines sur l'affinité des conjugués à l'héparine, mais aussi sur leur hydrophobicité. Il faut savoir que, plus

l'espacement entre les charges est grand, plus l'affinité augmente, plus l'hydrophobicité augmente et plus l'efficacité de correction diminue.

D'une manière très intéressante, le remplacement de l'espaceur **Ahx** par un autre de la même taille contenant un acide aminé hydrophobe affecte dramatiquement l'efficacité de correction. L'optimum d'activité est obtenu avec le conjugué (R-Ahx-R)$_4$-PMO. En se basant sur ces résultats, qui mettent le point sur l'importance de l'affinité et de l'hydrophobicité des conjugués aux constituants de la membrane pour la délivrance de PMO correcteur d'épissage, nous proposons le modèle suivant (Figure 24).

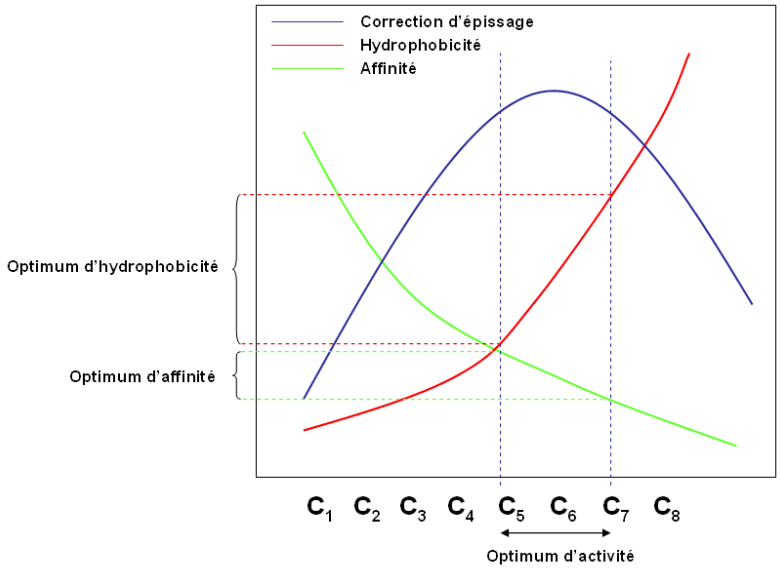

Figure 24 : *Modèle descriptif de l'importance de l'affinité et de l'hydrophobicité des conjugués pour la délivrance d'analogues d'oligonucléotides antisens.*

Un autre peptide a été sélectionné dans le cadre d'un travail de collaboration avec l'équipe du Dr. M. J. Gait. Ce peptide est le R$_6$Pen. Couplé à un PNA correcteur d'épissage, ce peptide permet une correction d'épissage en absence d'agent endosomolytique supérieure à celle obtenue avec (R-Ahx-R)$_4$-PNA.

Les études de structure activité sur ce conjugué ont montré que l'extension R$_6$ est nécessaire et suffisante pour avoir une efficacité de correction significative. Les faibles activités observées en présence des conjugués R$_3$Pen-PNA et R$_9$Pen-PNA correcteurs d'épissage sont probablement la conséquence d'une différence dans leur affinité par rapport à celle du R$_6$Pen-

PNA. De plus, l'espacement entre les groupements guanidiniums des arginines du R_6Pen-PNA par des spacers **Ahx** augmente l'efficacité de correction d'une manière significative. D'une manière très intéressante, et connaissant le rôle dramatique de l'hydrophobicité des conjugués dans ce modèle de correction, la substitution du résidu hydrophobe $\mathbf{W_{48}}$ de la pénétratine par un acide aminé moins hydrophobe **L** améliore l'activité de correction. Bien que l'étude structure-activité de ce peptide ne soit pas achevée, nous disposons actuellement de dérivés de ce peptide entrainant une correction d'épissage avec des EC_{50} d'environ 0,2µM. Toutefois, une perméabilisation des membranes à des concentrations > 2,5µM a été observée avec ces conjugués.

Une autre partie de l'étude de structure-activité concerne l'importance du mode de couplage entre le peptide de délivrance et l'analogue antisens correcteur d'épissage. Il était généralement proposé qu'un couplage par un lien réductible permette une correction plus efficace. En effet, une fois que les conjugués sont internalisés, une bonne partie d'entre eux reste séquestrée dans les vésicules d'endocytoses. Un couplage par pont disulfure réductible permet de libérer l'oligonucléotide correcteur d'épissage, même si le vecteur peptidique reste accroché à la membrane. Nos expériences faites en collaboration avec l'équipe du Dr. M. J. Gait (Cambridge) ont indiqué qu'un couplage par pont disulfure entre le peptide de délivrance et l'analogue antisens augmente légèrement l'efficacité de correction par rapport au lien stable. Ce résultat a été confirmé par nos travaux de collaboration avec l'équipe du Dr. J. Oehlke (Berlin) sur le peptide amphipathique MAP.

L'étude faite avec le MAP (Model Amphipathic Peptide) en collaboration avec l'équipe du Dr. J. Oehlke (Berlin) a montré l'efficacité du conjugué KLA-PNA pour promouvoir l'efficacité de l'épissage sans addition de chloroquine comme agent de déstabilisation des endosomes. De plus, la substitution des lysines **K** (chargées +) par des glutamates **E** (chargées -) abolit la correction de l'épissage, malgré la conservation de la structure en hélice α-amphipathique. Cette mutation affecte éventuellement l'internalisation cellulaire. Le remplacement des **K** par des **R** diminue significativement l'effet de correction, ce qui peut être la conséquence d'une augmentation d'affinité aux héparanes sulfates. Ce qui est très surprenant dans ce travail est que la correction d'épissage dépend de l'orientation du couplage. En effet, le couplage d'analogues antisens à l'extrémité N terminal du MAP est beaucoup plus efficace qu'un couplage en C terminal.

Malgré l'efficacité de ces différents conjugués, (R-Ahx-R)$_4$-PMO, R_6Pen-PNA et KLA-PNA en l'absence d'agent endosomolytique, l'addition de chloroquine améliore significativement la correction de l'épissage, argument complémentaire de leur séquestration dans les vésicules d'endocytose. Dans le même ordre d'idées, l'étude de la distribution intracellulaire de conjugués (R-Ahx-R)$_4$-PMO ou KLA-PNA marqués par des fluorochromes indique une localisation vésiculaire.

Tous ces résultats mettent l'accent sur deux critères très importants pour l'efficacité de la correction d'épissage : l'affinité pour les héparanes sulfates et l'hydrophobicité des conjugués. De plus et comme nous l'avons déjà décrit, l'espacement entre les charges qui régule l'affinité et l'hydrophobicité du peptide vecteur sont importants.

Connaissant l'importance des interactions électrostatiques dans l'internalisation cellulaire des peptides vecteurs, la cationisation directe des analogues antisens pourrait constituer une intéressante stratégie d'auto-vectorisation. Les collaborations avec l'équipe du Dr. J. J. Vasseur (Montpellier) et l'équipe du Prof. K. Ganesh (Pune) ont permis d'évaluer l'efficacité de deux types de modifications : la guanidylation des antisens et la cationisation des PNA (PNAs contraints). Certains de ces analogues ont une affinité plus importante pour une séquence complémentaire d'ARN, propriété avantageuse pour des oligonucléotides antisens agissant par blocage stérique. Malheureusement, pour l'une comme pour l'autre, les modifications ne se font avec un bon rendement que sur les monomères avec une thymine comme base. Une optimisation des procédés de synthèse est en cours afin d'améliorer le rendement et la qualité du produit à tester dans le modèle de correction d'épissage.

Nous poursuivrons l'optimisation de nos vecteurs peptidiques de délivrance avec pour objectif un meilleur relargage des vésicules d'endocytose. Rappelons ici que les vecteurs les plus efficaces dont nous disposions restent pour large part associés à des vésicules d'endocytose. Nous estimions néammoins ce travail suffisamment avancé pour envisager à court terme des applications à d'autres modèles biologiques pour le transport d'oligonucléotides correcteurs d'épissage ou pour d'autres biomolécules.
Un des modèles les plus étudiés est celui des régulateurs d'apoptose Bcl-x, de la famille Bcl-2 (Figure 25).

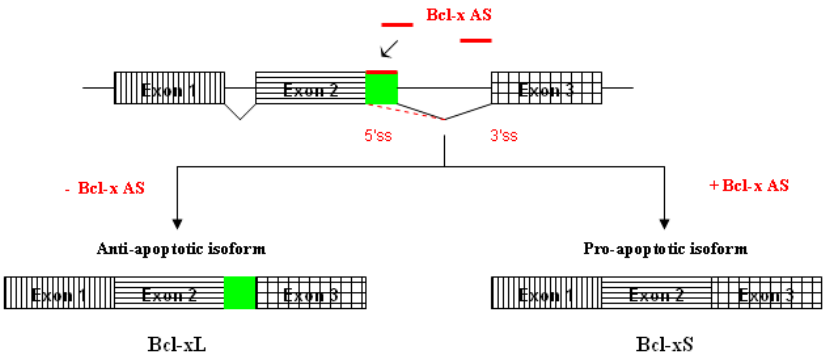

Figure 25 : *Modèle d'épissage alternatif du gène Bcl -X*

Un épissage alternatif des gènes de Bcl-x donne naissance à deux protéines, Bcl-xL et Bcl-xS, dont les propriétés sont antagonistes (Boise et al. 1993). L'expression préférentielle du variant Bcl-xL dans de nombreux cancers (Krajewska et al. 1996; Marone et al. 1998; Nuessler et al. 1999) rend les cellules tumorales résistantes à la chimiothérapie (Simonian et al. 1997). A l'inverse, la surexpression du variant pro-apoptotique Bcl-xS sensibilise les cellules tumorales à la chimiothérapie. Le traitement de cellules tumorales par des antisens permet d'augmenter l'expression de Bcl-xS et de diminuer celle de Bcl-xL, favorisant ainsi la mort par apoptose des cellules cancéreuses (Mercatante et al. 2001; Wacheck et Zangemeister-Wittke 2006).

Un aspect très important est la possibilité d'utiliser ces peptides in vivo dans des modèles à relevance clinique. Une collaboration avec une équipe de biophysiciens du NIH (confidentielle) pourrait permettre d'affiner les études de structure-activité de ces conjugués. Cette équipe vient de mettre en évidence une déstabilisation pH dépendante par le peptide Tat de vésicules lipidiques synthétiques dont la composition reflète celle des endosomes. Nous nous proposons d'évaluer sur ce modèle le potentiel de déstabilisation pH-dépendant de conjugués issus de nos études structure-activité afin de déterminer dans quelle mesure l'efficacité de correction d'épissage et de déstabilisation membranaire pH-dépendant sont liées.

Les travaux de l'équipe du Dr. P. Iversen (AVIBiopharma) sur des modèles animaux de correction d'épissage chez la souris β-thalassémique, de saut d'exon dans le cas de la dystrophie musculaire chez la souris *mdx* ou le chien (DMD : Duchenne Muscular Dystrophy) ou d'inhibition de la réplication virale chez la souris (SARS : Severe acute respiratory

syndrome coronavirus) sont très encourageants(Fletcher et al. 2007; Moulton et al. 2007). Ces résultats témoignent d'une large biodisponibilité tissulaire du conjugué $(R\text{-}Ahx\text{-}R)_4$-PMO, d'une efficacité significative après une injection intrapéritonéale chez la souris, et d'une stabilité métabolique satisfaisante dans le sérum (Youngblood et al. 2007). Ce conjugué exhibe néanmoins une cytotoxicité à forte concentration (Dr. H. Moulton, communication personnelle), ce qui nous amène à poursuivre nos travaux d'optimisation du conjugué $(R\text{-}Ahx\text{-}R)_4$-PMO avec nos collaborateurs d'AVIBiopharma. L'optimisation des deux peptides $(R\text{-}Ahx\text{-}R)_4$ et R_6Pen à la recherche d'une EC_{50} réduite et leur ciblage vers le tissu d'intérêt sont les deux points principaux en cours d'étude.

Références

Références

1. Abes, R., Arzumanov, A. A., Moulton, H., Abes, S., Ivanova, G. D., Iversen, P. L., Gait, M. J., et Lebleu, B. **(sous presse)**. Cell penetrating peptide-based delivery of oligonucleotides: an overview. *Biochem Soc Trans.*

2. Abes, S., Moulton, H., Turner, J., Clair, P., Richard, J. P., Iversen, P., Gait, M. J., et Lebleu, B. **(2007)**. Peptide-based delivery of nucleic acids: design, mechanism of uptake and applications to splice-correcting oligonucleotides. *Biochem Soc Trans.* ***35****(Pt 1): 53-55*.

3. Abes, S., Moulton, H. M., Clair, P., Prevot, P., Youngblood, D. S., Wu, R. P., Iversen, P. L., et Lebleu, B. **(2006)**. Vectorization of morpholino oligomers by the (R-Ahx-R)4 peptide allows efficient splicing correction in the absence of endosomolytic agents. *J Control Release.* ***116****(3): 304-313*.

4. Abes, S., Richard, J. P., Thierry, A. R., Clair, P., et Lebleu, B. **(2007)**. Tat-Derived Cell-Penetrating Peptides: Discovery, Mechanism of Cell Uptake, and Applications to the Delivery of Oligonucleotides. *Handbook of Cell-Penetrating Peptides (second edition). 29-42*.

5. Abes, S., Williams, D., Prevot, P., Thierry, A., Gait, M. J., et Lebleu, B. **(2006)**. Endosome trapping limits the efficiency of splicing correction by PNA-oligolysine conjugates. *J Control Release.* ***110****(3): 595-604*.

6. Agrawal, S., Temsamani, J., Galbraith, W., et Tang, J. **(1995)**. Pharmacokinetics of antisense oligonucleotides. *Clin Pharmacokinet.* ***28****(1): 7-16*.

7. Akhtar, S., et Juliano, R. L. **(1992)**. Cellular uptake and intracellular fate of antisense oligonucleotides. *Trends Cell Biol.* ***2****(5): 139-144*.

8. Al-Awqati, Q. **(1986)**. Proton-translocating ATPases. *Annu Rev Cell Biol.* ***2****(179-199*.

9. Andres, E., et Dimarcq, J. L. **(2007)**. [Cationic antimicrobial peptides: from innate immunity study to drug development. Up date.]. *Med Mal Infect.* ***37****(4): 194-199*.

10. Anson, D. S. **(2004)**. The use of retroviral vectors for gene therapy-what are the risks? A review of retroviral pathogenesis and its relevance to retroviral vector-mediated gene delivery. *Genet Vaccines Ther.* ***2****(1): 9*.

11. Arnold, L. J. J. **(1985)**. Polylysine-drug conjugates. *Methods Enzymol.* ***112****(270-285*.

12. Arzumanov, A., Walsh, A. P., Rajwanshi, V. K., Kumar, R., Wengel, J., et Gait, M. J. **(2001)**. Inhibition of HIV-1 Tat-dependent trans activation by steric block chimeric 2'-O-methyl/LNA oligoribonucleotides. *Biochemistry.* ***40****(48): 14645-14654*.

13. Astriab-Fisher, A., Sergueev, D., Fisher, M., Shaw, B. R., et Juliano, R. L. **(2002)**. Conjugates of antisense oligonucleotides with the Tat and antennapedia cell-penetrating peptides: effects on cellular uptake, binding to target sequences, and biologic actions. *Pharm Res.* ***19****(6): 744-754*.

14. Astriab-Fisher, A., Sergueev, D. S., Fisher, M., Shaw, B. R., et Juliano, R. L. **(2000)**. Antisense inhibition of P-glycoprotein expression using peptide-oligonucleotide conjugates. *Biochem Pharmacol.* ***60****(1): 83-90*.

15. Barawkar, D. A., et Bruice, T. C. **(1998)**. Synthesis, biophysical properties, and nuclease resistance properties of mixed backbone oligodeoxynucleotides containing cationic internucleoside guanidinium linkages: deoxynucleic guanidine/DNA chimeras. *Proc Natl Acad Sci U S A.* ***95****(19): 11047-11052*.

16. Begley, R., Liron, T., Baryza, J., et Mochly-Rosen, D. **(2004)**. Biodistribution of intracellularly acting peptides conjugated reversibly to Tat. *Biochem Biophys Res Commun*. ***318****(4): 949-954*.

17. Beltinger, C., Saragovi, H. U., Smith, R. M., LeSauteur, L., Shah, N., DeDionisio, L., Christensen, L., Raible, A., Jarett, L., et Gewirtz, A. M. **(1995)**. Binding, uptake, and intracellular trafficking of phosphorothioate-modified oligodeoxynucleotides. *J Clin Invest.* ***94****(4): 1814-1823*.

18. Benmerah, A., et Lamaze, C. **(2002)**. Endocytose: chaque voie compte! *MEDECINE/SCIENCES.* ***18****(1126-1136*.

19. Bergan, R., Hakim, F., Schwartz, G. N., Kyle, E., Cepada, R., Szabo, J. M., Fowler, D., Gress, R., et Neckers, L. **(1996)**. Electroporation of synthetic oligodeoxynucleotides: a novel technique for ex vivo bone marrow purging. *Blood.* ***88****(2): 731-741*.

20. Boise, L. H., Gonzalez-Garcia, M., Postema, C. E., Ding, L., Lindsten, T., Turka, L. A., Mao, X., Nunez, G., et Thompson, C. B. **(1993)**. bcl-x, a bcl-2-related gene that functions as a dominant regulator of apoptotic cell death. *Cell.* ***74****(4): 597-608*.

21. Brown, D. A., Kang, S. H., Gryaznov, S. M., DeDionisio, L., Heidenreich, O., Sullivan, S., Xu, X., et Nerenberg, M. I. **(1994)**. Effect of phosphorothioate modification of oligodeoxynucleotides on specific protein binding. *J Biol Chem.* ***269****(43): 26801-26805*.

22. Budker, V. G., Knorre, D. G., et Vlassov, V. V. **(1992)**. Cell membranes as barriers for antisense constructions. *Antisense Res Dev.* ***2****(2): 177-184*.

23. Butler, M., Stecker, K., et Bennett, C. F. **(1997)**. Cellular distribution of phosphorothioate oligodeoxynucleotides in normal rodent tissues. *Lab Invest.* ***77****(4): 379-388*.

24. Campbell, J. M., Bacon, T. A., et Wickstrom, E. **(1990)**. Oligodeoxynucleoside phosphorothioate stability in subcellular extracts, culture media, sera and cerebrospinal fluid. *J Biochem Biophys Methods.* ***20****(3): 259-267*.

25. Caron, N. J., Quenneville, S. P., et Tremblay, J. P. **(2004)**. Endosome disruption enhances the functional nuclear delivery of Tat-fusion proteins. *Biochem Biophys Res Commun.* ***319****(1): 12-20*.

26. Cavazzana-Calvo, M., et Fischer, A. **(2004)**. Efficacy of gene therapy for SCID is being confirmed. *Lancet.* ***364****(9452): 2155-2156*.

27. Ceruzzi, M., Draper, K., et Schwartz, J. **(1990)**. Natural and Phosphorothioate-Modified Oligodeoxyribonucleotides Exhibit a Non-Random Cellular Distribution. *Nucleosides, Nucleotides and Nucleic Acids.* ***9****(5): 679-695*.

28. Chan, D. I., Prenner, E. J., et Vogel, H. J. **(2006)**. Tryptophan- and arginine-rich antimicrobial peptides: structures and mechanisms of action. *Biochim Biophys Acta*. ***1758****(9): 1184-1202*.

29. Chellaiah, M. A., Soga, N., Swanson, S., McAllister, S., Alvarez, U., Wang, D., Dowdy, S. F., et Hruska, K. A. **(2000)**. Rho-A is critical for osteoclast podosome organization, motility, and bone resorption. *J Biol Chem.* ***275****(16): 11993-12002*.

30. Chen, Y. N., Sharma, S. K., Ramsey, T. M., Jiang, L., Martin, M. S., Baker, K., Adams, P. D., Bair, K. W., et Kaelin, W. G., Jr. **(1999)**. Selective killing of transformed cells by cyclin/cyclin-dependent kinase 2 antagonists. *Proc Natl Acad Sci U S A.* ***96****(8): 4325-4329*.

31. Ciftci, K., et Levy, R. J. **(2001)**. Enhanced plasmid DNA transfection with lysosomotropic agents in cultured fibroblasts. *Int J Pharm.* ***218****(1-2): 81-92*.

32. Clarenc, J. P., Lebleu, B., et Leonetti, J. P. **(1993)**. Characterization of the nuclear binding sites of oligodeoxyribonucleotides and their analogs. *J Biol Chem.* ***268****(8): 5600-5604*.

33. Clark, R. E. **(1995)**. Poor cellular uptake of antisense oligodeoxynucleotides: an obstacle to their use in chronic myeloid leukaemia. *Leuk Lymphoma.* ***19****((3-4)): 189-195*.

34. Cossum, P. A., Sasmor, H., Dellinger, D., Truong, L., Cummins, L., Owens, S. R., Markham, P. M., Shea, J. P., et Crooke, S. **(1993)**. Disposition of the 14C-labeled phosphorothioate oligonucleotide ISIS 2105 after intravenous administration to rats. *J Pharmacol Exp Ther*. ***267****(3): 1181-1190*.

35. Crooke, S. T. **(2004)**. Progress in antisense technology. *Annu Rev Med.* ***55****(61-95*.

36. Cutrona, G., Carpaneto, E. M., Ulivi, M., Roncella, S., Landt, O., Ferrarini, M., et Boffa, L. C. **(2000)**. Effects in live cells of a c-myc anti-gene PNA linked to a nuclear localization signal. *Nat Biotechnol.* ***18****(3): 300-303*.

37. D'Costa, M., Kumar, V., et Ganesh, K. N. **(2001)**. Aminoethylprolyl (aep) PNA: mixed purine/pyrimidine oligomers and binding orientation preferences for PNA:DNA duplex formation. *Org Lett.* ***3****(9): 1281-1284*.

38. Dash, P., Lotan, I., Knapp, M., Kandel, E. R., et Goelet, P. **(1987)**. Selective elimination of mRNAs in vivo: complementary oligodeoxynucleotides promote RNA degradation by an RNase H-like activity. *Proc Natl Acad Sci U S A.* ***84****(22): 7896-7900*.

39. Dass, C. R. **(2002)**. Cytotoxicity issues pertinent to lipoplex-mediated gene therapy in-vivo. *J Pharm Pharmacol.* ***54****(5): 593-601*.

40. Day, F. H., Zhang, Y., Clair, P., Grabstein, K. H., Mazel, M., Rees, A. R., Kaczorek, M., et Temsamani, J. **(2003)**. Induction of antigen-specific CTL responses using antigens conjugated to short peptide vectors. *J Immunol.* ***170****(3): 1498-1503*.

41. de Diesbach, P., Berens, C., N'Kuli, F., Monsigny, M., Sonveaux, E., Wattiez, R., et Courtoy, P. J. **(2000)**. Identification, purification and partial characterisation of an oligonucleotide receptor in membranes of HepG2 cells. *Nucleic Acids Res.* ***28****(4): 868-874*.

42. de Diesbach, P., N'Kuli, F., Berens, C., Sonveaux, E., Monsigny, M., Roche, A. C., et Courtoy, P. J. **(2002)**. Receptor-mediated endocytosis of phosphodiester oligonucleotides in the HepG2 cell line: evidence for non-conventional intracellular trafficking. *Nucleic Acids Res.* ***30****(7): 1512-1521*.

43. de Duve, C., de Barsy, T., Poole, B., Trouet, A., Tulkens, P., et Van Hoof, F. **(1974)**. Commentary. Lysosomotropic agents. *Biochem Pharmacol.* ***23****(18): 2495-2531*.

44. Debart, F., Abes, S., Deglane, G., Moulton, H. M., Clair, P., Gait, M. J., Vasseur, J. J., et Lebleu, B. **(2007)**. Chemical modifications to improve the cellular uptake of oligonucleotides. *Curr Top Med Chem.* ***7****(7): 727-737*.

45. Debart, F., Abes, S., Deglane, G., Moulton, H. M., Clair, P., Gait, M. J., Vasseur, J. J., et Lebleu, B. **(sous presse)**. Chemical Modifications to Improve the Cellular Uptake of Oligonucleotides. *Current Topics in Medicinal Chemistry.*

46. Deglane, G., Abes, S., Michel, T., Prevot, P., Vives, E., Debart, F., Barvik, I., Lebleu, B., et Vasseur, J. J. **(2006)**. Impact of the guanidinium group on hybridization and cellular uptake of cationic oligonucleotides. *Chembiochem.* ***7****(4): 684-692*.

47. Derossi, D., Calvet, S., Trembleau, A., Brunissen, A., Chassaing, G., et Prochiantz, A. **(1996)**. Cell internalization of the third helix of the Antennapedia homeodomain is receptor-independent. *J Biol Chem.* ***271****(30): 18188-18193*.

48. Derossi, D., Joliot, A. H., Chassaing, G., et Prochiantz, A. **(1994)**. The third helix of the Antennapedia homeodomain translocates through biological membranes. *J Biol Chem.* ***269****(14): 10444-10450*.

49. Deshayes, S., Heitz, A., Morris, M. C., Charnet, P., Divita, G., et Heitz, F. **(2004)**. Insight into the mechanism of internalization of the cell-penetrating carrier peptide Pep-1 through conformational analysis. *Biochemistry.* ***43****(6): 1449-1457*.

50. Dietz, G. P., et Bahr, M. **(2004)**. Delivery of bioactive molecules into the cell: the Trojan horse approach. *Mol Cell Neurosci.* ***27****(2): 85-131*.

51. Dimitrov, D. S. **(2000)**. Cell biology of virus entry. *Cell.* ***101****(7): 697-702*.

52. DiPaola, M., et Maxfield, F. R. **(1984)**. Conformational changes in the receptors for epidermal growth factor and asialoglycoproteins induced by the mildly acidic pH found in endocytic vesicles. *J Biol Chem.* ***259****(14): 9163-9171*.

53. Doherty, T., Waring, A. J., et Hong, M. **(2006)**. Peptide-lipid interactions of the beta-hairpin antimicrobial peptide tachyplesin and its linear derivatives from solid-state NMR. *Biochim Biophys Acta.* ***1758****(9): 1285-1291*.

54. Doherty, T., Waring, A. J., et Hong, M. **(2006)**. Membrane-bound conformation and topology of the antimicrobial peptide tachyplesin I by solid-state NMR. *Biochemistry.* ***45****(44): 13323-13330*.

55. Dragulescu-Andrasi, A., Zhou, P., He, G., et Ly, D. H. **(2005)**. Cell-permeable GPNA with appropriate backbone stereochemistry and spacing binds sequence-specifically to RNA. *Chem Commun (Camb). 2): 244-246*.

56. Drin, G., Cottin, S., Blanc, E., Rees, A. R., et Temsamani, J. **(2003)**. Studies on the internalization mechanism of cationic cell-penetrating peptides. *J Biol Chem.* ***278****(33): 31192-31201*.

57. Drin, G., et Temsamani, J. **(2002)**. Translocation of protegrin I through phospholipid membranes: role of peptide folding. *Biochim Biophys Acta.* ***1559****(2): 160-170*.

58. Eckstein, F. **(2000)**. Phosphorothioate oligodeoxynucleotides: what is their origin and what is unique about them? *Antisense Nucleic Acid Drug Dev.* ***10****(2): 117-121*.

59. Eguchi, A., Akuta, T., Okuyama, H., Senda, T., Yokoi, H., Inokuchi, H., Fujita, S., Hayakawa, T., Takeda, K., Hasegawa, M., et Nakanishi, M. **(2001)**. Protein transduction domain of HIV-1 Tat protein promotes efficient delivery of DNA into mammalian cells. *J Biol Chem.* ***276****(28): 26204-26210*.

60. El-Andaloussi, S., Holm, T., et Langel, U. **(2005)**. Cell-penetrating peptides: mechanisms and applications. *Curr Pharm Des.* ***11****(28): 3597-3611*.

61. Elliott, G., et O'Hare, P. **(1997)**. Intercellular trafficking and protein delivery by a herpesvirus structural protein. *Cell.* ***88****(2): 223-233*.

62. Ellis, J., et Bernstein, A. **(1989)**. Retrovirus vectors containing an internal attachment site: evidence that circles are not intermediates to murine retrovirus integration. *J Virol.* ***63****(6): 2844-2846*.

63. Eum, W. S., Kim, D. W., Hwang, I. K., Yoo, K. Y., Kang, T. C., Jang, S. H., Choi, H. S., Choi, S. H., Kim, Y. H., Kim, S. Y., Kwon, H. Y., Kang, J. H., Kwon, O. S., Cho, S. W., Lee, K. S., Park, J., Won, M. H., et Choi, S. Y. **(2004)**. In vivo protein transduction: biologically active intact pep-1-superoxide dismutase fusion protein efficiently protects against ischemic insult. *Free Radic Biol Med. **37**(10): 1656-1669*.

64. Felgner, P. L., Gadek, T. R., Holm, M., Roman, R., Chan, H. W., Wenz, M., Northrop, J. P., Ringold, G. M., et Danielsen, M. **(1987)**. Lipofection: a highly efficient, lipid-mediated DNA-transfection procedure. *Proc Natl Acad Sci U S A. **84**(21): 7413-7417*.

65. Ferkol, T., Pellicena-Palle, A., Eckman, E., Perales, J. C., Trzaska, T., Tosi, M., Redline, R., et Davis, P. B. **(1996)**. Immunologic responses to gene transfer into mice via the polymeric immunoglobulin receptor. *Gene Ther. **3**(8): 669-678*.

66. Filipowicz, W. **(2005)**. RNAi: the nuts and bolts of the RISC machine. *Cell. **122**(1): 17-20*.

67. Fischer, D., Bieber, T., Li, Y., Elsasser, H. P., et Kissel, T. **(1999)**. A novel non-viral vector for DNA delivery based on low molecular weight, branched polyethylenimine: effect of molecular weight on transfection efficiency and cytotoxicity. *Pharm Res. **16**(8): 1273-1279*.

68. Fisher, L., Soomets, U., Cortes Toro, V., Chilton, L., Jiang, Y., Langel, U., et Iverfeldt, K. **(2004)**. Cellular delivery of a double-stranded oligonucleotide NFkappaB decoy by hybridization to complementary PNA linked to a cell-penetrating peptide. *Gene Ther. **11**(16): 1264-1272*.

69. Flanagan, W. M., et Wagner, R. W. **(1997)**. Potent and selective gene inhibition using antisense oligodeoxynucleotides. *Mol Cell Biochem. **172**(1-2): 213-225*.

70. Fletcher, S., Honeyman, K., Fall, A. M., Harding, P. L., Johnsen, R. D., Steinhaus, J. P., Moulton, H. M., Iversen, P. L., et Wilton, S. D. **(2007)**. Morpholino Oligomer-Mediated Exon Skipping Averts the Onset of Dystrophic Pathology in the mdx Mouse. *Mol Ther 15(9):1587-92.*

71. Folini, M., Berg, K., Millo, E., Villa, R., Prasmickaite, L., Daidone, M. G., Benatti, U., et Zaffaroni, N. **(2003)**. Photochemical internalization of a peptide nucleic acid targeting the catalytic subunit of human telomerase. *Cancer Res. **63**(13): 3490-3494*.

72. Frankel, A. D., et Pabo, C. O. **(1988)**. Cellular uptake of the tat protein from human immunodeficiency virus. *Cell. **55**(6): 1189-1193*.

73. Fredericksen, B. L., Wei, B. L., Yao, J., Luo, T., et Garcia, J. V. **(2002)**. Inhibition of endosomal/lysosomal degradation increases the infectivity of human immunodeficiency virus. *J Virol. **76**(22): 11440-11446*.

74. Friend, D. S., Papahadjopoulos, D., et Debs, R. J. **(1996)**. Endocytosis and intracellular processing accompanying transfection mediated by cationic liposomes. *Biochim Biophys Acta. **1278**(1): 41-50*.

75. Fuchs, S. M., et Raines, R. T. **(2004)**. Pathway for polyarginine entry into mammalian cells. *Biochemistry. **43**(9): 2438-2444*.

76. Futaki, S. **(2002)**. Arginine-rich peptides: potential for intracellular delivery of macromolecules and the mystery of the translocation mechanisms. *Int J Pharm. **245**(1-2): 1-7*.

77. Futaki, S., Ohashi, W., Suzuki, T., Niwa, M., Tanaka, S., Ueda, K., Harashima, H., et Sugiura, Y. **(2001)**. Stearylated arginine-rich peptides: a new class of transfection systems. *Bioconjug Chem. **12**(6): 1005-1011*.

78. Gao, W. Y., Storm, C., Egan, W., et Cheng, Y. C. **(1993)**. Cellular pharmacology of phosphorothioate homooligodeoxynucleotides in human cells. *Mol Pharmacol.* ***43****(1): 45-50*.

79. Garcia-Blanco, M. A., Baraniak, A. P., et Lasda, E. L. **(2004)**. Alternative splicing in disease and therapy. *Nat Biotechnol.* ***22****(5): 535-546*.

80. Gehring, W. J., Qian, Y. Q., Billeter, M., Furukubo-Tokunaga, K., Schier, A. F., Resendez-Perez, D., Affolter, M., Otting, G., et Wuthrich, K. **(1994)**. Homeodomain-DNA recognition. *Cell.* ***78****(2): 211-223*.

81. Geselowitz, D. A., et Neckers, L. M. **(1992)**. Analysis of oligonucleotide binding, internalization, and intracellular trafficking utilizing a novel radiolabeled crosslinker. *Antisense Res Dev.* ***2****(1): 17-25*.

82. Gewirtz, A. M., Sokol, D. L., et Ratajczak, M. Z. **(1998)**. Nucleic acid therapeutics: state of the art and future prospects. *Blood.* ***92****(3): 712-736*.

83. Godbey, W. T., Wu, K. K., Hirasaki, G. J., et Mikos, A. G. **(1999)**. Improved packing of poly(ethylenimine)/DNA complexes increases transfection efficiency. *Gene Ther.* ***6****(8): 1380-1388*.

84. Godbey, W. T., Wu, K. K., et Mikos, A. G. **(1999)**. Size matters: molecular weight affects the efficiency of poly(ethylenimine) as a gene delivery vehicle. *J Biomed Mater Res.* ***45****(3): 268-275*.

85. Goun, E. A., Pillow, T. H., Jones, L. R., Rothbard, J. B., et Wender, P. A. **(2006)**. Molecular transporters: synthesis of oligoguanidinium transporters and their application to drug delivery and real-time imaging. *Chembiochem.* ***7****(10): 1497-1515*.

86. Govindaraju, T., Gonnade, R. G., Bhadbhade, M. M., Kumar, V. A., et Ganesh, K. N. **(2003)**. (1S,2R/1R,2S)-ainocyclohexyl glycyl thymine PNA: synthesis, monomer crystal structures, and DNA/RNA hybridization studies. *Org Lett.* ***5****(17): 3013-3016*.

87. Govindaraju, T., Kumar, V. A., et Ganesh, K. N. **(2004)**. (1S,2R/1R,2S)-cis-cyclopentyl PNAs (cpPNAs) as constrained PNA analogues: synthesis and evaluation of aeg-cpPNA chimera and stereopreferences in hybridization with DNA/RNA. *J Org Chem.* ***69****(17): 5725-5734*.

88. Green, M., et Loewenstein, P. M. **(1988)**. Autonomous functional domains of chemically synthesized human immunodeficiency virus tat trans-activator protein. *Cell.* ***55****(6): 1179-1188*.

89. Guild, B. C., Mulligan, R. C., Gros, P., et Housman, D. E. **(1988)**. Retroviral transfer of a murine cDNA for multidrug resistance confers pleiotropic drug resistance to cells without prior drug selection. *Proc Natl Acad Sci U S A.* ***85****(5): 1595-1599*.

90. Guvakova, M. A., Yakubov, L. A., Vlodavsky, I., Tonkinson, J. L., et Stein, C. A. **(1995)**. Phosphorothioate oligodeoxynucleotides bind to basic fibroblast growth factor, inhibit its binding to cell surface receptors, and remove it from low affinity binding sites on extracellular matrix. *J Biol Chem.* ***270****(6): 2620-2627*.

91. Hanss, B., Leal-Pinto, E., Bruggeman, L. A., Copeland, T. D., et Klotman, P. E. **(1998)**. Identification and characterization of a cell membrane nucleic acid channel. *Proc Natl Acad Sci U S A.* ***95****(4): 1921-1926*.

92. Harford, J., Wolkoff, A. W., Ashwell, G., et Klausner, R. D. **(1983)**. Monensin inhibits intracellular dissociation of asialoglycoproteins from their receptor. *J Cell Biol.* ***96****(6): 1824-1828*.

93. Hariton-Gazal, E., Feder, R., Mor, A., Graessmann, A., Brack-Werner, R., Jans, D., Gilon, C., et Loyter, A. **(2002)**. Targeting of nonkaryophilic cell-permeable peptides into the nuclei of intact cells by covalently attached nuclear localization signals. *Biochemistry. **41**(29): 9208-9214*.

94. Hendrie, P. C., et Russell, D. W. **(2005)**. Gene targeting with viral vectors. *Mol Ther. **12**(1): 9-17*.

95. Henriques, S. T., et Castanho, M. A. **(2004)**. Consequences of nonlytic membrane perturbation to the translocation of the cell penetrating peptide pep-1 in lipidic vesicles. *Biochemistry. **43**(30): 9716-9724*.

96. Henriques, S. T., Melo, M. N., et Castanho, M. A. **(2006)**. Cell-penetrating peptides and antimicrobial peptides: how different are they? *Biochem J. **399**(1): 1-7*.

97. Hoke, G. D., Draper, K., Freier, S. M., Gonzalez, C., Driver, V. B., Zounes, M. C., et Ecker, D. J. **(1991)**. Effects of phosphorothioate capping on antisense oligonucleotide stability, hybridization and antiviral efficacy versus herpes simplex virus infection. *Nucleic Acids Res. **19**(20): 5743-5748*.

98. Isin, B., Doruker, P., et Bahar, I. **(2002)**. Functional motions of influenza virus hemagglutinin: a structure-based analytical approach. *Biophys J. **82**(2): 569-581*.

99. Iversen, P. L., Copple, B. L., et Tewary, H. K. **(1995)**. Pharmacology and toxicology of phosphorothioate oligonucleotides in the mouse, rat, monkey and man. *Toxicol Lett. **82-83**(425-430*.

100. Izant, J. G., et Weintraub, H. **(1984)**. Inhibition of thymidine kinase gene expression by anti-sense RNA: a molecular approach to genetic analysis. *Cell. **36**(4): 1007-1015*.

101. Jarver, P., et Langel, U. **(2004)**. The use of cell-penetrating peptides as a tool for gene regulation. *Drug Discov Today. **9**(9): 395-402*.

102. Joliot, A., Pernelle, C., Deagostini-Bazin, H., et Prochiantz, A. **(1991)**. Antennapedia homeobox peptide regulates neural morphogenesis. *Proc Natl Acad Sci U S A. **88**(5): 1864-1868*.

103. Josephson, L., Tung, C. H., Moore, A., et Weissleder, R. **(1999)**. High-efficiency intracellular magnetic labeling with novel superparamagnetic-Tat peptide conjugates. *Bioconjug Chem. **10**(2): 186-191*.

104. Kang, S. H., Cho, M. J., et Kole, R. **(1998)**. Up-regulation of luciferase gene expression with antisense oligonucleotides: implications and applications in functional assay development. *Biochemistry. **37**(18): 6235-6239*.

105. Kaushik, N., Basu, A., et Pandey, V. N. **(2002)**. Inhibition of HIV-1 replication by anti-trans-activation responsive polyamide nucleotide analog. *Antiviral Res. **56**(1): 13-27*.

106. Kim, Y. H., Park, J. H., Lee, M., Kim, Y. H., Park, T. G., et Kim, S. W. **(2005)**. Polyethylenimine with acid-labile linkages as a biodegradable gene carrier. *J Control Release. **103**(1): 209-219*.

107. Kobayashi, S., Chikushi, A., Tougu, S., Imura, Y., Nishida, M., Yano, Y., et Matsuzaki, K. **(2004)**. Membrane translocation mechanism of the antimicrobial peptide buforin 2. *Biochemistry. **43**(49): 15610-15616*.

108. Kola, I., et Sumarsono, S. H. **(1995)**. Microinjection of in vitro transcribed RNA and antisense oligonucleotides in mouse oocytes and early embryos to study the gain- and loss-of-function of genes. *Methods Mol Biol. **37**(135-149*.

109. Kole, R., Williams, T., et Cohen, L. **(2004)**. RNA modulation, repair and remodeling by splice switching oligonucleotides. *Acta Biochim Pol.* ***51****(2): 373-378*.

110. Krajewska, M., Krajewski, S., Epstein, J. I., Shabaik, A., Sauvageot, J., Song, K., Kitada, S., et Reed, J. C. **(1996)**. Immunohistochemical analysis of bcl-2, bax, bcl-X, and mcl-1 expression in prostate cancers. *Am J Pathol.* ***148****(5): 1567-1576*.

111. Kraus, L. M. **(1961)**. Formation of different haemoglobins in tissue culture of human bone marrow treated with human deoxyribonucleic acid. *Nature.* ***192****(1055-1057*.

112. Kurreck, J. **(2003)**. Antisense technologies. Improvement through novel chemical modifications. *Eur J Biochem.* ***270****(8): 1628-1644*.

113. Lam, K. L., Ishitsuka, Y., Cheng, Y., Chien, K., Waring, A. J., Lehrer, R. I., et Lee, K. Y. **(2006)**. Mechanism of supported membrane disruption by antimicrobial peptide protegrin-1. *J Phys Chem B Condens Matter Mater Surf Interfaces Biophys.* ***110****(42): 21282-21286*.

114. Langel, U., Pooga, M., Kairane, C., Zilmer, M., et Bartfai, T. **(1996)**. A galanin-mastoparan chimeric peptide activates the Na+,K(+)-ATPase and reverses its inhibition by ouabain. *Regul Pept.* ***62****(1): 47-52*.

115. Lau, W. L., Ege, D. S., Lear, J. D., Hammer, D. A., et DeGrado, W. F. **(2004)**. Oligomerization of fusogenic peptides promotes membrane fusion by enhancing membrane destabilization. *Biophys J.* ***86****(1 Pt 1): 272-284*.

116. Lemaitre, M., Bayard, B., et Lebleu, B. **(1987)**. Specific antiviral activity of a poly(L-lysine)-conjugated oligodeoxyribonucleotide sequence complementary to vesicular stomatitis virus N protein mRNA initiation site. *Proc Natl Acad Sci U S A.* ***84****(3): 648-652*.

117. Leonetti, J. P., Degols, G., et Lebleu, B. **(1990)**. Biological activity of oligonucleotide-poly(L-lysine) conjugates: mechanism of cell uptake. *Bioconjug Chem.* ***1****(2): 149-153*.

118. Leonetti, J. P., Mechti, N., Degols, G., Gagnor, C., et Lebleu, B. **(1991)**. Intracellular distribution of microinjected antisense oligonucleotides. *Proc Natl Acad Sci U S A.* ***88****(7): 2702-2706*.

119. Leonetti, J. P., Rayner, B., Lemaitre, M., Gagnor, C., Milhaud, P. G., Imbach, J. L., et Lebleu, B. **(1988)**. Antiviral activity of conjugates between poly(L-lysine) and synthetic oligodeoxyribonucleotides. *Gene.* ***72****(1-2): 323-332*.

120. Levin, A. A. **(1999)**. A review of the issues in the pharmacokinetics and toxicology of phosphorothioate antisense oligonucleotides. *Biochim Biophys Acta.* ***1489****(1): 69-84*.

121. Li, Q. X., Tan, P., Ke, N., et Wong-Staal, F. **(2007)**. Ribozyme technology for cancer gene target identification and validation. *Adv Cancer Res.* ***96****(103-143*.

122. Li, W., Nicol, F., et Szoka, F. C., Jr. **(2004)**. GALA: a designed synthetic pH-responsive amphipathic peptide with applications in drug and gene delivery. *Adv Drug Deliv Rev.* ***56****(7): 967-985*.

123. Lonkar, P. S., Ganesh, K. N., et Kumar, V. A. **(2004)**. Chimeric (aeg-pyrrolidine)PNAs: synthesis and stereo-discriminative duplex binding with DNA/RNA. *Org Biomol Chem.* ***2****(18): 2604-2611*.

124. Lundberg, P., Magzoub, M., Lindberg, M., Hallbrink, M., Jarvet, J., Eriksson, L. E., Langel, U., et Graslund, A. **(2002)**. Cell membrane translocation of the N-terminal (1-28) part of the prion protein. *Biochem Biophys Res Commun.* ***299****(1): 85-90*.

125. Luo, D., et Saltzman, W. M. **(2000)**. Synthetic DNA delivery systems. *Nat Biotechnol.* ***18****(1): 33-37*.

126. Lv, H., Zhang, S., Wang, B., Cui, S., et Yan, J. **(2006)**. Toxicity of cationic lipids and cationic polymers in gene delivery. *J Control Release.* ***114****(1): 100-109*.

127. Mai, J. C., Shen, H., Watkins, S. C., Cheng, T., et Robbins, P. D. **(2002)**. Efficiency of protein transduction is cell type-dependent and is enhanced by dextran sulfate. *J Biol Chem.* ***277****(33): 30208-30218*.

128. Maier, M. A., Barber-Peoc'h, I., et Manoharan, M. **(2002)**. Postsynthetic guanidinylation of primary amino groups in the minor and major grooves of oligonucleotides. *Tetrahedron Letters.* ***43****(42): 7613-7616*.

129. Maiolo, J. R., 3rd., Ottinger, E. A., et Ferrer, M. **(2004)**. Specific redistribution of cell-penetrating peptides from endosomes to the cytoplasm and nucleus upon laser illumination. *J Am Chem Soc.* ***126****(47): 15376-15377*.

130. Mancheno-Corvo, P., et Martin-Duque, P. **(2006)**. Viral gene therapy. *Clin Transl Oncol.* ***8****(12): 858-867*.

131. Mano, M., Henriques, A., Paiva, A., Prieto, M., Gavilanes, F., Simoes, S., et Pedroso de Lima, M. C. **(2006)**. Cellular uptake of S413-PV peptide occurs upon conformational changes induced by peptide-membrane interactions. *Biochim Biophys Acta.* ***1758****(3): 336-346*.

132. Marone, M., Scambia, G., Mozzetti, S., Ferrandina, G., Iacovella, S., De Pasqua, A., Benedetti-Panici, P., et Mancuso, S. **(1998)**. bcl-2, bax, bcl-XL, and bcl-XS expression in normal and neoplastic ovarian tissues. *Clin Cancer Res.* ***4****(2): 517-524*.

133. Matsukura, M., Shinozuka, K., Zon, G., Mitsuya, H., Reitz, M., Cohen, J. S., et Broder, S. **(1987)**. Phosphorothioate analogs of oligodeoxynucleotides: inhibitors of replication and cytopathic effects of human immunodeficiency virus. *Proc Natl Acad Sci U S A.* ***84****(21): 7706-7710*.

134. Matsushita, M., Noguchi, H., Lu, Y. F., Tomizawa, K., Michiue, H., Li, S. T., Hirose, K., Bonner-Weir, S., et Matsui, H. **(2004)**. Photo-acceleration of protein release from endosome in the protein transduction system. *FEBS Lett.* ***572****(1-3): 221-226*.

135. Matsuzaki, K. **(1998)**. Magainins as paradigm for the mode of action of pore forming polypeptides. *Biochim Biophys Acta.* ***1376****(3): 391-400*.

136. Matsuzaki, K., Murase, O., Fujii, N., et Miyajima, K. **(1995)**. Translocation of a channel-forming antimicrobial peptide, magainin 2, across lipid bilayers by forming a pore. *Biochemistry.* ***34****(19): 6521-6526*.

137. Matzura, H., et Eckstein, F. **(1968)**. A polyribonucleotide containing alternation P=O and P=S linkages. *Eur J Biochem.* ***3****(4): 448-452*.

138. Mercatante, D. R., Mohler, J. L., et Kole, R. **(2002)**. Cellular response to an antisense-mediated shift of Bcl-x pre-mRNA splicing and antineoplastic agents. *J Biol Chem.* ***277****(51): 49374-49382*.

139. Mercatante, D. R., Sazani, P., et Kole, R. **(2001)**. Modification of alternative splicing by antisense oligonucleotides as a potential chemotherapy for cancer and other diseases. *Curr Cancer Drug Targets.* ***1****(3): 211-230*.

140. Mercatante, D. R., Sazani, P., et Kole, R. **(2001)**. Modification of alternative splicing by antisense oligonucleotides as a potential chemotherapy for cancer and other diseases. *Curr Cancer Drug Targets.* ***1****(3): 211-230*.

141. Michel, T., Martinand-Mari, C., Debart, F., Lebleu, B., Robbins, I., et Vasseur, J. J. **(2003)**. Cationic phosphoramidate alpha-oligonucleotides efficiently target single-stranded DNA and RNA and inhibit hepatitis C virus IRES-mediated translation. *Nucleic Acids Res.* ***31****(18): 5282-5290*.

142. Midoux, P., Kichler, A., Boutin, V., Maurizot, J. C., et Monsigny, M. **(1998)**. Membrane permeabilization and efficient gene transfer by a peptide containing several histidines. *Bioconjug Chem.* ***9****(2): 260-267*.

143. Miller, A. D., Miller, D. G., Garcia, J. V., et Lynch, C. M. **(1993)**. Use of retroviral vectors for gene transfer and expression. *Methods Enzymol.* ***217****(581-599*.

144. Minshull, J., et Hunt, T. **(1986)**. The use of single-stranded DNA and RNase H to promote quantitative 'hybrid arrest of translation' of mRNA/DNA hybrids in reticulocyte lysate cell-free translations. *Nucleic Acids Res.* ***14****(16): 6433-6451*.

145. Mitchell, D. J., Kim, D. T., Steinman, L., Fathman, C. G., et Rothbard, J. B. **(2000)**. Polyarginine enters cells more efficiently than other polycationic homopolymers. *J Pept Res.* ***56****(5): 318-325*.

146. Mizuguchi, H., et Hayakawa, T. **(2004)**. Targeted adenovirus vectors. *Hum Gene Ther.* ***15****(11): 1034-1044*.

147. Mizuno, T., Chou, M. Y., et M., I. **(1984)**. A unique mechanism regulating gene expression: translational inhibition by a complementary RNA transcript (micRNA). *Proc Natl Acad Sci U S A.* ***81****(7): 1966-1970*.

148. Morris, M. C., Chaloin, L., Choob, M., Archdeacon, J., Heitz, F., et Divita, G. **(2004)**. Combination of a new generation of PNAs with a peptide-based carrier enables efficient targeting of cell cycle progression. *Gene Ther*. ***11****(9): 757-764*.

149. Morris, M. C., Chaloin, L., Mery, J., Heitz, F., et Divita, G. **(1999)**. A novel potent strategy for gene delivery using a single peptide vector as a carrier. *Nucleic Acids Res.* ***27****(17): 3510-3517*.

150. Morris, M. C., Depollier, J., Mery, J., Heitz, F., et Divita, G. **(2001)**. A peptide carrier for the delivery of biologically active proteins into mammalian cells. *Nat Biotechnol.* ***19****(12): 1173-1176*.

151. Morris, M. C., Vidal, P., Chaloin, L., Heitz, F., et Divita, G. **(1997)**. A new peptide vector for efficient delivery of oligonucleotides into mammalian cells. *Nucleic Acids Res.* ***15****(14): 2730-2736*.

152. Moulton, H. M., Fletcher, S., Neuman, B. W., McClorey, G., Stein, D. A., Abes, S., Wilton, S. D., Buchmeier, M. J., Lebleu, B., et Iversen, P. L. **(2007)**. Cell-penetrating peptide-morpholino conjugates alter pre-mRNA splicing of DMD (Duchenne muscular dystrophy) and inhibit murine coronavirus replication in vivo. *Biochem Soc Trans.* ***35****(Pt 4): 826-828*.

153. Moulton, H. M., Hase, M. C., Smith, K. M., et Iversen, P. L. **(2003)**. HIV Tat peptide enhances cellular delivery of antisense morpholino oligomers. *Antisense Nucleic Acid Drug Dev.* ***13****(1): 31-43*.

154. Nelson, M. H., Stein, D. A., Kroeker, A. D., Hatlevig, S. A., Iversen, P. L., et Moulton, H. M. **(2005)**. Arginine-rich peptide conjugation to morpholino oligomers: effects on antisense activity and specificity. *Bioconjug Chem.* ***16****(4): 959-966*.

155. Nelson, N. **(1987)**. The vacuolar proton-ATPase of eukaryotic cells. *Bioessays.* ***7****(6): 251-254*.

156. Niesner, U., Halin, C., Lozzi, L., Gunthert, M., Neri, P., Wunderli-Allenspach, H., Zardi, L., et Neri, D. **(2002)**. Quantitation of the tumor-targeting properties of antibody fragments conjugated to cell-permeating HIV-1 TAT peptides. *Bioconjug Chem.* ***13****(4): 729-736*.

157. Nuessler, V., Stotzer, O., Gullis, E., Pelka-Fleischer, R., Pogrebniak, A., Gieseler, F., et Wilmanns, W. **(1999)**. Bcl-2, bax and bcl-xL expression in human sensitive and resistant leukemia cell lines. *Leukemia.* ***13****(11): 1864-1872*.

158. Oehlke, J., Scheller, A., Wiesner, B., Krause, E., Beyermann, M., Klauschenz, E., Melzig, M., et Bienert, M. **(1998)**. Cellular uptake of an alpha-helical amphipathic model peptide with the potential to deliver polar compounds into the cell interior non-endocytically. *Biochim Biophys Acta.* ***1414****(1-2): 127-139*.

159. Oehlke, J., Wallukat, G., Wolf, Y., Ehrlich, A., Wiesner, B., Berger, H., et Bienert, M. **(2004)**. Enhancement of intracellular concentration and biological activity of PNA after conjugation with a cell-penetrating synthetic model peptide. *Eur J Biochem.* ***271****(14): 3043-3049*.

160. Ohmori, N., Niidome, T., Wada, A., Hirayama, T., Hatakeyama, T., et Aoyagi, H. **(1997)**. The enhancing effect of anionic alpha-helical peptide on cationic peptide-mediating transfection systems. *Biochem Biophys Res Commun.* ***235****(3): 726-729*.

161. Ohsaki, M., Okuda, T., Wada, A., Hirayama, T., Niidome, T., et Aoyagi, H. **(2002)**. In vitro gene transfection using dendritic poly(L-lysine). *Bioconjug Chem.* ***13****(3): 510-517*.

162. Okuda, T., Sugiyama, A., Niidome, T., et Aoyagi, H. **(2004)**. Characters of dendritic poly(L-lysine) analogues with the terminal lysines replaced with arginines and histidines as gene carriers in vitro. *Biomaterials.* ***25****(3): 537-544*.

163. Park, C. B., Kim, H. S., et Kim, S. C. **(1998)**. Mechanism of action of the antimicrobial peptide buforin II: buforin II kills microorganisms by penetrating the cell membrane and inhibiting cellular functions. *Biochem Biophys Res Commun.* ***244****(1): 253-257*.

164. Paterson, B. M., Roberts, B. E., et Kuff, E. L. **(1977)**. Structural gene identification and mapping by DNA-mRNA hybrid-arrested cell-free translation. *Proc Natl Acad Sci U S A.* ***74****(10): 4370-4374*.

165. Pecheur, E. I., Sainte-Marie, J., Bienven e, A., et Hoekstra, D. **(1999)**. Peptides and membrane fusion: towards an understanding of the molecular mechanism of protein-induced fusion. *J Membr Biol.* ***167****(1): 1-17*.

166. Peitz, M., Pfannkuche, K., Rajewsky, K., et Edenhofer, F. **(2002)**. Ability of the hydrophobic FGF and basic TAT peptides to promote cellular uptake of recombinant Cre recombinase: a tool for efficient genetic engineering of mammalian genomes. *Proc Natl Acad Sci U S A.* ***99****(7): 4489-4494*.

167. Perales, J. C., Ferkol, T., Molas, M., et Hanson, R. W. **(1994)**. An evaluation of receptor-mediated gene transfer using synthetic DNA-ligand complexes. *Eur J Biochem.* ***226****(2): 255-266*.

168. Pichon, C., Freulon, I., Midoux, P., Mayer, R., Monsigny, M., et Roche, A. C. **(1997)**. Cytosolic and nuclear delivery of oligonucleotides mediated by an amphiphilic anionic peptide. *Antisense Nucleic Acid Drug Dev.* ***4****(335-343*.

169. Pichon, C., Goncalves, C., et Midoux, P. **(2001)**. Histidine-rich peptides and polymers for nucleic acids delivery. *Adv Drug Deliv Rev.* ***53****(1): 75-94*.

170. Pillai, R. S. **(2005)**. MicroRNA function: multiple mechanisms for a tiny RNA? *RNA.* ***11****(12): 1753-1761*.

171. Pooga, M., Hallbrink, M., Zorko, M., et Langel, U. **(1998)**. Cell penetration by transportan. *FASEB J.* ***12****(1): 67-77*.

172. Pooga, M., Kut, C., Kihlmark, M., Hallbrink, M., Fernaeus, S., Raid, R., Land, T., Hallberg, E., Bartfai, T., et Langel, U. **(2001)**. Cellular translocation of proteins by transportan. *Faseb J.* ***15****(8): 1451-1453*.

173. Pooga, M., Lindgren, M., Hallbrink, M., Brakenhielm, E., et Langel, U. **(1998)**. Galanin-based peptides, galparan and transportan, with receptor-dependent and independent activities. *Ann N Y Acad Sci.* ***863****(450-453*.

174. Prochiantz, A. **(1996)**. Getting hydrophilic compounds into cells: lessons from homeopeptides. *Curr Opin Neurobiol.* ***6****(5): 629-634*.

175. Pujals, S., Fernandez-Carneado, J., Lopez-Iglesias, C., Kogan, M. J., et Giralt, E. **(2006)**. Mechanistic aspects of CPP-mediated intracellular drug delivery: relevance of CPP self-assembly. *Biochim Biophys Acta.* ***1758****(3): 264-279*.

176. Que-Gewirth, N. S., et Sullenger, B. A. **(2007)**. Gene therapy progress and prospects: RNA aptamers. *Gene Ther.* ***14****(4): 283-291*.

177. Raso, V., Brown, M., McGrath, J., Liu, S., et Stafford, W. F. **(1997)**. Antibodies capable of releasing diphtheria toxin in response to the low pH found in endosomes. *J Biol Chem.* ***272****(44): 27618-27622*.

178. Resina, S., Kole, R., Travo, A., Lebleu, B., et Thierry, A. R. **(2007)**. Switching on transgene expression by correcting aberrant splicing using multi-targeting steric-blocking oligonucleotides. *J Gene Med.* ***9****(6): 498-510*.

179. Richard, J. P., Melikov, K., Brooks, H., Prevot, P., Lebleu, B., et Chernomordik, L. V. **(2005)**. Cellular uptake of unconjugated TAT peptide involves clathrin-dependent endocytosis and heparan sulfate receptors. *J Biol Chem.* ***280****(15): 15300-15306*.

180. Richard, J. P., Melikov, K., Vives, E., Ramos, C., Verbeure, B., Gait, M. J., Chernomordik, L. V., et Lebleu, B. **(2003)**. Cell-penetrating peptides. A reevaluation of the mechanism of cellular uptake. *J Biol Chem.* ***278****(1): 585-590*.

181. Robles, J., Grandas, A., et Pedroso, E. **(2001)**. Synthesis of modified oligonucleotides containing 4-guanidino-2-pyrimidinone nucleobases. *Tetrahedron.* ***57****(1): 179-194*.

182. Rockwell, P., O'Connor, W. J., King, K., Goldstein, N. I., Zhang, L. M., et Stein, C. A. **(1997)**. Cell-surface perturbations of the epidermal growth factor and vascular endothelial growth factor receptors by phosphorothioate oligodeoxynucleotides. *Proc Natl Acad Sci U S A.* ***94****(12): 6523-6528*.

183. Roe, T., Reynolds, T. C., Yu, G., et Brown, P. O. **(1993)**. Integration of murine leukemia virus DNA depends on mitosis. *EMBO J.* ***12****(5): 2099-2108*.

184. Roig, V., et Asseline, U. **(2003)**. Oligo-2'-deoxyribonucleotides containing uracil modified at the 5-position with linkers ending with guanidinium groups. *J Am Chem Soc.* ***125****(15): 4416-4417*.

185. Roosjen, A., misterová, J., Driessen, C., Anders, J. T., Wagenaar, A., Hoekstra, D., Hulst, R., et Engberts, J. B. F. N. **(2002)**. Synthesis and Characteristics of Biodegradable Pyridinium Amphiphiles Used for in vitro DNA Delivery. *European Journal of Organic Chemistry.* ***2002****(7): 1271-1277*.

186. Root, C. N., Wills, E. G., McNair, L. L., et Whittaker, G. R. **(2000)**. Entry of influenza viruses into cells is inhibited by a highly specific protein kinase C inhibitor. *J Gen Virol.* ***81****(Pt 11): 2697-2705*.

187. Rothbard, J. B., Garlington, S., Lin, Q., Kirschberg, T., Kreider, E., McGrane, P., Wender, P. A., et Khavari, P. A. **(2000)**. Conjugation of arginine oligomers to cyclosporin A facilitates topical delivery and inhibition of inflammation. *Nat Med.* ***6****(11): 1253-1257*.

188. Rothbard, J. B., Jessop, T. C., Lewis, R. S., Murray, B. A., et Wender, P. A. **(2004)**. Role of membrane potential and hydrogen bonding in the mechanism of translocation of guanidinium-rich peptides into cells. *J Am Chem Soc.* ***126****(31): 9506-9507*.

189. Rothbard, J. B., Kreider, E., VanDeusen, C. L., Wright, L., Wylie, B. L., et Wender, P. A. **(2002)**. Arginine-rich molecular transporters for drug delivery: role of backbone spacing in cellular uptake. *J Med Chem.* ***45****(17): 3612-3618*.

190. Rousselle, C., Clair, P., Smirnova, M., Kolesnikov, Y., Pasternak, G. W., Gac-Breton, S., Rees, A. R., Scherrmann, J. M., et Temsamani, J. **(2003)**. Improved brain uptake and pharmacological activity of dalargin using a peptide-vector-mediated strategy. *J Pharmacol Exp Ther.* ***306****(1): 371-376.*

191. Ryser, H. J., et Shen, W. C. **(1978)**. Conjugation of methotrexate to poly(L-lysine) increases drug transport and overcomes drug resistance in cultured cells. *Proc Natl Acad Sci U S A.* ***75****(8): 3867-3870*.

192. Sandgren, S., Cheng, F., et Belting, M. **(2002)**. Nuclear targeting of macromolecular polyanions by an HIV-Tat derived peptide. Role for cell-surface proteoglycans. *J Biol Chem.* ***277****(41): 38877-38883*.

193. Sandgren, S., Wittrup, A., Cheng, F., Jonsson, M., Eklund, E., Busch, S., et Belting, M. **(2004)**. The human antimicrobial peptide LL-37 transfers extracellular DNA plasmid to the nuclear compartment of mammalian cells via lipid rafts and proteoglycan-dependent endocytosis. *J Biol Chem.* ***279****(17): 17951-17956*.

194. Sandvig, K., et Olsnes, S. **(1981)**. Rapid entry of nicked diphtheria toxin into cells at low pH. Characterization of the entry process and effects of low pH on the toxin molecule. *J Biol Chem.* ***256****(17): 9068-9076*.

195. Sandvig, K., et van Deurs, B. **(2005)**. Delivery into cells: lessons learned from plant and bacterial toxins. *Gene Ther.* ***12****(11): 865-872*.

196. Sazani, P., Gemignani, F., Kang, S. H., Maier, M. A., Manoharan, M., Persmark, M., Bortner, D., et Kole, R. **(2002)**. Systemically delivered antisense oligomers upregulate gene expression in mouse tissues. *Nat Biotechnol.* ***20****(12): 1228-1233*.

197. Sazani, P., Kang, S. H., Maier, M. A., Wei, C., Dillman, J., Summerton, J., Manoharan, M., et Kole, R. **(2001)**. Nuclear antisense effects of neutral, anionic and cationic oligonucleotide analogs. *Nucleic Acids Res.* ***29****(19): 3965-3974*.

198. Schmidt, M. C., Rothen-Rutishauser, B., Rist, B., Beck-Sickinger, A., Wunderli-Allenspach, H., Rubas, W., Sadee, W., et Merkle, H. P. **(1998)**. Translocation of human calcitonin in respiratory nasal epithelium is associated with self-assembly in lipid membrane. *Biochemistry.* ***37****(47): 16582-16590*.

199. Shen, W. C., et Ryser, H. J. **(1981)**. Poly(L-lysine) has different membrane transport and drug-carrier properties when complexed with heparin. *Proc Natl Acad Sci U S A.* ***78****(12): 7589-7593*.

200. Shi, F., et Hoekstra, D. **(2004)**. Effective intracellular delivery of oligonucleotides in order to make sense of antisense. *J Control Release.* ***97****(2): 189-209*.

201. Shiraishi, T., et Nielsen, P. E. **(2006)**. Photochemically enhanced cellular delivery of cell penetrating peptide-PNA conjugates. *FEBS Lett.* ***580****(5): 1451-1456*.

202. Simeoni, F., Morris, M. C., Heitz, F., et Divita, G. **(2003)**. Insight into the mechanism of the peptide-based gene delivery system MPG: implications for delivery of siRNA into mammalian cells. *Nucleic Acids Res.* ***31****(11): 2717-2724*.

203. Simonian, P. L., Grillot, D. A., et Nunez, G. **(1997)**. Bcl-2 and Bcl-XL can differentially block chemotherapy-induced cell death. *Blood.* ***90****(3): 1208-1216*.

204. Simons, R. W., et Kleckner, N. **(1983)**. Translational control of IS10 transposition. *Cell.* ***34****(2): 683-691*.

205. Siwkowski, A. M., Malik, L., Esau, C. C., Maier, M. A., Wancewicz, E. V., Albertshofer, K., Monia, B. P., Bennett, C. F., et Eldrup, A. B. **(2004)**. Identification and functional validation of PNAs that inhibit murine CD40 expression by redirection of splicing. *Nucleic Acids Res.* ***32****(9): 2695-2706*.

206. Snyder, E. L., Meade, B. R., Saenz, C. C., et Dowdy, S. F. **(2004)**. Treatment of terminal peritoneal carcinomatosis by a transducible p53-activating peptide. *PLoS Biol.* ***2****(2): E36*.

207. Solodin, I., Brown, C. S., Bruno, M. S., Chow, C. Y., Jang, E. H., Debs, R. J., et Heath, T. D. **(1995)**. A novel series of amphiphilic imidazolinium compounds for in vitro and in vivo gene delivery. *Biochemistry.* ***34****(41): 13537-13544*.

208. Soomets, U., Lindgren, M., Gallet, X., Hallbrink, M., Elmquist, A., Balaspiri, L., Zorko, M., Pooga, M., Brasseur, R., et Langel, U. **(2000)**. Deletion analogues of transportan. *Biochim Biophys Acta.* ***1467****(1): 165-176*.

209. Srinivasan, S. K., et Iversen, P. L. **(1995)**. Review of in vivo pharmacokinetics and toxicology of phosphorothioate oligonucleotides. *J Clin Lab Anal.* ***9****(2): 129-137*.

210. Suzuki, T., Futaki, S., Niwa, M., Tanaka, S., Ueda, K., et Sugiura, Y. **(2002)**. Possible existence of common internalization mechanisms among arginine-rich peptides. *J Biol Chem.* ***277****(4): 2437-2443*.

211. Takeshima, K., Chikushi, A., Lee, K. K., Yonehara, S., et Matsuzaki, K. **(2003)**. Translocation of analogues of the antimicrobial peptides magainin and buforin across human cell membranes. *J Biol Chem.* ***278****(2): 1310-1315*.

212. Taylor, S. I., et Leventhal, S. **(1983)**. Defect in cooperativity in insulin receptors from a patient with a congenital form of extreme insulin resistance. *J Clin Invest.* ***71****(6): 1676-1685*.

213. Temsamani, J., Kubert, M., Tang, J., Padmapriya, A., et Agrawal, S. **(1994)**. Cellular uptake of oligodeoxynucleotide phosphorothioates and their analogs. *Antisense Res Dev.* ***4****(1): 35-42*.

214. Thierry, A. R., Abes, S., Resina, S., Travo, A., Richard, J. P., Prevot, P., et Lebleu, B. **(2006)**. Comparison of basic peptides- and lipid-based strategies for the delivery of splice correcting oligonucleotides. *Biochim Biophys Acta.* ***1758****(3): 364-374*.

215. Thierry, A. R., Abes, S., Resina, S., Travo, A., Richard, J. P., Prevot, P., et Lebleu, B. **(2006)**. Comparison of basic peptides- and lipid-based strategies for the delivery of splice correcting oligonucleotides. *Biochim Biophys Acta.* ***1758****(3): 364-374*.

216. Thierry, A. R., Vives, E., Richard, J. P., Prevot, P., Martinand-Mari, C., Robbins, I., et Lebleu, B. **(2003)**. Cellular uptake and intracellular fate of antisense oligonucleotides. *Curr Opin Mol Ther. **5**(2): 133-138.*

217. Thoren, P. E., Persson, D., Isakson, P., Goksor, M., Onfelt, A., et Norden, B. **(2003)**. Uptake of analogs of penetratin, Tat(48-60) and oligoarginine in live cells. *Biochem Biophys Res Commun. **307**(1): 100-107.*

218. Thoren, P. E., Persson, D., Karlsson, M., et Norden, B. **(2000)**. The antennapedia peptide penetratin translocates across lipid bilayers - the first direct observation. *FEBS Lett. **482**(3): 265-268.*

219. Torchilin, V. P. **(2006)**. Recent approaches to intracellular delivery of drugs and DNA and organelle targeting. *Annu Rev Biomed Eng. **8**(343-375.*

220. Tung, C. H., Mueller, S., et Weissleder, R. **(2002)**. Novel branching membrane translocational peptide as gene delivery vector. *Bioorg Med Chem. **10**(11): 3609-3614.*

221. Turner, J. J., Arzumanov, A. A., et Gait, M. J. **(2005)**. Synthesis, cellular uptake and HIV-1 Tat-dependent trans-activation inhibition activity of oligonucleotide analogues disulphide-conjugated to cell-penetrating peptides. *Nucleic Acids Res. **33**(1): 27-42.*

222. Turner, J. J., Ivanova, G. D., Verbeure, B., Williams, D., Arzumanov, A. A., Abes, S., Lebleu, B., et Gait, M. J. **(2005)**. Cell-penetrating peptide conjugates of peptide nucleic acids (PNA) as inhibitors of HIV-1 Tat-dependent trans-activation in cells. *Nucleic Acids Res. **33**(21): 6837-6849.*

223. Tycko, B., DiPaola, M., Yamashiro, D. J., Fluss, S., et Maxfield, F. R. **(1983)**. Acidification of endocytic vesicles and the intracellular pathways of ligands and receptors. *Ann N Y Acad Sci. **421**(424-433.*

224. Tycko, B., et Maxfield, F. R. **(1982)**. Rapid acidification of endocytic vesicles containing alpha 2-macroglobulin. *Cell. **28**(3): 643-651.*

225. Van Renswoude, J., Bridges, K. R., Harford, J. B., et Klausner, R. D. **(1982)**. Receptor-mediated endocytosis of transferrin and the uptake of fe in K562 cells: identification of a nonlysosomal acidic compartment. *Proc Natl Acad Sci U S A. **79**(20): 6186-6190.*

226. Venables, J. P. **(2004)**. Aberrant and alternative splicing in cancer. *Cancer Res. **64**(21): 7647-7654.*

227. Venables, J. P. **(2006)**. Unbalanced alternative splicing and its significance in cancer. *Bioessays. **28**(4): 378-386.*

228. Vendeville, A., Rayne, F., Bonhoure, A., Bettache, N., Montcourrier, P., et Beaumelle, B. **(2004)**. HIV-1 Tat enters T cells using coated pits before translocating from acidified endosomes and eliciting biological responses. *Mol Biol Cell. **15**(5): 2347-2360.*

229. Villa, R., Folini, M., Lualdi, S., Veronese, S., Daidone, M. G., et Zaffaroni, N. **(2000)**. Inhibition of telomerase activity by a cell-penetrating peptide nucleic acid construct in human melanoma cells. *FEBS Lett. **473**(2): 241-248.*

230. Violini, S., Sharma, V., Prior, J. L., Dyszlewski, M., et Piwnica-Worms, D. **(2002)**. Evidence for a plasma membrane-mediated permeability barrier to Tat basic domain in well-differentiated epithelial cells: lack of correlation with heparan sulfate. *Biochemistry. **41**(42): 12652-12661.*

231. Vives, E., Brodin, P., et Lebleu, B. **(1997)**. A truncated HIV-1 Tat protein basic domain rapidly translocates through the plasma membrane and accumulates in the cell nucleus. *J Biol Chem.* ***272****(25): 16010-16017*.

232. Vives, E., Granier, C., Prevot, P., et Lebleu, B. **(1997)**. Structure activity relationship study of the plasma membrane translocating potential of a short peptide from HIV-1 Tat protein. *Lettres Peptide Sci.* ***4****(429-436*.

233. Wacheck, V., et Zangemeister-Wittke, U. **(2006)**. Antisense molecules for targeted cancer therapy. *Crit Rev Oncol Hematol.* ***59****(1): 65-73*.

234. Wadia, J. S., Stan, R. V., et Dowdy, S. F. **(2004)**. Transducible TAT-HA fusogenic peptide enhances escape of TAT-fusion proteins after lipid raft macropinocytosis. *Nat Med.* ***10****(3): 310-315*.

235. Wagner, E. **(1999)**. Application of membrane-active peptides for nonviral gene delivery. *Adv Drug Deliv Rev.* ***38****(3): 279-289*.

236. Walder, R. Y., et Walder, J. A. **(1988)**. Role of RNase H in hybrid-arrested translation by antisense oligonucleotides. *Proc Natl Acad Sci U S A.* ***85****(14): 5011-5015*.

237. Wasungu, L., et Hoekstra, D. **(2006)**. Cationic lipids, lipoplexes and intracellular delivery of genes. *J Control Release.* ***116****(2): 255-264*.

238. Wender, P. A., Mitchell, D. J., Pattabiraman, K., Pelkey, E. T., Steinman, L., et Rothbard, J. B. **(2000)**. The design, synthesis, and evaluation of molecules that enable or enhance cellular uptake: peptoid molecular transporters. *Proc Natl Acad Sci U S A.* ***97****(24): 13003-13008*.

239. Wiethoff, C. M., et Middaugh, C. R. **(2003)**. Barriers to nonviral gene delivery. *J Pharm Sci.* ***92****(2): 203-217*.

240. Wolf, Y., Pritz, S., Abes, S., Bienert, M., Lebleu, B., et Oehlke, J. **(2006)**. Structural requirements for cellular uptake and antisense activity of peptide nucleic acids conjugated with various peptides. *Biochemistry.* ***45****(50): 14944-14954*.

241. Wu, G. Y., et Wu, C. H. **(1987)**. Receptor-mediated in vitro gene transformation by a soluble DNA carrier system. *J Biol Chem.* ***262****(10): 4429-4432*.

242. Wu, N., et Ataai, M. M. **(2000)**. Production of viral vectors for gene therapy applications. *Curr Opin Biotechnol.* ***11****(2): 205-208*.

243. Yamashiro, D. J., Fluss, S. R., et Maxfield, F. R. **(1983)**. Acidification of endocytic vesicles by an ATP-dependent proton pump. *J Cell Biol.* ***97****(3): 929-934*.

244. Yamashiro, D. J., et Maxfield, F. R. **(1984)**. Acidification of endocytic compartments and the intracellular pathways of ligands and receptors. *J Cell Biochem.* ***26****(4): 231-246*.

245. Yamashiro, D. J., et Maxfield, F. R. **(1987)**. Acidification of morphologically distinct endosomes in mutant and wild-type Chinese hamster ovary cells. *J Cell Biol.* ***105****(6 Pt 1): 2723-2733*.

246. Ye, D., Xu, D., Singer, A. U., et Juliano, R. L. **(2002)**. Evaluation of strategies for the intracellular delivery of proteins. *Pharm Res.* ***19****(9): 1302-1309*.

247. Yi, Y., Hahm, S. H., et Lee, K. H. **(2005)**. Retroviral gene therapy: safety issues and possible solutions. *Curr Gene Ther.* ***5****(1): 25-35*.

248. Youngblood, D. S., Hatlevig, S. A., Hassinger, J. N., Iversen, P. L., et Moulton, H. M. **(2007)**. Stability of cell-penetrating peptide-morpholino oligomer conjugates in human serum and in cells. *Bioconjug Chem.* ***18****(1): 50-60*.

249. Zamecnik, P. C., et Stephenson, M. L. **(1978)**. Inhibition of Rous sarcoma virus replication and cell transformation by a specific oligodeoxynucleotide. *Proc Natl Acad Sci U S A.* ***75****(1): 280-284*.

250. Zasloff, M. **(1987)**. Magainins, a class of antimicrobial peptides from Xenopus skin: isolation, characterization of two active forms, and partial cDNA sequence of a precursor. *Proc Natl Acad Sci U S A.* ***84****(15): 5449-5453*.

251. Zhang, X., et Godbey, W. T. **(2006)**. Viral vectors for gene delivery in tissue engineering. *Adv Drug Deliv Rev.* ***58****(4): 515-534*.

252. Zhou, P., Wang, M., Du, L., Fisher, G. W., Waggoner, A., et Ly, D. H. **(2003)**. Novel binding and efficient cellular uptake of guanidine-based peptide nucleic acids (GPNA). *J Am Chem Soc.* ***125****(23): 6878-6879*.

253. Zorko, M., Pooga, M., Saar, K., Rezaei, K., et Langel, U. **(1998)**. Differential regulation of GTPase activity by mastoparan and galparan. *Arch Biochem Biophys.* ***349****(2): 321-328*.

Auteur : Saïd ABES

Année : 2007

Titre : Optimisation des vecteurs peptidiques : Application à la délivrance d'analogues d'oligonucléotides à visée thérapeutique (PNA et PMO)

Résumé :
Les oligonucléotides antisens possèdent un immense potentiel thérapeutique. Cependant, la faible efficacité avec laquelle ils traversent les membranes biologiques limite leur utilisation. De nombreuses stratégies de délivrances ont été proposées pour contourner ce problème mais la plupart restent peu adaptées à une utilisation *in vivo*. Durant cette dernière décennie, plusieurs peptides capables de traverser la membrane plasmique ont été caractérisés. Regroupés sous le nom de Cell Penetrating Peptide, ces peptides sont polycationiques et parfois amphipatiques. Nos travaux d'évaluation de ces CPPs dans le modèle cellulaire de correction d'épissage indiquent que ces vecteurs, couplé à des PNA ou PMO, restent bloqués dans les vésicules d'endocytose. L'utilisation d'agents endosomolytiques comme la chloroquine, libère ces conjugués améliorant ainsi l'efficacité de la correction d'épissage. D'une manière générale, il est admis que le développement de nouveaux peptides vecteurs présentant une propriété endosomolytique intrinsèque constituerait une avancée majeure dans le domaine de la délivrance. Deux conjugués (R-Ahx-R)$_4$-PMO et R_6Pen-PNA corrigent efficacement l'épissage sans addition de chloroquine. Ces conjugués sont internalisés dans les cellules par un mécanisme endocytotique. Les études de structure activité ont indiqué une corrélation entre l'affinité des conjugués aux héparanes sulfates ainsi que de leur hydrophobicité et l'efficacité de correction. Les travaux sur les modèles animaux ont montré une large biodisponibilité du conjugué (R-Ahx-R)$_4$-PMO. Nos collaborations continuent pour améliorer ces deux peptides de délivrance.

Mots-clés
Antisens, peptides vecteurs (CPP), correction d'épissage et cancer

Title: Cell Penetrating Peptide optimization: Application to delivery of steric block oligonucleotide analogues (PNA, PMO)

Abstract :
Antisense oligonucleotides have a large therapeutic potential. However, the low effectiveness with which they cross biological membranes limits their clinical development. Many delivery strategies were proposed to circumvent this problem but the majority remain inadapted to an *in vivo* use. During this last decade, several peptides able to cross the plasma membrane were characterized. Gathered under the name of Cell Penetrating Peptides, these peptides are polycationic and sometimes amphipatic. Our work, using luciferase splice correction cells model, indicates that these CPPs and their conjugates to PNA or PMO remain blocked in endocytic vesicles. Endosomolytic agents, like chloroquine, promote the endosomal escape and improves the splice correcting efficiency. It is now admitted that the development of new peptides vectors with an intrinsic endosomolytic property would constitute a major step in the field of the delivery. Two conjugates, (R-Ahx-R)$_4$-PMO and R_6Pen-PNA, effectively correct splicing without addition of chloroquine. The mechanistic studies indicate that these conjugates are internalised in the cells by an endocytotic mechanism. The structure-activiy studies indicate a correlation between the affinity of CPP-ON to the heparan sulphate as well as theirs hydrophobicities and the effectiveness of correction. Work on the animals models showed a broad biodisponibility of (R-Ahx-R)$_4$-PMO.

Keywords : Steric block oligonucleotide analogues, Cell Penetrating Peptide, Splice correction and cancer

CNRS UMR5235, Dynamique des interactions membranaires normales et pathologiques. Département de défenses antivirales et antitumorales. Université Montpellier 2, Place Eugène Bataillon, 34095 Montpellier Cedex 5, France